

**INSTRUMENTATION SYSTEMS FOR POST-TENSIONED
SEGMENTAL BOX GIRDER BRIDGES**

APPROVED:

John E. Breen

Michael E. Kreger

to my family

**INSTRUMENTATION SYSTEMS FOR POST-TENSIONED
SEGMENTAL BOX GIRDER BRIDGES**

by

José Antonio Arréllaga Acosta, B.S.C.E.

THESIS

Presented to the Faculty of the Graduate School of
The University of Texas at Austin
in Partial Fulfillment
of the Requirements
for the Degree of
MASTER OF SCIENCE IN ENGINEERING

THE UNIVERSITY OF TEXAS AT AUSTIN

December 1991

ACKNOWLEDGEMENTS

This report is based on research conducted at the Phil M. Ferguson Structural Engineering Laboratory at the Balcones Research Center of the University of Texas at Austin. Financial support for the project was provided by the Texas State Department of Public Transportation (TSDHPT), and the Federal Highway Administration.

The present investigation was supervised by Dr. John E. Breen and Dr. Michael E. Kreger. The friendship and guidance provided by both advisors is highly valued. In particular, Dr. Breen's strong commitments to improving the general understanding of civil engineering structures, and to the ultimate building of a better society provided great technical as well as moral support. In addition to the direct project advisors, the helpful guidance provided by Dr. Karl H. Frank is gratefully appreciated.

Engineers from the Bridge Division of the sponsoring agency (TSDHPT) provided constant support and helpful contributions to the present project. My special thanks to Alan Matejowsky, Pat Bachman, and Greg Freeby.

I would also like to thank other people devoted to the enhancements of our engineering knowledge, particularly Carin Roberts whose endless help and cheerful support contributed to the realization of this project. The friendship and the collaboration of numerous Ferguson Lab. (FSEL) students is also well respected. My special thanks to a group of great colleagues and friends from FSEL: Sergio Alcocer, Asit Baxi, Hakim Bouadi, Brian Falconer, Reed Freeman, "Cliffy" Hall, Todd and Karen Helwig, Aziz Hindi, Gilberto Leiva, Francisco "Paco" Noyola, José Pincheira, Brock Radloff, Mike Rung, Bruce "The King" Russell, Dean Van Landuyt, Gregor Wollmann, and Les Zumbrennen.

The assistance of the excellent staff of Ferguson Laboratory was also a factor of great help to the present project. Two outstanding individuals deserve special merits: Wayne Fontenot and Johaan Ernest. The experienced technical background combined with the endless wills of Johaan and Wayne was always helpful for materializing any new idea. The help and friendship of other hard working people from Ferguson Lab. is also much appreciated. My very special thanks to Laurie Golding, April Jenkins, Jean Gherke, Sharon Cunningham, Blake Stassney, Pat Ball, and Wayne Little.

The extensive coverage and the very nature of the present project also required the direct interaction and help of several entities and people from outside the laboratory, particularly:

Austin Bridge and Road Co. of San Antonio: the support and interest expressed by numerous staff engineers greatly helped to smooth out the initial instrumentation details. My personal gratitude to Ron Ladewig, Greg Creamer, Jorge Hinojosa, David Hartmann, Mike Pettit, and Harold Steckle. The company is also thanked for their contributions of prestressing strand materials, for lending of their testing equipment and facilities in San Antonio, and for their continuous support to the ongoing instrumentation project.

Sika, Inc.: sample epoxy resins and a considerable discount for the large purchase of the epoxies to be used for the instrumentation project in San Antonio Y were donated by the Testing Department of this Company. In particular, the valued assistance and understanding of Mr. Frank Dominico is gratefully appreciated.

Viscosity Oil Company: the cooperation of Chuck Novak, and the donation of the Visconorust PT1001 grease is also recognized with appreciation.

Finally, but never lastly, my most profound feelings of gratitude are devoted to my family for their loving care and understanding. My parents, Víctor Hugo and María Mercedes, always provided all they had for the education and well being of their children. Their nobility and love is a tough challenge for the future relationships with my own children. The sincere moral and economical support of each one of my brothers have continuously strengthened my goals of furthering my education. I am very grateful to each one of them. My wife, has faithfully supported my work and studies. I will always be indebted to her for such a loveful and understanding companionship.

José Arréllaga

Austin, Texas

October 28, 1991

TABLE OF CONTENTS

Chapter 1. INTRODUCTION	1
1.1 Prestressed Concrete Segmental Box Girder Bridges	1
1.1.1 Definition.....	2
1.1.2 History of Development	2
1.1.2.1 Prestressed Concrete	3
1.1.2.2 Segmental Construction	9
1.1.3 Construction Methods	15
1.1.4 Future Trends.....	17
1.1.4.1 External Prestressing Tendons	18
1.1.4.2 New Geometries	18
1.1.4.3 Improved Materials.....	23
1.2 Need for the Instrumentation of Bridge Structures	27
1.3 Objective and Scope of the Present Study.....	29
1.3.1 Detailed Instrumentation Objectives.....	30
1.3.2 Present Study Summary	32
1.4 The San Antonio Y Project.....	34
1.4.1 Description of the Structure.....	35
1.4.2 Fabrication of Segments.....	42
1.4.3 Erection Systems.....	42
Chapter 2. PREVIOUS RESEARCH AND PUBLICATIONS	49
2.1 General.....	49
2.2 Turkey Run Bridge.....	50
2.3 Denny Creek Viaduct	52
2.4 CALTRANS Segmental Box Girder Bridges	56
2.5 River Torridge Bridge (England).....	59
2.6 James River Bridge	63
2.7 Highway Bridges in Nevada	68
2.8 Other Projects.....	72
2.8.1 Prestressed Concrete Bridges in Japan.....	73

2.8.2	Kishwaukee River Bridge.....	74
2.8.3	Pelotas River Bridge (Brazil)	74
2.8.4	Concrete Bridges in Switzerland	75
2.8.5	Concrete Bridges in Portugal.....	76
Chapter 3. STATE-OF-THE-ART INSTRUMENTATION SYSTEMS.....		78
3.1	Concrete Strains	78
3.1.1	Objectives	80
3.1.2	Embedment Systems	82
3.1.2.1	Vibrating Wire Strain Gages	83
3.1.2.2	Electrical Resistance Strain Gages	84
3.1.2.3	Carlson Elastic Wire Strain Meters	88
3.1.3	Surface Strain Systems.....	89
3.1.3.1	Mechanical Devices.....	89
3.1.3.2	Vibrating Wire Strain Gages	94
3.1.3.3	Electrical Resistance Strain Gages	94
3.1.3.4	Fiber Optical Strain Gages	95
3.2	Prestressing Steel Strains/Loads	99
3.2.1	Objectives	99
3.2.2	Strain Measuring Devices.....	99
3.2.2.1	Electrical Resistance Strain Gages	101
3.2.2.2	Other Systems.....	105
3.2.3	Load Measuring Devices.....	105
3.2.3.1	Calibrated Hydraulic Jacks	105
3.2.3.2	Load Cells	107
3.2.3.3	Cable Tensiometers	110
3.3	Span Deflections	116
3.3.1	Objectives	117
3.3.2	Base Line Methods.....	118
3.3.3	Hydrostatic Methods	123
3.3.4	Surveying Methods	125
3.4	Thermal Variations.....	128

3.4.1 Objectives	129
3.4.2 Concrete Temperature.....	130
3.4.2.1 Thermocouples	131
3.4.2.2 Thermistors.....	135
3.4.2.3 Other Systems.....	136
3.4.3 Solar Radiation	137
3.5 Other Measurements.....	139
3.5.1 Calibrated Crack Monitors	140
3.5.2 Caliper Gages.....	141
3.6 Data Acquisition Systems.....	142
Chapter 4. TRIALS OF INSTRUMENTATION SYSTEMS	146
4.1 Criteria for Selecting the Final Instrumentation Systems	146
4.2 Concrete Strain Measurements	147
4.2.1 Demec Gages: Bonding Methods	148
4.2.1.1 Ease of Installation	148
4.2.1.2 Long-Term Stability	151
4.2.2 Demec Gages: Increases in Operating Speed.....	155
4.2.3 Demec Gages: Repeatability	159
4.3 Prestressing Steel Strain/Load Measurements	160
4.3.1 Electrical Resistance Strain Gages	161
4.3.1.1 Improvements in Signal Stability	161
4.3.1.2 Single Strand Tests	169
4.3.1.3 Multi-Strand Tendon Tests.....	187
4.3.2 Epoxy Sleeves.....	200
4.3.2.1 Single Strand Tests	207
4.3.2.2 Multi-Strand Tendon Tests.....	220
4.3.2.3 Other Tests	235
4.4 Span Deflection Measurements	244
4.4.1 Line Tensioning Systems	245
4.4.1.1 Systems Investigated.....	246
4.4.1.2 Short Span Test Setup.....	246

4.4.1.3	Short Span Test Results	247
4.4.2	Reading Systems	248
4.4.3	Short Span Performance of Final System.....	258
4.4.4	Field Performance of Final System.....	260
4.4.4.1	Installation and Operation.....	260
4.4.4.2	Measuring Times	267
4.4.4.3	Repeatability of Readings	268
4.4.4.4	Stability of Readings.....	269
4.5	Data Acquisition System	277
Chapter 5. RECOMMENDED APPLICATIONS.....		281
5.1	Demec Extensometers	281
5.1.1	Installation of Locating Points.....	281
5.1.2	Corrections for Temperature Differentials	282
5.1.3	Operating Instructions	283
5.1.3.1	Repeatability.....	284
5.1.3.2	Handling and Storage.....	285
5.2	Electrical Resistance Strain Gages.....	285
5.2.1	System Selection.....	285
5.2.2	Use in Prestressing Steel Tendons	286
5.2.3	Use in Reinforcing Steel Bars	290
5.3	Epoxy Sleeves	291
5.3.1	Multi-Strain Tendon Systems	292
5.3.2	Data Reduction Process.....	294
5.4	Calibration of Hydraulic Jacks.....	295
5.5	Span Deflections	296
5.5.1	System Description and Selection	297
5.5.1.1	Base Lines	299
5.5.1.2	Live End Stations.....	299
5.5.1.3	Dead End Stations.....	300
5.5.1.4	Reading Stations	300
5.5.1.5	Portable Reading Units	301

5.5.2	Field Installation	301
5.5.3	Operation and Storage	302
5.6	Thermal Measurements	303
5.6.1	Concrete Temperature	303
5.6.2	Solar Radiation	305
5.7	Material Tests	305
5.7.1	Concrete	306
5.7.2	Prestressing Steel	308
5.7.2.1	Epoxy Sleeves	308
5.7.2.2	Electrical Resistance Strain Gages	309
5.7.3	Reinforcing Steel	310
5.8	Other Measurements	311
5.8.1	Joint Openings	311
5.8.2	Bearing Pad Deformations	312
Chapter 6. CONCLUSIONS AND FINAL RECOMMENDATIONS		313
6.1	General Conclusions and Recommendations	313
6.1.1	Demec Extensometers	313
6.1.2	Electrical Resistance Strain Gages	314
6.1.3	Epoxy Sleeve Systems	317
6.1.4	Base Line Methods	318
6.1.5	Automated Data Acquisition System	320
6.2	Future Research Needs	320
Appendix A. Survey of Segmental Concrete Box Girder Bridges		324
Appendix B. Schematic of Data Acquisition System		342
Appendix C. Special Provisions for Bridge Instrumentation		367
References		370
Bibliography		378

List of Tables

Table	Page
1.1 Average bridge length and range for various methods of construction	17
3.1 Technical data of typical vibrating wire strain gages for embedment in concrete.....	84
3.2 Technical data of original Mustran Cells	87
3.3 Technical data of other strain gages for embedment in concrete	89
3.4 Technical data for typical Demec extensometers	93
3.5 Current prices of Whittemore gages (from Soiltest, Inc.).....	93
3.6 Technical data for typical surface-mounted vibrating wire strain gages	95
3.7 Technical data of surface bonded foil electrical resistance strain gages	96
3.8 Technical data for ER-Load cells	108
3.9 Commonly available thermocouple wires, insulations, and overbraidings (from Omega Eng., Inc.).....	132
3.10 Typical costs of a thermocouple system for use in concrete structures (from Omega Eng., Inc. prices from late 1990)	133
3.11 Late 1990 prices for data acquisition components offered by Campbell Scientific, Inc.	144
4.1 Ease of installation of different bonding methods of Demec locating points ...	149
4.2 Description of systems tested for long-term stability.....	152
4.3 Final report on long-term stability of Demec guiding systems	153
4.4 Descriptions of single strand tests	170
5.1 Suggested ER-Gage systems.....	286

List of Figures

Figures	Page
1.1 Classification of layouts of longitudinal prestressing tendons of box girder bridges.....	4
1.2a Cross-section geometry of typical concrete segments outside the U.S.....	5
1.2b Cross-section geometry of typical concrete segments in the U.S.....	6
1.3 Bridge systems built by combination of concrete segments and longitudinal tendons	7
1.4 Evolution of concrete box girder segments (after Schlaich [10]).....	11
1.5 Influence of maximum span length on construction method of segmental concrete bridges	19
1.6 La Ferté Saint-Aubin Bridge (France), mixed system with concrete deck and stiffened metallic webs (after Virlogeux [14])	20
1.7 Cognac Bridge (France), mixed system with concrete deck and corrugated steel webs (after Mathivat [26])	21
1.8 Arbois Bridge (France), mixed system with concrete deck and webs of plane steel trusses (after Virlogeux [13]).....	22
1.9 Bubiyan Bridge (Kuwait), concrete segments with prestressed concrete triangular trusses (after Raspaud [25])	24
1.10 Entreprises Quillery (France), proposal of concrete segments with trapezoidal concrete webs (after Mathivat [26]).....	25
1.11 Viaduct de Maupré (France), mixed system with concrete deck, corrugated steel webs, and longitudinal steel tubing (after [13, 15])	26
1.12 Phases and location of the San Antonio Y Project.....	34
1.13 Finished phase of the San Antonio Y Segmental Project.....	36
1.14 Overall layout of Project II-C	37
1.15a Typical segment dimensions for spans A-43 and A-44 (segments type III)	38
1.15b Longitudinal post-tensioning layouts for spans A-43 and A-44 (type III segments)	39
1.15c Typical segment dimensions for spans C-9 and C-11 (segments type I)	40

1.15b	Longitudinal post-tensioning layouts for spans C-9 and C-11 (type I segments)	41
1.16	Assembling of new-cast segment	43
1.17	View of recently cast segment (used to match-cast the new segment)	43
1.18	Lowering of reinforcement cages in the stationary casting beds	44
1.19	Final installation of prestressing steel ducts in short line casting bed	44
1.20	Prestressing of transverse tendons in casting bed	45
1.21	Concrete work	45
1.22	General view of casting yard operations	46
1.23	Storage area in casting yard	46
1.24	Austin Bridge Company's erection truss	47
1.25	H. P. Zachry Construction's erection truss	47
3.1	Strain errors produced from <i>inclusion effect</i> of different materials and sizes (after Bakoss [59])	82
3.2	Typical commercial embedment type vibrating wire gages	85
3.3	Typical sister bar vibrating wire strain gage (after Dunicliff [60])	86
3.4	Concrete embedment strain gages based on the electrical resistance technology	90
3.5	Typical Carlson Elastic Wire Meter (courtesy of B. R. Jones and Assoc., Inc.)	91
3.6	Demec Extensometer (after Dunicliff [60])	92
3.7	Principle of interferometric fiber optic sensors	98
3.8	Principle of reference optical fiber sensors	98
3.9	Electrical resistance foil gage bonded to single wire of strand	102
3.10	Stress-strain plot of single prestressing strand with 6 ER-gages (after Yates [73])	103
3.11	Calibrated hydraulic jack for field measurement of tendon loads	107
3.12	Electrical resistance load cells with central holes (from Geokon's catalog)	108
3.13	Schematic of a typical electrical resistance load cell (after Dunicliff [60])	109
3.14	Freyssinet's Flat Jack (from Freyssinet's catalog)	110
3.15	Freyssinet's Tensiomag system (from Freyssinet's catalog)	112
3.16	Operation principle of Tensiomag (from Freyssinet's catalog)	113

3.17	DynaTension System (from DynaTension's catalog).....	114
3.18	Cable Tensiometer (after Dunnicliff [60]).....	115
3.19	Fulmer Tension Meter (after Hanna [78]).....	116
3.20	Kuhlman Beam from California D. O. T. (after Richardson [44]).....	116
3.21	Pauw-Breen original base line system.....	120
3.22	Bradberry-Breen modifications of the base line system	122
3.23	Law of communicating vessels	124
3.24	Sample layouts and final measuring pot of the hydrostatic leveling system (after Markey [53]).....	126
3.25	Basic operation of surveying methods for measuring span deflections (after Bradberry [81]).....	127
3.26	Factors influencing the thermal response of segmental box girder bridges	129
3.27	Principle of operation of thermocouples	131
3.28	Typical thermocouple system for field instrumentation projects	134
3.29	Typical thermistor for concrete embedment (from B. R. Jones catalog).....	135
3.30	LI-200SZ Pyranometer	138
3.31	Typical dimensions of calibrated crack monitors (Avongard products)	140
3.32	Avongard calibrated crack monitor.....	141
4.1	Concrete embedment method	150
4.2	Inserts for drilled concrete methods	151
4.3	Long-term stability of specimen #2	154
4.4	Modified Demec Extensometer	156
4.5	Location of Demec points on test span C-35.....	157
4.6	Comparison of reading speed of modified and standard Demec gages	158
4.7	Installation of the electrical resistance strain gages for TEST 1S (similar to TEST 4S)	172
4.8	Single strand TEST 1S	173
4.9	Single strand TEST 2S	174
4.10	Analytical approximation of a prestressing strand's apparent modulus of elasticity as determined by electrical resistance strain gages bonded to individual wires	175
4.11	Stress-strain curves for TEST 1S on ½ " ϕ strand specimen from roll "A"	179

4.12	Stress-strain curves for TEST 2S on first ½ " ϕ strand specimen from roll "B"	180
4.13	Stress-strain curves for TEST 3S on second ½ " ϕ strand specimen from roll "B"	181
4.14	Stress-strain curves for first loading cycle of TEST 4S on 0.6" ϕ strand specimen from roll "C"	182
4.15	Stress-strain curves for second loading cycle of TEST 4S on 0.6" ϕ strand specimen from roll "C"	183
4.16	Summary of stress-strain average curves of single strand tests with ER-gages	184
4.17	Statistical analysis of electrical resistance strain gage results from tests on ½ " ϕ strand specimens from roll "B"	185
4.18	Statistical analysis of electrical resistance strain gage results from tests on 0.6" ϕ strand specimen from roll "C"	186
4.19	General schematic of TEST 1T and TEST 2T.....	192
4.20	General schematic of TEST 3T and TEST 4T.....	192
4.21	Stress-strain plots of individual ER-gages for TEST 1T.....	193
4.22	Stress-strain plots of individual ER-gages for TEST 2T.....	194
4.23	Summary of stress-strain average curves of TESTs 1T and 2T.....	195
4.24	Statistical analysis of electrical resistance strain gage results from tendon TESTs 1T and 2T with ½ " ϕ strands.....	196
4.25	Stress-strain plots of individual ER-gages for TEST 3T.....	201
4.26	Stress-strain plots of individual ER-gages for TEST 4T.....	202
4.27	Average stress-strain plots of the ER-gages for each loading cycle of TEST 3T.....	203
4.28	Average stress-strain plots of the ER-gages for each loading cycle of TEST 4T.....	204
4.29	Comparison of average stress-strain plots of the ER-gages of TESTs 3T and 4T.....	205
4.30	Statistical analysis of ER-gage results from tendon TESTs 3T and 4T on 19-0.6" diameter strands	206
4.31	Schematic of the epoxy sleeve systems used in single strand tests	212

4.32	Stress-strain plots for TEST 1ES on ½ " ϕ strand specimen from strand roll "B"	213
4.33	Stress-strain plots for TEST 2ES on ½ " ϕ strand specimen from strand roll "B"	214
4.34	Stress-strain plots for first loading cycle of TEST 3ES on 0.6" ϕ strand specimen from roll "C"	215
4.35	Stress-strain plots for second loading cycle of TEST 3ES on 0.6" ϕ strand specimen from roll "C"	216
4.36	Summary of stress-strain average plots of single strand tests with epoxy sleeves.....	217
4.37	Statistical analysis of epoxy sleeve results from tests on ½ " ϕ strand specimens from roll "B"	218
4.38	Statistical analysis of epoxy sleeve results from tests on the 0.6" ϕ strand specimen from roll "C"	219
4.39	Construction steps of the epoxy sleeve system used in TEST 2T	222
4.40	Epoxy leaks in TEST 2T	223
4.41	Problems for finding the zero stress reading in epoxy sleeve systems	225
4.42	Stress-strain plots of individual epoxy sleeve reading locations for TEST 1T ..	228
4.43	Stress-strain plots of individual epoxy sleeve reading locations for TEST 2T ..	229
4.44	Summary of stress-strain average plots for TESTs 1T and 2T.....	230
4.45	Statistical analysis of epoxy sleeve results from tendon TESTs 1T and 2T with ½ " ϕ strands.....	231
4.46	Possible stress distributions in a typical epoxy collar	232
4.47	Epoxy sleeve measuring systems	232
4.48	Stress-strain plots of individual epoxy sleeve reading locations for TEST 3T ..	236
4.49	Stress-strain plots of individual epoxy sleeve reading locations for TEST 4T ..	237
4.50	Summary of stress-strain average plots for TESTs 3T and 4T.....	238
4.51	Statistical analysis of epoxy sleeve results from tendon TESTs 3T and 4T on 19-0.6" diameter strands	239
4.52	Short-term creep TEST 1C	242
4.53	Grouting component of the epoxy sleeve system for multi-strand tendons	243
4.54	Live end tensioning mechanism type I.....	249

4.55	Live end tensioning mechanism type II	250
4.56	Live end tensioning mechanism type III	251
4.57	Live end tensioning mechanism type IV	252
4.58	Typical dead end anchorage	253
4.59	Typical short span test setup of deflection measuring systems	254
4.60	Comparison of performances of line tensioning methods	255
4.61	Portable reading unit of deflection measuring system (during installation to reading position).....	258
4.62	Portable reading unit of deflection measuring system (located in reading position)	259
4.63	Overall performance of final deflection measuring system during short span test	261
4.64	Reading errors of final deflection measuring system during short span test.....	262
4.65	Repeatability errors of final deflection measuring system during short span test using two different operators.....	263
4.66	System setup inside box girder bridge.....	265
4.67	Live end anchor and calibrated weight inside the box girder bridge.....	266
4.68	Digital scale measuring unit, mini-printer processor, and voltmeter during sample reading operation inside box girder bridge.....	266
4.69	Repeatability errors of final deflection measuring system during field test	272
4.70a	Measured and calculated deflections of span C-35.....	273
4.70b	Measured and calculated deflections of span C-35.....	274
4.71a	Measured and calculated vertical movements of span C-35 at different construction stages	275
4.71b	Measured and calculated vertical movements of span C-35 at different construction stages	276
4.72	Three-leadwire, quarter-bridge Wheatstone completion circuit required for most data-loggers	277
5.1	Installation of recommended Demec gages guiding system	282
5.2	Schematic of the final epoxy sleeve system for multi-strand tendons.....	292
5.3	Typical types of platen to simulate uneven bedding (after Littlejohn [76])	296
5.4	Components of base line system designed for typical spans of the San	

Antonio Y bridges	298
5.5 Installation of a series of thermocouple wires across the thickness of a concrete member	304
5.6 Schematic of finished single strand epoxy sleeve systems.....	310

CHAPTER 1 INTRODUCTION

1.1 Prestressed Concrete Segmental Box Girder Bridges

This relatively new bridge technology in the United States has been steadily gaining popularity and momentum since its introduction in 1972. It has become a major contender for all medium to long span bridge competitions. Statistics from May 1989 provided by the National Bridge Inventory (NBI) indicate that the rate of growth of prestressed concrete bridges (in general) greatly exceeds the growth of other bridge types such as those of structural steel, reinforced concrete, and timber which are actually declining [1]. An increasingly large contribution to this overall growth is attributed to the segmental concrete technology.

The segmental construction of concrete box girder bridges represents one of the most fascinating examples of the advancement of structural engineering towards the 21st century. Improved efficiency of materials, better handling of environmental concerns during construction and improved aesthetics, along with the inherent safety and durability of the structures, have become new requirements for future structural designs. Reviews of the concept and constant development of segmental concrete bridge structures suggest that refinements of this technology are still underway. Further research and surveillance programs are important tools for future advances.

Several research studies have been reported throughout the United States and various European countries concerning the behavior of different components of segmental box girder bridges. A great amount of work has also been published in reference to field monitoring of bridge structures [Bibliog. - Section XI]. However, only a small percentage of these investigations have been successfully implemented and reported in recent years. Most past investigations were centralized on individual areas of interest such as temperature gradients, concrete creep and shrinkage investigations, and/or deflection measurements. With the constant advancement of segmental box girder bridge technology and the increasing concern for durability of these structures, there is presently a higher priority given to the field investigation and surveillance of future bridge projects in many industrialized countries. Reports of methods

of surveillance and maintenance programs for bridge structures have been recently published in Europe and the United States. Furthermore, some new field instrumentation projects are now in the final stages of their development process.

A general overview of the prestressed concrete segmental box-girder technology in terms of its history of development, present concept, construction methods and future trends is necessary to understand the evolution process and to stress the importance of this particular area of structural engineering. A basic knowledge of historical achievements of all engineering structures, and particularly the development of segmental box girder bridges, is important to structural engineers. Historical knowledge provides an initial understanding of the evolution of the structural forms that were finally implemented in successful applications and those that were avoided because of inadequate behavior. Another interesting appeal of historical studies is to find how famous designers and builders succeeded in developing efficient, economical and aesthetically attractive structures in spite of the limitations in scientific laws of behavior, materials, technology and funding.

1.1.1 Definition

Prestressed concrete segmental box girder bridges are made up of short concrete segments either precast or cast-in-situ, joined together by longitudinal post-tensioning of internal, external, or mixed tendons. The different classifications of tendon layouts that are currently being used for the arrangement of longitudinal tendons are shown in Fig. 1.1. The cross section geometry of concrete segments has varied widely from single to multiple cells and with straight or sloping webs, as shown in Fig. 1.2a and Fig. 1.2b.

It is of particular importance to notice that these different types of concrete segments and variations of longitudinal tendons may comprise major structural components of various types of bridge structural systems. Besides the widely used continuous box girder bridge on multiple direct supports, other bridges have been built with the combination of the segmental concrete technology and varying arrangements of longitudinal tendons. Most of those other bridge structural systems are shown in Fig. 1.3.

1.1.2 History of Development

Some comprehensive reports of historical note on prestressed concrete and segmental

concrete bridges have been previously presented by several authors. The more detailed observations from Powell et al. [2], Podolny and Muller [3], Billington [4,9] and Menn [27] are combined in this section. As mentioned earlier, the purpose of the following historical compilation is to provide an awareness of the different steps involved in the evolution of efficient structural forms in the segmental box girder bridge technology.

In order to organize the historical events, the history of the development of prestressed concrete segmental box girder bridges is directly related to:

- a) the independent advancements of materials and techniques used for prestressing, and
- b) the development of the technology of segmental construction of concrete bridges.

1.1.2.1 Prestressed concrete. With respect to the prestressing technology, the basic concept of introducing initial compressive stresses in concrete so as to avoid exceeding its tensile stress limitations dates back to the late 19th century [5]. One of the earliest attempts at introducing artificial prestressing forces in concrete occurred in the United States in 1886. P. H. Jackson from California tightened steel tie rods in concrete arches to use them as floor slabs. A few years later, in 1888, W. Döring from Germany patented a system that reduced concrete cracking in floor slabs by means of prestressing wires embedded in concrete. However, the most important advances in prestressed concrete did not occur until 40 years later.

The earliest rudimentary form of "prestressed concrete" technique applied to bridges is probably represented by the three-span arches of "Le Veudre Bridge" over the Allier River in France, built by the well known French engineer Eugène Freyssinet and completed in 1910 [4]. This particular bridge introduced an ingenious initial solution to the poorly known problem of creep of concrete structures. Through a previous 164ft test-span of a concrete arch Freyssinet started to visualize a continuous contraction of the compressed concrete under sustained loading, ie. concrete creep. To account for future unwanted deflections due to possible creep in the concrete of the main 238ft span of Le Veudre, Freyssinet left an opening at the crown of the arch where he later installed some jacks. These jacks were used after the occurrence of most concrete creep when deflections of up to 130mm were observed. Pushing the two halves of the arch apart Freyssinet restored the bridge to its original profile and introduced externally induced horizontal compressive forces in the concrete. These midspan hinges were later concreted transforming the spans into two-hinged arches.

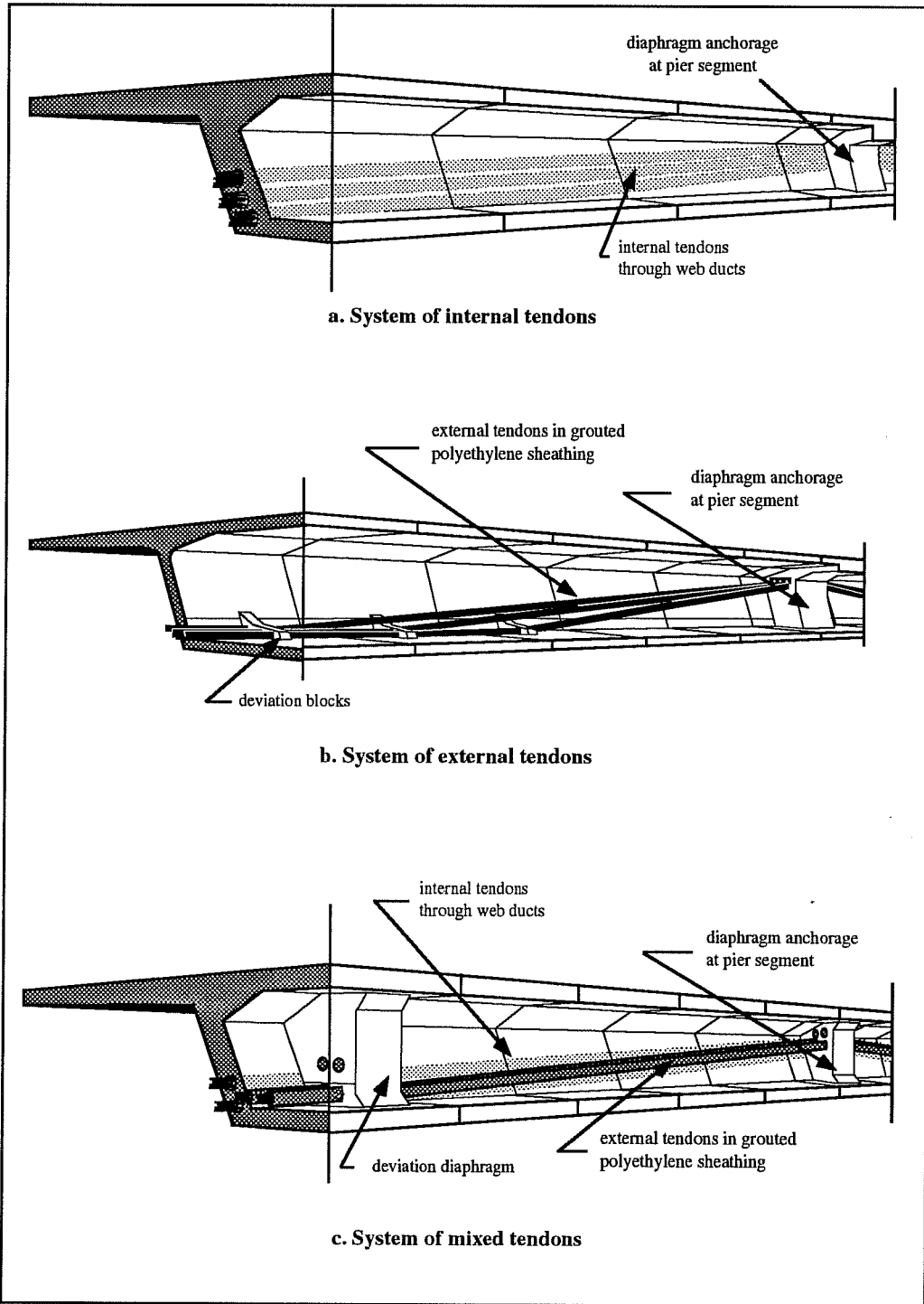


Figure 1.1 Classification of layouts of longitudinal prestressing tendons of box girder bridges.

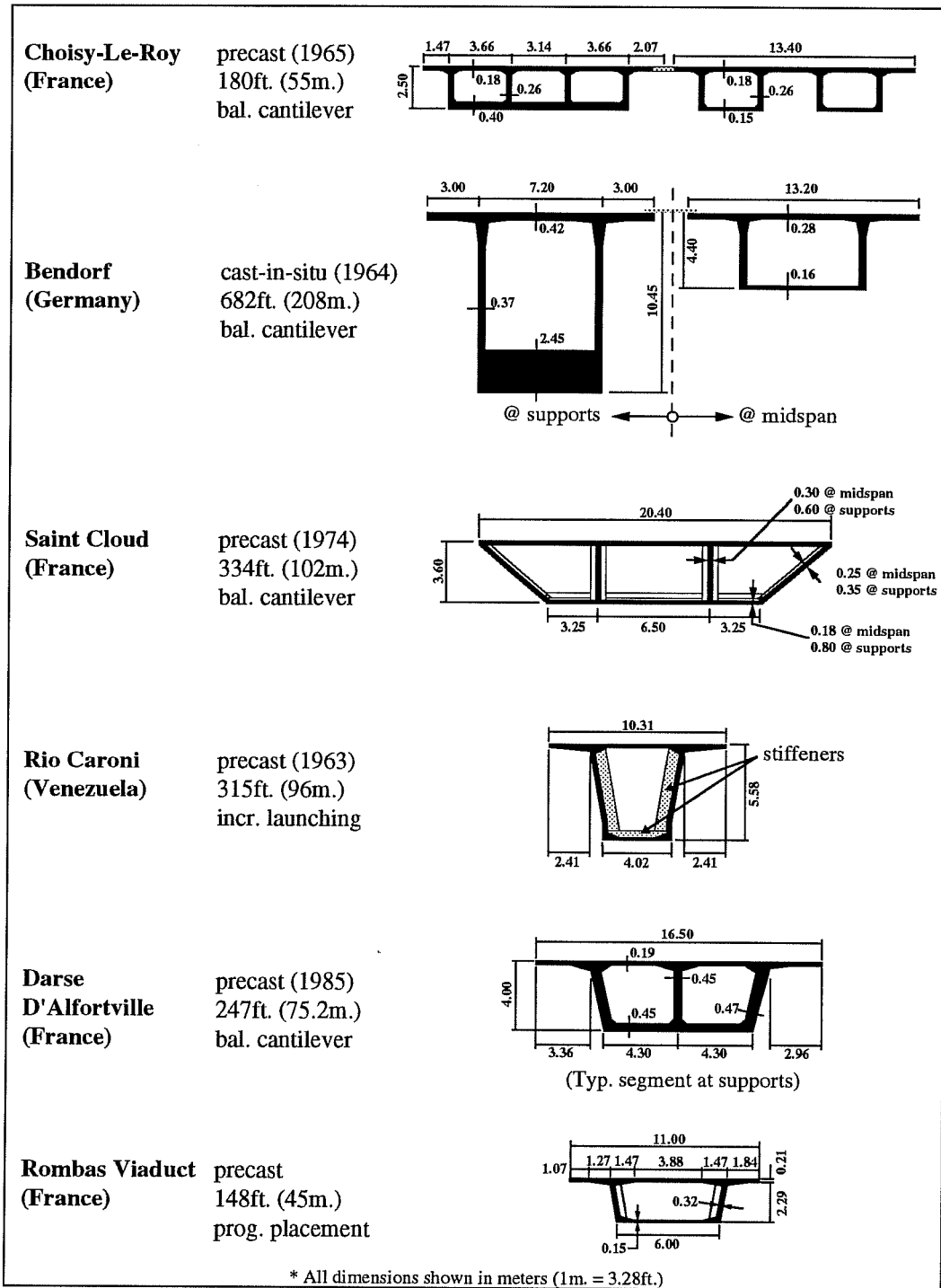


Figure 1.2a Cross-section geometry of typical concrete segments outside the US.

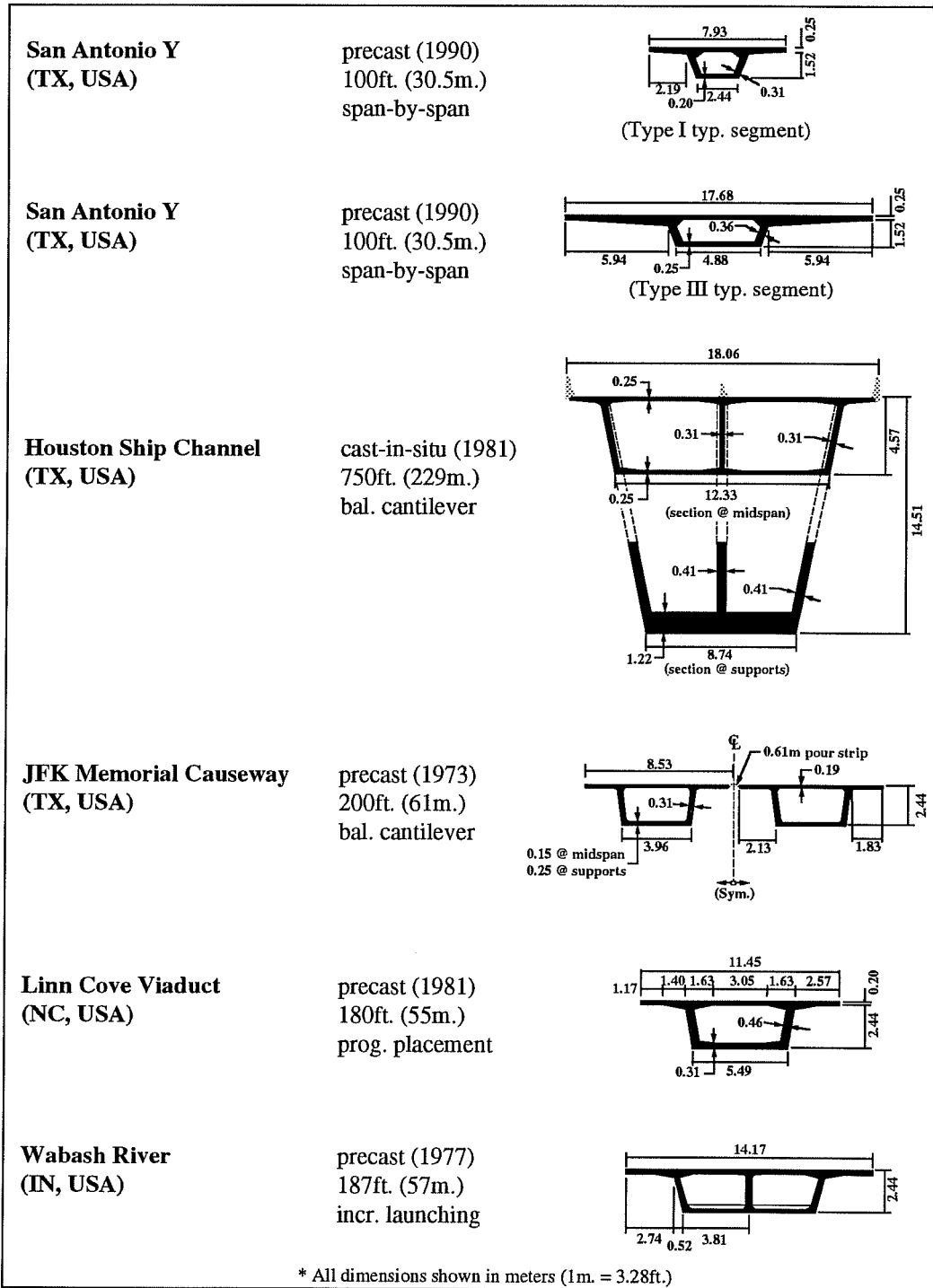


Figure 1.2b Cross-section geometry of typical concrete segments in the US.

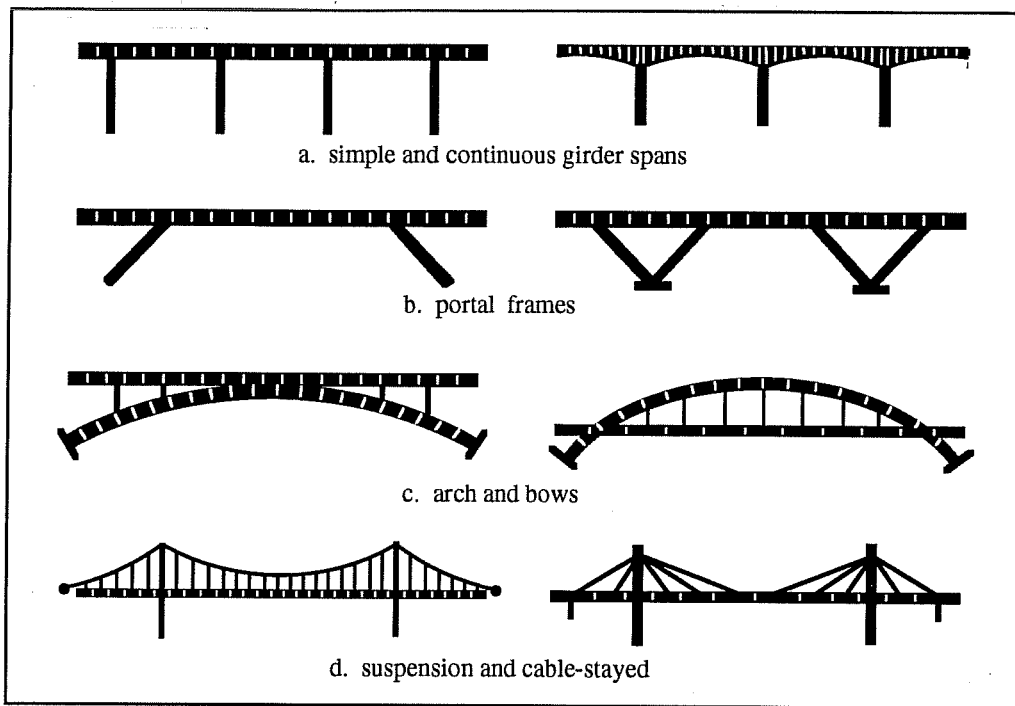


Figure 1.3 Bridge systems built by combination of concrete segments and longitudinal tendons.

Freyssinet continued with his studies of creep in concrete. Out of these studies, he visualized the basic ideas for prestressing that led him to patent the technology in October of 1928 [4].

Other European engineers also envisioned the great benefits of prestressed concrete bridges. In Germany, Franz Dischinger designed the Saale-brücke with external prestressing tendons that consisted of large diameter bars made of low-strength steel with butt-welded threaded couplings [2]. Finished in 1928, the Saale-brücke spanned 200ft over the Saale River in Alsleben and is considered to be the first modern prestressed concrete bridge in the world [2]. It also represents the first application of external prestressing in bridge structures. A highway bridge at Aue in Saxony (completed in 1937), and the Warthe-brücke in Potzdam (unfinished at outbreak of war in 1939) followed with applications of Dischinger's technology. However, these structures experienced large displacements and cracking due to the lower strength (about 60ksi.) of the prestressing rods used by Dischinger. After 25 years of service of these bridges, creep and shrinkage of concrete as well as steel relaxation introduced large prestressing losses which amounted to a loss of about 75% of their original prestress level [2]. The large displacements

(up to 200mm) and cracking of these structures made Dischinger aware of the effects of concrete creep and shrinkage, and their adverse influence on prestress losses, especially when using low strength prestressing tendons.

The revolution which launched prestressed concrete as a major construction method for bridge structures did not occur until reliable and more economical methods for prestressing and for anchorage of high strength tendons were introduced around the 1940s. Several new systems became available. In 1939, Eugène Freyssinet developed conical wedges for end anchorages, as well as double-acting jacks which tensioned the prestressing wires and thrust male cones into female receptacles for anchoring them. Freyssinet also fostered the original idea of "full prestressing" where concrete tension at service load state was completely eliminated by prestressing forces.

A few years after E. Freyssinet's patent, and induced by the impossibility to obtain Freyssinet's devices due to the occupation of Belgium, a new system was developed. Professor Gustave Magnel envisioned the Magnel-Blaton System (also known as the "Belgian Sandwich") wherein two wires were stretched at a time and anchored with a simple metal wedge at each end. One of the main advantages of this method was that it allowed for the use of cables containing a large number of prestressed wires. Up to 64-0.2in. ϕ wires capable of applying a compressive force of 214tons. have been used [28]. Slightly later, a new system was developed in the British Isles and became known as the Gifford-Udall System which used individual steel anchors with two-part wedges for anchoring the wires [6].

By the end of the 1940s one of Professor F. Dischinger's students, Ulrich Finsterwalder, invented the DYWIDAG system as it is known today. A different technique known as the LEOBA System was developed by Fritz Leonhardt and Willy Baur of Germany. They used strands made of high-strength steel wires placed inside of ducts and wrapped around concrete stressing blocks at the ends of the bridge [27].

In Switzerland, M. Birkenmaier, A. Brandestini and M. R. Rös developed the BBRV Prestressing System in 1948. It consisted of high-strength steel wires which were individually anchored by means of cold-formed buttonheads [27].

An ingenious technique for post-tensioning external tendons was introduced in 1951 with the Vaux-Sur-Seine bridge in France. A pair of bundles of prestressing wires were stressed simultaneously with low capacity jacks that pushed them apart against nearby

diaphragm deviators. These tendons were then held in their final position by a permanent concrete chock [2].

Further advances of prestressing technology came in the form of:

- improvements/modifications of the original systems already mentioned,
- appearance of new materials, and
- better understanding of the theory of prestressed concrete.

Modifications of the initial prestressing concepts started around 1946. P. W. Abeles originated the arguments against E. Freyssinet's ideas of "full prestressing." He discussed the advantages of reducing the prestressing levels of the tendons and of combining prestressed and non-prestressed tendons so as to obtain more economical structures. Small concrete tensile stresses at service loads would be permitted and allowed to be carried by mild reinforcement. However, the modern concepts of "partial prestressing" (or "limited prestressing" as called in Germany) were not introduced until 1968 in Switzerland. This theory eliminated the need for calculating concrete tensile stresses under service loads. Resistance at ultimate limit state was instead calculated considering both prestressing steel and mild reinforcing steel [27].

Progress towards simpler models for prestressed concrete design and construction continued until the present time. The latest advance in this area is the introduction of the theory of "structural concrete," as proposed by A.S.G. Bruggeling in 1987 [29]. The theory is based on the needs for unifying the different approaches to each type of concrete structure, from non-reinforced applications to those of mixed non-prestressed, prestressed, and post-tensioned reinforcement [30]. Prestressing is introduced as an artificial loading for the cases where prestressing could be profitable. In the United States, the "structural concrete approach" promoted by Breen [31] is basically aimed towards the same simplification and unification goals of Bruggeling's ideas. However, Breen emphasizes the needs for more global attention to load paths and deformation restraints in the preliminary design stage, instead of the emphasis in current designs of sectional load effects and load resistances [31]. This new model of "Structural Concrete" could open new ways for the development of simplified design and construction processes, imposing direct benefits to the entire concrete industry.

1.1.2.2 Segmental Construction. The initial concepts of segmental construction of bridges is much older than concrete. Some indications of very early applications by the Chinese in the 7th century have been reported [7]. However it was not until much later, in the 12th century, when

the first construction with flat segmental arches was recorded [8]. These early examples of segmental construction techniques were the bridges built by the monastic order of the Fratres Pontifices, of which their first one probably was over the Rhône River in Avignon, France --the famous Pont D'Avignon-- built during 1177-1185 [8]. Reinforced concrete later replaced the stones and bricks of earlier bridges. A major step occurred with the introduction of the more efficient hollow box girder concrete cross sections in the construction of arch bridges [9]. Since their introduction, concrete box girder sections used for arch bridges were designed to distribute the loads more efficiently. In these arch-bridges, the deck slab and thin box walls of the concrete sections could carry their own loads in addition to helping carry the lighter bottom arch slab.

Probably the first reinforced concrete box-girder arch bridge was the Inn River Bridge at Zuoz, Switzerland. Finished in October of 1901, this three-hinged arch bridge was designed and built by the famous Swiss bridge engineer Robert Maillart [9]. Maillart used his newly patented "bridge form" on other occasions, such as for the three-hinged arch bridges at Billwil (1904), and Tavanasa (1905) [9]. Other early applications of box girder bridges were François Hennebique's Risorgimento Bridge built in 1911 in Rome, Italy. This was another example of a three-hinged reinforced concrete arch bridge with box girder sections [10].

Later, with the combination of modern techniques of prestressed concrete, the box girder cross sections became part of the new prestressed concrete bridges often built by the segmental construction techniques. Jörg Schlaich in "Concrete Box Girders" [10] has presented an interesting graphical description related to the evolution of box-girders stating that they evolved structurally from the hollow cell deck bridge or the T-beam bridge, as shown in Fig. 1.4.

Further advances of prestressing and segmental construction techniques, along with the developments of new materials, the shortages of manual labor and the destruction of major bridges across Europe during World War II, all contributed to the final development of the prestressing technology and the segmental construction of bridges. In the second half of the 1900s, engineers thus evolved prestressed concrete segmental technology from the resources and needs of their time. Since their origin, prestressed concrete segmental box girder bridges have always been distinguished for revolutionizing the structural efficiency achieved in the use of materials, time and labor.

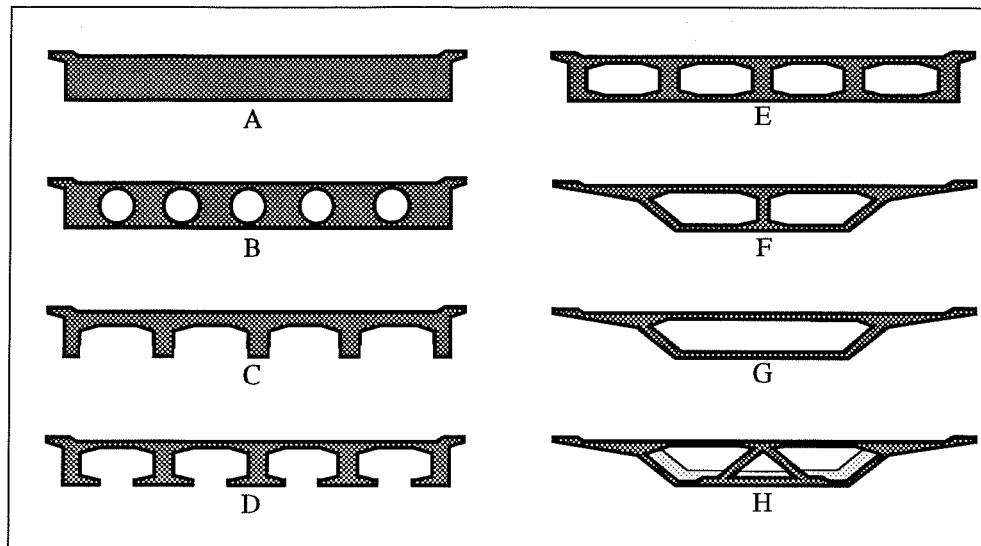


Figure 1.4 Evolution of concrete box girder segments (after Schlaich [10]).

A new achievement in the history of segmental construction of bridges was the idea of using concrete segments that were precast earlier, moved to their final position, and post-tensioned together to form the final bridge structure. E. Freyssinet was the first to use this methodology in his bridge over the Marne River at Luzancy which was finished in 1946 with a span length of 180ft [3]. The great benefit introduced by this new practice of precasting some bridge components was achieved by the increase in speed of the overall bridge construction process provided by the faster method of erection, and by the usage of repetitive industrialized manufacturing techniques. After continued development of the technology, precasting is now preferred because it allows for a better control of concrete quality and strength. Precasting also reduces the adverse effects of concrete creep and shrinkage since the bridge segments are usually quite mature before being erected. Five more bridges over the Marne River were built by Freyssinet. These were typically made of precast three-celled box-girder segments of 8ft lengths and 245ft spans.

In Belgium, Gustave Magnel designed and built the first continuous prestressed concrete box-girder bridge in the world in 1948. The Saclyn Bridge over the river Maas was made of three-celled concrete box girders forming two typical spans of 206ft [27].

The next advancement in the segmental construction of bridges was introduced by Ulrich Finsterwalder in Germany. The 1951 completion of the Lahn River bridge at Balduistein

marked the introduction of the first modern cast-in-place balanced cantilever bridge (main span length of 203ft). Other impressive bridges were built in Germany by the same technique [3]. This construction technique was not introduced in the United States until 1974. Pine Valley Creek bridge in San Diego, California, was the first segmental, prestressed concrete, cast-in-place balanced cantilever bridge in the United States. This bridge had a 450ft main span, and a total length of 1,741ft. It was designed by the California Department of Transportation [3]. This type of segmental bridge achieved quite impressive span lengths. The longest one to date is the 853ft centerspan of the Gateway Bridge in Brisbane, Australia, finished in 1986 [37].

Freyssinet and other French engineers continued with their applications of precast concrete. The first prestressed concrete bridges built in cantilever with precast segments appeared in France and the USSR in the 60s. One important bridge of this group is Choisy-le-Roi bridge over the Seine River in France, designed by Jean Müller. Finished in 1965 with spans of 123, 180, and 123ft it is the first epoxy jointed match-cast segmental box girder bridge in the world. The Olerón Island Bridge in France is another example of an epoxy jointed segmental box girder bridge. However, this particular bridge is important since it was the first to use an overhead steel launching truss (or steel launching girder) for the balanced cantilever erection of its segments. Precast segments for this 9,840ft long bridge structure were transported over the already completed portion and erected using the steel launching truss.

The first segmental concrete bridge in the United States is the JFK Memorial Causeway Bridge opened to traffic in early 1973 in Corpus Christi, Texas. It is made of twin single-cell concrete box girder segments erected in balanced cantilever forming three spans of 100, 200, and 100ft. It was designed by the Bridge Division of the Texas State Department of Highways and Public Transportation and with assistance by a research team from the University of Texas at Austin [32].

The span-by-span method of construction of segmental, prestressed concrete bridges was first used for the Untermarchtal Bridge over the Danube river, Germany. Fritz Leonhardt was responsible for the design and construction of this 1,096ft long, 5-span continuous girder bridge [27].

In the United States the span-by-span method of construction was first implemented for the Denny Creek Bridge in the State of Washington. This bridge completed in 1980 was built with cast-in-place concrete segments. It traverses a steep forested slope, crossing a deep ravine

and an avalanche path. The ecological and environmental sensitivity of the area made the span-by-span construction with a launching truss and movable scaffolding the most adequate. This structure, made of 20 spans with typical lengths of 188ft and a total length of 3,620ft, was designed by Dyckerhoff and Widmann in the United States [3].

The first use of precast concrete segments for a bridge built by the span-by-span method in the United States is the Long Key Bridge in the Florida Keys. Typical span lengths of 118ft make up the 12,160ft of this bridge structure that was completed in 1981. Of particular interest among the Florida Keys bridges is the 35,863ft Seven Mile Bridge, the longest segmental concrete bridge in the world to date. These bridges designed by Figg and Muller Engineers, Inc. successfully re-introduced the old concepts of external prestressing tendons.

Fritz Leonhardt is also responsible for developing the incremental launching method, his second innovation in the construction of segmental bridges. In 1964 he completed the world's first incrementally launched bridge over the Río Caroni in Venezuela. With typical spans of 315ft, a total length of 1,575ft was pushed to its final position from one abutment [33]. Although popular in Germany and much of Europe, this method of bridge construction has only been used twice in the United States. The Wabash River Bridge carrying U.S. I-74 near Covington, Indiana is the first incrementally launched bridge in the U. S. Completed in 1978, this bridge has typical spans of 187ft and a total length of 950ft [3]. The second bridge of this type is presently under construction over the Caguana River, in Puerto Rico. Slightly longer spans of 230ft typical lengths will extend for a total distance of 1,260ft [34].

Segmental, prestressed concrete bridges extended their range into longer span bridges with the construction of the first modern segmental, prestressed concrete, cable-stayed bridge in the world. The bridge over Lake Maracaibo in Venezuela, designed by Riccardo Morandi and finished in 1962, has a main span of 770ft [3]. However, the first use of this concept for concrete bridge structures actually occurred in 1925 when Eduardo Torroja built the Tempul Aqueduct over the Guadalete River in Spain [35]. This technology has been extensively improved with the latest segmental and prestressed concrete developments. Various impressive long-span cable-stayed concrete bridges were built in the United States and throughout the world in recent times. The first modern segmental, prestressed concrete cable-stayed bridge in the United States is the Pasco-Kennewick Bridge over the Columbia River, in the State of Washington. Finished in May 1978, the Pasco Kennewick Bridge was designed by Arvid Grant

& Associates, Inc. of Olympia, Washington, with collaborations of Leonhardt and Andra of Stuttgart, Germany. This bridge has a main cable-stayed span of 981ft [3]. Currently, the longest spanning concrete structure in the world is the Barrios de Luna cable-stayed bridge in León, Spain. Finished in 1983, this bridge has a main span of 1,444ft. It was designed by Carlos Fernández Casado S.A. of Spain [27]. In the State of Texas, the first concrete cable-stayed bridge is the Neches River Bridge in Port Arthur, finished in late 1990. This bridge, designed by Figg and Muller Engineers, has a centerspan of 640ft with backstay spans of 280 and 140ft [36].

Since Robert Maillart's first use of concrete box-girders for the segmental construction of arch bridges in 1901, the technology has improved considerably. E. Freyssinet introduced prestressed concrete segmental arch bridges with the Luzancy Bridge over the Marne River in France in 1946. Thereafter, concrete segmental arches have alternated with cable-stayed bridges as the longest spanning concrete structures in the world. Yugoslavia currently has the longest spanning concrete arch bridge, the Krk Island Bridge in the Adriatic Sea. It has a main arch span of 1,280ft and it was completed in 1979 [27]. In the United States this type of segmental construction has not been used as widely as in Europe. The George Westinghouse Bridge in Pittsburgh, Pennsylvania is the only representative in the country. It was finished in 1931 with reinforced concrete box-girder arch forms. Its main span of 440ft held the record span length of concrete bridges in the country for over 40 years.

A review of the literature suggested in the Bibliography of the present study was developed so as to form a database of most reported segmental concrete bridges around the world. This is included in Appendix A of this report. Bridges are separated by their method of construction, place of construction, and organized from shortest to longest span lengths. Notes regarding statistical facts and well-known designers are also included where necessary and available. Contradicting claims were often found in different reports. Most of these cases were compared with construction news magazines or books that provided broader details about the conflicting structures so as to establish a better organization of facts. Part of these disagreements were directly related to wording or interpretation of construction methods. These conflicts were solved according to the present author's judgement.

As a general summary of the historical facts, prestressed concrete segmental box girder bridge technology has achieved its modern strong competitive position through fuller

understanding of the techniques for prestressing the concrete, the combination of higher strength materials, advances in concrete technology, and with discoveries of new usages and combinations of box-girder segments (made of precast and cast-in-situ concrete). The final developments that tied together all these independent technological advances were the surge of ingenious construction methods. The different methods of erection of concrete segments show the versatility of these bridge structures which can adapt to the most demanding limitations of the environment, right of way, or aesthetical appearance.

1.1.3 Construction Methods

The overall construction procedure for this type of bridge is an important factor that actually must be considered in the design phase, where all possible construction loads have to be taken into account. During the actual fabrication and erection of the segments one important concern is the technological knowledge of the constructors, since it has been found that the segmental concrete technology can be a major economical threat to inexperienced builders [18]. In an attempt to reduce costs to contractors through savings in reusable forms, reusable installations and equipment, the Federal Highway Administration sponsored a study by T. Y. Lin and Assoc. of the feasibility for standardizing prestressed concrete segmental box girder bridges [11]. The study was also aimed at simplifying and improving the application and design of these type of bridges. The final report presented a broad analysis of segmental box girder technology up to 1982. An initial standardization of particular cases of segmental box-girder sections was suggested. The authors claimed that the flexibility of these ideas could help the industry achieve greater usage, safety and economy in future segmental projects. However, the present author considers that standardization could hurt the segmental concrete technology if it limits two of its main characteristics, which are its versatility of construction, and its freedom of form and shape --that provide variation of aesthetic impact.

Several factors come into play in the decision for the optimal construction method to be used on a particular segmental box girder bridge. The most influencing factors are probably the overall bridge length and the maximum span length which usually limit the construction method in terms of cost effectiveness. As mentioned earlier, segmental concrete bridges have been able to adapt to significant environmental restrictions and right-of-way limitations. These special circumstances can impose additional important factors for deciding the actual construction

method of certain bridge structures. The most commonly used methods of segmental construction are the following:

1. Span-by-span methods;
2. Incremental launching methods;
3. Balanced cantilever methods, precast and cast-in-place; and
4. Progressive placing methods.

Other systems such as cable stayed and arch bridges are usually built by one of the above mentioned methods. For some bridge projects a combination of the above mentioned erection systems have given the most cost effective solution [19]. However, most projects usually utilize only one single construction method. The versatility of traditional segmental construction operations has also allowed ample room for innovations and variations of techniques. An example of creativity and efficiency in erection systems has been shown recently in the construction of the bridges that carry U.S. Highway 36 across the Illinois River. Thirteen approach spans initially designed to be erected in balanced cantilever were more economically cast-in-situ in full span length on the ground, between piers. They were subsequently raised to final position and post-tensioned longitudinally [20].

A detailed description of each traditional method of construction of segmental bridges can be found in several books and publications [Bibliog. - Section VI]. This report, however, stresses the influence of maximum span length and total bridge length on choice of construction method as viewed from an economical standpoint. An approximate distribution of the construction methods used for segmental bridges with respect to maximum span length in America (mainly in the United States), Europe and Australia is presented in Fig. 1.5. This has been carefully prepared from the survey of bridges included in Appendix A (in turn based on the Bibliography of this report). The general correspondence of the ranges in these different continents is a good indication of the overall economic importance of the span length factor. In general, the shorter ranges of incremental launching and segmental arches in America show the narrower applications of these construction methods, and not a limitation of span lengths as compared to European practices. The influence of the second most important factor, the total bridge length, is shown approximately in Table 1.1. A brief study of these two controlling factors will be helpful for determining a good initial estimate of the most economical construction method for each particular project. Obviously, other construction restrictions such

as height limits, environmental concerns, right-of-way limitations and special aesthetics will also become a deciding factor for the selection of the most competitive and appropriate system.

With respect to the span-by-span method, it is evident that it is most economic on relatively short structures with several repetitive spans. This is the case of the San Antonio Y elevated highway project. It fits very well the average historical format with its 100-110ft (30.5-33.5m.) span lengths and 23,750ft (7,240m.) total bridge length. A more detailed description of this structure follows in Section 1.4.

Construction Methods	Length Range [meters]		Avg. Length [meters]	
	America	Europe/Aust.	America	Europe/Aust.
a. Span-by-Span	379-10,931	281-8,000	3,160	1,462
b. Incremental Launching	289-480	85-1,161	385	443
c. Progressive Placing	139-379	217-327	226	254
d. Bal. Cantilever (precast)	110-8,240	130-3,200	826	858
e. Bal. Cantilever (cast-in-situ)	97-680	122-1,710	383	495
f. Cable Stayed	279-1,495	197-639	635	405
g. Segmental Arches	213-552	70-580	332	275

Table 1.1 Average bridge length and range for various methods of construction.

As mentioned earlier, the segmental construction of bridges can actually include other bridge systems such as the cable-stayed and arch type built with concrete segments and longitudinal prestressing. They are compared in Fig. 1.5 to the traditional box girders to indicate the longer spans achieved by these type of segmental concrete bridges. Usage of hollow precast concrete segments often erected by tie-back methods have also helped the economical reintroduction of aesthetically appealing arch bridges by eliminating more elaborate construction methods.

1.1.4 Future Trends

The latest developments in the field of prestressed concrete segmental box girder bridges have been marked by the effective re-introduction of external prestressing tendons, the surge of new geometries for the box girder segments, and the introduction of improved materials in terms of concrete and prestressing tendons.

1.1.4.1 External Prestressing Tendons. Recent improvements in the protection, deviation, and anchorage of external tendons have contributed to the new success of the rather old idea of external prestressing [24]. The understanding of the behavior and analysis of externally prestressed concrete bridges has been widely investigated in the past few years and has greatly contributed to its further development. The latest evolution of the external prestressing technology is best represented by the systems of mixed tendons [Fig. 1.1 (c)], where internal and external tendons are combined so as to improve ductility, as well as impact and seismic resistance (as in the case of the San Antonio Y project).

A comprehensive discussion of the advantages and disadvantages of the external prestressing technology was presented by Powell and should be referred to for further details [2]. Many reports about recent advances in external prestressed tendon bridge technology were recently compiled in the American Concrete Institute publication SP-120 which presents articles about developments, analysis, and construction practices [24].

1.1.4.2 New Geometries. Recent geometries of segmental box girder bridges are all characterized by the introduction of thinner webs, sometimes by using truss-like segments, or mixed segments with steel webs. In most concrete segments the webs represent 30% to 40% of the total weight. They often produce an inefficient distribution of the material by decreasing the geometric efficiency of the cross section. The decrease in thickness of the webs therefore represents two major improvements: less weight of the actual segments and better geometric efficiency of the materials. There were several attempts to produce major decreases in the web thickness. The use of external prestressing of longitudinal tendons which reduces web thickness required for placement and compaction of concrete is one important tool for this goal. Some designers have proposed a combination of external prestressing along with vertical prestressing of the webs [15]. Others combined external prestressing with "mixed structures" where they replaced the heavy concrete webs by some lighter material such as stiffened metallic plates (Fig. 1.6), corrugated steel plates (Fig. 1.7), or plane steel trusses (Fig. 1.8). The French company of *Entreprise Bouygues* developed webs made of prestressed concrete trusses with a spatial triangulation, also combined with external prestressing (Fig. 1.9).

These different segment geometries have been evaluated and reported to present various inconveniences. The economic advantages of the steel-concrete "mixed structures" could not be completely proven since all applications were based on experimental structures that

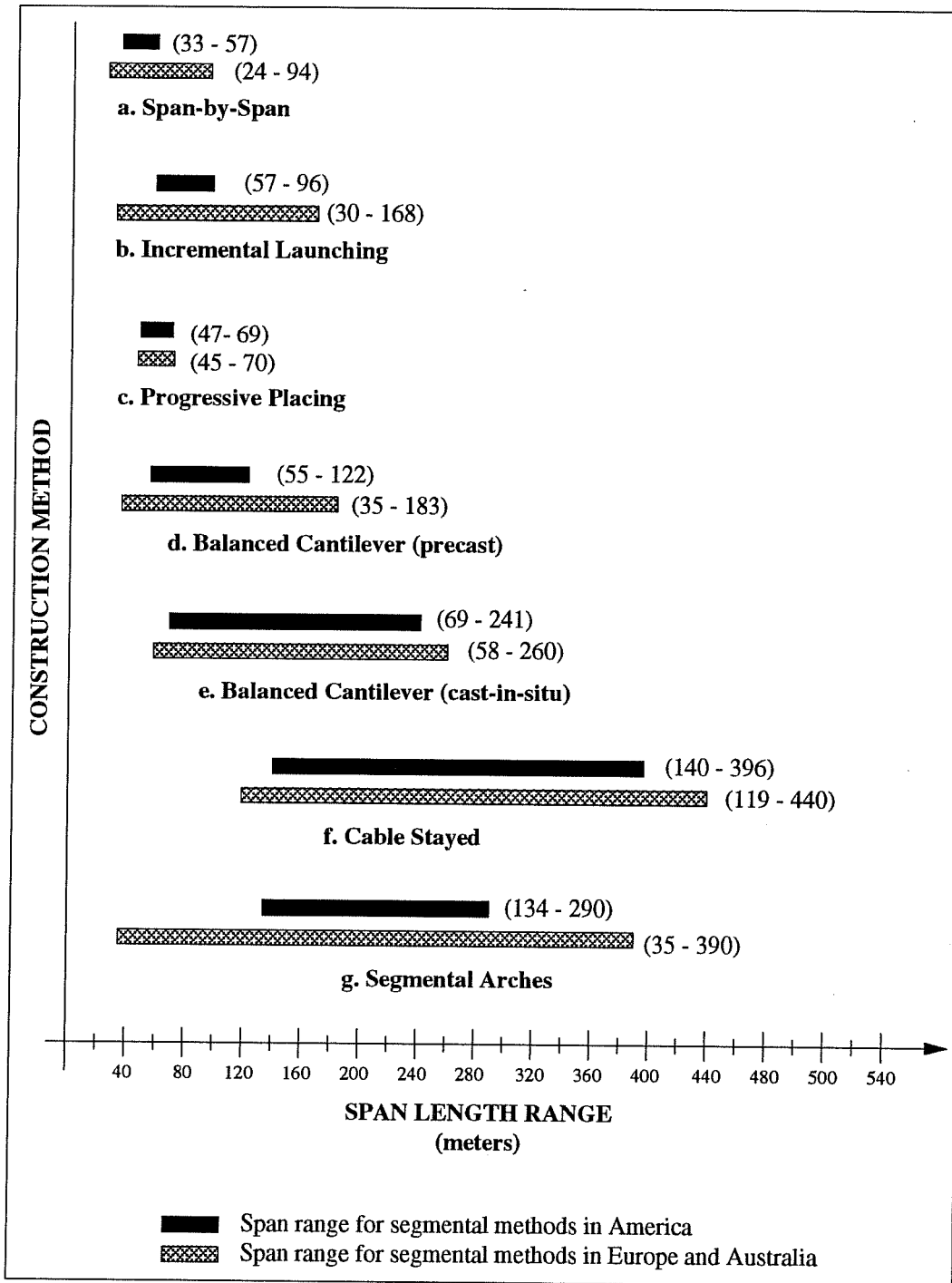
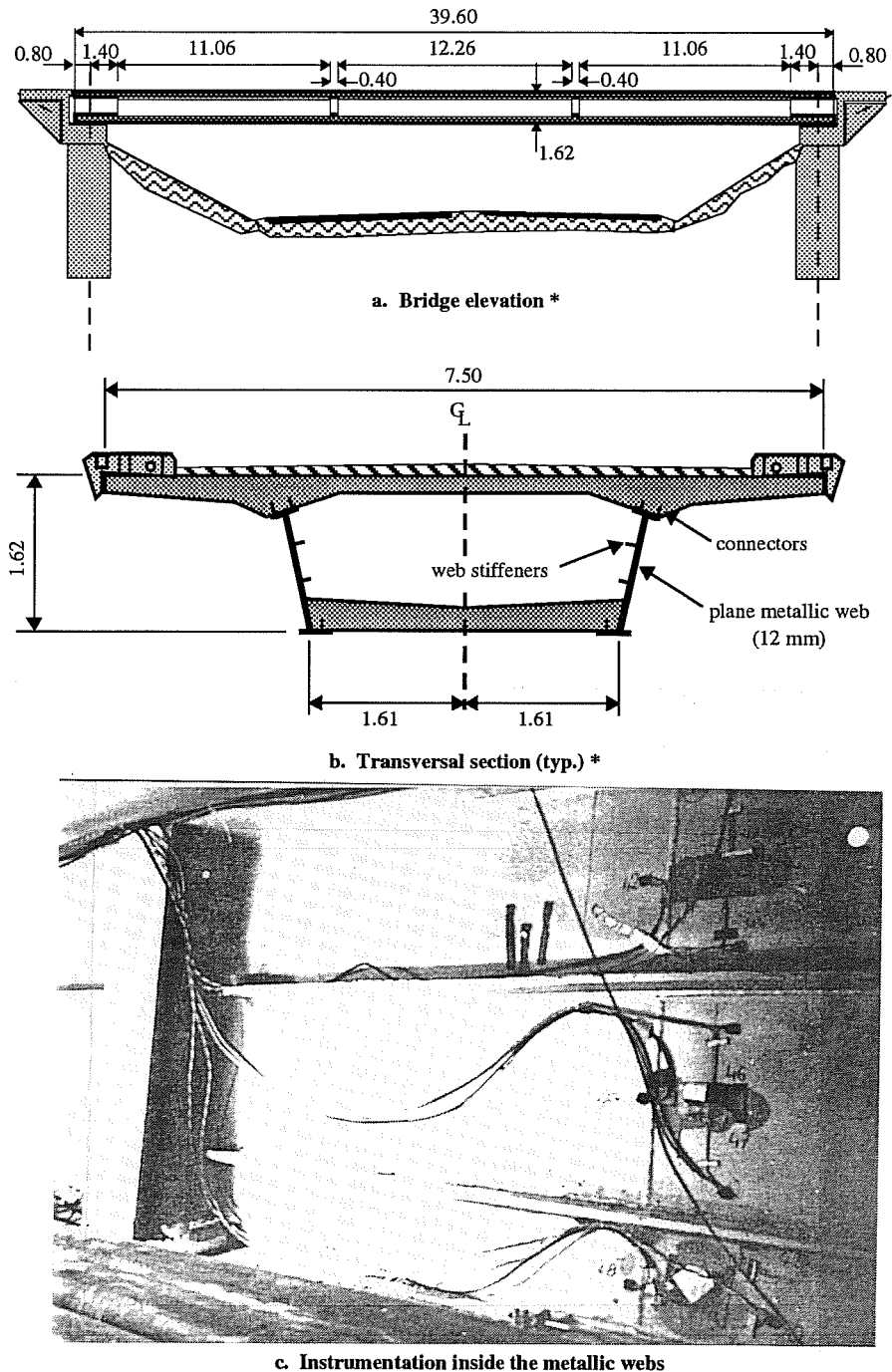
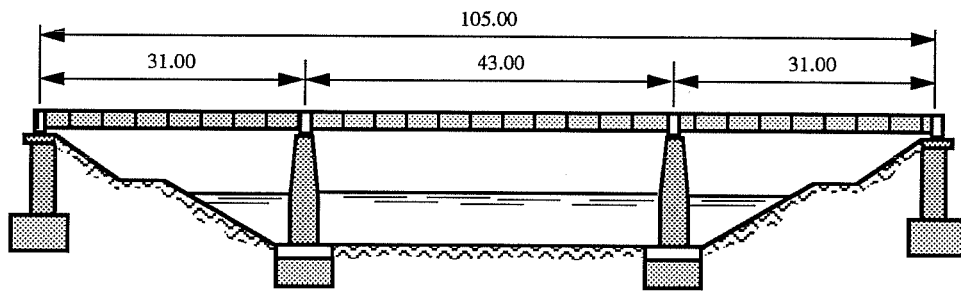


Figure 1.5 Influence of maximum span length on construction method of segmental concrete bridges

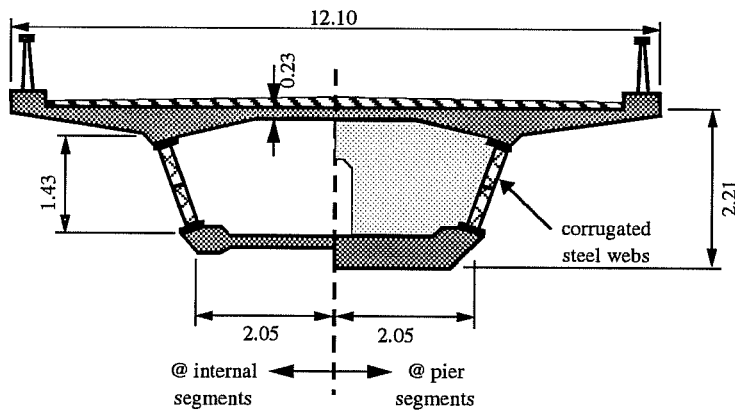


* All dimensions shown in meters
(1m.=3.28ft.)

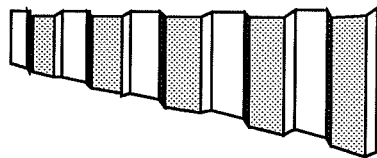
Figure 1.6 La Ferté Saint-Aubin Bridge (France), mixed system with concrete deck and stiffened metallic webs (after Virlogeux [14]).



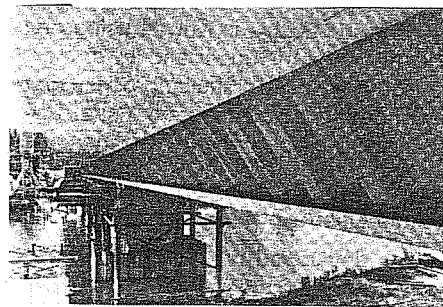
a. Bridge elevation *



b. Transversal section (typ.) *



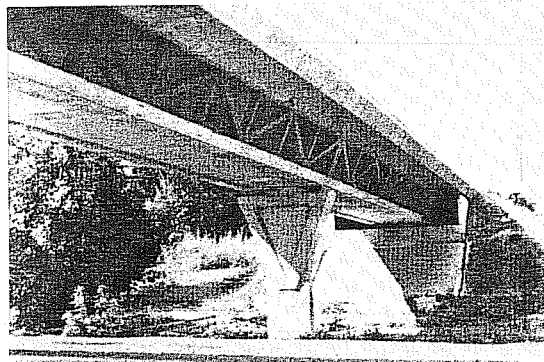
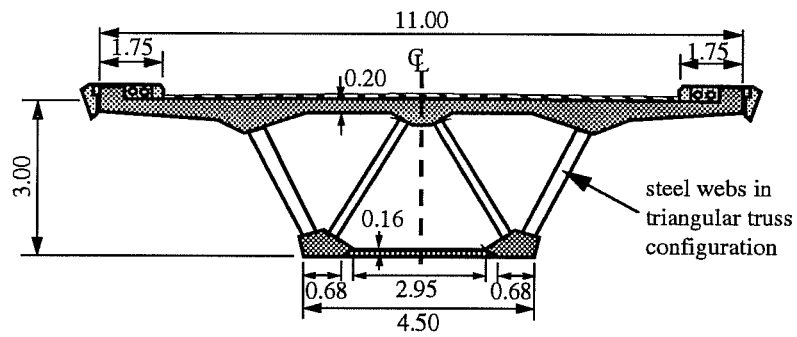
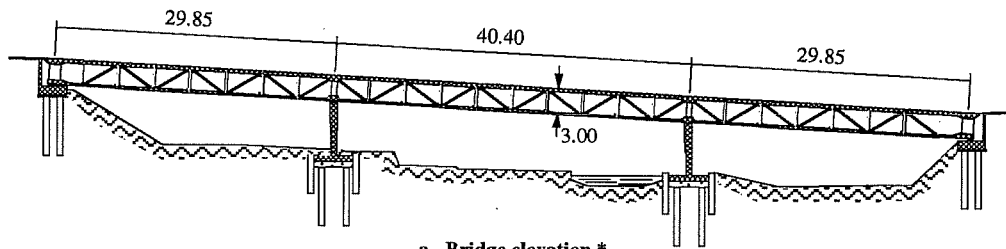
c. Corrugated steel used in webs



d. View of the finished structure

* All dimensions shown in meters
(1m.=3.28ft.)

Figure 1.7 Cognac Bridge (France), mixed system with concrete deck and corrugated steel webs (after Mathivat [26]).



* All dimensions shown in meters
(1m.=3.28ft.)

Figure 1.8 Arbois Bridge (France), mixed system with concrete deck and webs of plane steel trusses (after Virlogeux [13]).

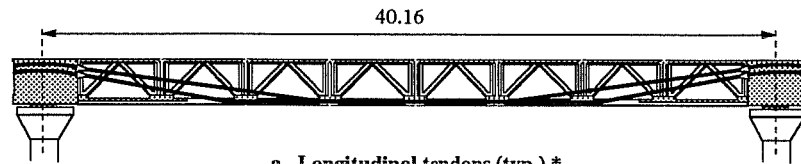
were let without much competition [15]. After redistribution of stresses due to concrete creep (under the effect of large longitudinal forces) a major share of the compression forces in the concrete could be transferred to the steel webs. These compression forces in the steel would require costly vertical and horizontal stiffening of the web members. With respect to the segments with concrete trusses, the main problem lies in the difficult technology of construction, and the necessity for tighter geometry control in the fabrication of the trusses, which could lead to problems of durability if overlooked [15].

More recent proposals from *Entreprises Quillery* in France suggested the use of trapezoidal concrete webs, as shown in Fig. 1.10. These forms have been envisioned so as to diminish the weight of the segments, improve the geometric efficiency of the cross-section, and facilitate the deviation of the longitudinal external prestressing tendons [15]. One last form of segment evolution, proposed by *Entreprises Campenon Bernard* in France, is the segment with triangular cross-section shown in Fig. 1.11. The Viaduct de Maupré, designed and built by Campenon Bernard, replaced the lower concrete deck by a steel tubing filled with concrete. The webs were made of corrugated steel plates and the structure was post-tensioned with external prestressing tendons.

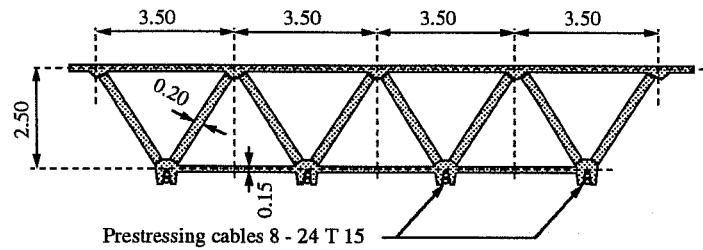
From this brief overview of the evolution of the new geometries of concrete segments, it is clearly seen that the "best" form is still under development. Only with thorough observations of the behavior of these new structures can present technology be improved. This is why the instrumentation of new bridge structures is not only important but necessary for refining the knowledge of their behavior and their performance.

1.1.4.3 Improved Materials. Important advances that will also help the segmental bridge technology consist of recent material developments in terms of concrete with much higher compressive strengths and innovations in the prestressing system technology. Concrete strengths of 70MPa. (10ksi.) have been reported as commercially feasible by the usage of microsilica fume additives and high-range water-reducing admixtures [17]. On the other hand, the evolution in the technology of prestressing systems has not only been in reaching higher tensile strengths with longer strand sizes but also in developing better corrosion protection schemes.

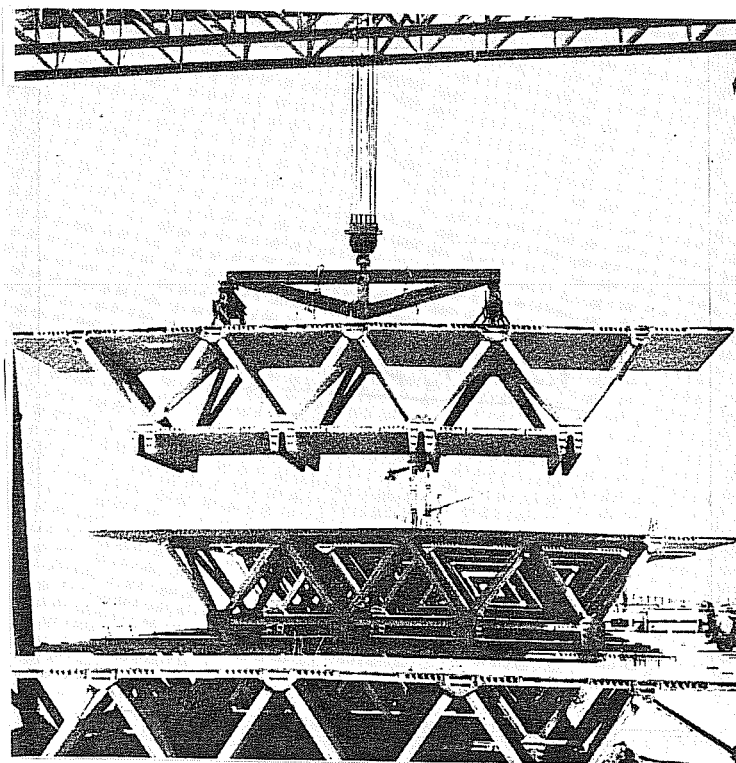
Limited introduction of steel strands of 2,100MPa. (300ksi.) has been reported recently at the FIP International Congress at Hamburg [17]. In the important area of corrosion resistance



a. Longitudinal tendons (typ.) *



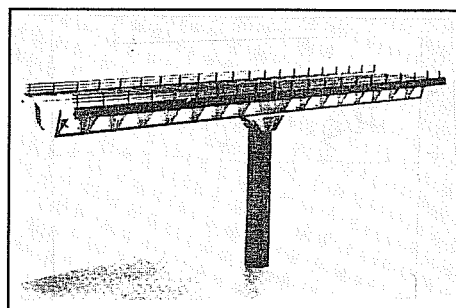
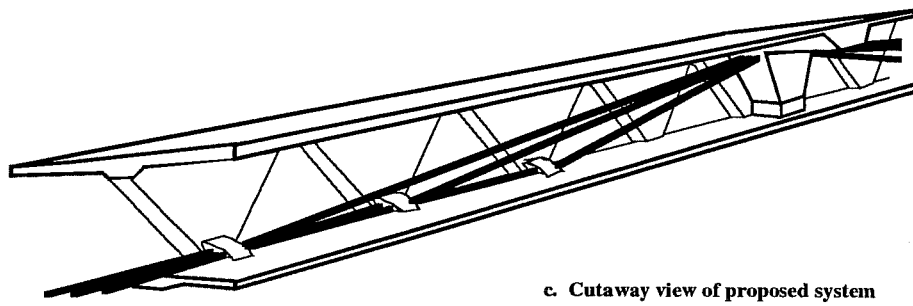
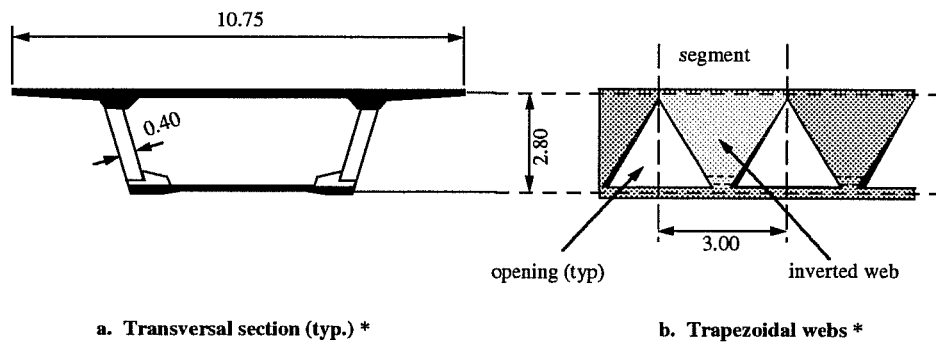
b. Transversal section (typ.) *



b. View of finished segments

* All dimensions shown in meters
(1m.=3.28ft.)

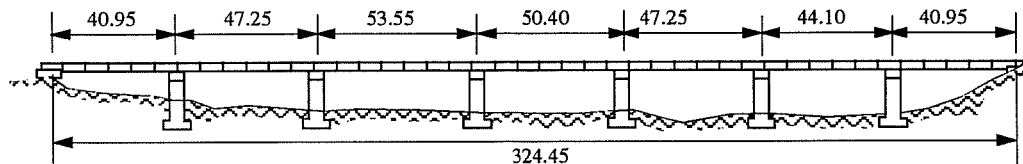
Figure 1.9 Bubiyan Bridge (Kuwait), concrete segments with prestressed concrete triangular trusses (after Raspaud [25]).



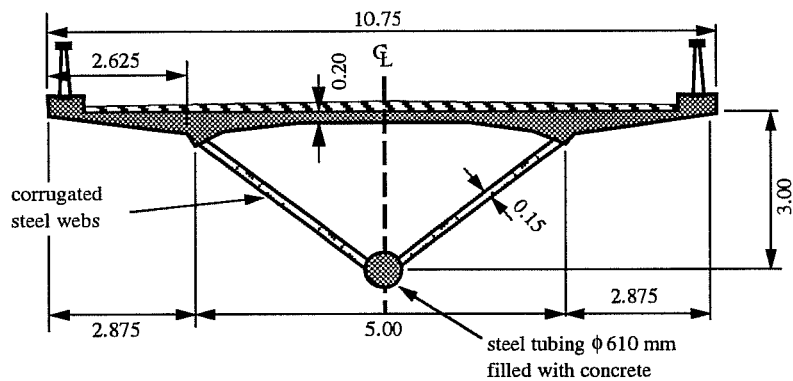
d. Proposal for the Viaducts of Sylans and Glacieres (France)

* All dimensions shown in meters
(1m.=3.28ft.)

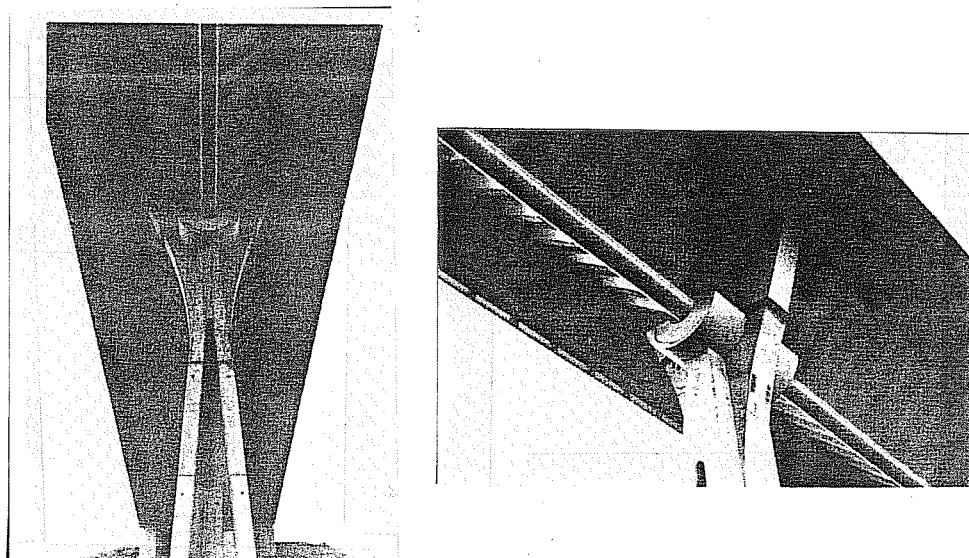
Figure 1.10 Entreprises Quillery (France), proposal of concrete segments with trapezoidal concrete webs (after Mathivat [26]).



a. Bridge elevation *



b. Transversal section (typ.) *



c. Views of the finished structure

* All dimensions shown in meters
(1m.=3.28ft.)

Figure 1.11 Viaduct de Maupré (France), mixed system with concrete deck, corrugated steel webs, and longitudinal steel tubing (after [13, 15]).

of steel strands, two new developments have been reported. First is the limited introduction of epoxy-coated prestressing strands in the United States by Florida Wire and Cable, and second is the advanced American and European studies aimed at improving the technology for electrically isolating prestressing tendons [17, 21]. Morris Schupack from the United States patented a system for electrically isolating unbonded tendons in buildings in 1986 [38]. This can be modified for applications in segmental bridges so as to provide one of the best protections for aggressive environments. Almost foolproof corrosion protection for systems of unbonded tendons is now available for a small additional expense, considering the total cost of a bridge structure [38].

The latest innovation in prestressing strands is probably represented by the development of composite strands made of fiberglass and Kevlar. Experimental applications were successfully completed in the Ulenbergstrasse and Marienfelde bridge projects in Germany [22]. In the United States, the latest development of non-metallic prestressing tendon technology was recently reported by C. Dolan from the University of Delaware [39]. In general, these new non-metallic tendons offer several advantages such as corrosion resistance, linear behavior up to failure, and the possibility for accurately monitoring the stress-strain response of the tendons and for effectively determining the location of any eventual failure along their full length. Drawbacks of the technology are related to low strains to failure, no ductility, lack of knowledge about long term performance in actual bridge structures, and the cost and availability of the special stressing equipment, anchorage systems, and actual tendons outside the European market. At present time no practical use of non-metallic tendons is expected, but with further research these systems could become competitive for applications in aggressive environments.

1.2 Need for the Instrumentation of Bridge Structures

The complete cost for developing an adequate instrumentation system for a large bridge structure is generally only a small percentage of the total expenditure for the finished bridge project. In the particular case of the San Antonio Y project, the estimated cost of the complete instrumentation system reported herein barely reaches 0.65% of the lowest bid price for phase II-C alone --not considering design, maintenance, and other general costs. Sometimes owners wish to avoid these expenditures by diminishing the importance of such investigations or simply

to avoid further expenditures for an already costly project. However, the instrumentation of bridge structures should be considered in any future project which involves new or novel developments. The usefulness of this practice is obvious and the small initial expenditure can be easily overshadowed by the large amount of knowledge that can be generated with a well thought out instrumentation program, even if the results only confirm design assumptions.

Beginning with the construction process for a bridge structure --even during the precasting of segments in the yard-- instrumentation systems can provide help to contractors by supplying valuable information about the general conditions of the concrete, such as strength, creep, shrinkage, and inner temperature. During the initial erection of segments and thereafter until the end of the service life of the structure, designers will obtain valuable information concerning the actual behavior of the structures to check important design assumptions. Direct benefit to the owners can also be obtained by combining the instrumentation systems with the surveillance program for the structure. A well planned bridge instrumentation system can greatly help maintenance checks by making it possible to check important variables that are currently overlooked. Examples of these variables are effective prestress level in tendons, and tendency towards joint openings. Such instrumentation checks should be coordinated with the overall maintenance/inspection program. Users also benefit from the added factor of safety and the possible increase in the life span of future structures through proper maintenance records and improved designs.

In summary, the importance of instrumenting bridge structures can be seen within the following areas:

- feedback to contractors and designers,
- check of current design assumptions,
- check of overall structural behavior,
- further usage of instruments as maintenance tools, and
- increase in the life span of structures.

A more detailed description of the objectives of the particular instrumentation for the San Antonio Y project is given in Section 1.3.1 of this report. Details about the specific areas of concern, and methods for monitoring performance and final areas of instrumentation are also included in that section.

1.3 Objective and Scope of the Present Study

The objectives for this portion of the instrumentation program developed for the Texas SDHPT elevated highway project in San Antonio were to:

- (a) prepare a state-of-the-art survey of current literature related to all aspects of the design, construction, instrumentation, and surveillance of segmental box girder bridges (Bibliography),
- (b) study available reports of previous full-scale instrumentation programs along with their successes and failures so as to avoid previous mistakes and to select areas that need improvement (Chapter 2),
- (c) select the major areas of segmental technology and behavior required for better understanding so as to determine the properties that will need to be measured (Section 1.3.1),
- (d) select the most appropriate instrumentation systems available as indicated from the survey of existing monitoring devices (Chapter 3),
- (e) develop improved instrumentation systems and test all new monitoring devices to be suggested for final use (Chapter 4),
- (f) prepare the specific installation special provisions included in the bid package for the last phase of the San Antonio Y project (Appendix C), and
- (g) include a comprehensive list of recommendations for the proper application of the instrumentation systems to be utilized in the San Antonio Y project (Chapter 5).

It is important to stress here the orderly participation which designers, contractors and research investigators followed in this project. This produced an organized special provision for the bid document specification package that should alleviate future unwanted claims for extra compensation due to interference with construction operations. Development of future full-scale instrumentation systems should follow the same early decision process so as to avoid any misunderstandings during the installation of instruments, the reading operations and during possible testing programs on the finished structure.

This initial phase of the overall project was restricted to the preparation and fine tuning of an instrumentation system for the final phase of the San Antonio Y elevated highways. Future phases of this study currently underway at the Phil M. Ferguson Structural Engineering Laboratory (FSEL) will perform the installation of the proposed instruments, the acquisition and reduction of

data, and develop final recommendations based on the observed behavior of the structure. However, a general description of the initial areas of interest to be monitored in the San Antonio project is included in this report in Section 1.3.1.

1.3.1 Detailed Instrumentation Objectives

The main instrumentation objectives of the San Antonio Y program were established based on areas of uncertainty concerning the AASHTO Interim Design and Construction Provisions for Segmental Box Girder Construction [40]. These areas are notable because professional judgement was used in the absence of actual data to develop the specification provisions. The overall instrumentation project will address these areas where data is lacking, instrument an actual bridge structure, and propose modifications to the specification where necessary. It is also within the goals of the overall project to develop a tentative instrumentation program for the proposed U.S. 183 bridge project to be built in Austin, Texas, near the research laboratory. The performance of the different instrumentation systems along with the experience of the researchers will provide a good basis for the preparation of a second major instrumentation project of a bridge structure.

The final data and recommendations that will arise from the overall project are beyond the scope of this initial report. The actual extent of work covered in the present report is described in Section 1.3.2.

The initial areas of interest for this instrumentation project are the following:

- (1) Prestress losses for external tendon systems, as affected by
 - standard anchorage losses,
 - effects of tendon stressing sequence,
 - friction losses at pier segments and at deviators, and
 - long-term behavior of the finished structure (creep-shrinkage-relaxation effects).
- (2) Effects of environmental conditions on the magnitude and distribution of temperature in the box girder segments, and bridge behavior due to these thermal gradients, determined by:
 - temperature distribution across the cross section of the box girders,
 - temperature distribution through the web, top and bottom deck slabs, and

- variations in deflection of spans, support reactions, and concrete strains.
 - The related environmental conditions to be measured are: direct solar radiation on top deck slab, ambient air temperature inside and outside box girders, and concrete temperature;
- (3) Transverse diffusion of external post-tensioning forces during stressing of the main longitudinal tendons (internal and external), obtained by observing the:
- web strain profile during stressing operations,
 - local reinforcement strains at anchorage zones and at deviators, and
 - transverse distribution of stresses (strains) across the top deck slab.
- (4) Effects of construction loads on partially finished structure, as measured by:
- the deflection of the erection falsework during construction operations,
 - concrete strains, tendon stresses, and deflections at times of unusual construction loads, such as erection crane and haul trucks on previously finished spans,
 - the impact of the construction sequence on continuous spans, and
 - long-term deflections at different time intervals.
- (5) Anchorage zones and deviator details, as measured by:
- non-prestressed reinforcing steel strains, and
 - visual inspections of these areas for cracking.
- (6) Efficiency of joints of precast segments, as measured by:
- movement of segments at the joints, and
 - type of epoxy used in the joints.
- (7) Study of effective flange widths, as measured by:
- concrete strain distributions across top and bottom flanges, and
 - overall deflection of the structure.
- (8) Banana shaped segment phenomenon, as measured by:
- temperature distribution in the concrete of new cast and match cast segments,
 - deformations of match cast segment, and
 - environmental conditions at time of study.
- (9) Behavior of the "Poor-boy" Continuous Unit, as measured by:
- span deflections,
 - concrete strains in top deck slab closure pour, and

- movement of the spans at the bearing pads over interior pier.

The study of all of the above mentioned areas of interest will require measurements of the following properties:

1. Concrete Strains.
2. Prestressing Steel Strains/Loads.
3. Reinforcing Steel Strains.
4. Span Deflections.
5. Concrete Temperatures.
6. Environmental factors: mainly solar radiation and ambient air temperatures.
7. Joint Openings.
8. Bearing Pad Movements.
9. Material characteristics of concrete, reinforcing steel, and post-tensioning steel.

Available instrumentation systems for monitoring these different properties are discussed in the present report. New systems were developed as found necessary. A multi-channel battery-operated data acquisition system was also tested for the automated recording of most measurements to be made in the present project. The present report describes:

- a review of available instrumentation systems,
- the refinement of available instrumentation systems,
- the development of new instrumentation systems,
- the operation check of certain systems, and
- final recommendations for their application in the San Antonio Y Project and in future full-scale studies of bridge structures.

1.3.2 Present Study Summary

In order to improve the understanding of the true behavior of this type of structure, an extensive instrumentation program for full-scale prestressed concrete box girder bridges has been developed and is introduced in this report. To fully understand the significance of these structures, the present study introduces the segmental concrete technology by summarizing its definition, development, and future trends in the industry due to technological advancements. The importance for bridge instrumentation programs and the detailed instrumentation objectives along with a general description of the major areas of instrumentation were further explained in

Chapter 1. Finally, this first chapter introduces the particular structure for which the present instrumentation program has been developed. Details concerning its location, geometry, current methods of construction of segments and erection systems are provided in Section 1.4.

A great amount of time was initially spent on an extensive literature review of the different segmental bridge instrumentation programs that have been reported in the past. These are mainly located in the United States but there are some references to European programs. Some reports of previous field studies concerning instrumentation techniques for concrete box girder type segmental bridges are reviewed in Chapter 2. The idea behind this study was to evade previous problems encountered in similar full-scale bridge instrumentations programs by developing, if necessary, some alternative methods for obtaining more favorable results. Chapter 3 presents a survey of the state-of-the-art instrumentation techniques and equipment that are commonly used in structural engineering applications, and particularly in full-scale investigations of bridge structures. Based on historical performance, degree of acquaintance with the technology, costs, ease of use, and availability of systems, some of the instrumentation systems were selected for further evaluations in actual test applications. These evaluation trials, and refinement of systems are reported with details in Chapter 4. A final recommendation for the application of the recommended systems in the San Antonio Y project is presented in Chapter 5. Finally, Chapter 6 summarizes the findings and suggests future investigations related to instrumentation systems for segmental box girder bridges.

A bibliography of relevant information and studies about segmental concrete box girder bridges is incorporated at the end of this report in order to aid future investigations of these structures. The suggested literature is separated into several areas of interest for ease in locating the most appropriate source of information. This is the final product of the extensive initial literature review process. Searches were conducted at the collections of The University of Texas Library System, as well as international computerized databases such as TRIS-Engineering Service (Transportation Research Information System), and CONTENDEX-Engineering Index. Other smaller databases were used. NTIS (National Technical Internal Service) provided information of reports that were the product of unclassified U. S. Government funded research in the area of transportation. Finally, TTS (Technology Transfer System) provided access to abstracts of all research reports funded by the Texas State Department of Highways and Public Transportation (Texas SDHPT).

1.4 The San Antonio Y Project

Located in the heart of one of the major cities of the United States, this project has been called the Y Project because of the geometric shape of the two main interstate highways on which the double decking work is being developed. The relative location and major phases of

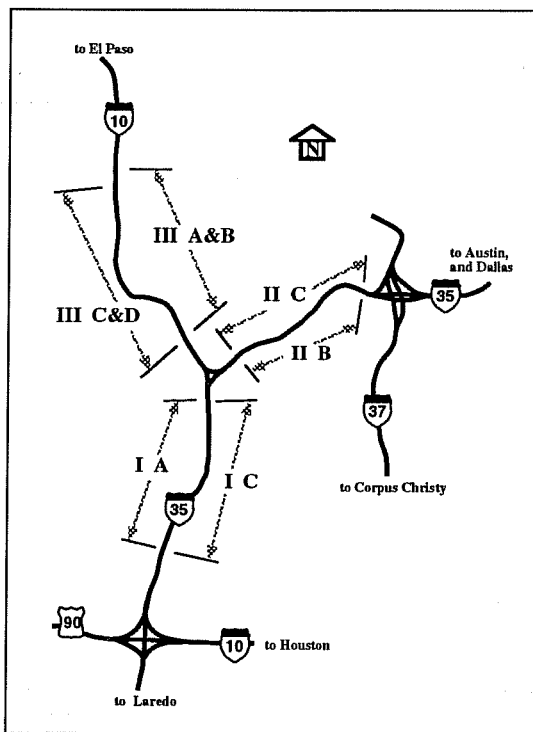


Figure 1.12 Phases and location of the San Antonio Y Project.

construction as prepared by the Texas State Department of Highways and Public Transportation (SDHPT) are shown on Figure 1.12.

This 10-mile project will add six lanes to U.S. Highways I-10 and I-35 near the central business district. About 6 miles of the new roadway will be elevated, and three-quarters of this will be erected with precast post-tensioned segmental box girder segments adding up to a total of 3.1 million square-ft.

Several restrictions limited the possibilities of competitive bridge systems that could be used for this project. The most important requirements were: (1) minimum purchase of right-of-way; (2) minimum disturbances of current traffic flow during construction; and (3) needs for an

aesthetically pleasing structure. Since most portions of I-10 and I-35 in downtown San Antonio were built in the early 1950s, some important commercial developments surged along their right-of-way and severely limited a horizontal type of expansion of these highways. The traffic on these highways almost doubled their original design limits and new lanes were needed to increase their capacity. However, they had to be added without severely disrupting the traffic flow during construction. Finally, San Antonio is a city which relies heavily on the tourist industry of its central business district area. It could not afford an unsightly bridge structure. This imposed severe restrictions against unappealing designs.

The post-tensioned segmental box-girder bridge alternative, built by the span-by-span method, not only pleased the sentiments of the public but also presented the least disruption of traffic, and became the most economical system for the San Antonio Y project. Final costs of construction were recently reported at about \$36 per square foot of completed bridge deck [23].

Large concrete masses or dark areas usually associated with prestressed concrete girders were avoided by the elegant, uncluttered, segmental box-girders with long cantilevered wings and small modern piers (Fig. 1.13). The finished San Antonio Y project will undoubtedly become a great model for future elevated highway designs in this country.

1.4.1 Description of the Structure

Phase II-C of the San Antonio Y project was let in mid-October of 1990 in Austin, Texas. The lowest bid, at \$51.987 million dollars, belonged to *Austin Bridge Company* who also was responsible for the construction of phases I-A and I-C (see Fig. 1.12). The second lowest bid, offered by *H. P. Zachry Construction Company*, was \$59.76 million dollars. Original designs for these phases were developed by the Bridge Division of the Texas Highway Department.

Phase II-C is formed by 108 spans with span lengths varying from 60 to 115ft. A total of 401,530 square feet of finished bridge area comprises this phase of the San Antonio Y Project.

After consideration of factors such as ease of access to the finished spans, type of concrete segments, and approximate time of construction, spans A-43, A-44, C-11 and C-9 were selected as the best candidates for the installation of the various instrumentation systems. A more detailed layout of this phase is shown in Figure 1.14, where the selected spans to be instrumented are blown up for better view. Spans A-43 and A-44 were both designed with the same type of segments (type III) characterized by their long cantilever wings, wider bottom soffit, and wider top deck. Overall dimensions of type III segments are shown in Fig. 1.15a. These two spans are composed of six external tendons deviated at third points by full segment diaphragms, as shown in Figure 1.15b. The cantilevered wings have four straight longitudinal tendons, along with transverse prestressing tendons consisting of single ½ in. ϕ strands, spaced 5in. on center. This spacing is reduced to 3 ½ in. for segments adjacent to the piers.

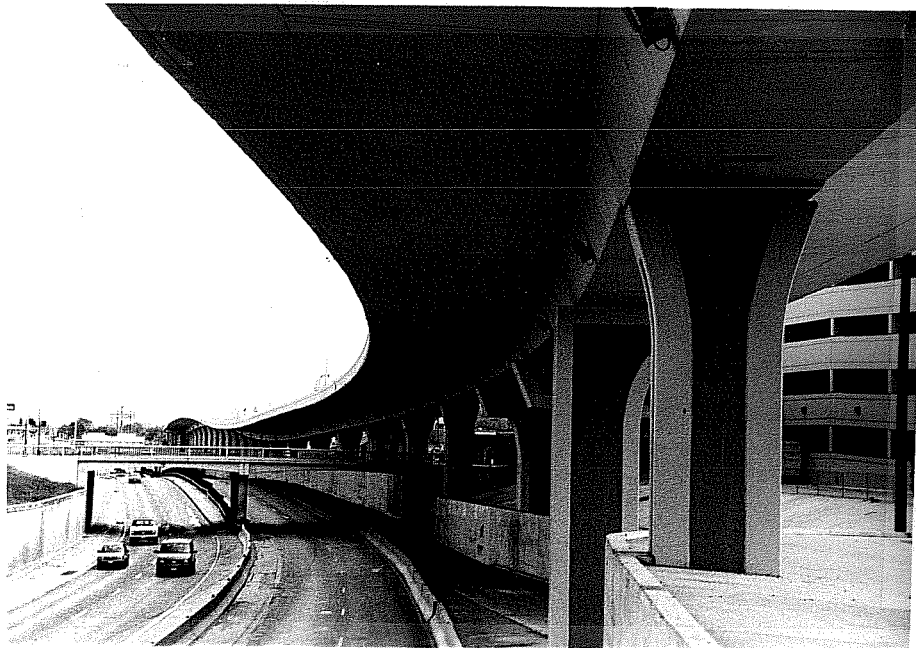


Figure 1.13 Finished phase of the San Antonio Y Segmental Project.

Spans C-11 and C-9 are made of type I segments which are much narrower in the soffit and top deck slabs (see Fig. 1.15c). These spans were initially designed with four external tendons deviated at third points by full segment diaphragms. A recent redesign by the contractor proposes deviation saddles (deviation blocks) in these spans. These are expected to provide savings in material and special formwork. They also help reduce the dead load on the final structure and avoid geometric problems of pass-through external tendons. These were reviewed and accepted by the Texas Highway Department. The smaller cantilevered wings of these spans were designed with two straight longitudinal tendons and transverse prestressed tendons made of single $\frac{1}{2}$ in. strands spaced 9in. on center. The segments in span C-11 are slightly truncated on one side of the wings. This side will eventually be connected to the adjacent mainline span. Dual-box behavior will be studied at this location and will be compared to the behavior of single boxes. Span C-9 was selected because it is one of the "poor-boy" continuous spans. A less extensive instrumentation scheme was thus prepared for this particular span.

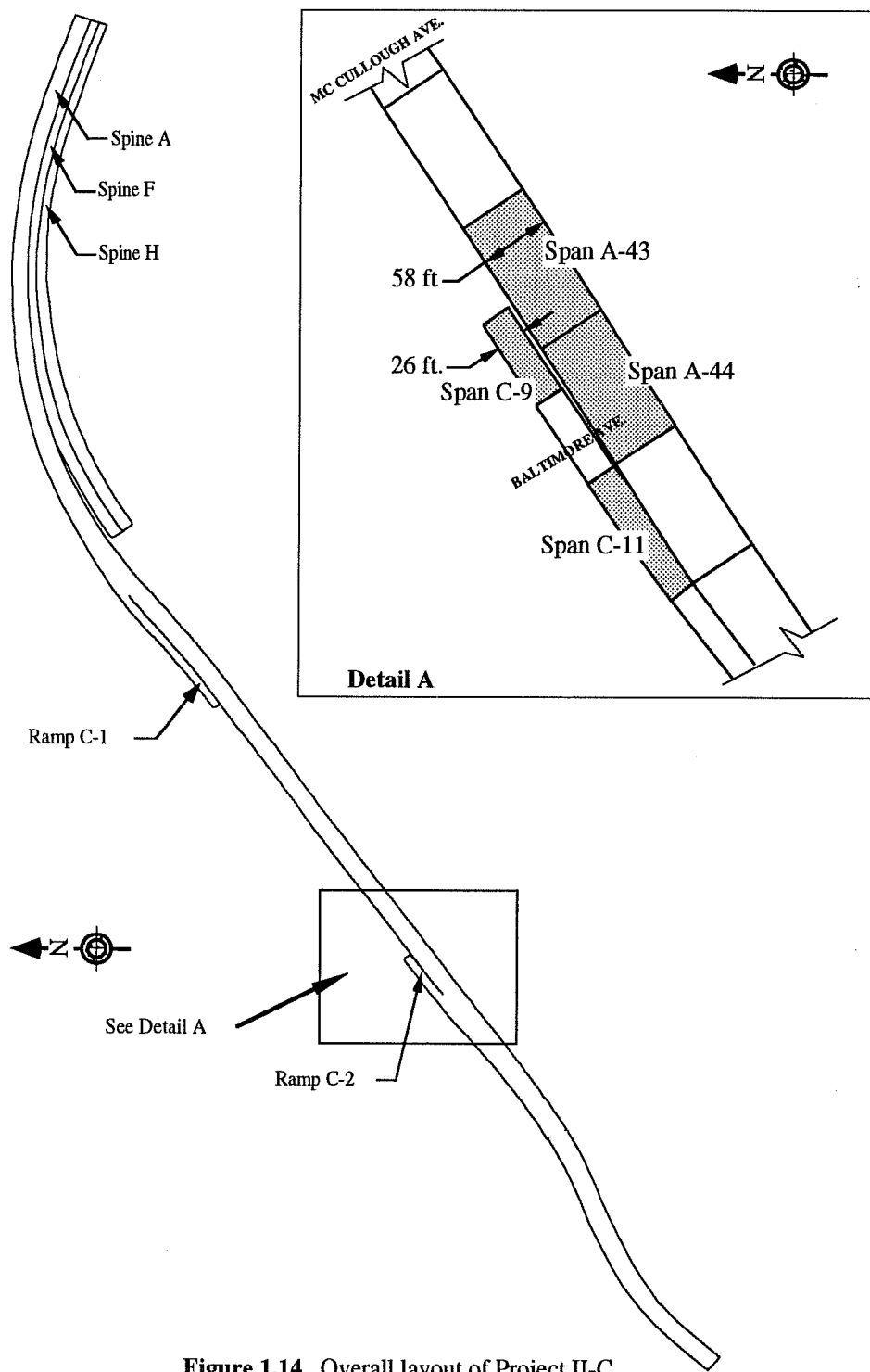
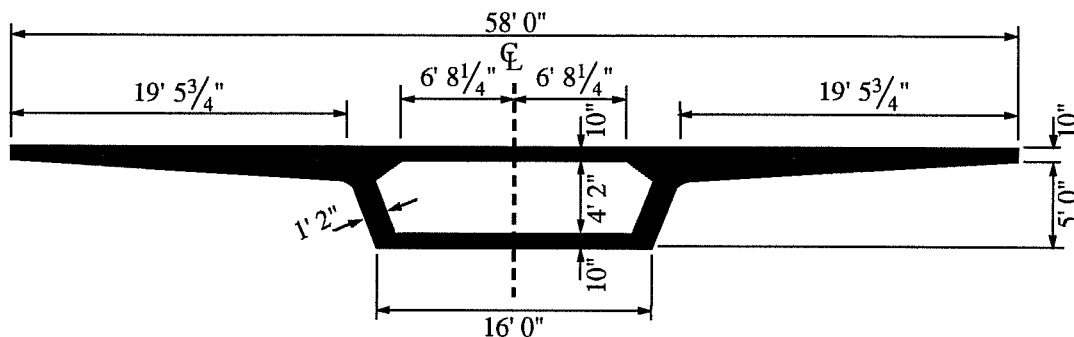
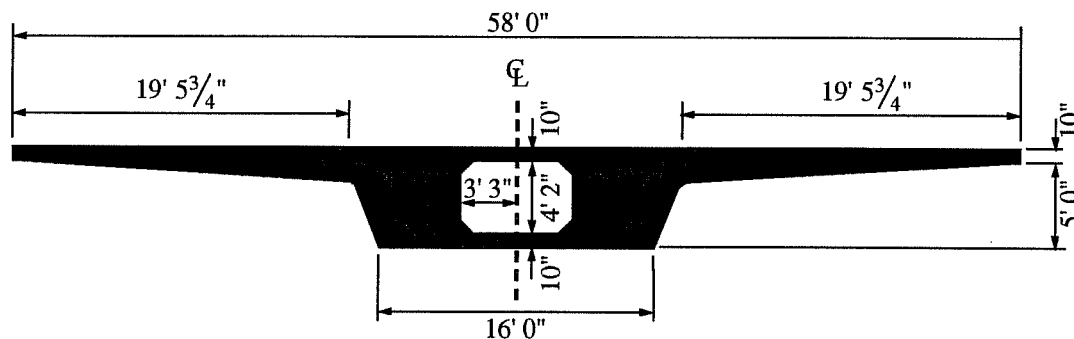


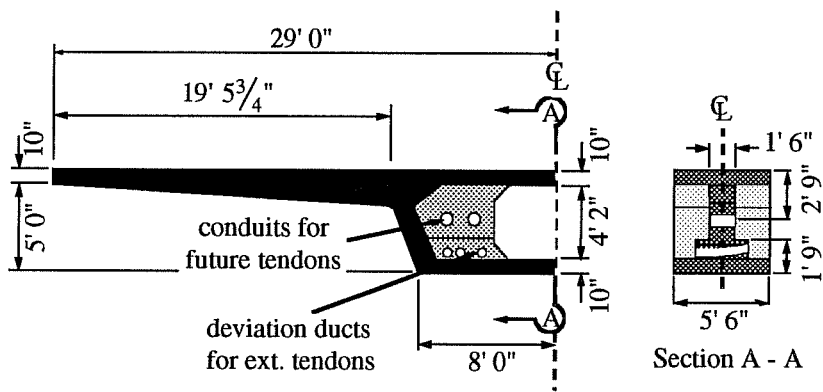
Figure 1.14 Overall layout of Project II-C.



a. Superstructure segment (typ.) - elevation view



b. Interior pier segment (typ.) - elevation view



c. Deviator diaphragm (typ.) - elevation view

Figure 1.15a Typical segment dimensions for spans A-43 and A-44 (segments type III)

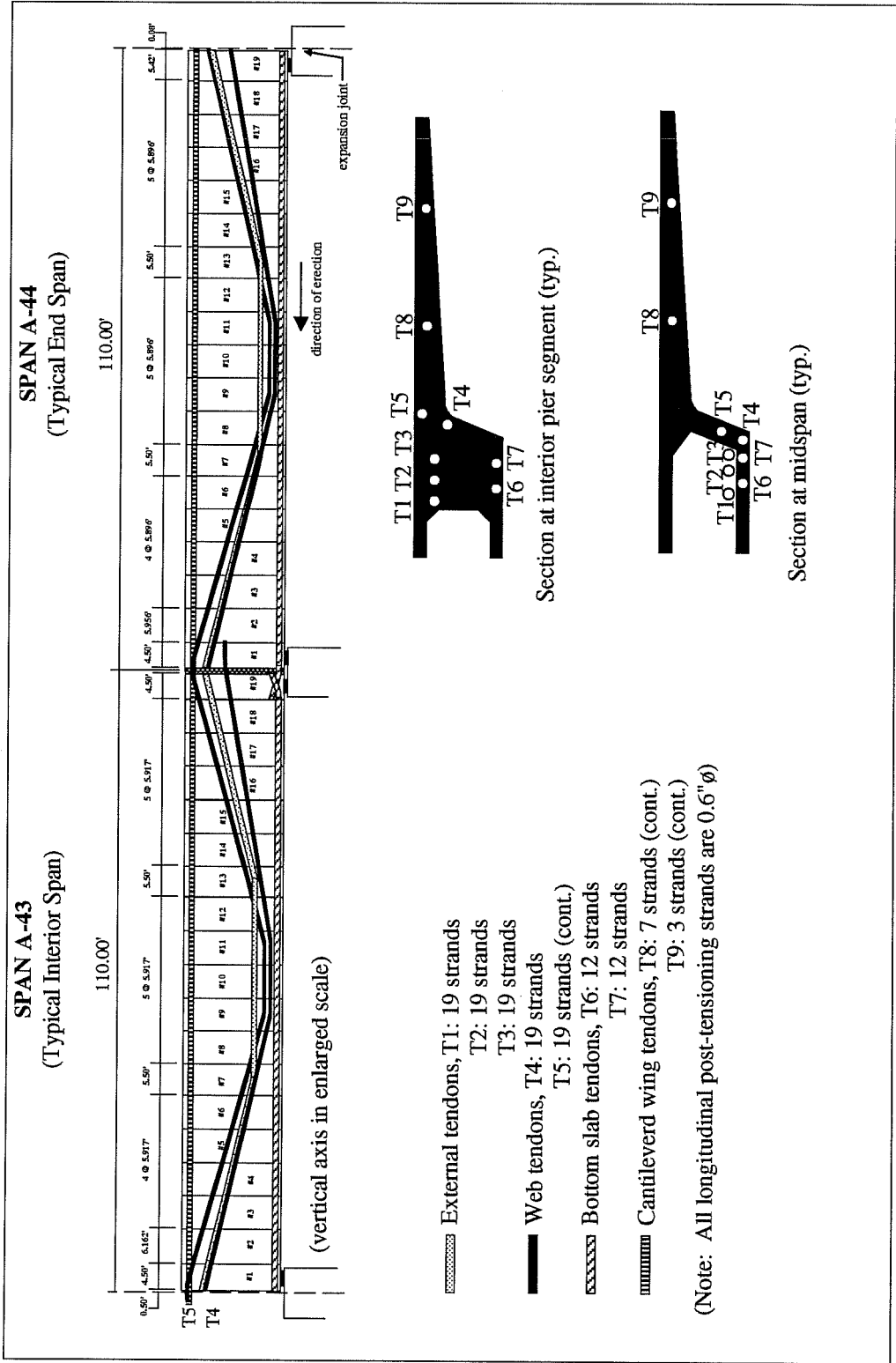
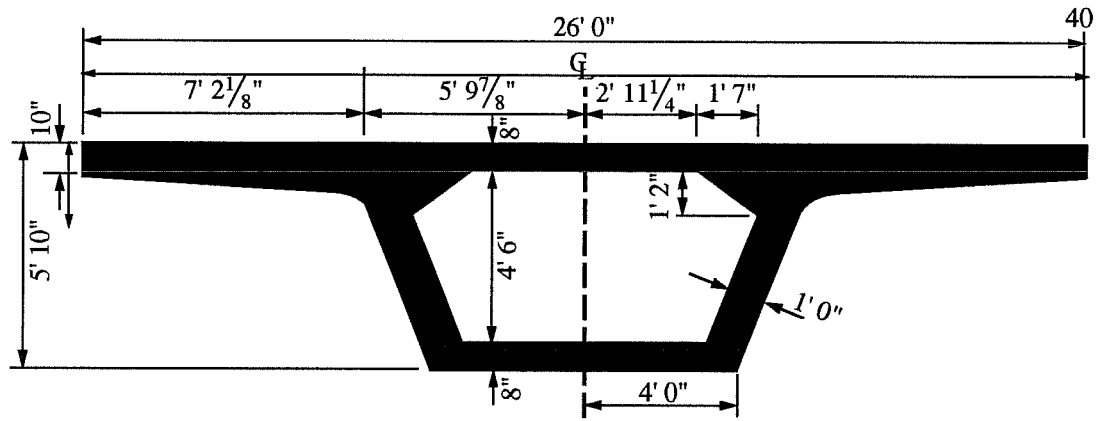
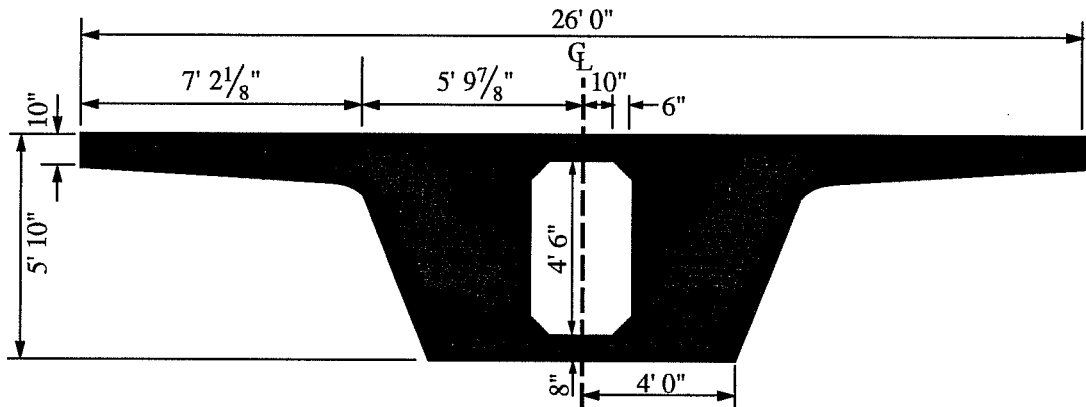


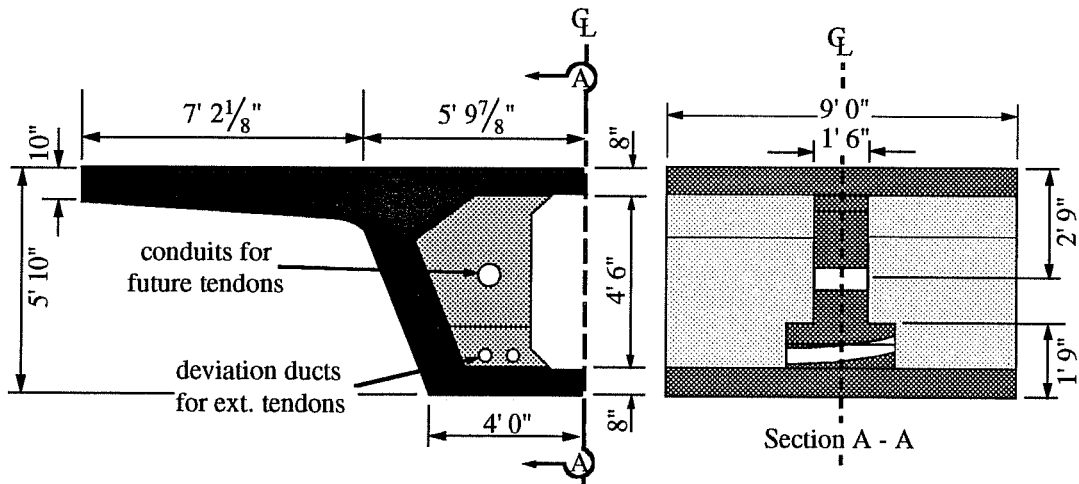
Figure 1.15b Longitudinal post-tensioning layouts for spans A-43 and A-44 (type III segments).



a. Superstructure segment (typ.) - elevation view



b. Interior pier segment (typ.) - elevation view



c. Deviator diaphragm (typ.) - elevation view

Figure 1.15c Typical segment dimensions for spans C-9 and C-11 (segments type I)

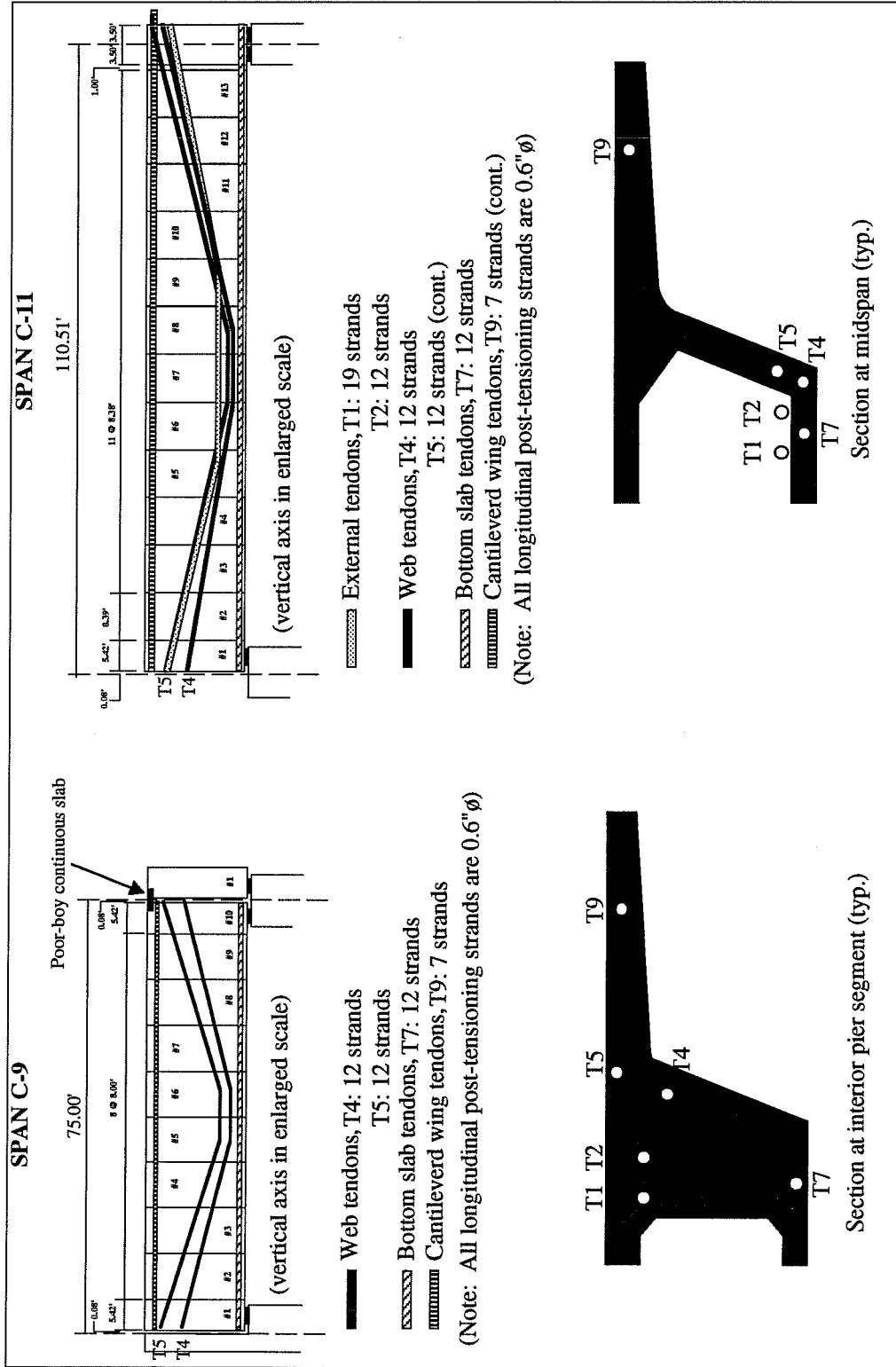


Figure 1.15d Longitudinal Post-tensioning layouts for spans C-9 and C-11 (type I segments).

1.4.2 Fabrication of Segments

The selected system for fabricating the precast segments used on all previous phases of the San Antonio Y project was the short line match-cast method. The short line method (shown in Figs. 1.16 - 1.17) uses a single stationary set of forms to match cast the segments. Recently cast segments are slid forward and used to match cast the following ones in the same order as they are to be placed in the actual bridge structure. Complex horizontal, vertical and rotational alignments are possible by adjusting the position of the matching segment. These positions must be set accurately since a check of the alignment of the span is not made until final erection of the segments. On their previous phases (I-A and I-C) of the San Antonio Y project, Austin Bridge Company had 9 stationary casting machines in their casting yard and was able to produce 7.5 segments per day at their top rate. The production for phase II-C is expected to be improved to 9 segments per day with the same number of stationary beds. Special cases, such as piers and deviator segments, slows down considerably the daily productivity. *Prescon Corporation*, which built phase III-A&B, had 10 casting beds and reached a peak production of 10 segments per day with the helpful addition of a third tower crane in their casting yard.

The segment reinforcement cages were initially fabricated outside the casting bed and later moved into it for adding the final reinforcement, tendon ducts and for performing the prestressing of transverse tendons. This sequential procedure can be seen in Figures 1.18 through 1.22 taken from Austin Bridge Company's casting yard.

All segments were later stored in the yard for a varying amount of time, usually between 4 to 8 weeks, before being transported to the structure for erection. However, due to the usual early start of casting at the casting yard, some segments waited for up to 6 months before erection. These initially long waiting periods were reported by both Austin Bridge Company and Prescon Corporation. An overview of Austin Bridge's casting yard storage area can be seen in Fig. 1.23.

1.4.3 Erection Systems

All previous phases of the Y project were erected with the span-by-span method using slightly different types of steel falsework girders and high capacity cranes. Austin Bridge Company had up to three similar erection trusses (Fig. 1.24) for phases I-A and I-C.

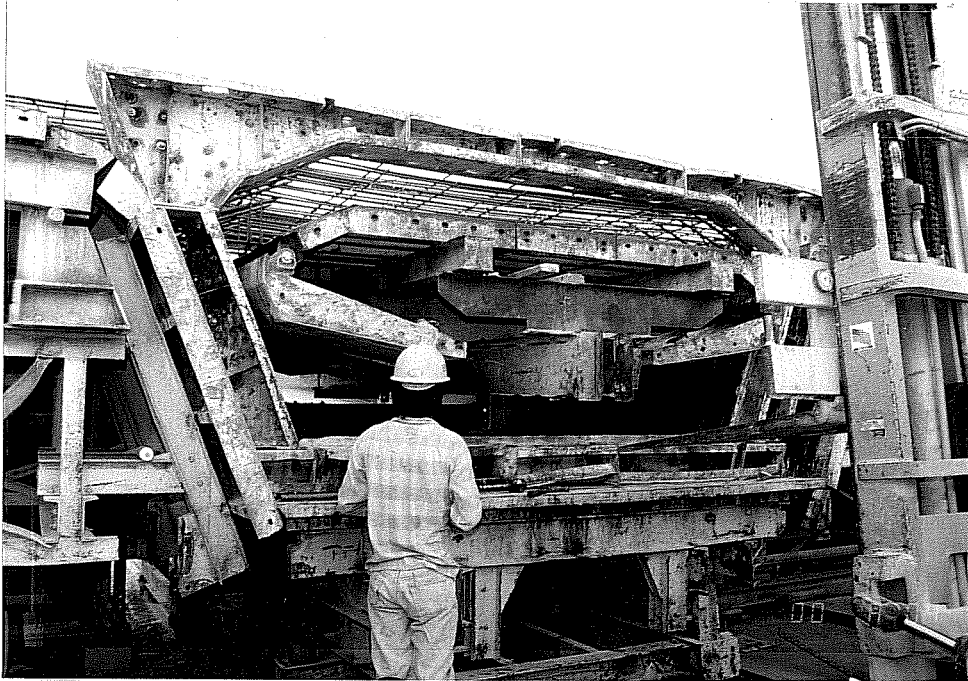


Figure 1.16 Assembling of new-cast segment.

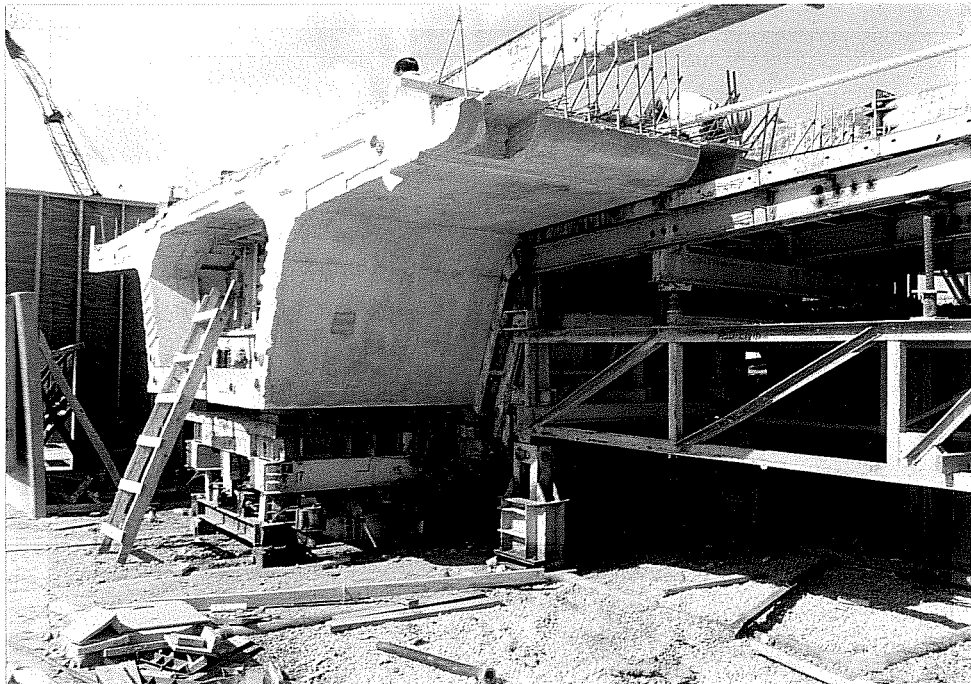


Figure 1.17 View of recently cast segment (used to match-cast the new segment).

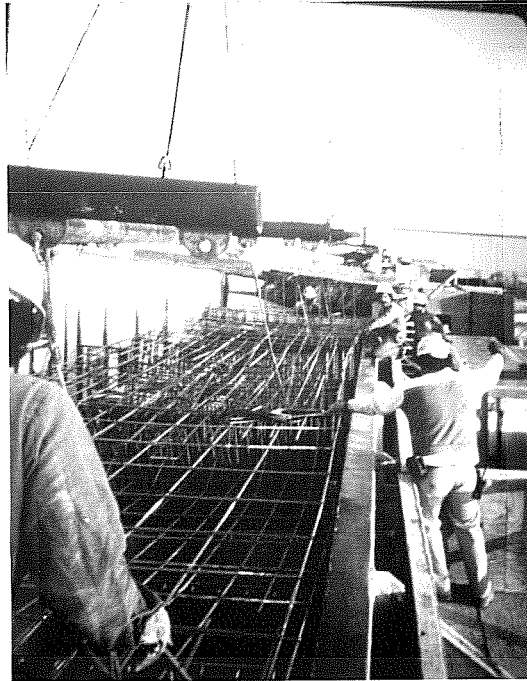


Figure 1.18 Lowering of reinforcement cages in the stationary casting beds.

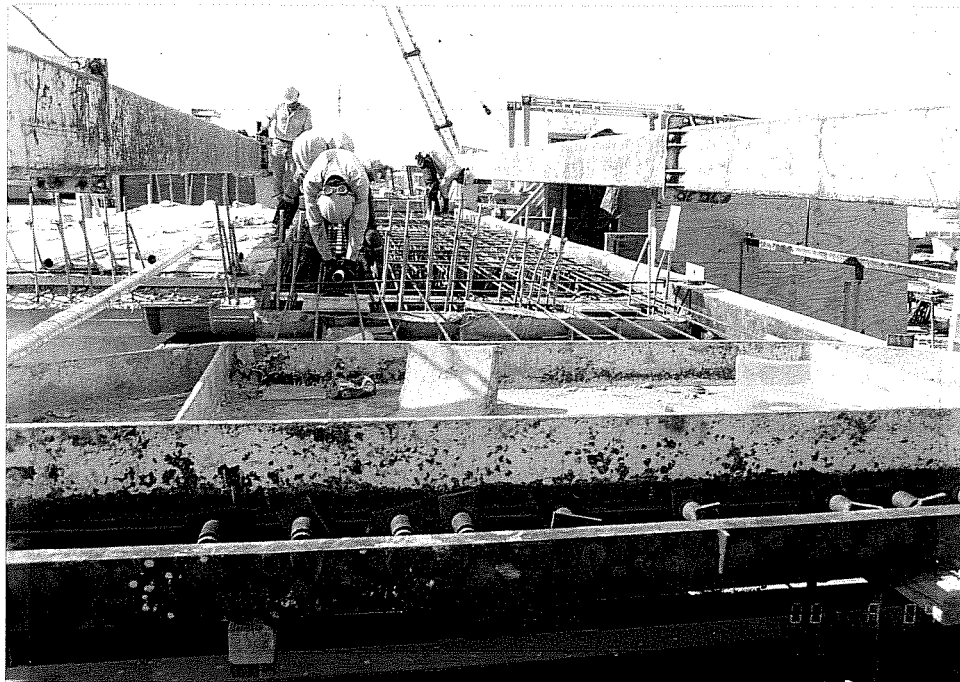


Figure 1.19 Final installation of prestressing steel ducts in short line casting bed.



Figure 1.20 Prestressing of transverse tendons in casting bed.

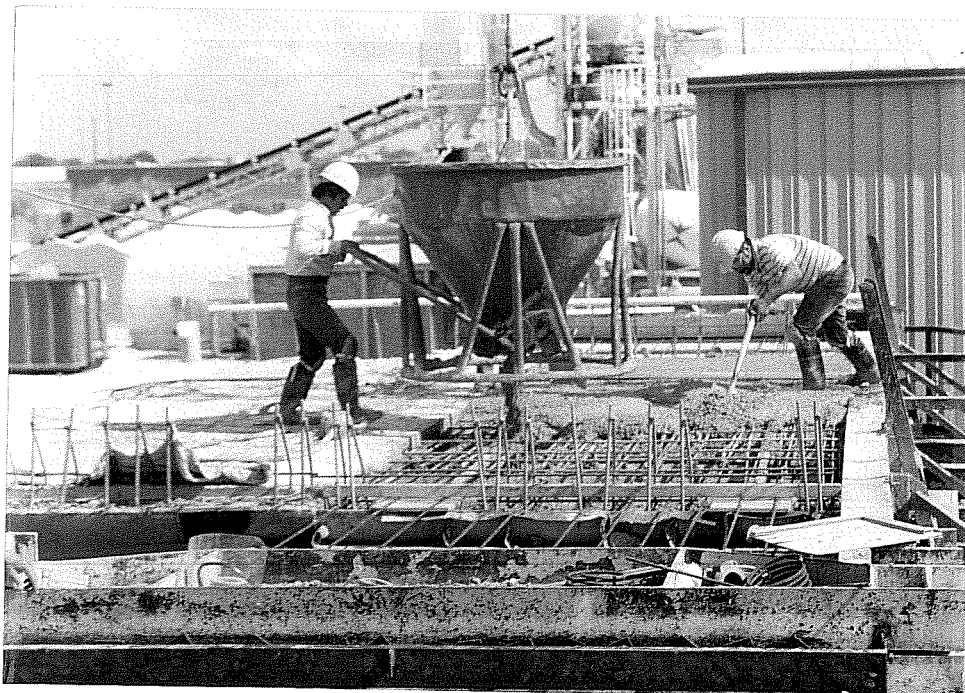


Figure 1.21 Concrete work.

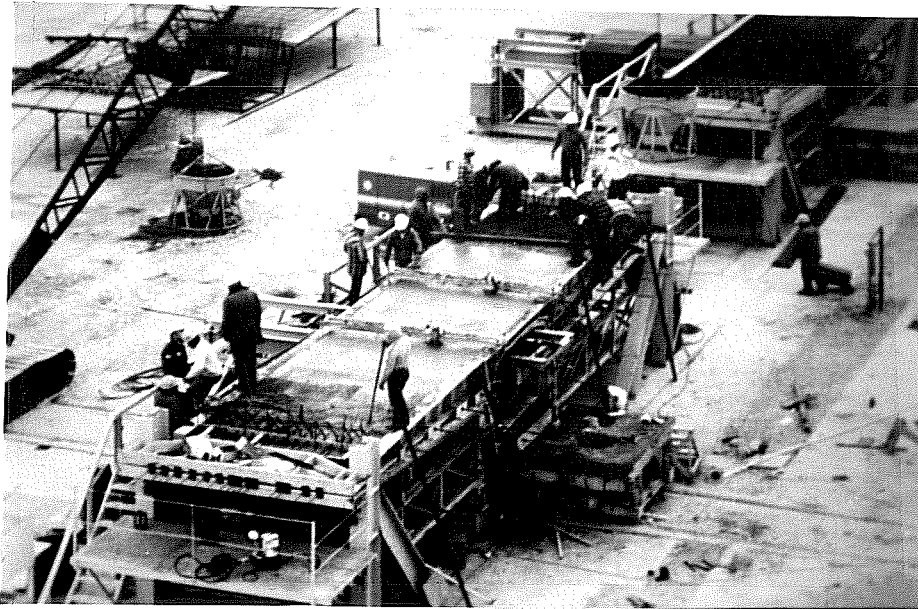


Figure 1.22 General view of casting yard operations.



Figure 1.23 Storage area in casting yard.



Figure 1.24 Austin Bridge Company's erection truss.



Figure 1.25 H. P. Zachry Construction's erection truss.

Austin Bridge Company was able to achieve an average speed of 4 spans per week with the two operating trusses. Their third erection truss was reserved for emergency situations. For spans providing clear advancement of trusses, with no straddle bents, no cantilever piers, and no unexpected problems, a top erection speed of 7 spans per week was obtained.

Prescon Corporation had a single light-weight erection truss and reached a top performance of about a span per week while constructing phases III-A and III-B of the San Antonio Y project. The truss designed by the third contractor, H. P. Zachry Construction Company, for phase III-C&D was much lighter in appearance (Fig. 1.25). They introduced the innovative idea of using externally stressed cables in a truss configuration to regulate the shape of the overall steel truss according to its loading status. With two of these cable-stressed trusses they were able to achieve an average speed of 3.5 to 4 spans per week.

CHAPTER 2

PREVIOUS RESEARCH AND PUBLICATIONS

2.1 General

Since the first large-scale introduction of the segmental box girder technology in the United States in 1973 several research projects and actual field investigations of their behavior have been developed around the country. Most investigations performed by universities and research laboratories have produced a steady supply of well documented reports about their testing program, review of related literature, test results, and recommendations. A large array of the available literature was reviewed by the present researchers and is only listed in the Bibliography of the present report. These research reports are not included within the present review. However, all reviewed literature included in the Bibliography and that provided helpful information related to instrumentation systems is properly referenced in Chapters 3 and 4 of the present report.

Large scale investigations involving the actual field instrumentation of segmental box girder bridges did not produce such a high number of accessible reports. This was partly due to the relatively low number of field investigations and partly due to the cancellation of certain programs. A number of field instrumentation projects were announced at the time of erection of new segmental concrete bridges but no further reports later became available. Some of the programs that were actually implemented and properly reported were reviewed by the present researchers and are included in this chapter. The following review is concentrated on the performance of the instrumentation systems that were utilized. However, the type of structure investigated, general project objectives, and areas of study are also mentioned in the present review. These reviews are not intended to be very specific but are rather intended to help save time and effort of future researchers involved in projects similar to the San Antonio Y bridge field investigation program.

A smaller number of other bridge structures instrumented with a relatively smaller field program were also investigated due to their novel instrumentation systems or long timeframe of the investigation program. Some of them are reported at the end of Chapter 2.

Finally, instrumentation systems used in completely different fields of engineering were also reviewed to check their possible applicability to the present project. In particular, several reports from geotechnical field investigations were very helpful. However, these reports are not included in the present chapter but are referenced where appropriate in Chapters 3 and 4.

2.2 Turkey Run Bridge

This is probably one of the first field instrumented segmental concrete bridge structures in the United States. Completed in 1978, this bridge erected in balanced cantilever is composed of two 180ft spans with a twin box girder cross section. Each box girder is 21ft wide. A 4ft cast-in-place slab was used as a cold joint between each pair of segments. Lap splices of steel reinforcing bars represented the continuity of bond between the transverse reinforcement of twin segments. These single cell segments were precast near the bridge site following a short-line casting method (match-casting technology). The bridge is located in Parke County, Indiana.

A field instrumentation program for this bridge was conducted by Purdue University in cooperation with the Indiana State Highway Commission. A final report was published in 1977 [41]. However, this report only contained information about the initial areas of concern, a detailed suggestion of load test methods, preliminary analytical studies, selection of appropriate sensors, and their locations in the bridge structure. An additional phase of the project was in charge of the actual data recording, analysis of measured results, and comparison of calculated results with two methods of elastic analysis. Information related to the performance of the different sensors was thus not included in the presently reviewed final report.

The basic objectives of the Turkey Run bridge instrumentation program were the following:

- a. Gather information on the transverse bending tractions in the box beam cross-sections (indirectly measuring the adequacy of the cast-in-place joint between twin box girders).
- b. Measure the thermal gradients existing between top and bottom slabs.
- c. Study the long-term creep deformations arising after erection.

Instrumentation systems used for reaching the above mentioned project objectives consisted of:

- a. Electrical resistance strain gages (120Ω): some of them spot welded to transverse reinforcing bars and others epoxy bonded to the concrete surface.

- b. Thermistors: each embedded at mid-depth of the top and the bottom slabs (centered between webs). Four segments were instrumented, thus using eight thermistors.
- c. Whittemore mechanical extensometers (@10in. gage length): locating points were epoxy bonded to the top of the bottom slab and bottom of the top slab of the two pier segments.

The Turkey Run bridge field instrumentation program was evidently not a very extensive study considering its limited objectives and consequent number of installed sensors. Although the final report included valid provisions for improving the long-term behavior of the electrical resistance sensors, the mentioned guidelines are not considered sufficient to provide an acceptable long-term performance of the strain gages and the thermistors. The few included recommendations related to the electrical resistance sensors were:

- the use of three-leadwire quarter-bridge Wheatstone completion gages for the strain gages,
- calculation of desensitized gage factors for long leadwire lengths, and
- reduction of strain errors associated with transverse strains.

A lack of details surrounded the description of the data acquisition system, especially the type of care that was taken for reducing errors related to the variation in contact resistances at the connectors. Also, no description of the temperature compensation method existing at the strain gage level was included (the three-leadwire, quarter bridge completion circuit only accounts for temperature compensation of the leadwires). Furthermore, some of the electrical resistance strain gages were epoxy bonded to concrete surfaces softened with a different layer of epoxy. This only seems appropriate for short-term laboratory controlled investigations. The epoxy bond is unlikely to last a long-term investigation under aggressive environmental field conditions. Errors can also be introduced if the base layer of epoxy is made too thick. This is because the temperature induced strains of the epoxy cover can vary differently than the covered concrete surface.

The last concern about the described system is related to the stability of the locating points of the Whittemore strain gages. Previous field instrumentation programs have reported several problems associated with the effectiveness of the epoxy bonds of mechanical extensometer locating points in concrete surfaces.

Although not located by the present researcher, it is presumed that an additional final report exists with the conclusions from this particular project and some information about the performance of the sensors. An analysis of this information could evidently have been helpful for determining more appropriate conclusions about the adequacy of the implemented instrumentation system.

2.3 Denny Creek Viaduct

The Denny Creek Viaduct is located a few miles west of Snoqualmie Pass and carries the westbound traffic of I-90 directed towards Seattle, Washington. The complete segmental box girder bridge structure is made of 20 spans extending for a total length of 3,620ft. In this structure, 16 spans have typical lengths of 188ft and the other 4 have varying lengths from about 143.5ft to 166ft. The single celled box girder segments used on all spans are 16ft wide at the bottom slab, 14.5ft wide at each cantilevering deck, and 9ft deep. The box girder segments, designed to carry three lanes of traffic, have a total top deck slab width of 52ft.

This bridge completed in 1982, represents the first United States application of the span-by-span method of construction. A moving scaffold was used to allow construction from the top of the piers, without the use of ground supported falsework (mainly due to restrictions imposed by the environmentally sensitive forested area of the Cascade Mountains). The construction of the superstructure was performed in three stages. In the first stage, a 330ft long movable launching truss enabled the construction of the bottom slab and webs. After translation of the Stage I launching truss to the next span, steel formwork supported on the cured and longitudinally stressed bottom slab was used to cast the Stage II top deck slab section located between the two webs. Finally, the Stage III cantilevered wings of the top deck slab were cast on formwork supported by a movable falsework riding on the finished Stage II portion of the top deck slab.

The field instrumentation project of the Denny Creek bridge was developed in two phases. In the first field instrumentation phase, the principal instrumentation design process, installation, and measurements during the construction process were developed by researchers from Construction Technology Laboratories (CTL). Their final report [42] covered the following instrumentation-related areas:

- Type of sensors utilized for measuring concrete strains, concrete temperatures and concrete surface strains on three bridge sections (located near the pier, near quarter span, and at mid-span).
- Description and results of the 37 measurement dates taken for an approximate period of one year since Stage I casting of the instrumented span.
- Description of accompanying laboratory material tests of concrete specimens.

The main objective of the initial study was to determine the short term time-dependent behavior of this type of structure. Particular areas of interest were related to the effects of creep, shrinkage, and temperature. However, most of their findings were later questioned in a review performed by researchers from the University of Washington in charge of the second phase of the field instrumentation process [43]. This final phase continued the measurements initiated by CTL, performed additional measurements of transverse deflections, bearing movements, and some meteorological conditions of the site (wind speed and ambient air temperatures). They also attempted to introduce an automated data acquisition system. Their final report was published in June 1983 [43]. This report contained:

- a critical review of the initial CTL findings (which were actually reproduced in Appendix E of the second phase report),
- an extensive review of literature related to creep and shrinkage, analytical methods for the design of roadway slabs and box-girders, and thermal studies in box girder bridges,
- descriptions of a live load testing program of the finished structure, and
- final observations determined from the original CTL and additional University of Washington measurements, and from the live load testing program.

The second phase report can be helpful to future field instrumentation programs since it contained some valuable recommendations. The report presented helpful findings related to thermal stresses and monolithic behavior of stage constructed box girder cross-sections. However, the findings from the live load test should only be analyzed as behavioral trends. The measured quantities seem questionable due to the low instrumentation accuracy (in relation to the total variation of the measured quantities) and due to accidental loads occurring during the actual test.

Although the second phase of the project continued with the original measurements performed by CTL, the readings were not executed in a uniform manner. Most readings of the second phase were performed between July and August of 1982. Only four measurements were taken between the last reading performed by CTL (the 37th reading on August 1, 1980) and the first July

1982 reading performed in the second phase (the 42nd reading on July 9, 1982). Slightly over 90% of the second phase readings (42 through 89) were performed between July 9 and August 14 of 1982. The lack of uniformity of this investigation and the relatively small amount of valuable data related to the long-term behavior limited the extent of the findings.

The instrumentation systems used in this project included the following sensors:

- a. *Carlson Elastic Wire Strain Meters*: fourteen meters were embedded in each one of the three instrumented cross-sections (totalling 42 sensors). Although not reported, from the published data it can be concluded that only three sensors failed and two others worked intermittently. This is actually a relatively good performance considering the four year instrumentation period. Carlson Meters were used for both measurements of concrete strains and readings of internal concrete temperatures.
- b. *Whittemore Mechanical Extensometers*: pairs of locating discs were epoxy bonded to thirteen concrete surface locations (five on top of the top deck slab and the rest around the inner surfaces of the box girder section). All of these gages were found ineffective in the second phase of the project (approximately a year after initial installation). Although not explained, it is presumed that the epoxy bond of the locating points did not perform as well as planned.
- c. *Expansion Joint Movements*: horizontal displacements were measured between the top bearing portion attached to the superstructure and the bottom one attached to the abutment. The nature of the bearings permitted this simple but precise measurement. The exact method for performing these measurements was not reported. However, it seems that two simple permanent reference marks (one on each portion of the bearing) were used to measure relative displacements. However, as mentioned by the second phase project researchers the only problem with this simple method is the difficulty in determining which component of the horizontal movement is due to temperature and which is due to creep and shrinkage shortening.
- d. *Ambient Air Temperature*: measurements of ambient air temperature inside and outside the box girders were initially performed with mercury thermometers. Thermocouple wires were later implemented for measuring ambient air temperatures and concrete surface temperatures.
- e. *Total Wind Run*: a portable weather station was used for measuring wind speed, wind direction, and ambient air temperature.

f. Transverse Vertical Movements: the vertical movements of a cross-section located near the expansion joint were measured with respect to the abutment level. However, these measurements were only performed during the live load test. Mechanical dial indicators with 1/1000in. resolution were successfully used for this purpose.

g. Electrical Resistance Strain Gages: some gages of the foil type were attempted to be installed during the second phase project. However, partly due to unexpected problems with the data acquisition system these sensors were not effective. The type of gages that were designed for installation, their method of installation, and their locations are unknown.

g. Data Acquisition System: it is assumed that all readings were performed with standard portable reading units (for the Carlson Meters). It seems that the contact resistance of the different connections to the meters did not vary widely in the four year instrumentation period. An automated data acquisition system was attempted to be used in the second phase of the project. However, numerous complications voided the effectiveness of such an expensive system (that consumed more than 60% of the total direct expenses of the project). The main complications were related to the appearance of a high level of noise in the electrical resistance readings of the Carlson Meters. Noise could have been related to several sources: the type of Wheatstone bridge circuit, high electromagnetism in the bridge structure, long and poorly protected leadwires, and temperature variations. Other inconveniences were found during the modification of the originally purchased AC-powered data acquisition system to a battery operated unit. Since it was not designed for battery use, the system consumed too much power for long unattended usage. Problems were also encountered in the lack of compatibility between the data acquisition unit with the storage unit (more programming was thought to be required to obtain the proper communication between the two systems).

The honest self-criticism of the researchers in charge of the second phase of the Denny Creek bridge instrumentation project led them to provide several useful recommendations for future similar undertakings. Their most important recommendations were actually followed by the present researchers and were related to:

- The need for a conservative preparation of the overall instrumentation project starting from the design phase as well as a direct dialogue between researchers, designers, and finally, contractors.

- The need for initially preparing an extensive review of the current state-of-the-art instrumentation systems along with a review of published results from previous laboratory applications of the selected sensors. Also an investigation of the long-term stability according to the review of previous field applications of the selected sensors was recommended.
- Compatibility between the data acquisition, recording, and power supply units was encouraged to be checked before the actual purchasing of the equipment. Also the security of instrumentation equipment to be left on site was recommended to be considered in advance.

Other individual reports about the findings from the Denny Creek field investigations were published in known civil engineering publications. However, these were more limited to particular areas of the project and were based on the same measurements included in the previously mentioned references.

2.4 CALTRANS Segmental Box Girder Bridges

This was a very limited field instrumentation project since it only monitored stresses of individual $\frac{1}{2}$ " ϕ stress-relieved prestressing strands installed inside single cells of certain box girder bridges. However, the field instrumentation project was carried out over a period of ten years and involved several novel load measuring devices that seemed to have worked at acceptable levels of accuracy over the long instrumentation period.

A total of six multi-celled segmental box girder bridges located around the central California area (San Francisco, Fresno, Sacramento) were used for this research project. One of the bridges is a 160ft single span cast-in-place segmental concrete bridge and the other five are cast-in-place two span structures varying in length from 240ft to 316ft (span lengths varying from 112ft to 157ft). Four $\frac{1}{2}$ " ϕ stress-relieved strands were installed inside a single box girder cell and anchored at the exterior face of the end diaphragms of each bridge structure. The project's objective was to study the actual prestress loss occurring in the installed strands due to causes other than friction and anchorage seating of the strands. This was carried out due to the increase of the "lump sum" loss estimates of the late 1971 AASHTO Interim Specifications for Highway Bridges. The lump sum stresses were increased from 25ksi (established by the previous 1961

AASHTO code) to a level ranging from 32ksi to 49ksi as calculated for 270ksi stress-relieved strands (but with allowances of $6\sqrt{f_c}$ maximum tensile stresses in the concrete). The six bridges were erected between 1971 and 1972 and the test strands were installed at about the same time of stressing of longitudinal tendons. The project was carried out by numerous researchers from the California Department of Transportation (CALTRANS) and a final report was published in June of 1984 [44].

Innovative load measuring devices were implemented throughout the study. However, most of these devices are only applicable to single prestressing strands. The following is a review of the load measuring sensors used in this study:

- a. *Compression Load Cell*: during initial stressing operations of each strand, loads were recorded at the live end with a calibrated electrical resistance load cell (30kip. capacity) connected to a portable battery operated strain indicator. During load cell calibration with a vertical loading machine, it was determined that the cell readings reported regular errors of about 0.08kip. and maximum error of 0.16kip. These errors only corresponded to 0.3% and 0.6% of a 25kip. load. The load cell was mounted externally around the strand, between the hydraulic jack and the "pulling" wedges. This enabled the cell to be free after strand seating was performed at the other end of the hydraulic jack.
- b. *Hydraulic Load Cell*: this was only used in one particular test location (on all four strands used at the location) and abandoned in later tests due to the great fluctuations observed in the readings from this sensor. According to the descriptions provided in the final report it seems that this particular sensor consisted of an early type of electrical resistance based pressure transducer connected to an independent portable strain indicator box. With the present knowledge of pressure transducers, the observed load fluctuations could have been related to internal friction in the hydraulic jack, and to some eventual hydraulic fluid leaks at the different connections to the hoses.
- c. *Tension Load Cells*: this was a single strand "coupler" permanently installed at an intermediate cross-section of only one of the test strands. From the given descriptions, it seems that this was an electrical resistance load cell of the tension type. The average of two tension load cell readings obtained in 12 load steps were compared to the corresponding compression load cell readings. A small regular variation of about 50lb was reported. However, the readings of the tension load cell were discontinued after three years of operation without any further explana-

tions. No safe conclusions about its long-term stability could be given. It is probable that large electrical resistance variations occurred in the long-term readings due to moisture intrusion, temperature differentials, or electrical contact resistance variations.

d. Kuhlman Beam: a mechanical "strand stress beam" was developed by a CALTRANS engineer (H. F. Kuhlman) and subsequently built by other staff members. The operation of this instrument is based on the flexural beam concept. With readings from electrical resistance strain gages arranged in a certain pattern in the Kuhlman Beam and with a proper calibration curve, this instrument provides fairly accurate tension measurements of single prestressing strands. For a load of 25kips, an average from 81 field calibration tension evaluations of the CALTRANS tests established a 6.5% accuracy for 100% confidence level (2.8% accuracy for 95% confidence level). The accuracy level of previous laboratory investigations was calculated at 1.6% for a 95% confidence level and for the same 25kips tension load. However, the rated accuracies were reported very dependent on the skill of the operators. It must also be mentioned that these were initial accuracy levels and do not represent the long-term behavior of the sensors. The long-term data provided by Richardson [44] cannot adequately represent the actual long-term accuracy of the Kuhlman Beam since no considerably better sensor readings were taken. The present author considers it unlikely that the Kuhlman Beam maintained its original level of accuracy. This is mainly because of the difficulty for avoiding electrical resistance variations induced by temperature differentials or varying electrical connections. However, the CALTRANS report showed that the long-term accuracy did not vary widely from the initial values obtained during sensor calibration. Another interesting aspect related to the behavior of the Kuhlman Beam was the slightly different calibration curve that was obtained for each strand tested. This either implied small variations in the strand materials or low reproduction of measurements by different operators.

e. Vibra Tension Model ET-U (known with the name of Vemco): this was the second portable instrument used for measuring intermediate tension loads in the individual strands. These sensors were originally manufactured by Vemco Industries, Inc., of San Francisco, California. It is presently manufactured by Smiser Industries, Inc. of Houston, Texas, under the name of DynaTension PTM-100. This electronic instrument measured the fundamental frequency of a vibrating strand. This along with manually introduced data about the particular instrumented strand provided a fairly accurate strand load value. Two parameters were introduced in the

portable readout unit: the strand's free length (also called vibration length) and its weight per unit length. The vibration length was determined according to the free distance between two firm supports of the strand. These strand supports were either "natural" such as in the case of anchorage and deviators, or "artificial" when special wooden structures were made for the particular objective of shortening the vibration length of a strand (since the ideal vibration length was around 20ft). The weight per unit length of the strand was actually a very important parameter that also depended on the scale used for the tension readings. It was usually evaluated according to calibration readings performed during strand stressing operations. Two different portable devices were used for readings of the natural frequency: a proximity-type and a contact-type transducer. CALTRANS provided an initial accuracy level of 2% for a 100% confidence level and 1.2% for a 95% confidence level (based on 88 field calibrations of 24 test strands). As with the Kuhlman Beam, the *Vemco* sensor long-term accuracy could not be adequately determined. However, due to the higher stability of frequency signals the present author considers this to be a very stable sensor.

In general, the information provided by the CALTRANS studies were very useful for providing a clear information about the behavior of different load measuring sensors for single prestressing strands. However, the use of such devices is very limited and evidently incompatible with multi-strand tendons.

2.5 River Torridge Bridge (England)

The River Torridge Bridge is a segmental concrete box girder bridge structure located near Bideford, North Devon, Great Britain. It is composed of eight spans totalling 645m (2,116ft), with three major spans of 90m (295ft). The single celled box girder segments used on its three major spans have a variable depth of 6m (19.7ft) to 3m (9.8ft), a total deck width of 13.3m (43.6ft) and a bottom slab width of 6m (19.7ft).

The bridge, opened to traffic in May of 1987, was erected according to the balanced cantilever method using precast segments with epoxy joints. These segments were cast in a short-line bed (using the match-casting technology) in a casting yard located on site. Segments were transported to the top of the finished spans and a steel launching girder was used for erect-

ing them in a double cantilever from each pier segment. Adjacent cantilevers were made continuous at midspan with a cast-in-situ joint and additional longitudinal prestressing.

The field instrumentation project of the River Torridge bridge is the initial part of an extensive program involving two other similar bridge structures in Great Britain. The research was carried out by investigators from the University of Bristol. Only their two initial reports were available but it is possible that new ones were recently published. The first report [12] provided an extensive review of the segmental construction of concrete bridges. Particular areas of interest were:

- The currently used segmental construction methods.
- Structural analysis methods for concrete bridges.
- An extensive current literature review of time-dependent behavior of concrete, particularly creep, shrinkage, and elastic strain.
- An extensive current literature review of factors involving time-dependent prestressing losses.
- A review of the thermal effects on concrete and particularly on segmental box girder bridges.
- A general literature review of previous experimental research of segmental bridges.

The second report [45] provided detailed information of the field instrumentation project of the River Torridge bridge structure. This report contained a description of the complete instrumentation program along with the original concrete strain measurements obtained over a 15 month period (starting at a few days after casting of the instrumented segments up to the completion of the bridge). Temperature readings for the same time period and a description of the material property data of samples taken from the instrumented segments were given. Brief information regarding the design and construction of the River Torridge bridge was also included.

The main objectives of the overall instrumentation program were (i) to conduct field measurements on prestressed concrete segmental bridges, (ii) to establish short and long term behavior of the concrete used in the instrumented bridges, and (iii) to develop computerized methods of analysis that predict the structural behavior of segmental bridges during construction and throughout their service life (this based on the observed short and long term behavior).

Four segments belonging to a single half span were fully instrumented with devices to obtain concrete strains and temperature. Sensors used for the instrumentation of the River Torridge bridge were the following:

- a. Vibrating Wire Strain Gages:* the gages used were manufactured in England by Gage Technique, Ltd. and were of the type TES/5.5. These were 140mm (5.5in.) gages generally used for embedment in concrete. They were selected due to their proven long term signal stability, robustness, and unaffected performance from gage disconnections (or variation in contact electrical resistances). A total of 122 vibrating wire strain gages were installed in the instrumented span of the River Torridge bridge. Only one of these gages failed after installation and no additional gages seemed to have failed after fifteen months of operation. Groups of three vibrating wire strain gages were placed in 120° rosette arrangements before installation in the two segments near the pier. Twelve rosettes were installed in each of the two segments near the pier. The rosettes were equally distributed around the two webs, the portion of the top deck slab between the webs, and the bottom slab. These gages provided additional information about the in-plane shear strains around the box section. In most segments a pair of single longitudinal vibrating wire strain gages were installed at two locations on each cantilever wing (one near the tip and one at the web connection). In the two segments near mid-span additional longitudinal gages were installed around the box section (instead of the rosettes). A few transverse strain gages were also installed in the last two segments, one across the top deck slab near the tip of a cantilever wing, one across a web thickness, and a last one across the bottom slab. The gages were normally secured to small reinforcing bars to prevent their movement during concrete placement. The vibrating wire strain gages were additionally protected by a light gage steel wire mesh. The leadwires were properly secured to the main steel reinforcement of each segment and brought out on the inside surface of either web as convenient. The researchers used a portable, battery-operated readout unit with an 8-channel rotary switch for monitoring the vibrating wire strain readings. According to their initial reports, the vibrating wire strain gages provided very reliable and stable measurements of concrete strains during the reported time period.
- b. Thermocouple Wires:* copper-constantan thermocouple wires of gage size 17 were used for embedment in concrete. Although misprinted as a Type "K" thermocouple in the field report, this combination of metals actually corresponds to a Type "T" thermocouple wire. About 42

thermocouple wires were installed at locations near the middle of each cantilever wing, and in the middle of the top deck slab, the bottom slab, and the two webs. In each location, the thermocouples were distributed at different depths in the concrete. Four wires were used in the 250mm (9.8in.) wide top and bottom slab sections. Five wires were used in the 350mm (13.8in.) wide cantilever wing sections, and seven wires were used in the 450mm (17.7in.) web sections. All thermocouple wires corresponding to a single width were tightly secured to a small plastic rod that was in turn tied to the main steel reinforcement. This enabled the gages to remain in place during concrete placing. The thermocouple wires were read with a portable, battery-operated, self-compensating digital electronic thermometer with a sensitivity of $\pm 0.1^{\circ}\text{C}$. This device also had an eight channel rotary switch to speed up the readings of several channels. Although not indicated in the report, it seems that all thermocouple channels were operational at fifteen months after their installation.

c. Meteorological Data: these consisted of relative humidity and average air temperature readings. Both were not measured on site but at a meteorological station located only 12 miles from the project. Despite the use of measurements obtained from a meteorological weather station, no readings of average solar radiation variations were reported. It is very possible that this parameter was actually not measured at the particular location.

d. Material Tests: first of all, the project researchers gathered very detailed information regarding the mix constituents of the concrete used in the instrumented spans. A large number of prisms and 150mm (5.9in.) control tubes were cast using concrete from two of the four instrumented segments. These were used to measure the following time-dependent concrete properties: compressive strength, modulus of elasticity, Poisson's ratio and coefficient of thermal expansion. Measurements were taken at 28, 90, 180, 240, and 365 days after casting. The concrete prisms were used to measure long term time-dependent strains. They were instrumented with a single axial vibrating wire strain gage. Some of the specimens were stored outdoors (protected from direct sunlight and rain) to monitor long term shrinkage. Others were stored indoors in a temperature controlled room (23°C and 85% relative humidity) for estimating creep and shrinkage properties under average British conditions. No material property data was needed for the mild steel nor the prestressing steel reinforcement.

Finally, the second report of the River Torridge bridge [45] provides good details and illustrations about the instrumentation systems used in the project. It also provides the original con-

crete strain and average temperature readings for the first fifteen months of the project. However, no discussion or conclusion about the measured data or the performance of the instrumentation systems was given. From the measured data it can be concluded that in general the sensors used in the field project were very appropriate. However, a simple automated data acquisition system would have considerably increased the ease of reading operations and subsequent handling of the recorded data. It would have also enabled an increase of data points without a corresponding increase in recording efforts. Finally, an automated data acquisition system would have considerably decreased the existence of operator errors.

2.6 James River Bridge

According to the final design plans [46], this is a segmental concrete box girder structure that carries I-295 over the James River near Richmond, Virginia. The complete bridge structure includes three 150ft approach spans on each side of the river and a 630ft cable-stayed main river span. Precast segments were used on all seven continuous spans. The transverse cross section of each span included twin single celled box girders each of about 58ft top deck width, 12ft depth, and 18ft bottom slab width. A unique type of delta frame assembly was used to adjoin every other pair of twin box girder segments of the central three spans to properly anchor the stay cables and distribute their concentrated loads. Twenty six stay cables arranged in a plane harp configuration and composed of 72 to 90 seven wire 0.6in. ϕ prestressing strands were used in the main river span. The cables were stressed to a maximum of $0.45f_{pu}$ and enclosed in polyethylene ducts. The segments of the side spans were erected following the span-by-span method. The cable-stayed main river span was erected in cantilever from the two central piers.

An extensive field instrumentation project was prepared before the start of construction operations by researchers from the Virginia Transportation Research Council (an organization partly dependent on the University of Virginia). The project was developed with the direct sponsorship of the Virginia Department of Transportation. An initial progress report was published in April of 1988 [46]. This report included:

- A brief summary of the James River bridge structure (according to final design plans).
- A description of the project objectives.

- A brief description and analysis of some possible sensors that can be utilized for fulfilling the original project objectives. Specific instrumentation systems under study were related to available methods for determining average stay cable stresses, methods for determining concrete strain, internal concrete temperature, and the description of a complex data acquisition system.

Since very few actual cable stayed bridges have been successfully instrumented in the past, the James River field project was fully prepared for measuring the typical live load stress ranges of two critical cable stays. Also among the project objectives was the desire to measure the magnitude of the torques introduced in the box girder segments as a result of varying service loads and eccentric stay cable forces. The project was also designed to measure temperature gradients in a selected box girder segment, an individual section of the pylon, and in the gaged stay cables. This was partly done to compensate for temperature differentials at the level of the electrical resistance strain gages and partly to observe the temperature gradients across the box girder segments of the pylons and of the bridge deck. A final objective of the project was to evaluate the structural performance of the delta frame assemblies that connect the twin box girder segments to the central, single plane, stay cable system. The project researchers wanted to observe the performance of the delta frame system in distributing the concentrated stay cable forces in the two supported box girder segments. Project researchers claimed that the James River structure is the first bridge constructed with the delta frame concept.

The interim report describes a review of numerous currently available sensors that were investigated prior to making the final decisions. The selection of the most adequate sensors was based on specific requirements of: long-term reliability (i.e. stability), speed of measurements (preferably in the order of fractions of a second, to allow for the determination of live load responses), ability to maintain the original structural integrity of the instrumented members, and ease of installation to avoid conflicts with the normal construction procedures. A wide margin of choices evidently existed at the beginning of the project since the total cost of the complete system was not directly included within the most important limitations.

The most adequate sensors complying to the requirements of the James River bridge instrumentation project were the following:

a. Electrical Resistance Strain Gages in Stay Cables: the stay cable stressing operations need to be known to determine the adequacy of the instrumentation system. Individual strands of the

stay cables are initially pretensioned to a low stress level (usually around $0.10f_{pu}$) against the back of the multi-strand hydraulic jack. This prevents overstressing of the strands during final stressing due to uneven lengths, differential anchorage, and/or varying internal friction at deviators and between strands. The multi-strand jack is finally used to simultaneously stress all strands to the design stress level (about $0.45f_{pu}$ in this case). The instrumenting of individual strands with electrical resistance strain gages would thus provide a good estimate of the average tendon stress. The interim report suggested to bond four pairs of electrical resistance strain gages to diametrically opposed strands of each cross section of the three stay cables to be monitored (one located closest to the pylon, one closest to midspan, and one midway between the previous two). Each pair of gages was in turn designed to be bonded to opposite wires of each instrumented strand (however, laying in the same accessible face of each strand). Gages suggested for use were manufactured by Measurements Group, Inc. and were of the type 062AP. Their bonding method was suggested to be done with a two-part epoxy resin coded AE-10 and manufactured by the same company. The actual electrical resistance of the gages, the resistor and backing material types, and their type of quarter bridge connection were not disclosed. Since the interim report repeatedly mentioned the necessity of installing thermocouple wires near the gages, it seems that these were not of the temperature compensated type. It also seems unclear if temperature compensated three-leadwire systems were used for the quarter bridge Wheatstone completion circuits. However, detailed provisions were made for the proper installation and moisture protection of the gages since the instrumented cable stays had to be subsequently grouted with code recommended pressures (up to 100psi). The present author considers that the described gage protection scheme seems to have doubtful stability since no previous laboratory tests of high-pressure grouted strands bonded and protected with the same method were performed by the James River project researchers.

b. Electrical Resistance Strain Gages in Box Girders: the primary method for monitoring concrete strains was the "sister bar" (or "dummy bar") system. A single temperature compensated electrical resistance strain gage composed of a 90° rosette (actually composed of two gages at 90° angles with each other) was recommended to be carefully bonded in the middle of a 4ft long #5 steel reinforcing bar. Placing the pair of 90° rosette gages in different legs of the Wheatstone bridge would effectively compensate for transverse strains. Careful detailing of

the gage installation, bonding method, and type of leadwire was provided in the Interim Report. The dummy reinforcing bars were suggested to be installed in three different box girder segments located near the pylon, near midspan, and at the point midway between the two previous segments. Ten longitudinally oriented dummy bars were designed to be equidistantly embedded in the top deck slab of each twin box girder section. Three longitudinally oriented dummy bars were designed for each bottom slab, and a three-bar rosette was designed to be placed in the middle of each web. The instrumented segment near the pylon was slightly different than the other two since additional three-bar rosettes were also designed for the top and bottom slabs. The envisioned dummy bar system seems appropriate to the present author. However, the use of the 90° rosette electrical resistance strain gages seems unnecessary since only small errors would be introduced by creep of the gages and transverse strains.

c. Electrical Resistance Strain Gages in the Pylon: two pylon sections were also recommended to be instrumented with the same dummy bar system to be used in the box girder segments. The sections to be monitored were the cast-in-situ pylon section located at bridge deck level, and the precast segment supporting stay cable S7 (approximately located at mid-height of the pylon above the deck level). The cast-in-situ section was designed to be instrumented with 10 vertical bars located around its periphery. The precast section had two additional dummy bars: one vertically oriented located at the center of the segment, and a horizontally oriented bar located at about the same place (directly below the stay cable S7 deviation saddle). Presumably the same 90° rosette gages described in (b) were also designed for use in the pylons.

d. Mechanical Extensometers: Whittemore mechanical extensometers of 10in. gage lengths providing a resolution of 10µε were recommended to measure concrete surface strains. These sensors will be used as a backup of the electrical resistance based dummy bars located in the box girder segments, and as a method for roughly measuring the structural adequacy of the delta frame assembly (at two critical locations, one near midspan and one at a quarter point). The locating points for the Whittemore extensometers were recommended to be inserted into drilled holes in the cured concrete and bonded with a rapid-curing, shrinkage-compensated, hydraulic cement (such as Duracal). This was thought to decrease the temperature related errors since the cement based mortar will have an expansion coefficient closer to the underlying

concrete than that of an epoxy resin. However, the present author believes that the error introduced by the different thermal coefficient of the epoxy and the concrete should not be large when the epoxy resin is used in conjunction with some type of mechanical anchorages. It is doubtful that the Duracal system would be stable for long-term readings under typical field environmental conditions.

- e. *Thermocouple Wires:* standard type "T" (copper-constantan), 24 AWG thermocouple wire were recommended. Two structural components were suggested to be instrumented: the previously described precast pylon segment corresponding to stay cable S7 (located at about mid-height of the pylon), and a quarter-span segment. Nineteen thermocouple wire locations were selected for the pylon segment. The twin box-girder cross section was envisioned to be instrumented with about thirty thermocouple wires located at three or four different levels through the thickness of the top and bottom deck slabs. To ensure the correct positioning of the wires, provisions were given to pre-attach each set of gages --corresponding to a certain slab thickness-- to small polyethylene ducts that should in turn be tied to the steel reinforcement cages. Finally, some thermocouple wires were also recommended to be installed near the electrical resistance gages of the stay cables to compensate the measured strains for temperature differentials.
- f. *Data Acquisition System:* a very complex system was designed for the automated acquisition of the data generated by all electrical sensors: strain gages and thermocouples. Provisions were also made to build a versatile system that can handle other type of sensors in future projects. The selected automated data acquisition system (ADAS) was manufactured by John Fluke Company and is based on a Helios main controller used to communicate with several remote scanning extender chassis. The remote scanning units were recommended to avoid having great lengths of leadwires coming from each remote sensor to the location of the main controller. Long leadwires can produce unwanted desensitization of the electrical resistance strain signals and increased costs. The connection of the remote scanning units to the main controller utilizes standard RS-422 communication cables and does not suffer desensitization problems since the data is transferred in digital form. However, analog to digital converters are thus needed at each remote scanning unit and at the main controller scanning unit. Temporary data storage will be performed by the Helios controller and permanent storage by the hard disc of a PC computer preferably located at the offices of the Virginia Department of Transportation (in Richmond). The PC

was planned to communicate with the Helios through two modems (caller and receiver) using a dedicated phone line to be installed in the box girder structure. All scanning units and the main controller located inside the box girders of the James River bridge are to be operated by AC power. Extensive provisions for preventing problems related to power surges, power outages, and lightning strikes were presented in the Interim Report. Although not mentioned the total cost of such an ideal automated data acquisition system seems quite large to the present author. It will be interesting to check the final design and the actual performance of the proposed system. Other projects have reportedly failed in the automatization of low electrical resistance signals due to the high comparative amount of electrical noise introduced to the system. A reduced laboratory simulation of the proposed system would have been ideal before engaging considerably larger amounts of time and money.

The Interim Report of the project [46] should be referred to for a more detailed review of the location and installation of the different sensors. The actual field performance of the proposed instrumentation systems during installation and construction of the instrumented span should be included in future reports from the investigating agency. To the knowledge of the present author no further data is presently available.

2.7 Highway Bridges in Nevada

Two concrete box girder bridges were recently instrumented in the State of Nevada. The first structure was the Sunset Road Interchange located in Henderson (instrumented in May 1988), and the second one was the Golden Valley Interchange near Reno (instrumented in September 1988). The Sunset Road Interchange bridge is a 195ft, single span, multi celled box girder structure with a total top deck slab width of 121ft. The twelve internal cells of its cross section are separated @ 8ft 8in. (center to center distance between the 12in. thick, intermediate, vertical webs) and the two external cells have a bottom width of 7ft 2in. The constant depth of the box girders is 8ft and each internal vertical web carries four internal tendons composed of either 29- or 30-½in. f low-relaxation 7-wire prestressing strands.

The Golden Valley Interchange bridge is composed of two multi-celled box girders extending on a single span of 155ft. Each box girder has three internal cells separated @ 7ft 6in.

(center to center distance between the 12in. thick, intermediate, vertical webs) and two external cells with a bottom width of 5ft 6in. The total top deck slab width is 45ft and the constant box girder depth is 7ft. Each one of the three intermediate vertical webs carries three tendons composed of 31-, 19- or 18-½ in. ϕ low-relaxation 7-wire prestressing strands.

The construction process of both structures was very similar. A staged construction procedure of full-span sections was followed. The stages consisted of consecutive castings of the bottom slab, the webs, and the top slab.

The complete field instrumentation project of both bridges was conducted by researchers from the Civil Engineering Department of the University of Nevada at Reno. The project was sponsored by the Bridge Division of the Nevada Department of Transportation (NDOT). It included four specific objectives that were defined by the project researchers [47].

The first part of this project involved the field measurement of average prestress losses of selected internal tendons of each one of the above mentioned structures. The period covered by the final project report [47] only involved the measurements taken in the first year after initial stressing of the tendons. This short monitoring time was thought enough to cover the first research objective since most prestress losses tend to occur early in the life of a structure. However, considering reports from previous stress loss studies it is unlikely that a one year measurement program could provide a relatively good prediction of the 40 or 50 year tendon stress losses. In fact, the project researchers recommended a continuation of the monitoring process to better predict the total prestress losses expected to be found at the end of the design life of the structures. Extremely dry weather occurred in the second half of the first measurement year and this produced much larger measured losses than the theoretical values.

A second objective of the instrumentation program was to determine the adequacy of the current design codes, since most of them were essentially developed according to data obtained from other parts of the United States. The State of Nevada presents a very different climate than most other places in the country.

A third objective of the report was to compare the measured anchorage set losses with design code values. Finally, the project was interested in determining if concrete surface strain data could be used to estimate the average prestress losses of fully bonded internal tendons.

The measurements needed for fulfilling the project objectives consisted of average tendon stresses, concrete surface strains, and corresponding studies of material properties of con-

crete and prestressing steel. The researchers monitored the average stresses of four tendons on each bridge structure: two located on a typical vertical interior web and the other two on a typical inclined exterior web. Square blockouts of about 1.5ft x 1.5ft were prepared on each instrumented web at transverse sections located near midspan. The different sensors were installed on selected prestressing strands and on web surfaces near the blockouts.

The following sensors were used in this instrumentation program:

a. Electrical Resistance Strain Gages: three 120Ω bonded type foil gages of the type EA-06-230DS-120 manufactured by Measurements Group, Inc. were installed on three different wires of a single strand of each tendon. Having four tendons instrumented in each bridge, a total of 12 gages provided the information related to average tendon stress losses. All gages were bonded with a cyanoacrylate adhesive also offered by Measurements Group, Inc. (M-Bond 200, similar to a Super Glue). Gage protection against moisture was accomplished by covering the gage and soldered leadwire assembly with Teflon tape and a top cover of butyl rubber compound. Temperature compensation was accomplished by installing a "sister gage" bonded to an unstressed prestressing wire located near the instrumented tendons. Practically all twelve electrical resistance strain gages installed in the Sunset Road Interchange (the first instrumented bridge) were damaged during the pressure grouting process. A different method to prevent the grout from reaching the location of the electrical resistance strain gages was used on the Golden Valley Interchange bridge. However, 25% of the installed gages were still damaged during the grouting process (3 damaged gages out of the original 12). The investigators also reported that most of the gages experienced false strain readings subsequent to the grouting process. The present author believes that this can be related to temperature differentials in the grout and in the instrumented strands. The surviving 9 electrical resistance strain gages seemed to have produced stable readings until the last measurement day, at about 15 months after their initial installation. However, it is doubtful that the cyanoacrylate bond of these gages can last for much longer instrumentation periods. Another interesting observation of this project is that only a single strand was instrumented on each tendon. A comparison of the average stress losses measured in each one of the four instrumented tendons still showed large standard deviations from the average stress values. The present author believes that a better average stress loss for each tendon could have been measured if the strain gages were installed on different strands instead of on different wires of the same strand.

- b. Mechanical Extensometers:* a Soiltest CT-171 Multi-Position Strain Gage of 10in. gage length was used for measuring concrete surface strains of the two instrumented webs in the Sunset Road Interchange bridge. However, these strain measurements were not accurate enough due to the short gage length and because the measuring points were located too close to the concrete blockouts in the webs (less than two wall thicknesses from the blockouts). A 30in. mechanical gage of the same type was used in the Golden Valley Interchange bridge. Although more sensitive and better positioned than the previous attempt, these measurements were still found too crude to predict average tendon stress losses. As in similar past investigations, all locating points for the mechanical extensometers were installed with an epoxy resin adhesive. Both mechanical extensometers had a dial indicator sensitive to 1/10,000in. movements. This should have provided a 4µε sensitivity on the 30in. gage.
- c. Material tests:* only concrete material properties were determined for this project. However, the final report leads one to believe that the only measured concrete properties consisted of compressive strengths at 7 and 28 days. Values for ultimate shrinkage strain and ultimate creep coefficient seem to have been taken from literature suggestions (ACI 209 method). The prestressing strand material properties were provided by the strand manufacturers and no actual material tests were performed on samples taken from the different strand rolls used for the instrumented tendons.
- d. Anchorage Set Measurements:* these were simply performed by taking electrical resistance strain gage readings before and after seating the instrumented tendons. Very good agreement was found between the average of the measured values and the code predicted losses (using the PCI method).
- e. Time-Dependent Deflections:* these were measured on both bridges with a surveying level and a Philadelphia rod. The rod was positioned at two or three locations of the midspan cross-section and over the bridge abutments. Relative vertical movements with respect to the abutment level were thus computed. Short and long term accuracy obtained in these measurements was unknown. However, the deflection curves seem to indicate that a maximum accuracy of about 1/10in. was obtained. This level of accuracy is in close agreement with other field instrumentation projects that used similar deflection measuring systems.

f. Data Acquisition System: an automated data acquisition system (ADAS) based on a Hewlett Packard computer of the series HP-9000 was used for this project. The HP-3497A Data Acquisition/ Control Unit, the HP-3456A Digital Voltmeter, the HP-6227B Dual DC Power Supply, and a parallel printer were also connected to the computer. A user friendly program was written to scan the different strain gage channels at pre-determined intervals. Quarter bridge Wheatstone completion circuits were used. However, it is unknown if these were arranged for two or three strain gage leadwires (to compensate for temperature differentials in the leadwires). This ADAS seems to be AC powered and was probably only operated for short-term intervals of a few days at a time.

The project researchers provided valuable recommendations for future similar instrumentation projects. The following observations were particularly interesting:

- More involved accompanying concrete material test studies were recommended to be carried out along with future field instrumentation projects. These tests would provide better information regarding concrete creep and shrinkage.
- Due to the uncontrolled climatic conditions of field projects, the monitoring sensors were recommended to be read or scanned more frequently than would normally be required for a laboratory investigation. They suggested an optimum one hour period between scans during each measurement day.
- They also recommended the use of a larger number of electrical resistance strain gages due to their wide scatter. This was mainly attributed to the large gage sensitivity and the harsh field environment. However, the present author strongly believes that not only these two factors contributed to the large deviations of the gage readings. Stress differentials among instrumented strands of multi-strand tendons can also be particularly large in field structures of this type.

2.8 Other Projects

Several other small field investigation projects were carried out around the world [see Bibliography, Section XI]. Most of these projects were not as extensive as the ones described

earlier in this chapter. However, some of the smaller field instrumentation projects for segmental box girder are reviewed briefly here to provide an overall idea of the extent of the past investigations, the sensors used, and the time frame of the monitoring periods.

2.8.1 Prestressed Concrete Bridges in Japan

Several segmental concrete box girder bridges were instrumented in Japan from the middle of the 60s. and into the first half of the 70s. A total of four box girder highway bridges and a single box girder railway bridge were monitored for vertical movements [48]. A total of 21 prestressed concrete bridges, including 11 of the box girder type, were also instrumented for concrete creep and shrinkage [49]. The majority of the instrumented box girder highway bridges had the following characteristics:

- erected in balanced cantilever from the piers.
- made of cast-in-situ box girder segments,
- composed of single cells and variable depths, and
- all the larger spans had a midspan hinge.

The monitoring program was carried out since it was known that this type of bridge was particularly susceptible to excessive deflections mainly attributed to creep and shrinkage of concrete and to prestressing steel relaxation. The deflection measuring system was based on the surveying technique and had consequently low levels of accuracy. Vertical deflection measurements relative to the pier segments were taken at different positions in the midspan segment of each bridge structure. The measurements were carried out for periods extending up to four and a half years. Only a few data points were taken in such a long period of time. However, the measured data was in approximately good agreement with the movements predicted with analytical methods. However, this seems strange since too many factors can control the measured deflections of such bridges.

Carlson elastic wire meters embedded in the concrete webs were used to determine the elastic properties of concrete. One interesting procedure followed in these studies was the determination of shrinkage measurements by installing the Carlson gages transverse in an unstressed concrete block located in the web or in the bottom slab of the instrumented bridges. In some cases this procedure showed a considerable scatter of the maximum concrete shrinkage strains determined by gages installed at different ends of the same bridge. This was attributed to

the different shading and air movement that existed between the two instrumented webs. The Japanese researchers determined that very few Carlson gages were damaged or rendered ineffective during the relatively long instrumentation period.

2.8.2 Kishwaukee River Bridge

This is a segmental concrete box girder bridge that carries four lanes of US-51 over the Kishwaukee River, located about four miles south of Rockford, Illinois. The structure is actually made of two similar parallel box girder bridges extending five spans each (three central spans of 250ft and two of 170ft). All spans were erected with precast segments in balanced cantilever with a launching girder. The box girders were single cell with a 41ft top deck slab width, 11ft 4in. constant depth, and 20ft 8in. bottom slab width.

Three cross sections of a single span for segments located near the pier, and at half and quarter span were instrumented with Whittemore mechanical extensometers and Carlson elastic wire meters [50]. A total of eight Carlson gages were embedded around the box girder section of each instrumented segment. The guiding points of the mechanical strain gages were bonded at about the same locations as the Carlson meters. They were presumably used as a backup system in case of failure of the electrical resistance meters. Both instruments provided consistent and similar results for the complete measurement period that extended slightly over two years.

Concrete material properties of specimens taken from the instrumented spans were also investigated. A total of 35 concrete cylinders were taken from each instrumented segment. The physical properties investigated were the variation of compressive strength, modulus of elasticity, Poisson's ratio, and coefficient of thermal expansion with time. Additional creep and shrinkage cylinders were installed outdoors and others in a temperature controlled environment. A good correlation of measured and calculated deformations was found when the concrete material properties were based on the specimens stored outdoors.

2.8.3 Pelotas River Bridge (Brazil)

This is a segmental concrete box girder bridge built in progressive cantilever from the abutments and with a hinge at midspan. The bridge has a center span of 620ft over the Pelotas River in southern Brazil, and two side spans of 294ft each. The bridge was erected in 1966 and

data was available about its initial leveling. This is a particularly interesting field instrumentation project since vertical deflection measurements were subsequently taken in four other time periods in 1968, 1971/72, 1974/75, and finally in 1978. A twelve year bridge deflection curve was thus prepared by independent researchers from Brazil [51]. The vertical movements were measured with a Wild N2 level and a surveying rod. Since the measured magnitude of deflections was quite large, the utilized sensors had the appropriate level of accuracy. A very large deflection of 450mm (17.7in.) was measured in the middle of the center span after twelve years of service. Large daily temperature-induced deflections of up to 57mm (2.2in.) were also measured.

Temperature readings on the concrete surface of the top and bottom slabs were measured with lightly embedded mercury thermometers. A maximum differential temperature of 17°C (30.6°F) was recorded. Despite the excessive creep deflections and temperature induced movements, load tests determined that the measured properties had apparently no adverse effect on the ultimate strength of the structure.

2.8.4 Concrete Bridges in Switzerland

Several concrete box girder bridges have been recently instrumented with a novel instrumentation system for measuring vertical span movements in Switzerland [52]. Researchers from the Ecole Polytechnique Fédérale de Lausanne developed an accurate, low-cost, and relatively easy to make, install, and operate deflection measuring system [53, 54]. The system is based on the hydrostatic principle of communicating vessels. According to its creators, their initial field studies reported an accuracy of $\pm 0.5\text{mm}$ ($\pm 0.02\text{in.}$) per circuit. However, the present author strongly believes that such an accuracy level will be hard to obtain in long-term measurements.

The reviewed references [53, 54] provide several details related to the construction, installation, and operation of the hydrostatic leveling system. The given sensor represents a plausible effort made to minimize total instrumentation costs while maintaining satisfactory levels of accuracy and stability.

2.8.5 Concrete Bridges in Portugal

Researchers from the *Laboratório Nacional de Engenharia Civil* performed several field measurements of strains and stresses in concrete bridges during the 50s and 60s. A report about their creep and shrinkage findings was published in the final report of the 1970 IABSE Symposium in Madrid [106]. It is mentioned here due to their unique method employed for identifying strains induced from stress, creep, shrinkage, and temperature (as measured by acoustic strain gages embedded in concrete).

The exact type and operation of the acoustic strain gages was described in a different paper and was not investigated by the present author. However, their particular method of placement in the investigated concrete bridges was closely reviewed. The same method can be performed with new types of concrete embedment gages (such as Carlson Elastic Wire Meters or Modified Mustran Cells). The Portuguese investigators placed the strain gages in the concrete structures in three different conditions: a) active, b) compensating, and c) controlled.

The active gages were directly embedded in concrete with no additional equipment. They thus measured total concrete strains. The compensating gages were installed inside double-wall cylindrical boxes made of thin copper sheet. The cylindrical boxes were open on one side (say at the bottom) and the gages were installed in the longitudinal direction (parallel with the lateral surfaces of the cylinder). The deformations of the side walls and the top of these boxes thus avoided the action of stresses on the compensating gages.

Finally, the controlled gages were installed inside similar double-wall cylindrical boxes (as the ones used for the compensating gages). However, a metallic cushion filled with oil was placed at the top of these boxes. These metallic cushions acted as internal jacks that were used to apply a known pressure to the gages located inside the cylindrical boxes. By controlling the pressure of oil in the cushion, mechanical tests of the concrete inside the structure --particularly creep tests-- were performed with excellent results.

A direct measurement of stress-induced strains --without knowing the mechanical properties of the concrete-- could be obtained by installing an active and a controlled gage at about the same location in the structure. Moreover, if the pressure in the hydraulic cushion is varied in such a way that the strains indicated by both the active and the controlled gages are permanently equal, the applied pressure approximately corresponds --without further corrections-- to the existing stress.

However, the Portuguese field investigations considered it preferable to perform creep tests by keeping a constant pressure on the controlled gages. These creep tests had the great advantage of close similitude between the conditions around the active and the controlled gages. The system permits a very accurate correction of total strains, and if similar thermal and hygrometric conditions are maintained around all three gages, the accuracy of the measured results will only depend on the accuracy of the strain gages. To prevent similar thermal conditions in gages installed in thin concrete webs, the investigators substituted simple thermal and hygrometric insulations for the cylindrical boxes.

Their measured results were in close agreement with values obtained from accompanying material tests and others calculated with the CEB-FIP code of the time. The only reported problem of the instrumentation system was the rupture of the metallic cushion of one of the controlled gages. This reviewed application can be helpful for future field investigations requiring a higher level of accuracy in the concrete strain/stress measurements. However, the method can be expensive for large full-scale investigations.

CHAPTER 3

STATE-OF-THE-ART INSTRUMENTATION SYSTEMS

3.1 Concrete Strains

Strains in concrete are seldom used directly in structural engineering design computations. They are often used by designers for estimating the state of stress in many types of structures, since the ability of a material to carry applied loads is normally expressed in terms of stress. The knowledge of local stresses in concrete structures is necessary for designing structural components which will use the least amount of material at their greatest efficiency.

Stress is a basic mathematical concept --force over a unit area-- and not amenable to measurement. With the understanding of Hooke's law, the measurement of the physical entity of strain of materials is an important tool for engineering research. The relationship between strain and stress, known as the "modulus of elasticity" (or Young's modulus of elasticity), is linear at service loading states for most structural engineering materials. The average intensity of stress in a body subjected to some external loads can therefore be estimated by measuring the resulting strains and multiplying them by the known modulus of elasticity of the material.

In the particular case of concrete structures, estimating of concrete stresses is quite difficult due to three complicating factors:

1. Inaccurate modulus of elasticity.
2. Presence of strains not directly related to stress.
3. Measurement of local strain variations.

Inaccurate Modulus of Elasticity. It is difficult to get a good estimate of the modulus of elasticity of composite materials such as concrete. Significant errors can result from this uncertainty. Between two different concrete batches, variations of the modulus of elasticity are widespread and obvious. Even for the same concrete batch, factors such as air voids, trapped moisture, and variation in compaction and curing conditions can also influence the modulus of elasticity from one point to another. For the particular case of segmental concrete bridge structures, concrete specimens used to indicate the modulus of elasticity would need to be taken out

of each different region of each segment where strains are to be measured if a high level of precision is to be attained. The level of compaction of the concrete in the actual element to be studied also needs to be simulated as closely as possible. However, in precast concrete segments where the level of control is greater than cast-in-place segments, the modulus should not present such a wide variation from one point to another.

Published data from a previous field instrumentation program of a segmental prestressed concrete bridge [55] was evaluated by the present researchers. Values for the concrete modulus of elasticity of twelve 6in. x 12in. control cylinders taken from three different segments (different concrete batches) of a single span were obtained following ASTM Specification C39 [56]. This small sample showed a maximum $\pm 10\%$ variation of the average concrete modulus of elasticity considered for the analytical studies. However, when only considering control cylinders taken from casting of each instrumented segment, the variation of the average modulus was calculated at $\pm 2\%$. This is in accordance with initial tests of control cylinders taken from the San Antonio Y project, where the variation of the average segment modulus seems to be near 1.7%.

Presence of strains not directly related to stress. With respect to strain variations, not all strains in concrete are induced by external load related stress. Other influencing factors are:

- (a) Creep (changes of strain under a constant state of stress).
- (b) Shrinkage and swelling (changes in strain due to moisture changes in the concrete).
- (c) Temperature (changes in strain due to temperature variations in the concrete and in the strain gage material).
- (d) Volume changes (changes in strain due to dimensional changes in the concrete that are self-generated, not due to temperature, moisture changes, or stress).
- (e) Curing effects (changes which occur during concrete curing).

In prestressed concrete structures creep is one of the most influential factors. Previous studies reflect that the importance of creep increases substantially when stresses are above about 60% of the ultimate strength of the concrete [57]. The duration of the instrumentation program is another important consideration to have in mind when dealing with creep and shrinkage strains. If the research is limited in time, creep and shrinkage induced strains in concrete may not significantly influence the final results.

The rate of creep and shrinkage of concrete structures are known to be modified by several factors [58]. These are mix design parameters, type of aggregate, fineness of cement, and environmental conditions during and after set (such as relative humidity, moisture content, ambient air temperature, etc.). The companion material tests of concrete, specified under "Recommended Applications" in Section 5.7.1 of this report, are included so as to more accurately determine the actual state of stress of the instrumented spans of the San Antonio Y structure.

In precast segmental bridge construction, changes due to shrinkage should be smaller than cast-in-place structures. This is because much of the shrinkage strain of precast segments occurs in very early periods, while they are kept in the storage yard. The level of creep in cast-in-place structures also tends to be much higher than in precast structures, which are more mature when stressed. This is because concrete loaded at a young age creeps more than older concrete. It is therefore concluded that in precast segmental bridge structures, and for the duration of a field instrumentation project, only creep and not shrinkage is expected to become a major factor.

Measurement of local strain variations. Finally, due to the non-homogeneity of concrete, local variations of strains occur from one point to another. As a general rule most investigations in structural concrete are designed to measure average strains thus avoiding the errors introduced by local variations of the material. Past investigations related to this effect suggest the use of gage lengths of at least 5 times the maximum aggregate dimension [59]. These gage lengths should be able to allow strain measurements without significant errors due to local variations in the concrete material.

3.1.1 Objectives

The basic goal of this section is to investigate the availability and performance of the most widely used methods for monitoring concrete strains in structures. The only way to measure this property of concrete is with the usage of "strain gages."

There are several types and variations of strain gages available. One of the best classifications has been proposed by Dunnycliff [60] who divided them in two groups:

1. Embedment strain gages.
2. Surface strain gages.

For the examination of performance of strain gages some qualifications must be met. An interesting description of necessary conditions for an "ideal" strain gage was proposed by Perry and Lissner [61]. These conditions, along with an explanation are:

1. Extremely small size. This is necessary in order to avoid modifying the actual behavior of the element to be instrumented.
2. Insignificant mass. This is also necessary to avoid modifying the actual behavior of the element to be instrumented.
3. Easy to attach to the member being analyzed. This is mainly for practicality.
4. Highly sensitive to strain. The possibility of measuring strain with extra sensitivity is desirable.
5. Unaffected by temperature, vibration, humidity, or other ambient conditions likely to be encountered in testing elements under service loads. This is to avoid measuring strains induced by factors other than applied loads.
6. Capable of indicating both static and dynamic strains.
7. Capable of remote indication and recording. This enhances the practicality of measuring and analyzing data.
8. Inexpensive.
9. Characterized by an infinitesimal gage length. By definition, strains are usually related to a single point in an element.

This review of an "ideal" gage provides an understanding of the ultimate objectives pursued by instrumentation engineers. The following survey of available concrete strain instrumentation devices explains the most important characteristics of each system, along with known data about their performance.

3.1.2 Embedment Systems.

Instruments that are embedded in concrete to measure stress through bonding introduce a new source of error known as the *inclusion effect*. A disturbance of the actual strain field could be caused by the inclusion of a strain gage in the concrete. The measured strains could be significantly different than the ones that would occur if the gage were not present. The degree

of disturbance of actual strains due to the inclusion effect is directly related to the relative ratio of gage to concrete stiffness [59].

Tests related to the inclusion effect of strain gages embedded in concrete were reported by Loh [62]. A generally good conformance is achieved by a gage that has a similar modulus to the concrete surrounding it. In these cases, the strain measurements will be correct. When the stiffnesses are different, some errors will be introduced. Their magnitude will then depend on the geometry of the gage. The stiffness of a gage is usually expressed in terms of the modulus of elasticity of a material which would form a solid cylinder of the same stiffness as the gage, when this cylinder has a diameter equal to the outside diameter of the tube of the gage.

A graphical description of the inclusion effect based on Loh's analytical expressions was prepared by Bakoss [59] and is shown in Figure 3.1.

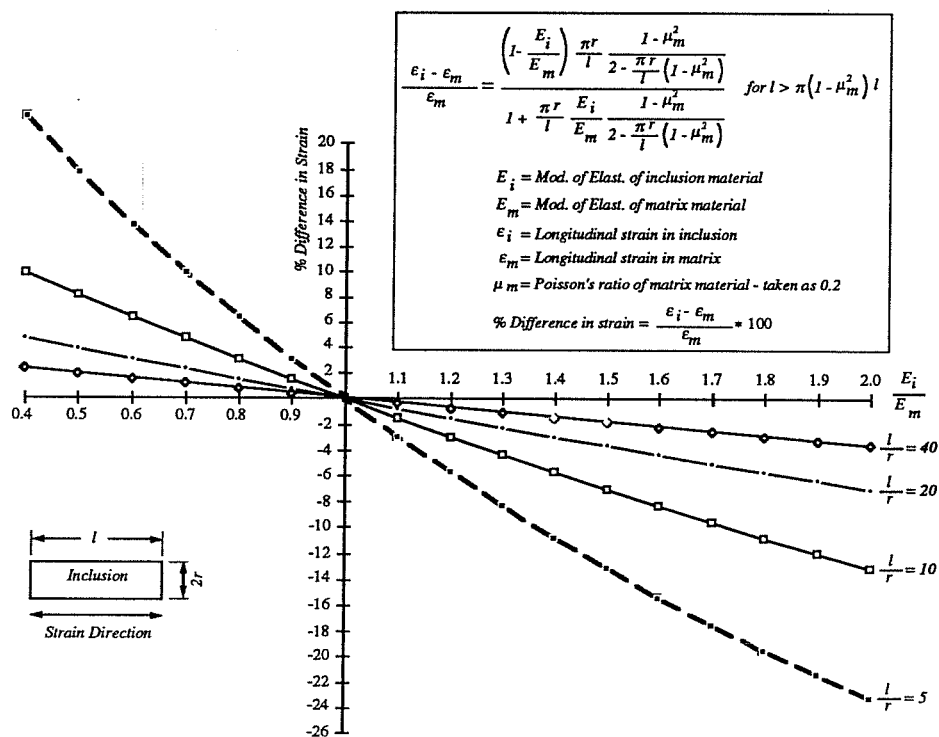


Figure 3.1 Strain errors produced from inclusion effect of different materials and sizes (after Bakoss [59]).

The analytical formulas included in the graph of Figure 3.1 are approximate and based on a linear-elastic behavior of the materials. The graph relates the longitudinal axial strain in a

cylindrical inclusion (strain gage) to the longitudinal strain which would occur in the same direction in the matrix material if the inclusion were not present.

Several strain gages of the embedment type were initially reviewed for this project. The main details of each system evaluated are provided here.

3.1.2.1 Vibrating Wire Strain Gages. These are the usually preferred type of gages for most long-term instrumentation programs due to their good performance and stability. However, their greatest disadvantage is their high cost which becomes a concern for large instrumentation projects. An important addition to the total cost for implementing vibrating wire gages for an instrumentation project is the need of special readout units. This could be expensive if portability and automated multi-channel operations are desired.

The vibrating wire technology measures strain from variations in the natural frequency of a high-strength steel wire. An advantage of these gages is that variations in resistance of the lead wires do not affect the readings of frequency. Inclusion effects are also minimized since most commercial vibrating wire gages have similar relative stiffness to that of commonly used concrete materials. Signal long-term stability is not a major concern for these type of gages. Previous studies indicate negligible long-term zero drifts [45, 59]. However, small sources of zero drift are still possible due to wire corrosion, creep of the vibrating wire under tension, external source of gage vibration, or slippage at the wire clamping points [60]. A summary of the main technical characteristics of typical commercial vibrating wire strain gages is shown in Table 3.1.

There are two different classes of gages that are based on the vibrating wire technology, the commercial prefabricated gages and the sister bar type of gages (sometimes called *rebar strainmeters*). A schematic and sample of the first type of gage are shown in Fig. 3.2. The usual configuration of a sister bar type of vibrating wire gage is presented in Fig. 3.3. Several companies offer vibrating wire strain gages, some of them are:

1. Rocrest, Inc., Irad Gage Division, 7 Pond Street, Plattsburgh, NY 12901. Current telephone (518) 561-3300.
2. Geokon, Inc., 48 Spencer Street, Lebanon, NH 03766. Current telephone (603) 448-1562.
3. Gage Technique Ltd., P.O.Box 30, Trowbridge, Wilts BA14 8YD, England, Great Britain.

Gage Manufacturer:	Irad Gage		Geokon, Inc.	
Distributor:	Roctest, Inc.		Geokon, Inc.	
Gage Model:	EM-5	EM-3	VCE-4200	VCE-4210
Current Cost (p/unit):	≈\$150.00	≈\$200.00	≈\$95.00	≈\$275.00
Gage Length (in):	6.63	3.63	6	10
Flange Diameter (in):	0.875	0.875	0.75	2
Strain Range (μϵ):	±3000	±3000	±1500	±1500
Avg. Sensitivity (μϵ):	0.3	0.2	1	0.5
System Accuracy Range (μϵ):	±5-50			

Table 3.1 Technical data of typical vibrating wire strain gages for embedment in concrete.

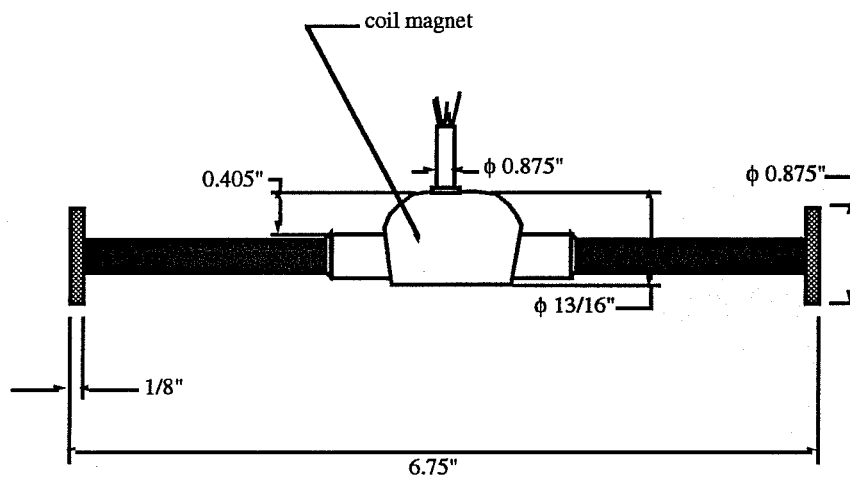
3.1.2.2 Electrical Resistance Strain Gages. These gages are the basic component of many concrete strain measuring devices. The electrical resistance gaging technology is explained below to review the most important factors regulating the sensitivity, accuracy, and long term stability of this type of measuring device.

Electrical resistance gages are basically formed by an electrical conductor bonded to a backup matrix material. This material is in turn bonded to the element to be instrumented. As this element deforms, the matrix material and conductor are strained causing a resistance change in the conductor. This resistance change is measured when a current is sent through the conductor. The change in resistance is directly proportional to the change in length. This relationship between resistance change (ΔR) and change in length (ΔL) is provided by the gage factor (GF) as follows:

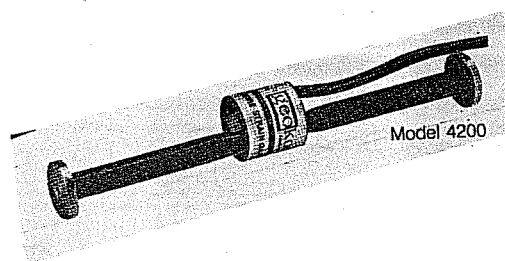
$$\frac{\Delta R}{R_0} = \frac{\Delta L}{L_0} * GF$$

The gage factor is a measure of sensitivity of the strain gage. It is influenced by several external conditions normally provided by the gage manufacturer.

Most concrete embedment strain gages based on electrical resistance foil gages are relatively inexpensive. One problem is that very strict guidelines for installation and moisture protection must be followed to achieve satisfactory long-term stability. Varying degrees of errors can also occur due to the previously mentioned *inclusion effect*. Other gages within this group consist of: Mustran Cells and Plastic Encased Embedment Gages.



a. Dimensions of Irad Gage Model EM-5 (courtesy of Roctest, Inc.)



b. Standard Geokon gage Model VCE-4200 (courtesy of Geokon, Inc.)

Figure 3.2 Typical commercial embedment type vibrating wire gages.

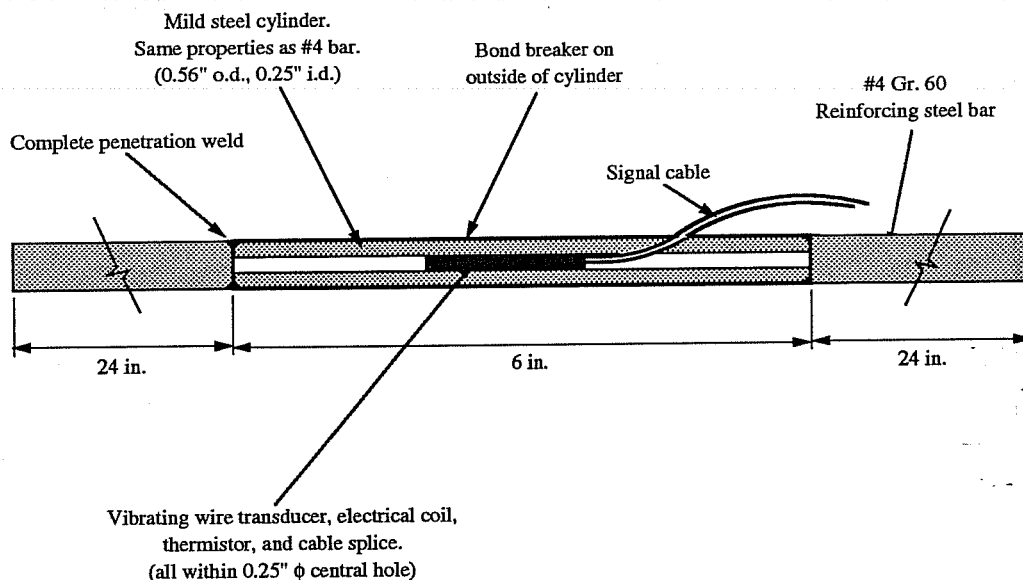


Figure 3.3 Typical sister bar vibrating wire strain gage (after Dunning [60]).

Mustran Cells. These were originally developed by L. Reese and student researchers from the Center for Highway Research of the University of Texas at Austin. The original name stands for *Multiplying strain transducers* [63]. They are based on electrical resistance strain gages bonded to specially fabricated steel bars with 1/4" threaded ends. In the design phase of these gages very careful measures were taken to match the relative stiffness of the gage with the average stiffness of concrete. This reduces the errors from the *inclusion effect* to a minimum.

Mustran Cells were reported to have worked well in drilled shaft tests performed by its creators [63]. Acceptably low levels of gage drift were encountered in the initial applications. However, long-term stability of these gages could be difficult and costly to obtain. Table 3.2 shows approximate technical data for the original Mustran Cells, as reported by the manufacturers. Costs are excluded since no correct estimates are presently available. The multiplication of strains and the robustness of the cells present two great advantages for structural investigations in large concrete elements.

The original design of the Mustran Cells seems expensive and complicated, particularly in the moisture protection system based on liquid nitrogen pressure. This gage protection scheme can probably be replaced by a more easily applicable method such as any of the epoxy

based moisture and physical protection methods suggested by leading electrical resistance strain gage manufacturers. Due to their size, the original cells are limited to applications in large concrete structures. This imposes another limitation for their effective use in segmental concrete box-girder bridge structures.

Gage Model:	Type I	Type II
Active Gage Length (in):	7	8.5
Flange Diameter (in):	2.5	2.5
Strain Range ($\mu\epsilon$):	1500	1500
Avg. Sensitivity ($\mu\epsilon$):	1	1
System Accuracy Range ($\mu\epsilon$):	$\pm 10-50$	

Table 3.2 Technical data of original Mustran Cells.

Smaller, cheaper, less complicated gages can be easily built based on the original Mustran Cell design procedure and the new moisture protection methods. However, further detailed testing of any modified Mustran Cell system would be necessary to determine their sensitivity, gage factor, and

accuracy. Illustrations of the original Mustran Cells and an example of a modified system used on previous projects at Ferguson Structural Engineering Laboratory are shown in Figure 3.4. Although these gages are not commercially available, they could be easily manufactured in-house at most structural engineering laboratories.

Plastic Encased Embedment Gages. (Also described as *Embedment Gages* by some researchers, and as *Polyester Mold Gages* by some manufacturers.) These gages consist of a standard wire-type resistance strain gage attached to leadwires, and hermetically sealed between thin resin plates. These plastic plates are usually coated with a rough grid surface to provide good bond. They are longer than traditional foil electrical resistance strain gages, and they are specifically manufactured for embedment in large structural concrete masses where uniaxial strains are expected --such as columns, piles, or drilled shafts.

Problems related to gage drift (due to temperature) and moisture penetration --causing low resistance to ground-- were reported in previous studies [64]. These studies have also concluded that the method of compensating temperature effects with a "dummy" un-strained gage was not an effective alternative. Further tests with carefully sealed dummy gages confirmed these conclusions [63]. Investigations are still needed for developing an effective method of temperature compensation and for reducing the drift of these gages.

The level of accuracy of the system can be improved by precasting them into small concrete cylinders, as suggested by Vijayvergiya [64]. However, as with other electrical resis-

tance strain gages, these can only be reliable for short term investigations.

A widely known manufacturer of these type of gages is Tokyo Sokki Kenkyujo Co. (TML) represented in the United States by Texas Measurements, Inc., P.O. Box 2618, College Station, TX 77841. Current telephone: (409) 764-0442.

3.1.2.3 Carlson Elastic Wire Strain Meters. These gages are also based on direct measurements of variations in the electrical resistance of an electrical conductor. In this case however, the conductor is an unbonded elastic wire, as shown in Figure 3.5. These devices are characterized by their long-term stability. To improve their stability and moisture protection the elastic wires are heat treated during manufacturing and the complete inner tubing is filled with oil and hermetically sealed. The main longitudinal body of the sensor is covered by a smooth PVC tubing to prevent bonding with concrete. Since the main frame of the sensor is made of steel, very small temperature corrections need to be made to account for the difference of thermal coefficients of expansion between steel and the surrounding concrete. This is only necessary when very precise measurements are important.

The instrument's design uses two separate elastic wires, one providing increased resistances with increasing strain while the other one indicates decreased values with increasing strains. Measuring the ratio of these two resistances maximizes accuracy and reduces temperature effects. These are claimed to be the most widely used concrete strain measuring devices in this country [60]. However, their elevated cost is a limiting factor for large instrumentation projects. Carlson Elastic Wire Strain Meters are mostly used in 8, 10, or 20in. gage lengths. Smaller, more economical gages are available in 4, 8, and 10in. gage lengths. Technical data for the most widely used gages are indicated in Table 3.3.

These gages can be purchased from:

1. Carlson Instruments, Inc., 1190-C Dell Avenue, Campbell, CA 95008.
Current telephone: (408) 374-8959.
2. B.R. Jones & Assoc., P.O. Box 38, Normangee, TX 77871. Current telephone: (409) 396-9291.
3. Texas Measurements, Inc., P.O. Box 2618, College Station, TX 77841. Current telephone: (409) 764-0442.

Gage Type:	Polyester Mold		Carlson Strain Meter	
Gage Manufacturer:	TML		Carlson/R.S.T. Inst., Inc.	
Distributor:	Texas Measurements, Inc.		B.R.Jones & Assoc., Inc.	
Gage Model:	PML-60	PML-120	A10	M10
Current Cost (p/unit):	≈\$15	≈\$25	≈\$207.00	≈\$127.00
Gage Length:	125mm	125mm	10in	10in
Gage Width:	13mm	13mm	1.19in	0.88in
Strain Range (μϵ):	20000	20000	2100	1600
Avg. Sensitivity (μϵ):	1	1	2.9	5.8
System Accuracy Range (μϵ):	±10-50		±20-75	

Table 3.3 Technical data of other strain gages for embedment in concrete.

3.1.3 Surface Strain Systems

Problems related to the *inclusion effect* are negligible in surface-mounted concrete strain gages. In general, most gages within this category provide slightly less accuracy and sensitivity than the embedment gages but they usually have larger strain ranges. Gages of this type were separated according to their method of measuring strains into mechanical, vibrating wire, and electrical resistance devices.

3.1.3.1 Mechanical Devices. This is one of the most widely used classes of devices for measuring strains in concrete. Advantages similar for all gages within this group are related to their simple behavior, low cost, robustness, ease of installation, and lack of special waterproofing procedures. Problems are related to the need for adequate access to the element to be instrumented, lack of automated readouts, and lower accuracy. Reported devices representing this group are composed of Demec Extensometers and Whittemore Gages.

Demec Extensometers. Their name is derived from *demountable mechanical* extensometers and were developed by the Cement and Concrete Association in England [60]. As shown in Figure 3.6, they consist of an invar bar with conical locating points at each end --one fixed and the other one pivoting on a knife edge. The pivoting movement is transmitted to a 0.002mm resolution dial indicator via a lever arm.

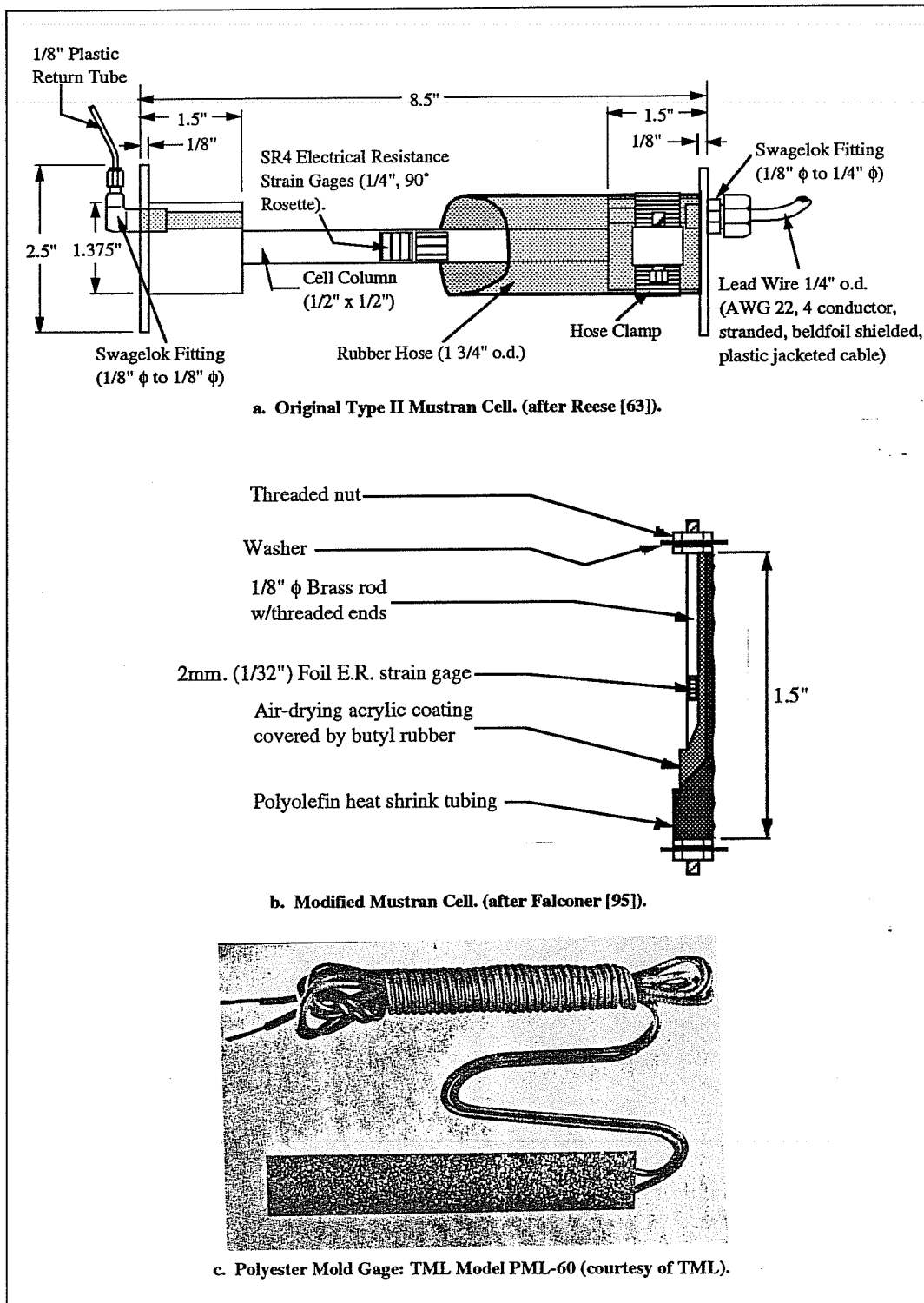


Figure 3.4 Concrete embedment strain gages based on the electrical resistance technology.

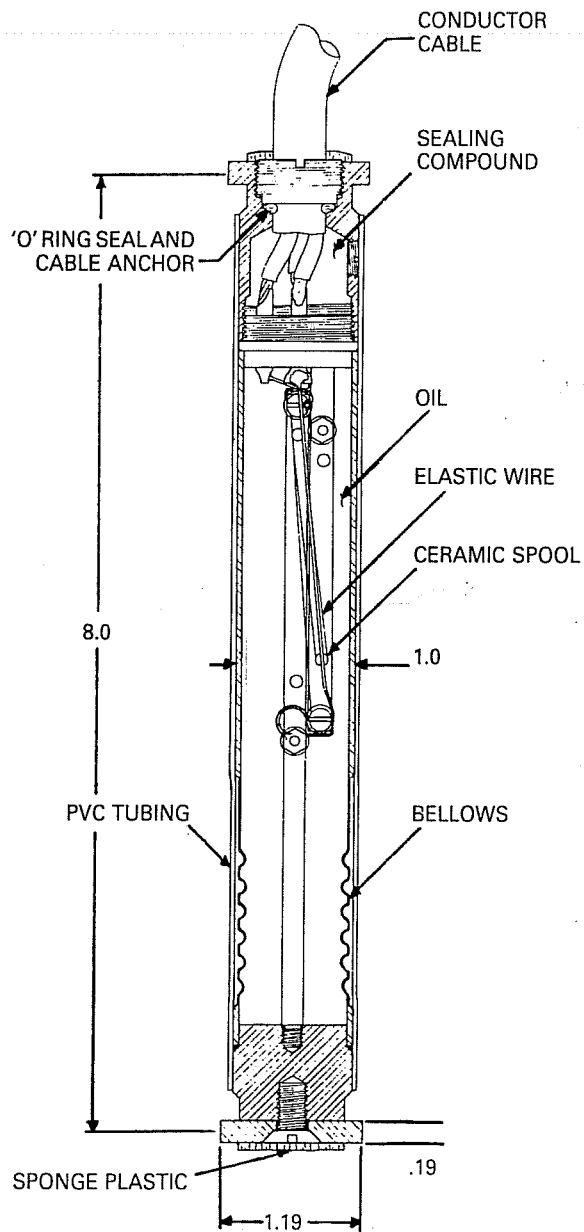


Figure 3.5 Typical Carlson Elastic Wire Meter (courtesy of B. R. Jones and Assoc., Inc.)

Gages are usually custom manufactured for each order and could have different gage lengths. The most common gages are of 100, 200, and 400mm lengths. An important disadvantage of these gages is related to their manufacture and availability. The only place of manufacture is in England and it can take 3 to 6 months for completing a purchase order from the United States (from time ordered to time of receiving the gage). Experiences of the present author with these gages also demonstrated that the spring at the pivoting end can wear out within a few years of field use, and the gage would have to be recalibrated for useful accuracy.

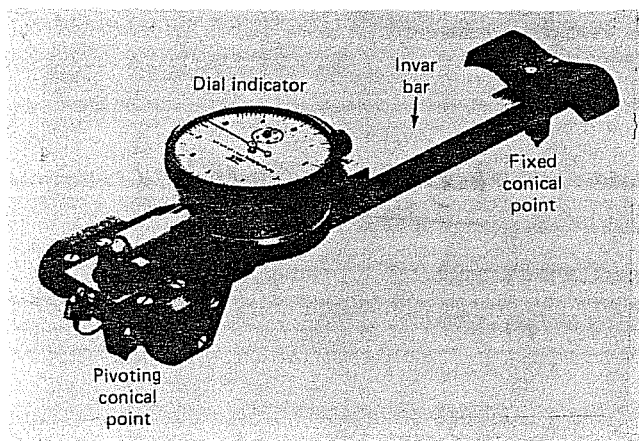


Figure 3.6 Demec Extensometer (after Dunicliff [60]).

A separate invar bar is supplied with each gage so as to measure a standard reference reading. Temperature strains of the Demec extensometer and zero drift are minimized by recording initial measurements of the standard reference bar and surface temperature measurements in the concrete. Small stainless steel locating discs with a central conical indentation are installed on the surface of the element to be measured. These are supplied by the gage manufacturer in standard circular stainless steel units of 6mm diameter, and 1mm thickness. The present researchers were able to produce satisfactory guides for the Demec extensometers by other methods detailed in Section 4.2.1. Long-term stability of these gages is feasible but also depends on the bonding method of the locating discs to the concrete surface. The actual level of accuracy varies according to gage length and reading carefulness. For 200mm gages --with standard sensitivities of $8.1\mu\epsilon$ -- accuracies of $16\mu\epsilon$ have been found feasible in field measurements. Technical data for typical Demec extensometers are included in Table 3.4.

The only manufacturer known by the present author for these gages is W. H. Mayes and Son (Windsor) Ltd., Vansittart Estate, Arthur Road, Windsor, Berkshire, SL4 1SD, England, Great Britain. Their current telephone is 44-753-864756.

Gage Manufacturer:	W.H. Mayes and Son (Windsor) Ltd.		
Gage Model:	100	200	400
Current Cost (p/unit, inc. standard bar):	≈\$902.00	≈\$950.00	≈\$1064.00
Gage Length (mm):	100	200	400
Strain Range (μϵ):	±50000	±20250	±10000
Avg. Sensitivity (μϵ):	20	8.1	4
System Accuracy Range (μϵ):	±12-60		

Table 3.4 Technical data for typical Demec extensometers.

Whittemore Gages. These are similar to Demec extensometers, but provide a significantly lower degree of accuracy [60]. They were formerly manufactured and marketed by Baldwin-Lima-Hamilton Corporation (now BLH Corp.). The new generation of Whittemore gages are now manufactured by Soiltest, Inc., and available in 4, 6, 8, and 10in. gage lengths. These gages are marketed under the name of *Multi-Position Strain Gages*. Their advertised average sensitivity is of $\approx 50\mu\epsilon$. As with the Demec extensometers, *Multi-Position Gages* are built around a calibrated dial indicator with a 0.002mm reading resolution. Their frame is different since they are made of aluminum-magnesium alloy. Invar master bars can be purchased separately for checking master settings of the main gage. When using these gages extra care should be given to temperature induced strains in the gage itself, the concrete, and in the master reference bar since all will be different. Previous applications of these mechanical gages to prestressed concrete I-girder bridges reported some difficulties due to temperature differentials between the top surface of the bridge and underneath [65].

Multi-Position Strain Gage (Eng. Units):	\$680.00
Invar Master Bar (English Units):	\$121.00
Strain Gage Punch Bar:	\$171.00
Contact Points:	\$13.00
Brass Inserts (100 units):	\$82.00
Contact Seats:	\$3.00

Table 3.5 Current prices of Whittemore gages (from Soiltest, Inc.).

Other problems such as long-term stability of the guiding points, and mechanical wear with time are also present in these type of strain gages. One great advantage of Whittemore gages over Demec extensometers is their availability, since they are stocked in the United States.

These gages can be obtained from Soiltest, Inc., Materials Testing Division, 2205 Lee Street, Evanston, IL 60202. Their current telephone is (800) 323-1242. Current prices for these gages are shown in Table 3.5.

3.1.3.2 Vibrating Wire Strain Gages. These are based on the same principle previously described in Section 3.1.2.1. They are normally attached to the concrete's surface by bolting to precast threaded studs or holes. Their long-term stability is more severely dependant on the method of attachment of the gages than on zero drift of the vibrating wire, since frequency readings are very stable. Surface mounted vibrating wire gages are costly, with prices similar to those of the embedment gages. The elevated price of these gages is a considerable limitation for their use in large instrumentation projects.

Most of these gages are provided with a mechanism for adjusting the initial tension in the vibrating wire. Wire tension is regulated according to the expected range of strains to be measured in the concrete surface. An additional device incorporated with most commercial gages is a thermistor that supplies simultaneous temperature data at each reading. Data from typical gage manufacturers is shown in Table 3.6. These gages could be obtained from the same manufacturers previously listed in the section of vibrating wire embedment gages.

3.1.3.3 Electrical Resistance Strain Gages. Some of the foil type electrical resistance gages are directly bonded to specially prepared concrete surfaces. Due to the method of preparation of the concrete surface and the difficulty of protecting the gages against external elements, bonded foil type gages are only reliable for short-term measurements. These gages also have the same problems previously outlined for the electrical resistance strain gage technology in Section 3.1.2.2.

Concrete surface preparation is usually done by vigorously removing all loose particles on a surface about 1in. larger than each dimension of the gage that is being used. Sometimes light sanding is required. A thin film of a normal set epoxy that hardens at ambient temperature is placed as the base for the strain gage. Once the epoxy has hardened, standard cyanoacrilate adhesives provided by gage manufacturers can be used for final bonding of the gage to the prepared surface. This surface preparation is not stable for long-term measurements. It is only recommended for a maximum of one or two weeks, provided that the installed system is not subjected to large temperature differentials. After installing the gage and leadwires a moisture and physical protection system should be used around the final system.

Since these gages are for direct bonding to the concrete surface, their size is longer than regular foil gages. The rule of thumb for using a concrete gage of about 5 times the diameter of the largest aggregate requires gage lengths of 2 to 5in. Longer gage lengths are usually better for full-scale investigations since a better average strain behavior can be measured. Typical data from leading electrical resistance strain gage manufacturers is shown in Table 3.7.

Gage Manufacturer:	Irad Gage		Geokon, Inc.	
Distributor:	Roctest, Inc.		Geokon, Inc.	
Gage Model:	SM-5A	SM-5B	VSM-4000	VK-4100
Current Cost (p/unit):	≈\$140.00	≈\$250.00	≈\$95.00	≈\$95.00
Gage Length (in):	5.88	5.08	5.875	2
Thermistor (yes or no):	Y	Y	Y	Y
Strain Range (µε):	3300	3300	3000	2500
Avg. Sensitivity (µε):	0.3	0.3	1	0.5
System Accuracy Range (µε):	±5-50			

Table 3.6 Technical data for typical surface-mounted vibrating wire strain gages.

3.1.3.4 Fiber Optical Strain Gages. These gages have not yet been used for measuring strain in concrete structures. Originally developed as a prototype for measurements in very aggressive environments (in terms of temperature and electromagnetic fields), commercial use of this technology can be expected in the near future. Several approaches to measuring strain could be followed by the principles of fiber optics. Two different fiber optical devices were investigated during the present survey of state-of-the-art systems for measuring strain.

Extensive research for a possible commercialization of a particular type of fiber optical gage is presently under development in the mechanical engineering department of The University of Texas at Austin --under the direction of A. B. Buckman. Initial reports of the status of this research are expected to be published by August of 1991.

A different fiber optical gage has been developed and successfully tested in a parallel study performed by the Center for Electromechanics (CEM) from the University of Texas at Austin [66]. This is among the first successful experimental applications of a fiber optical strain

gage based on the principle of interferometry. Most previous reports consisted of prototype models and of studies of gage accuracy and sensitivity.

Gage Manufacturer:	Measurements Group Vishay		Tokyo Sokki Kenkyujo Co., Ltd.	
Distributor:	Micro Measurements Division		Texas Measurements, Inc.	
Gage Model:	20CBW	40CBY	PL-90	PL-120
Current Cost (p/unit):	≈\$17.00	≈\$34.00	≈\$4.00	≈\$6.00
Gage Length:	2in	4in	60mm	120mm
Matrix Width:	0.32in	0.33in	8mm	8mm
Strain Range (μϵ):	up to 20,000		up to 2,000	
Avg. Sensitivity (μϵ):	1	1	1	1
System Accuracy Range (μϵ):	±1-5 (short-term only)			

Table 3.7 Technical data of surface bonded foil electrical resistance strain gages.

The basic principle of operation of interferometric fiber optic strain gages is shown in Figure 3.7. A laser beam --with sufficient coherent light length-- is launched into a directional coupler. This coupler splits the light beam into two others of approximately the same intensity, and propagates them into two similar lengths of single-mode fibers. Both light beams later reflect off the mirrored path ends and return to the directional coupler to recombine as the interfered output. This output produces visible fringes on certain devices such as oscilloscopes. If the optical pathlength through one fiber is changed with respect to the other, the fringes will shift. This amount of fringe shift is proportional to the relative change in optical pathlengths. By observing the motion of fringes in the oscilloscope, the optical pathlength changes can be determined with great accuracy. Simple studies on prototype tests of these gages reported up to 0.4μϵ accuracies [67]. No valid range of accuracy was obtained from CEM's fiber optic strain gage since only a single successful test was performed to date. However, the gage along with the reading equipment utilized had sensitivities in the order of 0.1μϵ.

Present technology for these gages only allows them to be used for short-term dynamic tests. The phase shifts on the fringes of the oscilloscopes need to be counted as the test is being performed, and no recording or automated systems are presently available for unattended operation. A second disadvantage is the very brittle consistency of the fibers. During bonding of the

fibers used in the CEM testing program, only one out of three survived installation. The fibers also need physical protection along their full length. Johnson, from CEM, threaded the fibers through a small heat shrink type of plastic, but this was still quite delicate [66]. However delicate, these gages have one of the highest levels of strain sensitivity and can be used in extreme environmental and electromagnetical conditions. The tests at CEM required maximum temperature ranges of -196°C to 200°C , under a maximum magnetic field of 30Tesla in a 30ms. timeframe. The surviving fiber optic gage only failed at failure of the specimen [66].

A different approach to fiber optical strain gage measurements was developed by Strabag Bau-AG in Germany [68]. Since optical fibers are characterized for having excellent light permeability, the amount of light attenuation due to mechanical constraints in bonded parts of the fibers is used for measuring strains. A graphical description of the main components of this system is shown in Figure 3.8. The optical fiber is bonded to the material to be instrumented at a certain location along its length. Infrared light rays are emitted from one end of the fiber while a receiver at the other end measures the amount of light that passes through. Elongation of the bonded part of the fiber causes transverse shortening according to Poisson's law. This decrease of the wire's diameter is measured by the amount of light that passes to the receiver, provided that no other physical damage caused any additional light passage restriction. This technology has been tested in full-scale structures. However, these were prototypes with new optical fiber prestressing tendons that incorporated the gages at their center [69].

The greatest advantage of this type of fiber optical gage is their suitability for long-term instrumentation projects, and their adequacy for automated data recording. Presently these gages are only included as part of the optical fiber prestressing strands manufactured by the same company. It is possible to have further uses of this system on other continuums. This approach to a workable fiber-optical strain gaging system is also growing at a fast pace. Further developments for standard structural applications should come soon in the near future.

With proper time both of these optical strain gaging technologies could develop into practical systems for field applications. They have been examined in this review of the current state-of-the-art as a way of addressing future trends of the strain gaging technology.

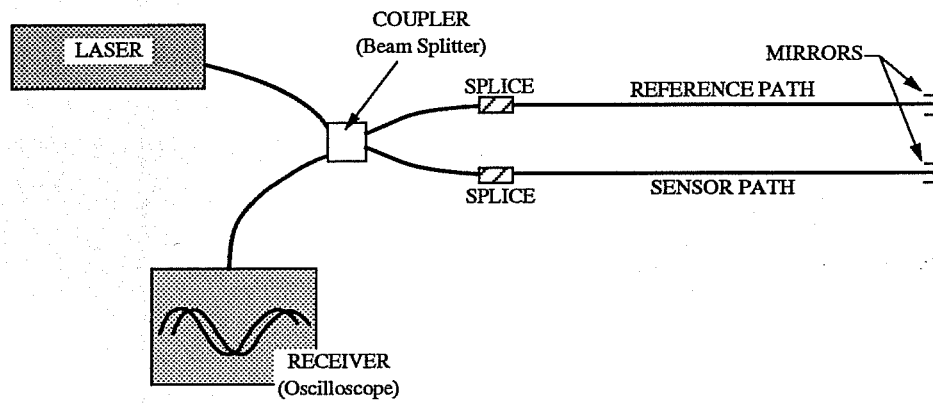


Figure 3.7 Principle of interferometric fiber optic sensors.

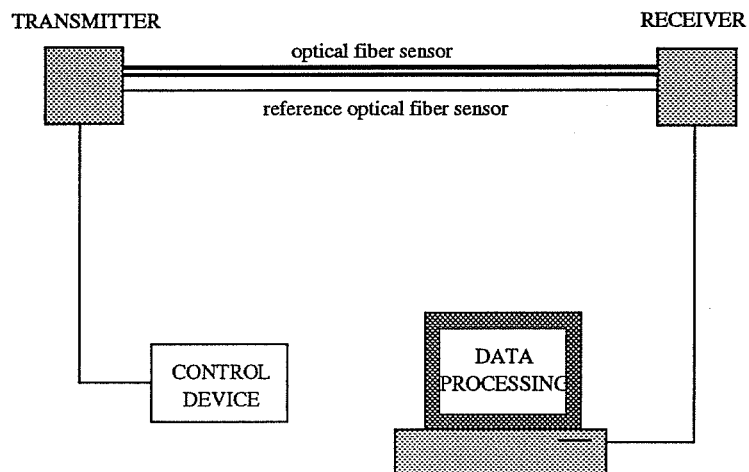


Figure 3.8 Principle of reference optical fiber sensors.

3.2 Prestressing Steel Strains/Loads

Accurate field measurements of strains or loads at different cross-sections of prestressing steel strands embedded in grout or concrete has been difficult to achieve in an effective manner. However, several devices were used in the past with acceptable levels of success. A careful review of these devices is necessary due to the importance of the accurate determination of the state of stress of prestressing strands or tendons.

3.2.1 Objectives

The interest of this section is to review some of the devices that have been commonly used for the measurement of strain or load in prestressing strands. This review's final objective is to help select the most appropriate instruments for the measurement of loads at different cross-sections of external and internal prestressing tendons used in concrete segmental box girder bridges. The selection process is completed in Chapter 4, where chosen systems are evaluated and refined in trial tests of performances.

In most cases, the load level in prestressing steel strands is measured indirectly by strain gages or directly --only at live or dead ends- by load cells or calibrated hydraulic jacks. Available instrumentation systems can thus be separated into two groups: indirect strain measuring devices and direct load measuring devices. A description of several commonly used instruments corresponding to each one of these two groups is included in the present chapter. Although load cells and some of the other mechanical systems cannot be used for measuring stresses at intermediate cross sections of multi-strand tendons (essential in studies of local stress losses), they are presented here for complementing the information in this broad area of measurements. They were also investigated to evaluate the possibility of modifying their original design in order to use them under different geometric conditions.

3.2.2 Strain Measuring Devices

The most commonly used device for measuring strains in prestressing strands is the foil type electrical resistance strain gage. Mechanical instrumentation devices for measuring strains are also available. However, most of these are quite rare and are only utilized by prestressing

strand manufacturers. A review of these novel methods is still important to expand the knowledge of techniques that can be used for measuring strains in prestressing strands.

Two factors complicate the correct estimation of the stress level on a certain cross section of a prestressing strand. These factors, influencing all types of strain measuring devices surveyed in this section, are:

1. Inaccurate modulus of elasticity of the prestressing strand, and
2. Inability to measure stress losses due to steel relaxation.

Inaccurate Modulus of Elasticity. Due to manufacturing tolerances in the diameter of each wire of a 7-wire strand and in the pitch of the six outer wires, a strand's modulus of elasticity can vary up to 2.4% among two different specimens. Since fabricators usually provide load-elongation curves based on the average of the last 30 to 50 tests of similar strands, a maximum error of 2.5% has been suggested in their modulus of elasticity [70]. It is the present author's experience that this error in the calculation of strand stresses can be increased considerably when a different instrumentation system is used for measuring strains in the field. If the manufacturer furnished modulus of elasticity is used with a testing program that measures strains with standard bonded foil electrical resistance strain gages, load errors of up to 10% can be experienced. This is because manufacturers use a completely different instrumentation system for obtaining their strand's load-elongation curves. It is therefore usually suggested that individual strands be calibrated according to each type of instrumentation system to be utilized in the field. Different modulus of elasticity would thus be obtained according to the method of measurement of strains. The resulting field measurements should be quite accurate provided that calibration was carefully done in laboratory conditions, and using a properly installed instrumentation system.

Losses from Steel Relaxation. Using strain gages or mechanical elongation instruments will, by definition, not measure the load changes due to steel relaxation. According to its definition, steel relaxation implies time-dependent losses of prestress that occur under a constant state of strain in the strands. An accurate analytical procedure should be followed to calculate steel relaxation losses at different time stages when using strain gages for measuring a strand's load. Previous research studies from the University of Queensland in Australia have reported some differences between code established relaxation losses and their test results [71]. They have found that analytical models of most international codes of the time ignored the relaxation losses

occurring in the first one or two minutes after stressing. However, comparison of their results against some of those code values only showed small disagreements. A maximum difference of 2.75% on the estimation of the actual load at 1000hr for a low relaxation strand initially stressed to $0.8f_{pu}$ was reported [71]. The current CEB-FIP Model Code introduced modifications to their computation of losses due to steel relaxation [72]. Comparisons between the CEB-FIP 1990 Model Code and the Australian research shows only 0.5% difference for the same conditions established above. Relationship between the University of Queensland research results and the Interim AASHTO Specifications for Segmental Bridges [40] establishes a difference of 1.7% for the same case compared earlier. However, in general the instrumentation system and the conclusions reached by the Australian research seems adequate. Strand instrumentation projects requiring more precise estimations of load levels should follow their recommendations.

3.2.2.1 Electrical Resistance Strain Gages. These are the most popular devices used for the measurement of strains in structural elements. Their overall method of operation has been previously described in Section 3.1.2.2 of this report. Several types of strain gages are presently available. They vary according to size, geometry, materials, and rated electrical resistance. A large selection of gages, completion circuits, data acquisition systems, and bonding methods have been previously used in research and field applications. Exact description of the gages, their method of installation, and other technical data is avoided in the present report due to the large differences among each application. However, brief reviews of overall system performance will greatly contribute to the process of selecting devices that can be refined in further trial tests.

As shown in Figure 3.9, a foil electrical resistance gage is generally bonded to an individual wire of a 7-wire prestressing strand. A problem evident with this arrangement is that the gage gives the measurement of strains experienced by an individual outer wire, as opposed to the average cross-sectional strains in the strand. Standard stressing equipment used in construction operations can vary widely in the gripping force exerted to individual wires of a prestressing strand. This is generally understood to be the cause of different levels of stress in each wire of a strand, especially at initial stressing loads.

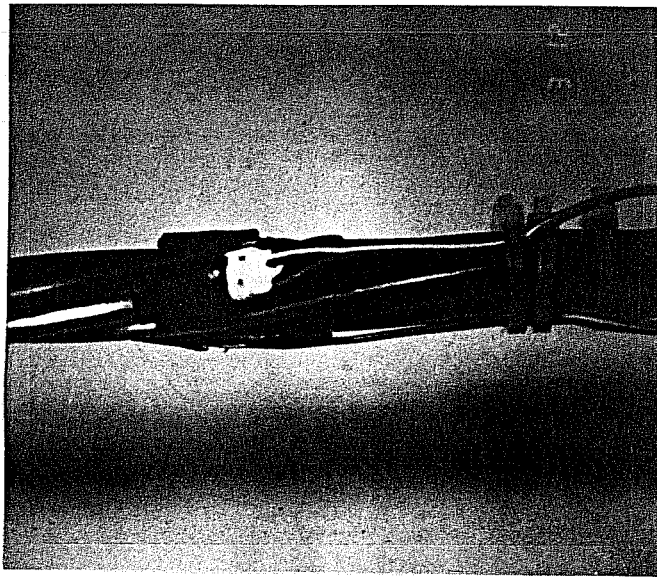


Figure 3.9 Electrical resistance foil gage bonded to single wire of strand.

Yates [73] reviewed the degree of influence of this factor on sets of fully instrumented strands. A general result from his research in this area is included in Figure 3.10. Nominal strand stress is plotted against measured strain for each exterior wire of a $\frac{1}{2}$ " ϕ Grade 270, stress relieved strand. He used 6 standard ER-gages bonded to each one of the outer wires of the strand. His test specimens were loaded on a specially fabricated stressing system for external tests of prestressing strands. Loads were obtained with a pair of center-hole load cells provided at each end of the calibrating bench. Yates also used $\frac{1}{2}$ " ϕ individual prestressing anchors to secure the specimen at the ends of the loading machine.

Observations from Figure 3.10 indicate that each wire experiences a different level of strain during the initial stressing operation. It is also noticeable that once each wire is fully anchored, the subsequent strain increases are more linear and stable. The slopes of each wire are approximately equal. The measurement of strains from a single wire can thus produce considerable levels of error if the absolute values are used. To reduce these errors, Yates ignored all readings corresponding to low stress levels. He suggested that only the readings for stresses higher than 50ksi ($\approx 0.20f_{pu}$) should be considered for the preparation of a linear calibration curve [73]. In a study of a box-girder bridge model, MacGregor [74] followed Yates' procedure of ignoring low stress readings. He also performed a linear regression of average gage data values with respect to live end loads obtained during stressing operations. These lines

he later transformed into straight lines of equal slope passing through the origin of the coordinates. With this method he corrected the offset of each strain data value obtained from each gaged cross-section of the external prestressing tendons [74]. After this procedure for correction of initial strain readings, MacGregor established the level of stress at each position based on the calibrated modulus of elasticity that he previously obtained from his material tests (different than manufacturer data). Other researchers further suggested the installation of two ER-gages bonded to diametrically opposed wires of a single strand. This was thought to provide a more representative average modulus of elasticity for the actual field tests [46].

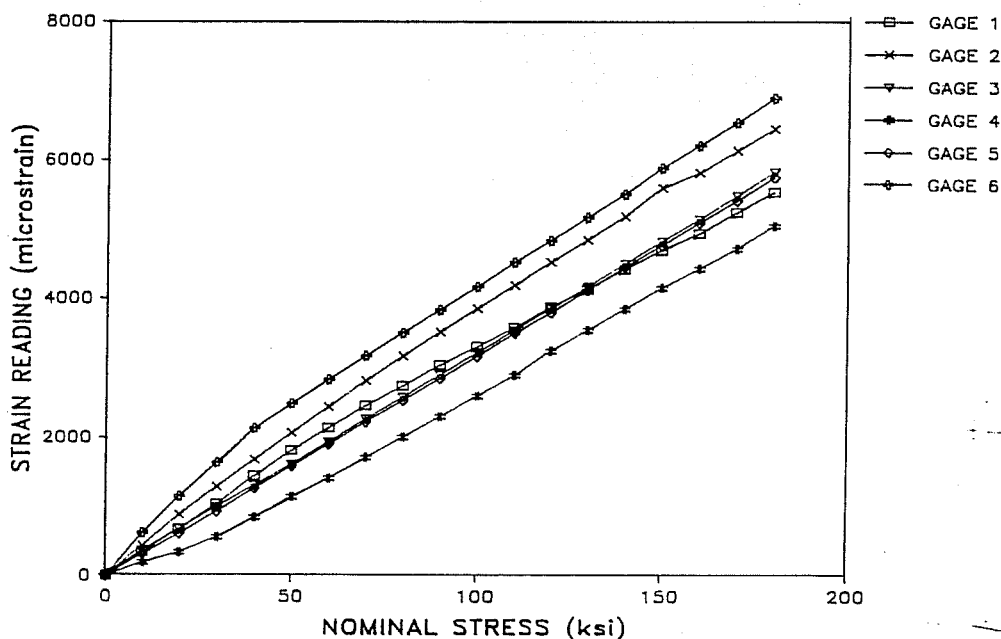


Figure 3.10 Stress-strain plot of single prestressing strand with 6 ER-gages (after Yates [73]).

In multi-strand tendons the averaging of cross-sectional stresses determined from single wire strains becomes even less acceptable than for single prestressing strands. Individual stresses on each strand of a multi-strand tendon can vary considerably. The stress level on each strand varies according to the efficiency of the live end grips, the total strand length (in turn dependant on the degree of twisting of each strand), and the amount of frictional losses across path changes. McGregor followed his previously outlined procedure to obtain a better estimate of the average tendon stress level at each instrumented cross-section [74]. Obviously, an increase in

the number of instrumented strands at each tendon cross-section will also increase the accuracy of the modified average tendon stresses. However, for large instrumentation projects this is an expensive alternative.

Another important problem associated with electrical resistance gages is related to their long-term stability. Several factors can influence the long-term performance of ER-gages. Among the most important ones are:

- a. Partial debonding of gages with time influenced by large temperature differentials, attacks from aggressive environments, and/or fatigue loadings.
- b. Variation of electrical resistance due to accidental grounding of leadwires or moisture increases.
- c. Temperature variation on long leadwires, gages and connectors.
- d. Variation of parasitic resistance in switches or connectors (influenced by moisture or temperature differentials).

Each one of the above listed topics should be carefully addressed in any serious long-term instrumentation program which includes electrical resistance strain gages. The overall performance of strain gages based on measurements of variation of electrical resistance signals has not been very successful for long periods of time. A large number of the reviewed research studies have reported serious problems with their electrical resistance strain gages (either Carlson elastic wire meters or bonded foil gages). As established earlier, it is not the objective of this section to address each individual case. The main input from previous research failures at this time is only needed for the objective evaluation of this particular method of measurement.

Among the best benefits of using electrical resistance strain gages is the possibility for automated multi-channel data acquisition, recording, and reduction. The ability for remote readings is another important benefit inherent to ER-gages. This type of gage is also quite accurate and precise. Sensitivities of $1\mu\epsilon$ are possible with most gages and standard reading units. Short-term accuracy of $5\mu\epsilon$ can be achieved with proper gage installation and operation. Strain ranges of up to $3000\mu\epsilon$ are typical with most strain gages suited for prestressing strands. Finally, the cost of electrical resistance strain gages is relatively low. However, the backup equipment such as portable readout units, extra wire, bridge completion circuits, or any multi-channel automated readout unit can be expensive.

3.2.2.2 Other Systems. Most of the other systems relating strains to stresses in prestressing strands are mechanical. Due to their high costs these mechanical extensometers are mainly used by strand manufacturers for their modulus of elasticity and ultimate strength tests. One of the major problems with these devices is related to the mechanical method of gripping each test strand. Any slip or rotation of the strand's wires at the end of the extensometers will throw off the accuracy of the measurements. Two mechanical extensometers were mentioned to be the best performers and most widely used devices [70]. These are known as the *50" Double Dial Extensometer* and the *Tinius Olsen Extensometer*. The first extensometer uses a pair of dial indicators with sensitivities of 0.001in. thus providing an accuracy of $20\mu\epsilon$ for the 50in. gage length system. Replacing the dial indicators by more sensitive devices of 0.001mm resolution (≈ 0.00004 in.) can substantially improve their accuracy to a few microstrains. Although not investigated, the accuracy of the other device should be quite similar. Preston [70] also provided several details of the *50" Double Dial Extensometer* which can be easily fabricated at a machine shop.

A newer device known as the *Wallace No-Contact Extensometer* has also been reported by Preston [70]. This expensive equipment is based on optical reading devices which lock the contact points without any influence from slippage or rotation of individual strand wires. In 1984 Preston was quoted a price of \$16,565.00 (plus freight and installation) for 7-wire strand testing equipment of this type. Values for level of accuracy of these machines were not investigated. They have been distributed in the United States by: Testing Machines Inc., 400 Bayview Ave., Amityville, New York 11701; telephone: (516) 842-5400 [70].

3.2.3 Load Measuring Devices

As mentioned earlier, the largest problem with these systems is related to their geometric requirements. In most cases these instruments are required to be positioned at the ends of the prestressing strands or tendons, thus limiting the versatility of their possible measurements. Innovative techniques surged within this area of measurements, but the efficiency of most of these novel systems is still uncertain. This section presents reviews of some of the most important devices available to date. Other devices that are no longer marketed were also investigated due to their unusual and innovative measuring technique.

3.2.3.1 Calibrated Hydraulic Jacks. These are the most commonly used tools for measuring

strand or tendon loads during normal construction operations. It is customary with hydraulic jacks to also check the elongation of the strand at each loading operation. This is a more rudimentary measuring technique, but probably sufficient for fast approximations of standard loads. A sample field use of a calibrated hydraulic jack with a single pressure dial gage is shown in Figure 3.11. Problems directly influencing the degree of accuracy achieved by this form of measurement were reported by Dunnicliff [60]. They consist of load misalignments, off-center loading, internal friction in the jack, hydraulic pressure losses at higher loads, temperature changes, and resolution of dial gages. In addition, an incorrect calibration of the jack can further reduce the accuracy of measurements.

Hydraulic jack calibration under laboratory conditions can be substantially different than a normal field application. One important difference is that in the laboratory, and on a high-quality vertical loading machine, the jacks are loaded with spherical swivel heads and rigid bearing plates. In the field, the centerline of the tendons being stressed can be at an angle with respect to the centerline of the loading jack. This will therefore produce a higher degree of internal friction between the piston and the cylinder of the jack, and thus a variation from the "real" load in the prestressing tendons. In the field of geotechnical engineering there are several reports about errors introduced by load misalignment and eccentric loading on calibrated hydraulic pressure jacks. Fellenius [75] claimed that overestimations of up to 15% of the applied load can be found in the loading stage when comparing hydraulic jack loads with load cell data. This seems too high according to previous experience with tests developed at Ferguson Structural Engineering Laboratory (FSEL). Probably the calibration of the jacks and load cells used by Fellenius were not accurate and this contributed to such a high error percentage. In any case, the existence of some errors in hydraulic pressure jacks is undoubted and can be minimized by proper system calibration. Littlejohn [76] suggested an ideal method for calibrating hydraulic jacks and load cells. Due to its importance, his method is fully reproduced in Section 5.4 of the present report as the ideal calibrating procedure for the jacks to be used in the instrumented spans of the San Antonio Y structure.

The resolution of readings with calibrated hydraulic jacks directly depends on the resolution of the pressure dial indicators. Beyond the usage of higher resolution dial indicators, another solution to this complication can be the use of pressure transducers. Remote readouts and automated systems for data acquisition, retrieval, and analysis can also be implemented with

most types of pressure transducers and data acquisition systems. Pressure transducers, along with the complete system to be utilized for stressing and readouts, should be properly calibrated in order to achieve useful levels of accuracy.

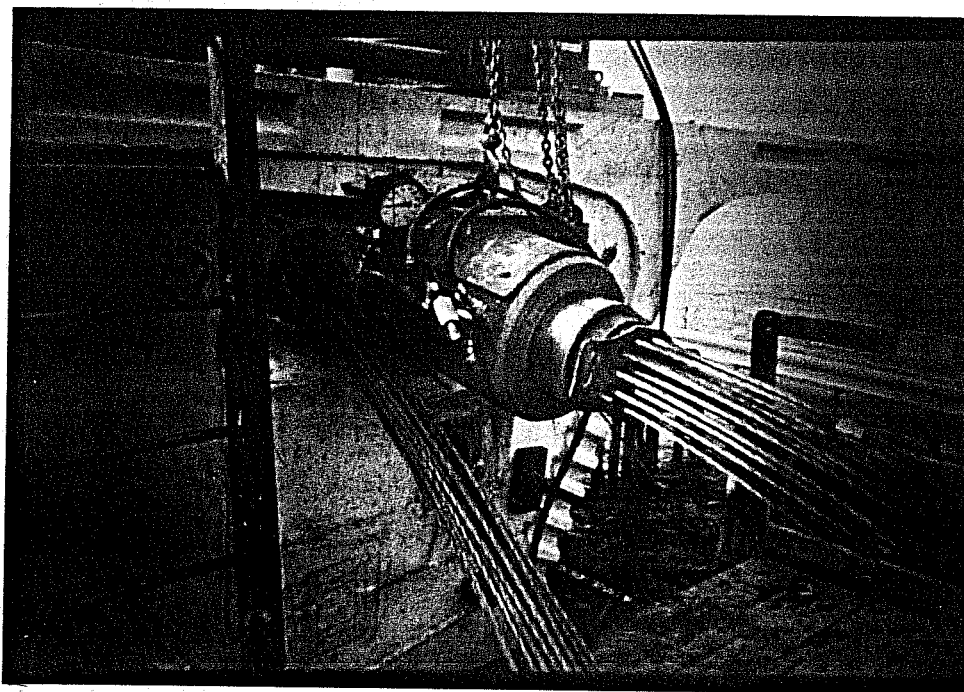


Figure 3.11 Calibrated hydraulic jack for field measurement of tendon loads.

3.2.3.2 Load Cells. These are popular for most loading operations of prestressing strands or tendons in laboratory testing operations. They obviously present the same geometric inconveniences as calibrated hydraulic jacks. Their level of accuracy also depends on their proper calibration so as to reproduce field conditions of load misalignments, off-center loadings, and temperature. Load cells should be calibrated according to the same guidelines previously mentioned for hydraulic jacks (included in Section 5.4 of the present report). There are many different types of load cells and they vary according to their basic method of operation. Load cells can be based on electrical resistance technology, hydraulic pressure, mechanical methods, vibrating wire technology, and even photoelastic principles.

Electrical Resistance Load Cells. These are the most popular type of load cells, probably due to their high accuracy and lower cost. Cells used for measuring loads on prestressing strands and tendons are of the center-hole type (Figure 3.12). A typical schematic for commercial de-

signs of electrical resistance load cells is shown in Figure 3.13. Individual ER-gages of the foil type are usually connected in a full Wheatstone bridge configuration and with some of the foil gages bonded so as to measure tangential strains. This is done in order to reduce errors from load-misalignments and off-center loadings.

The costs of these cells are considerable and can limit their field application (see Table 3.8). These cells can be reused when implemented as a check of stressing forces at the live end of the tendons. However, they are only used once when installed at the dead end of tendons or when monitoring vertical reactions at the supports of bridge structures. Allowance for proper fitting

must be made in box-girder bridges when they are to be left on site permanently. Their size is a limiting factor since minimum heights of ≈ 3 in. are necessary even for the small type of cells. Most of the problems previously outlined with respect to the long-term stability of electrical resistance foil gages are also applicable to ER-load cells. Although moisture protection is better achieved in load cells, some manufacturers do not provide waterproofed equipment which is essential for long-term projects.

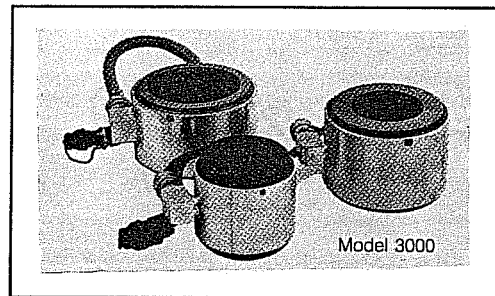


Figure 3.12 Electrical resistance load cells with central holes (from Geokon's catalog).

Load Cell Manufacturer:	Geokon, Inc.	
Distributor:	Geokon, Inc.	
Current Cost (p/unit):	\approx \$700.00	\approx \$1200.00
Load Cell Model:	3000-400-4.0	3000-400-6.0
Load Range (Tons):	181	200+
Sensitivity (kg):	13	45
Central Hole Diameter (in):	4	6
System Accuracy Range (%):	$\pm 2-5$	

Table 3.8 Technical data for ER-load cells.

load cells would be satisfactory. With a drop in accuracy, some electrical resistance based load cells can also be custom manufactured and tested in laboratory conditions. Barker, Reese et al. built a simple load cell called a *bottomhole cell* that provided good results for measuring

This type of load cell is strongly recommended to be used as a check of calibrated hydraulic jack loads and not as an instrument to monitor the load variations in tendons over the life of a structure. Load cells can also be a good solution for checking reactions at the supports of bridge structures. In these cases the less expensive solid

loads at the bottom of drilled shafts [63]. A similar load cell can be fabricated for measuring vertical reactions at the supports of bridge structures.

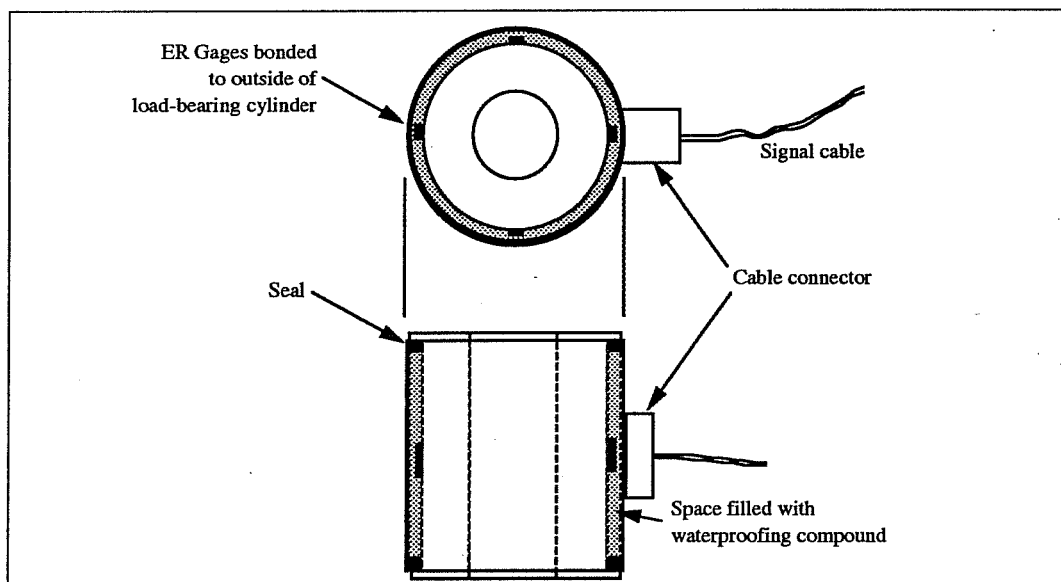


Figure 3.13 Schematic of a typical electrical resistance load cell (after Dunniclif [60]).

Hydraulic Load Cells. Most hydraulic load cells are similar in size to electrical resistance load cells. Their largest difference is in their method of operation. Hydraulic load cells use pressure transducers to measure loads. These transducers can vary in type of operation including pneumatics, semiconductor strain gages, electrical resistance strain gages, or vibrating wires. Their degree of accuracy is much higher than that of the load cells themselves. Larger errors are introduced from internal friction of the cell components and from eccentric loadings. Due to their lower accuracy, these gages are usually not recommended as the sole device for measuring jacking loads.

An innovative variation of the technology of *Earth Pressure Cells* commonly offered by most instrumentation companies is represented by Freyssinet's *Flat Jacks*. These operate similarly to hydraulic load cells, are conveniently smaller, and besides their original use to implement small jacking movements they can also be used to monitor large loads. These jacks are offered in different sizes --directly related to jacking capacities-- and seem to be ideal for monitoring the vertical reaction forces at the supports of bridge structures. A typical jack is shown in Figure 3.14. Costs, availability, and technical data of these jacks could not be readily obtained

from Freyssinet at the present time. Due to the simplicity of the *flat jack* technology the present author believes that they can be a competitive system for measuring vertical reaction forces in most segmental bridges.

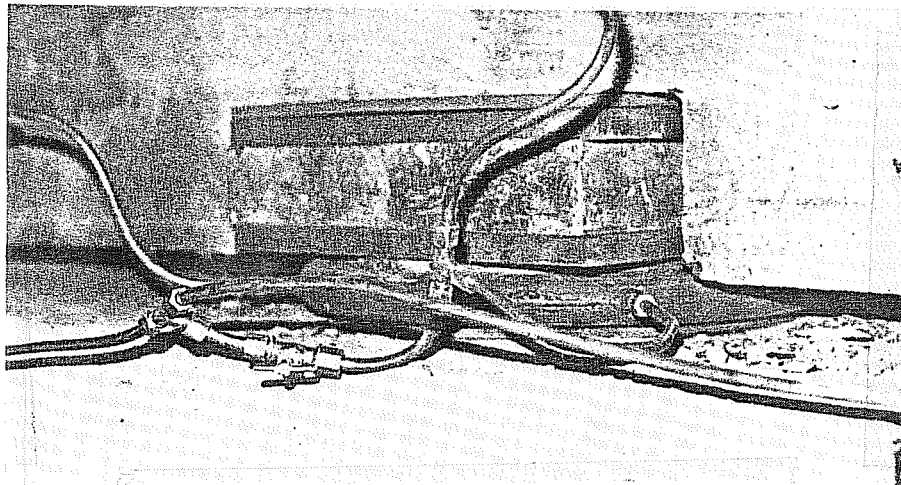


Figure 3.14 Freyssinet's Flat Jack (from Freyssinet's catalog).

Other Load Cells. There are also reports of load cells based on photoelastic fringes and mechanical methods. These load cells do not allow for remote reading operations, have stricter geometric requirements, and are usually less accurate than the first ones reviewed in the present section. However, advantages of these systems consist of their extra stiffness for field operations, and their good performance for long-term measurements.

An indirect method for monitoring the approximate load variations at bridge supports is to measure the deformations of the bearing pads. A simple method for performing this type of measurement is to use high accuracy (resolutions of 5/10,000in.) caliper gages. These gages can measure height variations between two reference points mechanically anchored and epoxy bonded to the bottom face of the pier segment and the actual pier. The first field implementation of a system of this type is being prepared for the instrumented spans of the San Antonio Y project. Results of the accuracy and the performance of such an innovative system are therefore not available at the present time.

3.2.3.3 Cable Tensiometers. Systems designed to measure the tension in a cable are the Tensiomag, DynaTension, Cable Tensiometer, and the Fulmer Tension Meter. Most of these instruments are made for single strands or cables. Some of them are not readily available in this country. However, an understanding of their behavior is important for avoiding past errors and

enhancing future developments.

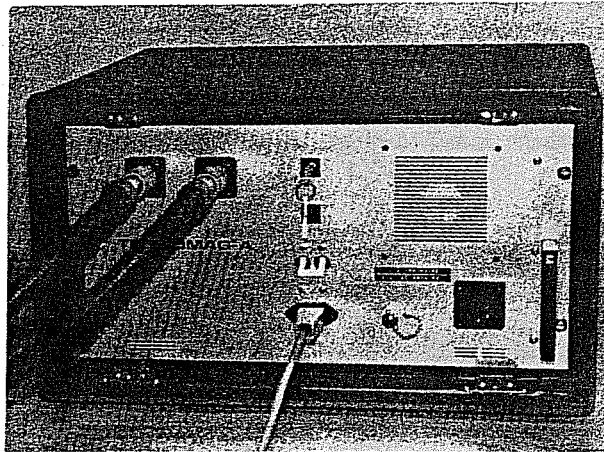
Tensiomag. These devices are offered by Freyssinet International. They are the only ones --within the present category-- that can be used in multi-strand tendons. They consist of steel jackets with a central hole and a separate readout unit (Figure 3.15). The operation of the Tensiomag is based on the directly reversible variation of the incremental magnetic permeability of steel with respect to applied mechanical stress. The sensing device is made of a special transformer. When steel --such as a prestressing strand-- is placed in its inner core it serves as a connection between the primary and secondary windings of the transformer (Figure 3.16). When the primary winding is supplied with an electric current it produces a magnetization in the steel and an electric signal is emitted from the secondary winding. This signal is dependant on the magnetic state of the tendon and thus on the stress imposed on it [88].

The reported sensitivity of this system is on the order of $\pm 25 \text{ N/mm}^2$ ($\pm 145 \text{ psi}$) [88]. The main advantage is that it can be placed at several cross sections along the length of the longitudinal (internal as well as external) prestressing tendons of segmental box girder bridges. It is of sturdy construction and is reported to have good long-term stability. Another interesting characteristic is that it measures the average tendon stress at each cross-section, and not single stresses related to individual wires of a strand. Laboratory accuracy for multi-strand tendon tests were reported between 2% to 3% when using 12-0.6" ϕ strands [88].

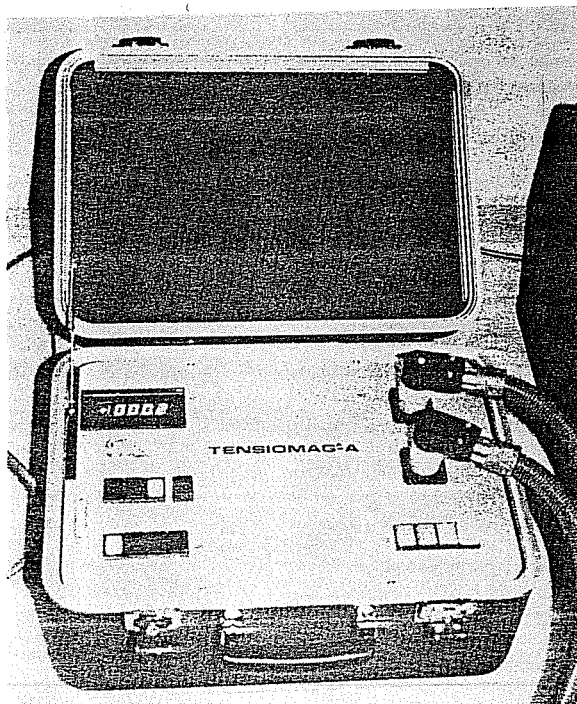
Costs and availability of devices able to measure tendons made of up to 19 - 0.6" ϕ strands could not be obtained from the manufacturers. However, it seems that a complete set of sensor, power unit and readout box can be expensive. No reports of previous usage for field studies in the U.S. were found in the literature review prepared for this study. It is also believed by the present author that for the long-term usage the amount of magnetic permeability creep of prestressing strands can introduce much larger errors than originally reported in the manufacturer catalog. The system is also not portable in the sense that it cannot be removed from a tendon without previous destressing of the tendon. A final disadvantage of the system is the need for preparing calibration curves according to each configuration where it is designed to be installed.



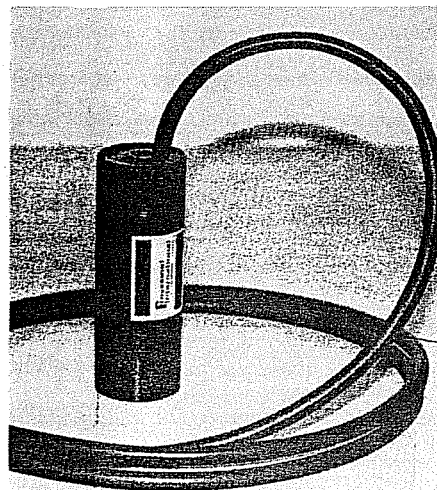
a. Sensor for multi-strand tendons.



b. Power supply unit.



c. Readout unit.



d. Sensor for single strands.

Figure 3.15 Freyssinet's Tensiomag system (from Freyssinet's catalog).

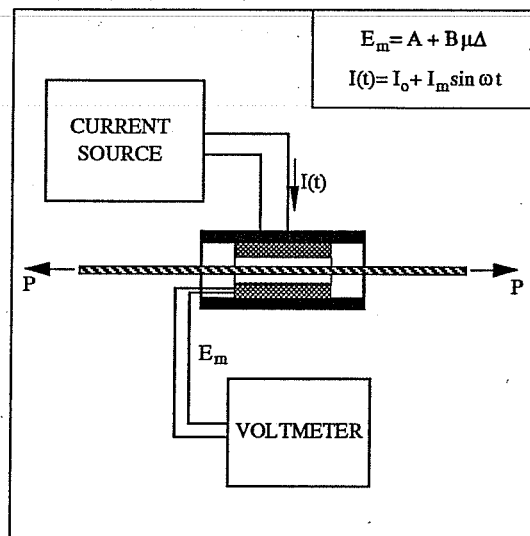


Figure 3.16 Operation principle of Tensiomag (from Freyssinet's catalog).

DynaTension. These are made for measurements of loads on single strands or cables. The method of operation consists of relating the fundamental frequency of vibration of strands and cables to the applied tension. This is based on the principle that the natural frequency of a length of cable between two nodes is directly proportional to the tension of the cable. It is simple to install and use. A proximity-type or a contact-type transducer is installed near or around the single strand or cable. Information regarding the free length of the strand and its weight per unit length is introduced in the portable readout unit. A scale and a multiplying factor are selected according to the expected level of measurements. A simple tap on the free length of cable will produce a vibration that is in turn measured by the *DynaTension* and related to tension according to the input data. These devices do not need recalibration with use, and are unaffected by weather, cable lubricants, dirt, or overloads. The workable range is rated up to 4,000kips and can accept cables weighing up to 80.5lb/ft. The manufacturer reported accuracies of $\pm 2\%$ and resolutions of 0.33% with this system. A sample portable readout box and two different types of sensors are included in Figure 3.17.

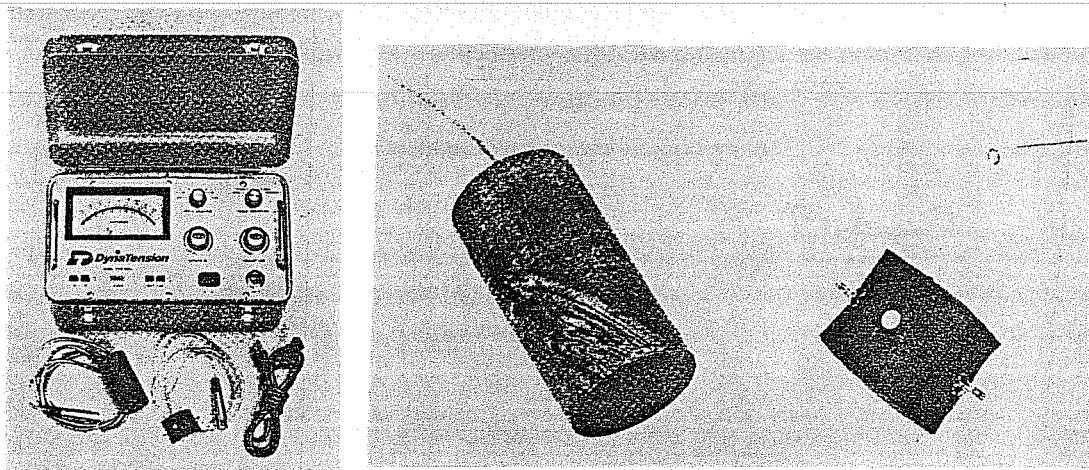


Figure 3.17 DynaTension System (from DynaTension's catalog).

An original version of the *DynaTension* has been previously used on extensive tests performed by the California Department of Transportation in 1984 [44]. Their system, then known as *Vemco*, has been reported to work well and with an initial accuracy of 2% at 100% confidence level. The *Vemco* and the *DynaTension* systems lacked the portability problem associated with the *Tensiomag*, since both can be clamped and removed from any location along the free length of a single strand.

The most important handicap of the *DynaTension* is related to its inability to measure loads on multi-strand tendons. Its cost is quite high; the complete system (including two sensors and a portable readout box) has been rated at \$7,000.00 in late 1990. It can be purchased from Smiser Industries, Inc., 9215 Solon Unit D-2, Houston, Texas 77064; current telephone: (713) - 890-6007.

Cable Tensiometer. This device was manufactured by Roctest, Inc. It is currently unavailable due to certain operational irregularities found by the manufacturer. However, the method of operation is quite innovative. Load measurements are determined from a calibration curve based on the travel velocity of a wave generated by impact. An impactor and a detecting sensor are attached to a single cable at a distance of 5ft (Figure 3.18). The time of travel is then measured in a portable readout unit that is provided with the system. The original manufacturer's claim of accuracy and resolution is not repeated herein due to the failure reported in the original system. Evidently, this device is also limited to measurements in single cables or prestressing strands. Initial cost of the complete system and reports of previous usage are not

available. It is probable that a new instrumentation system based on this technology may appear in the future. However, the cost, ease of installation, and accuracy will have to be competitive with the *Tensiomag*, or the *DynaTension*. This system also has the same type of portability mentioned for the *DynaTension*.

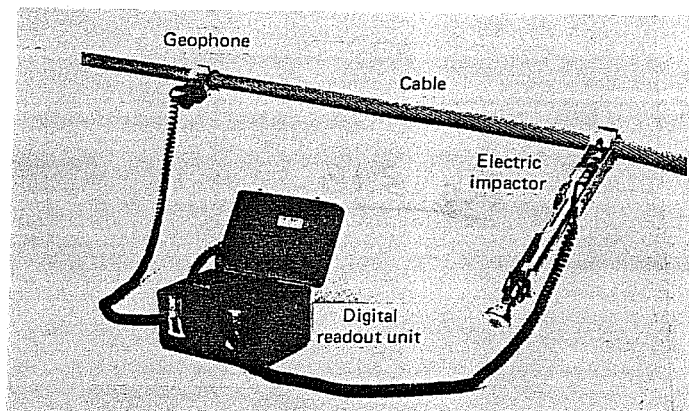


Figure 3.18 Cable Tensiometer (after Dunncliff [60]).

Fulmer Tension Meter. This is an example of a simple mechanical device that can be used for the measurement of loads on single prestressing strands or cables. The system in operation is shown in Figure 3.19. Its technique is simple. The eccentric wheel applies a deflecting force on a single strand causing the frame of the meter to bend in direct proportion to the applied force [78]. A calibration chart must be prepared for each strand type in order to obtain load measurements from the values of the dial indicator. The system accuracy has been rated at 5% on prestressing strands [60]. Besides its inability to measure multi-strand tendon loads, it also presents severe geometric restrictions for proper usage. As originally designed the system does not allow for remote reading operations. Similar devices evolved from the original *Fulmer Tension Meter*. One instrument known as the *Kuhlman Beam* --named to honor its creator-- has been fabricated and successfully used in field tests of the California Department of Transportation (Figure 3.20). Several improvements were introduced by the *Kuhlman Beam*. The most important ones are related to the reduction in size and the allowance for remote reading operations. Values for the initial level of accuracy of this device were reported around 6.5% and 2.8% for field tests with 100% and 95% confidence levels respectively [44]. However, the rated accuracy is strictly limited to the skill of the operators and the stability of the electrical resistance signals.

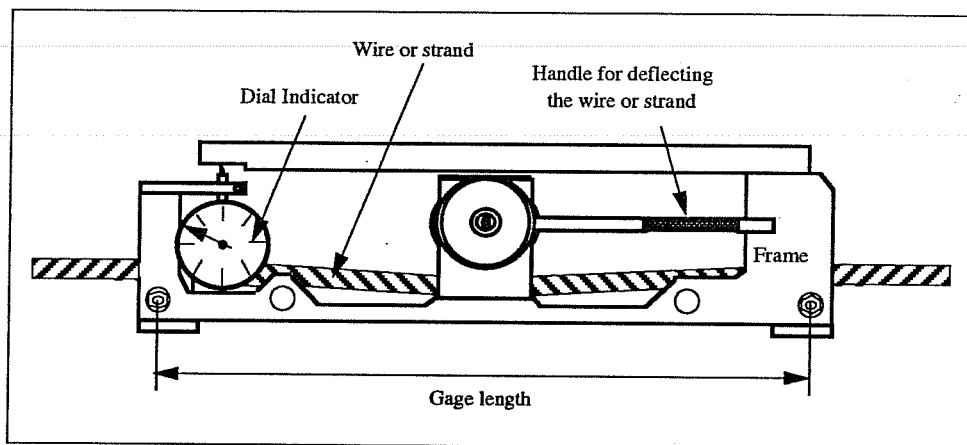


Figure 3.19 Fulmer Tension Meter (after Hanna [78]).

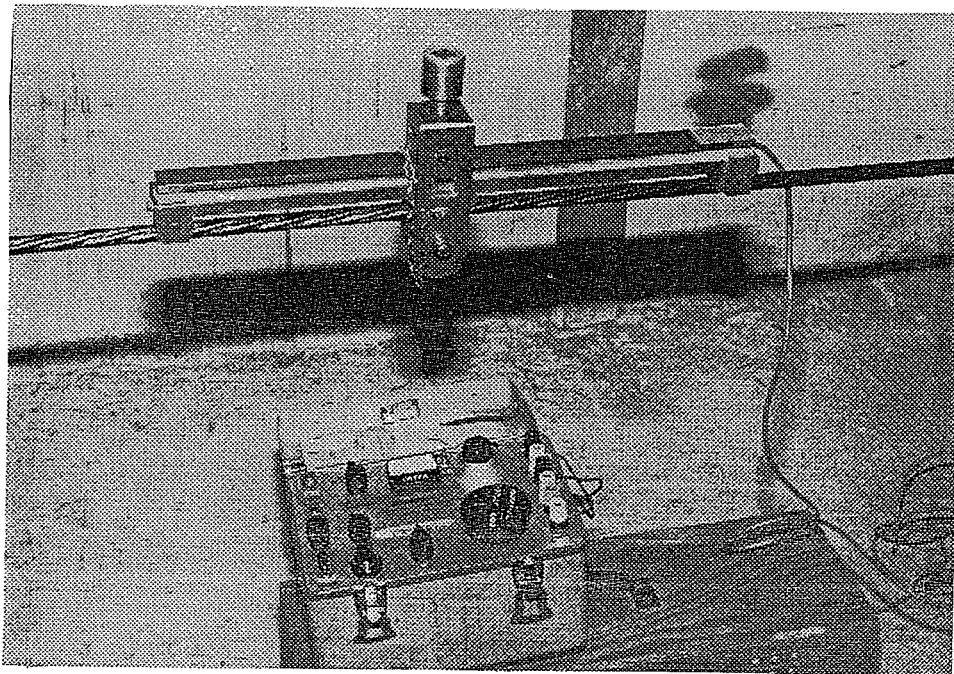


Figure 3.20 Kuhlman Beam from California D.O.T. (after Richardson [44]).

3.3 Span Deflections

Accurate measurements of vertical deformations are vital components of the required structural information for fully instrumented bridge spans, such as those to be studied in the San Antonio Y project. Individual measurements of span deflections are useful for checking certain

design assumptions for segmental concrete bridges, and to verify their structural safety and strength (through load tests which can be performed at any time during the life of the structures).

This type of measurement is not too difficult to perform, especially when compared to the cases of detecting strains or loads in concrete and prestressing strands. A variation in height is a relatively simple quantity to measure. However, some complications are usually added due to the large distances between the points that determine the reference line for vertical movements and the small magnitudes of expected displacements. The deflections of selected cross sections of a segmental bridge structure are mainly taken with respect to reference points located in the abutments or pier segments. The longitudinal distance between these two reference points is thus usually equal to several thousand times the maximum expected vertical movements of the instrumented cross section. For example, vertical movements of less than 1/10in. usually have to be measured during load tests with bridge spans of over 100ft in length.

Measurements of vertical deformations of prestressed concrete bridges have been frequently performed with surveying techniques (sometimes called *optical methods*). The results have often been poor or marginal [82]. The need for a higher level of accuracy has spurred studies of new methods within this area of measurements. Both mechanical and hydrostatic techniques have emerged as candidates for future deflection measuring systems. New devices -- based on these two technologies-- not only proved to be reliable and accurate, but also came with a reduction in the total cost of the old surveyor's leveling technique.

3.3.1 Objectives

An investigation of some devices used for measuring vertical deformations in spans of concrete bridge structures is introduced here. Existing techniques can be separated into three different classes, according to their basic method of measurements:

- base line methods,
- hydrostatic methods, and
- surveying methods.

Devices based on the first two methods were more carefully investigated due to their innovation, relatively good accuracy levels, and cost-effectiveness.

3.3.2 Base Line Methods

The original base line method used for measuring the relative vertical movements of certain points of a bridge span was developed in late 1959 by A. Pauw and J. Breen [79]. The method has the advantage of simplicity, good accuracy, and ease of use. It basically consisted of the mechanical measurement of vertical movements of specific span points from a firmly set reference line. Two slightly different systems were originally designed according to the needs for short and long term measurements of vertical movements of two prestressed concrete girders. The difference between the two measuring systems only consisted of the better protection techniques designed for the long-term readings.

The overall schematic of the original base line system is shown in Figure 3.21. The reference line for vertical movements was a tensioned wire stretched between two end brackets. In the temporary system, special plug inserts were cast into the top surface of the girders and above the bearing plates. These inserts were used to hold the bases of the anchorage brackets that were leveled to a fixed height between the mounting surface on the girder and the base line (as shown in Figure 3.21a). The bracket at the dead end was used as an anchorage for the wire, while the bracket at the live end had an arm and two grooved pulleys from which a calibrated 50lb weight was suspended. This was the method used to provide constant tension in the base line wire. The wire originally used consisted of #23 gage steel music wire (piano wire), stretched to 100ksi by the 50lb weight.

The only variation for the permanent system --used after the girders were in place on the abutments-- was that the dead and live end brackets were installed in anchorage boxes pre-cast in the inner faces of the end piers. The live end box had a detachable part with an additional grooved bearing that was used as a wire guide to hang the calibrated weight for the deflection readings (as shown in Figure 3.21b). The other notable characteristic was that both boxes had cover plates with rubber gasket seals to protect the anchorage parts from environmental conditions. A package of silica gel dehydrator was also placed inside each box to prevent rusting and corrosion of the moving parts.

Reference brass inserts were cast into the girders on top (for temporary readings) and bottom (for permanent readings) surfaces at the quarter- and center-points. For the deflection readings, the deflection meter (shown in Figure 3.21c) was installed on a precast set of brass inserts, and leveled with the third adjustable screw. The deflection meter consisted of a standard

12in. *Starrett* gage with a micrometer adjustment and with a vernier that allowed for a measurement accuracy of 1/1000in. The gage's extension arm and vibrating reed were used as a method for more accurately determining the contact of the gage with the base wire. When the movable head of the reed was brought into contact with the wire, the vibration of the reed was damped, thus giving a sensitive indication of position. The base plate of the deflection meter had a bubble level that was used to level the meter assembly to reproduce its previous measuring positions.

One system related problem described by Pauw and Breen consisted of the movements of the base line wire on windy days. A secondary source of errors, mainly for long term measurements, was that any variation of the friction of the pulleys implied a variation of the catenary shape of the reference line. Despite the inconveniences, the original investigators claimed to have reproduced measurements on the order of 2/1000in. [79]. However, it is the belief of the present author that this high level of accuracy is related to reproductions of a series of readings from each set position of the base line wire and deflection meter. The repeatability of readings at varying positions of the deflection meter must have been limited by the small angular movements of the base plate. The bubble level has a lower degree of accuracy than the vernier ruler, and small inclinations of say 0.25° at the base plate can produce height differentials of 0.0065in. at a set height of 10in. from the base plate.

However, the method still seems to be highly accurate and even with pessimistic observations it should be able to determine 1/100in. movements on still days and for long-term readings.

A slightly modified version of the original base line deflection method was later used on a field measurement of deflections of a prestressed concrete girder bridge during load testing operations [80]. However, one of the most detailed investigations for improvements of the original base line method was developed by Bradberry in 1986 [81]. Bradberry presented a good comparison of different systems available for measuring span deflections of prestressed concrete girders. After determining the general adequacy of the base line method for his particular tests, he proceeded to evaluate possible modifications of the original system in order to eliminate the pulleys and the 50lb weight while making it possible to easily reposition the base line. His final suggestions involved modifications of the base line tension adjusting method, and of the reading devices.

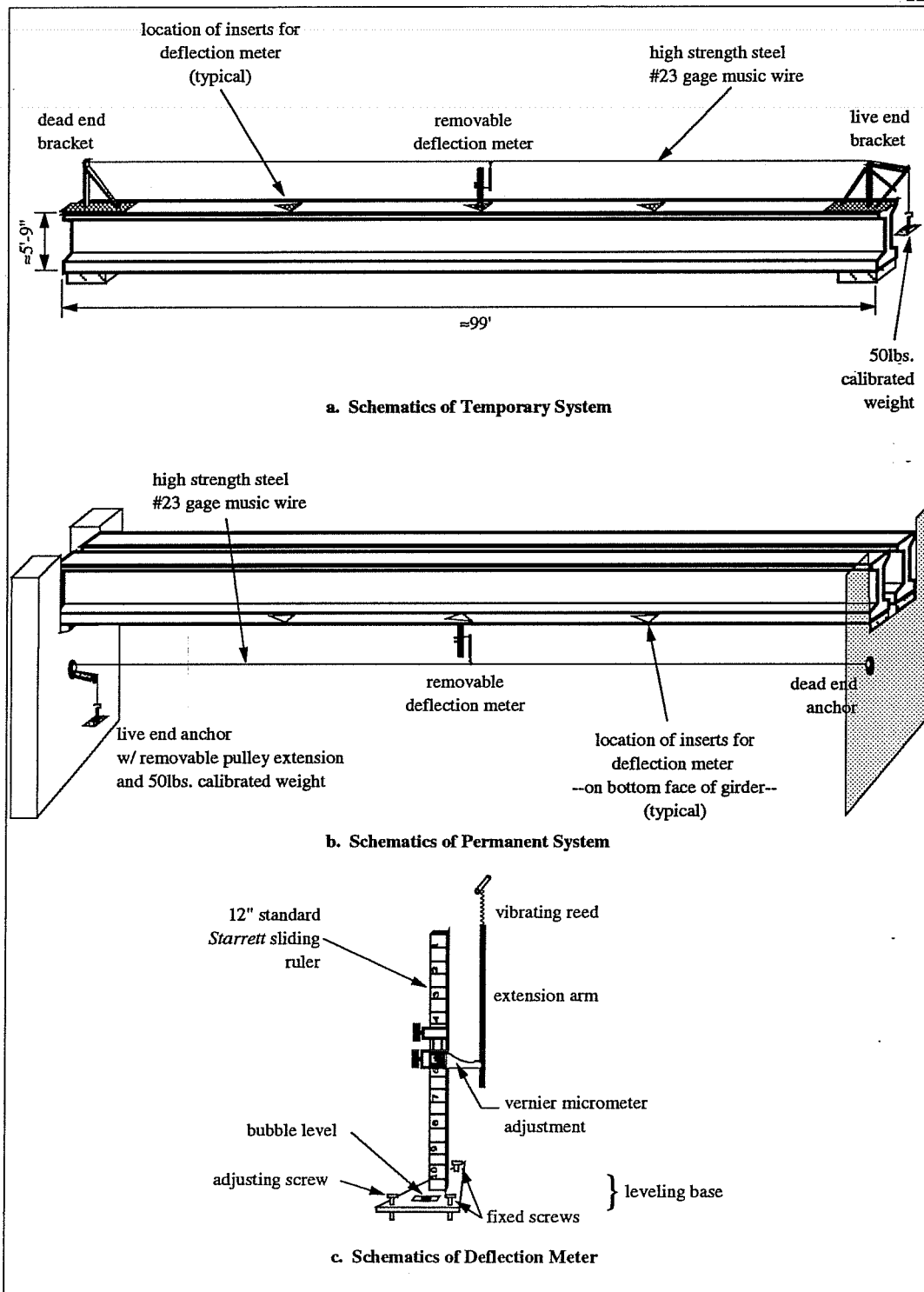


Figure 3.21 Pauw-Breen original base line system.

Bradberry designed wire anchorages that were ideal for imposing small load increments to the wire during the tension adjusting procedures. The live end anchor consisted of a $\frac{1}{2}$ " ϕ x $2\frac{1}{2}$ " bolt with a $\frac{3}{4}$ " H x $\frac{1}{8}$ " D shank recess, and a $\frac{1}{8}$ " ϕ hole for the passage of the base line wire. The recess provided a winding area for the excess wire obtained during the adjustment of tension. To adjust deflection readings according to the small movements of the wire at the live end, Bradberry installed an additional deflection measuring station next to the live end anchorage.

As an accurate method for reproducing the tension of the base line wire he suggested the following steps (refer to Figure 3.22):

- a. Initially adjust the base line wire tension by turning the live end anchor bolt like the frets of a guitar, controlling the tension initially "by sound."
- b. Hang a small calibrated load at mid-span section of the tensioned line and measure the resulting deflection increment.
- c. Repeat procedures a. and b. until obtaining a pre-determined line deflection increment for the calibrated load.

The reading devices used by Bradberry consisted of small mirrors located next to short pieces of calibrated rulers (with divisions of $\frac{1}{64}$ "). These two pieces were bonded to quarter-, center-, and live end-points on a side face of the girders. Two part epoxy products were used for the surface bond of the mirror and tape assembly to the concrete. Accurate readings were obtained with this simple system by aligning the mirror image of the taut base line wire with the position of the wire itself (see Figure 3.22).

Bradberry's evaluation of the overall performance of his instrumentation system indicated it highly satisfactory, recommending that it be used in future similar projects [81]. Although Bradberry considered that the final system had high levels of accuracy, an overall field accuracy value was not provided. However, this value was estimated to be close to half of the reading resolution of the system. This is approximately equal to half of the resolution of the calibrated rulers, or $\approx 8/1000$ in.

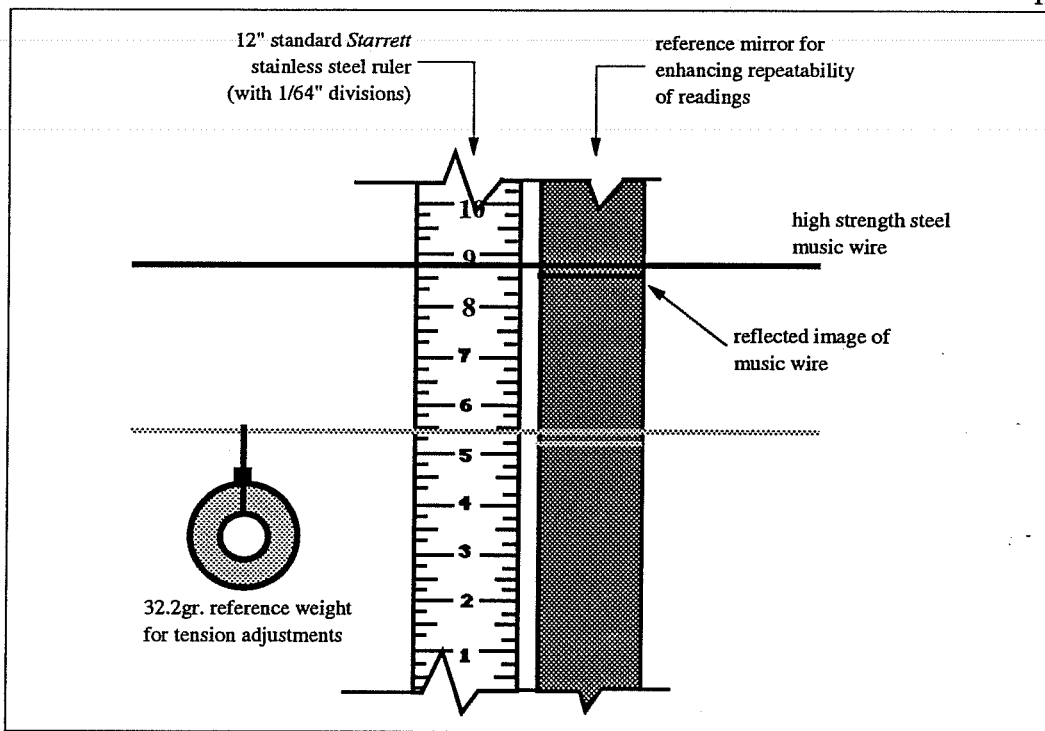


Figure 3.22 Bradberry-Breen modifications of the base line system.

Some possible complications of Bradberry's base line method were investigated by the present author and are related to the following points:

- Long-term problems can result from loosening of the epoxy bond of the tape and mirror assemblies installed at each reading station.
- The tension adjusting method suggested by Bradberry seems to be time consuming (mainly due to the trial and error procedures that need to be followed for obtaining accurate tension adjustments of the base wire).
- To anchor the dead and live end of the base wire, Bradberry installed bolts on the actual formwork of the girders. These bolt inserts attached to the formwork can be damaged during concrete vibration and depend on the approval of the contractors. The present project researchers investigated alternative solutions to this problem during the testing of anchoring systems for the locating discs of the Demec Extensometer. It was found that the best system consisted of a combination of mechanical stainless steel anchors and two-part epoxies (refer to Section 5.1.1).

- Wind induced vibration of the reference wire still presents an occasional inconvenience for this modified base line system.

Bradberry's reference to the difficulties in uncoiling long lengths of piano wire under time restricted situations is another complication that should also be considered in future applications of this modified base line system.

Finally, a common inconvenience of both base line methods is related to their basic incompatibility for allowing remote or automatic data recording operations. Despite this and the other previously mentioned problems, both systems evidently provide affordable levels of accuracy.

3.3.3 *Hydrostatic Methods*

Extensive research related to hydrostatic methods for measuring vertical deformations were investigated in Switzerland by Markey and Favre [53, 54]. Their final system suggested for field installation in box girder bridges is presented here.

The principle of operation of their system is based on the hydrostatic law of communicating vessels (Figure 3.23). This law is basically that at a state of equilibrium and when certain physical parameters are ideally equal, interconnected liquid surfaces lie at the same horizontal level. The most rudimentary case of a deflection measuring system based on this principle is the traditional hose level. A quite advanced version of the hose level is represented by the Swiss hydrostatic leveling system, which was specifically designed for field measurements in box girder bridges. The system is made of reading pots firmly installed in the inside face of the box girders and interconnected to each other by clear plastic tubing (as illustrated in Figure 3.24). Each reading pot is formed by a calibrated glass cylinder (2mm thick, and 20mm internal diameter) mounted to a metal stand that is in turn fixed to the internal walls of the box girder segments. The pots are hose clamped --with some type of rubber gaskets and adaptors-- to a clear plastic PVC tubing of 2mm thickness and 11mm internal diameter. Varying distances to the reference pots --usually installed at the pier segments-- can be obtained by splicing lengths of tubing through tapered hard plastic connectors and pairs of hose clamps. Circuit lengths of up to 100m were found to be reasonable limits to avoid complications of the measuring systems. However, the actual length of a circuit is usually regulated by the bridge geometry, as shown in the sample layouts of Figure 3.24. The communicating liquids suggested for use consist of

clean, demineralized water, isopropyl alcohol, or a 50/50 mix of both liquids.

Actual field applications of several models of the hydrostatic leveling concept imposed certain alterations of the original design envisioned by the developers of the system [53]. Their most adequate model was the one introduced in the present review. However, some

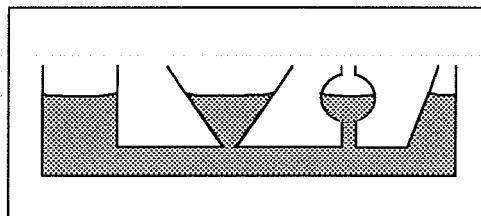


Figure 3.23 Law of communicating vessels.

important areas of concern still mentioned by system investigators were [53]:

- a. The communicating liquid. This needs to be non-homogeneous, preferably with a low variation of density with temperature, clear, and with a low freezing point and a high evaporation point. Non-homogeneous liquids introduce errors due to their unknown densities. Similarly, when temperature varies during a measurement, all liquids expand or contract thus introducing movements that must be accounted for during the data reduction process. Clear tubing and liquids are needed to help locate trapped air bubbles (which in certain cases can throw off the deflection readings). Finally, low freezing points are evidently necessary for preventing the liquid from freezing in low-temperature areas. On the other hand, a high point of evaporation is also desired to slow the rate of evaporation of the liquid during the summer temperatures of certain regions. Isopropyl alcohol was successfully used in the last applications of the leveling system. However, the investigators still recommended a search for more appropriate liquids.
- b. The reading system of the level of the liquid. Some physical properties of the liquids complicate the efficiency of an acceptable reading system for the hydrostatic leveling method. The first problem is the irregular surface of liquid levels in small tubes (property known as *capillary action*). This introduces some approximation to the exact location of the "meniscus" of the liquid level. A secondary problem is the need for using a high resolution scale or ruler that can accurately measure the small variations of the level of the meniscus of the liquid surface. The solution recommended by the Swiss researchers consisted of a calibrated clear glass cylinder --probably to the 1mm division marks-- from where measurements are taken by sighting a horizontal level at the plane at which the meniscus touches the glass walls.
- c. Infiltration of air bubbles in the liquids. When air bubbles are trapped in vertical lengths of

the tubing, they introduce vertical height differentials in the measuring systems. This is due to the negligible density and compressibility of air. Bubbles were found to be usually formed during the filling of the plastic tubes. This process was thus recommended to be performed at a laboratory, where the tubes can be pre-filled with the liquid and tightly corked to assure no entrained air in the system. When this process needs to be performed on site, however, all visible air bubbles must be carefully removed. To further avoid having air bubbles in longitudinal sections, an inverted "Y" shape of the plastic tubes at their connection to each measuring pot was recommended. This is because a natural evacuation of air bubbles can occur in vertical lengths. A secondary option only available when using water as the interconnecting fluid is to deaerate it by previous boiling.

- d. Movement of the liquid surface. Certain problems were reported due to the oscillations of the liquid after its installation in the tubes. On the other hand, traffic movement on top of the instrumented bridges did not cause oscillations in the liquid. Moreover, with the final hydrostatic leveling system the investigators reported that equilibrium of water was usually obtained within a matter of a few minutes.

The Swiss investigators claimed to have reached an accuracy of 0.5mm ($\approx 2/100$ in.) in their field applications on actual box girder bridges [54]. However, it is not clearly described how this accuracy was obtained nor the method for computing the "true" measurements of vertical movements of the instrumented spans. Most of the report about the field tests [54] deals with "deflection trends" and not with relative movements from specific reference points (such as the bridge abutments or the pier segments). However, it is still possible that a slightly modified hydrostatic leveling system could become an alternative for measuring relative vertical movements with a 1/100in. accuracy level.

3.3.4 *Surveying Methods*

These are probably the most traditional methods used for field monitoring of span deflections in bridges. The basic operation principle of the majority of these methods is illustrated in Figure 3.25. It consists of sighting leveling rods located on bench marks at different points along the top surface of the bridge. This is usually accomplished with high precision optical micrometer levels or theodolites.

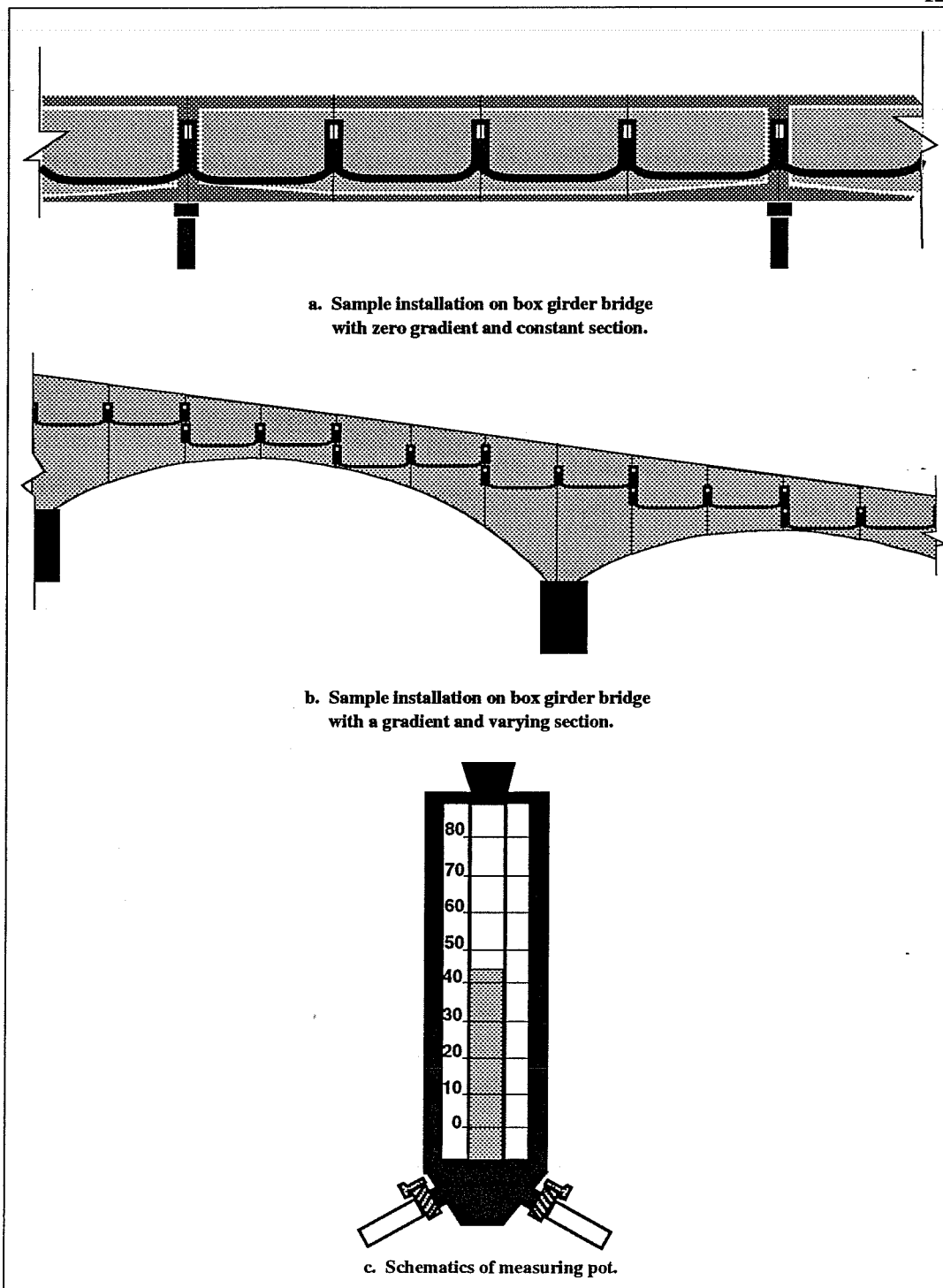


Figure 3.24 Sample layouts and final measuring pot of the hydrostatic leveling system (after Markey [53]).

The accuracy of this type of measurement depends on several factors:

- Resolution of the surveying instruments, either precision theodolites or electronic levels.
- Type of reference points used as guidance for the leveling rod.
- Experience of the survey crew.
- Efficiency of the surveying technique utilized by the crew.

A previous field investigation of vertical movements of two 100ft spans of a composite winged-girder concrete bridge at Bear Creek, Austin, Texas using experienced surveyors reported accuracies only to the 12/100in. level [82]. This is obviously a very large error when compared to the other methods previously investigated in the present survey.

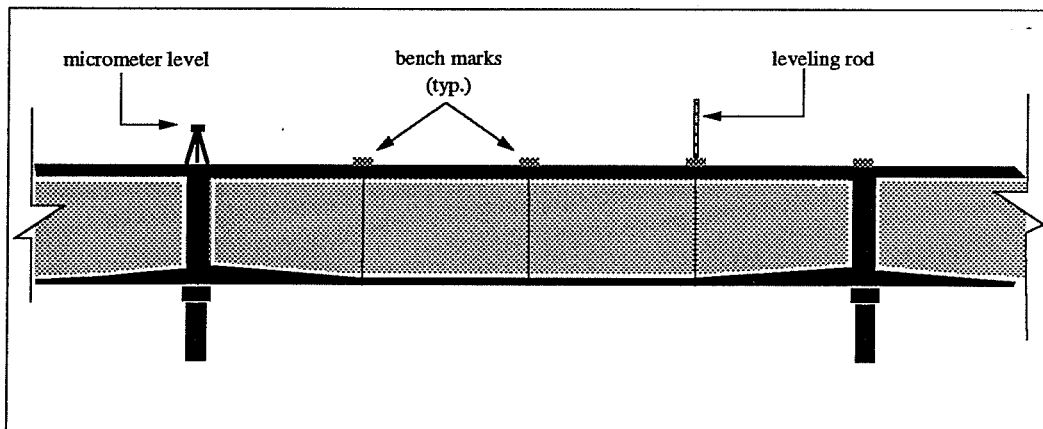


Figure 3.25 Basic operation of surveying methods for measuring span deflections (after Bradberry [81]).

In conclusion, the most important problems with this method of measurement are related to:

- Cost. Accurate bridge deflection measurements require surveying instruments of high resolution along with an experienced crew. Both of these requirements are costly.
- Accuracy. Even with state-of-the-art instruments and an experienced surveying crew it is highly unlikely that the method could reach an accuracy level of 1/100in.
- Weather protection. Readings during extreme temperatures (with substantial distortions due to heat reflections) and on rainy days can further limit the effectiveness of the measurements.

3.4 Thermal Variations

Measurements of the thermal characteristics of bridge structures has lately become an important component of field instrumentation projects. Thermally induced stresses in concrete bridge structures can contribute to cause various types of distress. This is particularly true for the latest type of segmental box girder bridges composed of design optimized sections or irregularly shaped sections (designed to impose a certain degree of aesthetic appeal). However, only in a few published cases were thermally induced stresses considered as the main cause of cracking or joint openings in concrete bridges [12, 83].

In segmental concrete box girder bridges thermally induced stresses can be significant in either the longitudinal or the transverse direction. In some precast segments, additional problems can result in the match-cast process due to the differential temperatures produced by the elevated and uneven heat of hydration between large and small concrete elements (webs, top and bottom slabs, and cantilever wings). It is thus essential for a field instrumentation system of a novel segmental box girder structure --such as the San Antonio Y project-- to measure the most important factors affecting the thermal response of the bridge.

Environmental factors, material properties, and geometric shapes can all influence the thermal response of a bridge structure. Some of these factors are shown in Figure 3.26. However, the most important mechanism of heat transfer in a bridge structure is usually considered to be the amount of solar radiation impinging upon the surface of the structure. This varies widely according to the angle at which the radiation passes through the atmosphere and the length of daylight. The intensity of solar radiation thus varies seasonally and daily (according to the time of day, degree of cloudiness, wind strength, etc). An amount of the total radiation that reaches a bridge's structure is reflected, and part is absorbed by the structure and converted into heat. The amount of absorbed solar radiation depends on the type of surfacing of the bridge structure, particularly its color. Darker colors tend to absorb more solar radiation. However, previous research showed that a concrete surface with asphalt blacktop usually yields 10% lower temperatures than uncovered gray concrete surfaces [83]. This was explained to be possibly due to the insulating effect of the blacktop layer of asphalt.

Another important source of heat exchange for a bridge structure is the temperature of

the surrounding atmosphere, which is transmitted to the concrete by convection and conduction (and is particularly dependent on wind speed and thermal conductivity of the material).

It will be helpful for designers to study the degree of influence that each one of the above mentioned factors (solar radiation and ambient temperature) has on the non-linear temperature distribution of the different members of a typical concrete segment. The measurement of concrete temperatures is therefore crucial for determining the results of the heat exchange process.

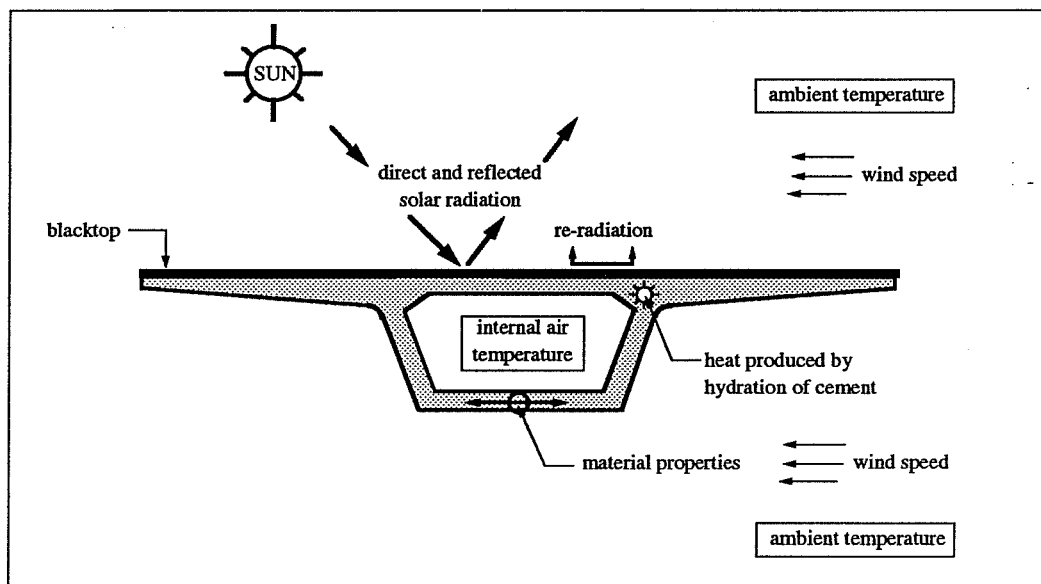


Figure 3.26 Factors influencing the thermal response of segmental box girder bridges.

3.4.1 Objectives

The interest of this section is to review some of the most popular instrumentation systems used for measuring concrete temperature and solar radiation. For each reviewed instrument, an evaluation of some of the most important information related to its method of installation, operation, and cost is included. Devices commonly available for measuring concrete temperature are included in Section 3.4.2, and a basic introduction to the measurement of solar radiation is included in Section 3.4.3. The final objective of this review is to help select the most appropriate devices for the instrumentation of concrete segmental box girder bridges.

High accuracy and sensitivity are not critical for these devices and their selection for a particular project is thus more dependent on cost, availability, and technological knowledge of

the instrumentation engineers. Another factor of importance is the long-term stability of the selected system. No trial tests were considered necessary among the reviewed instrumentation devices for concrete temperatures since some of them have showed outstanding behavior in several reviewed short to medium term instrumentation projects. However, the selected solar radiation instrumentation system was installed on top of a finished span of the San Antonio Y bridges to check its overall behavior. This single field test helped the present researchers to familiarize themselves with this seldom used instrumentation device. Since measurements were only performed for understanding the operation of the solar radiation measuring device, no valid test conclusions were reached and no trial test reports are thus included in Chapter 4. Only a few recommendations about the installation and maintenance are included in Chapter 5.

3.4.2 Concrete Temperature

In most field instrumentation projects of concrete bridges, measurements are needed to determine the type of temperature distribution occurring in different components of a structure and across the thicknesses of each individual component. However, temperature measurements can also be helpful for correcting other types of measurements. For instance, the hydraulic liquids inside commonly used jacks or some type of load cells can vary in volume according to the ambient temperature. Pressure variations of these devices may need to be corrected when large temperature differentials occur. The same is true for most of the other load or strain measuring devices. However, other methods for avoiding temperature related errors exist. Some instruments are made of materials that have very small thermal coefficients of expansion (such as Invar or Super-Invar) and other instruments use materials that approximately match the thermal coefficient of expansion of the surfaces they instrument (such as temperature compensated strain gages).

There are several instrumentation systems available for measuring temperature. The most widely used devices are:

- thermocouple wires,
- thermistors,
- resistance temperature devices, and
- vibrating wire temperature sensors.

3.4.2.1 Thermocouples. These are by far the most widely used devices for embedment in concrete structures. The operation of a thermocouple wire is simple. The voltage variations between two wires made of different materials and twisted together at one end is directly proportional to the temperature variations at the connection of the wires. The connection of the two wires (usually called the *measuring junction*) can be made either by twisting the wires together (see Figure 3.28c) or by fusing the two wire materials with an oxyacetylene flame. Both methods have worked well in previous instrumentation projects.

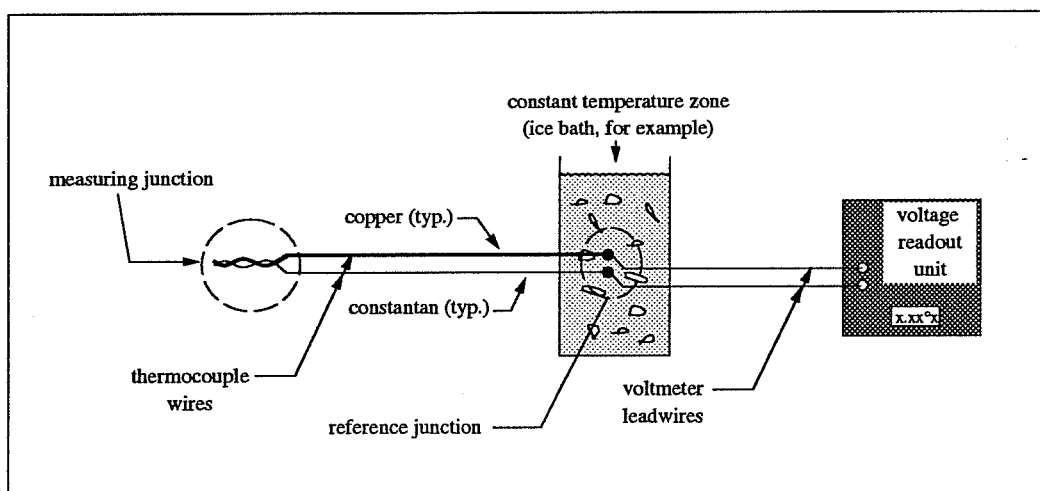


Figure 3.27 Principle of operation of thermocouples.

Measuring the voltage variations between the two thermocouple wires cannot be made with regular voltmeters. This is because the connections to the voltmeter leadwires would produce another thermocouple junction of dissimilar metals that will throw off the temperature measurements of the *measuring junction*. As shown in Figure 3.27, a reference temperature must be used at the connection of the voltmeter leadwires with the two thermocouple wires. Most of the measuring devices provided by thermocouple wire manufacturers have an electronically controlled constant-temperature zone where the *reference junction* is performed. Most readout devices thus permit direct connection to each one of the thermocouple wires (provided that they are compatible with the type of materials used in the thermocouple wires). Calibrating charts are standard for each type of thermocouple wire, temperature can thus be directly measured in °F or °C in most readout devices.

Several combinations of materials are available for thermocouple wires. The most common for embedment in concrete is copper-constantan (type T thermocouples). This is because both of these materials oxidize only mildly in aggressive environments such as concrete. Furthermore, thermocouple manufacturers also provide different types of insulating and overbraiding materials. Teflon is the preferred insulating material for concrete embedment due to its excellent moisture and abrasion resistance. Overbraiding of the thermocouple wires is optionally provided by most manufacturers. However, this is strongly suggested for field applications to increase the durability, flexibility, and abrasion protection of the thermocouple wires. Tinned copper overbraids are recommended due to their relatively low cost and good performance. For applications different than in concrete, literature or suggestions from thermocouple manufacturers should be consulted due to the wide variety of combinations that can be made with the currently available wires, insulations, and overbraids (see Table 3.9).

Thermocouple Wire Types:
Iron-Constantan (Type J)
Copper-Constantan (Type T)
Chromel-Constantan (Type E)
Chromel-Alumel (Type K)
Insulation Types:
Polymil Chloride
High-Temp. Glass
Kapton
Teflon/Neoflon
Silicone Rubber
Glass
Refrasil
Nextel
Overbraiding Types:
304 Stainless Steel
Inconel 600
Tinned Copper

Table 3.9 Commonly available thermocouple wires, insulations, and overbraids (from Omega Eng., Inc.).

Thermocouples are also widely preferred since they can measure a wide range of temperatures at an accuracy level that is usually around $\pm 1.0^{\circ}\text{C}$ ($\pm 1.8^{\circ}\text{F}$). This is practical for most structural engineering applications. Furthermore, there is a large selection of thermocouple readout equipment. Some are portable (battery operated) and can be used with specially manufactured multi-channel switching devices. A portable 19-channel switching device is shown in Figure 3.28(a). This was easily assembled at the research facility (FSEL) with parts purchased from Omega Engineering, Inc. A battery operated, standard portable readout unit (for Type J, K and T thermocouples) is also shown in Figure 3.28(b).

Another important characteristic of thermocouples is their excellent suitability for automatic data acquisition. Most data-logger manufacturers provide the necessary reference

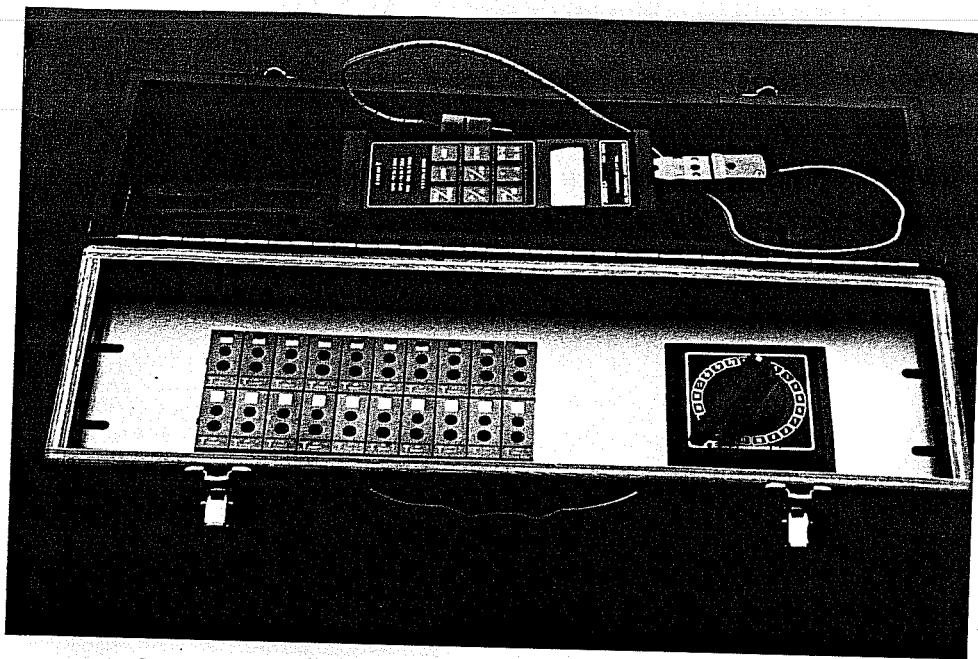
junctions and calibration charts for each thermocouple wire type as standard options to their equipment. However, certain data-loggers need to be programmed to be able to record the thermocouple measurements in $^{\circ}\text{F}$ or $^{\circ}\text{C}$.

Type T thermocouples with the proper protection and installation can have excellent stability in concrete. The manufacturer specified life of thermocouple systems with the proper insulation and overbraiding is usually around five years. However, in most of the reviewed field instrumentation projects much longer performance was obtained.

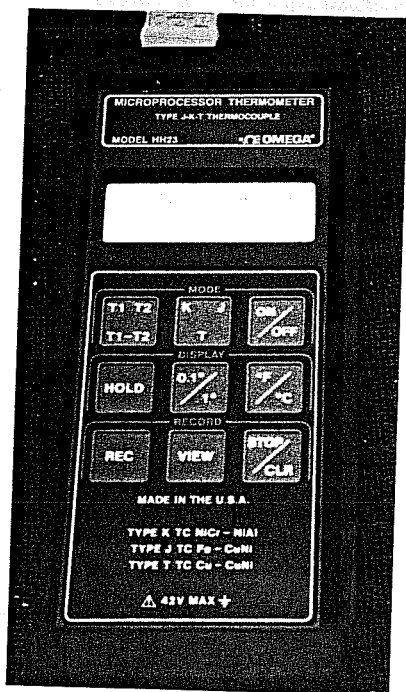
Typical costs of a standard thermocouple system for embedment in concrete and with a portable readout unit and multi-channel switching device are shown in Table 3.10. These prices are of late 1990 and obtained from Omega Engineering, Inc. They can be reached at: One Omega Dr., P. O. Box 4047, Stamford, CT. 06907. Their current telephone number is: (203) 359-1660.

a. Thermocouple Wire:	\$244.00
- Type T thermocouples	
- with Teflon/Neoflon Insulation	
- Size 20AWG	
- 500ft spools	
b. Thermocouple wire overbraids: (for the above listed wire description)	
- Tinned Copper	\$85.00
- 304 Stainless Steel	\$127.00
- Inconel 600	\$212.00
c. Quick disconnect connectors for Type T thermocouples (each)	\$1.80
d. Hand-held thermometer for Type J/K/T thermocouples (battery operated, Type HH-23)	\$189.00
e. 19-channel portable switching device for Type T thermocouples (assembled at research facility, cost not including labor)	\$300.00

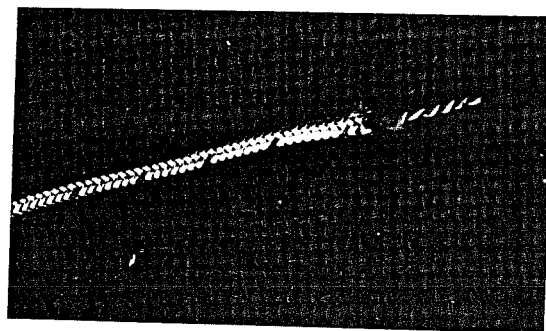
Table 3.10 Typical costs of a thermocouple system for use in concrete structures (from Omega Eng., Inc., prices from late 1990).



a. Portable multi-channel (19-channel) switching device for type T thermocouples.



b. Close-up of battery operated readout unit.



c. Close-up of a typical thermocouple measuring junction.

Figure 3.28 Typical thermocouple system for field instrumentation projects.

3.4.2.2 Thermistors. *Thermally sensitive resistors* are usually made of semiconductor materials that change their resistance with temperature (as shown in Figure 3.29). Absolute temperatures from thermistor resistance measurements (usually in Ohms) are obtained through manufacturer charts. However, most thermistor manufacturers provide readout devices that can directly show temperatures in °F or °C. These instruments are relatively cheap and provide great levels of stability and accuracy. They are available in different sizes and shapes, the smaller ones are more adequate for the temperature corrections of other instrumentation devices. However, they have also been commonly used for embedment in boreholes in geotechnical instrumentation projects.

The semiconductors of a thermistor are highly sensitive to temperature differentials, while the two leadwires --that connect them to the readout units-- are not as sensitive. This makes the thermistors to be highly accurate and stable devices. A usual degree of accuracy for thermistors is $\pm 0.1^{\circ}\text{C}$ ($\pm 0.2^{\circ}\text{F}$). The range of temperatures that can be measured at such an accuracy level is usually quite considerable. Most manufacturers can offer the mentioned level of accuracy for a -80°C to a $+75^{\circ}\text{C}$ (-112°F to $+167^{\circ}\text{F}$) temperature range. Two-conductor long leadwires can usually be used without a drop in accuracy since the resistance of the leadwires varies only slightly with temperature. However, the resistance created by long lengths of leadwires should be subtracted from the total resistance readings of the thermistors to obtain absolute temperatures.

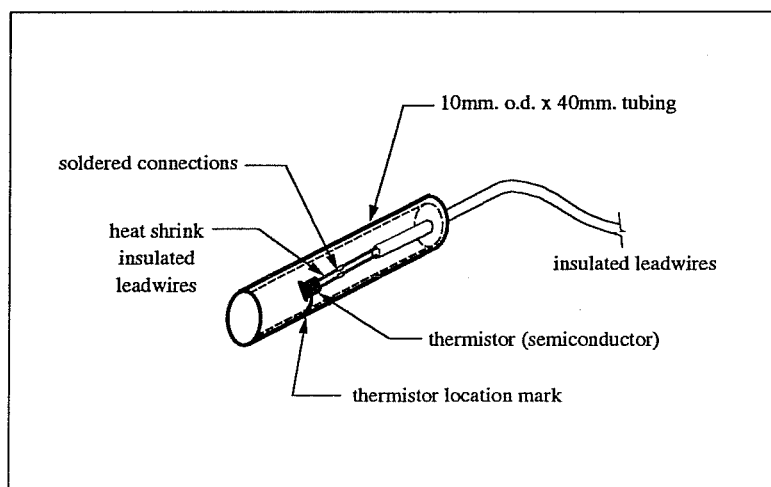


Figure 3.29 Typical thermistor for concrete embedment (from B.R. Jones Catalog).

The largest inconvenience with thermistors is their lower degree of compatibility with automated data acquisition systems. Since the variations of electrical resistance are quite large, only a few data-loggers supply the digital voltmeters necessary for obtaining such measurements. However, most manufacturers can provide affordable readout units, multi-channel switching devices, and data-loggers compatible to their thermistors. This type of thermometer can be purchased from several companies in the U.S.:

1. B.R. Jones & Assoc., P. O. Box 38, Normangee, TX 77871. Current telephone: (409) 396-9291.
2. Roctest, Inc., 7 Pond Street, Plattsburgh, N.Y. 12901-0118. Current telephone: (518) 561-1192.
3. Atkins, Technical, Inc., 3401 S.W. 40th. Blvd., Archer Interchange (I75), Gainesville, FL 32608. Current telephone: (904) 378-5555.

3.4.2.3 Other Systems. Less familiar systems for measuring temperature variations in concrete structures consist of resistance temperature devices and vibrating wire temperature sensors.

Resistance temperature devices (also known as RTD's) are simple metal wire resistors connected to a readout unit through a three leadwire system. As well as with the thermistors, these are also based on the principle that a wire's resistance varies in a directly proportional relationship with temperature. However, the temperature induced resistance variations of an RTD are much smaller than for the thermistors thus requiring the use of a three-leadwire, quarter-bridge Wheatstone bridge (necessary for avoiding the measurement of temperature differentials on the leadwires themselves). They are compatible with most automated data acquisition systems. However, since they require independent channels and quarter-bridge completion circuits, their application is more expensive than the other systems reviewed earlier in the present report. Manufacturers claim that these devices have excellent stability with time. In fact, their rated stability is usually in the neighborhood of 10 to 15 years. However, unless these devices are permanently connected to a portable readout unit or to an individual data acquisition channel, errors can occur due to leadwire effects. The exact electrical resistances produced at the connections of the leadwires of each RTD to the different channels of a data acquisition system cannot be accurately reproduced. A reduced accuracy level therefore exists

in most practical applications of the RTDs. Nevertheless, not considering leadwire effects results in an accuracy level that is usually about the same as obtained with thermistors ($\pm 0.1^{\circ}\text{C}$ or $\pm 0.2^{\circ}\text{F}$).

Vibrating wire temperature sensors can also be used for concrete embedment. One of the most familiar type of vibrating wire sensors is the previously reviewed Carlson Elastic Wire Meter. Although mainly used for measuring strains, this device provides the added benefit of measuring temperature.

Dedicated vibrating wire transducers also exist. They are usually made of a steel body to which a vibrating wire element is attached. The different coefficients of thermal expansion of the steel body and the vibrating wire enables a sensitive determination of temperature variations. Since signals consist of frequencies, no errors due to leadwire effects or other changes of resistance (caused by moisture penetration, temperature, or contact resistance) influence the stability and accuracy of these devices. The main problem related to these systems is that they are usually more expensive than the other temperature measuring devices that were reviewed here. Vibrating wire temperature sensors also require compatible readout units and data-loggers, which can be considerably expensive if non-compatible measurements of strain are performed for the same instrumentation project. High accuracy levels of less than $\pm 0.1^{\circ}\text{C}$ ($\pm 0.2^{\circ}\text{F}$) for temperature ranges of -40°C to $+160^{\circ}\text{C}$ (-40°F to $+320^{\circ}\text{F}$) can usually be obtained with these sensors.

3.4.3 Solar Radiation

Radiation is the transfer of energy produced by a disorganized propagation of photons. Any body continually radiates photons at random directions, phases and frequencies. Photons can travel in any wavelength of the electromagnetic wave spectrum. Only the photons travelling at a small part of the spectrum affect the human eyes as visible light. Available instrumentation devices for measuring the amount of radiation impinging upon a flat surface usually vary according to the range of the electromagnetic wave spectrum that they measure. Within them, the most accurate devices are those that use cosine corrected functions to account for the angular incidence of the radiation rays (coming from all angles of a hemisphere) on a flat surface.

Instruments that measure the solar radiation received from a whole hemisphere have the specific name of *pyranometers*. These instruments are suitable for measuring the energy flux

density of both direct beam and diffuse sky radiation passing through a horizontal plane of known unit area (thus measuring global sun plus sky radiation). In general, pyranometers are not generally useful when installed under artificial lighting or to measure reflected radiation. However, these devices are effective for most applications in concrete structures where the largest amount of radiation comes from direct solar rays. Some of them are even effective for more dedicated thermal engineering research (such as the *Eppley Precision Spectral Pyranometer*). These devices provide measurements of radiation density flux in units of $\text{cal}/(\text{m}^2 \times \text{min})$.

Only one type of pyranometer was actually purchased and operated by the present research project. This was the LI-200SZ Pyranometer Sensor manufactured by LI-COR Inc. (shown in Figure 3.30). The manufacturer is located at: 4421 Superior St., P.O.Box 4425, Lincoln, NE 68504. Their current telephone number: (402) 467-3576.

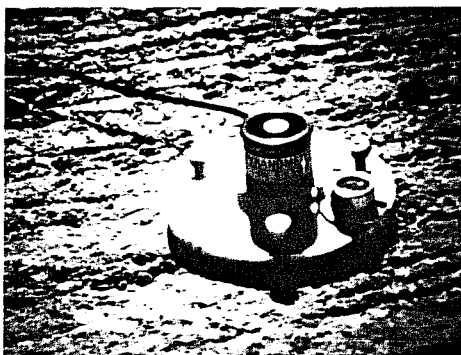


Figure 3.30 LI-200SZ Pyranometer.

The operation of this pyranometer is based on a silicon photodiode sensor. The spectral response of this sensor is not ideal since it measures a nonlinear response between 400nm to 1100nm (the ideal behavior would be to measure a constant spectral response from 280nm to 2800nm). However, this does not cause serious errors for the type of measurements to be performed at the San Antonio Y project. Optional

attachments to this pyranometer are a mounting and a leveling fixture. These are helpful for easier installation and operation of the devices. Pyranometers based on the silicon photodiode sensor are distinguished for their usually low cost. The LI-200SZ with a 30ft leadwire was purchased for \$200.00 in late 1990, and the corresponding mounting base and leveling fixture cost \$40.00.

Readings from the pyranometer are measured in the form of a current that varies with the solar radiation that impinges upon the silicon photodiode sensor. Pyranometer manufacturers usually provide special readout units for their products. However, most data-loggers can easily measure pyranometer currents by the voltage drop (in millivolts) across a fixed resistor (of no more than 147Ω) installed between the two poles of the coaxial cable provided with the LI-COR

pyranometer. The coaxial cable of the pyranometer can be purchased in different lengths, according to the distance from the sensor to the data-loggers. The largest inconvenience with this pyranometer is that it should be recalibrated by the manufacturer every two years (to keep the original absolute level of errors between $\pm 3\%$ and $\pm 5\%$).

3.5 Other Measurements

In segmental box girder bridges it is usually desirable to instrument critical joints between concrete segments to check if any displacements occur. Although not expected to move considerably in the San Antonio Y bridges, joints between certain segments have opened considerably in the earlier applications of this bridge technology [12]. Monitoring of displacements across the joint of two concrete segments is a simple measuring process that can be performed with relatively inexpensive instruments. A number of previous laboratory investigations related to box girder bridges have successfully used devices called *calibrated crack monitors* to measure these movements. These are introduced here in larger detail.

Another physical quantity usually desired to be measured in segmental concrete bridges is the load imposed to the supports of each span. These measurements can be easily achieved with most of the previously reviewed load cells (see Sections 3.2.3.1 and 3.2.3.2). However, in these cases the high-priced load cells would have to be left permanently in the bridge structures. This is a very expensive alternative for any large bridge instrumentation program. The present investigators thus avoided the use of load cells due to their elevated cost. However, these measurements can probably be indirectly determined by measuring the deformation of the neoprene bearing pads at each support. These measurements can be performed easily and at a very low cost with the help of high resolution caliper gages. This process is further explained in Section 3.5.2.

It is interesting to note that despite investigations in laboratory-controlled environments, most of the previously reviewed projects (mainly the field instrumentation projects) did not perform this kind of measurement. According to U.S. representatives of Freyssinet International, some European bridge structures implemented Freyssinet's *flat-jacks* to measure load variations in a few supports. However, no literature was obtained from these applications. Nevertheless, the *flat-jacks* were briefly reviewed in Section 3.2.3.2 of the present

report (within the load measuring devices).

3.5.1 Calibrated Crack Monitors

As their name implies, these gages have been traditionally marketed for measuring crack widths in concrete members. However, they can also be used very efficiently for the measurement of joint openings between concrete segments (which can basically be treated as cracks).

They are simple measuring devices composed of two Plexiglass acrylic plates of approximately 4in. L x 1¼ in. W (as shown in Figure 3.31). One of these plates is usually white with a black colored grid of 40mm x 20mm (calibrated in millimeters). The other plate is transparent and fits on top of the first one. This top plate has two red colored cross hairs centered over the zero marks of the bottom grid. The installation of the plates involves careful attachment to each side of a joint between two concrete segments. In short-term projects, the plates can be attached with any two-part epoxy adhesive. However, long-term projects should avoid this method of installation since epoxy adhesives have shown low long-term durability when used on concrete surfaces. An alternative is to use some type of mechanical anchoring devices combined with two-part epoxy products.

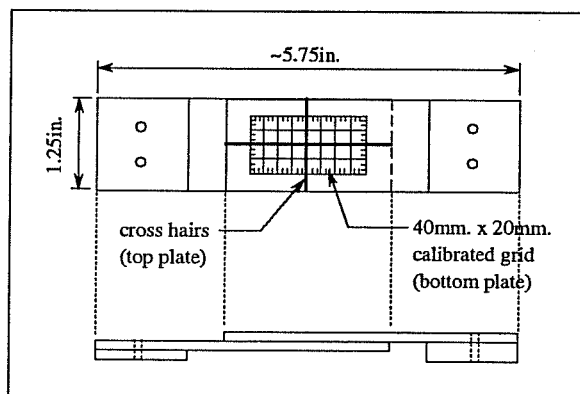


Figure 3.31 Typical dimensions of calibrated crack monitors (Avongard products).

Vertical and horizontal movements can be estimated to the ½ mm with these crack monitors. To obtain a greater degree of accuracy, mechanical strain measuring devices can also be employed at the same locations where the crack monitors are placed. A pair of Demec locating discs can be easily installed near each calibrated crack monitor.

The crack monitors have a registered patent in the U.S. and are manufactured by a single company. The lack of competition makes this product more expensive than expected. A single calibrated crack monitor cost \$12.50 in early 1991. They can be purchased

from Avongard Products U.S.A., located at: 2836 Osage, Waukegan, IL 60087. Their current telephone number is: (708) 244-6685.

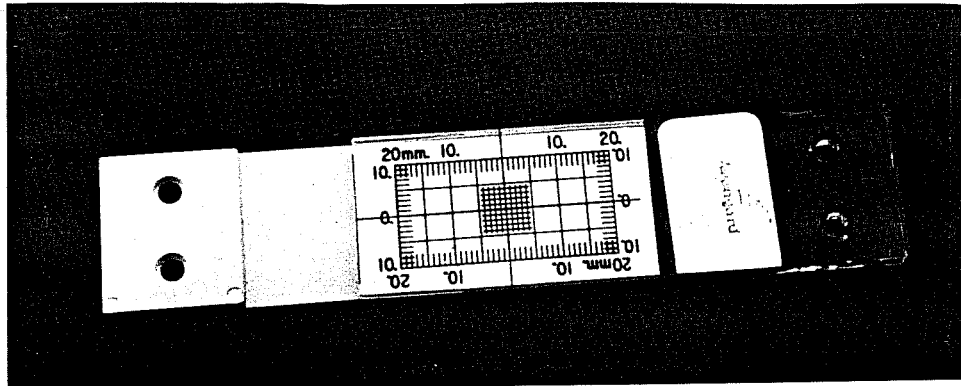


Figure 3.32 Avongard calibrated crack monitor.

3.5.2 Caliper Gages

These gages are usually present in every well equipped machine shop. They are used for the measurement of internal diameters of tubes, or for measuring internal grooves and recesses. They are offered in different gage lengths. The larger gages can be ideal for accurately measuring the vertical movements between the bottom of the pier segment and the top plane surface of the piers (as occurring near a neoprene bearing pad). The approximate behavior of the neoprene bearing pads can be obtained from their manufacturers. This information combined with measured vertical deformations can give an approximation of the loads imposed to each bearing pad. The accuracy of these loads will evidently be quite low. However, serious overloadings or loading differentials among the bearing pads of a single span are still expected to be determined with this type of measurement. None of the reviewed instrumentation projects --in laboratory as well as in field applications-- have applied these measurements before. The San Antonio Y project will provide the first conclusions about their use and applicability for a field instrumentation project.

Caliper gages can be obtained from most machine shop precision tool manufacturers. They are offered with digital readouts or with dial indicators. Resolutions of $5/10,000$ in. can be obtained with most gages. The larger calipers can measure movements of up to 0.8in. However, these larger calipers (of the dial indicator type) can cost up to \$400.00, and up to \$650.00 for digital calipers with $2/10,000$ in. resolution.

3.6 Data Acquisition Systems

This is usually the single most expensive investment of a dedicated instrumentation project. The function of data acquisition systems is to gather signals from different instrumentation devices, condition some of the collected signals, and record, transmit or display the processed data. Most of the reviewed field instrumentation projects used portable manual readout units in their data acquisition process. However, some field projects and most of the laboratory investigations used sophisticated automated data acquisition systems (sometimes referred to as ADAS).

Practically each instrumentation device previously reviewed is offered with a compatible portable manual readout unit. Some of these units can be combined with manually operated multi-channel switching devices. However, these systems are not recommended for large instrumentation projects employing several input channels that must be scanned at regular intervals. Manually obtained data needs to be keyed into electronic spreadsheets for final analysis. This introduces a new level of operational error and a time consuming operation for projects involving several instrumentation devices. A more important problem occurs with measurements of small electrical resistances --such as from ER-gages and load cells-- due to the variation of the contact resistance that occurs in the connections to each channel. In long-term readings, large errors can be introduced from the variation in the contact resistances of the connections. These electrical resistance variations can occur due to oxidization of terminals, temperature differentials, variation of the type of electrical contact produced by each connector, etc. The best way of avoiding these errors is by using permanent (i.e. for the duration of the project) connections to each channel. However, this is expensive and inefficient when a large number of channels are needed. A different solution is to use some other type of almost perfectly reproducible electrical contact. One electrical connection that can be reproduced accurately through different contacts is to immerse the connecting leadwires in a solution of mercury. This method is evidently impractical and dangerous due to the health threatening effects of mercury. However, an accurate reproduction of connections can also be obtained with gold-plated connectors (usually employed inside several multi-channel switching devices).

The best method for acquiring data from a large number of instrumentation devices is to use a commercial automated data acquisition system. There is a wide variety of systems

available, ranging from data-loggers to computer controlled data controllers. The data-loggers are characterized by simply scanning and recording data from different type of instruments at user programmable time intervals. Data can be recorded in internal random access memory (RAM-memory), hard disc memory, floppy disks, tape cartridges, or some systems can even be coupled with external modems and send data directly to a remote computer (located in a research laboratory for example) through a dedicated phone line. Prices of these systems vary widely according to the type and amount of data storage, number and type of devices that can be scanned, availability of internal programs (written in ROM modules and used to reduce data processing or programming), operating environment, etc.

Data controllers are similar to data-loggers but provide additional interfacing and basic programming that can control the operation of certain equipment based on the variations of the measured data. These are more sophisticated and expensive equipment and are seldom used in structural engineering investigations.

Battery operated data-loggers are usually preferred for field instrumentation projects. Only a few field projects can be supplied with a regular source of electricity. Even when electricity is available, provisions must be made to prevent voltage surges, voltage drops, or occasional power outages that can alter the normal operation of the system. Line stabilizers, surge suppressors, and uninterruptible backup power supplies should be used with expensive data acquisition systems connected to regular AC electricity (to protect their delicate internal circuitry).

The present project researchers investigated several types of available data acquisition systems. A portable data-logger was desirable because it would avoid the dependance on regular sources of electricity and the extra investments of power backup and system protection devices. Moreover, battery-powered data-loggers can usually be operated in harsher environmental conditions (in terms of moisture and temperature) than AC systems that are mainly designed for laboratory use.

After a review of previously used data-loggers and after an investigation of the currently available technology, the present researchers decided to purchase a low-cost system offered by Campbell Scientific. Part of the reason for purchasing this equipment was that a very efficient field system built around a portable data-logger was previously designed by researchers of the present laboratory [84]. The previous researchers considered the *Campbell Scientific 21X* to be a cost-efficient battery-powered type of data-logger. An extensive development of soft-

ware needed for interactive programming and data retrieval was prepared for this system. This software program was found incompatible for the presently desired application and the development of a new one would have considerably increased the final cost of the data acquisition system. However, Campbell Scientific recently developed a low-cost PC-compatible software kit that includes the necessary wiring for connecting their data-logger to the serial port of any personal computer. This kit also includes some basic software that helps considerably in the processes of programming, remote communication, and data retrieval of the data-loggers offered by this company. Costs of the purchased equipment from Campbell Scientific are included in Table 3.11. However, these costs do not include the extra equipment necessary for the construction of the field-operational data acquisition system built for the San Antonio Y project. Other expenditures were related to:

- the internal quarter bridge completion circuitry (necessary for the electrical resistance strain gages),
- high quality connectors (to ensure good resistance to moisture and physical damage),
- labor time needed for soldering the internal wiring of all data-logger channels to the proper poles in the connectors, and for construction of the box enclosure.

a. 21XL Micrologger (w/40K RAM & PROM module).	\$1900.00
b. 16-channel 4-wire input multiplexer (AM416, no enclosure).	\$475.00
c. Optically isolated RS-232 interface (to PC serial port).	\$130.00
d. Data acquisition software package.	\$200.00

Table 3.11 Late 1990 prices for data acquisition components offered by Campbell Scientific, Inc.

More details about the data acquisition system designed for the present instrumentation project are included in Section 4.5. Important wiring information about the quarter bridge Wheatstone completion circuits (designed by the present researchers) are also included in Appendix B. This information can be helpful for future similar projects since the completed system is between the most affordable ones considering the extensive number of quarter bridge ER-gage channels that it can handle.

Future instrumentation projects desiring different data-loggers can consult with several companies. First of all, most of the previously mentioned manufacturers of monitoring devices offer some type of data acquisition system. Other companies more dedicated to the production of data acquisition systems (rather than specific instrumentation devices) are:

1. Campbell Scientific, Inc., P. O. Box 551, Logan, UT 84321. Current telephone: (801) 753-2342.
2. Optim Electronics, Middlebrook Tech Park, 12401 Middlebrook Rd., Germantown, MA 20874. Current telephone: (301) 428-7200.
3. Hewlett-Packard, 1820 Embarcadero Road, Palo Alto, CA 94303.
4. National Instruments, 6504 Bridge Point Parkway, Austin, TX 78730-5039. Current telephone: (512) 794-0100.
5. Contec Microelectronics U.S.A., Inc., 2010 N. First Street, Suite 530, San Jose, CA 95131. Current telephone: (408) 436-0340.

CHAPTER 4

TRIALS OF INSTRUMENTATION SYSTEMS

4.1 Criteria for Selecting the Final Instrumentation Systems

As a general rule, a consistent set of factors were considered for selecting the final type of instruments to be tested in trial experimental conditions. The main factors of consideration were the following:

- (a) Stability for long-term performance. An important goal of the present project is to study the long-term behavior of concrete bridge structures. Selection of systems capable of achieving stable readings for a period of several years was considered necessary.
- (b) Robustness. This takes into account the field performance of each system. Robust instruments are preferred so as to withstand normal construction operations. Information related to this factor was obtained from previous research and reports of full-scale instrumentation programs.
- (c) Technological exposure. Systems that were previously used and readily available to the present project researchers were given extra consideration for trial tests.
- (d) Availability of support equipment. This was an important factor for automated readouts. Support equipment such as completion circuits, data acquisition systems, scanning systems, and/or instrumentation software is quite expensive. The availability of equipment at the research laboratory required only small investments for trial tests and refinement of technology. Several systems were chosen from this standpoint.
- (e) Cost. The large magnitude of the present project and its conservative operational budget influenced a decision towards the lowest priced instrumentation systems that satisfied the above mentioned conditions.

The level of accuracy of commercially available instruments is generally within the acceptable range for structural applications, provided that they are properly installed and operated. This is

based on the premise that all commercial instruments for measuring concrete strains, for example, should provide at least a minimum level of accuracy in order to be successfully marketed. Accuracy was thus not a very useful factor for comparison of candidate instrumentation systems. The behavior of most commercial instruments reviewed in Chapter 3 was checked in reports of previous full-scale investigations and laboratory research. These reviews helped to suggest better operating rules and to identify areas that needed improvement. Instruments reported to have failed in previous field studies were excluded from further trial tests, unless new technological developments were available.

Maximum range for measurements was also avoided as a factor of comparison since for full-scale instrumentation programs extreme ranges are not expected to occur. Properly sized commercial instruments normally provide a measurement range well within the elastic range of most structural materials. This factor was also avoided in the comparison of reviewed instrumentation systems.

All instrumentation systems evaluated for further trial tests had useful levels of accuracy and range of measurements.

A factor given careful consideration was the need for automated data logging operations. This would enable unattended scanning of selected sensors. Since the automatization of structural instruments is usually expensive, its application was considered with strict limitations to the areas where other methods were not feasible.

4.2 Concrete Strain Measurements

All concrete strain measuring devices reviewed in Section 3.1 were considered for testing trials. A simple method of analysis of systems was employed based on the selection criteria outlined in Section 4.1. Vibrating wire gages and Carlson meters were eliminated due to their high costs and because of unavailability of laboratory support equipment. Mechanical extensometers and Mustran Cells appeared to be the most satisfactory devices for the present project. Mustran Cells however, were set aside because of the high expenditure necessary for achieving long-term stability of the low electrical signals. Demec extensometers and Whittemore gages were serious contenders, but the availability of Demec extensometers at the research facility made this system the best one to choose for trial tests.

Demec mechanical extensometers were selected for refinement in the following areas:

- (a) More durable method of bonding locating discs to concrete surfaces.
- (b) Need for increasing the operating speed for taking measurements.
- (c) Better repeatability of readings.

4.2.1 Demec Gages: Bonding Methods

One of the main problems with Demec extensometers is directly related to the long-term stability of the guiding points bonded to the concrete's surface. Previous field studies found long-term stability problems with the frequently used method of surface glueing of locating discs provided by the gage manufacturer [80, 81].

Several methods for bonding locating discs of Demec gages to the concrete surface were therefore tested under laboratory and field conditions. The following is a general description of the different systems investigated:

I. Surface bond:

- with quick setting epoxy
- with cyanoacrilates

II. Concrete embedment bond:

- stainless steel bolts
- stainless steel pins

III. Drilled concrete bond:

- epoxied stainless steel bolts
- epoxied stainless steel pins
- mechanical wedging bolts
- mechanical nailed inserts

Some of the guide points for the Demec gages were custom made at Ferguson Laboratory. Bonding systems were evaluated in two areas of concern: ease of installation and long-term stability in aggressive environments.

4.2.1.1 Ease of Installation. In addition to actual installation problems, this factor also takes into account the difficulties encountered for the manufacture of the new Demec locating points. Several systems were found inadequate just after installation due to incorrect misalignment. Others did not survive through concrete casting and formwork stripping operations. The effec-

tiveness of the installed system is thus another factor of importance to be considered within the overall factor of ease of installation. A final analysis of the systems investigated in trial tests is shown in Table 4.1.

Surface bonding of the original Demec locating discs proved to be the best method with respect to ease of installation. They are easy to attach and provide one of the best final alignments. The movement of the pivoting endpoint of the Demec extensometer is restricted to a certain range. Good alignment of the guide points is thus necessary for measuring the full range of possible strains in the concrete specimens. Surface bonding of the original Demec locating discs also provided the least amount of concrete disruption.

Bonding Methods	Advantages	Disadvantages
Surface Bond	<ul style="list-style-type: none"> • Relatively cheap • No special manufacturing • No overlapping with construction operations • Short installation process • Least concrete disruption • No formwork modifications • Good final alignment 	<ul style="list-style-type: none"> • Long periods of time to receive locating discs from manufacturer • Loss of bond with time and exposure
Concrete Embedment	<ul style="list-style-type: none"> • Medium cost • Low concrete disruption 	<ul style="list-style-type: none"> • Requires special manufacture • Difficult installation process • Overlapping w/const. operations • Requires formwork modification • Poor final alignment • Problems at casting
Drilled Concrete	<ul style="list-style-type: none"> • Medium cost • No overlapping with construction operations • No formwork modifications 	<ul style="list-style-type: none"> • Requires special manufacture • Medium difficulty in installation process • Some chipping on concrete surface • High concrete disruption • Medium final alignment

Table 4.1 Ease of installation of different bonding methods of Demec locating points.

The initial specimens with concrete embedment systems had serious difficulties related to stability during concrete casting operations. Several methods to improve their formwork attachment were later designed. Labor intensive methods of installation that required drilling of the formwork had successful stability during concrete casting and formwork stripping. However, they had problems with the final alignment of the drilled Demec guide points. Even at the final testing of the most successful method of installation, four out of six guide points were out of range for the Demec gage. Drilling two off-centered indentations on each one of the custom manufactured inserts was later found to greatly reduce misalignment problems. A schematic of the final method used for embedment in concrete is shown in Figure 4.1.

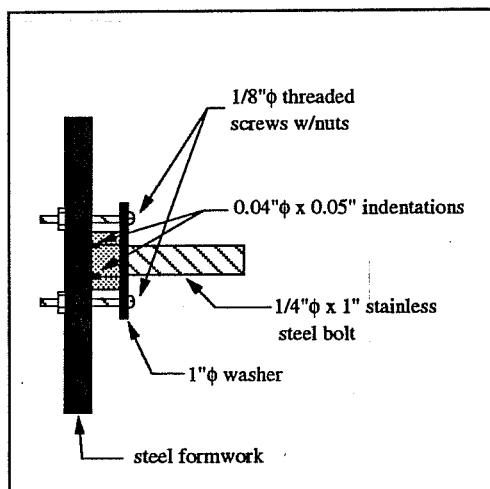


Figure 4.1 Concrete embedment method.

base of the drilled hole (≈ 0.05 "). These custom manufactured locating points did not cause a measurable decrease in reading accuracy. The same manufacturing system for custom guide points was also used in some specimens of the drilled concrete bonding methods. No major disturbances of the concrete were caused by embedment methods. Inclusion effects were also small since the strains of the inserted material were relatively small compared to the strains in the concrete between guide points.

Adequate performance was obtained with most drilled concrete methods. Some problems of chipping of the concrete's surface were found with systems that required larger diameter holes. Drilling in high strength concrete was performed with tungsten carbide masonry drill bits

Indentations used as guide points for the Demec gages were manufactured at the research facility. A drill press with precision finger chucks was used in the manufacturing process. The drill bits were of straight shank size 60 ($.040$ " ϕ) of ≈ 0.8 " usable flute length (stub length). Cobalt drill bits broke easily and only worked well for an average of 12 holes. Slightly more expensive tungsten carbide bits improved performance to 60-80 holes before breaking. Minimum drill depth was the depth at which the ends of the conical points from the Demec gages would reach the

and special electric hammer drills. In general, the final alignment of guide points was better than with embedment methods. Improved alignment was obtained with drilled inserts of smaller diameter. Drilling smaller holes was easier, produced low concrete disruption, improved accuracy, and provided less room for misalignment. A picture of the four types of inserts used in the drilled concrete systems is shown in Figure 4.2. Varying degrees of concrete disruption were introduced by these methods. The present investigation did not address their degree of influence but assumed this to be negligible for 200mm gage lengths. Certain errors were introduced with this assumption and more research can be helpful in this particular area.

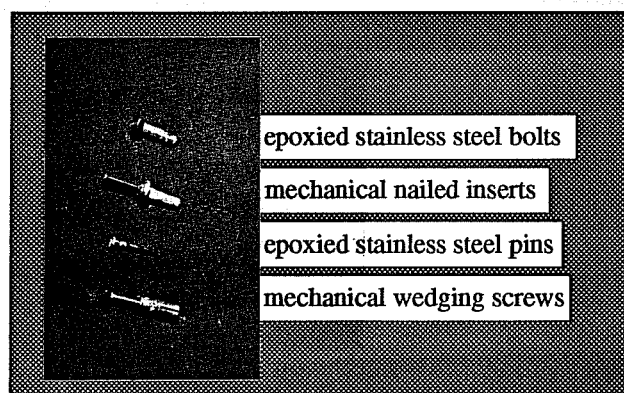


Figure 4.2 Inserts for drilled concrete methods

4.2.1.2 Long-Term Stability. This was a more important factor of consideration for the present investigations. Five 7"x13"x3" concrete specimens were cast with a design mix of $f'_c=5,500$ psi. A general description of the systems tested for long-term stability is included in Table 4.2. An indication of the size and type of inserts is also included in the same table. The systems of "Mechanical Stainless Steel Inserts" (Table 4.2: #3.1 & #3.2) and "Mechanical Wedging Bolts" (Table 4.2: #3.5 & #3.6) consisted of modified commercially available anchors for concrete. Anchors used were *Rawl Zamac Nailin* (stainless steel type w/mushroom head) of $1/4"$ ϕ x 1" for systems #3.1 and #3.2, and *Hilti Quick Bolts* (also stainless steel) of $1/4"$ ϕ x 1" for systems #3.5 and #3.6. Locating indentations for the Demec gages were drilled at the laboratory under the same procedures outlined in Section 4.2.1.1.

Systems of "Stainless Steel Pins" (Table 4.2: #2.3 and #3.3) consisted of original Demec discs welded in the laboratory to stainless steel rods of 1/8"φ x 1" lengths. Special stainless steel rods were used for the welding process to avoid corrosion at the welds. Finished samples of each one of these special systems were shown in Figure 4.2. The epoxy used for bonding complied with Texas Highway Department Type V Specifications [85]. Tests were performed with *Industrial Coating Model A-103* two-part epoxy donated by the Material Testing Division of the Texas Highway Department.

SYSTEM CODE: NUMBER & NAME	INSERT DESCRIPTION	BONDING METHOD
1. Surface Bond: 1.1 Epoxied Demec Discs	Orig. Demec Discs	Type IV Epoxy
2. Concrete Embedment Bond: 2.1 Stainless Steel Bolts 2.2 Non-Stainless Steel Bolts 2.3 Stainless Steel Pins	1/4"φ x 1" 1/4"φ x 1" 1/8"φ x 1"	Precast Precast Precast
3. Drilled Concrete Bond: 3.1 Epoxied & Mechanical Stainless Steel Inserts 3.2 Mech. Stainless Steel Inserts 3.3 Epoxied Stainless Steel Pins 3.4 Epoxied Stainless Steel Bolts 3.5 Epoxied Mech. Stainless Steel Wedging Bolts 3.6 Mech. Stainless Steel Wedg. Bolts	1/4"φ x 1" 1/4"φ x 1" 1/8"φ x 1" 1/4"φ x 1" 1/4"φ x 1" 1/4"φ x 1"	Type V Epoxy & Mechanical Anchorage Mechanical Anchorage Type V Epoxy Type V Epoxy Type V Epoxy & Mechanical Anchorage Type V Epoxy

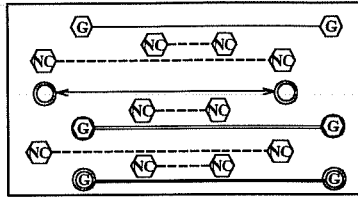
Table 4.2 Description of systems tested for long-term stability.

Long-term stability testing was performed according to ASTM Specification D-2933-74 (1986) "Corrosion Resistance of Coated Steel Specimens (Cyclic Method)" [86]. Thirty five freeze-thaw cycles with a salt-water solution were performed on the five concrete test specimens. According to specifications, this was approximately equivalent to more severe conditions than two years of inland Florida exposure. After this initial cycling the specimens were left outside the laboratory for a period of one year. A final report of the failures and problems encountered with the different systems is included in Table 4.3.

SYSTEM CODE (Table 4.2)	ORIGINAL QUANTITY TESTED (& gage length)	SPECIMEN	STABILITY REPORT:		
			AFTER CASTING	AFTER FREEZE/ THAW	AFTER ONE YEAR
1.1	2-100mm	3	OK	OK	2-Debonded
2.1	2-200mm	1 & 3	1-Bad	OK	OK
2.2	3-100mm	4 & 5	1-Bad	OK	OK
	3-200mm	2 & 3	OK	3-Corr	--
2.3	3-100mm	2	3-Bad	3-Corr	--
	2-200mm	1 & 3	1-Bad	OK	1-Scaled
	3-100mm	4 & 5	1-Bad	OK	OK
3.1	2-200mm	1 & 2	OK	OK	OK
3.2	3-100mm	4 & 5	2-Bad	OK	OK
	2-200mm	1 & 2	OK	OK	OK
3.3	3-100mm	4 & 5	2-Bad	OK	OK
	2-200mm	1 & 3	OK	OK	OK
3.4	3-100mm	4 & 5	OK	OK	OK
	2-200mm	1 & 2	OK	OK	OK
3.5	6-100mm	4 & 5	OK	OK	OK
	2-200mm	2 & 3	OK	OK	1-Corroded
3.6	1-200mm	3	OK	OK	OK
	3-100mm	5	OK	OK	OK

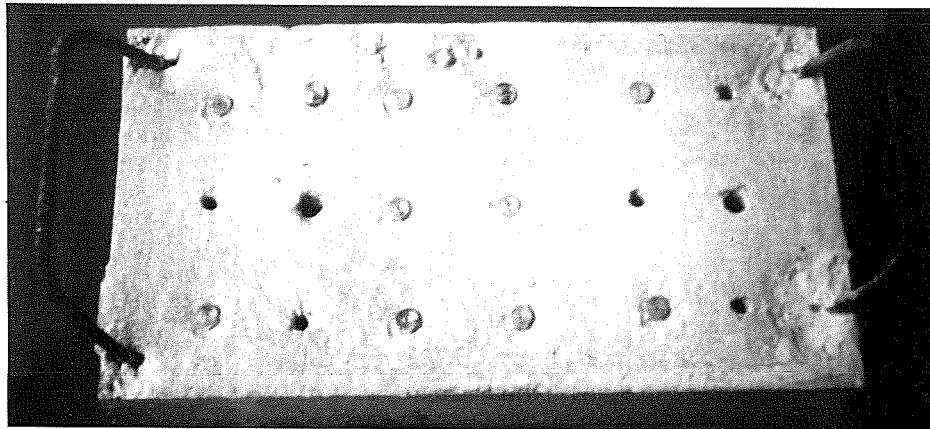
Table 4.3 Final report on long-term stability of Demec guiding systems

All of the non-stainless steel systems were corroded at the end of the cyclic period (≈ 2 years equivalent exposure). Some of these systems were still giving reasonable readings. However, at the end of one year exposure (equivalent to a three year period) all readings became unstable. More than 43% of the original number of concrete embedment systems were initially cast out of range, while only 15% of the drilled concrete systems were misaligned at initial setting. Surface bonded Demec discs worked well initially. However, at the end of the three year equivalent testing period some of them started debonding. A graphic report of the conditions of the systems on Specimen #2 throughout testing is shown in Figure 4.3. Darkened systems in the pictures represent the corroded non-stainless steel bolts.

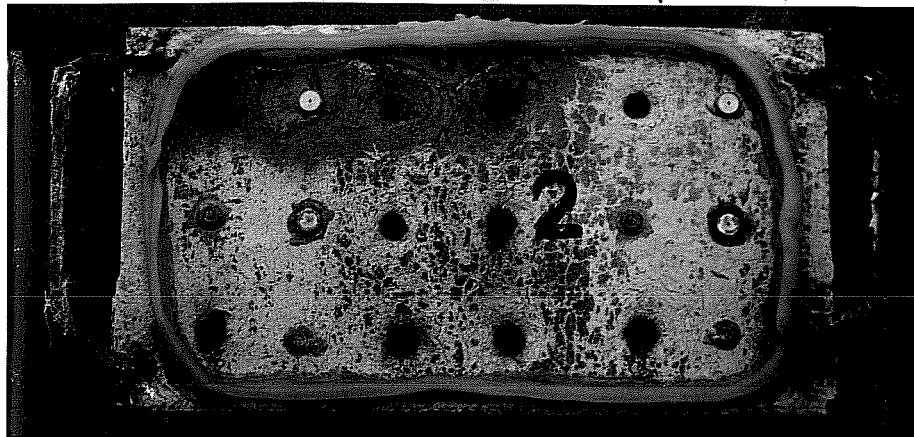


- (NC)— : Non-Stainless Steel Bolts (code #2.2)
- (G)— : Epoxyed Mechanical Wedging Bolts (code #3.5)
- (G)— : Epoxyed Mechanical Stainless Steel Inserts (code #3.1)
- (G)— : Mechanical Stainless Steel Inserts (code #3.2)
- (G)— : Epoxyed Stainless Steel Bolts (code #3.4)

a. Description of Bonding Systems



b. Initial Specimen



c. Specimen after Three-Year Tests

Figure 4.3 Long-term stability of specimen #2.

Results from these tests of Demec systems suggested that drilled concrete methods are more appropriate for long-term instrumentation projects. The stiffness of drilled concrete methods was considered to be an added factor of security for acceptable long-term behavior. Stainless steel inserts (Table 4.2: #3.1) were finally selected as the most adequate system.

Although cheaper and easier to install, surface bonding systems were not selected since they become unbonded with time. Wear and tear from periodic measurements was also considered to be a secondary factor influencing the long-term behavior of surface bonded systems. This factor was not properly reproduced on the test specimens and could have been the reason for such a relatively long stability of the surface bonded systems. Systems based on embedment methods were too complicated to install, and they also presented serious problems of initial misalignment of locating points.

4.2.2 Demec Gages: Increases in Operating Speed

All demec extensometers are furnished with a high resolution dial indicator mounted to the top of their frame, as previously shown in Fig. 3.6. A considerable amount of time is usually necessary for the reading process of a group of gage points, since very careful attention must be taken to avoid reading errors. Even for experienced people this reading process takes up some valuable time due to the small guide marks on the dial indicators. The present researchers attempted to find an automated method or set of instructions that would speed up the reading process without increasing the randomly occurring reading errors. The system that was finally envisioned involved the replacement of the original dial indicator by a "friendlier" digital indicator now available in the market. This was assumed to be an obvious growth of the old mechanical technology.

The original dial indicators of the Demec extensometers are custom built for the Demec gage manufacturer based on standard dimensions of commercially available dial indicators. Demec dial indicators have a 0.5in. range and a 0.002mm (0.000787in.) reading resolution. The project researchers used a *Mitutoyo Digimatic Indicator Model 543-135* as a replacement. The installation of this new system only required special machining for the four mounting screws at the base. The new digital indicator was slightly larger, but it fit well in the flat mounting plate of the Demec extensometer. The final system is shown in Figure 4.4.

Proper usage of the new system would have required a careful recalibration of the extensometer so as to find the new gage factor. However, to carry out the initial goals of the present testing phase (i.e. to examine speed in reading operations) a recalibration was not necessary.

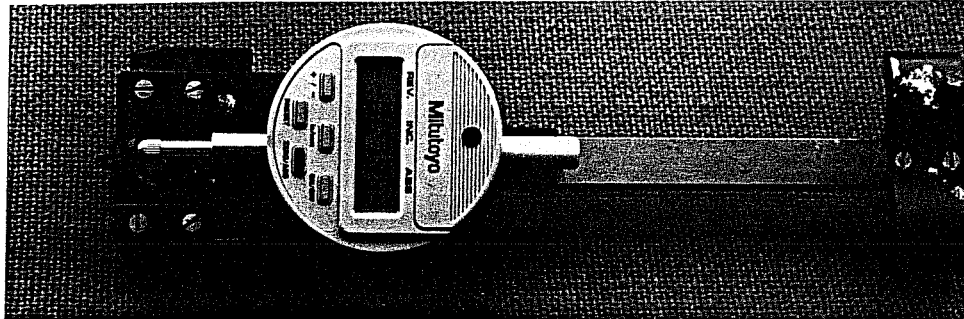


Figure 4.4 Modified Demec Extensometer.

Tests were performed with a field investigation of span C-35 of Phase I-C of the San Antonio Y elevated highway project. Sets of thirteen, nine and five Demec locating discs were distributed in three different cross sections on the top surface of the 100ft span as shown in Figure 4.5. All gage points were the standard Demec locating discs directly bonded to the concrete with quick setting epoxy resins. No sophisticated bonding methods were used since the test involved only short-term measurements. It was the intention of this testing trial to observe the daily variation of surface strains in the concrete due to temperature, and to observe the performance of the modified Demec extensometer. Both Demec extensometers used, standard and modified, were of 200mm gage length. Readings from the modified --but uncalibrated-- Demec extensometer were not accurate and were taken for the sole purpose of addressing speed improvements.

Test results, shown in Figure 4.6, show a consistent increase in speed of the reading operations of the modified gage. Each vertical scale value on this graph represents the time necessary for performing a single strain reading (as averaged from a series of 13 readings). It was safely concluded from this initial test that digital dial indicators provide an average 22% increase in speed for a single reading step. As shown in Figure 4.6, this amounts to about 2.6sec of an average 11.6sec standard Demec reading. This benefit is consistent with the increase in cost, since the addition of the digital indicator represented a 20% increment of the original cost of the 200mm Demec gage (about ≈\$194.00 price increase).

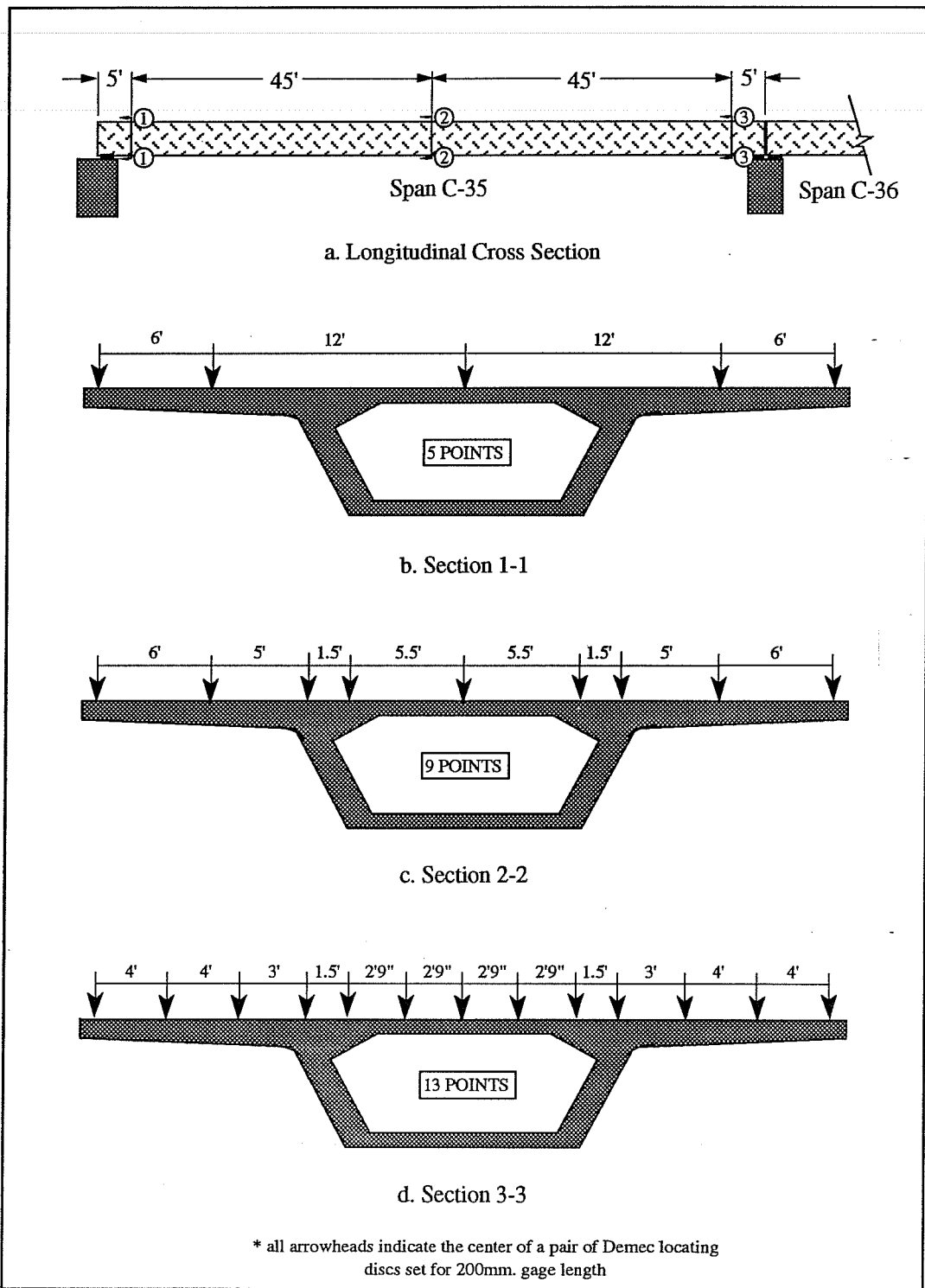


Figure 4.5 Location of Demec points on test span C-35.

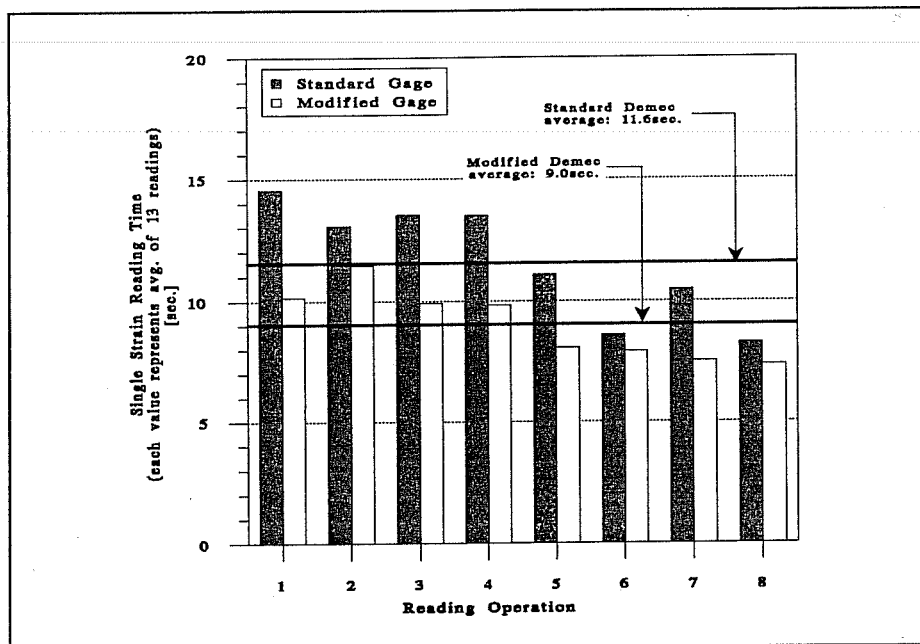


Figure 4.6 Comparison of reading speed of modified and standard Demec gages.

The reduction of random reading errors of the modified Demec extensometer represents a secondary factor of benefit. This was not addressed by the present researchers and is recommended for further study.

After a thorough investigation of newer digital dial indicators, models providing better resolution were found available. The indicator used for the reading speed tests had a 0.0127mm (0.005in.) resolution, much cruder than the 0.002mm (0.0008in.) resolution of the original Demec dial indicators. Digital dial indicators with much higher precision were investigated. The *Mitutoyo Digimatic Indicator Model 543-180* provides a resolution of 0.0001mm (0.00005in.). If properly installed and calibrated, these digital indicators can achieve a considerable improvement on the original sensitivity of the standard Demec extensometers. The present researchers performed no tests related to improvements of sensitivity, but strongly recommend them for future investigations. The higher resolution indicator represents 34% cost of the original price of a 200mm Demec extensometer (\approx \$320.00). Installation costs were calculated at 10% increase (\approx \$100.00), and calibration would require an additional investment of 32% of the gage price (\approx \$304.00). This total investment of 76% of the original 200mm gage price can be cost effective by the addition of the following benefits:

- (a) Improved sensitivity (in the order of 100 to 200%).

- (b) Faster operation (about 20% per reading step).
- (c) Reduced possibility for random reading errors.

Two methods of gage calibration were considered by the present project researchers:

- (a) Shipment of complete modified gage to the original manufacturer in England for purposes of recalibration, or
- (b) Construction of a gage calibration device based on a workable model designed by Pauw and Breen for The University of Missouri [87].

The use of either of these two methods for proper gage calibration would have required longer time than available. Time and budget limitations precluded the use of modified Demec extensometers with digital dial indicators in the present project.

4.2.3 Demec Gages: Repeatability

The 200mm Demec extensometers have been found to reach $16\mu\epsilon$ in reading repeatability when special care was followed in the reading operations.

Throughout the different tests performed with Demec gages, the following factors were found to influence the repeatability of gage readings:

- (a) Positioning of the Demec extensometer with respect to the locating points. Variations between the two possible locations of the Demec gage on each set of locating points introduced small errors. These were probably associated with irregularities in the geometry of the gage and the conical holes in the locating points.
- (b) Variations of gage pressure while holding in place to obtain strain readings. This is particularly important for inclined surfaces, when some pressure must be exerted on the gage to make it fit well in the conical holes of the locating points. Errors due to this factor increase if different operators alternate gage readings. Different operators should standardize their gage pressure for readings on inclined surfaces. For horizontal surfaces the only pressure should be the weight of the gage itself. This will minimize errors due to pressure differentials between different operators.

4.3 Prestressing Steel Strain/Load Measurements

Only two devices were found acceptable for measuring strains or loads at different cross-sections of multi-strand tendons. These devices consisted of the Tensiomag load-measuring system and the bonded foil type of electrical resistance strain gages.

The present researchers tried to obtain more data about Freyssinet's Tensiomag. Representatives of Freyssinet International in the United States were contacted several times to obtain information about their product's accuracy, geometric requirements and price. A few months later, only basic information was provided by the manufacturer's representative in this country. A catalog and a published report of tests and explanation of behavior were later obtained from other sources [88]. Although conversation was established several times with Freyssinet's technical engineers, no information on costs and availability has been obtained to date.

The article published in IABSE Proceedings reported that Tensiomag cells have not been used in tendons composed of more than 12 - 0.6" ϕ 7-wire prestressing strands. However, most of the external and internal tendons for the San Antonio Y bridges were designed for 12 to 19 - 0.6" ϕ 7-wire strands. Another problem related to this system is the lack of portability of the cells, since the only method for moving these devices is by detensioning the tendons to which they are installed.

Without a field report of system reliability, lack of portability, and no serious interest from the manufacturers, the present author recommended to avoid the use of Tensiomag load cells for the San Antonio Y Project.

The only other system with proven reliability and behavior is electrical resistance strain gages. Although several complications are tied to this technology, advances in this field of measurements have been remarkable and some workable system was thought possible. Another factor helping the refinement of this technology was that trial test costs were expected to be minimal since all completion circuits, portable readout boxes, automated scanning units, and data reduction software were readily available at the research facility.

However, the present research team's awareness of the poor long-term performance of electrical resistance gages influenced a decision for finding a secondary "back-up" system for measuring tendon stresses. Tensiomag cells were considered an unreliable and probably expensive possibility. Since no other commercially manufactured devices were available, a new de-

vice --known as the Epoxy Sleeve System-- was developed. Final manufacturing details, operation and trial tests of this new system are included in Section 4.3.2.

4.3.1 Electrical Resistance Strain Gages

These gages comprised the primary system envisioned for obtaining stresses at different cross-sections of prestressing tendons. Trial tests were performed in order to get a better understanding of the current technology and to improve the application of bonded foil type electrical resistance strain gages. The studies were concentrated in the following areas:

- a. Improvements necessary for acceptable long term stability of signals.
- b. Stress differences between wires of a single prestressing strand.
- c. Stress differences among strands in multi-strand tendons.

Final recommendations with respect to the most appropriate type, installation and use of this system of measurements in field studies of segmental box girder bridges with internal and external tendons are included in Chapter 5.

4.3.1.1 Improvements in Signal Stability. Available reports of previous instrumentation projects involving electrical resistance strain gages were carefully reviewed. This was done in order to address the possible causes of failure or success of each program. Factors that directly affected the resulting stability of these gages were studied individually. A thorough investigation of manufacturer technical reports on electrical strain gaging technology helped considerably in the preparation of this section [89].

The following conditions can influence the long-term behavior of bonded foil electrical resistance strain gages:

- a. Width of backup gage matrix.
- b. Material of gage matrix and conductor.
- c. Gage rated resistance and excitation level.
- d. Bonding system and installation.
- e. Moisture protection system for aggressive environments.
- f. Gage completion circuit.
- g. Leadwires.
- h. Connectors used for automated multi-channel scanning systems.

a. Gage Size. The most important dimension regulating maximum size is the width of the backup matrix of the resistors. Most previous researchers at Ferguson Laboratories have used Measurements Group gages of the size type 062AP (matrix size: 6.6mm L x 4.1mm W). *TML* gages size type FLE-1 (matrix size: 5mm L x 2.5mm W) were also popular for laboratory applications. In the present trial tests the project researchers decided to compare three different types of gages. Measurements Group gages of sizes 062AQ (6.6mm L x 3.8mm W), 125BZ (7.4mm L x 3.3mm W) and the previously mentioned 062AP were studied for ease of installation on individual wires of 0.6" ϕ 7-wire prestressing strands. After individual applications for the experimental trials, narrower gages were found easier to install and are recommended for future use. Although slightly longer, the 125BZ gages performed the best during the installation process and provided the least amount of problems with improper bonding of the sharply curved sides. *TML* manufactured gages were not investigated. However, the size type FLE-1 should also provide acceptable results.

b. Gage Material. It is important to choose the most appropriate material for the gage's conductor and backup matrix in order to reduce errors associated with temperature differentials. Obviously, more accurate conductor materials will be those for which temperature differentials have smaller effects on their electrical resistance properties. These special conductors of low resistance variations with temperature fluctuations are available for a considerable increase in cost. Their price can be as much as double the price of conductors of "moderate" accuracy.

An important effect of temperature fluctuations consists of the linear variation of the length of the prestressing strand. This increase or decrease in strand length is measured as stress-induced strain by the bonded foil gages unless it is properly accounted for. The resistivity of the strain gage's conductor wire also varies with temperature, and this is also measured as stress-induced strain by the gage readout units. Temperature induced strains in the strand and in the gages are commonly known as *apparent strains*.

The first method of compensating for temperature was the use of a "dummy" unstressed strain gage bonded to the same material --but unstressed-- and at the same environmental condition as the principal gages. Compensation was then achieved by installing both gages on opposite legs of a Wheatstone bridge circuit in order to cancel their strains. This is possible to be implemented with measurements in prestressing strands by gaging a small unstressed strand specimen located next to each instrumented cross section of the stressed strand. However, this

procedure would increase final instrumentation costs to a large degree due to the addition of the extra gage, and due to the additional Wheatstone bridge circuits in the data acquisition system.

The second method for avoiding apparent strains is to use temperature compensated strain gages currently offered by most gage manufacturers. Measurements Group offers two types of temperature self-compensating materials, constantan (A-alloy) and a more expensive modified karma (D-alloy). To compensate for strains suffered by the material where these gages are to be installed, strain manufacturers use an S-T-C (Self-Temperature-Compensation) number. This number matches the linear coefficient of expansion of most structural materials. For prestressing strands, an S-T-C factor of 09 approximates well the linear coefficient of expansion of high-strength steel (with $\alpha \approx 8$ PPM/°F).

Temperature compensated constantan gages provide the best behavior for smaller temperature variations. Inside the box-girders of the San Antonio Y segmental bridges a maximum temperature differential of 80°F is the most expected between top summer heat and the coolest measurement day in the fall. When bonded to high-strength steel, errors due to *apparent strains* from temperature differentials in the order of 80°F will only represent about 10 $\mu\epsilon$ for 09 S-T-C constantan gages. When high precision measurements are required, compensation for even such small differences can be done with the formula provided on each individual package of strain gages. Calibration formulas for 09 S-T-C gages are usually prepared from manufacturer tests on 304 Stainless Steel. They have a thermal expansion coefficient of about 9.6 PPM/°F, which is slightly higher than for the low-relaxation prestressing strands. The difference of 1.6 PPM/°F should not matter for the smaller temperature differentials expected for the present project. However, it was found that better performance can be provided by 06 S-T-C gages. Their calibration tests are usually made on 1008-1018 Steel with $\alpha=6.7$ PPM/°F thus providing an S-T-C mismatch of only 1.3 PPM/°F. These gages were therefore recommended for the present instrumentation project.

c. Gage Resistance and Excitation Level. Another inconvenience with electrical resistance measurements is that signals are usually quite small. This is worsened when the physical property to be measured varies only slightly, as is expected for the long term tendon stress fluctuations of the San Antonio Y structures. Even in cases of overloading of this type of structure, the stress variations on the tendons are expected to be small. MacGregor's model study of an external tendon segmental box-girder bridge found a maximum stress increase of only 5ksi for

factored design live load plus impact, and up to 8ksi for cracking loads [74]. To successfully measure and distinguish these small movements with electrical resistance strain gages it is necessary to have stronger electrical signals. An easy way to achieve this is by using slightly higher resistance strain gages and their corresponding higher excitation levels. Most previous short-term static testing of structures used lower 120Ω strain gages. The present project researchers decided to use the next standard gage resistance of 350Ω . Gage resistances above 350Ω are not standard but still available at higher prices and lower turn-around times.

The most appropriate excitation for strain gages depends on gage rated resistance, gage size, and type of material to be instrumented. For Measurements Group gages of the type EA-125BZ-350 (Option LE) bonded to high-strength steel of prestressing strands (which provide a good level of heat dissipation) an optimum excitation level of 4 to 5V was calculated from manufacturer tables [90]. Conservatively, an excitation level of 4.5V would prevent self-heating strains in these gages.

d. Bonding System. Cyanoacrilate (i.e. Super Glue) type of adhesives are usually the preferred bonding system due to their ease of installation. Most previous short-term laboratory tests investigated have used the M-Bond 200 cyanoacrilates from Measurements Group. As easy and fast as they are to use, cyanoacrilates are not recommended for long-term projects due to their lower bond life. More durable epoxy-based glues should be used when stability for longer periods of time is desired. Besides higher costs, added complications of epoxy glues are their slower drying period and stricter installation requirements. During installation of gages with epoxy adhesives, an evenly distributed surface pressure over the strain gages has to be exerted in the drying period to obtain proper bond. This is complicated by the small curved surfaces of individual prestressing strand wires and the tight arrangements of strands in a tendon.

Use of epoxy adhesives was investigated for the instrumentation of the San Antonio Y structure. The final type of adhesive selected for testing was Measurements Group's AE10 since it dries faster --at normal temperatures-- than other epoxies. For proper gage installation, a method of providing even drying pressure on the surface of the strain gages bonded to single wires of prestressing strands was also investigated. Small plastic molds of individual $0.6\text{''}\phi$ 7-wire prestressing strands were prefabricated with a special silicone. The product used for these molds was General Electric RTV-620 Silicone. Plastic silicone molds of $\approx 1\text{''}\phi$ were precast around small prestressing strand pieces and dried --keeping a vertical position of the strand

pieces-- at normal temperature for a period of 4 to 7 days. Cutting a longitudinal line on one side of the dried plastic molds enabled them to be easily pulled out in jackets of 1" to 1 ½" lengths. For tests on individual strands, these small jackets were fitted at the strain gage's location and even pressure was applied by tightening a small hose clamp around each jacket. The hose clamp tightening procedure should be carefully applied since high pressures can squeeze too much epoxy resin from underneath the foil gages. Ideally, the clamping pressure on the gages should be between 5 and 20psi. When using strain gages with pre-attached leadwires (Measurements Group Option LE) a small piece of Teflon tape or clear plastic sheet was placed between the leadwires and the instrumented surface of the strand. This was done before the installation of the silicone jackets in order to prevent bonding of the leadwires to the prestressing steel.

For multi-strand tendons the procedure was slightly different. Since the silicone jackets could not be wrapped all around individual strands, they were cut in three sections. These cuts were done in a way which ensured that a full wire's cross section would be in the middle of each piece. These smaller silicone pieces were later placed on top of each previously installed strain gage. A larger hose clamp placed around the cross section of the tendon was used for the application of even surface drying pressure on each strain gage. Trial tests with these systems performed well and installation was not difficult to carry out. However, practical experience and strain gage handling care of the operators played an important role for optimum installation. The largest problem with this bonding method was the long time period needed for proper epoxy drying. At normal temperatures ($\approx 75^{\circ}\text{F}$) the clamped gages must be dried for no less than five hours.

e. Moisture Protection System. Humidity protection of the gage is one of the most important factors because it has serious influences on the initial stability of the system. If excess humidity is present, three different effects are possible: an electrical short of lead wires, a gage resistance change due to electrochemical corrosion of the lead wires or foil, or a breakdown of the bonding material. Waterproofing must therefore provide a high degree of bond to the strain gage, and at the same time should not be stiff enough to cause resistance to movements of the instrumented surface.

Several methods for avoiding moisture intrusion in the strain gages have been used in the past. Yates achieved good performance by unwinding each individual wire of a strand, in-

stalling the gage and its protection scheme and later rewinding the whole system [73]. This is impractical for the present project where great lengths and number of strands are expected. Other methods have been used less successfully and are based on standard manufacturer recommendations. These performed poorly on most long-term projects. The combination of grouting of tendons and the very small tightly curved surfaces of individual wires of each strand becomes a highly aggressive environment for a proper gage protection scheme. Since prevention is a better technique for avoiding physical or moisture damage to strain gages, a method for maintaining a dry atmosphere around the gages by blocking off certain sections of external tendons during the grouting process was developed. In order to replace the grout as a corrosion protection system, these blocked sections of external tendons were protected against corrosion (after mounting of the gages) with high quality greases. Greases have the added benefit of enhancing the moisture protection of the strain gages, and they can be easily removed if a strain gage needs to be replaced in the future.

More elaborate schemes were investigated for protecting strain gages placed in areas that necessarily have to be grouted. Epoxy based coatings were found to work satisfactorily. The M-Coat J system from Measurements Group was characterized as having enough consistency to stay in place after placement. It also spread well in tight areas between strand wires. Before coating gages with M-Coat J epoxy a small piece of Teflon tape was usually placed on top of the installed gages to prevent a bond to their epoxy cover. After placement of the epoxy, liberal amounts of microcrystalline wax in a larger area around the epoxy was found to help the moisture protection scheme. These small wax plates were easily liquefied with air blow driers. Other moisture protection schemes based on nitrile rubbers did not work well in grouted environments.

f. Gage Completion Circuit. Different Wheatstone bridge completion circuits provide varying degrees of accuracy and cost. The most popular system for laboratory applications due to cost and ease of configuration consists of the quarter bridge circuits. Quarter bridge Wheatstone networks can have two or three leadwires attached to a single strain gage. This is important when long lead-wires are necessary, or when large temperature differentials are expected to occur during the test schedule. Both of these factors bear influence on the San Antonio Y instrumentation project. Leadwire lengths of up to 60ft are necessary and temperature differentials of up to 80°F are possible. Three-leadwire quarter bridge completion circuits directly compensate

for temperature differentials in the length of the wires, provided that both wires connected to the single strain gage terminal have the same length and undergo the same temperature differentials. This is a proven electrical characteristic of the Wheatstone bridge and no tests were performed between two- and three-leadwire quarter bridge circuits. Temperature compensation systems are strongly recommended for long-term instrumentation projects. A detailed explanation of the benefits and complications related to each possible completion circuit configuration was presented by Dunnicliff [60] and should be consulted when other circuits are under consideration.

g. Leadwires. Their selection is also important for final system stability. Factors influencing proper leadwire selection are physical protection and electrical noise reduction. Jackets around individual leadwires are necessary for physical protection. Electrical noise produced from large currents or electromagnetic sources can be diminished by threading individual leadwires in winding arrangements. This type of leadwire can be obtained from most electrical wire manufacturers. Trial tests were successfully performed with Belden conductors of the type 8771. These consisted of stranded tinned copper, polyethylene insulated conductor cables of size 22AWG (American Wire Gage). Added electrical noise reduction of the stranded three-leadwires was provided by an encapsulation of aluminum-polyester shield, and physical protection was provided by a chrome PVC jacket.

An important concern related to long lengths of leadwires is the introduction of an extra electrical resistance that dampens the readings of strain induced resistances. For the selected type of leadwires and strain gages, the original gage factor should be desensitized to account for long leadwire lengths. Strain gage manufacturers suggest the following procedure to quantify the effect of leadwire lengths [89]:

$$GF_D = GF_0 * \frac{R_G}{R_G + R_W}$$

GF_D = desensitized value of gage factor

GF_0 = original gage factor (provided by manufacturer)

R_G = gage resistance in Ohms

R_W = effective leadwire resistance (for a three leadwire quarter bridge configuration this should be the resistance of one single leadwire).

For the suggested gages of the type Micro Measurements EA-06-125BZ-350, Belden type 8771 leadwires, and for average lengths of 35ft expected for the present applications in the San Antonio Y bridges, the desensitized factor becomes:

$$GF_0 = 2.085$$

$$R_G = 350\Omega$$

$$R_W = 35 * 0.01474 = 0.5159\Omega$$

$$\therefore GF_D = 2.082$$

Evidently, neglecting this factor of correction only implies an error of 0.14% on each strain reading. Furthermore, this small error only influences absolute readings and not strain differentials.

h. Connectors. Another source of *parasitic resistances* comes from electrical resistance variations due to different connections of strain gage leadwires. A good connection of two electrical wires --with minimum losses in resistance-- is difficult to achieve. Moreover, an exact reproduction of a connection of two electrical wires is difficult to replicate. Factors affecting these two complications are not only related to physical differences in the connections but also due to temperature differentials. Evidently, the electrical resistance related to an individual connection at a point in time with one certain temperature will be different than the resistance of the same connection at a later time with a different temperature. This is because the resistivity of the connector's materials varies with temperature. One method of solution envisioned by the present researchers was to establish a "permanent" connection of all leadwires to each strain gage channel. Although this does not fully eliminate all *parasitic resistances*, it avoids the introduction of electrical resistance differentials due to varying physical connections. However, this is ineffective to achieve in multi-channel systems, since no connectors would imply a permanent readout unit for each channel. To make the system more effective, a high quality multi-channel switching device was purchased. This electronic device had the characteristic of reducing differences in electrical resistance variations during different scans by using gold-plated connectors. Temperature induced differentials were also minimized with these systems. The multi-channel switching device purchased was the *AMD-416 Multiplexer* manufactured by Campbell Instruments, Inc. This was also compatible with the electronic data acquisition system and is further described in Section 4.5 of this report.

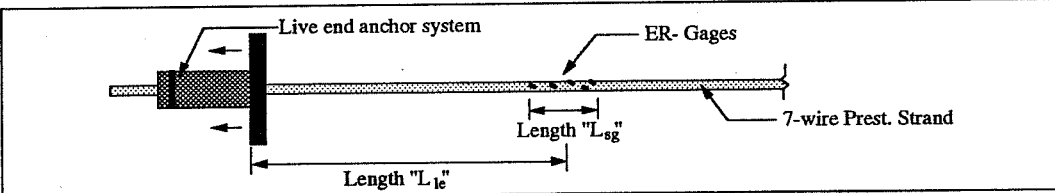
4.3.1.2 Single Strand Tests. Electrical resistance strain gages measure strains of individual wires of the prestressing strands to which they are bonded. Yates [73] indicated that the strains experienced by each wire of a 7-wire prestressing strand can vary substantially. A plot of his results for one particular strand test was previously included as Figure 3.10. Although each wire behaved differently at low stresses, the slopes of the best-fit lines of high stress data points seemed to be approximately the same. In most of these and other previous single strand tests, the "apparent" modulus of elasticity defined by the slope of the best-fit line of the stress-strain plot obtained from each electrical resistance strain gage was slightly larger than the manufacturer provided data.

The present researchers considered it necessary to perform a few more tests with electrical resistance strain gages bonded to single wires of prestressing strands to better understand their overall behavior. These tests were also performed to investigate the performance of various types of strain gages and bonding methods. Finally, it was desired to suggest a more standardized procedure for the data reduction process.

a. Test Descriptions. A total of four single strand tests were performed. Three strand specimens of approximately 3.5ft lengths were used in the first three tests. These specimens were taken from two different rolls of $\frac{1}{2}$ " ϕ 7-wire low-relaxation prestressing strands manufactured by Florida Wire and Cable Company. A 7ft specimen was used in the fourth single strand test. This specimen was taken from a roll of 0.6" ϕ 7-wire low-relaxation strand also manufactured by Florida Wire and Cable Company. Two loading cycles were performed in the final single strand test. Standard anchorage equipment used in all single strand tests consisted of 3-wedge anchor systems manufactured by Supreme Industries Inc. General descriptions related to the strain gages, their physical position, and the stressing system used for each test are included in Table 4.4.

Electrical resistance strain gages of the foil type were bonded to each one of the six external wires of each strand specimen. In TEST 1S and TEST 4S each set of six gages were carefully installed in one particular cross-section of the strands, as shown in Figure 4.7. The cross-sections passing through the middle of each gage had a longitudinal separation of less than 5mm (0.2in.). However, in the specimen used for TEST 2S and TEST 3S the gages were spread over a length of 10cm (4in.). Only gage #1 of TEST 1S was damaged during installation. The testing systems used for TEST 1S and TEST 2S are shown in Figures 4.8 and 4.9 respectively.

In most tests, strand strains were automatically scanned with a computer-controlled data acquisition system. However, a portable strain indicator box connected to a switch and balance unit was used in TEST 3S. Load levels were obtained either from the scale readings of a 60kip vertical loading machine (TESTs 1S and 2S) or from readings of an electrical resistance load cell (TESTs 3S and both loadings of TEST 4S) installed at one of the anchoring ends of the strands. All electrical measuring devices (strain gages and occasional load cell) were connected to the data acquisition system for the complete duration of each test. Errors due to temperature differentials were minimal due to the short duration of each test. Moreover, no errors due to existence of *parasitic resistances* were assumed to be present since the gages were permanently connected to the data acquisition system (i.e. for the complete duration of each test).



	TEST 1S	TEST 2S	TEST 3S	TEST 4S (a & b)
Strand Characteristics:				
a. Strand Roll	A	B	B	C
b. Diameter [in]	½	½	½	0.6
c. Type	7-wire, low-lax	7-wire, low-lax	7-wire, low-lax	7-wire, low-lax
ER- Gages:				
a. Manufacturer	Measurements Group	Measurements Group	Measurements Group	TML
b. Description	EA-06-125BZ-350	EA-06-062AQ-120	EA-06-062AQ-120	FLE-1 (120Ω)
c. Length "L _{sg} " [in]	0.5	4	4	0.5
d. Length "L _{le} " [in]	23	8	4	20
Stressing Method	Loading Machine	Loading Machine	Hydraulic Jack	Loading Machine

Table 4.4 Descriptions of single strand tests.

b. Data Reduction Method. Stress values of each strand were obtained by considering the nominal areas of 0.153in^2 and 0.215in^2 for the $\frac{1}{2}$ " ϕ and the 0.6 " ϕ strands respectively. Since no stress losses can be reasonably expected to occur between the instrumented section of the strand and the section where loads were measured, the corresponding values of stress and strain were plotted on a single σ - ϵ graph. A best-fit line was defined considering the data points of the σ - ϵ graph that corresponded to stresses between $0.20f_{pu}$ and $0.80f_{pu}$. This procedure thus

avoided the consideration of initial nonlinearities in the graph (usually occurring during seating of the strand specimen at the anchor ends). The slopes of the best-fit lines corresponding to each workable electrical resistance strain gage installed in each specimen were recorded. The prestressing strand's apparent modulus of elasticity was determined by the average of these slopes.

Since electrical resistance strain gages are installed at a certain angle from the longitudinal axis of a strand, it was expected to find a slightly different modulus of elasticity than determined by strand manufacturers. To help quantifying the possible value for the "apparent" modulus defined by an electrical resistance strain gage, an analytical study of the phenomena was performed. This study is summarized in Figure 4.10. The drawing in this figure represents a 7-wire prestressing strand specimen (drawn with an exaggerated high pitch and small wires to better show the extreme behavior). If this sample specimen were completely anchored at the beginning and at the end of the instrumented wire's single loop, the strand strains would be 3.7% to 6.4% higher than the single wire's strains (for the same stress level). This directly implies that the strand's modulus of elasticity is slightly smaller than the single wire's modulus due to their different geometric conditions.

As explained in Section 3.2.2, the modulus of elasticity tests performed by strand manufacturers approximately measure average strains of the whole strand, whereas the electrical resistance strain gage approximately measures a single wire's strain. This difference in testing devices combined with the theoretical example of Figure 4.10 show that it is expected that strands will have a slightly larger apparent modulus of elasticity when performing measurements with electrical resistance strain gages. It is difficult to accurately predict how much larger would the apparent modulus be (because other factors different than the strand pitch influence the results). However, to avoid a potential source of error it is strongly recommended to always perform material tests of the prestressing strand specimens with the same instrumentation devices that will be used either in the laboratory or in the field. In the data reduction process the "apparent" modulus determined by each instrumentation device should be used accordingly.

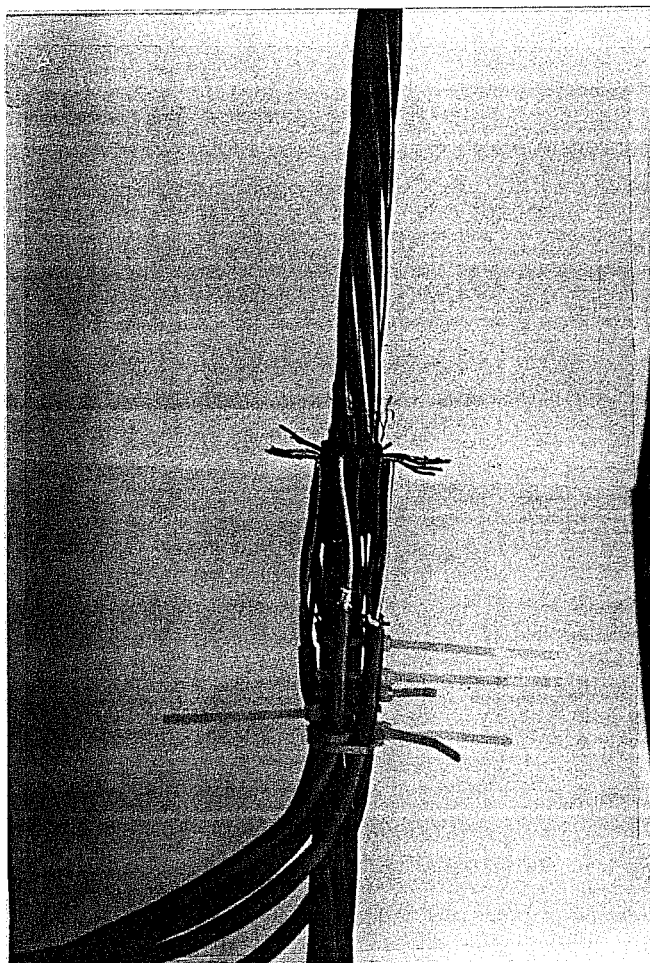


Figure 4.7 Installation of the electrical resistance strain gages for TEST 1S
(similar to TEST 4S).

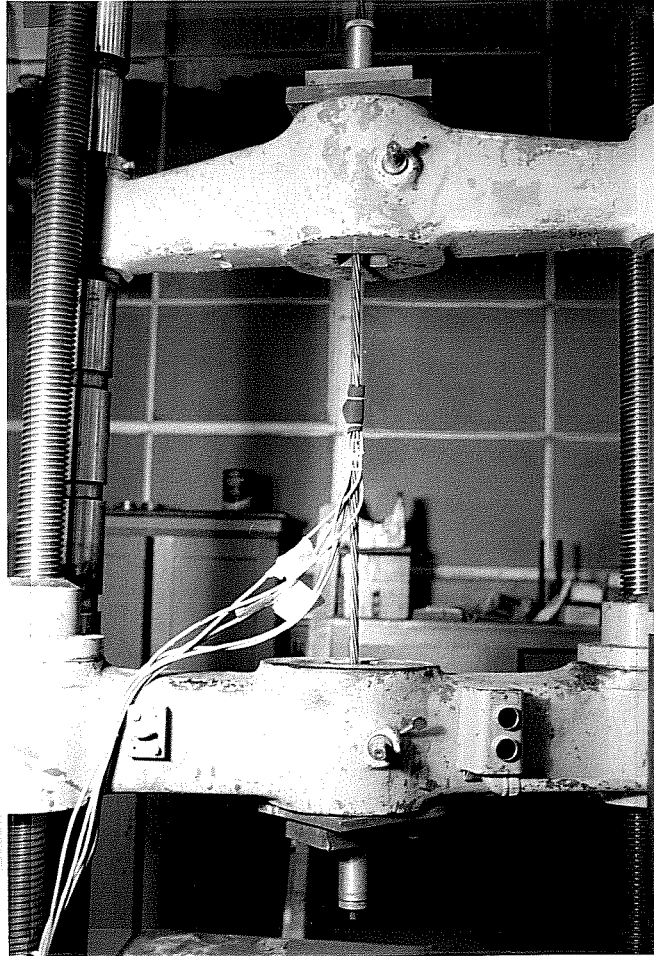


Figure 4.8 Single strand TEST 1S.

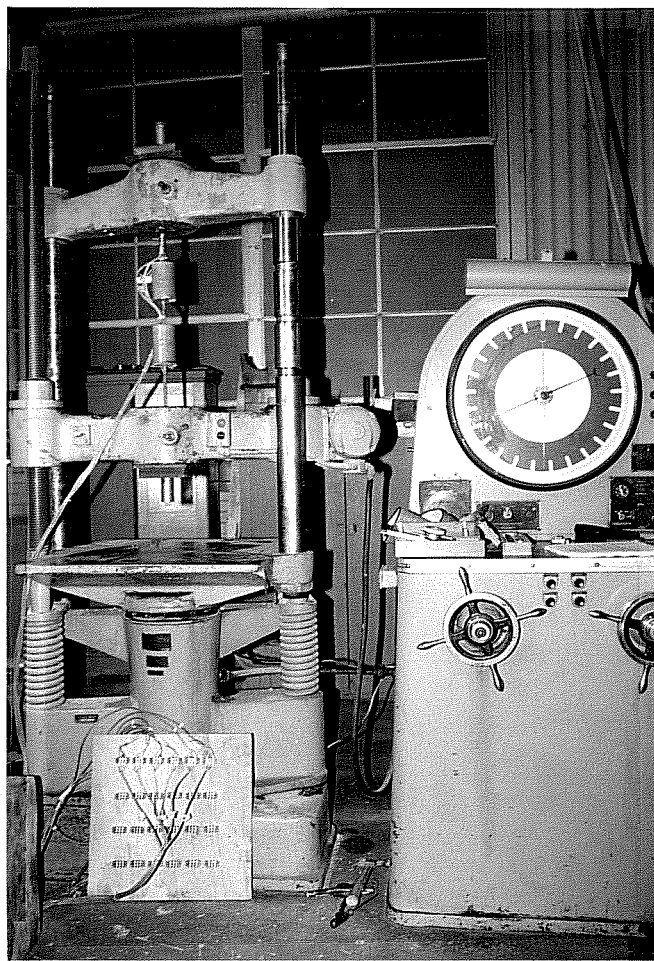
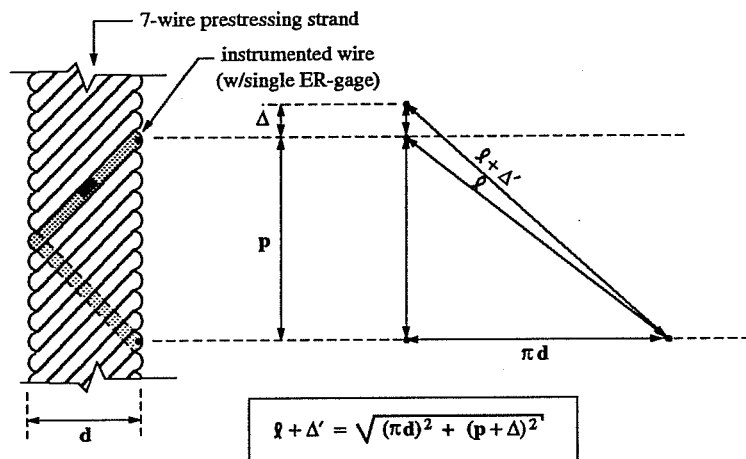


Figure 4.9 Single strand TEST 2S.



where:

l : length of instrumented wire corresponding to 1 revolution around the strand.

Δ : strand elongation.

Δ' : wire elongation.

ϵ : strand strain.

ϵ' : wire strain.

p : pitch of the strand.

d : nominal strand diameter.

* **Manufacturer tolerance in strand's pitch:** 12 to 16 strand diameters.

* **Effect on apparent modulus determined by electrical resistance strain gages:**

(same for $\frac{1}{2} \phi$ and 0.6ϕ strands)

Pitch	$\left(\frac{\epsilon'}{\epsilon} \right)$
12 d	0.936
16 d	0.963

Figure 4.10 Analytical approximation of a prestressing strand's apparent modulus of elasticity, as determined by electrical resistance strain gages bonded to individual wires.

c. Interpretation of Results. The measured behavior of the strand wires in each single strand test are plotted in Figures 4.11 through 4.16. Final statistics of the results from both tests performed with the specimens taken from strand roll "B" ($\frac{1}{2}$ " ϕ strand) are included in Figure 4.17. The statistics of the results from both tests with the single specimen from strand roll "C" (0.6" ϕ strand) are included in Figure 4.18.

In general, it was found that the variation of strain readings among the wires of each individual strand was considerably lower than the values obtained by Yates (previously shown in Figure 3.10). Differences between the present test results and those from Yates' are probably caused by a combination of the following factors:

- type of strand,
- type of anchorage,
- type of stressing system,
- distance from ER-gage to anchorage (" L_{1e} " on Table 4.4), and
- separation of ER-gages (" L_{sg} " on Table 4.4).

As mentioned earlier in this report, during initial stressing operations the wires of a prestressing strand are engaged at varying degrees of tightness by the stressing hardware. It is therefore logical to find large differences of stresses between wires. However, the present author believes that due to the helical arrangement of the wires the stress gradient between them should decrease at sections farther away from the anchorage ends. According to this train of thought, the wires should experience similar strains at sections beyond the "stress distribution length" from either end of the strand. The present test results agree with this hypothesis. TEST 1S and TEST 4Sb (second loading of the strand specimen of TEST 4S) had longer *stress distribution lengths* during testing. They also had very linear placement of the strain gages on a single cross-section of each strand specimen. The results from these two tests (shown in Figures 4.11 and 4.15) indicate quite similar behavior of the wires of each strand, even at low stress levels. Results from the other single strand tests indicate slightly irregular behavior at low stress levels, as shown in Figures 4.12, 4.13 and 4.14.

An interesting observation can be drawn from the results of TEST 4SA (Figure 4.14, first loading of the strand specimen of TEST 4S). One of the single strand anchorages of this test was accidentally left at an angle from the longitudinal axis of the strand thus causing certain wires to be stressed at a higher level than the others. The severity of this stress differential

between wires was not corrected by the long *stress distribution length* of this particular test setup. During the second loading of the same specimen --with the only difference of correcting the anchorage's positioning-- the wires behaved quite similarly (as shown in Figure 4.15).

The theory of stress distribution among the wires of a strand can thus be different in most practical applications of prestressing. Friction between strands and deviation ducts in multi-strand tendons, uneven strand lengths between anchor assemblies, and variations in the positioning of end anchors can all modify the redistribution of stresses among wires of each strand. But even with these unfavorable conditions, at high stress levels each wire should still behave similarly. This is partially addressed in the following section, where tests on multi-strand tendons deviated at small angles were performed.

A further analysis of the single strand test results was carried out to find the stress level at which all wires became engaged to the stressing hardware. Gradually eliminating low stress points and performing best line fits of the results from the single strand tests suggested that $0.20f_{pu}$ was a conservative low stress mark after which all wires strain more similarly. All data reductions were thus performed between this low level of stress and a stress level just below $0.80f_{pu}$ (to safely avoid measuring the plastic behavior of prestressing steel).

Interesting remarks can be drawn from the combined statistical analysis of the results of the tests performed with the strand specimens taken from rolls "B" and "C" (included in Figures 4.17 and 4.18). From the twelve statistical observations it was found that the variabilities of the average modulus of elasticity of the $\frac{1}{2}$ " ϕ and the 0.6" ϕ strand specimens were $\pm 1.91\%$ and $\pm 1.35\%$ respectively. In the tests with the 0.6" ϕ strand specimen the loads were computed from readings of a high definition electrical resistance load cell that was simultaneously scanned with the strain gages. This must have been one of the main reasons for improving the variability of the apparent modulus to under $\pm 1.5\%$. Future material tests are thus recommended to be performed with calibrated load cells scanned simultaneously with the electrical resistance strain gages.

Another comment from the statistical analysis of the test results is the slightly larger apparent modulus recorded by the electrical resistance strain gages. A manufacturer obtained modulus of elasticity of 29,100ksi was supplied with the prestressing strand roll "B" (used to take the two specimens for TESTs 2S and 3S). The statistics of Figure 4.17 indicate an apparent average modulus of 30,881ksi for the two specimens from this strand roll. This is 6.1% larger

than the manufacturer supplied value and still within the analytical range previously computed in Figure 4.10. No manufacturer value was obtained from the prestressing strand roll "C" (corresponding to the 0.6" ϕ strand specimen). However, the average apparent modulus (29,488ksi) is still slightly larger than the 28,900ksi to 29,100ksi typical range of manufacturer modulus.

d. Conclusions. The following conclusions can be drawn from the electrical resistance strain gages bonded to single prestressing strands:

- a. When all electrical resistance strain gages are installed at one particular cross-section and at an equal distance of no less than 24in. from the anchorage ends, the gages were found to measure similar values of strains (even at low stress levels).
- b. Calibrated load cells scanned at the same time as the electrical resistance strain gages were found to improve the variability of the average apparent modulus of elasticity obtained in the data reduction process. With calibrated load cells, the apparent modulus of elasticity determined by a single ER-gage was found more likely to be within $\pm 1.35\%$ of the average strand modulus.
- c. When computing the linear regression of measured data points on a σ - ϵ graph, it was found better to consider only the points that corresponded to stresses between $0.20f_{pu}$ and $0.80f_{pu}$. This prevented any consideration of errors related to the initial differential seating of the wires, or to the plastic behavior of the prestressing steel.
- d. The slopes of individual σ - ϵ lines (the "apparent" modulus of elasticity) obtained from the electrical resistance strain gages were found repeatedly higher than manufacturer given values. This is mainly attributed to the different measurement system used by strand manufacturers. Since most single strand tests are performed as material checks of the modulus of elasticity and the overall behavior of the strands from a particular structure, the measured "apparent" modulus of elasticity should be consistent with the instrumentation device to be used in the actual tests of the structure.

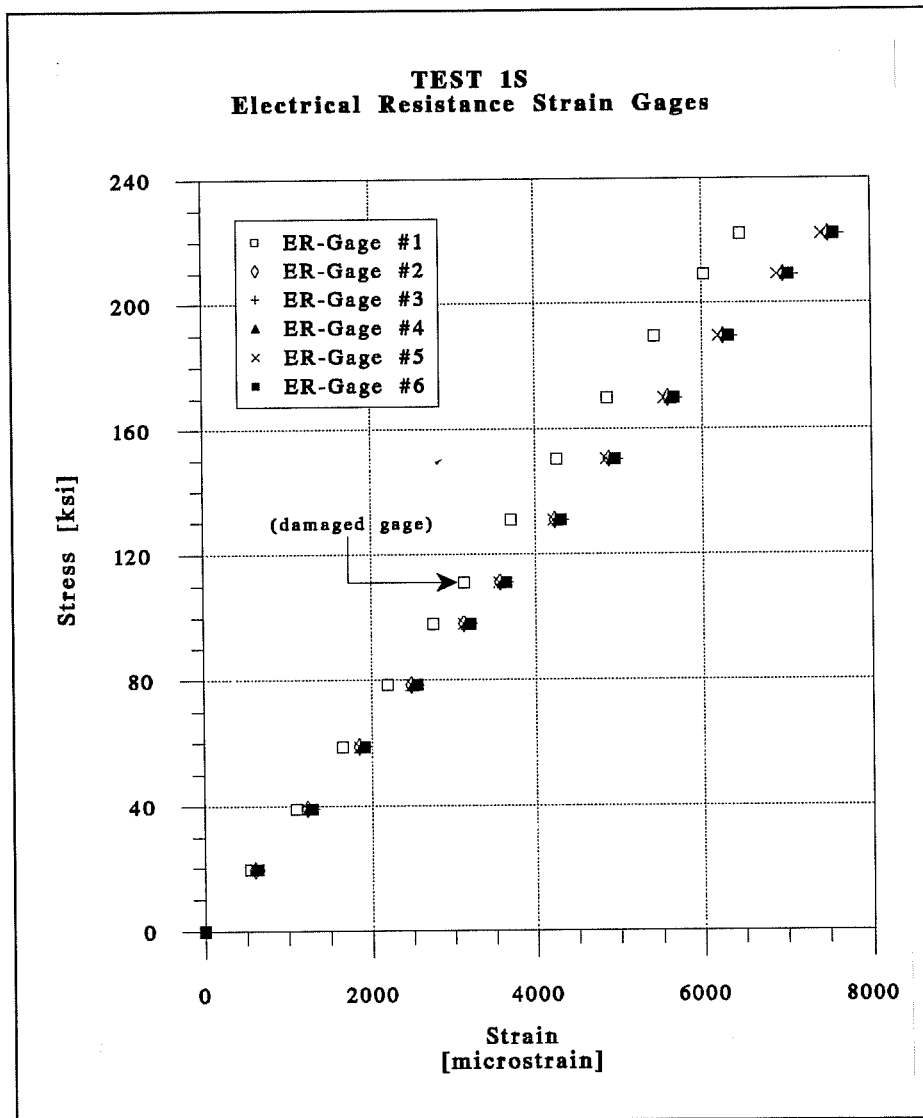


Figure 4.11 Stress-strain curves for TEST 1S on $\frac{1}{2}$ " ϕ strand specimen from roll "A".

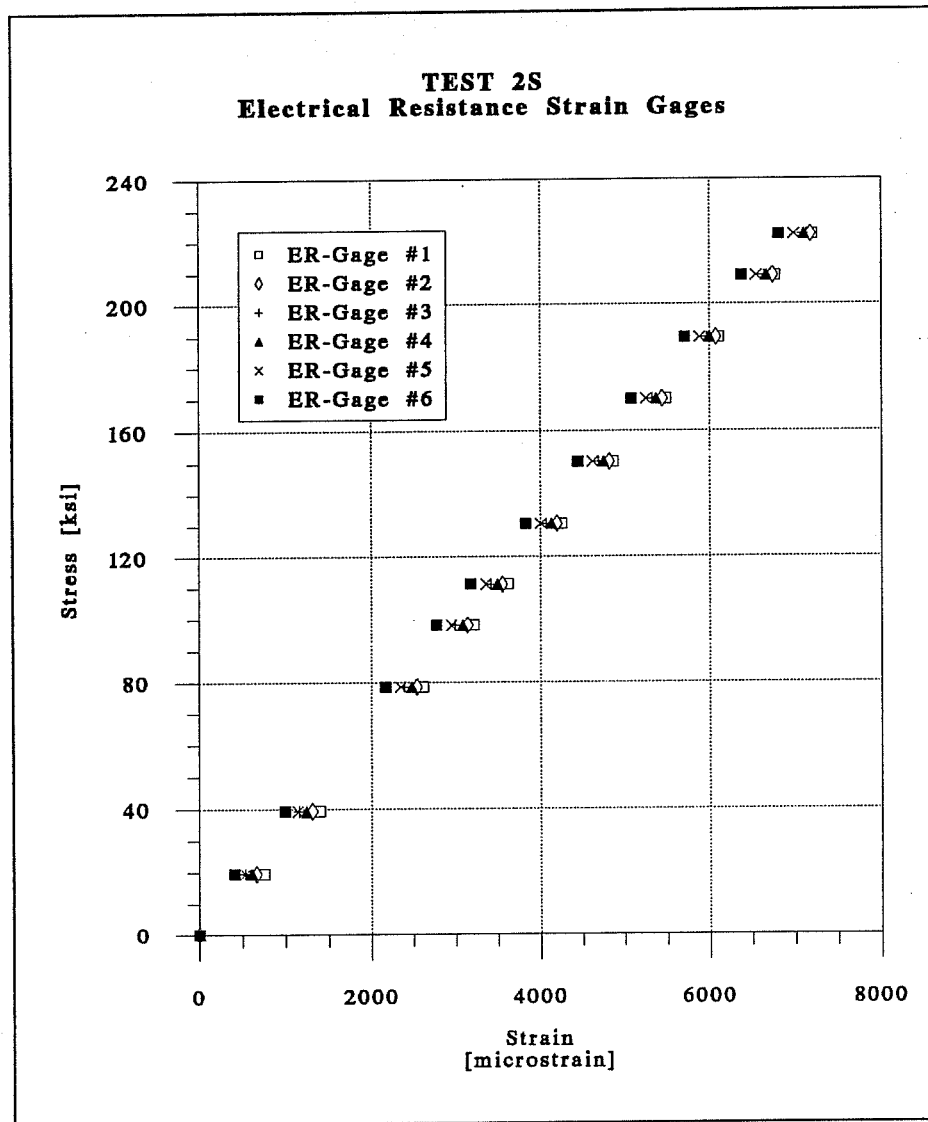


Figure 4.12 Stress-strain curves for TEST 2S on first $\frac{1}{2}$ " ϕ strand specimen from roll "B".

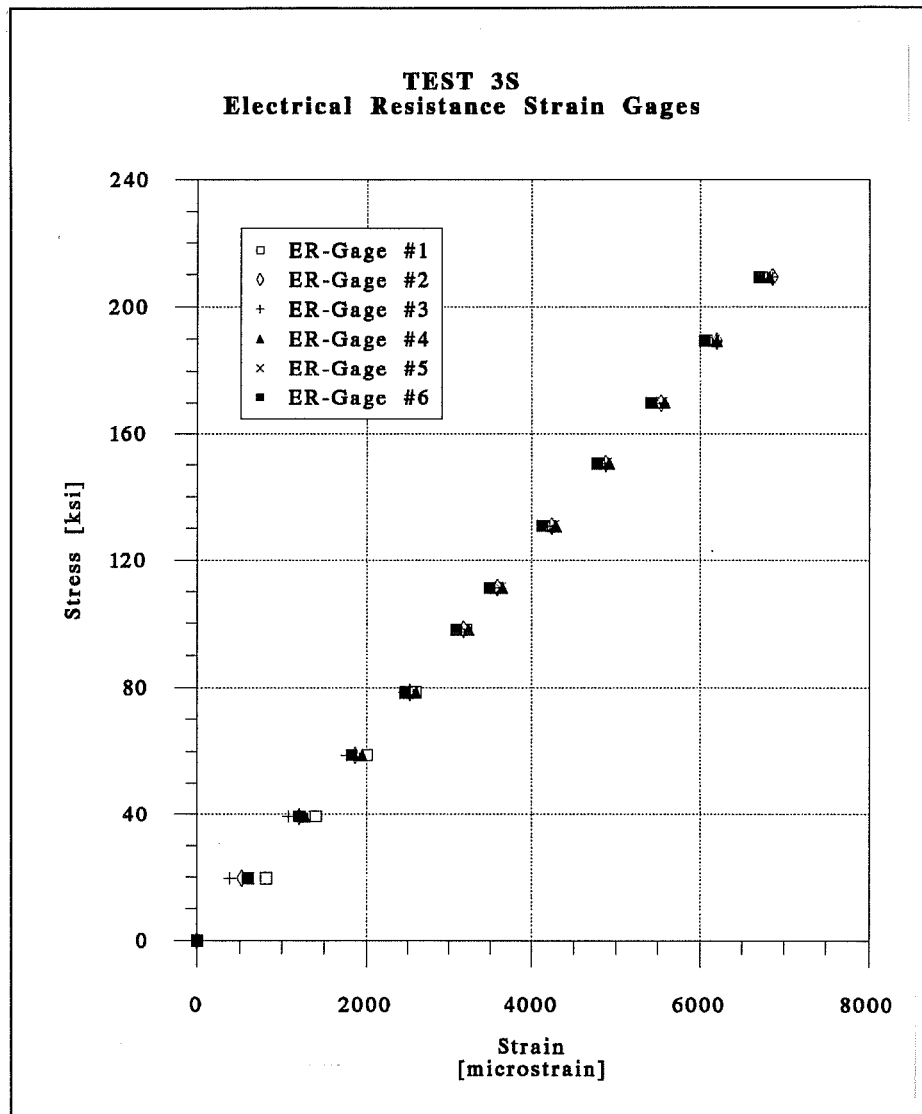


Figure 4.13 Stress-strain curves for TEST 3S on second $\frac{1}{2}$ " ϕ strand specimen from roll "B".

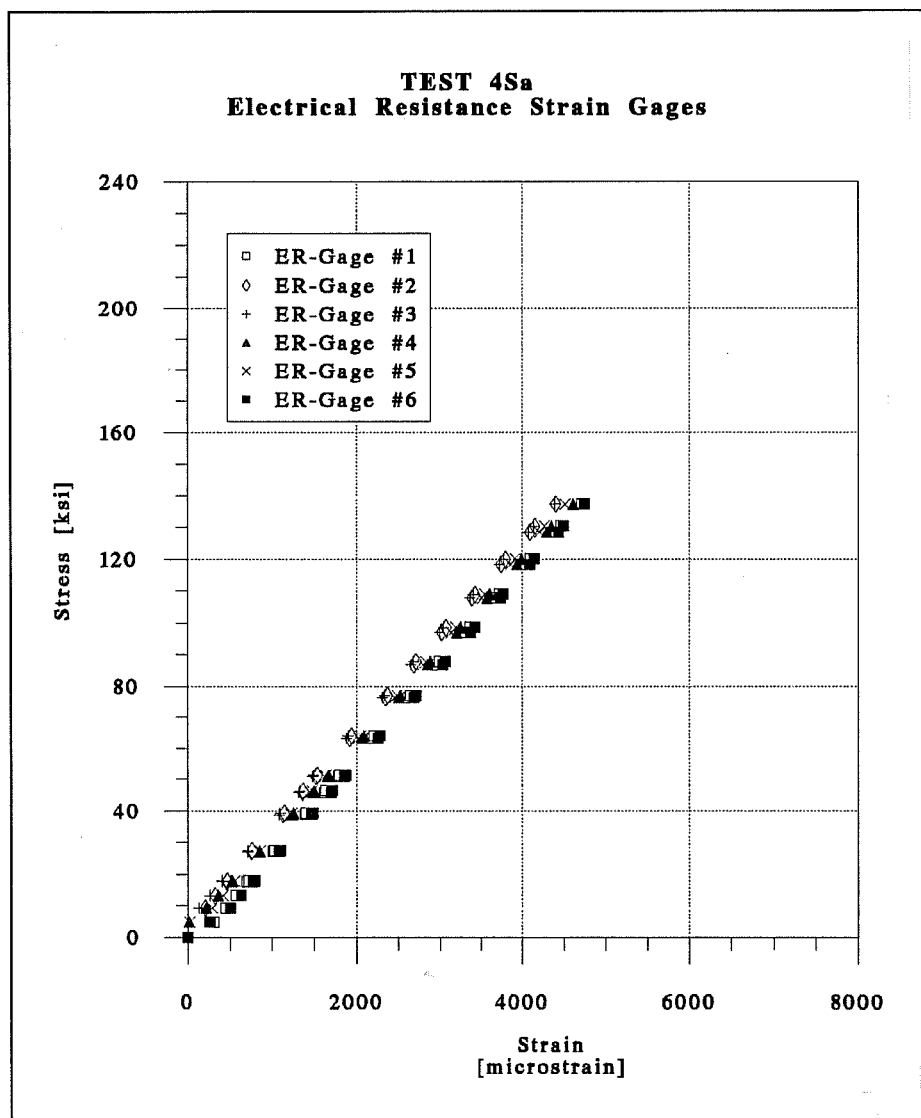


Figure 4.14 Stress-strain curves for first loading cycle of TEST 4S on 0.6" ϕ strand specimen from roll "C".

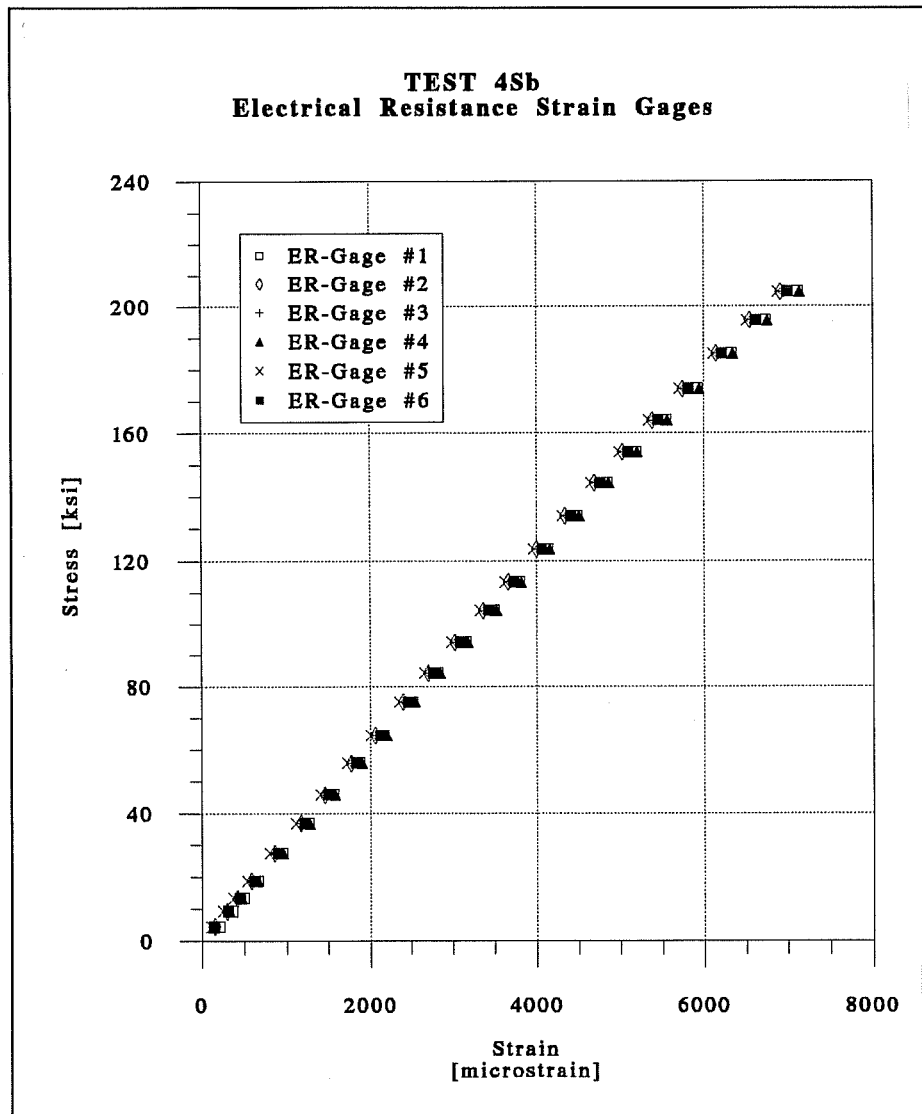


Figure 4.15 Stress-strain curves for second loading cycle of TEST 4S on 0.6" ϕ strand specimen from roll "C".

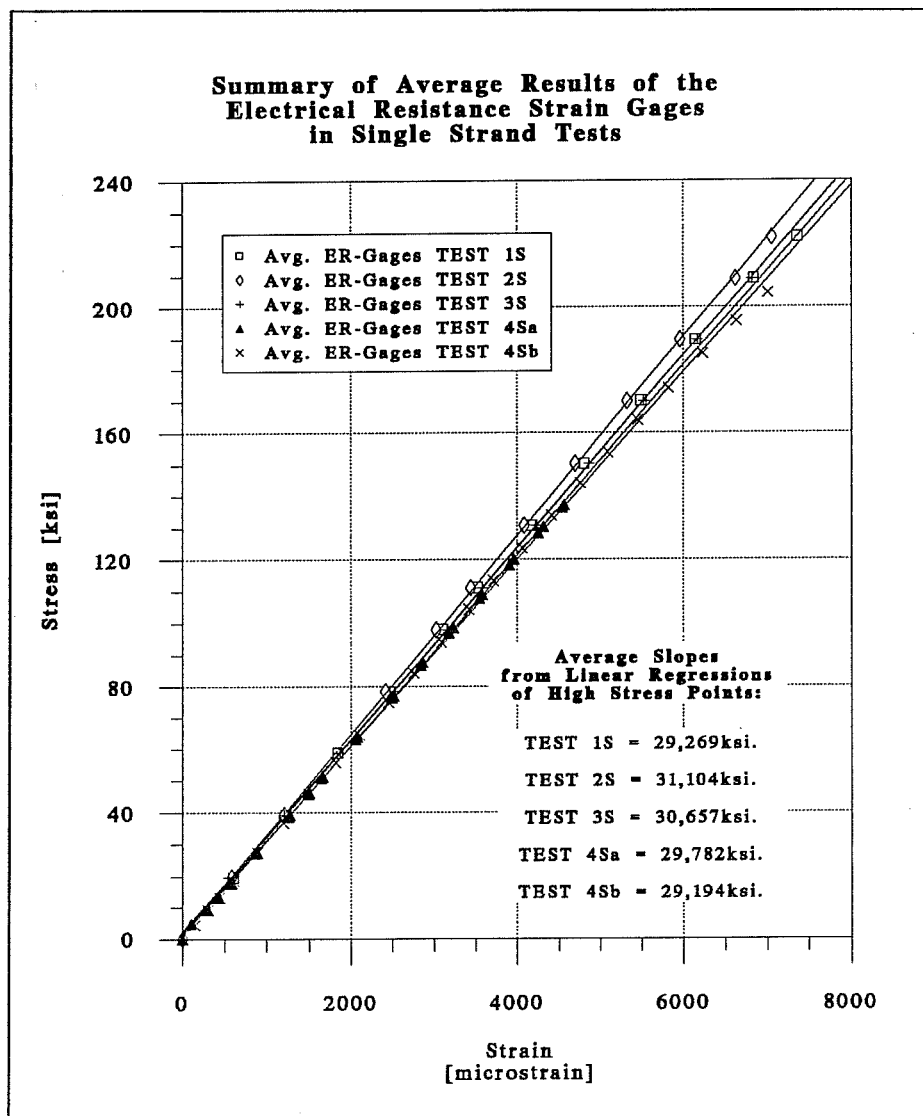


Figure 4.16 Summary of stress-strain average curves of single strand tests with ER-gages.

Summary of results from tests of specimens from strand roll "B" (½" diameter):

		Computed Modulus of Elasticity *		Statistics of ER-Gages (from both TESTS):
		[ksi]		
		TEST 2S	TEST 3S	
ER-Gage #1		31470	31838	
ER-Gage #2		31087	30172	
ER-Gage #3		30720	29548	
ER-Gage #4		31238	30796	
ER-Gage #5		31098	30743	
ER-Gage #6		31010	30846	
Statistics of ER-Gages (per TEST):	Min.:	30720	29548	29548
	Max.:	31470	31838	31838
	St. Dev.:	248	765	590
	Avg.:	31104	30657	30881
	Variability of Avg.**:	±0.80%	±2.49%	±1.91%

Notes:

* To obtain each computed modulus of elasticity, a best-fit line was performed only considering the measured data points that corresponded to stresses between 0.20fpu and 0.80fpu. No other manipulation of raw data was performed.

** The values corresponding to the variability of each given average were considered to be equal to the percentage of the ratios between the standard deviation of each set of slope observations and their corresponding average slope.

Figure 4.17 Statistical analysis of electrical resistance strain gage results from tests on ½ " ϕ strand specimens from roll "B".

Summary of results from tests of specimen from strand roll "C" (0.6" diameter):

		Computed Modulus of Elasticity *		
		[ksi]		
		TEST 4Sa	TEST 4Sb	
ER-Gage #1		29538	28860	
ER-Gage #2		30112	29433	
ER-Gage #3		29778	29220	
ER-Gage #4		29323	28969	
ER-Gage #5		29915	29351	
ER-Gage #6		30023	29330	
Statistics of ER-Gages (per TEST):				Statistics of ER-Gages (from both TESTS):
	Min.:	29323	28860	28860
	Max.:	30112	29433	30112
	St. Dev.:	302	229	399
	Avg.:	29782	29194	29488
	Variability of Avg.**:	±1.01%	±0.79%	±1.35%

Notes:

* To obtain each computed modulus of elasticity, a best-fit line was performed only considering the measured data points that corresponded to stresses between 0.20fpu and 0.80fpu. No other manipulation of raw data was performed.

** The values corresponding to the variability of each given average were considered to be equal to the percentage of the ratios between the standard deviation of each set of slope observations and their corresponding average slope.

Figure 4.18 Statistical analysis of electrical resistance strain gage results from tests on 0.6" ϕ strand specimen from roll "C".

4.3.1.3 Multi-Strand Tendon Tests. These tests were developed to check the performance of electrical resistance strain gages on multi-strand tendons. A technique for reducing the amount of stress differences among strands of typical prestressing tendons was also investigated.

Laboratory tests using short lengths of tendons can produce large stress differentials among each instrumented strand. This is mainly due to the following factors:

- Small differences in initial strand length. This is usually produced from irregular twisting of the strands as they are threaded through the test specimens.
- Small sliding movements of seating wedges before a strand is fully engaged by the anchorage hardware. During initial stressing it is unlikely that all strands will seat simultaneously in the stressing hardware. Small stress variations are thus expected.

Most laboratory instrumentation projects with prestressing tendons are carefully prepared so as to avoid overstressing individual strands. This is usually accomplished by initially stressing and seating each strand against the back of the multi-strand tendon jacking system. Stressing operations of most stay cables composed of multiple prestressing strands are usually performed in a similar way. However, this practice is not followed in field applications of prestressing tendons, where small variations in length among individual strands should not cause a major overstressing problem.

Four tests in two different testing setups were performed with electrical resistance strain gages of the bonded foil type. The description of each test, along with the most important findings follows.

a. Test Descriptions. The first two tendon tests (TEST 1T and TEST 2T) were developed in connection with a different study related to bonding of external tendons at deviators [91]. A tendon made of 7-½ " ϕ prestressing strands was used in TEST 1T, and a tendon made of 12-½ " ϕ prestressing strands was used in TEST 2T. A general description of the test setup is shown in Figure 4.19, where the position of the instrumentation system under study is also indicated. The epoxy sleeves (also shown in Figure 4.19) were a candidate instrumentation system investigated as a backup to the electrical resistance strain gages. This system is described fully in Section 4.3.2. One expected influence of the epoxy sleeves in the present tests was a "clamping" action on the strands, making them behave much more similarly during stressing

operations. If this linearization of results was possible, only a few ER-gages would be needed to accurately determine the average tendon stress of each instrumented section. The strain gages used in these tests were of the type EA-06-062AP-120 Option LE, made by Measurements Group (used due to the availability of supplies). Three ER-gages were bonded to easily accessible strands at a particular tendon cross-section of TEST 1T. Four ER-gages of the same type were used in TEST 2T. All of these electrical resistance strain gages performed satisfactorily during both tendon tests. No complicated provisions for long-term stability were implemented in these gages due to the short-term duration of the tests. Strand strains were automatically scanned with a computer-controlled data acquisition system. Corresponding live end load levels were scanned simultaneously by the data acquisition system. They were computed from readings of an electrical resistance pressure transducer installed in the pressure line of the hydraulic jack used for stressing the tendons.

TEST 3T and TEST 4T were performed to observe the more complicated behavior of tendons composed of 19-0.6" ϕ strands. Actual field operations were simulated in the threading and stressing operations of these tendons. In each test, the tendons were loaded in three different cycles from zero stress to about $0.85f_{pu}$. These tests were performed in San Antonio, on a testing setup (shown in Figure 4.20) built by Austin Bridge Co. to perform their regular modulus of elasticity tests. Austin Bridge Co. extended the use of their equipment, and also donated all the prestressing strands needed for these two tests. Two types of electrical resistance strain gages, and the final version of the epoxy sleeves were implemented. The strain gages used were of the type EA-06-125BZ-350 Option LE and EA-06-062AQ-350 Option LE, both manufactured by Measurements Group. In each one of these last two tendon tests, three ER-gages were bonded to selected strands at a particular tendon cross-section. Only one gage (ER-gage #2 of TEST 3T) was damaged before performing the actual tendon test. Strand strains were monitored using a portable strain indicator box that was coupled to a portable multi-channel switching device. Both were connected to the electrical resistance strain gages for the complete duration of each test. Loads were computed at the live ends from pressure readings of a calibrated hydraulic jack instrumented with a pair of dial indicators. As in the previous tendon tests, no provisions for long-term gage stability were necessary.

b. Data Reduction Method. In most laboratory and field investigations with instrumented tendons, load levels are measured at the live ends from readings of calibrated hydraulic jacks

equipped with pressure transducers (usually of the electrical resistance type). However, better accuracy of the stressing loads imposed on the tendons can be obtained with calibrated center-hole load cells. But these expensive devices must be permanently left in each one of the instrumented tendons when performing field measurements of actual structures. A more economical but complicated procedure can be to install temporary electrical resistance strain gages on selected strands at the stressing end of the tendons. These gages would have to be located at a carefully determined distance away from the stressing jacks, so as to avoid damaging or neutralizing them during stressing operations. Besides providing an accurate determination of tendon loads, these gages can also give information regarding the losses caused by internal friction in the stressing equipment.

Stressing loads of the instrumented spans of the San Antonio Y project will be obtained with electrical resistance pressure transducers installed in the calibrated hydraulic jacks. These pressure transducers will be scanned simultaneously with the electrical resistance strain gages located at selected intermediate cross-sections of the external tendons. The information available to the researcher will therefore consist of live end loads and corresponding cross-section strains of instrumented strands. The stress loss from the live end to each intermediate tendon cross-section is unknown but will be estimated using live end loads and cross-section strains. Another expected field complication is that the strands of each multi-strand tendon will probably behave erratically at low stress levels (mainly because of uneven strand anchorage and varying strand lengths).

Given these conditions, it was necessary to determine the best method for reducing the right information from the measured data. Several complicated procedures were investigated in the present project, and the most accurate data reduction method resulted to be one of the simplest to understand. A description of the data reduction procedure utilized for the present tendon tests and suggested for future investigations is included here.

Average tendon stress values at the live ends were obtained by considering the nominal areas of 0.153in^2 and 0.215in^2 for each one of the $\frac{1}{2}$ " ϕ and the 0.6" ϕ strands respectively. Strain readings from each ER-gage and their corresponding live end stresses computed from the pressure transducer (or dial indicator) readings were plotted on a σ - ϵ graph. For each ER-gage, a best fit line was computed considering the data points that corresponded to stresses between $0.20f_{pu}$ and $0.80f_{pu}$. The intersection of this best-fit line to the ϵ -axis was also computed. This

value --labeled " ϵ_0 "-- was considered to be the strain reading that corresponded to the zero stress level. Each measured value of strain was thus corrected by arithmetically subtracting the computed initial strain value (ϵ_0). Stress levels were then obtained by multiplying each corrected strain value by the apparent modulus of elasticity (previously obtained in the prestressing strand material tests). Stress losses produced in each loading step were estimated by comparing reduced stresses (of the intermediate ER-gages) with corresponding live end stresses (measured by the calibrated hydraulic jack). An estimate of the average tendon stress loss was calculated by the average of the intermediate loading step losses registered by each ER-gage (only comparing the intermediate stresses located between $0.20f_{pu}$ and $0.80f_{pu}$). However, a more accurate average of the stress loss from live end to each instrumented tendon cross-section was obtained by computing the ratio between the slope of the calculated best-fit line of each ER-gage with the slope obtained from the material tests of the prestressing strands (the apparent modulus of elasticity). When using more than a single ER-gage on an intermediate tendon cross-section, an even better estimate of the tendon stress loss was given by averaging the stress losses determined from the individual strain gages.

c. Interpretation of Results from TEST 1T and TEST 2T. Strain readings of each ER-gage of TEST 1T and TEST 2T were plotted against corresponding stress values computed from readings of a pressure transducer located at the live end. These plots are shown in Figures 4.21 and 4.22. The σ - ϵ curves of both plots are shifted away from the origin of coordinates because each prestressing strand was independently stressed to 20ksi in TEST 1T and to 40ksi in TEST 2T before the ER-gages were installed. This was done to prevent overstressing the individual strands (small differences in strand lengths can be critical when the tendon is relatively short and loaded to about 80% of its ultimate capacity). The best-fit lines (along with their calculated slopes) defined by the high stress data points of the σ - ϵ graphs of each ER-gage are also included in the plots of Figures 4.21 and 4.22.

The results from both tendon tests with $\frac{1}{2}$ " ϕ strands are drawn together on a single graph (shown in Figure 4.23) to compare their average behavior. Finally, a detailed statistical analysis of the results from both tests is included in Figure 4.24.

Material tests of a specimen taken from the same prestressing strand roll used for tendon TESTs 1T and 2T were described as strand TESTs 2S and 3S in the previous section (Section 4.3.1.2). As shown previously in Figure 4.17, the average apparent modulus of

elasticity obtained from the material test specimens was found to be equal to $\approx 30,900$ ksi. As explained in the data reduction process, this apparent modulus was the one used for determining the average stress losses occurring from the live end to the instrumented cross-section of each tendon.

The first observation that can be drawn from an examination of Figures 4.21 and 4.22 is the very similar strain levels exhibited among the instrumented strands of each tendon test. However, these similarities are largely attributed to the initial pretensioning of the strands (strands of TEST 1T and TEST 2T were pretensioned to 20ksi and 40ksi respectively before the ER-gages were installed). Despite this stress difference, a comparison of the average results from both tendon tests define two nearly parallel best-fit average lines (as shown in Figure 4.23).

The combined statistical analysis of the results from these first two tendon tests are shown in Figure 4.24. Interestingly, the variability of the combined average slope of all seven statistical observations from TESTs 1T and 2T was $\pm 1.57\%$ (as defined by the percentage of the ratio between the combined standard deviation and the average of all slope observations). This is a better level of variability than the $\pm 1.91\%$ previously obtained in the single strand tests (Fig. 4.17). It was therefore concluded that if a single electrical resistance strain gage was taken as a representation of the behavior of the whole tendon, the measured slope of the best-fit line will most likely lay within $\pm 1.57\%$ of the average tendon behavior.

Finally, the statistical analysis of the stress losses computed from the live end station to the instrumented cross-section of the tendon provided a 2.61% average loss value (as shown in Table B of Figure 4.24). Considering the location of the instrumented cross-section (at a length of straight tendon from the live end, as shown in Figure 4.19), this stress loss can only be attributed to internal friction occurring in the stressing equipment. However, it must also be considered that the average stress loss can vary $\pm 1.61\%$ (as indicated by the general standard deviation value included in Table B of Figure 4.24). Nevertheless, according to the present test results it is evident that certain losses occur in the stressing equipment. It will be interesting to have future projects investigate if these stress losses can be standardized for certain stressing equipment, or if stress loss ranges can be provided.

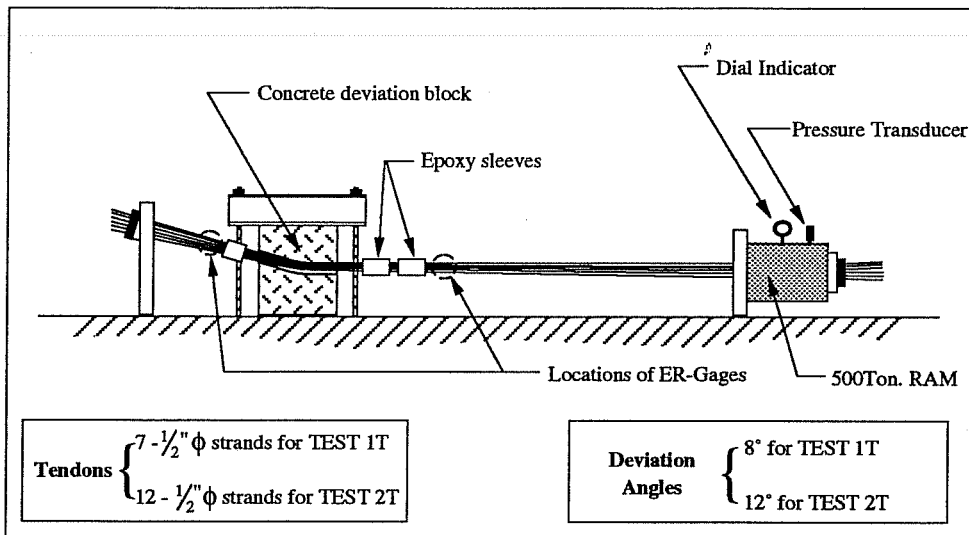


Figure 4.19 General schematic of TEST 1T and TEST 2T.

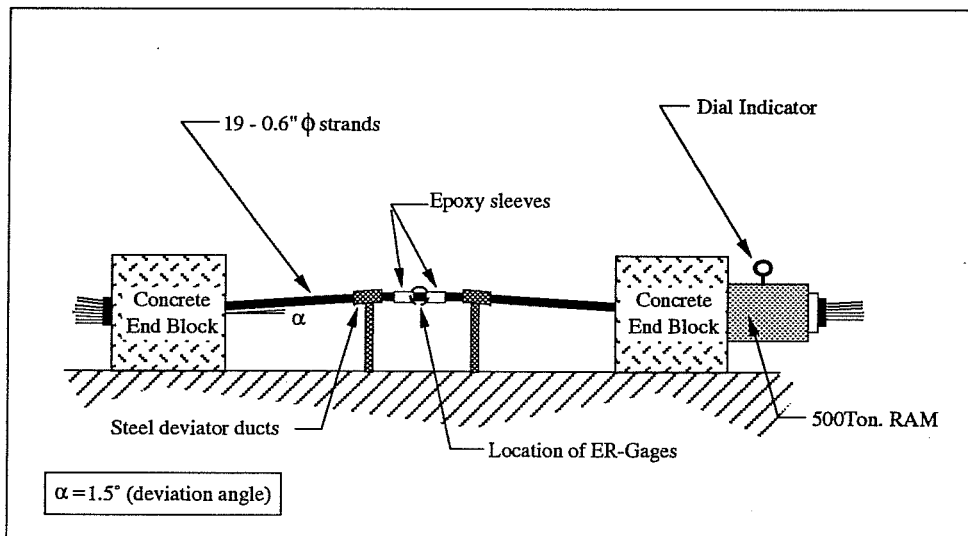


Figure 4.20 General schematic of TEST 3T and TEST 4T.

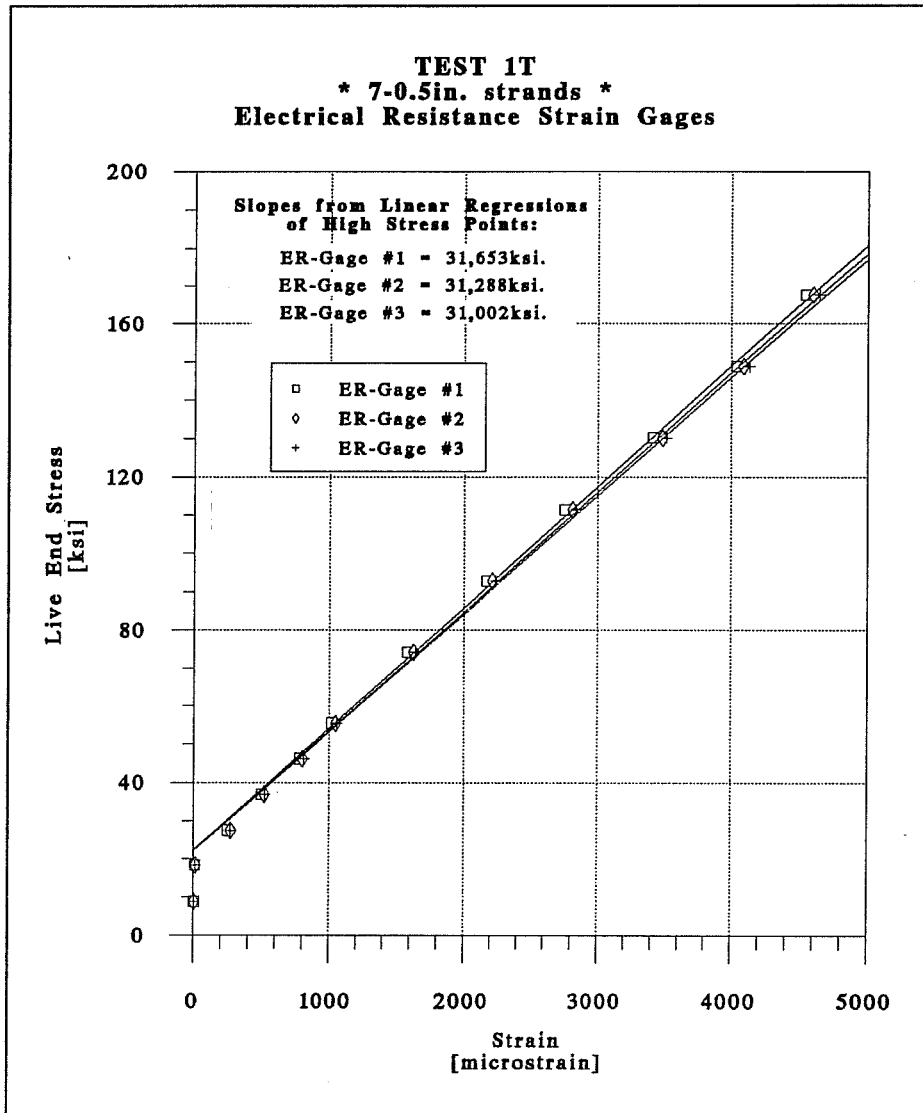


Figure 4.21 Stress-strain plots of individual ER-gages for TEST 1T.

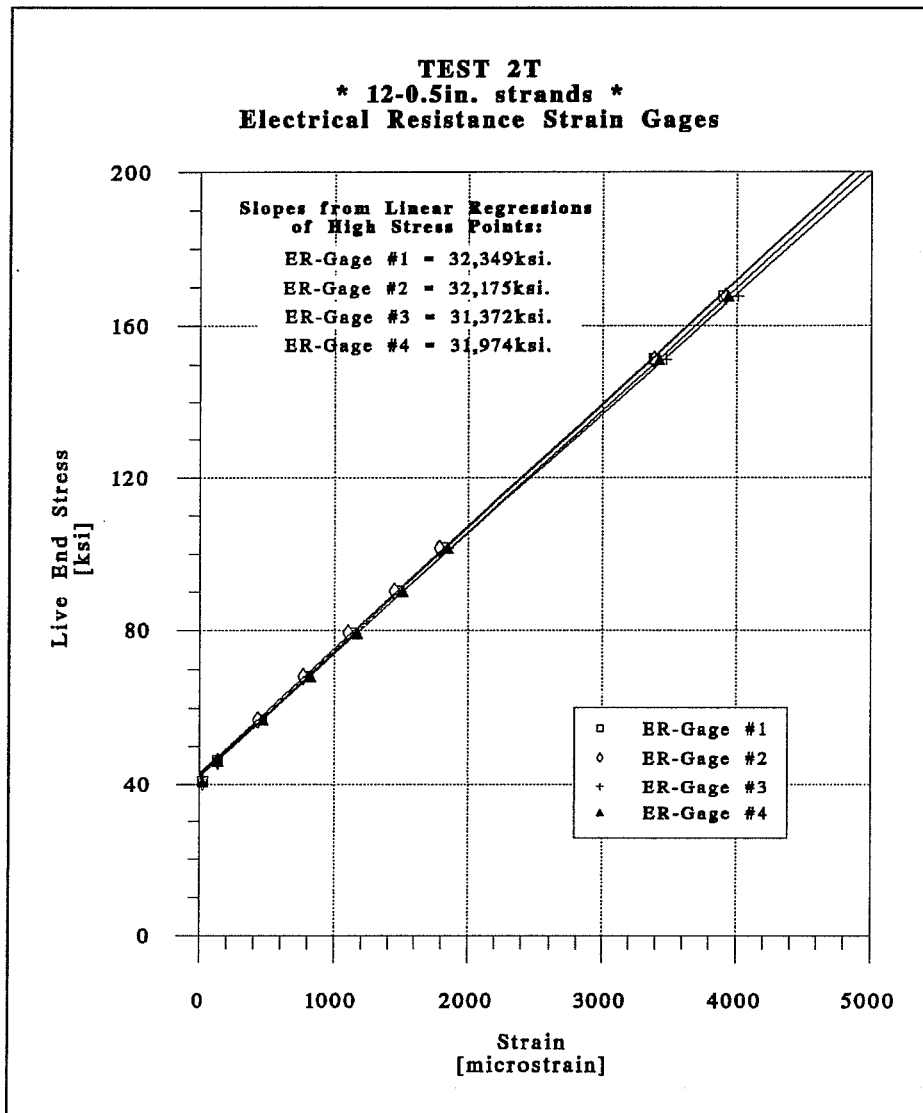


Figure 4.22 Stress-strain plots of individual ER-gages for TEST 2T.

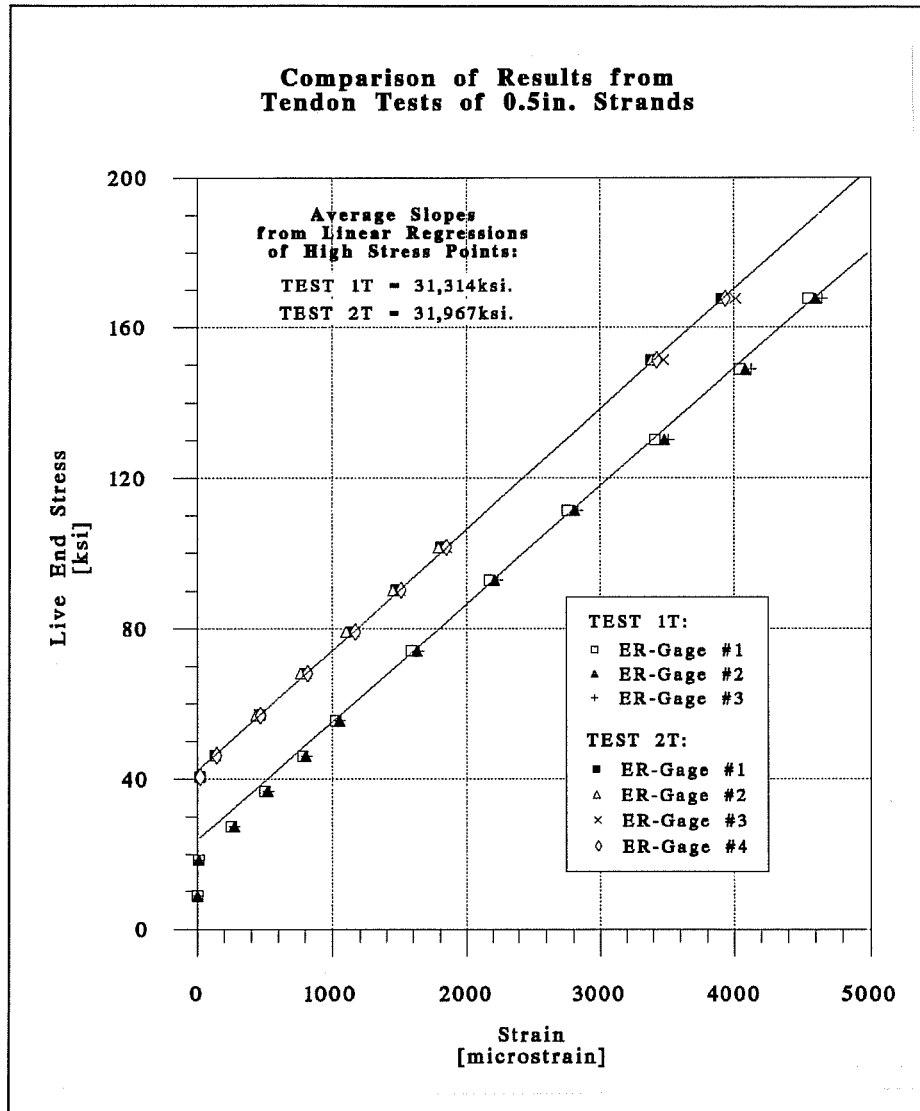


Figure 4.23 Summary of average stress-strain curves of TESTs 1T and 2T.

A. Summary of results from tests on tendons composed of 1/2" diameter strands:

		Slope of Best-Fit Line *		Statistics of ER-Gages (from both TESTS):
		[ksi]		
		TEST 1T	TEST 2T	
ER-Gage #1		31653	32349	
ER-Gage #2		31288	32175	
ER-Gage #3		31002	31372	
ER-Gage #4		(-)	31974	
Statistics of ER-Gages (per TEST):	Min.:	31002	31372	31002
	Max.:	31653	32349	32349
	St. Dev.:	326	426	498
	Avg.:	31314	31968	31688
Variability of Avg.**:		±1.04%	±1.33%	±1.57%

B. Summary of stress losses from tests on tendons composed of 1/2" diameter strands:

		Stress loss from live end ***		Statistics of ER-Gages (from both TESTS):
		[%]		
		TEST 1T	TEST 2T	
ER-Gage #1		2.50%	4.75%	
ER-Gage #2		1.32%	4.19%	
ER-Gage #3		0.39%	1.59%	
ER-Gage #4		(-)	3.54%	
Statistics of ER-Gages (per TEST):	Min. Loss:	0.39%	1.59%	0.39%
	Max. Loss:	2.50%	4.75%	4.75%
	St. Dev.:	1.06%	1.38%	1.61%
	Avg. Loss:	1.40%	3.52%	2.61%

Notes:

* The best-fit line of each ER-gage was computed only considering the measured data points that corresponded to stresses located between 0.20fpu and 0.80fpu. No other manipulation of raw data was performed.

** The values corresponding to the variability of each average slope were considered to be equal to the percentage of the ratios between the standard deviation of each set of slope observations and their corresponding average slope.

*** Losses were obtained by the ratio between the modulus of elasticity given on "A" and the "apparent" modulus determined from the material tests of strand specimens taken from the same prestressing strand roll used for these tendons ($E_{app}=30,881\text{ksi}$).

Figure 4.24 Statistical analysis of electrical resistance strain gage results from tendon TESTS 1T and 2T with 1/2" ϕ strands.

d. Conclusions from TEST 1T and TEST 2T. The following conclusions can be drawn from the electrical resistance strain gages installed in the first two tendon tests (composed of $\frac{1}{2}$ " ϕ prestressing strands):

- a. In most cases, the measured data of a field instrumentation program with multi-strand tendons is comprised of live end stresses and corresponding strains of individual prestressing strands located at intermediate tendon cross-sections. An appropriate data reduction method must be followed to obtain valuable information from the measured data. A data reduction method was suggested and successfully employed in multi-strand tendon tests.
- b. The average stress losses occurring between instrumented tendon cross-sections was measured with a $\pm 1.57\%$ accuracy when electrical resistance strain gages were only installed on 25% of the $\frac{1}{2}$ " ϕ strands of a tendon. However, this occurred when: (a) the suggested data reduction method and accompanying material tests were performed, and (b) the strands were individually pretensioned to a similar stress level in the back of the multi-strand tensioning system.
- c. Absolute stress losses of 2.61% ($\pm 1.61\%$) were found to occur due to internal friction of the stressing equipment used in the first two tendon tests. Although difficult to determine with great accuracy, these stress losses seem to be present in most stressing equipment and are recommended to be more carefully investigated in future projects.

e. Interpretation of Results from TEST 3T and TEST 4T. As mentioned earlier, three loading cycles from zero stress to $0.85f_{pu}$ were performed in tendon TESTs 3T and 4T. The strains measured from each one of the workable ER-gages of TEST 3T and TEST 4T were plotted against corresponding stress values computed from readings of a dial indicator located at the live end. Since the gages behaved similarly in all other cycles, only the results from the first loading cycles of TESTs 3T and 4T are given in Figures 4.25 and 4.26. However, the average instrumented strand behavior from each one of the three loading cycles of each test are compared in Figures 4.27 and 4.28. It must be mentioned that the electrical resistance strain gages used on these two tests were installed without an initial tendon stress.

The operations followed for the threading of the tendons and for the installation of the instrumentation devices during these tendon tests were performed with a close simulation of the actual field operations to be followed in the instrumented spans of the San Antonio Y project.

Also included in the plots of Figures 4.27 and 4.28 are the best-fit lines defined by the upper data points of the σ - ϵ graphs of each gage and for each loading cycle. Calculated values for the slopes of each one of these six lines are also shown in the same figures. The final average results from both tendon tests with 0.6" ϕ strands are put together in a single graph (shown in Figure 4.29) to compare their overall average behavior. Finally, a detailed statistical analysis from the results of both tendon tests is included in Figure 4.30.

No material tests were performed on specimens taken from the same prestressing strand roll used in TEST 3T and TEST 4T. Instead, the results obtained from material tests performed on a different 0.6" ϕ strand specimen (taken from a different strand roll) were used as background information for these last two tendon tests. The results from the single strand tests on 0.6" ϕ strands were explained earlier in Section 4.3.1.2, and the final average apparent modulus of elasticity was found to be equal to 29,488ksi (as previously shown in Figure 4.18). This apparent modulus of elasticity was used for the determination of the average stress losses that occurred from the live end to the instrumented cross-section of each tendon. Obviously, these stress losses are not representative of the "absolute" losses that actually occurred in the present test setup. This is because of the lack of material tests of specimens taken from the same prestressing strand roll used for the tendons of TEST 3T and TEST 4T. However, the only observation dependent on material tests of sample specimens taken from these two tendon tests is related to the absolute stress loss that occurred due to internal frictions in the stressing hardware and in the small deviation angles of the tendons. The present test results are still helpful for reaching important conclusions about the overall ER-gage performance, differences in the behavior of each instrumented strand, and performance of the backup tendon strain measuring system (the *epoxy sleeve* system described in Section 4.3.2).

An examination of Figures 4.25 and 4.26 yields the observation that each instrumented strand from the same test behaved similarly. The same behavior was found earlier in TESTs 1T and 2T. However, the present similarity of strand behavior seems to be related to the use of the epoxy sleeve system. As mentioned earlier, this novel tendon strain measuring system has the added benefit of producing a certain form of "clamping" action among all the prestressing

strands of the instrumented tendon. If all the prestressing strands of a tendon are completely clamped at two cross-sections separated by a small straight length, the strands between clamps will obviously strain similarly. Evidently, the epoxy sleeve system does not cause a "perfect clamp" to all the strands of a tendon and at all stress levels of the strands. However, it is possible that at low stress levels the epoxy sleeve system does efficiently clamp the prestressing strands located on the periphery of the tendon. All the ER-gages used in these last two tendon tests were located in between the two "clamps" of the epoxy sleeve systems.

A careful observation of Figures 4.25 and 4.26 gives an indication of the existence of this "clamping" effect of the epoxy sleeves. In the first loading cycle of TEST 3T (Figure 4.25), both electrical resistance strain gages --and thus the instrumented strands-- showed identical behavior until about the 110ksi stress level. Beyond this point the strands started straining slightly differently, thus indicating that the "clamp" was allowing some strand slippage to occur. A similar behavior can be seen in the first loading cycle of TEST 4T (Figure 4.26). However, in this case the strand to which ER-gage #2 was bonded started slipping from the very beginning. Observations of σ - ϵ plots from the two other loading cycles of each test indicated a similar behavior of the strands. It was therefore concluded that at stresses below 110ksi the epoxy sleeve system provided some degree of clamping to the prestressing strands located in the periphery of a tendon. This helped considerably the electrical resistance strain gages since by measuring fewer strand strains they still provided a good estimate of the average tendon behavior.

The comparisons of average tendon behavior for each loading cycle of each test (shown in Figures 4.27 through 4.29) indicated approximately equal average slopes of the best-fit lines. Indeed, the combined statistical analysis of the results from both tendon tests (shown in Figure 4.30) indicated a $\pm 2.61\%$ variability of the average of the slopes obtained from all best-fit lines. This seems to be an acceptable instrumentation behavior for predicting the average stresses of a tendon composed of 19 prestressing strands.

The statistics of stress losses from live end to the instrumented tendon cross-section (shown in Table B of Figure 4.30) are not absolute values. However, the standard deviation of all 15 observations indicates that the average prediction of stress loss --whatever its absolute value may be-- can vary $\pm 2.74\%$. This is a somewhat high range of variation of stress loss estimate considering that the expected losses to be measured in field instrumentation projects

should not considerably exceed such a range. However, this range of $\pm 2.74\%$ was reduced to $\pm 2.0\%$ when the best-fit line for each group of measured data was performed only considering the data points below $\approx 0.50f_{pu}$ (approximately when the strands started to slip in the epoxy sleeves).

f. Conclusions from TEST 3T and TEST 4T. The following conclusions can be drawn from the electrical resistance strain gages installed in the final tendon tests (composed of 19-0.6" ϕ prestressing strands):

- a. The backup instrumentation system for measuring average tendon strains (the epoxy sleeve system) was found to help considerably the ER-gage results by exerting a certain degree of "clamping" to all the prestressing strands of the tendon. This was particularly true for strands located in the outer periphery of the tendon and for stresses up to about 110ksi. However, it was also apparent that occasional strands disengaged from the epoxy "clamps" at lower stresses.
- b. The average stress losses occurring between instrumented tendon cross-sections were measured with a $\pm 2.74\%$ accuracy when electrical resistance strain gages were only installed to 16% of the 0.6" ϕ strands of a tendon. However, this occurred when: (a) the suggested data reduction method was performed, and (b) all the electrical resistance strain gages were bonded between the epoxy sleeves. The accuracy was further improved to $\pm 2.0\%$ by performing a data reduction considering only the data points located between $0.20f_{pu}$ and $0.50f_{pu}$.

4.3.2 Epoxy Sleeves

A mechanical backup system envisioned as an alternative method for measuring strand strains, and ultimately tendon loads at intermediate cross-sections was developed. Since no available system satisfied the backup requirements of the present instrumentation project, the epoxy sleeves were investigated as a new device for measuring loads in multi-strand tendons.

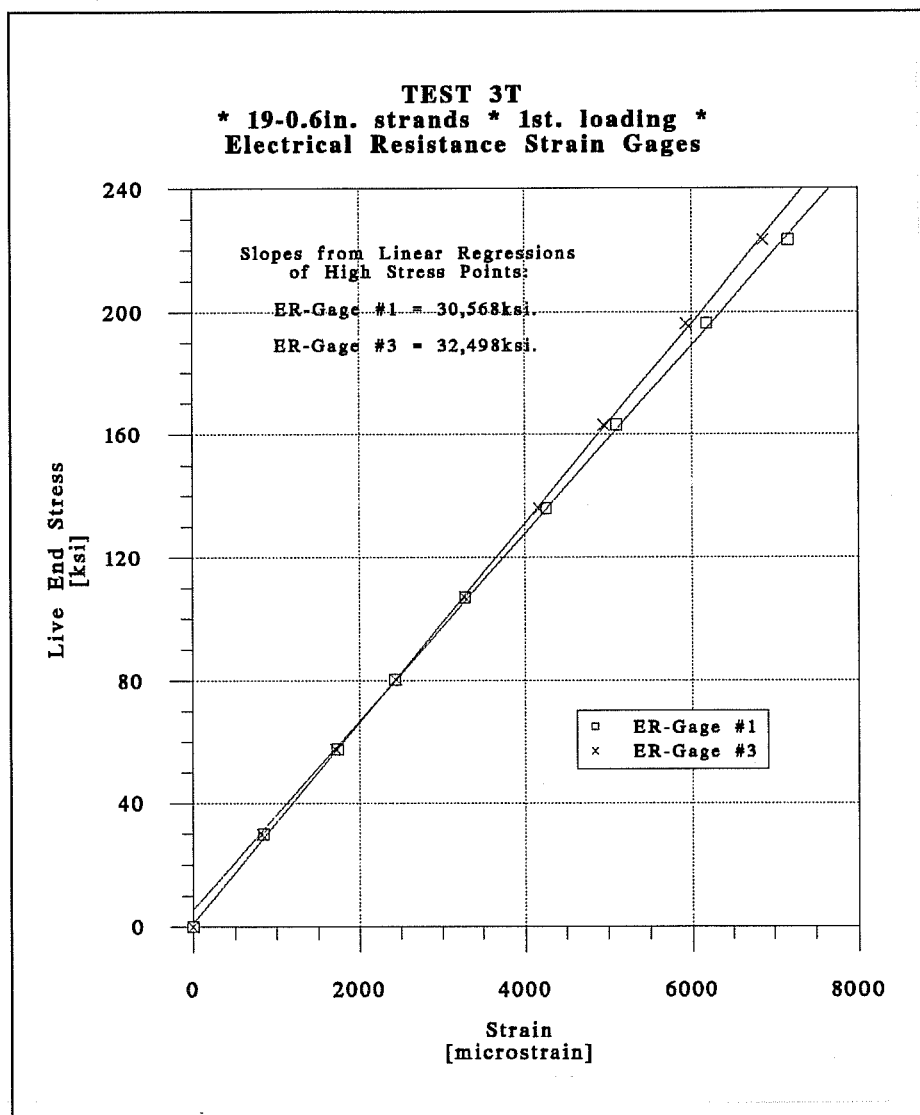


Figure 4.25 Stress-strain plots of individual ER-gages for TEST 3T.

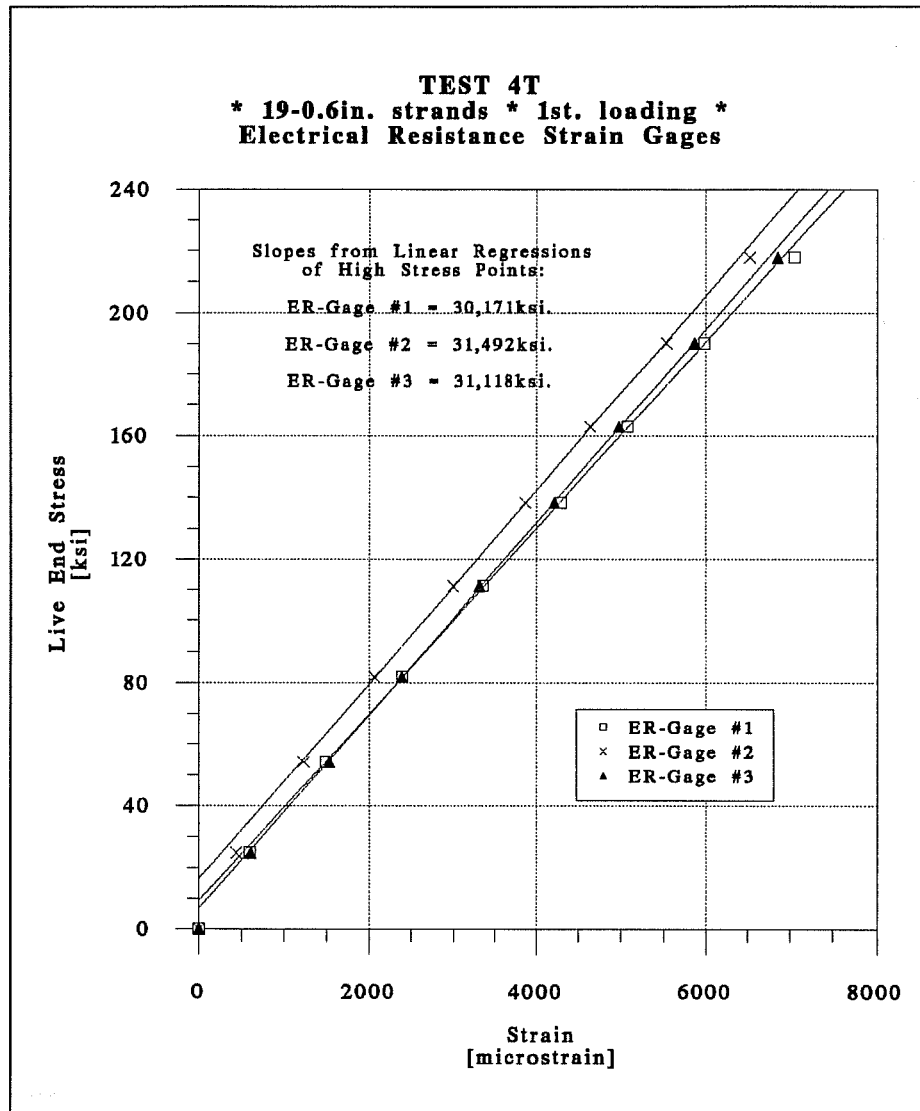


Figure 4.26 Stress-strain plots of individual ER-gages for TEST 4T.

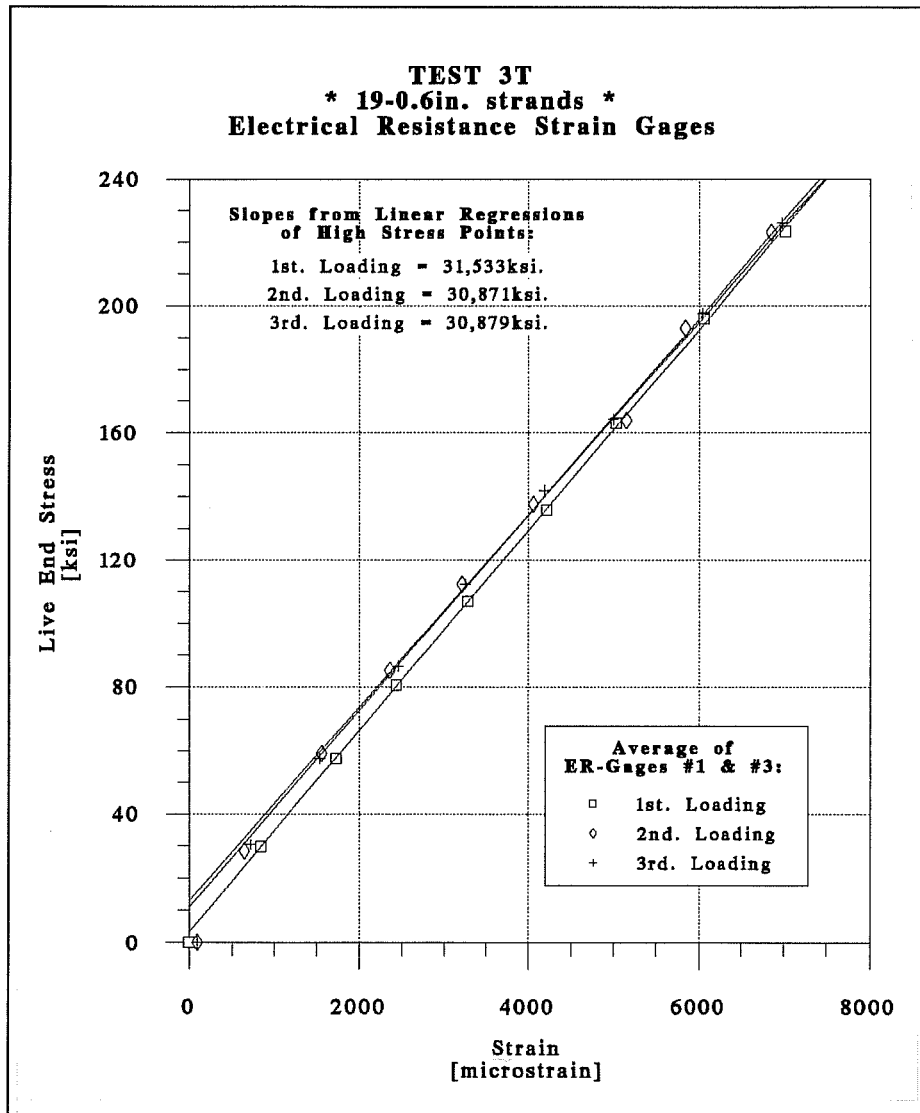


Figure 4.27 Average stress-strain plots of the ER-gages for each loading cycle of TEST 3T.

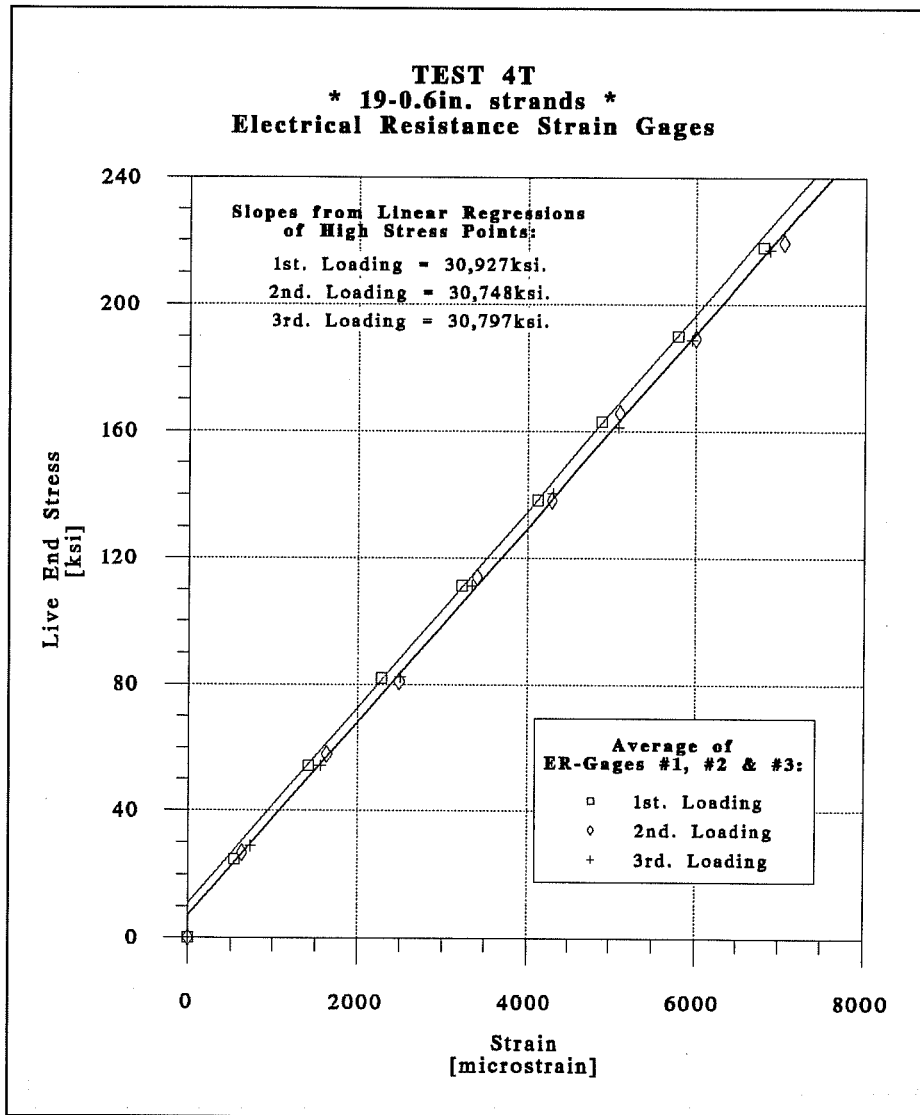


Figure 4.28 Average stress-strain plots of the ER-gages for each loading cycle of TEST 4T.

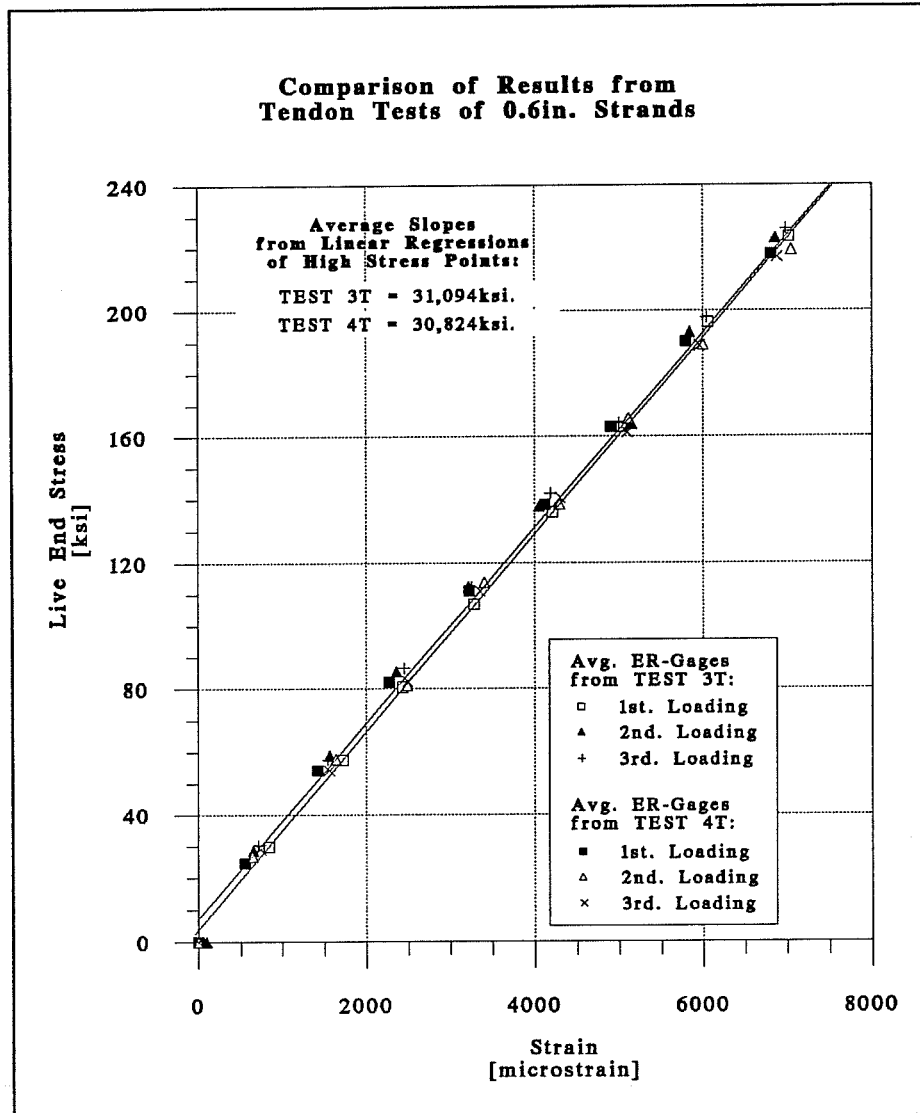


Figure 4.29 Comparison of average stress-strain plots of the ER-gages of TESTs 3T and 4T.

A. Summary of results from tests on tendons composed of 0.6" diameter strands:

	Slope of Best-Fit Line [ksi.]						Statistics of ER-Gages (per TEST):	Variability of Avg.:
	TEST 3T			TEST 4T				
	1st. Loading	2nd. Loading	3rd. Loading	1st. Loading	2nd. Loading	3rd. Loading		
ER-Gage #1	30568	30009	29625	30171	30097	30463	Statistics of ER-Gages (from both TESTS):	29625 32498 809 30932 ±2.61%
ER-Gage #2	(-)	(-)	(-)	31492	31056	30827		
ER-Gage #3	32498	31733	32133	31118	31092	31100		
Min.:		29625			30097			
Max.:		32498			31492			
St. Dev.:		1189			477			
Avg.:		31094			30824			
		±3.82%			±1.55%			

B. Summary of stress losses from tests on tendons composed of 0.6" diameter strands:

	Stress loss from live end (using E _{app} =29,488ksi.) [%]						Statistics of ER-Gages (from both TESTS):
	TEST 3T			TEST 4T			
	1st. Loading	2nd. Loading	3rd. Loading	1st. Loading	2nd. Loading	3rd. Loading	
ER-Gage #1	3.66%	1.77%	0.46%	2.32%	2.07%	3.31%	Statistics of ER-Gages (from both TESTS):
ER-Gage #2	(-)	(-)	(-)	6.80%	5.32%	4.54%	
ER-Gage #3	10.21%	7.61%	8.97%	5.53%	5.44%	5.47%	
Min. Loss:		0.46%			2.07%		
Max. Loss:		10.21%			6.80%		
St. Dev.:		4.03%			1.62%		
Avg. Loss:		5.45%			4.53%		

Figure 4.30 Statistical analysis of ER-gage results from tendon TESTS 3T and 4T on 19-0.6" diameter strands.

Tests were first performed using single strands so as to easily address the effectiveness of the system. After an analysis of the initial problems, slightly modified epoxy sleeve systems were investigated in further strand tests. For the San Antonio Y instrumentation project, these single strand tests with epoxy sleeves will only be performed as part of the material tests of prestressing strands. The final recommendations for these tests are therefore included within the recommended Material Tests in Section 5.7.2.1.

Larger epoxy sleeve systems were tested with the electrical resistance strain gages in the previously described multi-strand tendon tests. These tests also assisted to check the behavior of the new instrumentation system under large loads and stress differentials among strands. As explained previously, the first two tests were performed with tendons composed of 7 and 12 units of $\frac{1}{2}$ " ϕ low relaxation strands loaded to about $0.80f_{pu}$. After these initial tests, a final modified epoxy sleeve system was tested in the tendon tests of 19-0.6" ϕ low relaxation prestressing strands loaded to $0.85f_{pu}$. An analysis of the results related to the epoxy sleeve system used in multi-strand tendons is included in Section 4.3.2.2. The final epoxy sleeve system is also described in Section 5.3 as a recommended application for the field tests of the San Antonio Y structures.

4.3.2.1 Single Strand Tests. The envisioned operation of the epoxy sleeve system was based on the measurement of the elongations of a completely clamped section of a prestressing strand. The "clamping" of each wire of a prestressing strand was envisaged to be performed by high strength epoxy collars precast on two locations of the strand specimens. The gage length of the epoxy sleeve system was given by the center-to-center distance of the precast epoxy collars. Initial single strand tests were performed to check the overall system behavior and to determine the required diameter and gage length of the epoxy collars. The last three single strand tests were performed with the final version of the epoxy sleeve system. These last three tests are reported here.

a. Test Descriptions. The first two single strand epoxy sleeve tests were performed on $\frac{1}{2}$ " ϕ 7-wire low relaxation prestressing strand specimens taken from the same prestressing strand roll. These tests were coded TEST 1ES and TEST 2ES. The last single strand epoxy sleeve test was performed on a 0.6" ϕ 7-wire low relaxation prestressing strand specimen. Since two loading cycles were imposed on this final specimen, the present test results were coded TEST 3ESa and TEST 3ESb. Each one of these single strand epoxy sleeve tests corresponded to a previously

mentioned ER-gage single strand test (previously reported in Section 4.3.1.2). They are named differently here for organizational purposes to identify the study of specific results related to the performance of the epoxy sleeve system. Single strand tests 1ES and 2S, 2ES and 3S, 3ESa and 4SA, and 3ESb and 4Sb are thus the same.

Descriptions of the precast operations and dimensions of the epoxy sleeve systems used in these tests are shown in Figure 4.31. The only difference between the two epoxy sleeve systems described in Figure 4.31 is that a 200mm Demec extensometer was used in TESTs 1ES and 2ES, and a 400mm extensometer was used on both loadings of TEST 3ES.

Several types of two-part epoxy products were compared in the single strand tests. Two products with good performance were: Industrial Coating A-103 and Sikadur 32 Hi-Mod. Both of these epoxies comply with the requirements for a Type V Epoxy according to the Material Specifications of the Texas State Department of Highways and Public Transportation (TSDHPT) [85]. Most of the epoxy products used for these tests were donated by the Material Testing Laboratories of TSDHPT. A smaller amount of epoxy was also donated by the Testing Laboratory of Sika, Inc. from New Jersey. The epoxy sleeves of TEST 1ES were made with A-103 epoxy mixed with sand, and those of TEST 2ES and 3ES were made with Sikadur 32 Hi-Mod epoxy.

Testing was performed using a vertical loading machine, and the strand specimens were anchored with standard 3-wedge single strand anchorages. Strain readings from the epoxy sleeve system of TESTs 1ES and 2ES were taken with a 200mm Demec extensometer which had a resolution of $8\mu\epsilon$. Loads for TEST 1ES were registered from the scale readings of a 60kip. vertical loading machine. In TEST 2ES, loads were computed from strain readings of an electrical resistance load cell. The strain readings from the epoxy sleeve system of TEST 3ES were taken with a 400mm Demec extensometer of $4\mu\epsilon$ resolution. Load levels on both cycles of this final single strand test were also computed from strain readings of an electrical resistance load cell. Information concerning the prestressing strand specimens and the electrical resistance strain gages were mentioned previously in Section 4.3.1.2 and should be reviewed according to the mentioned correlation of test code names (1ES is 2S, 2ES is 3S, 3ESa is 4SA, and 3ESb is 4Sb).

b. Data Reduction Method. A similar method to that described previously in Section 4.3.1.2 was used for the data reduction of the measured epoxy sleeve strains. This method is explained

here for the particular case of epoxy sleeve readings. Stress values in each strand were obtained by considering the nominal areas of 0.153in^2 and 0.215in^2 for the $\frac{1}{2}$ " ϕ and the 0.6 " ϕ strands respectively. Since no stress losses can be reasonably expected to occur between the instrumented section of the strand and the section where loads were measured, the corresponding values of stress and strain were plotted on a single σ - ϵ graph. A best-fit line was defined considering the data points of the σ - ϵ graph that approximately corresponded to stresses between $0.20f_{pu}$ and $0.80f_{pu}$. This procedure thus avoided the consideration of initial nonlinearities in the graph (usually occurring during seating of the strand specimen at the anchor ends). As shown in Figure 4.31, one to four pairs of demec locating discs were installed in diametrically opposed locations around the epoxy collars. At each loading step, up to four different strain readings were thus obtained in each epoxy sleeve system according to the location of the Demec reference discs. The slopes of the best-fit lines corresponding to each epoxy sleeve reading location were recorded. The prestressing strand's apparent modulus of elasticity was determined by the average of these slopes.

Prestressing strand manufacturers usually perform their modulus of elasticity tests using a similar method --but with longer gage lengths-- as the epoxy sleeve system. It was therefore expected to find much closer values between the apparent modulus of elasticity determined from the epoxy sleeve system and that given by the strand manufacturer.

c. Interpretation of Results. Two pairs of locating discs were installed (for 200mm Demec extensometers) in different locations around the epoxy sleeves of TEST 1ES and TEST 2ES. The epoxy sleeves of TEST 3ES had four pairs of locating discs placed for 400mm Demec extensometers. Measured stress-strain values corresponding to each epoxy sleeve measuring location for each test (for each loading cycle of TEST 3ES) are plotted in Figures 4.32 through 4.35. For purposes of comparison, the average behavior observed by each corresponding set of electrical resistance strain gages are outlined in each one of these plots. The slopes obtained from the linear regression analysis of each σ - ϵ curve are also included in Figures 4.32 through 4.35. A final plot showing the averages of the epoxy sleeve readings of each single strand test is shown in Figure 4.36.

Statistics of the results from the tests performed with the $\frac{1}{2}$ " ϕ strand specimens (TESTs 1ES and 2ES) are included in Figure 4.37. Similarly, the statistics of the results from the tests performed with the 0.6 " ϕ specimen (both loading cycles of TEST 3ES) are included in

Figure 4.38. In each one of the tests with the $\frac{1}{2}$ " ϕ strand specimens (TESTs 1ES and 2ES), the apparent modulus of elasticity determined by each epoxy sleeve reading was smaller than the apparent modulus determined by the average of the ER-gages (Figures 4.32 and 4.33). Although significantly reduced, a similar trend of differences was found with the 0.6" ϕ strand specimen (as shown in Figures 4.34 and 4.35). It is thus evident that the type of instrumentation system used in the single strand tests plays an important role in the determination of the apparent modulus of elasticity. The average apparent modulus determined by the epoxy sleeve readings of TEST 1ES ($E_{app}=27,571\text{ksi}$, see Figures 4.32 and 4.36) was found to be 5.3% lower than the manufacturer modulus that was provided with the prestressing strand roll ($E=29,100\text{ksi}$). This difference was unexpectedly high and was presumably related to the use of a lower strength epoxy mix in the epoxy collars used for this particular test. The quality of the Industrial Coating A-103 two-part epoxy was considerably altered by the mixing of sand. The lower strength epoxy collars suffered several small tension cracks that may have caused the measurement of larger strains at each loading step.

Sand mixes were avoided in the following single strand tests. A strand specimen taken from the same roll as the specimen used in TEST 1ES was tested with a stronger epoxy mix in TEST 2ES. The average modulus of the epoxy sleeve readings of this second test ($E_{app}=29,504\text{ksi}$, see Figures 4.33 and 4.36) was in better agreement with the manufacturer provided modulus ($E=29,100\text{ksi}$).

No accurate conclusions can be drawn from the apparent modulus determined by the average of the epoxy sleeve readings from both loadings of the 0.6" ϕ strand. This is because no manufacturer modulus of elasticity was obtained with the prestressing strand roll from where this specimen was taken. However, the results of TESTs 3ESa and 3ESb were quite similar, as indicated by the 334ksi standard deviation of the eight different statistical observations (shown in Figure 4.38). The general average of the apparent modulus of these two tests was 29,261ksi. This average is just 227ksi smaller than the apparent modulus determined by the average of the ER-gages (29,488ksi, shown previously in Figure 4.18). This similarity of behavior between epoxy sleeve and ER-gage results can be seen easily in Figures 4.34 and 4.35.

The variability of the results of the epoxy sleeve system used in TESTs 3ESa and 3ESb was lower than the variability of the results of the ER-gages (TESTs 4Sa and 4Sb). The modulus obtained from a single epoxy sleeve location (in TESTs 3ESa and 3ESb) was found

more likely to be within $\pm 1.14\%$ of the average reading, whereas for a single ER-gage reading this value was ± 1.35 (for the same tests). In the first two single strand tests the variability of the results of the epoxy sleeve reading locations was much higher ($\pm 4.47\%$, as shown in Figure 4.37). It is probable that this effect was caused by the use of a lower resolution Demec extensometer (as explained earlier, a 200mm Demec extensometer of $8\mu\epsilon$ resolution was used in TESTs 1ES and 2ES, whereas TESTs 3ESa and 3ESb had a 400mm Demec of $4\mu\epsilon$ resolution). Another factor that could have influenced the difference in the homogeneity of the results of these single strand tests was the use of a high precision load cell in TESTs 3ESa and 3ESb. This cell helped determining more accurate loads at each measuring stage.

d. Conclusions. The following conclusions can be drawn from the epoxy sleeve systems installed in single prestressing strands:

- a. Low strength epoxy mixes (especially those with sand in the mix) were found to provide unreliable performance.
- b. The apparent modulus of elasticity determined from the epoxy sleeves was generally found similar to the manufacturer given values. In some cases, the epoxy sleeve apparent modulus was also found close to the apparent modulus determined by the electrical resistance strain gages. However, in average the measured results indicated that the type of instrumentation system used makes a difference in the determination of the apparent modulus of elasticity of the prestressing strand.
- c. The modulus of elasticity obtained from the data reduction of the readings from one location around a particular epoxy sleeve was very similar to the results obtained from other reading locations around the same epoxy sleeve. A single epoxy sleeve reading location was found to provide results that were around $\pm 1.14\%$ of the average apparent modulus of elasticity.
- d. Judging from the results and the repeatability of the epoxy sleeve readings in single strand tests, it was concluded that the epoxy sleeves provided an accurate instrumentation system for determining the load level at intermediate cross-sections of individual prestressing strands.

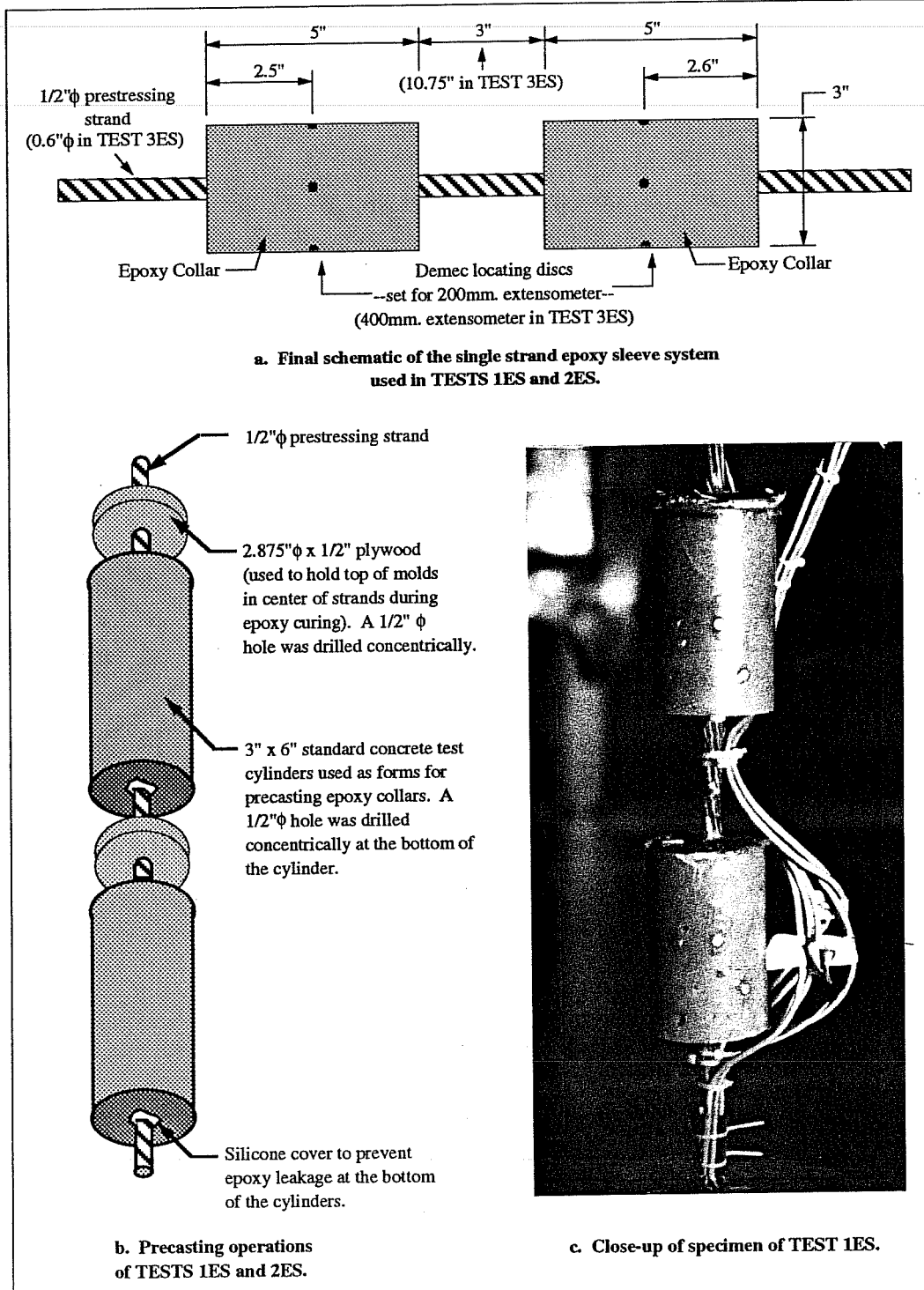


Figure 4.31 Schematic of the epoxy sleeve systems used in single strand tests.

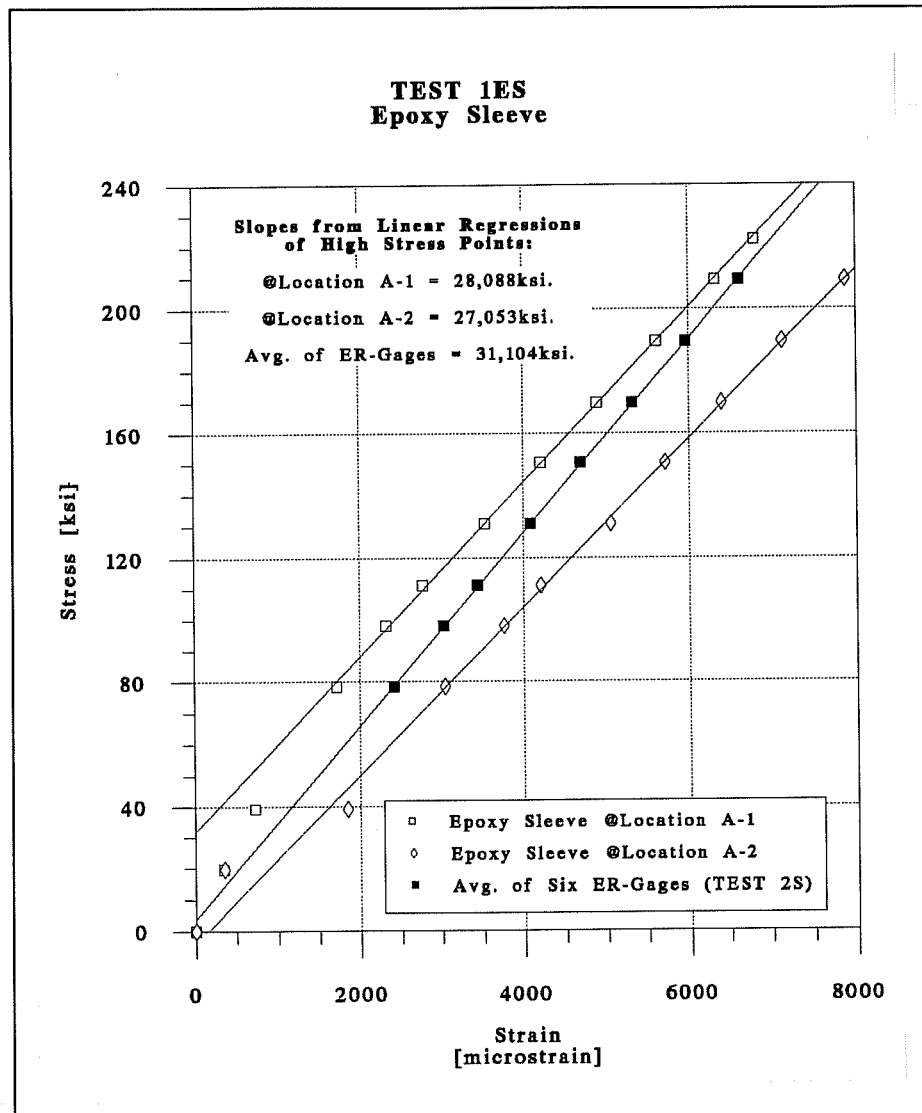


Figure 4.32 Stress-strain plots for TEST 1ES on $\frac{1}{2}$ " ϕ strand specimen from roll "B".

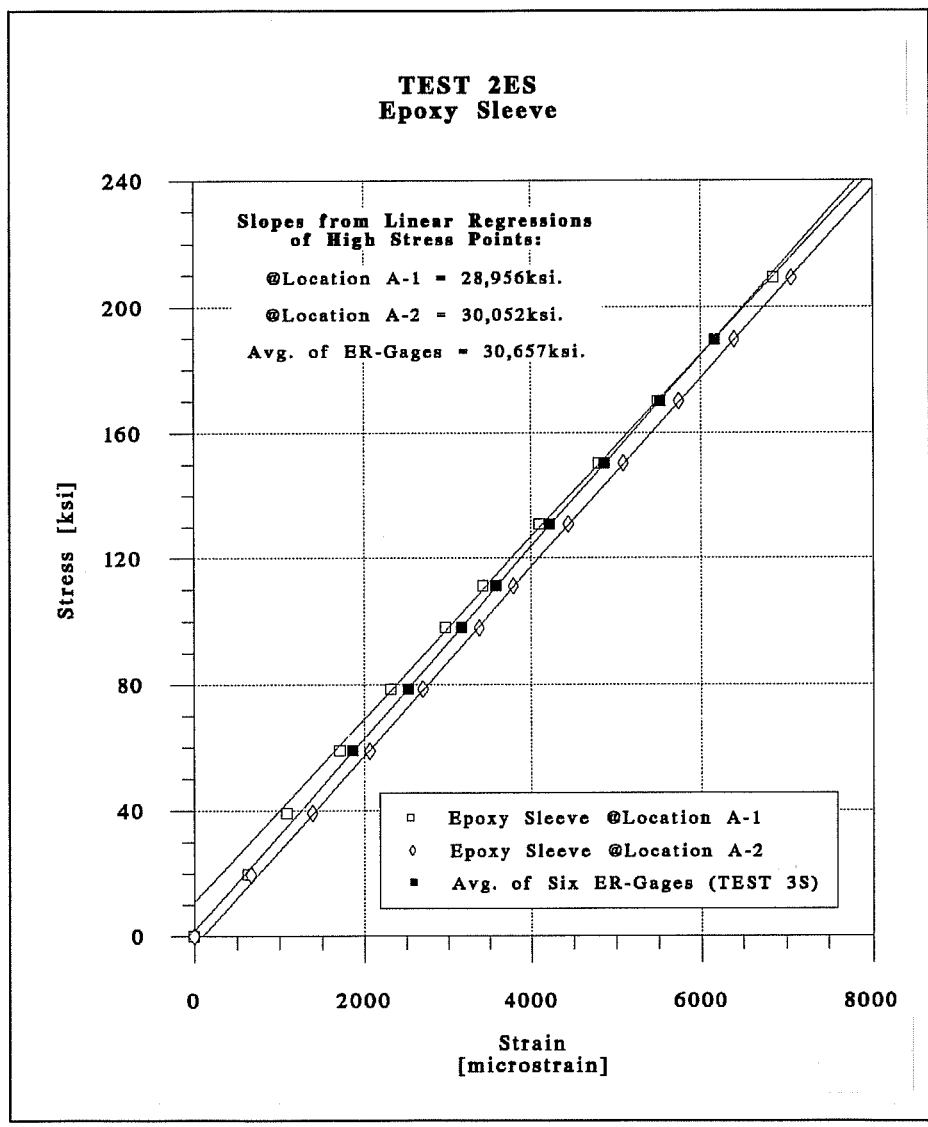


Figure 4.33 Stress-strain plots for TEST 2ES on 1/2 " ϕ strand specimen from roll "B".

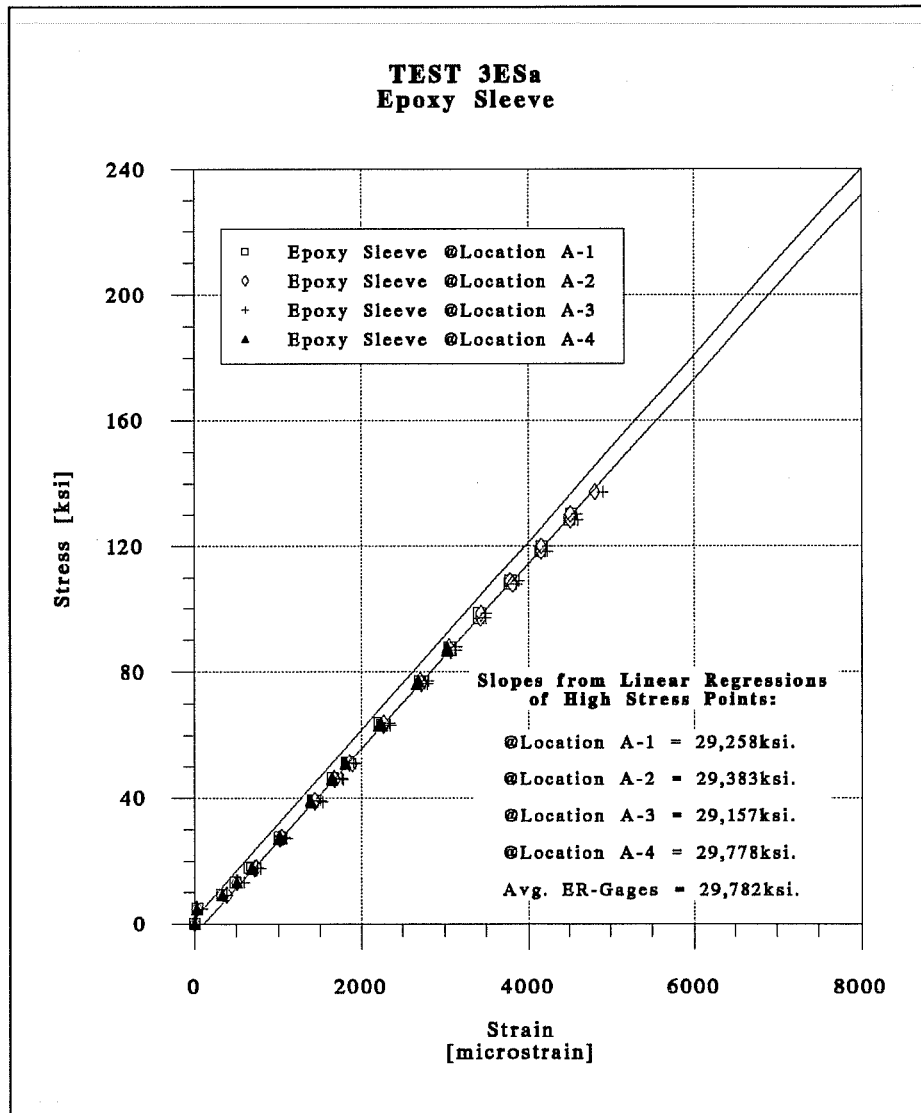


Figure 4.34 Stress-strain plots for first loading cycle of TEST 3ES on 0.6" ϕ strand specimen from roll "C".

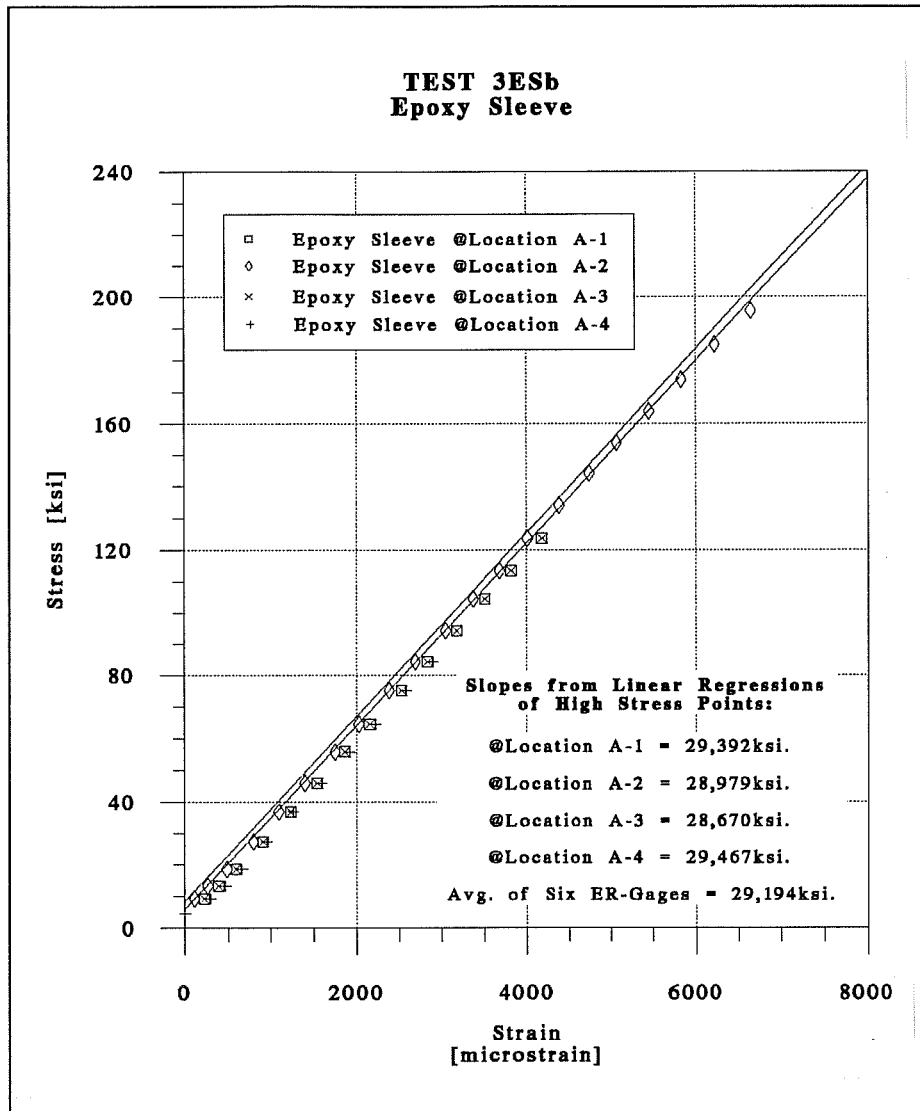


Figure 4.35 Stress-strain plots for second loading cycle of TEST 3ES on 0.6" ϕ strand specimen from roll "C".

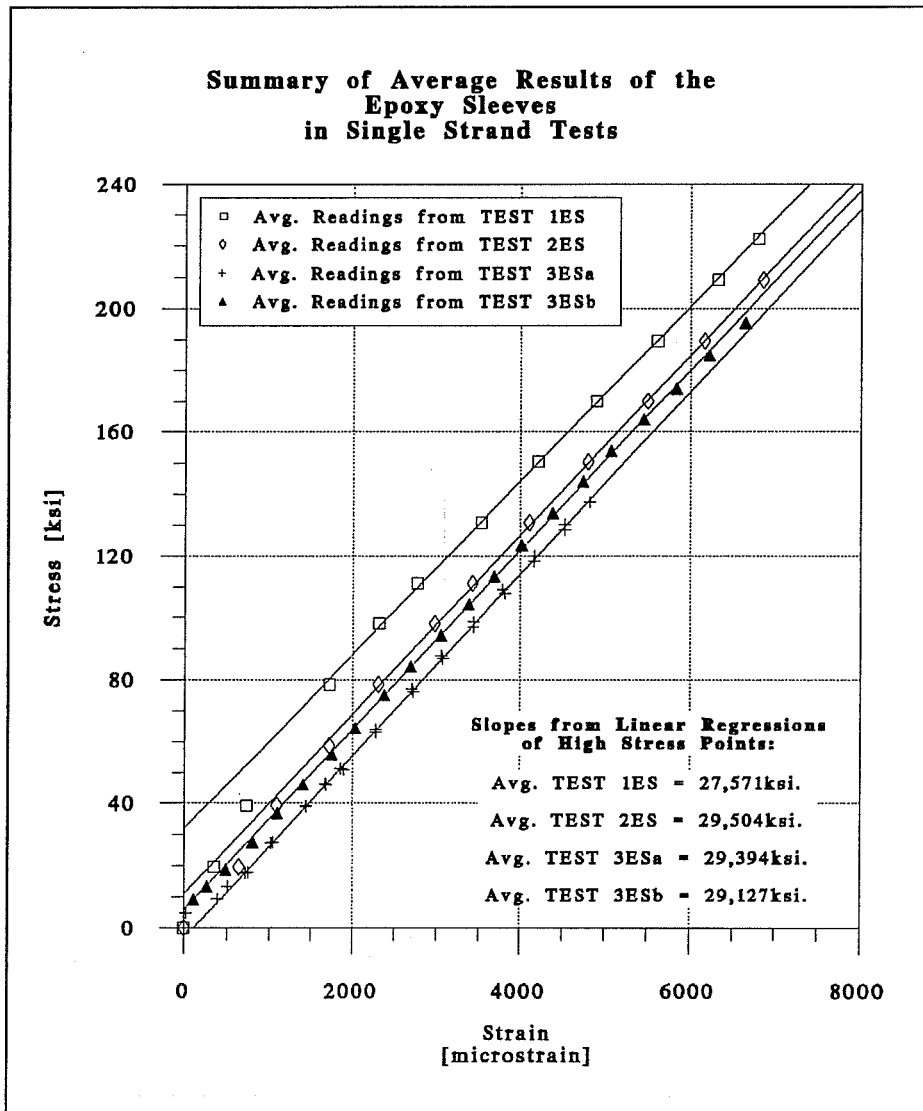


Figure 4.36 Summary of stress-strain average plots of single strand tests with epoxy sleeves.

Summary of results from tests of specimens from strand roll "B" (½" diameter):

		Computed Modulus of Elasticity *	
		[ksi]	
		TEST 1ES	TEST 2ES
	Epoxy Sleeve @Location A-1	28088	28956
	Epoxy Sleeve @Location A-2	27053	30052
Final Statistics (from both TESTS):	Min.:	27053	
	Max.:	30052	
	St. Dev.:	1275	
	Avg.:	28537	
	Variability of Avg.**:	±4.47%	

Notes:

* To obtain each computed modulus of elasticity, a best-fit line was computed considering only the measured data points that corresponded to stresses between 0.20fpu and 0.80fpu. No other manipulation of raw data was performed.

** The values corresponding to the variability of each given average were considered to be equal to the percentage of the ratios between the standard deviation of each set of slope observations and their corresponding average slope.

Figure 4.37 Statistical analysis of epoxy sleeve results from tests on ½ " ϕ strand specimens from roll "B".

Summary of results from tests of specimen from strand roll "C" (0.6" diameter):

		Computed Modulus of Elasticity *		Final Statistics (from both TESTS):
		[ksi]		
		TEST 3ESa	TEST 3ESb	
Epoxy Sleeve @Location A-1		29258	29392	
Epoxy Sleeve @Location A-2		29383	28979	
Epoxy Sleeve @Location A-3		29157	28670	
Epoxy Sleeve @Location A-4		29778	29467	
Final Statistics (per TEST):	Min.:	29157	28670	28670
	Max.:	29778	29467	29778
	St. Dev.:	272	373	334
	Avg.:	29394	29127	29261
	Variability of Avg.**:	±0.93%	±1.28%	±1.14%

Notes:

* To obtain each computed modulus of elasticity, a best-fit line was computed considering only the measured data points that corresponded to stresses between 0.20fpu and 0.80fpu. No other manipulation of raw data was performed.

** The values corresponding to the variability of each given average were considered to be equal to the percentage of the ratios between the standard deviation of each set of slope observations and their corresponding average slope.

Figure 4.38 Statistical analysis of epoxy sleeve results from tests on the 0.6" ϕ strand specimen from roll "C".

4.3.2.2 Multi-Strand Tendon Tests. As explained previously in Section 4.3.1.3, each strand of a multi-strand tendon experiences a different level of stress in most field applications. The epoxy sleeve system would then have to bond to each strand and adequately average their stresses for it to be successful in measuring tendon loads. Tests were thus performed on multi-strand tendons to check the performance of various sizes of epoxy sleeves. Initial tests were performed in 7- and 12- ½ " ϕ strands, and final tests were implemented on 19-0.6" ϕ strands.

a. Tests Descriptions. A sample preparation process for one of the epoxy sleeve systems used in the multi-strand tendon tests is included in Figure 4.39. Recommendations about the precast process and the installation of the final epoxy sleeve system in multi-strand tendons are included in Section 5.3.

The first two tendon tests of the epoxy sleeve system were TEST 1T and TEST 2T reported previously in the section of electrical resistance strain gages. For organizational purposes these tests were split according to the two measurement systems investigated. A general sketch of the testing setup has been shown already in Figure 4.11. The epoxy sleeves used in both of these tests were made with Industrial Coating A-103 Epoxy donated by the Material Testing Laboratories of TSDHPT.

The last two tendon tests, TEST 3T and TEST 4T, were also the same as those mentioned previously in the section on electrical resistance strain gages. The corresponding test setup was sketched in Figure 4.12. The epoxy resin used in TEST 3T consisted of Industrial Coating A-103 (Type V Epoxy Resin) also donated by the Materials Testing Laboratories of TSDHPT. The epoxy resin of TEST 4T was Sikadur 32 Hi-Mod. donated by Sika, Inc.

The molds for the epoxy collars consisted of 6in. o.d. standard PVC drainage pipes of 10in., 10in., 13in., and 13in. lengths corresponding to the 7-, 12- ½ " ϕ , and the two sets of 19-0.6" ϕ strands respectively (TESTs 1T, 2T, 3T and 4T). Each mold had a single longitudinal splitting cut and two 2in. x 1in. rectangular cuts located approximately in the middle of the cylinder, on both sides of the longitudinal cuts.

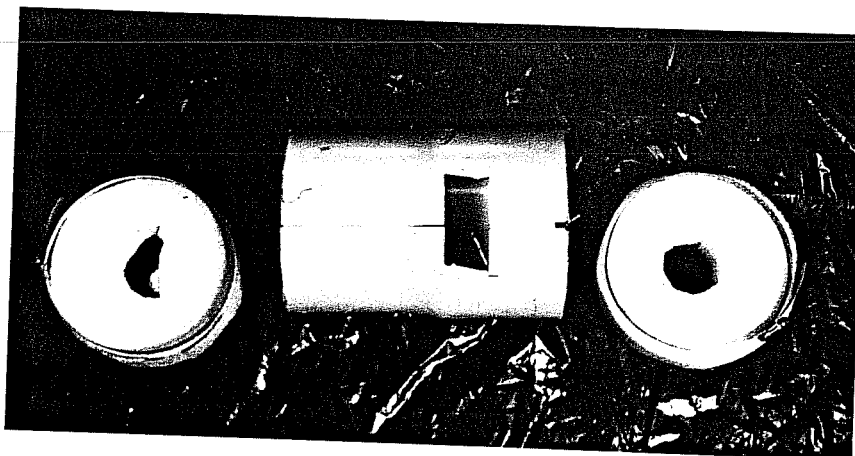
A pair of plastic foam pieces of 2in. thickness were cut in circular shapes of 6in. o.d. The middle of these pieces were in turn cut into the approximate shape of the tensioned tendons --but at a reduced size. These were used as end covers of the PVC cylinders. The final locations of the foam molds in the tendon were then calculated and marked. These marks indicated the cross-sections where silicone was to be injected: between, and around the

prestressing strands. This process was found to be critical and should be done very carefully. A large screwdriver was used as an aid for separating the strands to allow for the installation of silicone in the tight spaces at the center of the tendon. Once the silicone was placed between all the strands, the molds were installed in their marked locations. The ends of the PVC cylinders were in turn placed around the foam molds, making sure that the square holes of the cylinders were facing up. Large diameter hose clamps were finally used to tighten the PVC cylinders to the foam molds.

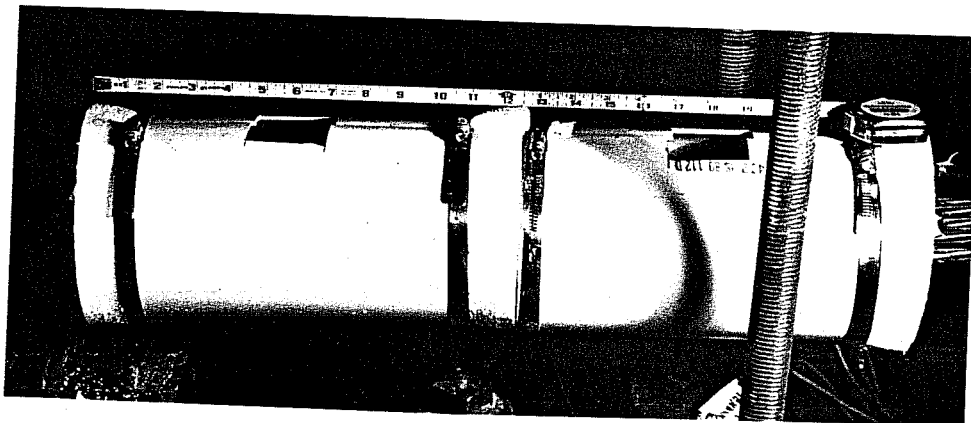
The strong tightening pressure of the hose clamps against the foam molds and the strands spread the silicone to less accessible areas between the strands. The excess silicone outside the foam molds was spread evenly around the outer surfaces of the strands. A 1hr drying period was the minimum allowed for curing time of the silicone in the strands. After proper mixing of the epoxy resins, they were poured in the square holes on the top part of the PVC cylinders. Lack of careful spreading of the silicone between strands resulted in several leaks in the epoxy collars of TEST 2T (see Figure 4.40). However, it was found that small leaks usually stopped quickly due to the quick hardening of the epoxy resins (caused by the overheating effect created by large volumes of epoxy).

The epoxy sleeves were given an average 8hr drying period at normal summer temperatures of $\approx 80^{\circ}\text{F}$. Once hardened, the PVC molds were separated from the epoxy collars in certain sections. Pairs of Demec locating points were installed directly on the epoxy collars, and on the PVC molds to compare measurements. The lack of longer gage lengths of Demec extensometers limited the tendon tests to a combination of 100mm and 200mm gage lengths. The 400mm Demec extensometer designed for the San Antonio Y field tests was received too late for use in these trials.

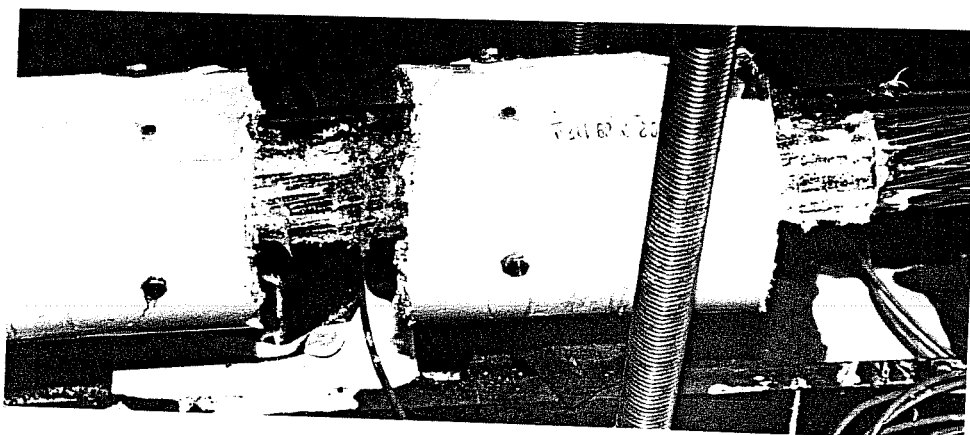
Tendon loading was performed up to $\approx 0.80f_{pu}$ for the $\frac{1}{2}$ " ϕ strands, and up to $\approx 0.85f_{pu}$ for the 0.6" ϕ strands. The loading steps were mostly done in 10kip increments for TEST 1T and 2T, and in 100kip increments for TEST 3T and 4T. At the time of each mechanical measurement of the strains at each instrumented location of the epoxy sleeves of TESTs 1T and 2T, the corresponding live end load levels were automatically scanned by a computer-controlled data acquisition system. Load levels were determined from readings of an electrical resistance pressure transducer installed in the pressure line of the hydraulic jack used for stressing the tendons. In TESTs 3T and 4T, loads were computed at the live ends from pressure readings of a



a. Molds for the epoxy sleeve.



b. Installed epoxy sleeve assembly.



c. Final gaged epoxy sleeve system.

Figure 4.39 Construction steps of the epoxy sleeve system used in TEST 2T.

calibrated hydraulic jack instrumented with a pair of dial indicators.

b. Data Reduction Method. A similar method to that described previously in Section 4.3.1.3 was used for the data reduction of the measured epoxy sleeve strains. This method is explained here for the particular case of the epoxy sleeve readings.

As mentioned earlier, stressing loads of the instrumented spans of the San Antonio Y project will be obtained with electrical resistance pressure transducers installed in the calibrated hydraulic jacks. These pressure transducers will be scanned at regular time intervals and will be related to the mechanical strain readings of the epoxy sleeves located at selected intermediate cross-sections of the external tendons (the stressing load will be maintained for about 20min. on each reading operation). The information available to the researcher will therefore consist of live end loads and corresponding cross-section strains of instrumented tendons. The stress loss from the live end to each intermediate tendon cross-section is unknown but will be estimated using live end loads and cross-section strains. Another expected field complication is that the strands of each multi-strand tendon will probably behave erratically at low stress levels (mainly because of uneven strand anchorage and varying strand lengths).

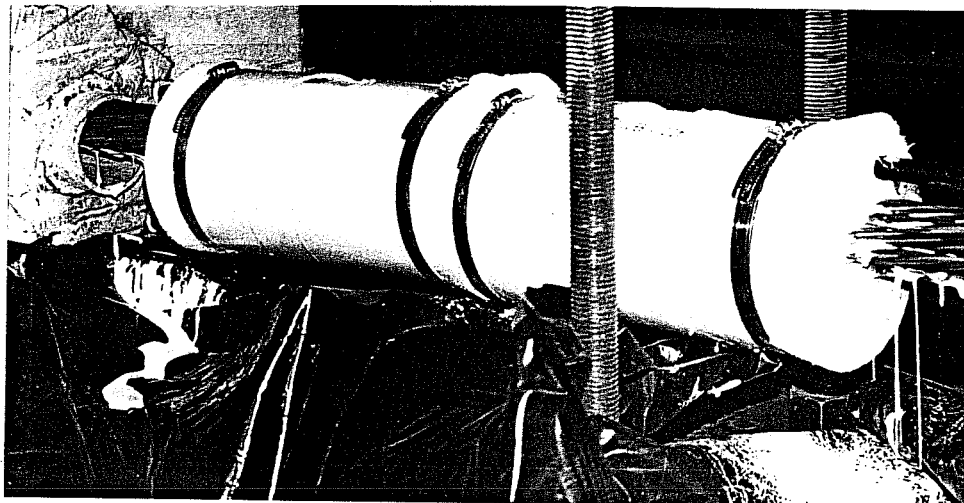


Figure 4.40 Epoxy leaks in TEST 2T.

The data reduction process suggested in this report is based on the same field conditions and available information expected for the San Antonio Y instrumentation project. Average tendon stress values at the live ends were obtained by considering the nominal areas of 0.153in^2 and 0.215in^2 for each one of the $\frac{1}{2}$ " ϕ and the 0.6 " ϕ strands respectively. Strains from each

reading location of each epoxy sleeve and their corresponding live end stresses computed from the pressure transducer (or dial indicator) readings were plotted on a σ - ϵ graph. For each reading location of each epoxy sleeve, a best-fit line was computed considering the data points that corresponded to stresses located between $0.20f_{pu}$ and $0.80f_{pu}$. The intersection of this best-fit line with the ϵ -axis was also computed. This value --labeled " ϵ_o "-- was considered to be the strain reading that corresponded to the zero stress level. Each measured value of strain was thus corrected by arithmetically subtracting the computed initial strain value (ϵ_o). Stress levels were then obtained by multiplying each corrected strain value by the apparent modulus of elasticity (previously obtained in the prestressing strand material tests). Stress losses produced in each loading step were estimated by comparing reduced stresses (of the intermediate epoxy sleeve system) with corresponding live end stresses (measured by the calibrated hydraulic jack). An estimate of the average tendon stress loss was calculated by the average of the intermediate loading step losses registered at each reading location of each epoxy sleeve (only comparing the intermediate stresses located between $0.20f_{pu}$ and $0.80f_{pu}$). However, a more accurate average of the stress loss from live end to each instrumented tendon cross-section was obtained by computing the ratio between the slope of the calculated best-fit line of each epoxy sleeve reading location with the slope obtained from the material tests of the prestressing strands (the apparent modulus of elasticity). When using more than a single reading location on each epoxy sleeve, an even better estimate of the tendon stress loss was given by averaging the stress losses determined from the individual reading locations.

The strain reading corresponding to the zero stress value (ϵ_o) of each epoxy sleeve system is particularly difficult to determine without a regression analysis of the measured data. A graphical description of the cause of this particular problem is shown in Figure 4.41. A proper data reduction process is thus very important for the case of strain readings from epoxy sleeve systems.

c. Interpretation of Results from TEST 1T and TEST 2T. Strains obtained from each reading location of the epoxy sleeves used for TEST 1T and TEST 2T were plotted against corresponding stress values computed from a pressure transducer located at the live end. These plots are shown in Figures 4.42 and 4.43. The σ - ϵ curves of both plots are shifted away from the origin of coordinates because each prestressing strand was independently stressed to 20ksi in TEST 1T, and to 40ksi in TEST 2T before the ER-gages were installed. This was done to

prevent overstressing the individual strands (small differences in strand lengths can be critical when the tendon is relatively short and loaded to about 80% of its ultimate capacity). The best-fit lines (along with their calculated slopes) defined by the high stress data points of the σ - ϵ graphs of each epoxy sleeve reading location are also included in the plots of Figures 4.42 and 4.43.

The results of both tendon tests with $\frac{1}{2}$ " ϕ strands are drawn together on a single graph (shown in Figure 4.44) to compare their average behavior. Finally, a detailed statistical analysis from the results of both tests is included in Figure 4.45.

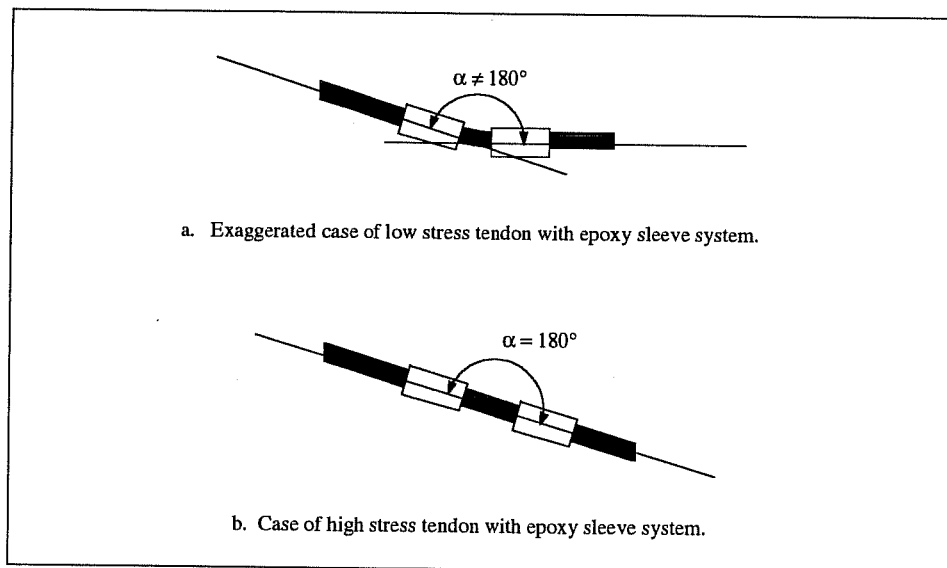


Figure 4.41 Problems for finding the zero stress reading in epoxy sleeve systems.

Material tests of a specimen taken from the same prestressing strand roll used for tendon TESTs 1T and 2T were included as strand TESTs 1ES and 2ES in the previous section (Section 4.3.2.1). As shown previously in the statistics of Figure 4.37, the average apparent modulus of elasticity obtained from the material test specimens was found to be equal to 28,537ksi. This apparent modulus was the one used for determining the average stress losses occurring from the live end to the instrumented cross-section of each tendon.

As shown in Figure 4.42, the strains measured in the three epoxy sleeve reading locations of TEST 1T at each loading step were quite similar to each other. In fact, the statistical analysis of the results of this test (shown in Figure 4.45) indicated a $\pm 1.12\%$

variability. This was an indication that the strains experienced at all locations around the epoxy sleeves were practically the same. Any single location can thus provide an accurate idea of the average strains determined by the epoxy sleeve system. A similar behavior occurred in the epoxy sleeves of TEST 2T (shown in Figure 4.43). In this second tendon test, although strains were similar at each loading step, the σ - ϵ curves were highly non-linear. This was caused by tension cracks that appeared around the epoxy sleeves of TEST 2T. As a reminder, this second test was performed on a tendon composed of a larger number of strands than the first tendon (12- $\frac{1}{2}$ " ϕ strands instead of the 7- $\frac{1}{2}$ " ϕ strands used in TEST 1T). The length of each epoxy collar of TEST 2T (about 7in.) and the type of epoxy resin employed (Industrial Coating A-103) were exactly the same as for TEST 1T. The results of these initial tests thus influenced certain modifications of the epoxy sleeve systems to be used in the future 19-0.6in. ϕ tendon tests: (a) the length of each epoxy collar should be increased to about 10in., and (b) a stronger epoxy resin (such as Sikadur 32 Hi-Mod) should be used.

The average results of TESTs 1T and 2T (performed in the same test setup) were both plotted in Figure 4.44. The best-fit lines --corresponding to the data points located between $0.20f_{pu}$ and $0.80f_{pu}$ -- of the average results were found to be quite similar. However, this particular occurrence is highly inconclusive due to the nonlinear behavior of the σ - ϵ response of TEST 2T (as shown in Figure 4.44).

An important characteristic of the behavior of the epoxy sleeves in TESTs 1T and 2T can be determined from the comparisons of the slopes of the best-fit lines of the epoxy sleeves and the corresponding best-fit lines of the ER-gages (Figures 4.42 and 4.43). In the statistical analysis of the results from the epoxy sleeve readings (shown in Figure 4.45), it is indicated that the slopes of the best-fit lines indicate average stress increases of 20% from the live end to the intermediate section instrumented with the epoxy sleeves. This obviously could not have occurred. In the data reduction process, it was found later that the small strain increases measured in the epoxy sleeves must have been directly related to: (a) the incorrect positioning of the Demec extensometers, and (b) the linear stress distribution occurring through the epoxy collars. The probable distribution of stresses in a typical epoxy collar is shown in Figure 4.46. The epoxy sleeve strains of TEST 1T and 2T were not measured from the center-to-center distance between the two epoxy collars but rather from about their nearest quarter points (as shown in Figure 4.47a). The internal strains between these points and the center points were

thus not measured in these tests and caused an "apparent" increase in stress. The system shown in Figure 4.47b was used in the following tendon tests (since the 400mm Demec extensometer was not yet available for testing). For the actual San Antonio Y field measurements, the system shown in Figure 4.47c was finally designed with the 400mm Demec extensometers.

d. Conclusions from TEST 1T and TEST 2T. The following conclusions can be drawn from the epoxy sleeves used in the first two tendon tests (composed of $\frac{1}{2}$ " ϕ prestressing strands):

- a. Strains were found to be very similar in different locations around the epoxy sleeves. According to results from TEST 1T, the measurement of strains in a single location of the epoxy sleeve will more likely give results that are within ± 1.12 of the average strains.
- b. The strength and the length of the epoxy used for the collars is critical for applications in tendons with a large number of strands. It was found that an epoxy collar length of 7in. was small for $12\text{-}\frac{1}{2}$ " ϕ strands. From the test results, a 10in. length was suggested as the minimum for the epoxy collars of tendons composed of $19\text{-}0.6$ " ϕ strands. It was also found important to carefully measure the right mixing amounts of each epoxy product.
- c. Absolute measurements from the epoxy sleeves of both initial tendon tests showed inconsistent strains when compared to the ER-gage measurements. A theoretical stress distribution in each epoxy collar was considered. This distribution suggested that future epoxy sleeve strains should be measured with a gage length equal to the center-to-center distance between each pair of epoxy collars.

e. Interpretation of Results from TEST 3T and TEST 4T. Three loading cycles from zero stress to $0.85f_{pu}$ were performed in tendon TESTs 3T and 4T. In each one of these two tendon tests, the strains measured from two epoxy sleeve reading locations were plotted against corresponding stress values computed from readings of a dial indicator located at the live end. Since the strains were found previously to be similar at different locations around each epoxy sleeve, readings from two locations were only taken in the first loading cycles of TESTs 3T and 4T. The σ - ϵ plots corresponding to each epoxy sleeve reading location and to each loading cycle of TESTs 3T and 4T are shown in Figures 4.48 and 4.49 respectively.

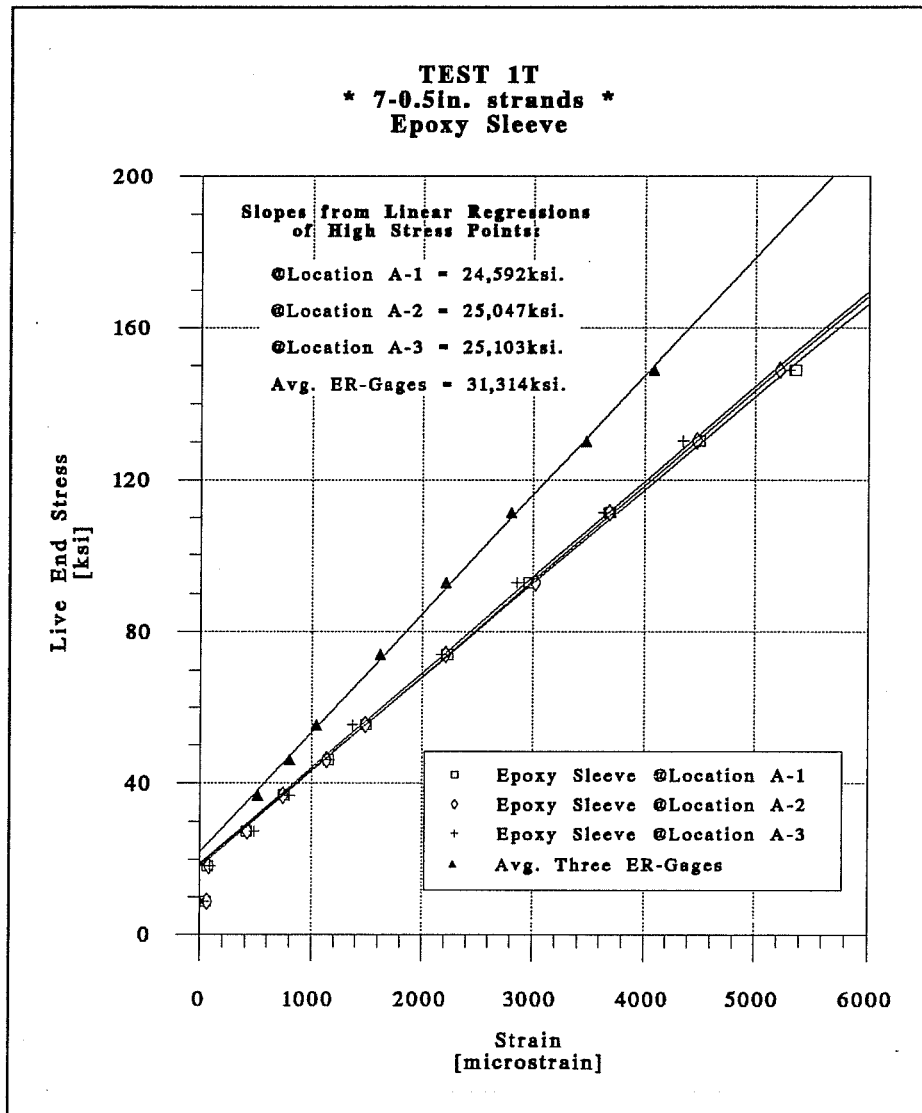


Figure 4.42 Stress-strain plots of individual epoxy sleeve reading locations for TEST 1T.

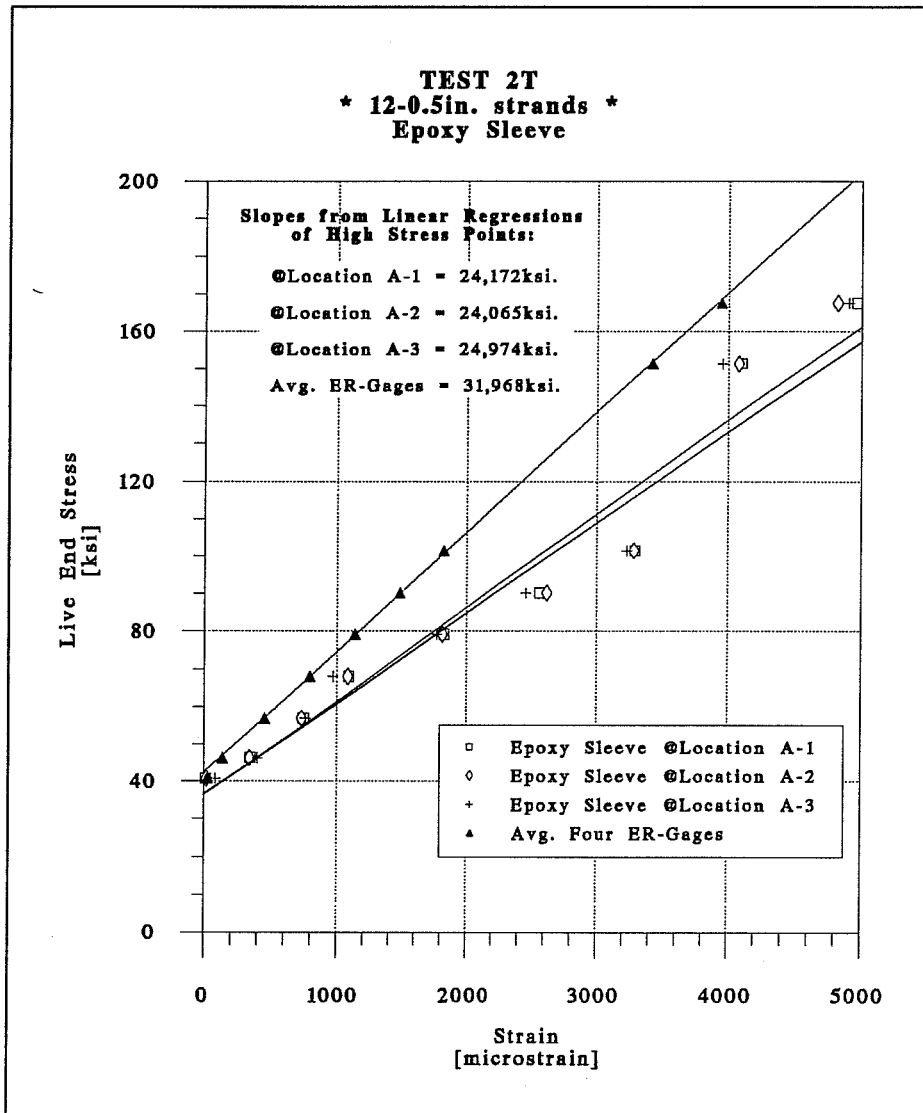


Figure 4.43 Stress-strain plots of individual epoxy sleeve reading locations for TEST 2T.

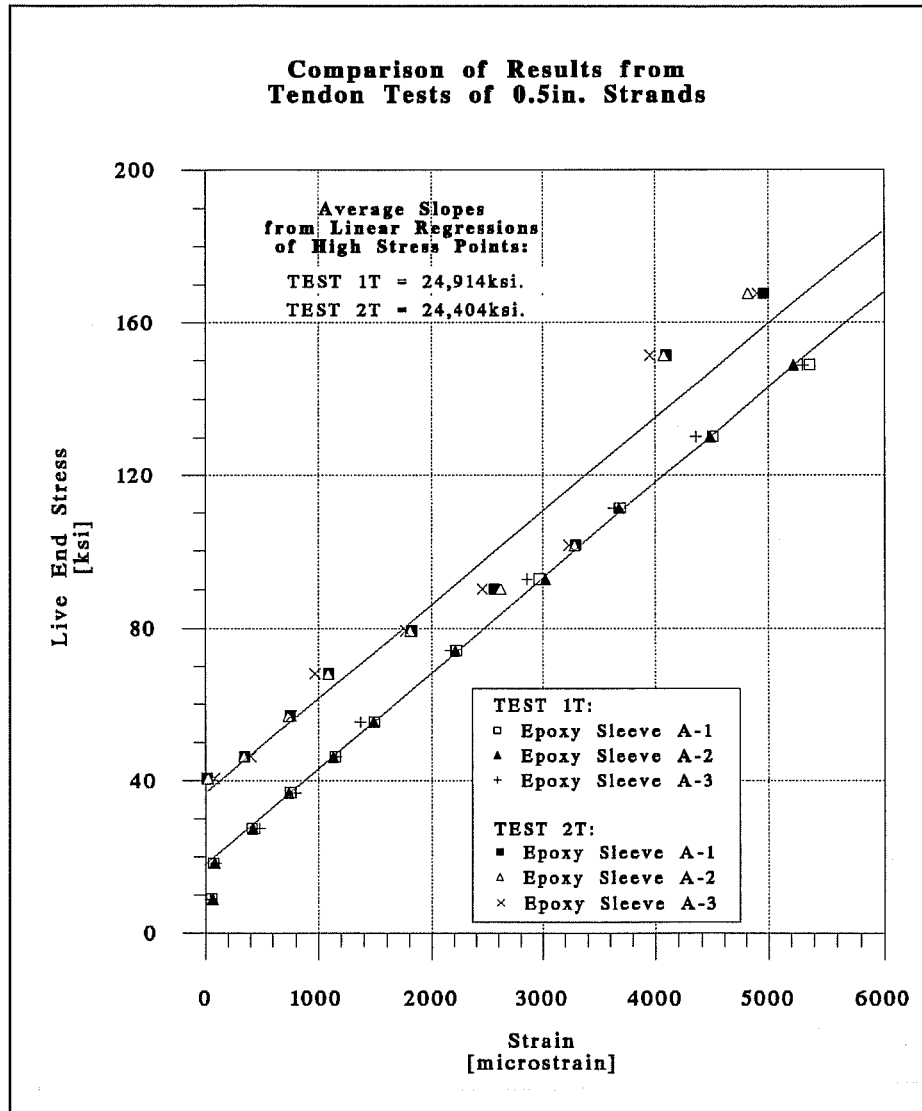


Figure 4.44 Summary of stress-strain average plots for TESTs 1T and 2T.

A. Summary of results from tests on tendons composed of ½" diameter strands:

		Slope of Best-Fit Line *		Statistics of Epoxy Sleeves (from both TESTS):
		[ksi]		
		TEST 1T	TEST 2T	
Epoxy Sleeve @ Location A-1		24592	24172	
Epoxy Sleeve @ Location A-2		25047	24065	
Epoxy Sleeve @ Location A-3		25103	24974	
Statistics of Epoxy Sleeves (per TEST):	Min.:	24592	24065	24065
	Max.:	25103	24974	25103
	St. Dev.:	280	497	456
	Avg.:	24914	24404	24659
	Variability of Avg.**:	±1.12%	±2.04%	±1.85%

B. Summary of stress losses from tests on tendons composed of ½" diameter strands:

		Stress loss from live end ***		Statistics of Epoxy Sleeves (from both TESTS):
		[%]		
		TEST 1T	TEST 2T	
Epoxy Sleeve @ Location A-1		-20.37%	-21.73%	
Epoxy Sleeve @ Location A-2		-18.89%	-22.07%	
Epoxy Sleeve @ Location A-3		(-)	-19.13%	
Statistics of Epoxy Sleeves (per TEST):	Min. Loss:	-20.37%	-22.07%	-22.07%
	Max. Loss:	-18.89%	-19.13%	-18.89%
	St. Dev.:	1.04%	1.61%	1.45%
	Avg. Loss:	-19.63%	-20.98%	-20.44%

Notes:

- * The best-fit line of each epoxy sleeve reading location was computed considering only the measured data points that corresponded to stresses located between 0.20fpu and 0.80fpu. No other manipulation of raw data was performed.
- ** The values corresponding to the variability of each average slope were considered to be equal to the percentage of the ratios between the standard deviation of each set of slope observations and their corresponding average slope.
- *** Losses were obtained by the ratio between the modulus of elasticity given on "A" and the "apparent" modulus determined from the material tests of strand specimens taken from the same prestressing strand roll used for these tendons ($E_{app}=28,537\text{ksi}$).

Figure 4.45 Statistical analysis of epoxy sleeve results from tendon TESTs 1T and 2T with ½" ϕ strands.

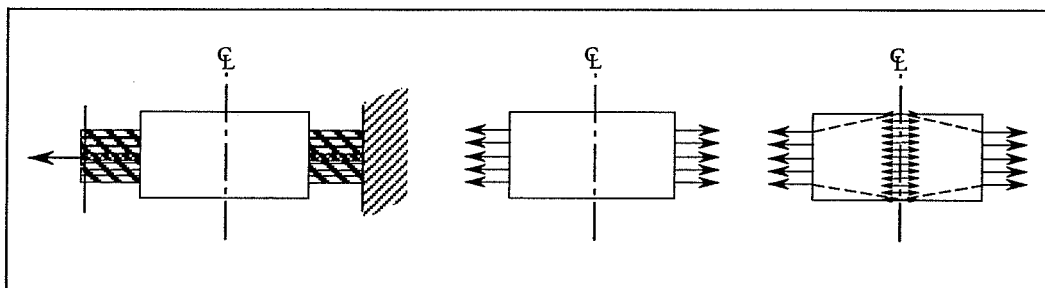


Figure 4.46 Possible stress distributions in a typical epoxy collar.

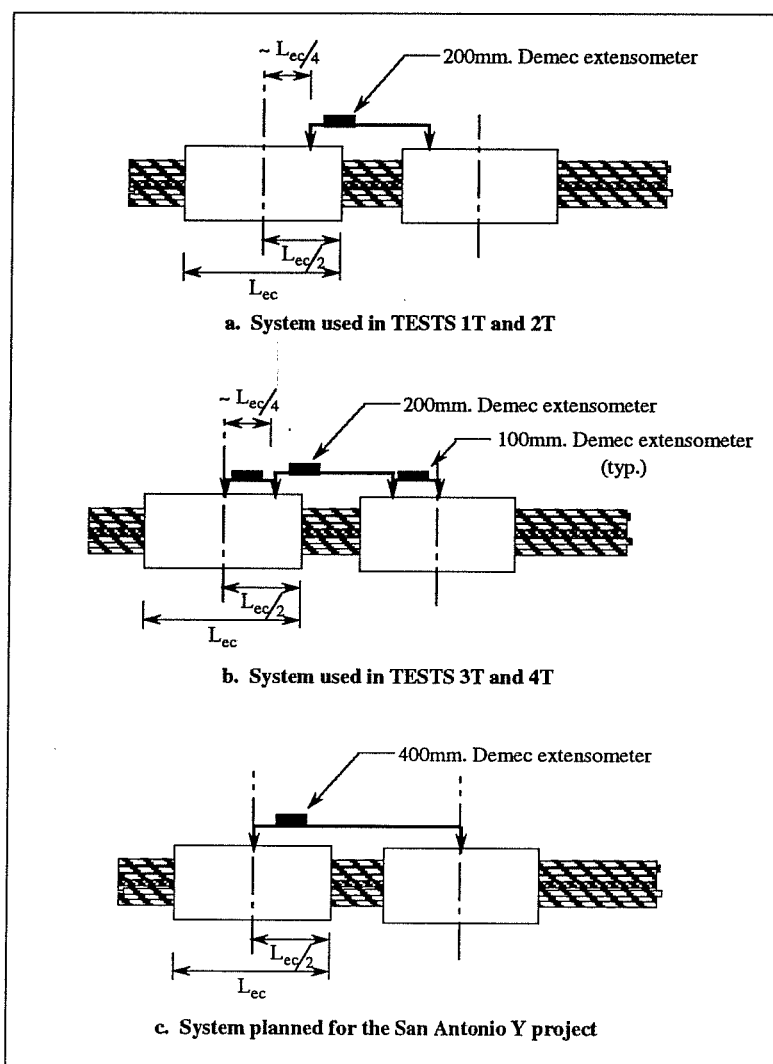


Figure 4.47 Epoxy sleeve measuring systems.

The average instrumented strand behavior of the three loading cycles of each test are compared in Figure 4.50. It must be mentioned that the epoxy sleeves used on these two tests were installed without an initial tendon stress (different than in the previous tendon TESTs 1T and 2T where initial stresses of 20ksi and 40ksi, respectively, were applied to the tendons before the installation of the epoxy sleeves). However, the plots of Figures 4.48 through 4.50 show irregular strain variations corresponding to the initial stress increases. This irregular behavior at low stress levels was related to the problem shown previously and explained in Figure 4.41.

Also included in the plots of Figures 4.48 through 4.50 are the corresponding average ER-gage results obtained for each test. Calculated values for the slopes of each one of the best-fit lines (for "high stress" data points) are also shown in the same figures. Finally, a detailed statistical analysis of the results from both tendon tests with 0.6" ϕ strands is included in Figure 4.51.

As mentioned previously in Section 4.3.1.3, no material tests were performed on specimens taken from the same prestressing strand roll used in TEST 3T and TEST 4T. The stress losses shown in Figure 4.51 are thus relative to the value used for the apparent modulus of elasticity (as determined by the epoxy sleeves). The apparent modulus used for stress loss computations was equal to 29,261ksi. This value was obtained from the average results of single strand TESTs 3ESa and 3ESb performed with a 0.6" ϕ prestressing strand specimen (shown previously in Figure 4.38).

The operations followed for the threading of the tendons and for the installation of the instrumentation devices during the present tests were performed with a close simulation of the actual field operations to be followed in the instrumented spans of the San Antonio Y project. As suggested by the first two tendon tests, the proper length of epoxy collars (of ≈ 10 in.) and Demec extensometers were used in the final tendon tests. Instead of the 400mm Demec extensometers, a proper gage length was achieved by using a combination of 200mm and 100mm Demec extensometers (as shown previously in Figure 4.47c).

Initial observation of Figure 4.48 reveals that the strains measured in the epoxy sleeve reading location A-1 during the first loading cycle of TEST 3T differ from the rest of the readings until ≈ 110 ksi. However, beyond this relatively high stress level the following four readings were quite linear. Strains measured in the same location (A-1) during the following loading cycles became linear at a slightly lower stress level (around 80ksi). In the data

reduction process, the straight lines corresponding to each epoxy sleeve reading location and loading cycle shown in Figure 4.48 were thus made to fit only the data points that were approximately linear. As shown in Figure 4.48, the slope of these lines was found to be approximately the same.

At each loading step of TEST 4T the strain readings were quite similar and approximately linear starting from ≈ 50 ksi (as shown in Figure 4.49). The straight lines corresponding to each one of these epoxy sleeve reading locations and loading cycles were thus made to fit only the data points located between 50ksi and 220ksi. The slope of these lines were also found to be approximately the same (as shown in Figure 4.49).

These initial observations from Figures 4.48 and 4.49 thus indicated that in the data reduction process of large multi-strand tendons it is best to perform the data reduction process only considering the data points that approximately increased linearly in the σ - ϵ graph.

The statistical analysis of the results from both of these tests (performed in the same test setup) indicated approximately equal average slopes of the best-fit lines. Indeed, the combined statistical analysis of the results from both tendon tests (shown in Figure 4.51) only indicated a $\pm 1.52\%$ variability among the eight statistical observations. This was a better instrumentation behavior than that obtained with the ER-gages (with a variability of ± 2.61 , as shown previously in Figure 4.30).

The statistics of stress losses from live end to the instrumented tendon cross-section (shown in Table B of Figure 4.51) are not absolute values. However, the standard deviation of all eight observations indicate that the average prediction of stress loss --whatever its absolute value may be-- can vary $\pm 1.66\%$. This is a much better stress loss estimate than that obtained with the ER-gages (that had an initial variation of $\pm 2.74\%$, as previously shown in Figure 4.30). In the setup of TESTs 3T and 4T, the relative tendon stress losses from live end to the instrumented cross-section computed by the average epoxy sleeve results and the average ER-gage results were $9.5\%(\pm 1.7\%)$ and $4.9\%(\pm 2.7\%)$ respectively. This difference of results was further lowered when the ER-gage strains were reduced only considering the data points below ≈ 0.50 fpu (which is the approximate stress level when the strands started to slip in the epoxy sleeve collars). With these new stress loss estimates, the average result from the ER-gages was increased to $5.6\%(\pm 2.0\%)$. There was a clear tendency of the ER-gage average stress loss estimate to increase towards the results of the epoxy sleeve system. This seems to indicate that

the epoxy sleeve system gives a more appropriate estimate of the average tendon stresses (and consequently stress losses). A second measured epoxy sleeve behavior supporting the previous hypothesis is that the standard deviation of the results obtained from the epoxy sleeve readings was smaller than that obtained from the ER-gages. However, to reach a more conclusive opinion new tests will need to be performed with a larger number of instrumented strands with electrical resistance strain gages.

f. Conclusions from TEST 3T and TEST 4T. The following conclusions can be drawn from the epoxy sleeves installed in the final tendon tests (composed of 19-0.6" ϕ prestressing strands):

- a. The data reduction process for epoxy sleeve readings of large multi-strand tendons was found to be performed best with strict consideration of the data points that approximately increased linearly in the σ - ϵ graphs. In most cases, linear behavior of the epoxy sleeve readings started around 50ksi. However, in some special cases linearity did not occur until 80ksi.
- b. A very small variability of results was found among the epoxy sleeve readings. Eight statistical observations only produced a standard deviation corresponding to a $\pm 1.52\%$ variation of the average slope of the best-fit line in the σ - ϵ graph. This resulted in better instrumentation behavior than for the ER-gages.
- c. The epoxy sleeve systems seemed to provide a better estimate of the average tendon stress than did the ER-gages. However, to reach a better conclusion new tests are recommended to be performed using multi-strand tendons instrumented with a larger number of ER-gages.

4.3.2.3 Other Tests. Two final tests were performed on the epoxy sleeves system: one related to creep behavior, and the other one to check the performance of the epoxy sleeves during grouting of the external tendons.

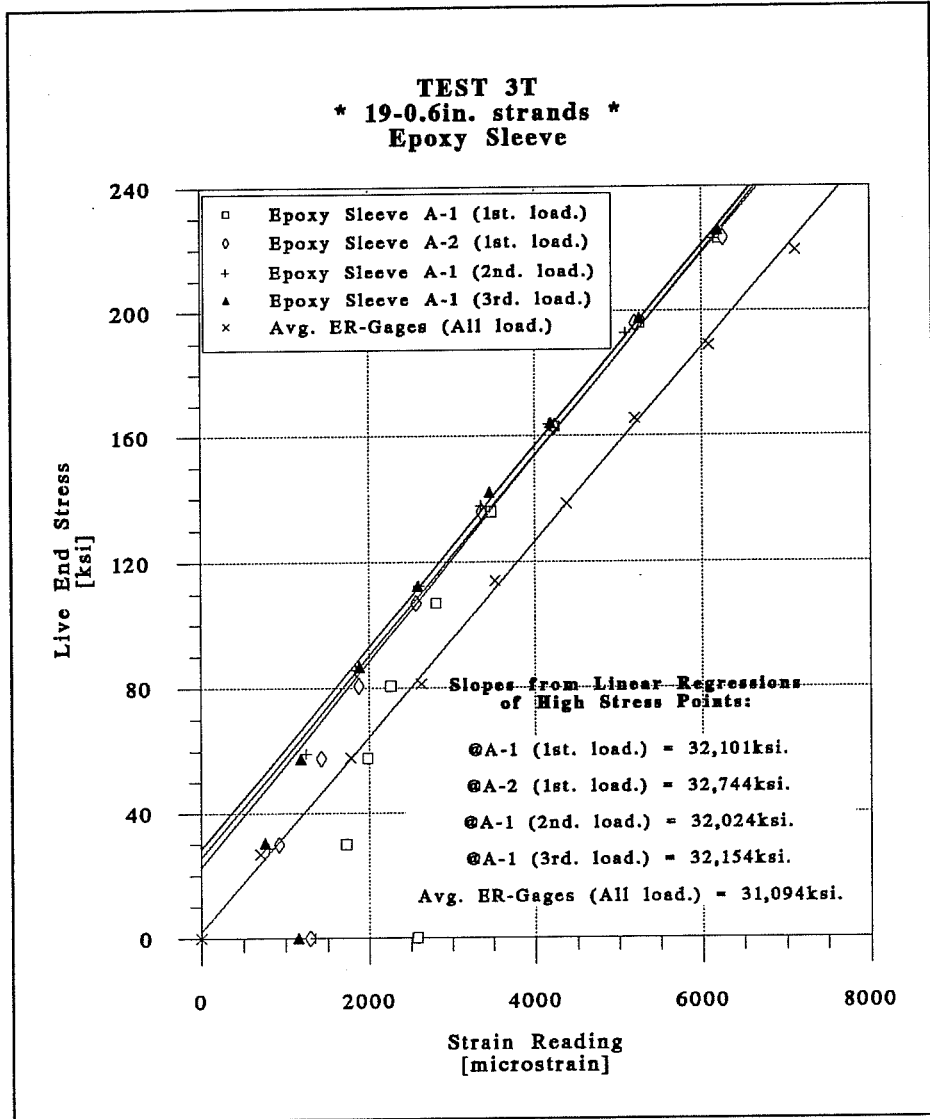


Figure 4.48. Stress-strain plots of individual epoxy sleeve reading locations for TEST 3T.

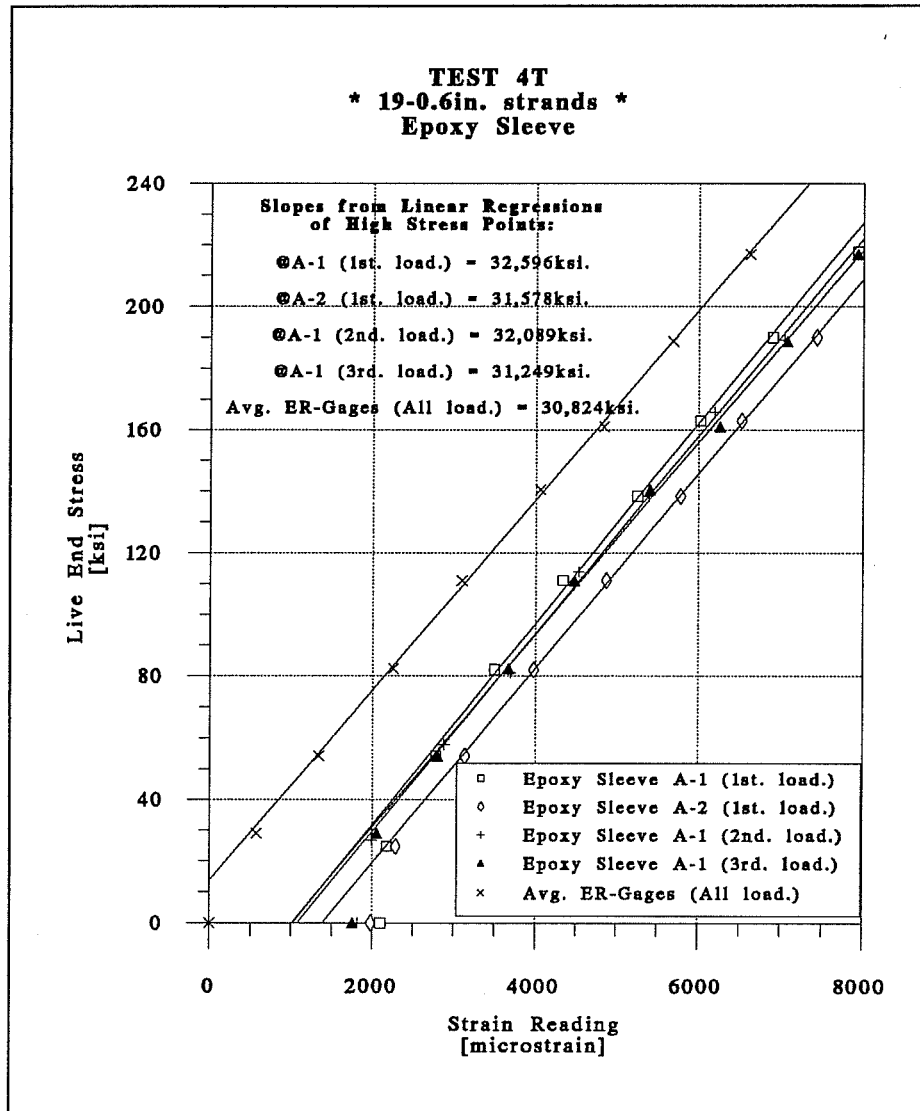


Figure 4.49 Stress-strain plots of individual epoxy sleeve reading locations for TEST 4T.

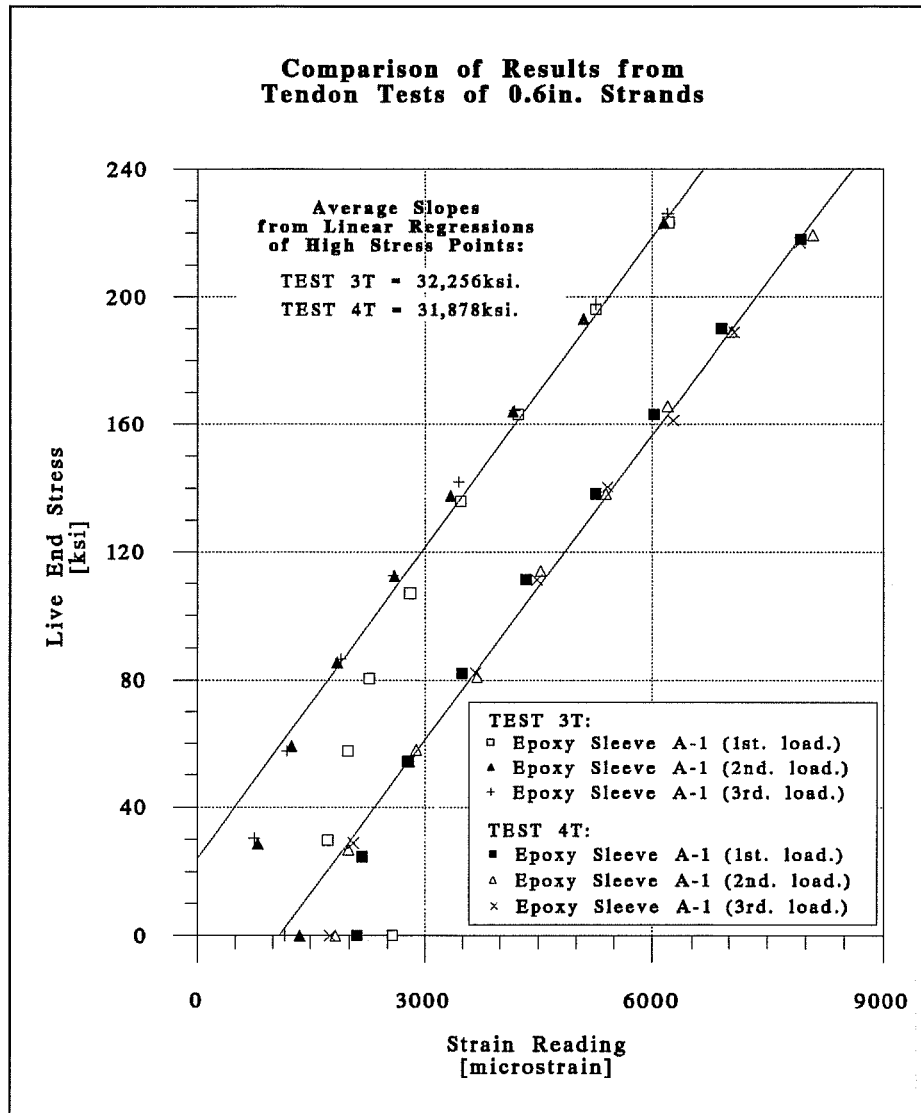


Figure 4.50 Summary of stress-strain average plots for TESTs 3T and 4T.

A. Summary of results from tests on tendons composed of 0.6" diameter strands:

		Slope of Best-Fit Line [ksf.]					
		TEST 3T			TEST 4T		
		1st. Loading	2nd. Loading	3rd. Loading	1st. Loading	2nd. Loading	3rd. Loading
Epoxy Sleeve @ Location A-1		32101	32024	32154	32596	32089	31249
Epoxy Sleeve @ Location A-2		32744	(-)	(-)	31578	(-)	(-)
Statistics of Epoxy Sleeves (per TEST):							
	Mln.:		32024			31249	31249
	Max.:		32744			32596	32744
	St. Dev.:		330			590	487
	Avg.:		32256			31878	32067
	Variability of Avg.:		±1.02%			±1.85%	±1.52%
							Statistics of Epoxy Sleeves (from both TESTS):

B. Summary of stress losses from tests on tendons composed of 0.6" diameter strands:

		Stress loss from live end (using E _{app} =29,261ksf.) [%]					
		TEST 3T			TEST 4T		
		1st. Loading	2nd. Loading	3rd. Loading	1st. Loading	2nd. Loading	3rd. Loading
Epoxy Sleeve @ Location A-1		9.71%	9.44%	9.89%	11.40%	9.66%	6.79%
Epoxy Sleeve @ Location A-2		11.90%	(-)	(-)	7.92%	(-)	(-)
Statistics of Epoxy Sleeves (per TEST):							
	Mln. Loss:		9.44%			6.79%	6.79%
	Max. Loss:		11.90%			11.40%	11.90%
	St. Dev.:		1.13%			2.02%	1.66%
	Avg. Loss:		10.23%			8.94%	9.59%
							Statistics of Epoxy Sleeves (from both TESTS):

Figure 4.51 Statistical analysis of epoxy sleeve results from tendon TESTS 3T and 4T on 19-0.6" diameter strands.

a. Creep Test. After consultations with epoxy manufacturers, particularly with technical engineers from Sika [92], they recommended that a check of the stability of the epoxy sleeve strain readings be performed. This was suggested since epoxy materials are known to strain plastically under stress. A single creep test was therefore performed on a ½ " ϕ 7-wire low-lax prestressing strand specimen, instrumented with 6 standard ER-gages and epoxy sleeves. The specimen was loaded to $0.80f_{pu}$ and properly seated, with the load cell registering a residual load of $0.70f_{pu}$ after seating. Nine readings of all ER-gages, epoxy sleeves, load cell, and ambient temperature were taken for a time period of 15 days after initial loading. A portable data acquisition system with multi-channel switching devices was connected to the load cell and strain gages for the duration of the experiment. A 200mm Demec extensometer with a resolution of $8\mu\epsilon$ was used for the epoxy sleeve readings.

Results from this test are shown in Figure 4.52. Epoxy sleeve readings were corrected for temperature differentials between the linear expansion of prestressing steel ($\alpha \approx 8.0 \times 10^{-6}$ $1/^\circ\text{F}$) and Invar steel ($\alpha \approx 0.8 \times 10^{-6}$ $1/^\circ\text{F}$). The electrical resistance strain gages were of the temperature compensated type (Measurements Group S-T-C type 06), thus no corrections for temperature were necessary for such small temperature variations.

The maximum error reading of $36\mu\epsilon$ in the epoxy sleeves system marked on the first measurement day of Figure 4.25 corresponds to only 1.05ksi in the prestressing strand. For a $0.70f_{pu}$ stress level in the strand, the highest epoxy sleeves measurement error implies only a 0.55% variation of stress --which is acceptable for field measurements. However, it was found that the measured error level of the epoxy sleeves is highly dependant on the reading resolution of the Demec extensometers. With Demec gages of higher resolutions --either 400mm or modified gages with high resolution digital indicators-- the results from this test would have indicated smaller errors than with the standard 200mm Demec extensometer.

As shown in Figure 4.25, the electrical resistance strain gages behaved well during the creep test. The largest measurement error of the ER-gages also occurred in the first measurement day and only corresponded to $10\mu\epsilon$. For practical matters, the ER-gages were not affected by creep of the gages and of the bonding agents during the short-term creep test.

b. Grouting Test. A secondary benefit of the epoxy sleeves system consists of their tight blocking of grout at intermediate sections of multi-strand tendons. It has always been difficult to provide a good mechanism for blocking grout at intermediate sections of external tendons.

However, the epoxy sleeve system seemed ideal for this purpose. It was therefore necessary to design and test a grouting by-pass system that could be implemented in external tendons of segmental concrete bridges.

The final version of the epoxy sleeves have an outer diameter of approximately 6in. However, the external tendons of the San Antonio Y bridges are initially designed to be protected by 4in. o.d. polyethylene ducts (PE ducts). A 6in. to 4in. o.d. rubber reducer used for standard drainage pipes was thus designed to be used with the epoxy sleeves to be placed in the San Antonio Y external tendons. These reducers are attached to the epoxy sleeves and PE ducts with hose clamps. A grouting test was performed to check how well the hose clamps of the reducers avoided any leakage during the high pressure grouting operations of the tendons. The tests were performed on a 7ft section of 12- ½ " ϕ strands instrumented with a standard epoxy sleeve system. Pressure was checked with a special gage. Water was used instead of grout. It was found that the hose clamp connections and the reducers performed well up to \approx 40psi. At higher pressures, failure was actually induced by a modeling error in the test setup and not by a poor connection. Due to the test setup problem, it was assumed that the grouting by-pass system could have still worked well for a 50% increase in pressure. It was finally safely suggested that a \approx 50psi pressure should be the maximum allowed during the grouting operations of the instrumented tendons.

Further innovations of the grouting components of the epoxy sleeves produced the final system that is shown in Figure 4.53. For each epoxy collar, a 1" ϕ hole was drilled on top of the PE duct, just before the 6in. to 4in. reducer. A standard 90° grouting attachment hose and valve system was then clamped on top of the drilled hole of the PE duct. This final setup is designed to allow normal grouting operations to be performed from any of the two grouting vents of each epoxy sleeve system. As mentioned earlier, the section of the tendons located between the epoxy sleeves will be later protected with a high-quality grease.

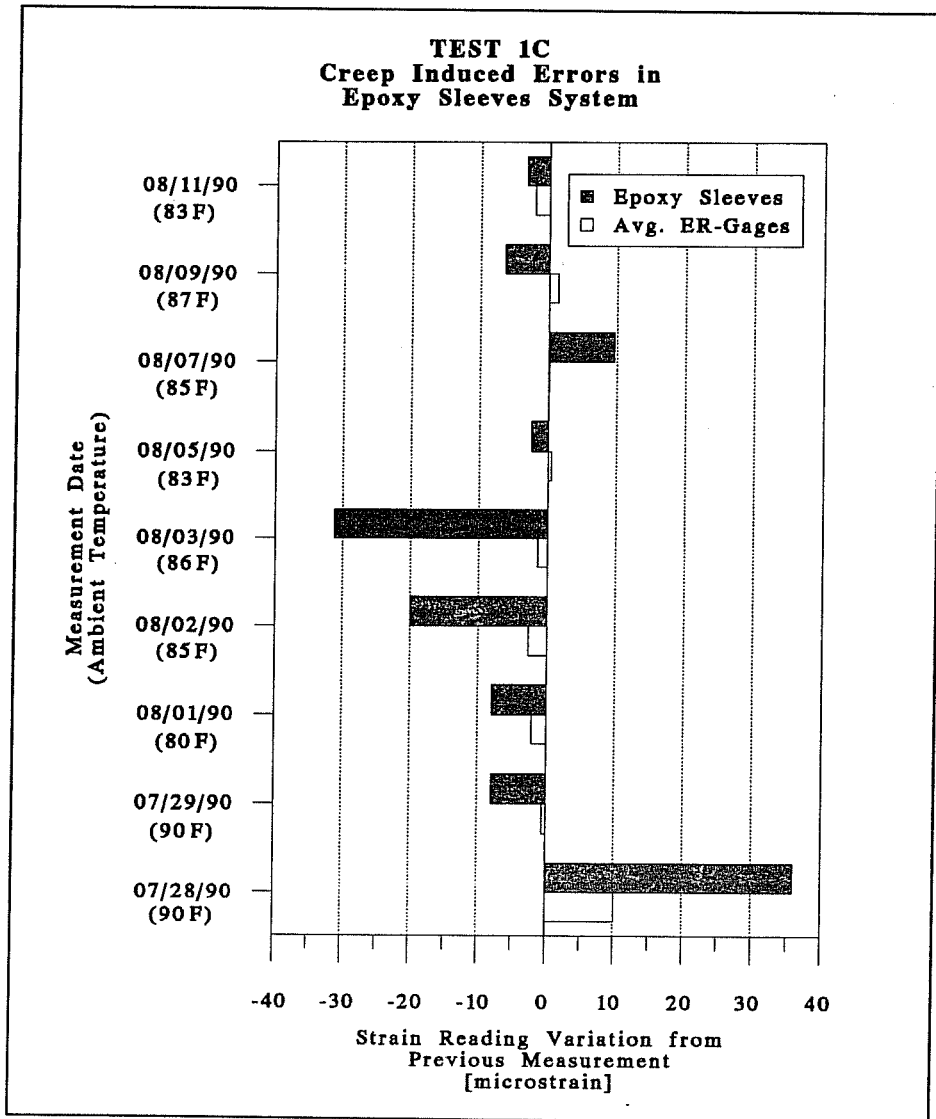


Figure 4.52 Short-term creep TEST 1C.

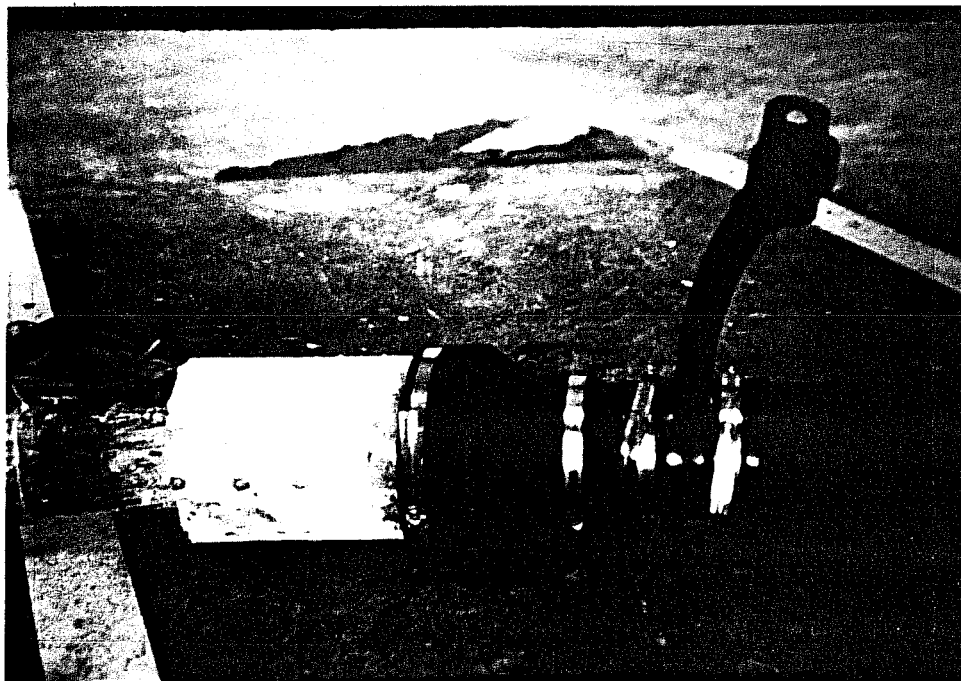


Figure 4.53 Grouting component of the epoxy sleeve system for multi-strand tendons.

4.4 Span Deflection Measurements

Only small ranges of deflections are anticipated during construction operations, service load conditions and long-term behavior of concrete segmental box girder bridges. Vertical movements during construction operations and due to long-term behavior were estimated by TSDHPT's computer analysis based on current AASHTO recommendations for the design of segmental concrete bridges. For the 110ft span A-44 of the San Antonio Y project, TSDHPT's computer-aided analysis calculated 0.182in. and 0.210in. mid-span upward camber variations after stressing each one of the following two continuous spans, A-43 and A-42 respectively. The analysis also predicted that the initial deflected shape of span A-44 should move a total of 0.571in. at the mid-span cross section after finishing all construction operations on continuous spans, after adding dead loads (including a 4in. overlay and the rails), and after accounting for prestress losses (at 199 days after erection). However, the mid-span vertical movement from day 200 to day 4000 was calculated at only 0.049in.

The temperature induced vertical movements calculated by TSDHPT's computer program showed only small variations. Results indicated a maximum daily movement of only 0.050in. at the center of the 110ft span.

Ranges of vertical movements due to high loadings were also investigated. Results from recent tests on a scale model of a segmental box girder bridge [74] found maximum service load deflections in the order of $L/6000$. If the same behavior occurs at the instrumented 110ft span of the San Antonio Y project, a 0.220in. mid-span downward deflection should be expected for full service loads.

For measuring vertical movements during construction operations or high service loadings it would appear that an accuracy of about 0.02in. may be acceptable. However, movements due to high loadings are rare and perhaps only present during specific load tests of a structure.

On the other hand, the very small vertical movements due to daily temperature variations and due to long-term effects can only be adequately measured with an instrumentation system of high accuracy and repeatability. The present testing trials were therefore seeking an instrument that would be able to provide a final accuracy of approximately 1/100in. and that can

be reliable over a long period of time. Secondary concerns for economics also influenced the final selection of the most adequate instrumentation system.

Only two of the reviewed systems from Section 3.3 complied with the present requirements of accuracy, stability, and cost (directly related to availability). The two acceptable systems were based on hydrostatic leveling techniques and on the modified base line methods. Hydrostatic devices were later canceled from further trial tests for the following reasons:

- lack of familiarity with the different aspects of this technology (i.e. construction, installation and operation of the measuring devices),
- concerns over evaporation and leakage problems in the very hot climate of San Antonio,
- the long-term accuracy of hydrostatic devices is still doubtful, and
- concerns over thermal effects.

With these considerations in mind, the present researchers opted to enhance the accuracy and ease of operation of the reviewed base line methods, and to check their performance in actual concrete structures.

Two components of the reviewed base line methods needing improvement were the method for adjusting the tension of the base line wire, and the type of measuring device used for the recording of small movements. Modifications of the line tensioning systems along with new measuring devices were investigated in trial tests. The overall performance of the most adequate system was finally checked in a short-span, short-term deflection test, followed by an actual field installation and test on a finished span of the San Antonio Y bridge project.

4.4.1 Line Tensioning Systems

As reviewed earlier in Section 3.3, two base line tensioning methods were used in past investigations with varying degrees of success. The first method consisted of the tension adjusting procedure introduced by Bradberry [81] and previously explained in Section 3.3.2. With this method, the tension of the base wire is adjusted according to the deflection imposed by a calibrated weight hung at mid-span (as shown in Figure 3.23). Although it was reported to have worked well in Bradberry's applications, the time needed to accurately adjust the tension in the wire was envisioned to be a major drawback when speed of measurements is a factor of

concern. Adding to the total measurement time required by this method is the need for checking vertical movements of the base wire at the live end anchor. These extra measurements are needed when using Bradberry's drilled bolt tensioning method because the height of the base wire usually varies at each turn of the bolt. All deflection readings are therefore corrected according to the initially measured position of the base wire at the live end anchor. The recording of this extra station readings thus increases the time required for taking all the deflection measurements and for carefully reducing the data.

The second system under consideration consisted of the constant weight method used by Pauw-Breen with the original base line system [79]. In this system, the catenary shape of the base wire is kept constant by the force produced from a calibrated weight hung at the live end station. From previous tests, it was found that the calibrated weight needs to be such that it stresses the base wire to 80% or 90% of its breaking strength. One problem mentioned by Pauw-Breen was the wind-induced oscillations of the base wire. However, when applied to measurements inside box girder bridges, climatic factors (especially wind) should not impose severe movements on the calibrated weight and base wire assembly. A second inconvenience to this method, however, was that any variations in the friction of the moving parts will produce a different catenary shape in the base wire. To decrease the degree of influence of this problem, high quality sealed bearings were purchased for the present trial tests. The outer circumference of each bearing was machined with a narrow groove that was used as a guide for the base wire.

Several line tensioning methods based on the two previously mentioned applications were investigated. The following sections describe the systems investigated, their test setup, and the findings from the trial tests performed in the laboratory (on short-span, short-term configurations).

4.4.1.1 Systems Investigated. Four devices were manufactured and tested in short span trial test configurations (22.7ft and 18.3ft). Although originally based on the two previous applications of the base line method, each tested line tensioning device evolved from observed behavioral errors found in the previous trial test. General schematics, along with the main problems and advantages of all the line tensioning systems investigated are included in Figures 4.54 through 4.58.

4.4.1.2 Short Span Test Setup. The short span tests were performed at the setup of an on-going investigation of bond behavior of prestressing strands in prestressed concrete girders [93,

94]. The schematic of a typical short span test setup is included in Figure 4.59. Each base line deflection system under consideration was installed on the top surface of the girder, directly above the supports. Four initial trial tests were performed by comparing the deflection system readings against the "real" beam deflections registered by a linear potentiometer automatically scanned with a computer-controlled data acquisition system. As shown in Figure 4.59, the linear potentiometer of the trial tests measured the deflections of the bottom surface of the girder, directly below the place where the deflection measuring systems were located. This was possibly not the same deflection as occurred at the top surface of the girder where the deflection systems were installed. However, since all trial tests were performed with the same reference, the errors introduced by the inadequate "real" pot deflection readings were approximately the same in each test.

Finally, these trial tests were also performed on a short term basis with a maximum duration under two hours. Therefore, no conclusions about the stability of the readings with time could be drawn.

4.4.1.3 Short Span Test Results. The most adequate tension adjusting method of the three types which were similar to Bradberry's consisted of the Type III system shown in Figure 4.56. The performance of this particular system was compared to the constant weight method of Figure 4.57 (system Type IV). Reading errors registered at each measuring stage during the short span test of system Type III were compared to those of the short span test of system Type IV. As shown in Figure 4.60, both line tensioning methods provided good levels of short-term accuracy. System Type III showed the single highest reading error of 0.021in. On the other hand, the largest reading error registered by the constant weight method was almost half of that, around 0.013in. Still, these two larger error extremes can be attributed to occasional operator misreadings or a similar type of accidental error. Ignoring the two sporadic errors, it is highly probable that both systems can achieve about the same level of accuracy. Moreover, the average absolute reading errors for Type III and Type IV were only 0.0052in. and 0.0045in. respectively.

Due to their resemblance in accuracy levels, installation, and manufacturing costs, the only difference between these two systems was therefore related to the level of difficulty of their tension adjusting procedures. System Type III required rather tedious procedures for adjusting the tension of the base wire. On the contrary, the constant weight method directly self-adjusted

the tension of the wire after each deflection of the girder (provided that the friction in the bearings was small enough to allow for the wire movements to occur). The high-quality sealed bearings were considered to have very low internal friction (enough to allow small movements to occur). More importantly, they were considered to have only a minimal variation of their friction coefficients with time. This quality of the bearings should therefore ensure a high level of repeatability of readings with time.

The tensioning system Type IV was therefore recommended as the most adequate method for the base line method of measurements of vertical deflections in box girder bridges. General recommendations about their manufacturing, installation and use are included in Section 5.5.

4.4.2 Reading Systems

Once again, the two different reading systems used by Bradberry [81] and Pauw-Breen [79] were the basic systems tested and modified during the present laboratory investigations.

Bradberry's reading system --previously shown in Figure 3.22-- was a small piece of a stainless steel high precision ruler bonded next to a similarly sized mirror. The mirror helped to accurately reproduce the same reading reference in the ruler (by taking each measurement when the base wire's image in the mirror was covered by the wire itself). This reading system was enhanced in the present project by purchasing stainless steel rulers with 1/100in. divisions. This barely perceptible level of reading resolution could be achieved by consistently reading the ruler mark defined by the top (or bottom) of the base wire, after proper alignment of the mirror image. However, the disadvantage of this method was the high occurrence of accidental reading errors. These were mainly due to the confusion associated with counting the number of 1/100in. divisions to each reading mark. Another concern was related to the time and effort required for recording each deflection, which involved careful concentration and single-eye sighting.

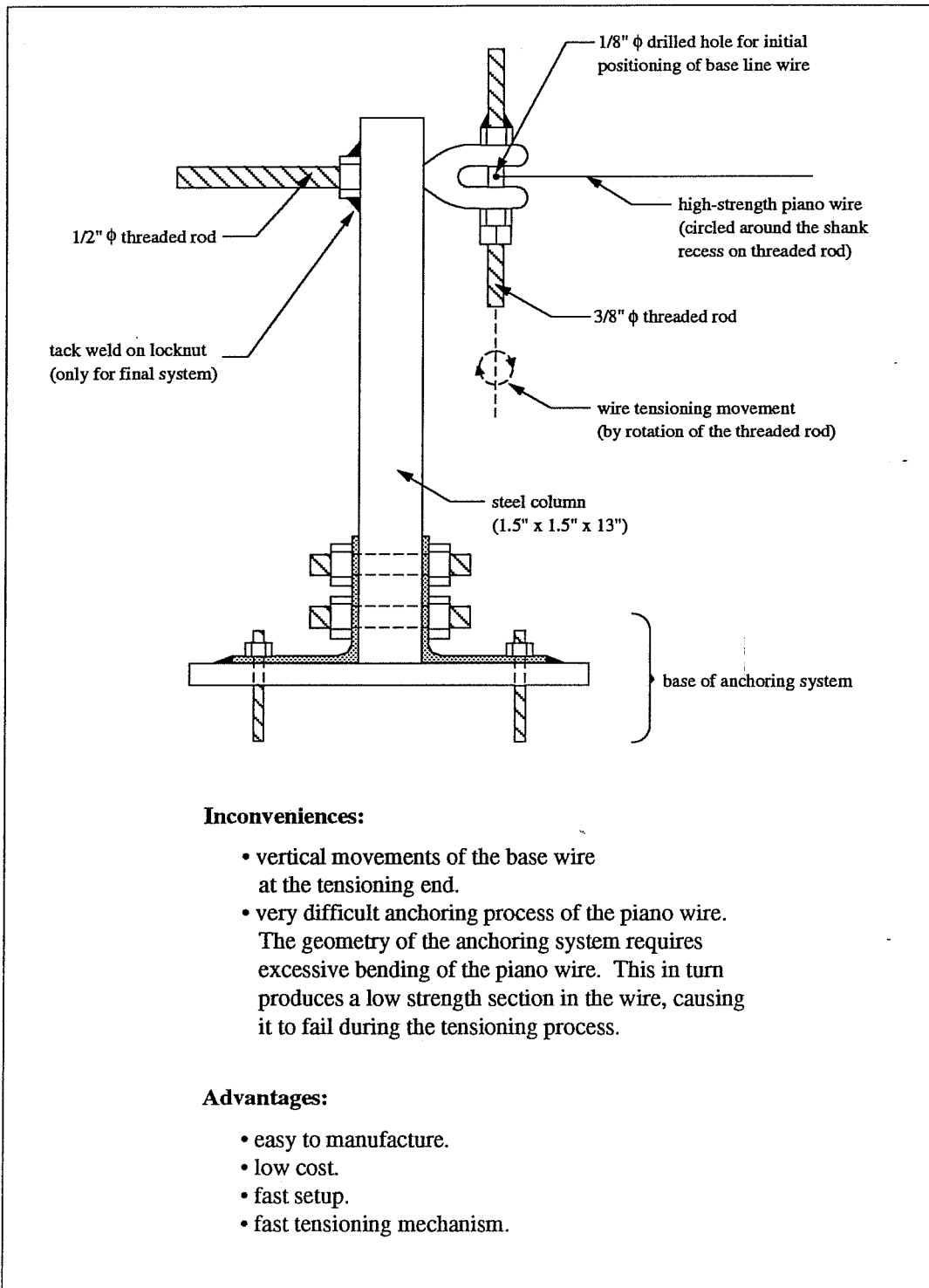


Figure 4.54 Live end tensioning mechanism type I.

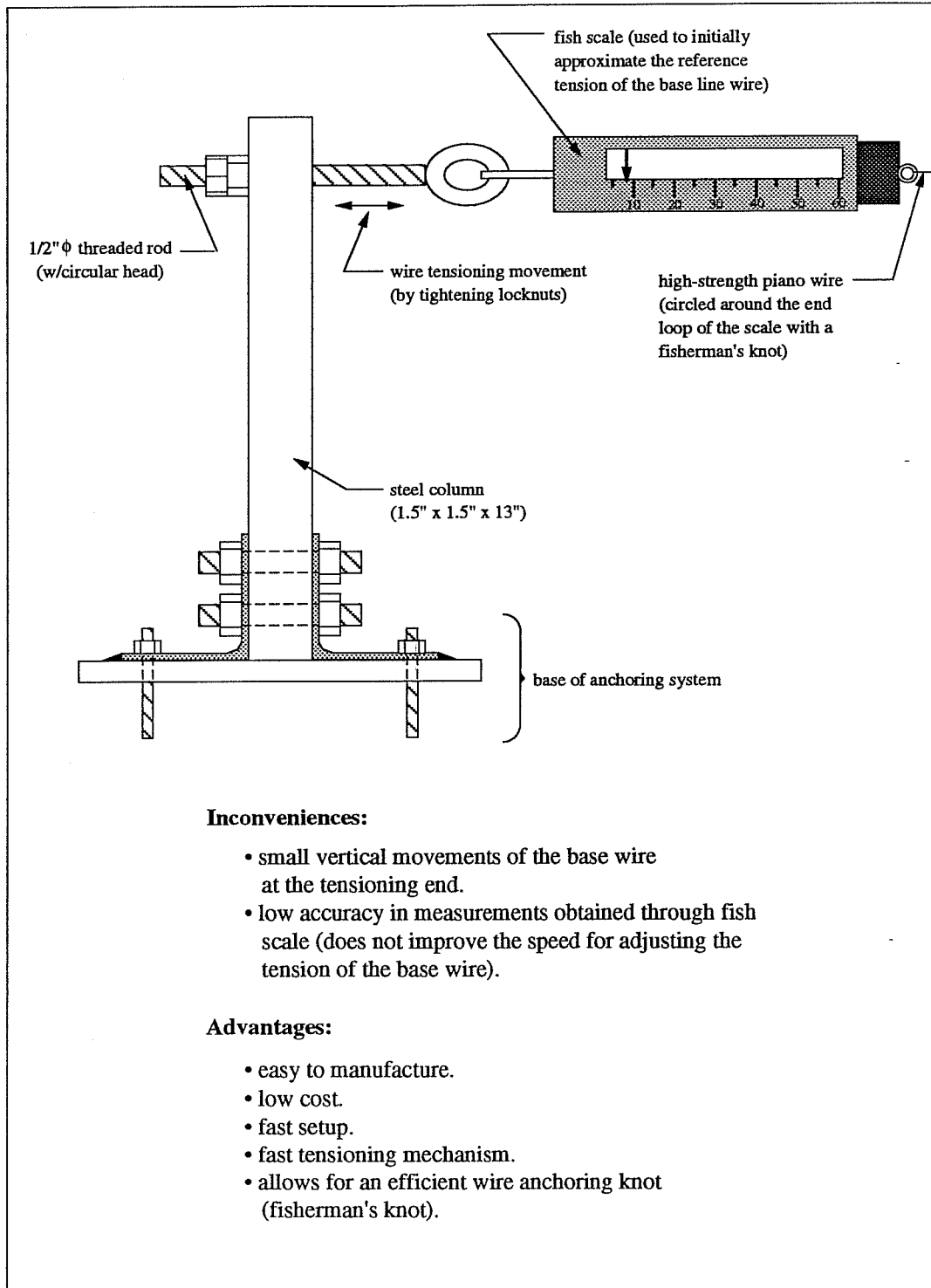


Figure 4.55 Live end tensioning mechanism type II.

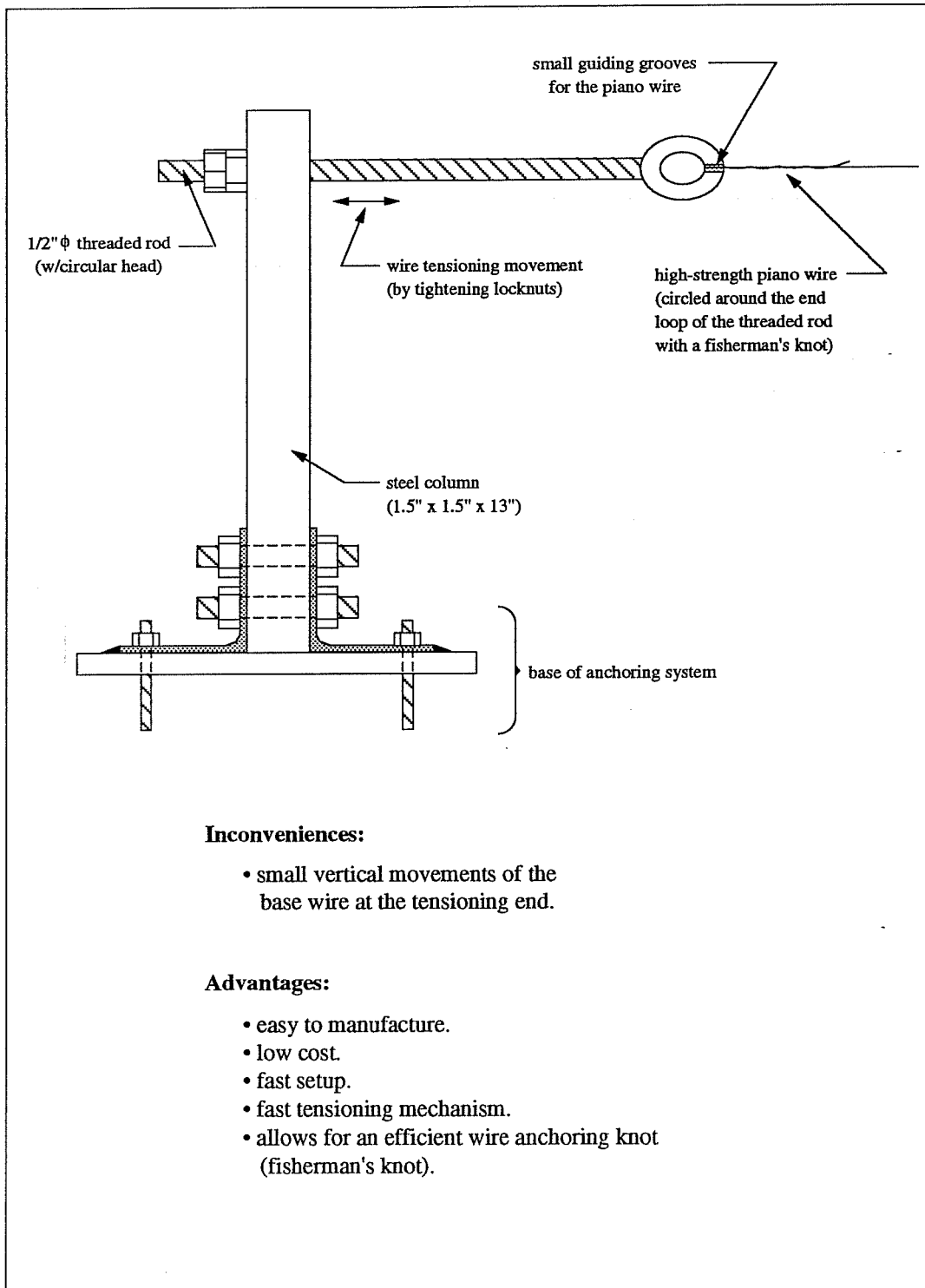


Figure 4.56 Live end tensioning mechanism type III.

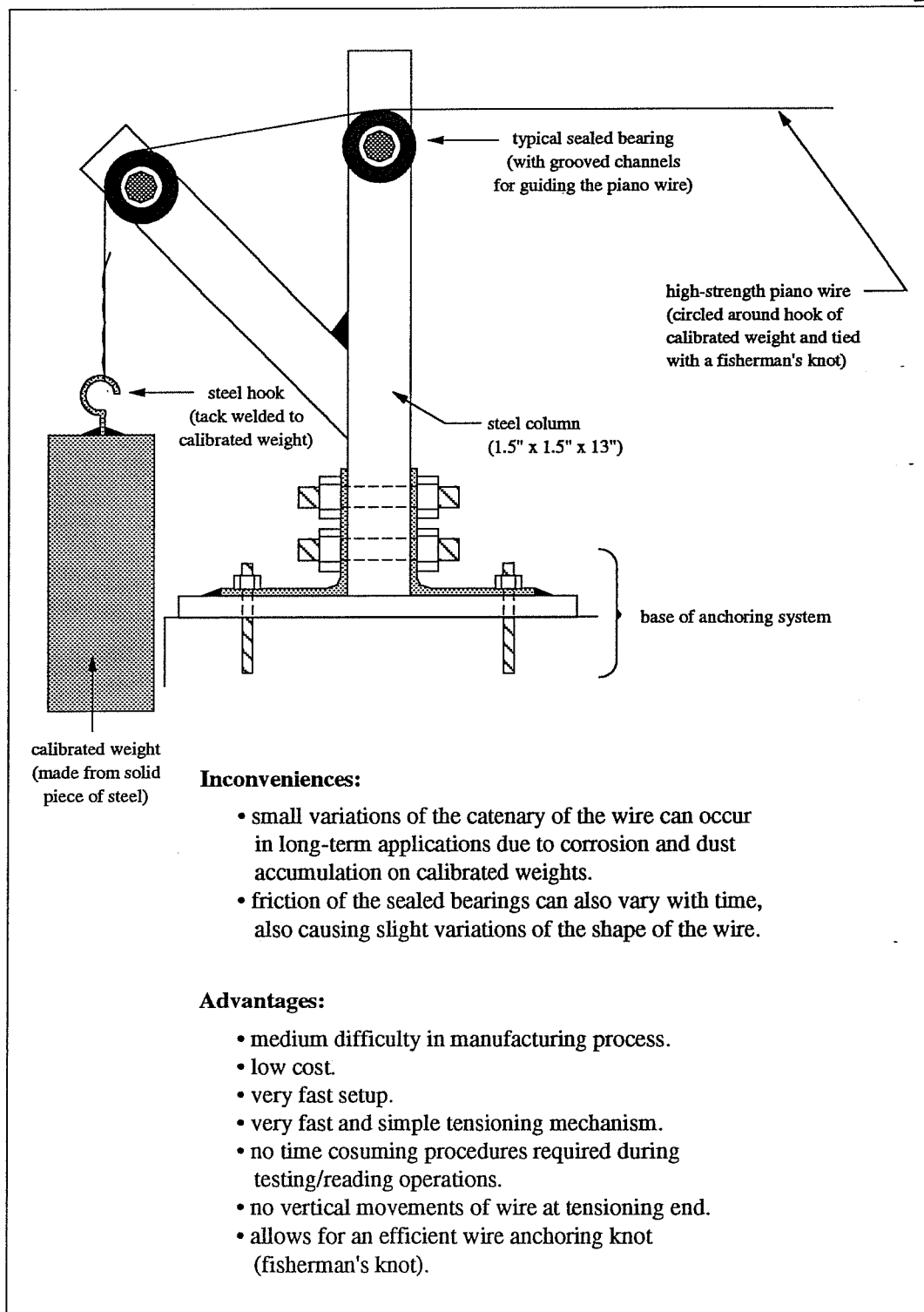


Figure 4.57 Live end tensioning mechanism type IV.

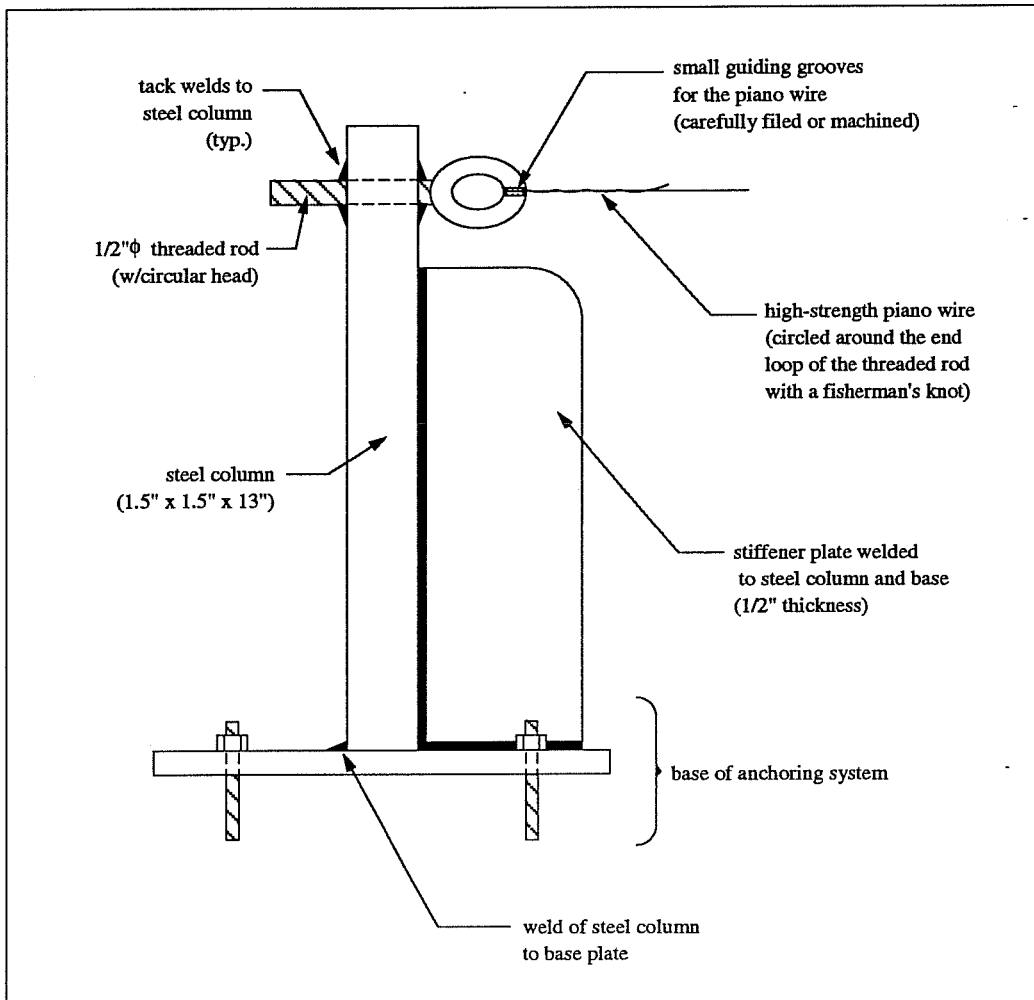


Figure 4.58 Typical dead end anchorage.

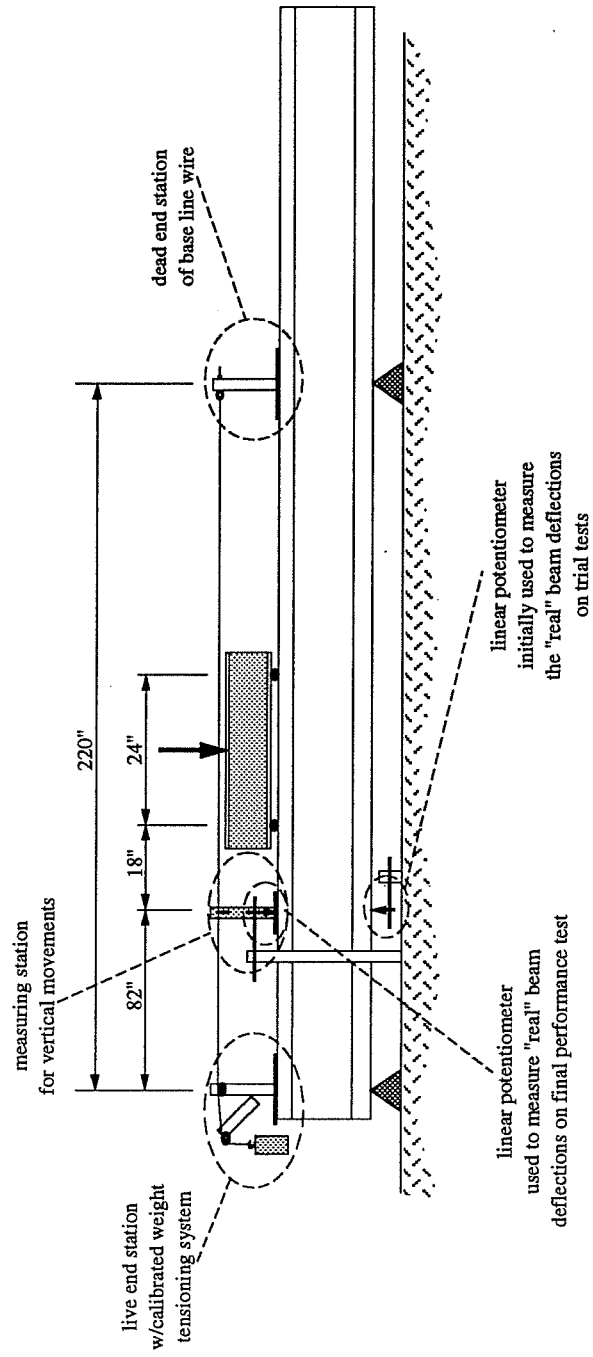


Figure 4.59 Typical short span test setup of deflection measuring systems.

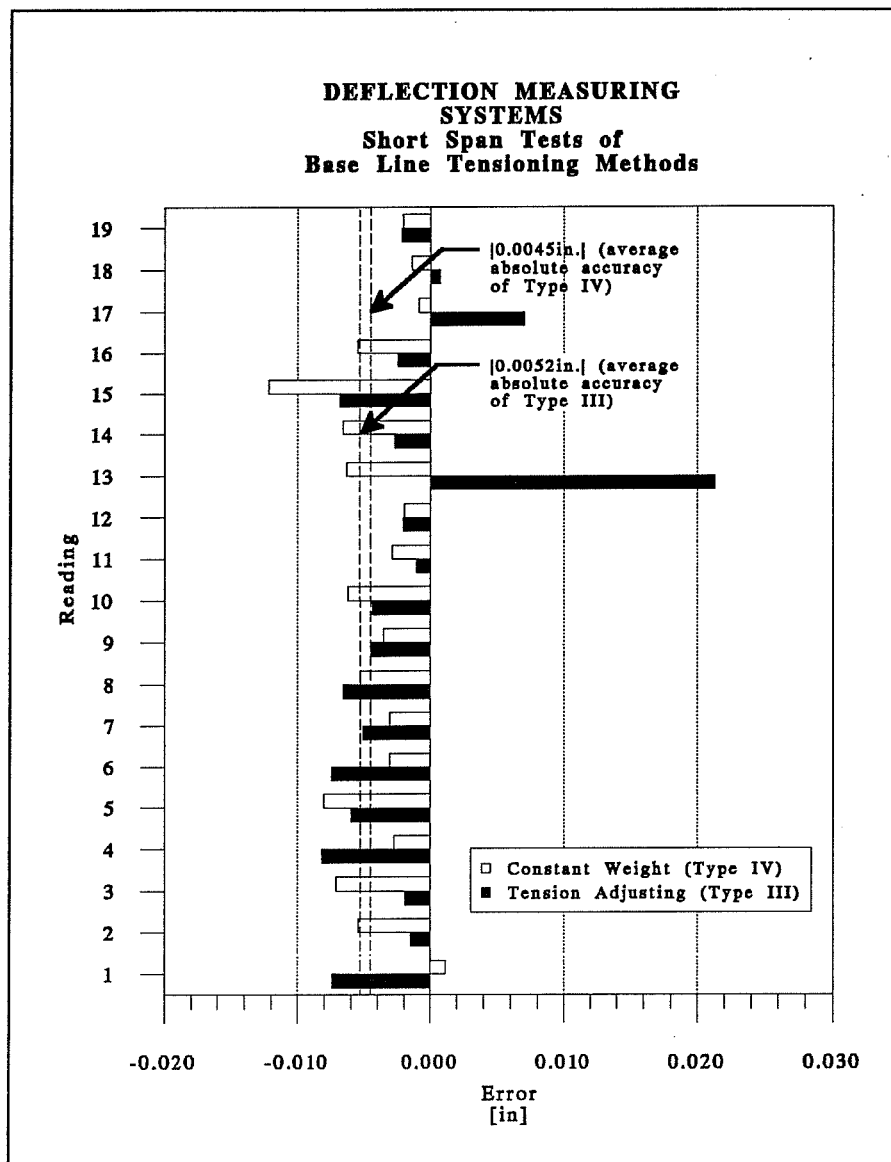


Figure 4.60 Comparison of performances of line tensioning methods.

In an ideal situation, the accuracy of the reading system based on the ruler and mirror assembly can only be improved to the lowest visible divisions of the ruler. Estimations of the 5/1000in. divisions of a ruler are highly unlikely to be visible, unless a system of magnifying glasses is used. And even then, the error would be transferred to the variations of the reference level (since the mirror image of the wire can probably move --unnoticeably-- more than 5/1000in.). This limitation of the ideal system based on the ruler and mirror assembly inspired the investigators to examine other reading devices that can allow more accurate ideal determinations of the position of the base wire.

Pauw-Breen used a reading unit made of a ruler coupled with a vernier scale that reached measurement accuracies of 1/1000in. [79]. The present investigators modernized this 1959 system model by replacing the old ruler by a currently available digital scale providing reading resolutions of 5/10,000in. The ruler used was a *Mitutoyo Digital Scale* with an 8in. gage length. An aluminum extension arm was machined to fit a pair of screw holes existing in the moving part of the digital scale. This extension arm helped reach the location of the base wire, and its wide section allowed enough room for accidental lateral misalignments of the wire. The digital ruler with the fixed extension arm was tightly mounted to a 1in. x 1in. x 13in. steel tube and a steel base. This deflection meter assembly would be expensive if it had to be permanently positioned at each reading station of each instrumented span. The digital scale alone was priced at \$150.00 in 1991. An alternative was to use a leveling base similar to that in Pauw & Breen's portable deflection meter [79]. This base was made with two fixed screws and one leveling screw that worked in conjunction with a bubble level. However, as mentioned in Section 3.3.2, the bubble level can substantially decrease the accuracy of the readings. Also, the leveling process of the meter at each measuring station can take long periods of time. A magnetic base was thus envisioned as a possible solution for the problems of accuracy and installation time. The foot of the steel tubing of the reading unit assembly (with the attached digital scale) was bolted to a strong magnet. The bench mark reading stations were therefore simplified to 4in. x 4in. x ½ in. square steel base plates secured to the concrete surface by four anchor bolts. A pair of guides were welded to the steel bases to reproduce the exact positioning of the magnets at each reading operation. The final system investigated is illustrated in Figures 4.61 and 4.62.

The next problem encountered with the new digital deflection system was the difficulty in determining the exact moment when the extension arm of the scale "touched" the base wire. Small digital scale induced pressure movements of 5/10,000in. or even 1/1,000in. of the base wire were easy to randomly produce from one reading to another. A consistent method for determining the exact moment when the scale touched the base wire was therefore needed. One solution that was successfully tested consisted of using a beeping sound that determined the electrical contact between the ruler's extension arm and the base line wire. This was an easy solution that only required the installation of a small electrical wire extending from the dead or live end station to a place near each measuring station. One terminal of a standard hand-held voltmeter was connected to the reading unit assembly and the other terminal to the wire that was stretched to the live end station (Figures 4.61 and 4.62). When the reading unit assembly made contact with the base line wire, a beep signaling the electrical shorting was produced by the voltmeter.

A final improvement in the deflection meter was the use of a semi-automated readout processor electrically connected to the digital scale. Digital scale manufacturers provide a mini processor that can store and print all readings of their digital scales by pressing a sensitive control switch located either at the scale or at the processor. This instrument is highly recommended for projects involving extensive deflection measurements because it provides several advantages:

- decreases the time necessary for sighting a reading and writing it on paper,
- can automatically store up to 11 readings from one single measuring position and print their statistical average (including maxima, minima, coefficients of variation, mean value, and standard deviation),
- eliminates reading errors of the operator (and errors due to illegible notes), and
- is battery operated and can be easily hand carried for field measurements.

The only disadvantage of the mini-processor is its cost. The *Mitutoyo Mini Processor BDP-100*, was priced at \$415.00 in July of 1991.

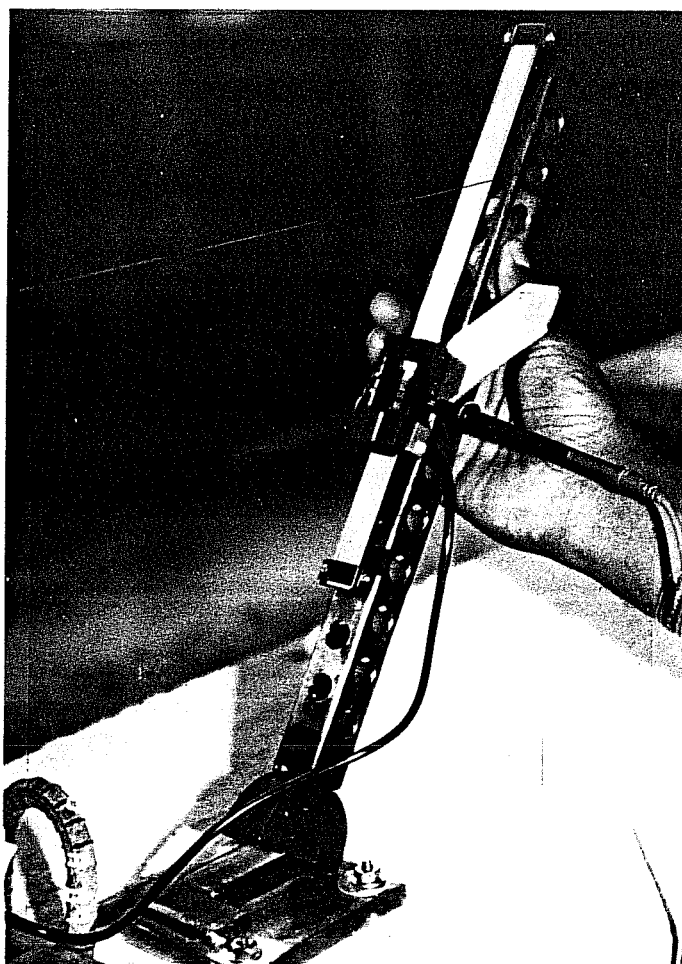


Figure 4.61 Portable reading unit of deflection measuring system (during installation to reading position).

4.4.3 Short Span Performance of Final System

The performance of the final version of the base line system with the digital scale, the magnetic base, and the electrical system for determining contact of wire and meter was evaluated in a final short span test. To check the accuracy of the readings, a linear potentiometer was installed next to the deflection meter station (as previously illustrated in Figure 4.59). The overall performance of the deflection meter during the complete loading test of the girder was compared to that of the linear potentiometer (which was automatically scanned with a computer-controlled data acquisition system). The result of this overall performance check is shown in Figure 4.63. Comparisons of each measurement obtained by the deflection

meter with the corresponding value from the linear potentiometer (considered as the "real" deflection) gives an idea of the final accuracy of the modified base line system. The result from this comparison is included in Figure 4.64. The highest reading error was 0.0082in. in the 14th reading. However, an average of the absolute reading errors indicates 0.0024in. errors for each reading operation.

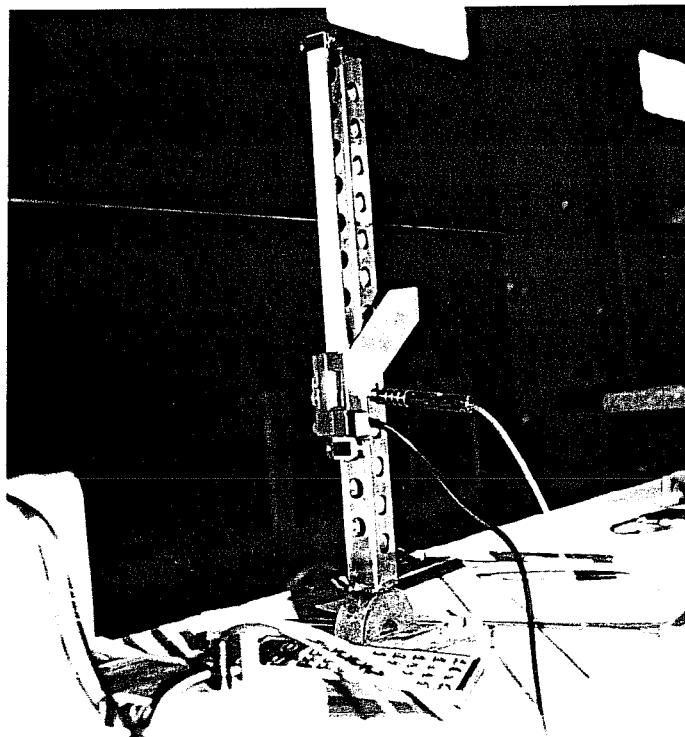


Figure 4.62 Portable reading unit of deflection measuring system (located in reading position).

Another noticeable behavior discovered by examining Figure 4.64 is the occurrence of the consistent errors for the last four readings. These readings corresponded to girder deflections higher than 0.5in. at the instrumented cross section. A possible cause of these errors is the slight rotational movements experienced by the base plate of the reading station. As the girder deflected, the 4in. x 4in. steel base plate approximately moved tangent to the deflected shape of the girder at the instrumented section. The portable digital scale assembly was therefore installed at a small angle away from the vertical position when high levels of deflections occurred at the girder's cross section. These errors are highly related to the

maximum range of deflections to be experienced by the instrumented girder or span. It is concluded that the smaller the vertical movements of the instrumented station, the higher the level of accuracy of the measuring system, and vice versa, higher movements should produce smaller accuracies. Still, as shown by this short span performance test, the maximum error of measurements taken beyond the cracking load of the concrete girder was well below the 1/100in. desired accuracy level.

The short term repeatability of measurements taken by two different operators during this short span test was also investigated. The absolute differences between immediate readings taken by the different operators are included in Figure 4.65. It can be seen that the average error was only |2/1000in.|. However, the highest repeatability error reached the |5/1000in.| level.

After examining the results of the final short span test it was concluded that the deflection measuring system provides an accuracy level that is much more sensitive than the desired 1/100in.

4.4.4 Field Performance of Final System

The last testing stage of the suggested base line system was performed at a finished 100ft typical span of Phase I-C of the San Antonio Y project. The overall accuracy of the deflection system was not addressed due to the difficulty for monitoring comparable "real" deflections of the structure. However, the field test was performed to indicate any other possible problems not envisioned during the installation and operation of the system.

Researchers evaluated the typical amount of time required for system installation, and for measuring span deflections at quarter- and mid-span stations. At the same time, the repeatability and the stability of the deflection readings were also investigated. These became a concern due to the longer spans of base line wire required for field measurements in actual bridges.

4.4.4.1 Installation and Operation. The system setup inside the concrete box girder bridge is illustrated in Figure 4.66. The instrumented span (C-35 of Project I-C) was the first one of six continuous spans. Indeed, a secondary factor influencing the selection of this particular span was the interest in investigating the trend of vertical movements caused by subsequent stressing of the other continuous spans.

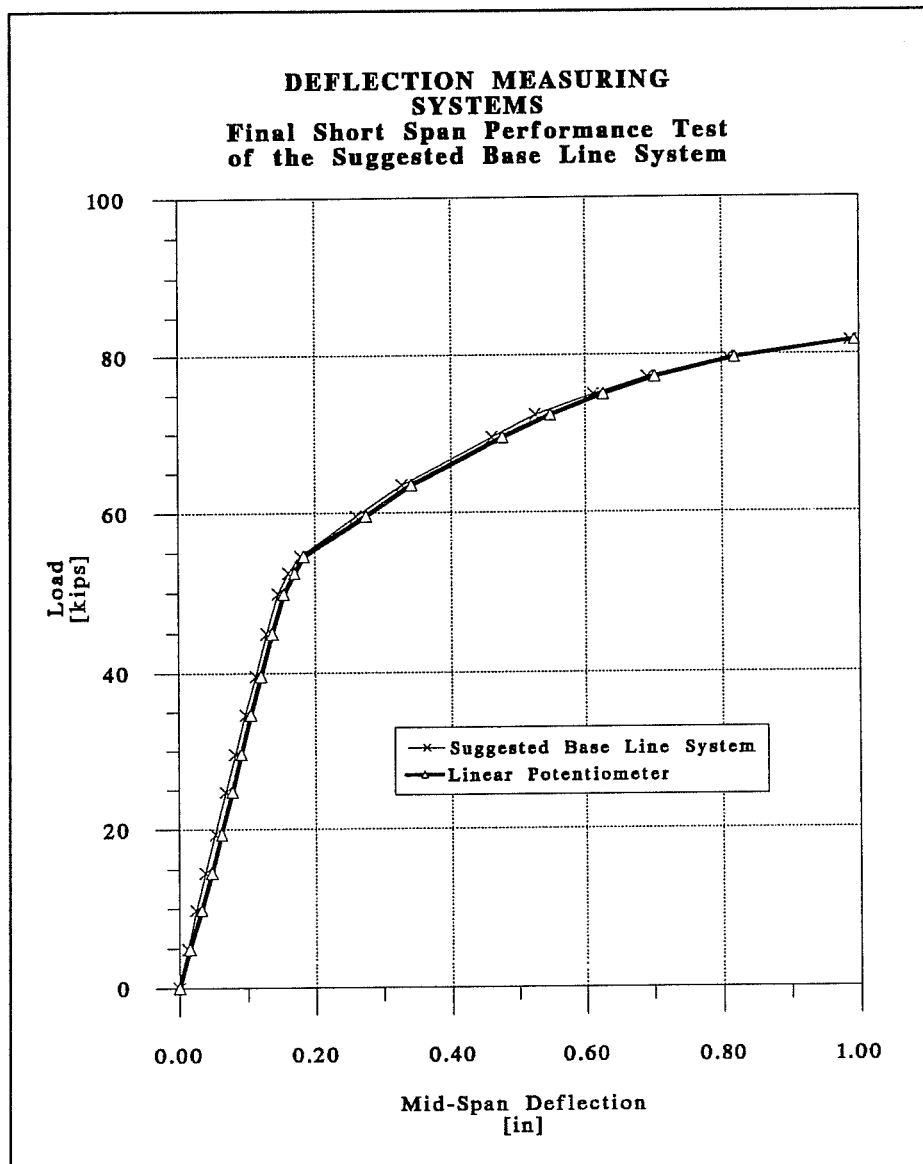


Figure 4.63 Overall performance of final deflection measuring system during short span test.

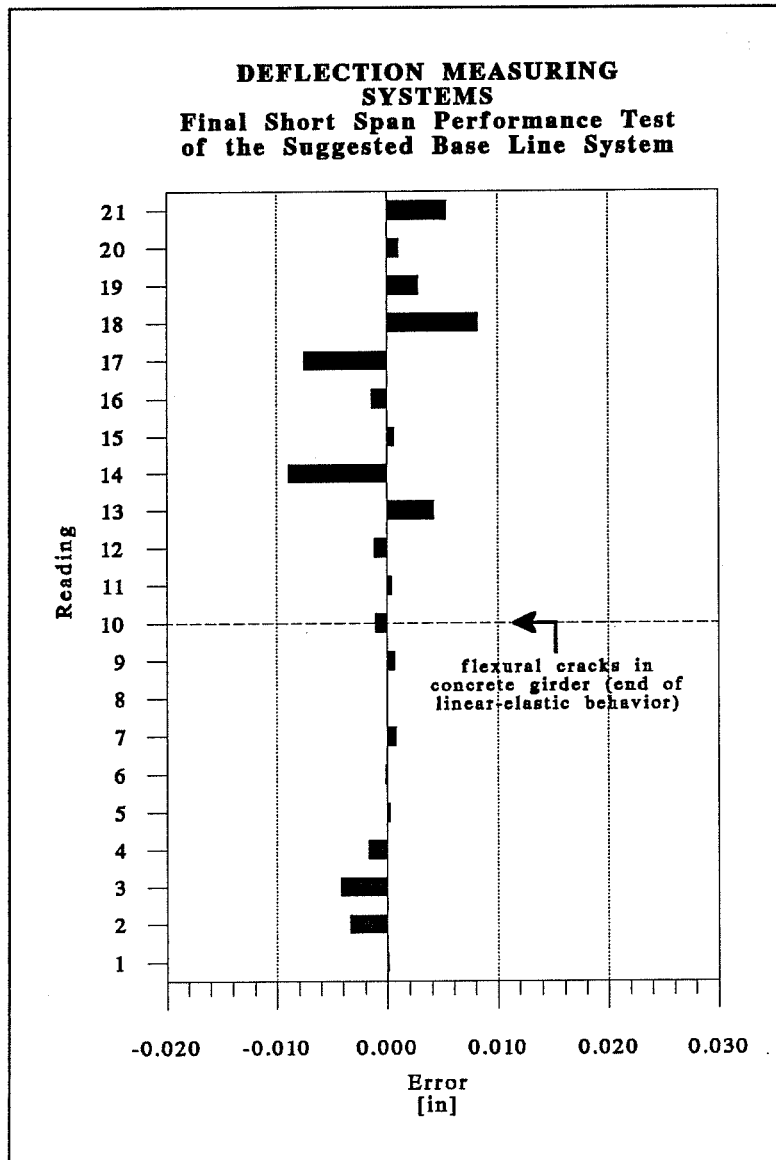


Figure 4.64 Reading errors of final deflection measuring system during short span test.

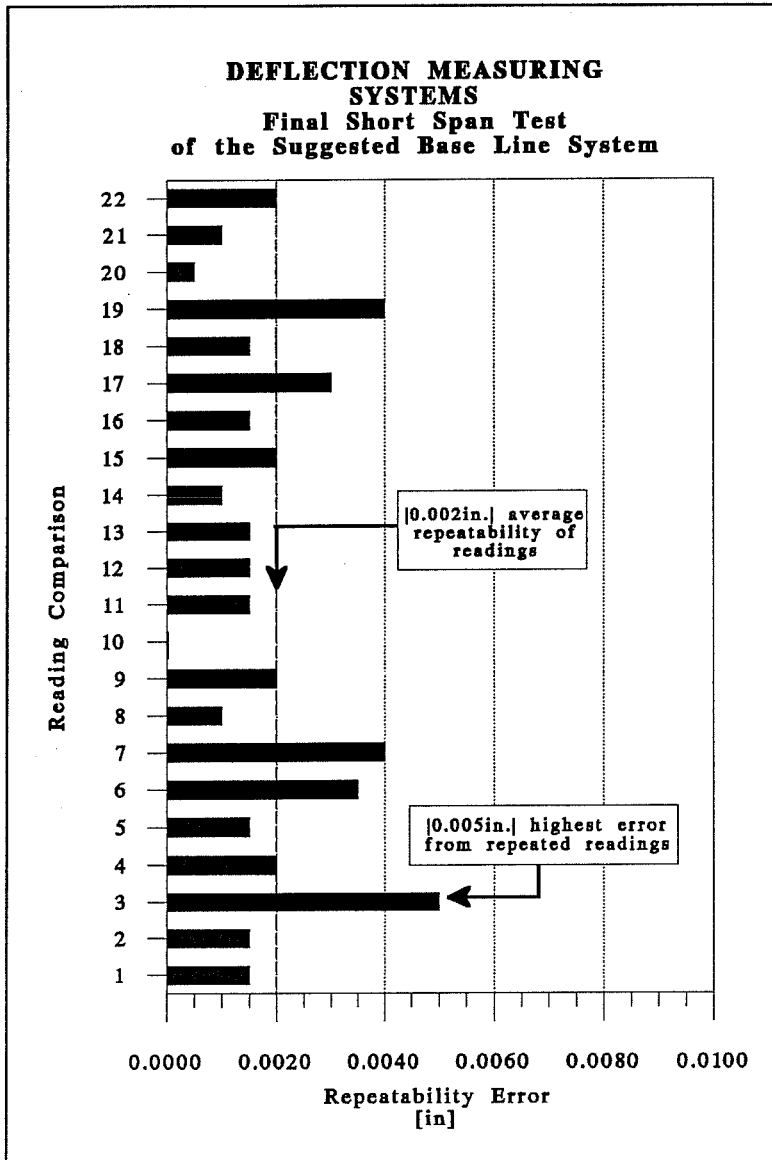


Figure 4.65 Repeatability errors of final deflection measuring system during short span test using two different operators.

The base plates of the reading stations --with the welded guides for correct positioning of the portable reading unit-- were installed on the bottom (inner) surface of the top deck slabs of selected box girder segments, at the approximate distances shown in Figure 4.66. The plates consisted of 4in. x 4in. x 3/8in. steel squares with four 5/16in. holes drilled at their corners. The plates were fixed to the structure by special 1/4in. ϕ x 2.25in. stainless steel mechanical anchors (manufactured by *Hilti*, of the type *Kwik Bolt II, AISI 304 & 316 Stainless Steel*, with 3/4in. thread length and requiring 1in. of embedment length in concrete).

Drilling of high strength concrete was easily achieved with a concrete vibrating drill and special tungsten carbide drill bits. The initial use of regular drill bits was terminated since this considerably increased the installation efforts. Furthermore, regular drill bits only lasted for 3 or 4 drilling operations in high-strength concrete.

Live and dead end anchor assemblies were welded to their steel base plates and were permanently installed on the instrumented structure. The steel bases were similar to those used at the reading stations. The live and dead end anchors were not installed directly above the supports in this trial application (as shown in Figure 4.66) because they were designed for pier segments with larger height clearances. An electrical wire was connected from the live end station to places near each measuring station. This was part of the mechanism that helped determine the time of contact of the base line wire and the extension arm of the digital scale.

Illustrations of the live end bracket assembly with the calibrated weight, and of a sample reading operation inside the box girder bridge are shown in Figures 4.67 and 4.68 respectively.

Despite the inconveniences produced by the small clearances existing inside the box girder segments (shown in Figures 4.66 and 4.68), the complete installation and the initial check of operation of the system was finished in approximately three hours.

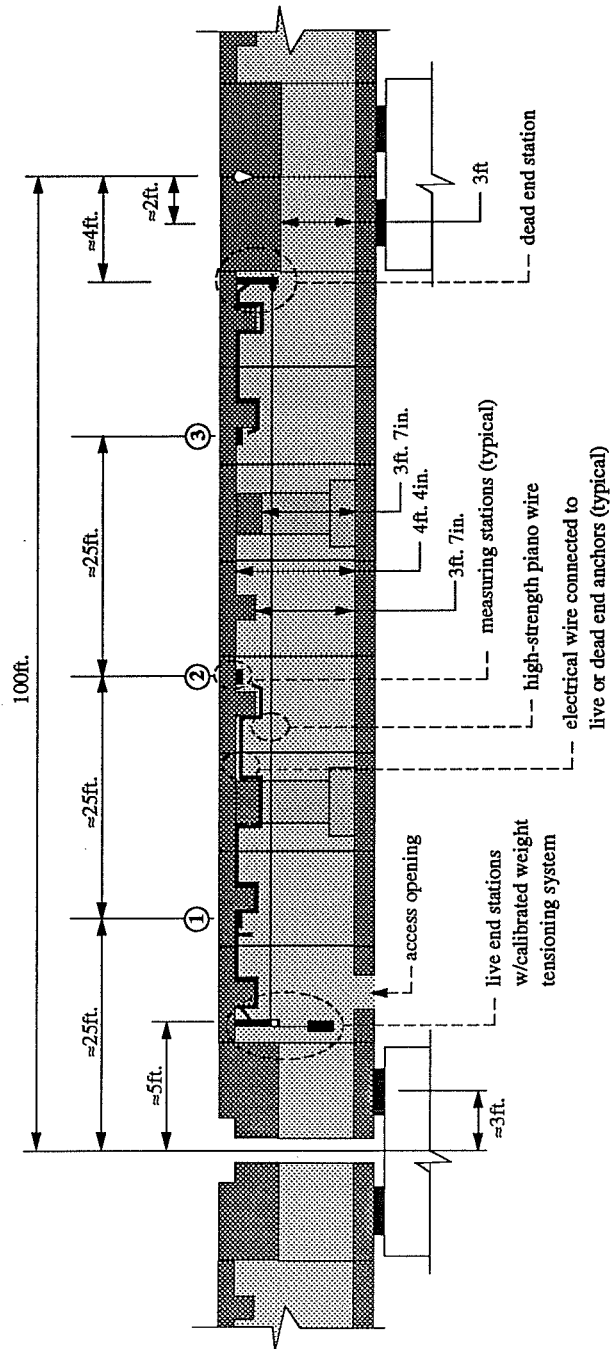


Figure 4.66 System setup inside box girder bridge

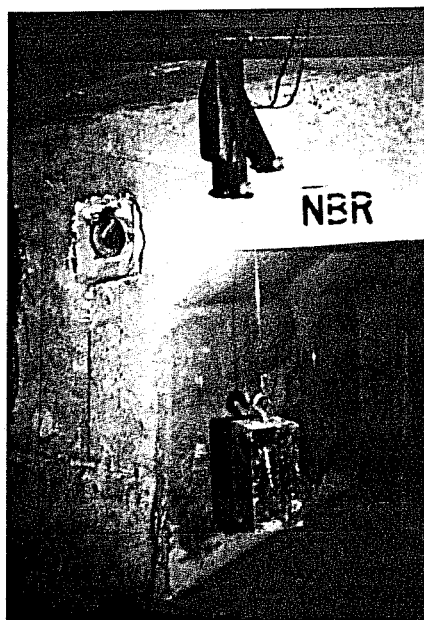


Figure 4.67 Live end anchor and calibrated weight inside the box girder bridge.



Figure 4.68 Digital scale measuring unit, mini-printer-processor, and voltmeter during sample reading operation inside box girder bridge.

4.4.4.2 Measuring Times. The components of the deflection system that were permanently left on site were the live and dead end anchors, and the steel bases of each measuring station. Each reading day therefore required the following operations:

- Installation of the piano wire from dead end to live end station, where it was connected to the calibrated weight and hung on bearing guides.
- Translation of hand-held voltmeter, portable reading unit, and mini-processor-printer (optional) to location of each one of the three reading stations.
- Connection of the terminals of the voltmeter. One to the reading unit, and the other one to the "live" wire located next to each reading station (and connected to the live end station).
- Recording of readings from each one of the three stations.

Two operators --individually and in pairs-- performed the outlined measuring day procedures on the single instrumented span. For a single operator, the total time employed varied from 18min. to 35min. However, when a pair of operators worked together, the total time employed ranged from 9min. to 15min.

One frequently difficult and time consuming operation consisted of the installation of the piano wire from the dead end to the live end station. Unwinding long lengths of piano wire inside a box girder bridge with low vertical clearance was difficult. However, this initial problem was later avoided by installing proper lengths of piano wire on a large diameter reel built in the laboratory. The piano wire was not left on site between measurements to avoid problems with the construction crew, and to avoid wire corrosion. The low clearance inside the instrumented box girder segments also contributed to increasing the total measuring time, and the effort required for moving along the span.

On the contrary, a decrease of the total reading time was provided by the mini-processor-printer, since it allowed for direct recording of several measurements at each reading station. This in turn produced more accurate reading averages and almost completely avoided reading errors from the operators.

In conclusion, the total time required for wire installation and recording of measurements at three stations of one 100ft span averaged 12min. and 28min. for two operators and one operator respectively. This provided that operators used properly coiled lengths of piano wire along with a mini-processor-printer.

4.4.4.3 Repeatability of Readings. After installing the deflection measuring system, the first investigation was to determine the accuracy at which measurements were repeated from one operator to another. For this purpose, the first operator took deflection readings of all three stations and immediately transferred the equipment to the second operator. Therefore, an average of 15min transpired between the first and the last reading of each station. No significant variation of the deflected shape of the instrumented span should have occurred in such a small lapse of time. The differences between each corresponding pair of measurements were therefore considered as repeatability errors of the system. Figure 4.69 shows the repeatability errors obtained from a comparison of 18 measurements. As expected, most of the largest errors from each measurement day were obtained at the mid-span station. However, the maximum error of $|0.0118\text{in.}|$ obtained in the fifth reading comparison was believed to have been caused by a different source. A heavy construction forklift was operating on top of the finished span, near the mid-span station, when the initial readings were taken. The machinery was not present during the station readings of the second operator. Ignoring this accidental error, the next poorest repeatable deflection reading only showed $\approx|5/1000\text{in.}|$ maximum disagreement. This is an acceptable degree of repeatability, and the recommended deflection measuring system is thus considered to be capable of determining $1/100\text{in.}$ movements.

Although far from "perfect," practice does improve the accuracy of the measurements. The last set of readings performed by the same operators indicated a much lower average error. It is therefore important to develop the experience of the operators by making them follow well defined standards while performing some initial sample measurements.

Observing Figure 4.69 and ignoring the reading discrepancy due to the live load, the next largest repeatability error occurred from comparisons of the mid-span measurements. These were evidently caused by the inaccurate determinations of the time when the deflection meter touched the base wire. The electrical-short-induced beeping of the voltmeter did not perform very efficiently. Furthermore, before the 10/11/90 set of readings in Figure 4.69, it was found that a new and unexpected electrical circuit existed between the live and dead end stations and each one of the anchor bolts of the measuring stations. This prevented the use of the voltmeter beeping system, and the readings were taken by sighting with one eye the instant when the extension arm of the digital scale touched the base wire. The $|0.0015\text{in.}|$ repeatability of these measurements was surprisingly high (see Figure 4.69). However, much more careful

and time consuming readings were necessary to be performed to obtain such high levels of repeatability.

It is still unknown what particular event caused the electrical shorting between the different stations. Although unlikely to occur, it is possible that each one of the anchored bolts of each one of the stations were embedded too deep in the segments and just reached the reinforcing bars. All of the bars of each segment have an electrical connection to each other. On the first two days of testing the segments were electrically isolated. However, on the third test day it seemed that the segments were probably electrically connected to the other segments at the time of installation of the metallic side railings along the wingtips at the top of the instrumented span. To prevent this problem, it is recommended that the anchors of each base plate be embedded to between 3/4in. and 7/8in. instead of the 1in. embedment length used in the trial field test.

4.4.4.4 Stability of Readings. It was beyond the budget of this study to prepare an accurate and stable system for measuring more "realistic" span deflections at the same locations of the measuring stations of the base line system. This was mainly because the accuracy of the comparable system would at least have to be better and more repeatable than the 5/1000in. short-span accuracy of the base line system. No comparable measurements were therefore made to evaluate the long span accuracy of the deflection system under investigation.

However, deflection measurements of the instrumented span were taken after each stressing operation of the following five continuous spans. Final measurements were also taken at 80 days after the erection of the instrumented span to verify the stability of the deflection measuring system.

To have some base of reference for the adequacy of the trend of measured vertical movements of the instrumented span, TSDHPT engineers performed a detailed computer analysis of the span and provided their results to the researchers. A graphical comparison of the measured and calculated deflection values at each instrumented station and after each specific construction operation is included in Figures 4.70a and 4.70b. Readings taken after stressing of the instrumented span C-35 were considered as the reference shape for all future readings. Similarly, the calculated shape after stressing of the instrumented span was also taken as reference for further calculated values of span deflections.

Despite the initial readings after stressing of the first continuous span (C-36), all the other measurements taken after erection of the following continuous spans showed noticeable discrepancies with the calculated estimates. At 80 days after erection of span C-35 though, the calculated values were once again close to the measured deflections (see Figure 4.41b). This was an interesting indication of a probable good performance of the deflection measuring system over an extended period of time. Furthermore, if the field measurements were indeed accurate, they also indicated a relatively good prediction of 80-day deflections by the analytical method used by TSDHPT's designers. However, considerable differences between calculated and measured deflections were noticed between erection stages of continuous spans. Part of these differences were induced by predicted small vertical movements of the reference line. These movements were produced because the live and dead end anchors of the base wire were not installed directly above the supports.

Another source of errors could have been produced by temperature induced vertical movements of the instrumented span. However, the field measurements corresponding to the erection stages of all continuous spans were approximately taken at the same time of the day and under similar ambient temperatures. The widest temperature difference occurred with the 80-day measurements that were taken at a lower ambient temperature.

To help determine the relevance of the predicted and measured deflection values, more graphical comparison plots are included in Figures 4.71a and 4.71b. Each vertical movement produced by a determined construction stage was plotted using as a reference the previously measured and calculated deflected shape of the instrumented span. Only comparison of vertical movements from the previous values are therefore plotted in Figures 4.71a and 4.71b. The graphics help one understand the overall adequacy of the trend followed by the measured vertical movements. They also show the slight inconsistency of the calculated values with the construction operation. For instance, from the deflected shape calculated after stressing span C-40 (@ ≈ 45 days after erection of span C-35) to a time of more than a month afterwards (@ ≈ 80 days after erection of span C-35) the calculated values show a small upward increase in the camber of the instrumented span --see stage (f) of Figure 4.71b. This evidently does not agree with the downward deflections expected to be caused by the small losses of prestressing forces in the tendons. This is a small but important example of one of the benefits that can be obtained with a field instrumentation program of segmental box girder bridges.

Factors influencing the long-term performance of the base line method were also investigated. Corrosion of the base plates at the measuring station was considered to be an important possible source of future problems. The final plates were therefore designed with non-corrosive *17-4 Stainless Steel*. Regular stainless steel plates were not used because these are not magnetic and would have not been compatible with the magnetic portable measuring unit. However, the bases of the live and dead end stations were designed with regular stainless steel plates.

Accidental damage of the dead or live end stations is possible during construction stages when different crews must travel inside the box girder segments. Each one of these stations --which are permanently left on site-- was therefore designed to be attached to the concrete with four strong mechanical anchor bolts that can also be installed with epoxy as an added factor of stability.

The final factor influencing the long-term stability of readings is the possible physical damage of the portable reading unit with the digital scale. Any accidental movement of the extension arm attached to the digital scale will produce considerable errors. This unit should thus be carefully handled and stored. In addition, a reference calibrator should be constructed so that if a new unit must be made, readings can be transferred.

In conclusion, the deflection measuring system designed for field use in selected fully instrumented spans of the San Antonio Y project is accurate and assumed to be stable for long term readings. The approximate short term accuracy of the selected system is expected to be $\approx 5/1000$ in. It is also considered possible to get close to a $1/100$ in. accuracy level for medium term readings of a few years. The system accuracy would be improved and reliability further assured if deflection measurements were also made at the dead and live end stations. It is possible that the disagreement between measured and calculated deformations in Fig. 4.71 were due to a shifting of the wire elevation at the right end of the base line. A more positive test should be included in actual field readings.

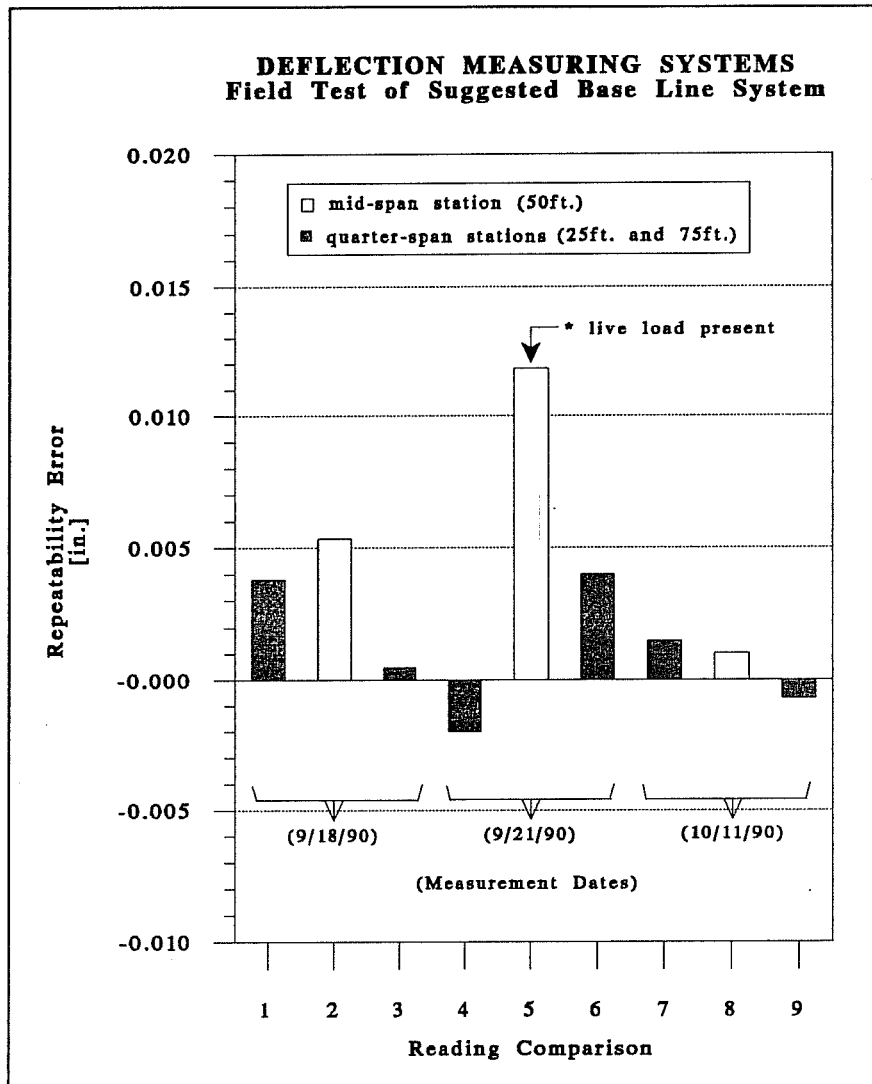


Figure 4.69 Repeatability errors of final deflection measuring system during field test.

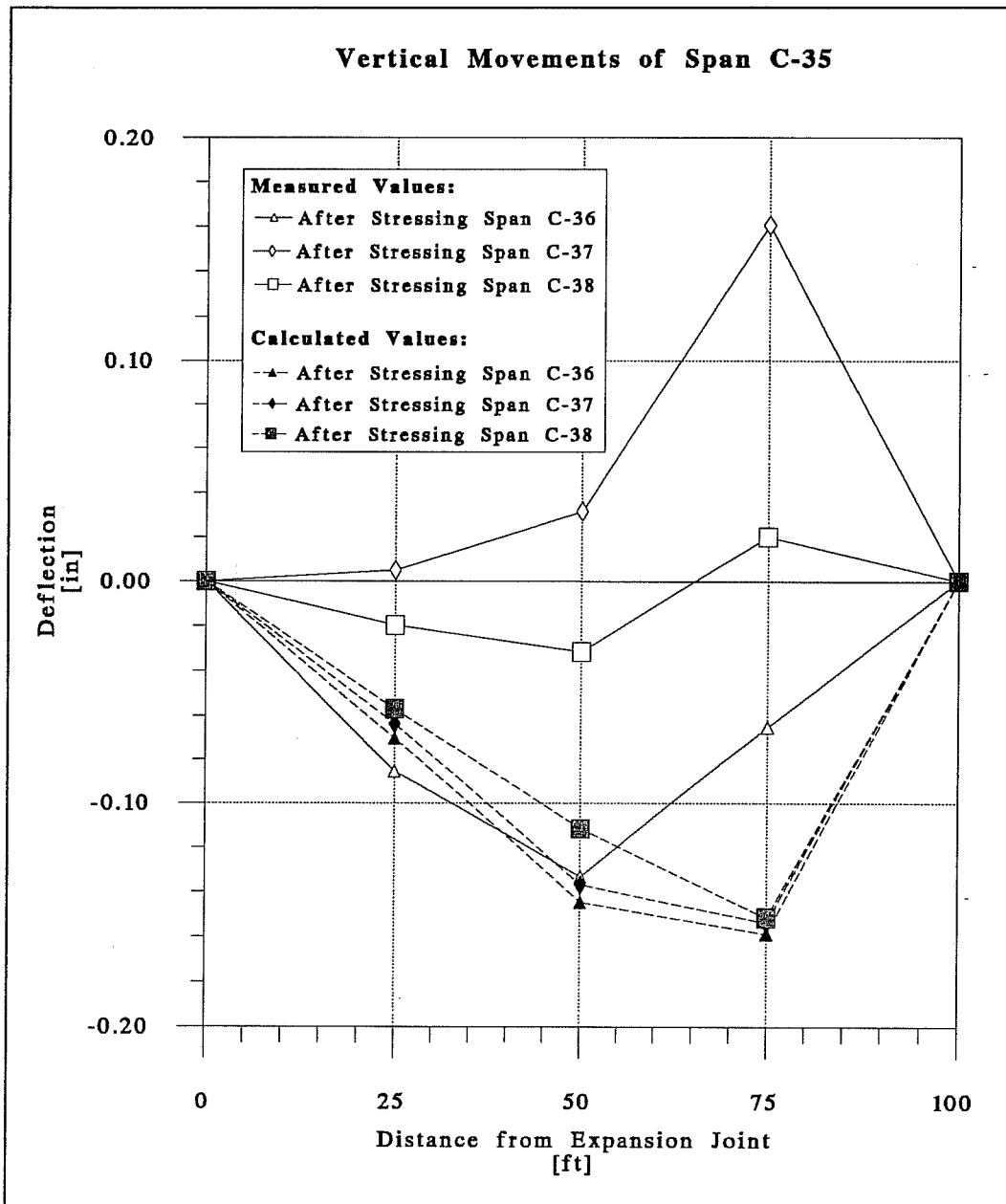


Figure 4.70a Measured and calculated deflections of span C-35.

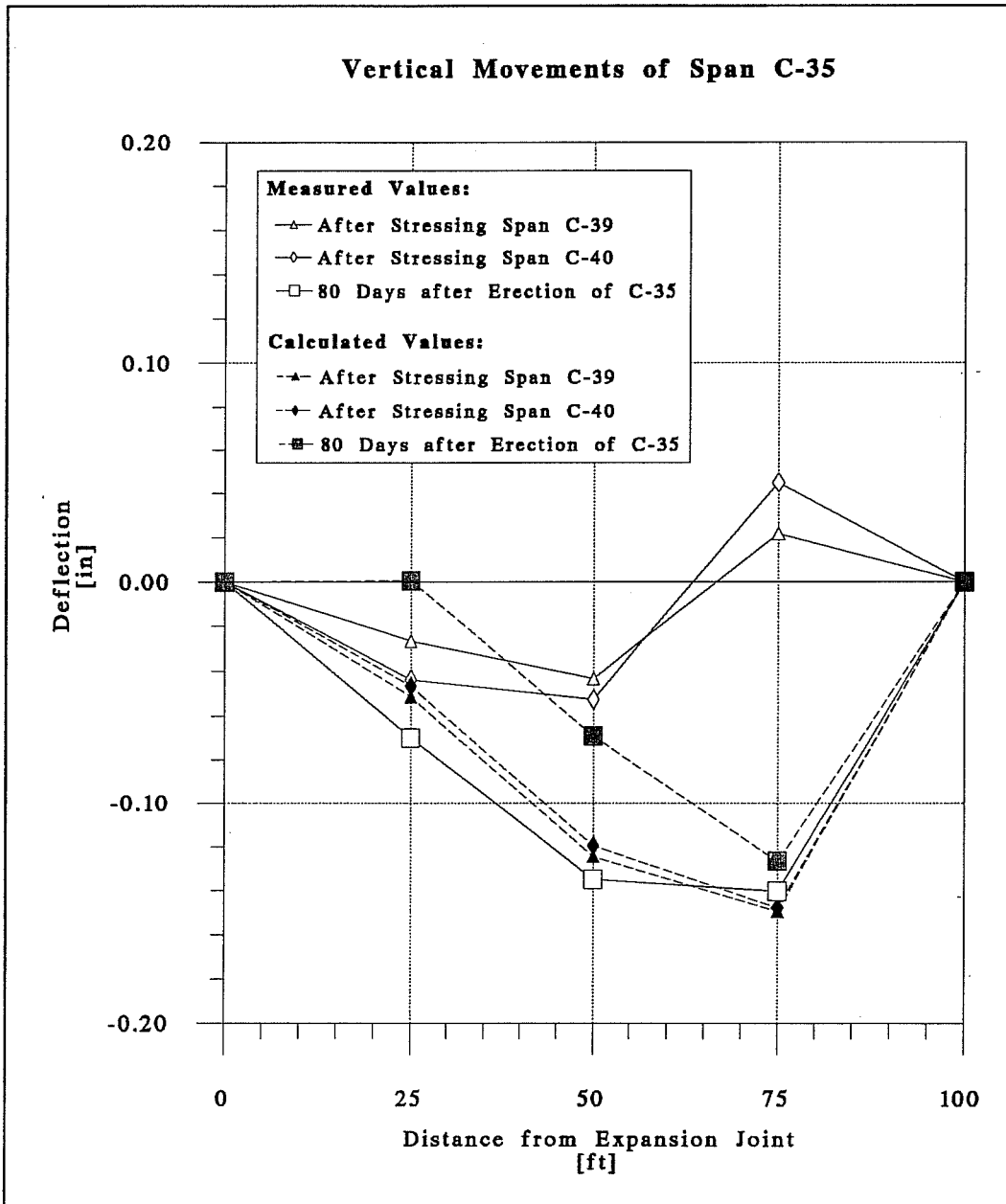


Figure 4.70b Measured and calculated deflections of span C-35.

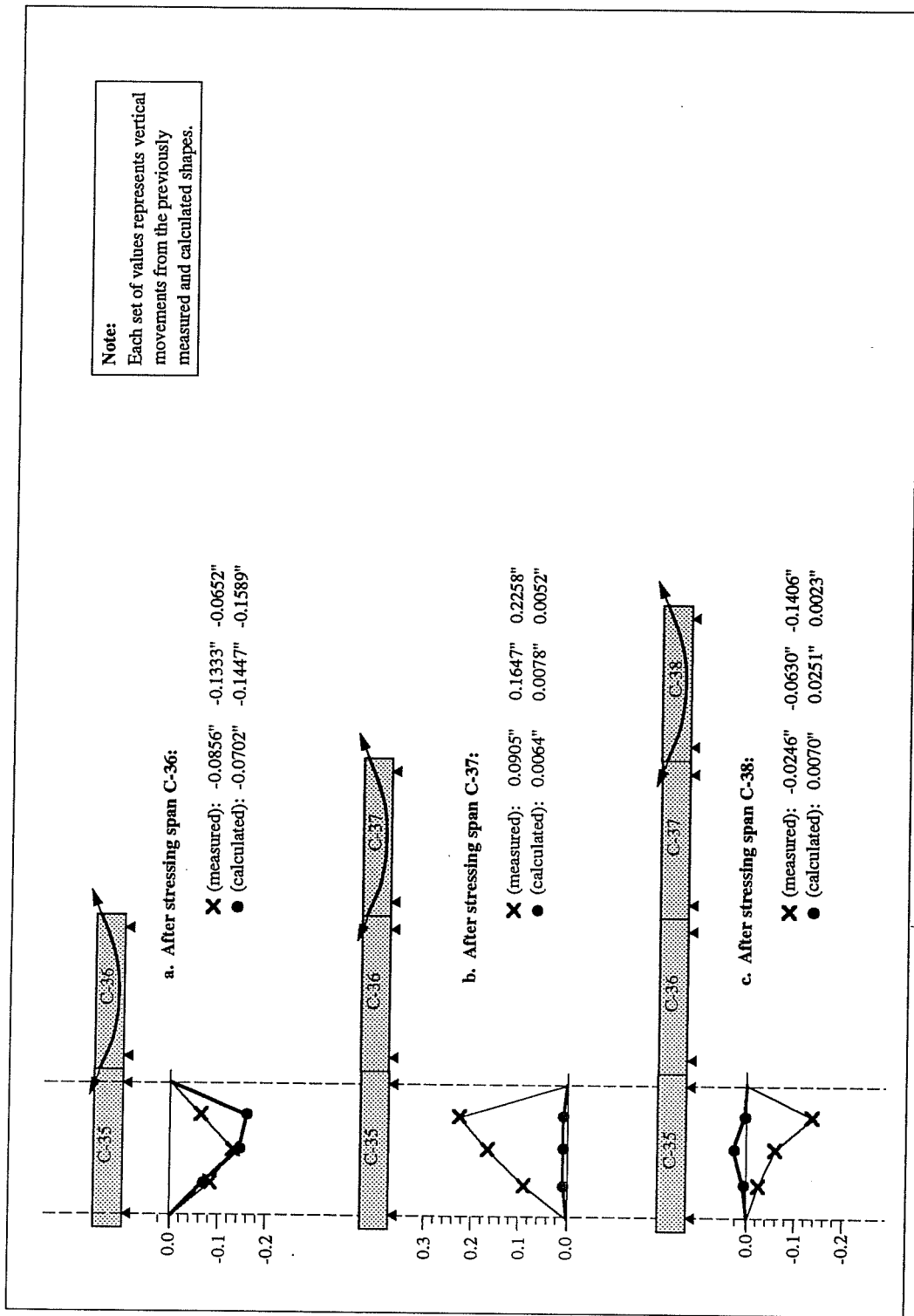


Figure 4.71a Measured and calculated vertical movements of span C-35 at different construction stages.

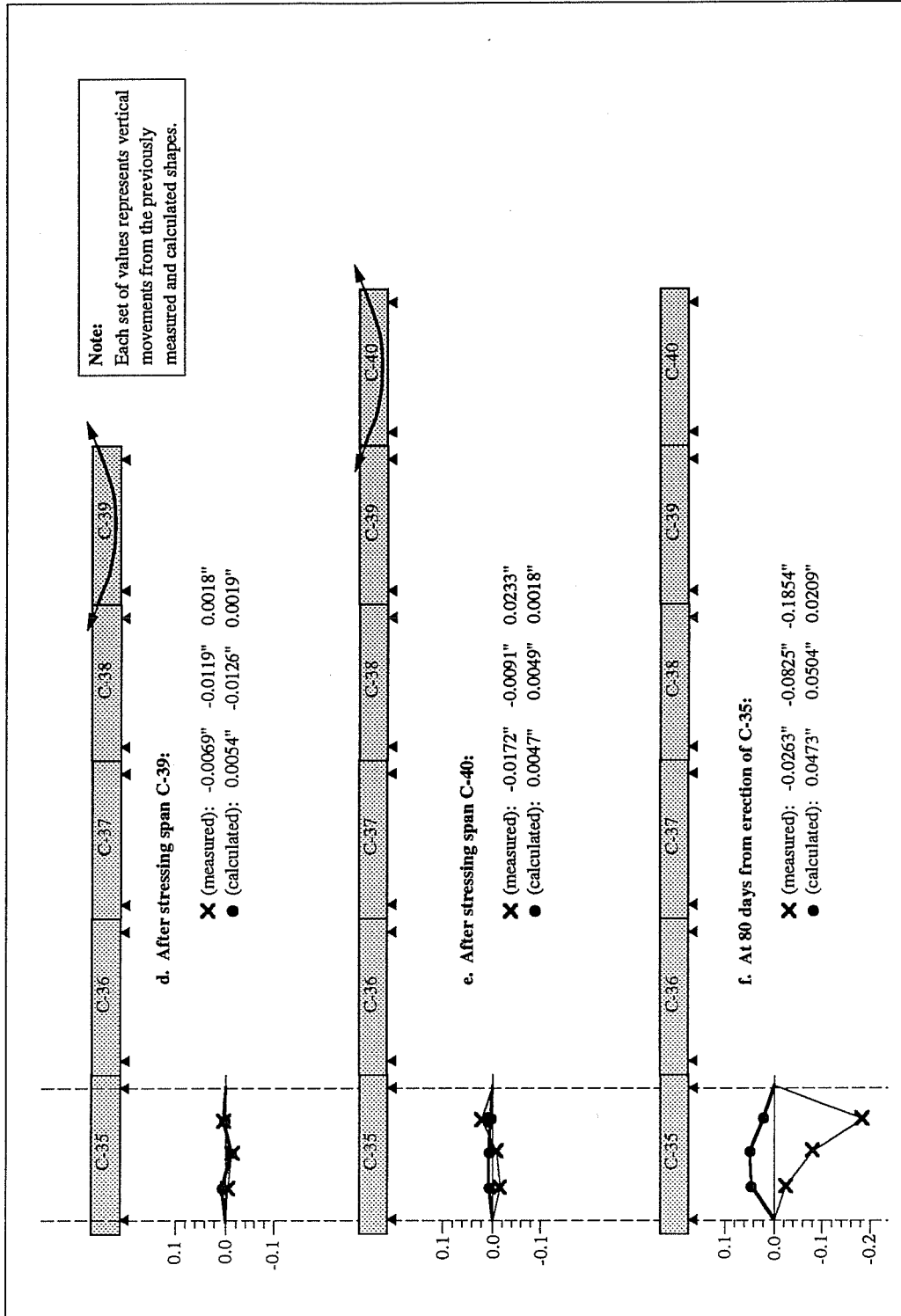


Figure 4.71b Measured and calculated vertical movements of span C-35 at different construction stages.

4.5 Data Acquisition System

As initially described in Section 3.6, a battery-powered data acquisition system based on the *Campbell Scientific 21X Micrologger* was purchased for the project. The following considerations influenced the decision for purchasing this particular system:

a. Factors supporting an automated system:

- operational errors are usually associated with the data recording procedures of manually operated systems,
- time consuming operations are involved in the data recording procedures of manual systems, and
- large long-term errors can be introduced due to the variation of contact resistances that occur in the connections of electrical resistance strain gage channels.

b. Factors supporting a battery-operated system:

- independence from a reliable source of AC electricity,
- avoidance of line stabilizers, surge suppressors and uninterruptible power supplies, and
- ability to operate in a harsher range of environmental conditions (in terms of moisture and temperature).

c. Factors supporting the Campbell Scientific equipment:

- data-loggers, PC-interfacing kit and software for programming and data retrieval all offered at low comparative costs,
- ability to work with a large number of ER-gage channels (with quarter bridge Wheatstone circuits),
- ability to accept input from a great variety of sensors, such as: thermocouples, LI-200SZ Pyranometer (for solar radiation measurements), ER-based strain gages, load cells and pressure transducers, LVDTs, etc.

Beyond the cost of the actual data-logger, multi-channel switching devices, PC interfacing kit, and data retrieval software, other important expenses are associated with the fabrication of the bridge completion circuits. The high sensitivity of the measurements related to variations of

electrical resistances (such as those of ER-gages) gave a priority to the automation of these particular channels. A very large number of electrical resistance strain gages were initially designed to be used in each instrumented span of the San Antonio Y project (up to 66 channels on two spans and up to 34 channels on the third one). However, this number is low when considering that all concrete strains were designed to be instrumented with mechanical extensometers. Most of the reviewed field instrumentation and laboratory projects also used an elevated number of electrical resistance sensors (when compared to the other devices that were used in the same project).

A certain type of Wheatstone completion circuit is necessary to be coupled with each channel of the data acquisition system to measure the very low electrical signals provided by the electrical resistance strain gages or load cells. Most of the ER-gages used in concrete structures are based on 120 Ω or 350 Ω resistors and require some type of Wheatstone bridge completion circuit (as previously explained in Part F of Section 4.3.1.1). The most widely used Wheatstone bridge for ER-gages is the three-leadwire, quarter-bridge completion circuit. To build this, it is necessary to have three high-precision resistors for each ER-gage channel (as shown in Figure 4.72). Similar precision resistors need to be installed in the same arm of the Wheatstone bridge where the electrical resistance strain gage is to be placed. The second arm is usually designed with the same resistors for simplicity. The 350 Ω (@0.01%) precision resistors cost about \$7.50 a piece (as of July 1990). Each completion circuit thus costs around \$22.50. Up to 16 quarter bridge channels were advertised to be handled by each AM416 relay multiplexer unit (this is the multi-channel switching unit that can be connected to the 21X data-logger). For the initially desired 166 quarter bridge completion circuits the total cost of completion circuits alone would have been about \$3,735.00. Evidently, the completion boxes would have comprised a highly-priced component of the instrumentation project.

As a savings alternative, the researchers investigated the possibility of directly wiring quarter bridge circuitry between the data-logger and each AM416 multiplexer. If this was possible then a single completion circuit could be used for each group of 16 ER-gage channels. The only disadvantage was that all 16 channels of each multiplexer wired in a quarter bridge configuration to the data-logger could not be used for other types of measurements.

An initial design of the envisioned quarter bridge circuitry was provided by the engineers of Campbell Scientific [101]. The researchers from FSEL learned the operation

principles of the data-logger and redesigned the original circuitry provided by Campbell Scientific [104]. The first finding was that a simple completion bridge can be formed between the data-logger and each multiplexer. A secondary, yet equally important, finding was that each multiplexer could actually handle double the 16 original number of quarter bridge channels mentioned by Campbell Scientific (provided that the data-logger is programmed and wired in accordance to the new design). With these findings, the total cost of the completion circuits necessary for the originally designed 166 ER-gage channels of the project was reduced from \$3,735.00 to \$360.00.

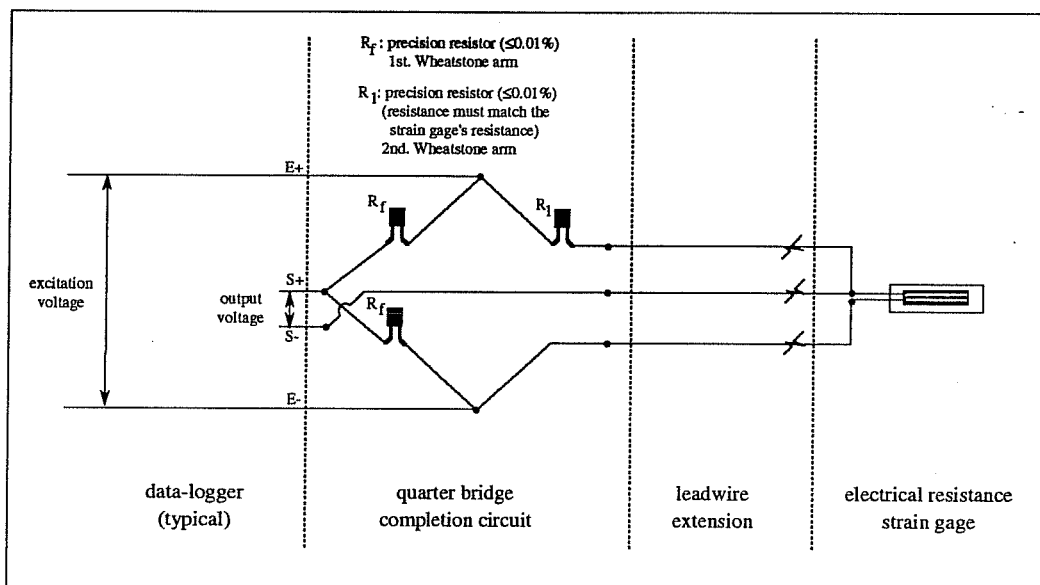


Figure 4.72 Three-leadwire, quarter-bridge Wheatstone completion circuit typically needed for most data-loggers

Three portable data acquisition systems were designed (one for each span to be instrumented). A general description of these systems is included here. However, a more detailed analysis of these systems is included in Appendix B.

The two larger data acquisition systems were similar. Each one of these two was composed of a single 21X Micrologger, two AM416 Multiplexers, and an internal PC Interface Kit. The third system only had a single AM416 Multiplexer since it was prepared for use in the span with less instrumentation. Each system was designed to be powered by an external hookup to a 12V marine-type battery that was calculated to last about two weeks at the scan rate,

excitation level, and number of channels to be used by each large-size data acquisition system. The final design included a provision for replacing the battery without cutting the power to the data-logger. This was accomplished by providing a secondary external battery port that can be connected to a replacement battery before cutting off the old one. The side panel of each system was also designed with two button-activated indicators. The first one was a voltmeter that checked the charge of the main battery, and the second one was a scan rate signal light that indicated if the system was properly scanning channels. These two control devices were incorporated based on a previous system designed by Post et al. [84].

In each system, all the connections to the different gage channels were designed with high quality silver-plated military standard Amphenol connectors. These were used to ensure the long-term stability of the external electrical connections. Heat shrink plastic tubes were used to cover all internal connections from the data-logger to the multiplexers and to the connectors. Special Polyethylene foam panels were used to enclose the data-logger and multiplexers inside each portable system. Packages of silica gel dehydrators were also placed inside each system to help prevent moisture accumulation. The portable boxes of each system were built at FSEL with ½ in. marine plywood sheets.

The small data acquisition system was completed first and it was checked on a short-term laboratory trial test using four 350Ω ER-gages. The gages were alternated through all the available channels of the system. This test showed that the system was completely functional. Initial tests were performed on one of the larger data acquisition systems and also indicated satisfactory behavior. All necessary details for the construction and operation of these systems are evaluated in Appendix B. These can be helpful for future similar endeavors.

CHAPTER 5

RECOMMENDED APPLICATIONS

5.1 Demec Extensometers

The selected method of monitoring concrete strains for this instrumentation project was based on the Demec Extensometer. Several recommendations for the proper operation of this type of instrument are summarized in this chapter. These guidelines originated from the testing trials reported previously in Chapter 4. Suggestions for future testing related to further improvements of this measurement technology are included in Section 6.2.

Standard Demec extensometers can have good stability of measurements and efficiency, provided that they are properly calibrated, installed and operated. Guidelines for achieving acceptable long-term stability of measurements with Demec extensometers are included in this section.

5.1.1 Installation of Locating Points

According to results from the trial tests reported in Section 4.2.1, the system of "Epoxyed Mechanical Stainless Steel Inserts" was selected as the most favorable for the present project.

Inserts recommended for use are the *Rawl Zamac Nailin* (stainless steel type w/mushroom head) 1/4"φ x 1" length (sold in boxes of 100 units). As shown in Figure 5.1, these devices are composed of a receptacle and a stainless steel nail insert. To use the *Nailin* as Demec locating discs requires pre-drilling of the indentations used as guiding points at the head of the stainless steel nails. Drilling should not be performed at the center location in the head of the inserts. Off-centered guiding holes allow better positioning of the nails so as to stay within the measurement range of the Demec gages. Drilling of the guiding holes is recommended to be performed in a drill press with special high precision adaptors. Use of a straight shank size 60 (.040"φ x 0.8" usable flute length) tungsten carbide bit gives good performance. A drilling depth of .05" should be the minimum for these indentations to prevent the points of the Demec gage from touching the steel at the base of the hole.

The heads of the pre-drilled stainless steel nails should be protected with a thick cloth during insertion, to prevent physical damage of the indentations. Concrete drilling is better performed with a tungsten carbide masonry drill bit ($1/4"$ ϕ , $\approx 2"$ usable flute length) and an electric hammer drill.

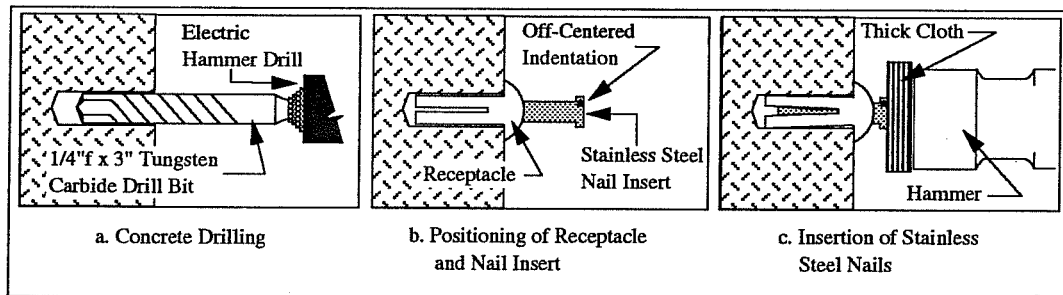


Figure 5.1 Installation of recommended Demec guiding system

Use of epoxy is encouraged. When utilized, epoxies complying with the Texas Highway Department Type V Epoxy Specifications should be used. *Industrial Coating A-103* two-part epoxy worked well in the trial tests.

5.1.2 Corrections for Temperature Differentials

Two important temperature related sources of errors should be avoided in field measurements of concrete strain with Demec extensometers.

First of all, in segmental box girder structures large temperature differentials are usually present between the top slab surface and the interior of the box girders. Errors associated with different temperature strains of the Demec extensometer, standard reference bar and concrete surface should be avoided.

Errors due to temperature could also be present if the different expansions of invar steel and concrete are not considered in the data reduction. This second problem is important in cases where extreme temperature differentials are expected, such as in long-term instrumentation projects. Long-term instrumentation projects in Texas can expect to find temperature differentials in the order of 80°F between summer and fall. This can introduce significant errors.

To avoid errors from temperature differentials, the following considerations are recommended:

1. The initial standard reference bar reading should be taken before the first set of locating point readings, but after the Demec extensometer and the standard reference bar have reached the same ambient temperature as the location of the first set of guiding points. For segmental box girder bridges, where one set of locating points is usually installed in the outside top deck slab and another in the inside of the box girders, two widely different ambient temperatures are usually present. When available reading time is an important factor, then two different sets of Demec extensometers and standard reference bars should be used. One set should be allowed to operate at standard ambient temperature on the inside of the box girder, and the other on the top surface.
2. The Demec extensometer and the standard reference gage are both made of invar steel. Thermal coefficient of expansion for invar is approximately 0.8×10^{-6} units per °F, and that of concrete varies from 5 to 6.5×10^{-6} units per °F. For each temperature differential of 10°F about $8 \mu\epsilon$ will be induced by temperature strains of the gage itself, and $50 \mu\epsilon$ to $65 \mu\epsilon$ due to expansion of concrete. The best method for avoiding differential expansion errors is to implement an organized set of reading operations and data reduction when utilizing Demec extensometers. A suggested methodology for reading operations is included in Section 5.1.3. Data reduction procedures can vary widely according to the researcher's depth of knowledge of standard electronic spreadsheets. Any method that follows a consistent reduction should be acceptable.

5.1.3 Operating Instructions

The following reading operations are suggested:

- a. Allow Demec extensometer and standard reference bar to achieve the same ambient temperature as the instrumented concrete surface.
- b. Set dial indicator of Demec at an initial value. This initial value should normally be the zero mark of the dial indicator.
- c. Get initial reference reading ($\epsilon_{st,0}$) of standard bar (use the average of three readings).
- d. Get readings from each instrumented location on the surface of the concrete ($\epsilon_{ci,0}$), again averaging a set of three readings if possible.

- e. Measure the average ambient temperature T_o , or concrete surface temperature at time of initial readings at location of first set of points.
- f. At a later time, after finishing the next set of readings (following steps a through e), the corrected concrete strain at each location of similar ambient temperature on the concrete surface can be obtained with the following formula:

$$\epsilon_{i\text{corr}} = (\epsilon_{ci,j} - \epsilon_{ci,o}) + (T_j - T_o) * (\alpha_{in} - \alpha_c) + (\epsilon_{st,j} - \epsilon_{st,o})$$

where:

$\epsilon_{i\text{corr}}$: corrected concrete strain differential of guiding point i ($\mu\epsilon$)

$\epsilon_{ci,j}$: jth concrete strain reading of guiding point i ($\mu\epsilon$)

$\epsilon_{ci,o}$: initial concrete strain reading of guiding point i ($\mu\epsilon$)

T_j : jth concrete surface temperature reading ($^{\circ}\text{F}$)

T_o : initial concrete surface temperature reading ($^{\circ}\text{F}$)

α_{in} : thermal coefficient of expansion of invar steel ($0.8 \mu\epsilon/^{\circ}\text{F}$)

α_c : thermal coefficient of expansion of concrete ($5.5 \mu\epsilon/^{\circ}\text{F}$, suggested)

$\epsilon_{st,j}$: jth strain reading of standard invar reference bar ($\mu\epsilon$)

$\epsilon_{st,o}$: initial strain reading of standard invar reference bar ($\mu\epsilon$)

Final operating recommendations of the Demec extensometers are related to:

- (a) Repeatability, and
- (b) Handling and Storage.

5.1.3.1 Repeatability. Gage readings should be performed following the most standardized methods of operation. This has been found to have a direct influence on the repeatability of gage readings [81]. Standards for reading operations should be set in the following areas:

1. The positioning of the Demec extensometer's fixed point should be the same for all subsequent readings of the same locating points. This avoids measuring strain related to differences in seating conditions.
2. Pressure on the Demec extensometer while reading the strain values at each point should be constant for all subsequent readings. For strain readings on horizontal surfaces it is recommended to avoid using any more pressure than the weight of the Demec extensometer (for 200mm or larger gages). On inclined surfaces, all operators in charge of strain readings should standardize the pressure exerted on

the Demec gage. This can be done by taking several successive readings at one particular location until all operators achieve strain values within the acceptable level of repeatability.

5.1.3.2 Handling and Storage. Demec gages should be treated with all the carefulness required for precision mechanical instruments. The spring at the pivoting ends wears out rapidly in field applications and recalibration is costly and time consuming. When the pivoting end is worn out, the old gage should be replaced with a recalibrated gage. Strain correction readings should be taken from each location with the new and old gages. Standard reference bars should also be kept clean and in good condition to avoid the introduction of wearing errors in the reference readings.

5.2 Electrical Resistance Strain Gages

The most important consideration investigated within this technology was the reliability of measurements for long-term testing applications. Several sources of literature about the electrical resistance strain gaging technology were reviewed. Short-term testing was performed to address problems with installation, moisture protection and actual performance in single strands and multi-strand tendons. The late completion of the purchasing and assembling of the data acquisition system prevented any long-term performance tests of the complete electrical resistance strain gaging system. In fact, the lack of long-term testing influenced the decision for accommodating a mechanical backup system for measuring multi-strand tendon loads.

Nevertheless, a detailed analysis of most of the factors related to long-term signal stability was reported in Section 4.3.1.1. This section presents a guideline for the proper ER-gage system selection and installation. Suggestions for a data reduction method are also mentioned. Electrical resistance strain gages were planned to be used in selected spans of the San Antonio Y project for the following objectives:

- long-term measurements of strains in steel tendons composed of 19- and 12- 0.6"φ prestressing strands.
- short-term measurements of strains in #3 to #7 steel reinforcing bars.

5.2.1 System Selection

It is important to select the most adequate gage, bonding agent, protection, wiring, and data retrieval systems according to the particular type of test to be performed. Literature from gage manufacturers concerning these factors is strongly recommended for applications different from those reviewed in this project. Table 5.1 shows the final systems recommended for the San Antonio Y project, and a summary of important guidelines.

I. GENERAL GUIDELINES	
ER-Gages:	
Length	≥0.29in. (7.4mm)
Width	≤0.13in. (3.3mm)
Material	Constantan (A-alloy)
Bonding agents	cyanoacrilates (short-term tests), epoxy (long-term tests).
Resistance	350Ω
Leadwires	stranded, shielded, three-leadwire conductors.
Completion circuit	quarter-bridge Wheatstone.
Connectors	simple (short-term tests), gold-plated (long-term tests).
Data Acquisition System	Battery operated (for field tests), permanently switched (throughout testing), multi-channel scanners.
II. FINAL SYSTEM	
ER-Gage	EA-06-125BZ-350 (Micro Measurements).
Leadwires	8771 (Belden Wire).
Bonding Agent	M-Bond 200 (short-term tests), M-Bond AE10 (long-term tests).
Excitation level	4.5V

Table 5.1 Suggested ER-Gage systems.

5.2.2 Use in Prestressing Steel Tendons.

1. Epoxy Preparation. The bottles of epoxy type AE-10/15 supplied by Micro Measurements come in volumes that produce large amounts of waste when installing a group of gages, especially if installation is done under hot Texas summer temperatures. This is because the adhesives completely harden in 10 to 20 minutes, therefore providing only short workable

times. It is recommended to separate each bottle of AE-10/15 resin (bottle with larger volume) into four other smaller, clean glass containers. Proper mixing can then be accomplished with one-fourth the volume of the hardener component, at the 5ml mark on the provided calibrated droppers.

2. Surface Preparation. This should be done according to technical suggestions from gage manufacturers [96]. A summary of the steps suggested for applications in prestressing wires follows:

- 2.1 Surface degreasing with CSM-1 degreaser sprayed on a strand section of 3-4in. length should be the first procedure.

- 2.2 Initial sanding with 120-grid sanding paper.

- 2.3 Final sanding with a smoother 400-grid silicon-carbide sanding paper.

- 2.4 Apply the cleaning solution (Conditioner A), avoiding drying on the finished surface. For drying purposes apply single strokes of clean cotton swabs.

- 2.5 Apply the surface conditioner (Neutralizer 5), also avoiding drying on the finished surface.

* Gage installation should follow as soon as possible.

3. Gage Installation. More detailed procedures are usually included in each package of epoxy adhesives. A modified summary from technical literature follows [97].

- 3.1 Remove the gage from the plastic envelope by carefully grasping the attached leadwires. Place the gage on a chemically clean surface with its top side up.

- 3.2 Bond a piece of cellophane tape to the top of the gage and carefully detach it from the clean surface by lifting it at a shallow angle, making sure the gage is glued to the tape.

- 3.3 Position the gage/tape assembly on the cleaned surface of the strands and tack down one end of the tape to the strand.

4. Epoxy Mixing and Placing. The instructions included with the adhesives [97] should be slightly modified to accommodate the approximate distribution of epoxy resin that was previously prepared. The following steps are now recommended:

- 4.1 Use calibrated droppers to insert 5ml. of the epoxy hardener in the center of the bottle of epoxy resin. Use the provided stirring rods to mix both solutions for a period of 3 to 5 minutes.

- 4.2 Lifting one end of the cellophane tape (at a shallow angle) coat the back of the gage and wire with a thin layer of mixed epoxy solution.
 - 4.3 With a clean gauze sponge slowly make a single wiping to bring the tape/gage assembly back to the final gage position.
 - 4.4 Lifting the end of the tape that corresponds to the pre-attached gage leadwires, position a small piece of Teflon tape to prevent a strong bond of the leadwires with the prestressing steel wire.
5. Gage Clamping. Use precast silicone pieces of the proper strand size to completely cover the installed gage (fabrication previously reviewed in Section 4.3.1.1 - Part C). Apply an approximate pressure of 5 to 20psi with a standard hose clamp. The epoxy solution should achieve good curing in 5hr at 75°F (for higher temperatures consult charts included in gage packages).
 6. Soldering and Gage Protection. The following instructions are suggested for gage protection in aggressive environments:
 - 6.1 Cover each one of the three leadwires (usually red, white and black) with the M-Coat B Solvent (white colored solution).
 - 6.2 Cut a piece of the FB rubber sealant (black colored) and install next to the end of the gage, under the gage's leadwires. This is done to prevent shorting with the prestressing steel wires. The size of the piece of rubber sealant should be enough to cover the spaces up to the middle of the two adjacent wires to the wire being gaged. Make sure that the rubber sealant covers the grooves between prestressing wires.
 - 6.3 Twist two conductors of the leadwires together (usually the red and white conductors) and cut all three conductors to a length of about ¼ in. Bend the conductor ends in 90° angles and place them tight against the previously installed rubber sealant.
 - 6.4 With small tweezers wrap each one of the two leadwires coming from the gage to each conductor placed on the rubber sealant surface. Make sure that no shorting of wires and specimen occurs. Finally solder both terminals.

- 6.5 Cover the complete assembly strain gage/soldered terminals with a coating of epoxy type M-Coat J-1. Let the coat cure for a day at normal 75°F temperature, or for two hours at 150°F (when using a blow drier).
 - 6.6 Use a larger layer of rubber sealant to cover the hardened system. Cover the gage system with a final coating of wax (Microcrystalline Wax W-1, melted with a blow drier).
7. Data Reduction. The following procedures are suggested for the data reduction process of each electrical resistance strain gage bonded to an individual prestressing strand located at an intermediate tendon cross-section:
- 7.1 Record the live end loads according to the readings obtained from pressure transducers installed in the calibrated hydraulic jacks used for initial stressing of the tendon. Compute the average tendon stresses at the live end by considering the nominal areas of the prestressing strands.
 - 7.2 Simultaneously scan the ER-gage and the live end pressure transducer at load intervals of no more than $0.08f_{pu}$ (about 20ksi). Plot the strain readings from the ER-gage and the corresponding live end stresses computed from the pressure transducer on a σ - ϵ graph. In this graph, find the best-fit line through the data points corresponding to live end stresses between $0.20f_{pu}$ and $0.80f_{pu}$. Find the intersection of the best-fit line with the strain axis (this is the strain reading that corresponds to the zero stress level). Subtract this zero strain reading from each one of the originally measured strain readings. Although it is likely to be positive, the zero strain reading can be either positive or negative and its sign should be considered for the correction of the original strain readings. The corrected strain values multiplied by the apparent modulus of elasticity (determined in the previously performed material tests with ER-gages) gives an approximate indication of the stress level of the intermediate tendon cross-section where the ER-gage is installed.
 - 7.3 A good approximation of the stress loss that occurs between the live end and the instrumented tendon cross-section is given by the ratio between the slope of the best-fit line (computed above in 7.2) and the apparent modulus of elasticity (computed from the material tests with ER-gages).

- 7.4 To establish stress losses from one ER-gage instrumented section to another follow a different data reduction procedure. Compute the average difference from each strain reading corresponding to stresses between $0.20f_{pu}$ and $0.80f_{pu}$ during the initial loading of the tendon. To find the average stress loss multiply the final averaged strain difference by the apparent modulus of elasticity of the prestressing strand (determined from the material tests with ER-gages, following Section 5.7.2.2).
- 7.5 In long-term tests, the effects of steel relaxation with time should be estimated according to current AASHTO [40] formulas (see Section 3.2.2).
- * When using epoxy sleeves, install the ER-gages in between each pair of epoxy collars. The epoxy collars were found to produce a certain degree of clamping to the prestressing strands and thus help averaging the tendon stresses between the strands (see Part E of Section 4.3.1.3). In the data reduction process, instead of considering the data points located between $0.20f_{pu}$ and $0.80f_{pu}$, only consider the linear data points that were obtained before the strands slipped in the epoxy sleeves. In the reported tendon tests, the stress level when strand slippage usually occurred was ≈ 110 ksi (see Part E of Section 4.3.1.3).

5.2.3 Use in Reinforcing Steel Bars.

Techniques related to the use of electrical resistance strain gages in steel reinforcing bars were not investigated due to the good performance reported in previous laboratory tests at Ferguson Laboratory. At the San Antonio Y structures, reinforcing bars are planned to be instrumented only for short-term investigations during initial loading of tendons. However, if long-term stability is also needed, then most recommendations established previously for the prestressing strands should be followed:

1. Epoxy Preparation. Same as in Section 5.2.2.
2. Surface Preparation. Modify instruction 2.1 in Section 5.2.2 as follows:
 - 2.1 Grind the ribs of the reinforcing bar leaving a smooth area for installation of the strain gage. Spray degreaser CSM-1 on a section slightly larger than the grind area.
3. Gage Installation. Same as in Section 5.2.2.
4. Epoxy Mixing and Placing. Same as in Section 5.2.2.

5. Gage Clamping. Modify. Cut a small piece of thin neoprene rubber (Measurements Group FN Neoprene Rubber) and cover the installed gage. Use an adequate hose clamp to exert an even pressure over the area of the gage. Follow the same curing conditions indicated in Section 5.2.2.
6. Soldering and Gage Protection. Same as in Section 5.2.2. Gage protection should work better considering the smoother surface of the reinforcing bars.
7. Data Reduction. Modify. When establishing load levels at each instrumented reinforcing bar, use the modulus of elasticity that was reduced from the steel reinforcing bar material tests and not the manufacturer values (see the Material Test Recommendations in Section 5.7.3).

5.3 Epoxy Sleeves

This is the mechanical system envisioned as a backup for measuring loads at intermediate sections of typical external tendons used in segmental box girder bridges. The system was selected due to the following benefits:

- it has a relatively low cost,
- probably provides a better estimate of average tendon cross-section stresses (at intermediate tendon sections) than the ER-gages,
- is a good method for blocking grout and protecting ER-gages, and
- produces an averaging effect of the stresses on the strands located between the epoxy collars (which helps ER-gages in the sense that a few instrumented strands can still provide a good approximation of the average tendon stresses).

At the same time, it is equally important to mention some of the problems related to this new measurement system:

- long-term stability of the system was not tested properly with fully modeled effects of creep, and temperature,
- epoxy fumes can become a problem for installation inside box girder bridges (especially when instrumenting several tendons), and

- tendon segments have to be grouted carefully at each intermediate location between epoxy sleeves.

5.3.1 Multi-Strand Tendon Systems

A step-by-step procedure for precasting and preparing the epoxy sleeves on 19-0.6" ϕ prestressing strands is described fully in this section (however, the pictures previously included in Figure 4.40 should greatly help understand the suggested fabrication process). Final dimensions of the finished epoxy sleeves system are included in Figure 5.2. The following steps are recommended to be followed in the fabrication and installation of multi-strand epoxy sleeves:

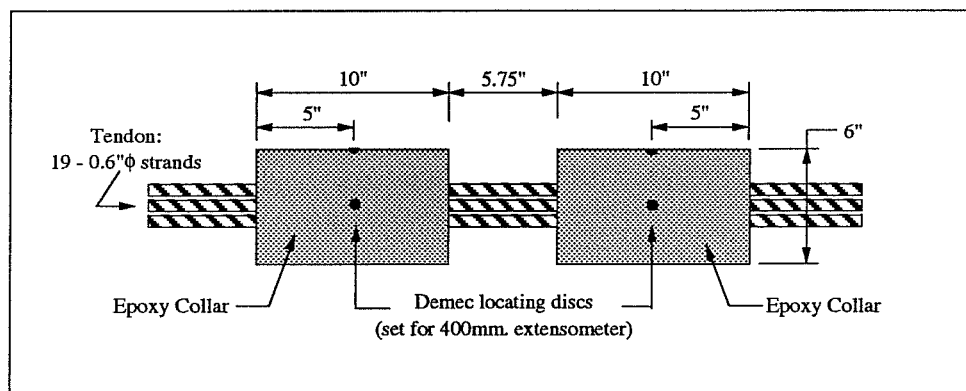


Figure 5.2 Schematic of the final epoxy sleeve system for multi-strand tendons.

1. Cut two 12in. long pieces of 6in. o.d. PVC drainage pipe to be used as cylinder molds for the epoxy collars. Standard 6in. x 12in. plastic cylinder molds for standard concrete compression tests also work well for this purpose (after cutting off the bottom of the mold).
2. Make a single longitudinal cut in the 12in. axis of each PVC mold. Also make rectangular cuts of approximately 2in. x 1in. at the middle of the cylinders, and on each side of the longitudinal cuts.
3. End caps of the molds for the epoxy collars should be prepared from 2in. thick foam panels. Two circles of 6in. o.d. should be cut from the foam panels, and an

approximate shape of the cross section of the tendons to be instrumented should be cut from the center of each one of these end covers.

4. A small initial load corresponding to $0.05f_{pu}$ should be applied to the tendons before installing the epoxy sleeves. This is necessary to shape the tendons according to the approximate configuration that they will take in their final loading stage.
5. The first step in the installation process of the epoxy collars is to mark the approximate places where the foam caps will be located. This should be done carefully to obtain the final dimensions of epoxy sleeves shown in Figure 5.2. The strands located at the cross-sections corresponding to the location of the foam caps should be well covered with silicone.
6. Foam caps should be placed in their final marked positions around the strands. The PVC cylinders should be placed around each pair of end caps, covering about an inch of each cap. This is necessary to allow enough room for a 10in. length between the inner faces of a pair of end caps.
7. A pair of hose clamps should be used for tightening the PVC molds against each foam cap and against the strands. This will further help spreading the silicone to the areas between strands that were not accessed during their initial installation. A final coating of silicone should be spread around the ends of each epoxy collar and strand. The silicone should be cured for no less than one hour before pouring the epoxy.
8. Epoxy should be poured in the top rectangular access holes of each collar. The large volume of epoxy contained in each collar induces a fast hardening process of the epoxy (due to self-heating effects produced by the high temperatures of large volumes of epoxy). However, the epoxy should be allowed to cure according to manufacturer recommended periods.
9. After taking the PVC molds from the epoxy collars, the proper Demec locating discs should be installed as close as possible to the positions shown in Figure 5.2. The suggestions for assuring the long-term stability of Demec locating discs included in Section 5.1.1 of this report should be followed. Also, 400mm Demec extensometers are recommended highly due to their higher reading resolution.

5.3.2 Data Reduction Process

A good recording of live end loads and corresponding epoxy sleeves strains is necessary for determining stress losses from the live end to the location of each pair of epoxy sleeves. The following procedures are suggested for the data reduction process of each pair of epoxy sleeves installed at an intermediate tendon cross-section:

- a. Record the live end loads according to the readings obtained from pressure transducers installed in the calibrated hydraulic jacks used for initial stressing of the instrumented tendon. Compute the average tendon stresses at the live end by considering the nominal areas of the prestressing strands.
- b. Record the epoxy sleeve strain and the corresponding live end pressure transducer readings at load intervals of no more than $0.08f_{pu}$ (about 20ksi). Plot the strain readings from the epoxy sleeve and the corresponding live end stresses computed from the pressure transducer on a σ - ϵ graph. In this graph, find the best-fit line through the data points that show approximately linear increases of stress and strain (in the tendon tests, these points usually corresponded to stresses between $0.20f_{pu}$ and $0.80f_{pu}$ --see Part E of Section 4.3.2.2). Find the intersection of the best-fit line with the strain axis (this is the strain reading that corresponds to the zero stress level). Subtract this zero strain reading from each one of the originally measured strain readings. Although most likely positive, the zero strain reading can be either positive or negative and its sign should be considered for the correction of the original strain readings. The corrected strain values multiplied by the apparent modulus of elasticity (determined in the previously performed material tests with epoxy sleeves) gives an approximate indication of the stress level of the intermediate tendon cross-section where the epoxy sleeve system was installed.
- c. A good average approximation of the stress loss that occurs between the live end and the instrumented tendon cross-section is given by the ratio between the slope of the best-fit line (computed above in "b") and the apparent modulus of elasticity (computed in the material tests with epoxy sleeves).

- d. To establish stress losses from one epoxy sleeve instrumented section to another follow a different data reduction procedure. Compute the average difference from each strain reading corresponding to stresses between $0.20f_{pu}$ and $0.80f_{pu}$ during the initial loading of the tendon. To find the average stress loss, multiply the final averaged strain difference by the apparent modulus of elasticity of the prestressing strand (determined from the material tests with epoxy sleeves, following Section 5.7.2.1).
- d. In long-term tests, the effects of steel relaxation with time should be estimated according to current AASHTO [40] formulas (see Section 3.2.2).

5.4 Calibration of Hydraulic Jacks

Properly calibrated hydraulic jacks are extremely important when these are the only source of measurement of live end loads during initial stressing of tendons. As initially discussed in Section 3.2.3.1, one method of calibration was presented by Littlejohn [76] and is a suggested procedure for the jacks to be used in the instrumented spans of the San Antonio Y structures. This rigorous calibration method must be followed when the hydraulic pressure in the jacks provide the only source of live end loads during initial stressing operations.

Although this technique was actually envisioned for load cells, it can also be implemented for hydraulic jacks. Littlejohn [76] suggested the following series of tests to simulate the service conditions to which the load cells may be subjected:

- (i) Routine calibration using centric loading and rigid flat platens at 20°C, say.
- (ii) As in (i) but using (a) concave inclined platens, (b) convex inclined platens, and (c) 0.3mm sheets with irregular spacing to simulate uneven bedding (Figure 5.3).
- (iii) Eccentric loading between rigid flat plates, with eccentric distance up to 10% cell diameter.
- (iv) If torsion is anticipated during service, an approximate torsion should be applied during a test between rigid flat platens to gauge the effect.
- (v) Inclined platens up to 1° with centric loading.
- (vi) On completion of the approximate series of tests, the cell should finally be subjected to a repeat routine calibration (i).

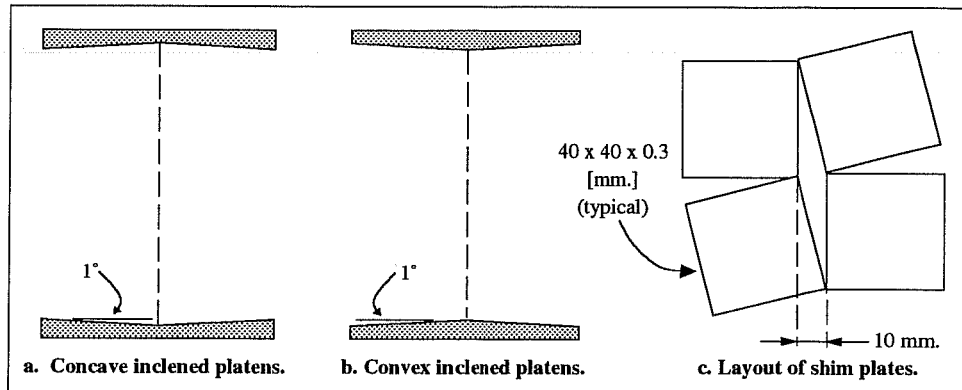


Figure 5.3 Typical types of platen to simulate uneven bedding (after Littlejohn [76]).

Littlejohn also suggested other conditions for this calibration to be appropriate [76]:

- Load cell should achieve room temperature before routine calibration.
- Centric loading should be performed using a loading machine with an absolute accuracy of 0.5% or less.
- If load cell was not in use, load cycle the cell over its full range until zero and maximum readings are consistent.
- Load increments and decrements of not more than 10% of cell's rated capacity.
- To measure temperature effects, perform centric loading tests at other temperatures.

Since the final objective for calibrating any load measuring device is to obtain more accurate readings during their service use, other authors [60, 75] suggest additional considerations:

- In normal field stressing of prestressing tendons, hydraulic jacks are usually in an active mode, yet during calibration the loading machine is the active device. To better model this field behavior, the hydraulic jacks should therefore be calibrated with their pistons in different extensions.
- Whenever possible, the complete system to be used in the field should also be used in the routine calibration process.

5.5 Span Deflections

The method suggested for performing this type of field measurement was designed in this research program based on improvements of a previously developed system. The base line

system suggested by Pauw-Breen [79] in 1959 was ideal for the present instrumentation program since it complied with most of the initial requirements. The main advantages of the final version of the base line system are:

- economical,
- easy to manufacture, install, and operate,
- accurate,
- good short to medium term stability, and
- simple technology.

Tests of this system were performed in laboratory controlled conditions on short spans of up to 22ft lengths. A final test was performed inside a selected 100ft span of the San Antonio Y structure. Results from these trial tests were included in Section 4.4. A final description of the base line system, and important suggestions for its proper selection, installation, and operation are included here.

5.5.1 System Description and Selection

The basic technology of the base line method for measuring span deflections in bridges is very simple. It consists of measuring vertical movements of selected points of a span with respect to a reference line strung between the abutments (or between locations just above the supports). The different components of this system, as designed for spans A-43 and A-44 of the San Antonio Y structure, are shown in Figure 5.4. A general description of the considerations that must be taken when designing each one of these components is included here.

5.5.1.1 Base Lines. High-strength piano wire is suggested to be used as the reference line for this type of measurement. Sizing of the piano wire is closely related to the span length of the structure to be instrumented. Piano wires are usually sold in 0.5lb rolls, so larger diameter wires have shorter lengths. For example, the maximum length of wires sold in 0.0310in. ϕ is \approx 200ft and for 0.0170in. ϕ is \approx 650ft. If the particular span to be instrumented is considerably longer than 110ft, say beyond 200ft, the proposed measurement system would need to be re-evaluated in terms of accuracy and repeatability of readings. The experience of the research team suggests that a 1/100in. level of repeatability and accuracy can still be obtained with spans up to 200ft length. Even for longer spans, it is likely that this system provides a better degree of accuracy than the traditional surveying methods.

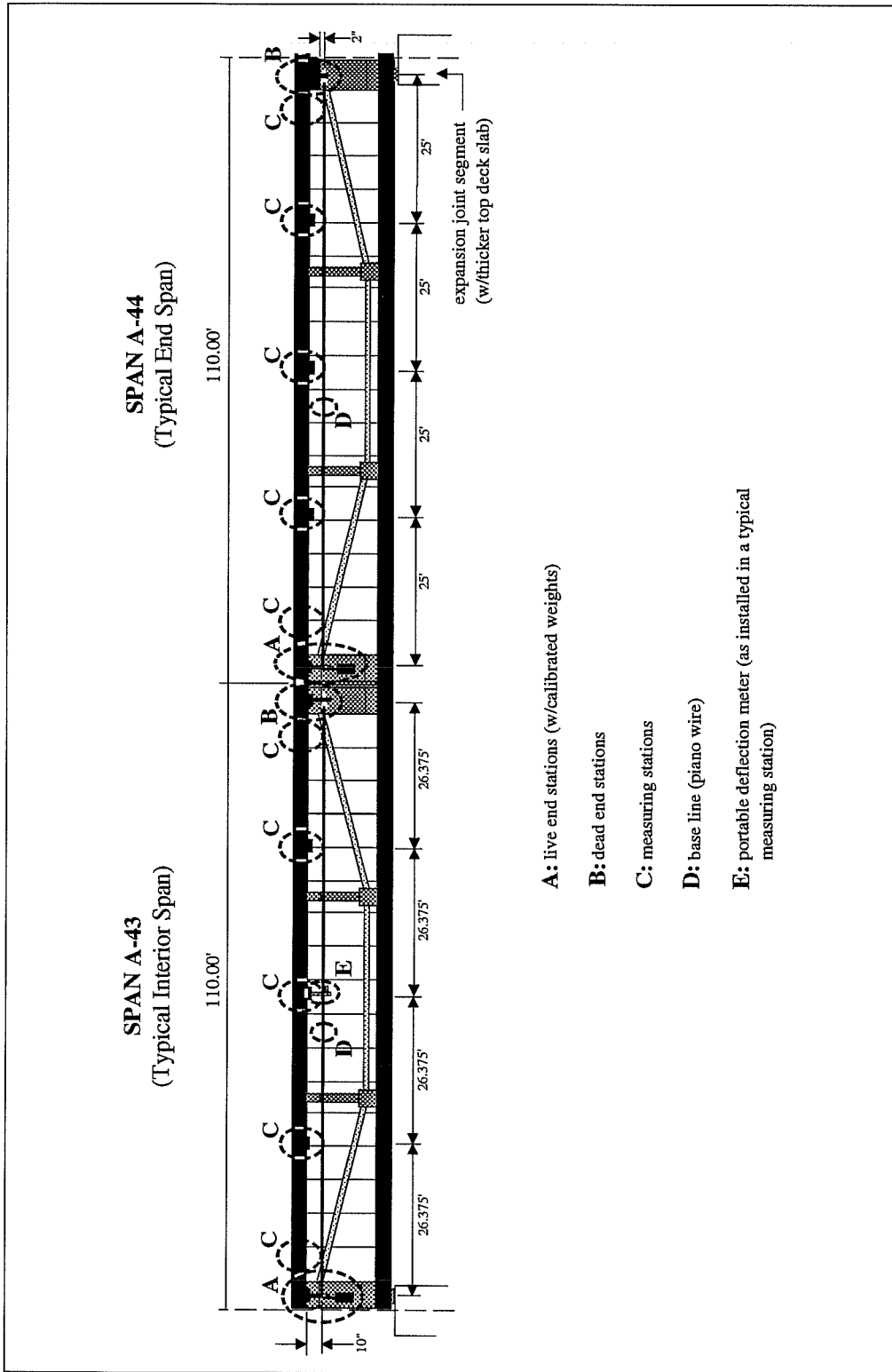


Figure 5.4 Components of base line system designed for typical spans of the San Antonio Y bridges.

A secondary factor regulating the ideal size of the piano wire is the portability of the calibrated weight that is hung at the live end (and used for stressing the wire). It is recommended to stress the piano wire to a level around 90% of its breaking strength. This is desired since small fluctuations of such a high level of stress should not provide any measurable variations in the catenary shape of the free length of the piano wire. To impose this level of stress in a piano wire requires heavy loads at the live end, for instance, the 0.0310in. ϕ wire needs ≈ 122 lb to reach 90% of its breaking strength. This kind of load is obviously difficult to handle and also requires strong anchorages for the live and dead end stations.

Consideration of both of these factors (the free length of the wire and the calibrated load) influenced the decision for recommending the 0.017in. ϕ piano wires. These are sold in ≈ 650 ft lengths and only need a 37lb weight to be stressed to 90% of the breaking strength. In the U.S., the place to purchase them is: *Schaff Piano Supply Co.*; located at: 451 Oakwood Rd., Lake Zurich, Illinois; Zip Code: 60047. The cost of piano wires is not a concern. As an example, in late 1990 each 0.5lb roll of 0.031in. ϕ piano wire was purchased for \$3.70.

5.5.1.2 Live End Stations. These are composed of steel base plates, steel columns, and sealed bearings (as shown in Figure 4.30). Smaller bases are preferred to minimize the rotational movements produced by the span deflections. When large span deflections occur (usually only during ultimate strength tests performed in a laboratory, or during service load tests performed in the field), small errors are introduced by the rotation of the base plates. However, using the same size plates at the live and dead end anchors, and installing them directly above the supports should help decrease these errors. A suggested size for the base plates at both end anchors is 4in. x 4in. x 3/8in. with 4-1/4in. ϕ holes drilled at their corners (for installation of the concrete anchorage bolts). These plates are recommended to be made of stainless steel members to avoid long-term corrosion problems.

The steel columns of the live ends should be made of regular steel tubing cut at variable heights. Square tubing of 1in. x 1in. (with $\approx 1/8$ in. thickness) is recommended. Column stiffener plates can also be used to assure that the columns are not bent by the tension of the base wire. The height of the tubing depends on the particular geometry of the span to be instrumented. For instance, the steel tubing at the dead end station of span A-44 had to be designed shorter than the other stations due to the increased thickness of the top deck slab at the expansion joint segment (see Figure 5.4). Whenever possible, it is suggested to minimize the height of steel columns to

decrease the errors attributed to rotations of the base plates. The steel tubes and optional stiffeners are recommended to be permanently welded to the base plates to avoid any accidental movements while left on site during construction operations. For this particular process, special stainless steel welding rods must be used (since the base plates are made of regular stainless steel).

The roller bearings are recommended to be of the sealed type to prevent friction variations with time. They should be tightly bolted to the steel columns. However, they should not be installed permanently to allow for their possible replacement in the future. An important characteristic of these bearings is that they should be grooved at the center of their outer circumference. These grooves should have $\approx 1/16$ in. depth and no more than $1/16$ in. width. They are recommended (one on each bearing) to serve as guides for the positioning of the base wires.

As mentioned earlier, the calibrated weights used to impose the proper level of stress to the base wires at the live end stations need to stress the wires to about 90% of their ultimate strength. A second condition in the design of these weights is that they should have a hook or a similar device helping to effectively anchor the piano wires.

5.5.1.3 Dead End Stations. These are similar to the live end stations, with the main difference that the bearings are replaced by a steel bolt with a circular loop at one end (as shown in Figures 4.28 and 4.29). This loop is ideal for anchoring the piano wire. An important consideration here is related to the type of knot used to anchor the piano wire to the steel loop. The traditional "fisherman's knot" worked the best in the trial tests with 0.017in. ϕ wires and is therefore recommended. Furthermore, to avoid having small vertical variations of the place where the piano wire is anchored to the dead end loop, it is strongly suggested to machine some small grooved guides at the dead end anchors.

5.5.1.4 Reading Stations. These are 4in. x 4in. x $1/4$ in. square plates of a special steel used as bases for the portable reading units. Small steel tabs are suggested to be welded to the top surface of these steel plates to serve as reference guides for the magnet of the portable reading unit. Four $1/4$ in. ϕ holes should also be drilled at each plate's corners for proper anchoring to the concrete. Another important characteristic related to these plates is that they cannot be made of regular stainless steel because it is not magnetic. As a solution, these plates should be made of *17-4 Stainless Steel* that is characterized by being magnetic and non-corrosive.

5.5.1.5 Portable Reading Units. These are made of a digital scale, a magnet, and a steel mounting column (as shown previously in Figures 4.61 and 4.62). The digital scales are recommended to have a 5/10,000in. resolution to obtain better levels of accuracy. A vernier adjustment would definitely improve the adequacy of the scale, however, it is not imperative (since a 5/1000in. accuracy was already obtained without a vernier micrometer). Digital scales of high resolution (at \approx 8in. lengths) are expensive. The scale to be used in the San Antonio Y instrumentation project is an 8in. *Mitutoyo Digital Scale* priced at \$150.00 in July of 1991. Other digital scales of better accuracy are also available but at higher cost. For instance, *Swiss Precision Instruments, Inc.* offers the *Digital Height Gages* of 12in., 18in. and 24in. lengths, and with 5/10,000in. accuracy levels for \$468.00, \$676.00 and \$815.00 respectively (priced in late 1990). These type of gages are specifically made for base line type of measurements and come with pre-attached extension arms and solid steel bases.

The digital scales (not purchased pre-assembled to a base and extension arm assembly, as in the case of the *Digital Height Gages*) should be tightly mounted (not permanently welded) to a steel column of the proper height. If solid, the weight of the steel column should be "lightened" by drilling several holes on all faces of the steel tubing (as shown in Figures 4.61 and 4.62). This is recommended as a method to decrease the downward force exerted by the weight of the portable unit on the magnetic bond system used at its base. An aluminum extension arm is also suggested to be mounted to the digital scale to allow for a wider range of lateral movements of the piano wire.

A strong magnet is suggested to be bolted to the base of the steel column. This method of securing the portable reading units to each reading station decreases considerably the total installation time and the portability of the reading stations without decreasing their accuracy and repeatability.

5.5.2 Field Installation

The field installation of the base line system components requires the use of two electrical tools: a vibrating concrete drill and a portable drop-light. The drill is necessary for the installation of all the anchor bolts. Special tungsten carbide drill bits are strongly recommended, since in the trial tests the regular bits only worked well for 3 to 4 operations in high strength concrete. The concrete anchorage bolts for the base plates of all stations should be made of

strong, non-corrosive elements. *Hilti Kwick Bolt II, AISI 304 & 316 Stainless Steel* of 1/4in. diameter and 3/4in. threaded ends are recommended. The embedment length of these bolts, however, should be carefully controlled to less than 7/8in. (ideally between 3/4in. and 7/8in.) to avoid establishing an electrical contact with the reinforcing bars. To increase the stability and mechanical strength of the anchor bolts, two-part epoxy mixes can also be used in their installation.

5.5.3 Operation and Storage

The first step for operation of the installed system is to tie the piano wire to the dead end station and unwind it to the live end station. The manufacturer-provided cage that holds each roll of piano wire is quite difficult to handle during the unwinding process of long lengths of wire. It is strongly recommended to manufacture a more practical piano wire cage assembly in the laboratory to prevent field problems. An important consideration for the handling of the piano wire is also to avoid producing any "kinks" due to excessive bending. When the piano wires are stressed to a level near their ultimate load, the locations damaged from excessive bending become critical failure areas where the wire fractures. The "fisherman's knot" worked well at preventing this from happening in the connection of the piano wire to the dead end and to the calibrated load.

After proper unwinding of the piano wire, make sure that the bearings are not bound (or tighter than usual). Use light machine oil on the bearings when measurements are taken after long periods of time. Place the piano wire over the guiding grooves in the bearings and hang the calibrated weight very slowly to prevent overstressing the wire.

Before taking readings, make sure that the base plate of each reading station is clean and free of any metal particles (stuck to the plate due to its small residual magnetism). Take several readings from each station, and when averaging the results, do not include obvious mis-readings. This is especially important when the method for determining the contact of the extension arm of the digital scale and the base wire is performed by single-eye sighting.

The portable reading unit should be stored and handled very carefully, as for any other high-precision instrument. Finally, it is strongly recommended that special light-weight, Styrofoam padded wooden cases be constructed for the portable reading units.

A battery-operated, portable, mini-processor-printer unit is suggested to be used for all the measurements. Most gage manufacturers provide a compatible processor that can be coupled with their digital gages. The use of the processor helps eliminating most operator errors and considerably increases the speed of measurements.

5.6 Thermal Measurements

The most important physical parameter within this area consists of concrete temperature measurements. Thermal measurements can provide important information about the nonlinear temperature distribution in the different elements of the box girder segments. They can also provide important information related to the temperature differentials existing between different parts of each segment during concrete curing (due to hydration of cement).

A second form of measurement suggested to be used in the instrumentation program for selected spans of the San Antonio Y project was the amount of solar radiation impinging upon the top deck slabs. This can be helpful for determining the amount of heat transfer produced from the inciding solar radiation. Measurements of concrete temperature and solar radiation can also be related to determine the percentage of the total radiation that is actually absorbed by the concrete surface and transformed into heat (before and after installation of the layer of asphalt).

Both of these measurements can be performed with low-cost instrumentation systems that are known to provide good levels of accuracy and stability.

5.6.1 Concrete Temperature

The devices selected for measuring temperature variations inside concrete members were thermocouple wires. Size 20AWG copper-constantan wires (thermocouple type "T") were selected due to their lower degree of oxidization and abrasion in aggressive environments. To further protect the thermocouple wires, it is recommended that they be insulated with Teflon/Neoflon compounds. These provide increased moisture protection and abrasion resistance. Finally, tinned copper overbraids are recommended for field applications to increase the physical protection and durability of the thermocouple wires. This type of overbraid is usually the least expensive and provides acceptable levels of protection.

To avoid any intermediate splices, the original thermocouple wires should be cut in proper lengths. Intermediate splices can form a secondary thermocouple junction that can introduce erroneous temperature readings. However, if splices become necessary, good recommendations can be obtained from most thermocouple manufacturers. The temperature measuring junction of copper-constantan thermocouple wires can be prepared by stranding both wires together or by fusing them with an oxyacetylene flame. To install a series of wires across the thickness of certain box girder sections, each wire should be tightly taped to a strong plastic rod that can serve as a stabilizing base for the wires. The rods can then be tied to neighboring reinforcing steel bars at the required locations (as shown in Figure 5.5). These plastic rods will therefore ensure that the thermocouple wires are kept at their predetermined locations during concrete casting. For individual thermocouple wires located along the bridge superstructure, high-strength fishing line can be used alternatively to tie each independent thermocouple to the reinforcing steel bars.

When a thermocouple wire is installed near the concrete surface that is instrumented with strain measuring devices, the thermocouple readings can provide important data for temperature induced strains in the concrete.

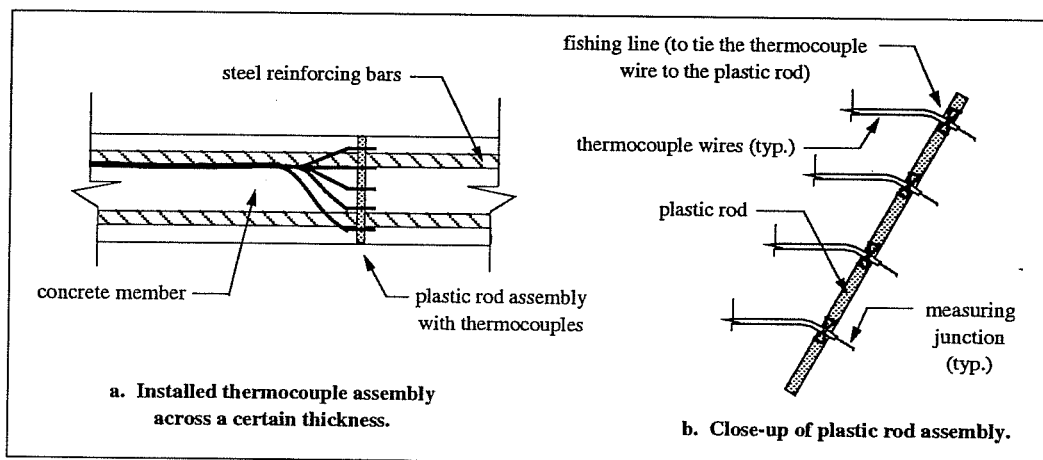


Figure 5.5 Installation of a series of thermocouple wires across the thickness of a concrete member.

Multi-channel switching devices are strongly recommended to be used in projects involving a considerable number of thermocouple wires. Since leadwire effects or contact resistance differentials do not decrease the accuracy of the thermocouples, highly sophisticated

automated data acquisition systems are seldom needed. Portable multi-channel rotary switching devices for up to 39 channels can be easily assembled in most research laboratories at a very low cost. Groups of thermocouple wires placed in different spans can be plugged and unplugged at various times when readings are needed. The only problem with these arrangements will be the slow oxidization process of the reading junction terminals of each pair of unprotected thermocouple wires. This can only become a problem for long-term projects. To decrease the oxidization process at the end of the thermocouple wires, each group of wires can be kept inside foam-filled boxes containing several packets of silica gel desiccants.

5.6.2 Solar Radiation

The device selected for measuring the amount of solar radiation impinging upon the top of the deck slabs was the LI-200SZ Silicon Photodiode Pyranometer. The operation of this device is relatively simple when connected to automated data-loggers. It can also be operated with a multimeter (measuring millivolts) provided that a 140Ω (max.) resistor is installed across the leads of the coaxial cable of the pyranometer. The millivolt output can be directly related to units of $cal/(m^2 \times min)$ by knowing the calibration constant of the pyranometer sensor.

The greatest inconvenience associated with the pyranometer is that it should be sent back to the manufacturer for recalibration every two years. It should also be stored and treated very carefully in order to maintain its original accuracy for each two year period. The top of the sensor should always be cleaned from dust before each operation. The pyranometer should be installed on a leveled surface. Leveling can be achieved easily with the optional mounting and leveling fixtures offered with the pyranometer. Finally, these devices are very sensitive to any form of shade. They should be positioned so they only become affected by shade provided by clouds and not shade induced by localized elements (such as construction machinery, trees, etc.).

5.7 Material Tests

Every well-thought structural instrumentation program must consider material tests to check values of several properties that cannot be accurately obtained with code-established empirical procedures. These tests are essential in concrete structures. The following suggestions have been prepared from a literature survey of past field investigations.

5.7.1 Concrete

Accompanying material tests of concrete are suggested as an aid for more accurately determining the state of stress of the instrumented spans of the San Antonio Y structure. These concrete tests are suggested for estimating the highly variable parameters of:

- modulus of elasticity, and
- creep and shrinkage.

Several factors have been found to influence the actual creep and shrinkage of concrete structures, most of these factors were already mentioned in Section 3.1. The influence of creep and shrinkage in segmental concrete bridges has been studied in several previous investigations. Most of these tests determined considerable creep and shrinkage strain variations among specimens stored inside, on top, and underneath the box girder segments. Bryant [98] found that specimens on top and under the box girders experienced similar creep, but those inside the bridge experienced 15% more creep. Shrinkage was found to be more dependent on location. The specimens inside the box girders had 100% more shrinkage than those on the top slab, and 25% more than specimens under the bridge [98]. Bryant also found that the CEB-FIP [99] and ACI [100] predictions for creep and shrinkage were both about 25% of the experimental values [98]. Although size of the concrete elements also plays an important role in creep and shrinkage test results, there is a well defined dependence on location that should be considered. Japanese shrinkage tests further found that unstressed web elements inside the same span of a box girder bridge but located at opposite ends had differences of up to 40% [49]. These previous tests suggest the following considerations for the concrete material tests of the San Antonio Y structures:

1. Creep Tests.

1.1 Cylindrical specimens (6in. x 12in.) should be taken during casting operations of each instrumented segment of the selected spans. These should be properly labeled and left near, or inside the box girder segments during the time they are in storage.

1.2 Creep specimens should be loaded on special frames that comply with ASTM C512 specifications [102]. Due to problems related to transportation, theft, and possible tinkering of creep frames left on the job site, these tests can be developed on a field outside the Austin laboratory facilities. The environmental conditions should be

similar to those in San Antonio. Creep specimens should be loaded as close as possible to the stressing day of corresponding spans. Properly calibrated load cells are highly recommended as load monitoring devices during initial loading of creep specimens.

- 1.3 Each specimen should be gaged in two diametrically opposite positions following the recommended procedures for 200mm Demec extensometers (see Section 5.1).

2. Shrinkage Tests.

- 2.1 Shrinkage specimens should be taken according to the locations where strain readings will be taken in the structure. The size of these specimens depends on the gage length of the instrumentation device to be used on them (which should be the same as the device to be used in the actual field measurements of concrete strains). Since 200mm Demec extensometers are planned to be used in the field measurements, 6in. x 12in. cylinders or 6in. x 12in. x 3in. rectangular beams are recommended. Each specimen should be properly labeled and should undergo similar environmental conditions as the sections of the structure that will be monitored. For example, specimens monitoring concrete behavior at inner web locations should be stored inside the box girders.

- 2.2 Each specimen should be gaged in at least two locations following the recommended procedures for assuring long-term stability of the locating points of 200mm Demec extensometers (see Section 5.1).

3. Modulus of Elasticity.

- 3.1 Specimens for these tests should be taken during casting operations of each instrumented segment of the selected spans. The size of these specimens usually depends on the most available testing machine. Since the contractor's San Antonio casting yard has a testing machine for 4in. x 8in. cylindrical specimens, this is the recommended size. This size of specimens also facilitates handling.

- 3.2 Tests should be performed at the following days:

- 7 days after casting,
- 28 days after casting,
- at day of initial stressing of tendons.

5.7.2 Prestressing Steel

Laboratory testing should be performed with at least two samples taken out of each prestressing strand roll to be used in the instrumented spans. The important parameters obtained from these tests consist of the values for the strand's modulus of elasticity determined by the epoxy sleeves and the electrical resistance strain gages. These two separate values can be obtained with single material tests of strand specimens instrumented with both measurement systems. General recommendations regarding the single strand material tests consist of the following:

- The length of the specimen directly depends on the testing machine to be used. A good rule is to use specimens no shorter than 4½ ft.
- Use standard single strand anchorage hardware. Pre-load the specimen to about $0.50f_{pu}$ to properly seat the wedges on each wire. Unload back to zero and start testing.
- A properly calibrated load cell or universal test machine should be used for obtaining corresponding live or dead end loads. Average strand stresses should be obtained by considering the nominal cross-sectional strand area.
- In the data reduction process, only consider the data points that correspond to stress values between 20% and 80% of ultimate.

5.7.2.1 Epoxy Sleeves. For the San Antonio Y instrumentation project, the single strand tests with epoxy sleeves will only be performed as material tests. These will be necessary for determining the modulus of elasticity that corresponds to the strain measurements from the epoxy sleeve system. The modulus determined from epoxy sleeve readings should only be slightly larger than that given by the strand manufacturer.

Two different setups can be followed according to the gage length of the Demec extensometer to be used in the field instrumentation project. Figure 5.6 helps illustrate these two possible systems. The following specific guidelines only apply to the shorter epoxy sleeve system. However, they can be easily modified for the longer one.

1. For ease of installation in structural engineering laboratories, the 3in. x 6in. standard plastic cylinders for concrete tests are ideal for single strand epoxy sleeve molds. The only modification is that a 0.5in. or 0.6in. diameter circle

- according to the size of strand being tested-- should be drilled at the bottom of each plastic mold.
2. To maintain concentricity the tops of the plastic molds with the prestressing strand, two 2.875in. o.d. circles should be cut from a 0.5in. thick plywood sheet. These plywood caps should have a central 0.5in. or 0.6in. diameter hole according to the size of the strand to be instrumented.
 3. Each mold and cap pair should be slipped onto the prestressing strand specimen and placed so as to have a space of approximately 2.75in. between the top of the lower plastic mold and the bottom of the upper plastic mold (10.5in. when using 400mm extensometers). The small spaces between the strand and the circular holes at the bottom of both molds should then be covered with silicone. A minimum drying period of one hour is recommended for the silicone.
 4. With the strand specimens in an upward position, the proper epoxy mix (same as that to be used in the actual field tests) should be poured into the plastic molds. The molds should only be filled up to a level 1in. below their tops. The minimum epoxy curing time suggested by the manufacturer should be followed.
 5. After cutting the plastic molds from the epoxy collars, at least two pairs of demec locating points should be placed around the sleeves according to the distances shown in Figure 5.6. Since only short term tests are necessary, these locating points can just be bonded to the surface of the epoxy collars.
 6. During testing, the strain readings of the epoxy sleeves should be taken very carefully, preferably according to the recommendations included in Section 5.1.3 for Demec extensometers.
 7. In the data reduction process, a straight line fit of all acceptable data should finally provide the average modulus of elasticity determined from the epoxy sleeve readings. This is the modulus that should be used for converting the modified field measurements of epoxy sleeve strain readings to average stresses.

5.7.2.2 Electrical Resistance Strain Gages. Material tests of prestressing strands with electrical resistance strain gages should be performed according to the following guidelines:

1. Each specimen should be gaged with a minimum of 4 ER-gages similar to those to be used for the actual field testing. Install these gages at one single cross-section in the

middle of the specimen, preferably between the two epoxy collars. If possible, also install every pair of gages on diametrically opposed wires of the prestressing strand.

2. In the data reduction process, compute the average of the strain readings obtained from each ER-gage and for each loading step. Make a linear regression of the acceptable data points, without requiring the line to pass through the origin of coordinates. Use the slope of this line as the modulus of elasticity for estimating stress levels from field strain readings of ER-gages.

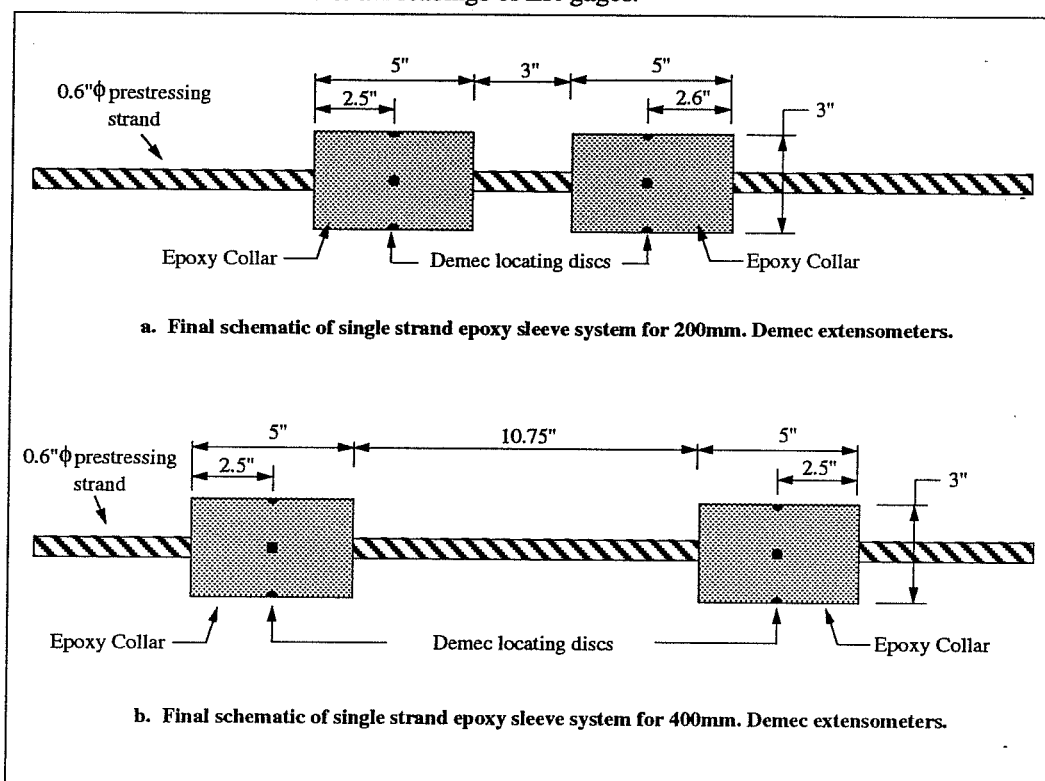


Figure 5.6 Schematic of finished single strand epoxy sleeve systems.

5.7.3 Reinforcing Steel

These material tests are expected to be much simpler than for concrete and prestressing steel. Reinforcing steel material tests are more important for laboratory testing of structural components, when specimens are usually loaded to failure. In most cases, the material tests of reinforcing bars reveal slightly different yield points. However, such a high level of stress is evidently not expected in field instrumentation projects of actual structures.

Some recommendations for these tests are:

- Specimens should be taken from the same batch of reinforcing steel bars that will be instrumented with strain gages.
- Instrumentation should consist of a single strain gage per specimen, installed according to the recommended procedures of Section 5.2.3.

5.8 Other Measurements

Other measurements recommended for segmental box girder bridges consist of joint openings and bearing pad deformations (as an indirect measurement of load at the supports). Devices suitable for these measurements were not investigated in great details and were not included in the state-of-the-art review of instrumentation systems. Part of the reason for not developing a large review is because these measurements are relatively simple and of a lesser degree of importance than the rest of the systems that were investigated.

5.8.1 Joint Openings

To measure any separation of segments across their joints, *calibrated crack monitors* are recommended to be used along with Demec extensometers. Locating these two systems across a joint will provide a reliable source of information about joint openings. Demec extensometers will provide a more accurate measurement of movements. However, the maximum measurable range of a Demec extensometer is very limited. In the unexpected case of large openings, the crack monitors will be essential instrumentation devices.

The calibrated crack monitors should be installed with some type of mechanical anchorage and two-part epoxy adhesives to ensure their long-term stability. The recommended methods from Section 5.1.1 should be used for anchoring the Demec locating discs near each crack monitor. Either the 100mm or the 200mm gage lengths of Demec extensometers will work well for these measurements. The operating instructions mentioned previously in Section 5.1.3 should be followed for these readings.

5.8.2 Bearing Pad Deformations

This is a novel application to be investigated for reliability in this instrumentation project. No trials have been made with this system and some rules and recommendations are expected to appear in the near future.

High resolution caliper gages can be ideally used for measuring the vertical deformations of the neoprene bearing pads located at the support of each span. This information, along with the material data for the neoprene pads can be helpful for determining the loads imposed at each support.

CHAPTER 6

CONCLUSIONS AND FINAL RECOMMENDATIONS

6.1 General Conclusions and Recommendations

An extensive literature review as well as laboratory and field investigations were conducted to develop a model full-scale instrumentation system for prestressed concrete segmental box girder bridges. In particular, ideal instrumentation systems were investigated for their installation in selected spans of the San Antonio Y Elevated Highway Project and as a backup for a possible future similar venture (the 183 Elevated Highway Project in Austin, Texas).

The laboratory and field testing program developed during the research study produced several conclusions about the investigated instrumentation systems. Most of these conclusions along with some recommendations were already included in Chapters 4 and 5. However, this section contains a summary of the most important findings along with certain recommendations related to the selection, installation, operation, and/or data reduction process of certain instrumentation systems.

6.1.1 Demec Extensometers

Tests of bonding methods of different types of locating discs used for Demec extensometers produced the following conclusions (Section 4.2.1):

1. Systems that were drilled in fresh concrete, epoxy bonded, and incorporated an additional mechanical anchorage had the best long-term stability for field applications.
2. Drilling holes larger than $\frac{1}{4}$ " ϕ caused considerable disturbance to the surrounding concrete surfaces and should be avoided in future projects.
3. Tungsten carbide drill bits caused the least amount of disturbance in young concrete and had the best performance for repeated drilling operations.
4. Non-stainless steel locating points showed considerable rusting and scaling in the long-term laboratory tests. However, they performed well for short-term applications in laboratory controlled environments.

5. Locating discs bonded with two-part epoxy resins to a concrete surface did not perform well. Most discs debonded due to extreme temperature differentials combined with the wear and tear produced by repeated measurements.

In further tests with Demec extensometers, a high resolution digital indicator was installed as a replacement of the original dial indicator of a 200mm Demec extensometer. The "modified Demec" showed an average reading speed increase of 20% of the time taken by the standard Demec extensometer (Section 4.2.2). Reduced random reading errors and improved sensitivity were also expected to be found in the modified Demec extensometers. However, these improvements were not investigated further.

Finally, the reading repeatability of a standard 200mm Demec extensometer was found to reach $16\mu\epsilon$ when special care was observed in the reading operations (Section 4.2.3).

6.1.2 Electrical Resistance Strain Gages

The review of available literature related to the electrical resistance strain gaging technology --of the foil type-- and its application in prestressing strands produced the following conclusions (Section 4.3.1.1):

1. Thinner gages perform better. A width of 0.13in. (3.3mm) is recommended to be considered as an upper limit.
2. Gages should preferably be of the temperature compensated type, approximately matching the linear coefficient of expansion of high-strength steel.
3. High-rated resistances with corresponding excitation voltages improve the signal-to-noise ratio of the electrical resistance gages. Since gages of resistances higher than 350Ω are not standard and consequently expensive, the 350Ω gages are recommended as the most appropriate.
4. Two-part epoxy resins are effective for use in gage bonding methods for long-term applications. Cyanoacrilates (i.e. Super Glues) are only recommended for short-term studies. The proper clamping pressure --in terms of pressure distribution and intensity-- should be applied to gages bonded with epoxy resins.
5. Good protection against moisture intrusion and physical damage is necessary when using bonded foil electrical resistance strain gages.

6. Three-leadwire, quarter-bridge Wheatstone completion circuits can provide a compensation for the temperature differentials suffered in the leadwires. This is strongly recommended for all future applications.
7. Leadwires used for electrical resistance strain gages should be threaded in a winding arrangement to reduce the influence of electrical noise produced from electromagnetic sources. They should also have proper physical protection from the environment in which they operate (especially when embedded in concrete). The extra electrical resistance produced by long leadwires should be considered according to the corresponding gage manufacturer formulas.
8. The electrical resistance strain gages should preferably be connected to the read-out units for the complete duration of the field tests. Multi-channel switching devices should have low connector resistance variations (usually accomplished by using gold-plated contacts).

Material tests of electrical resistance strain gages bonded to single strands produced the following conclusions (Section 4.3.1.2):

9. When all electrical resistance strain gages are installed at one particular cross-section and at an equal distance of no less than 24in. from the anchorage ends, the gages were found to measure similar values of strains (even at low stress levels).
10. Calibrated load cells scanned at the same time as the electrical resistance strain gages were found to improve the variability of the average apparent modulus of elasticity obtained in the data reduction process. With calibrated load cells, the apparent modulus of elasticity determined by a single electrical resistance strain gage was found more likely to be within $\pm 1.35\%$ of the average strand modulus.
11. When computing the linear regression of measured data points on a σ - ϵ graph, it was better to consider only the points that corresponded to stresses between $0.20f_{pu}$ and $0.80f_{pu}$. This prevented any consideration of errors related to the initial differential seating of the wires, or to the plastic behavior of the prestressing steel.
12. The slope of σ - ϵ lines (the "apparent" modulus of elasticity) obtained from the electrical resistance strain gages was found repeatedly to be higher than

manufacturer reported values. This is mainly attributed to the different measurement system used by strand manufacturers. Since most single strand tests are performed as material checks of the modulus of elasticity and the overall behavior of the strands from a particular structure, the measured "apparent" modulus of elasticity should be consistent with the instrumentation device to be used in the actual tests of the structure.

Tests of electrical resistance strain gages used in multi-strand tendons composed of $\frac{1}{2}$ " ϕ and 0.6" ϕ , 7-wire, low relaxation prestressing strands produced the following conclusions (Section 4.3.1.3):

13. In most cases, the measured data of a field instrumentation program with multi-strand tendons is comprised of live end stresses and corresponding strains of individual prestressing strands located at intermediate tendon cross-sections. An appropriate data reduction method must be followed to obtain valuable information from the measured data. A data reduction method was suggested and successfully employed in multi-strand tendon tests.
14. The average stress losses occurring between instrumented tendon cross-sections were measured with a $\pm 1.57\%$ accuracy when electrical resistance strain gages were only installed on 25% of the $\frac{1}{2}$ " ϕ strands of a tendon. However, this occurred when: (a) the suggested data reduction method and accompanying material tests were performed, and (b) the strands were individually pretensioned to a similar stress level at the anchor plate of the multi-strand tensioning system.
15. The average stress losses occurring between instrumented tendon cross-sections was measured with a $\pm 2.74\%$ accuracy when electrical resistance strain gages were only installed on 16% of the 0.6" ϕ strands of a tendon. However, this occurred when: (a) the suggested data reduction method was performed, and (b) all the electrical resistance strain gages were bonded between the epoxy clamps (of the epoxy sleeve system). The accuracy was further improved to $\pm 2.0\%$ by performing a data reduction considering only the data points located between $0.20f_{pu}$ and $0.50f_{pu}$.

6.1.3 Epoxy Sleeve Systems

Material tests of $\frac{1}{2}$ " ϕ and 0.6" ϕ prestressing strands instrumented with the epoxy sleeve system produced the following observations (Section 4.3.2.1):

1. Low strength epoxy mixes (especially those with sand in the mix) were found to provide unreliable results.
2. The apparent modulus of elasticity determined from the epoxy sleeves was generally found similar to the manufacturer given values. In some cases, the epoxy sleeve apparent modulus was also found close to the apparent modulus determined by the electrical resistance strain gages. The measured results indicated that the type of instrumentation system used plays an important role in the determination of the apparent modulus of elasticity of the prestressing strand.
3. The modulus of elasticity obtained from the data reduction of the readings from one location around a particular epoxy sleeve was very similar to the results obtained from other reading locations around the same epoxy sleeve. A single epoxy sleeve reading location was found to provide results that were around $\pm 1.14\%$ of the average apparent modulus of elasticity.
4. Judging from the results and the repeatability of the epoxy sleeve readings in single strand tests, it was concluded that the epoxy sleeves provided an accurate instrumentation system for determining the load level at intermediate cross-sections of individual prestressing strands.

Tests of the epoxy sleeve system installed in multi-strand tendons composed of $\frac{1}{2}$ " ϕ and 0.6" ϕ , 7-wire, low relaxation prestressing strands produced the following conclusions (Section 4.3.2.2):

5. The data reduction process for epoxy sleeve readings of large multi-strand tendons was found to be performed best with strict consideration of the data points that approximately increased linearly in the σ - ϵ graphs. In most cases, linear behavior of the epoxy sleeve readings started around 50ksi. However, in some special cases linearity did not occur until 80ksi.
6. A very small variability of results was found among the epoxy sleeve readings. Eight statistical observations only produced a standard deviation corresponding to

- a $\pm 1.52\%$ variation of the average slope of the best-fit line in the σ - ϵ graph. This implied a better sensor behavior than that of the electrical resistance strain gages.
7. The epoxy sleeve systems seemed to provide a better estimate of the average tendon stress than was provided by the electrical resistance strain gages. However, to reach a better conclusion new tests are recommended to be performed with multi-strand tendons instrumented with a larger number of strain gages.
 8. The epoxy sleeve system helped the operation of the electrical resistance strain gages when these were installed between the epoxy collars. This occurred mainly because of the "clamping" action exerted by the epoxy collars to the prestressing strands of the tendon. The clamping action was particularly noticeable for stresses up to about 110ksi. However, it was also apparent that occasional strands -- mainly those located in the center of the tendon's cross section-- disengaged earlier than those in the periphery (Section 4.3.1.3)

A short-term creep test of the epoxy sleeve system indicated that these sensors were not influenced considerably by the plastic creep experienced in the epoxy resins (Section 4.3.2.3). Final tests of the epoxy sleeve system indicated that they can work well with grouting pressures up to 50psi (Section 4.3.2.3). Leakage of the laboratory tested grouting system occurred at the connection between the PE duct pipe and the epoxy sleeve. This failure was actually induced by a testing error and a much different behavior can occur in the field application. The author believes that the epoxy sleeve system and its attachments can withstand more standard code-required pressures of ≈ 100 psi. The epoxy sleeve system is thus considered one of the best mechanisms for blocking grout at intermediate sections of external multi-strand tendons.

6.1.4 Base Line Methods

Three short-span tests of scaled prestressed concrete beams loaded to failure in a laboratory setting helped the evolution of the base line deflection measuring system. A final short-span test was performed with the ideal system recommended in Section 5.5. This final laboratory test of the ideal deflection measuring system installed in an 18ft span provided the following observations (Section 4.4.3):

1. The highest reading error was in the order of $\pm 8/1000$ in. However, an average of the absolute errors only indicated $\pm 2/1000$ in. error.
2. The repeatability of measurements taken by two different operators had a maximum error of $\pm 5/1000$ in. The average repeatability error was $\pm 2/1000$ in.

The suggested span deflection measuring system was later installed inside the box girder of a recently erected 100ft span of the San Antonio Y project. Span deflection measurements were taken during the erection of continuous spans and beyond for up to 80 days after the installation of the base line system. In general, the short to medium term performance of the span deflection measuring system was encouraging. Although not measured, it was estimated that the system can operate with a $\pm 1/100$ in. accuracy in a long-term application. The main conclusions taken from the field test were (Section 4.4.4):

3. The total time required for base line installation and recording of measurements on three stations of one 100ft span averaged 12min. and 28min. for two and one operator respectively (Section 4.4.4.2).
4. The repeatability of measurements taken by two different operators had a maximum error of $\pm 5.4/1000$ in. (Section 4.4.4.3).
5. Practice considerably improved the accuracy of the measurements. It is recommended to develop a well defined set of standards for performing the measurements. This is particularly important when more than one operator will be in charge of taking the measurements (Section 4.4.4.3).
6. To prevent electrical shorting of the portable readout unit with the mild reinforcement of the box girder segments, the anchorage nuts of the reading plates should be embedded to a depth of less than $7/8$ in. --ideally between $3/4$ in. and $7/8$ in (Section 4.4.4.3 and 5.5.2).
7. The 80-day deflection measurements correlated well with the calculated values obtained from the computer analysis performed by the bridge designers. However, measurements taken during the erection of continuous spans showed substantial disagreement with the computer data (Section 4.4.4.4). It is believed this can be improved by also taking measurements at the end stations.

6.1.5 Automated Data Acquisition System

A complex automated data acquisition system (ADAS) was developed throughout the project. Complete descriptions of the three independent ADAS are included in Section 4.5 and Appendix B. Initial tests of the system proved that they worked satisfactorily. However, some additional recommendations for future improvements are included in Section 6.2.

The developed ADAS is considered as a breakthrough in the technology due to its main characteristics:

- relatively simple operation,
- low-power consumption,
- fully portable (battery operated),
- capable of operating with multiple channels, and
- very economical total system cost.

6.2 Future Research Needs

Further improvement of several instrumentation systems reviewed in the present report are possible to be achieved with limited research investments. Benefits that can be obtained from improvements of the current technology of instrumentation systems are undisputed and extensive. Better understanding of the true behavior of civil structures in general can only be acquired with the proper tools for investigating full-scale structures. The following is a list of areas suggested for further investigations.

I. Concrete Strains

- 1.1 Modified Mustran Cells for embedment in concrete should be tried in future research investigations. Recent developments in the electrical resistance strain gaging technology should help to increase the long-term stability of strain signals. Modified Mustran Cells with shorter gage lengths and traditional epoxy based moisture protection systems should be investigated as a low cost, highly sensitive system for measuring concrete strains. Additional research is necessary to address

the long-term behavior, and cost benefits of modified Mustran Cells against other systems (Section 3.1.2.2).

- 1.2 The effect of drilling the finished concrete's surface to install Demec guiding systems disrupts the surrounding area (refer to Section 4.2.1.1). The number of errors introduced by this disruption should be addressed in a future investigation.
- 1.3 The modified Demec extensometers equipped with high precision digital dial indicators suggested in Chapter 4 can provide a major improvement of this mechanical gaging technology. Each one of the possible benefits outlined in Section 4.2.2 are recommended to be carefully evaluated in future research projects.
- 1.4 Fiber optical strain gages based on the technology of interferometry should be investigated further for embedment in concrete or bonding to prestressing strands (Section 3.1.3.4). Although having a very limited degree of success, recent developments of this technology include novel laboratory applications of fiber optic sensors embedded in concrete [103].

II Prestressing Steel Strains/Loads

- 2.1 Further research is necessary to investigate the possibility for standardizing the modulus of elasticity tests and data reduction methods for prestressing strands (Section 4.3.1.2).
- 2.2 Hydraulic jacks used in field applications and calibrated with pressure transducers or dial indicators usually present varying amounts of operational errors. These errors can be attributed to numerous causes: internal friction between jack components, load misalignments, off-center loadings, and/or temperature differentials between laboratory calibrations and field uses (Section 3.2.3.1). A series of tests are recommended to be performed to investigate if the internal stress losses of

certain stressing equipment can be standardized or if typical stress loss ranges can be determined (Section 4.3.1.3).

- 2.3 A more meaningful conclusion about the apparently accurate determination of average tendon stresses obtained by the epoxy sleeve system can be reached by performing additional tendon tests. In these multi-strand tendon tests, a large percentage of the strands are recommended to be instrumented with electrical resistance strain gages. This is necessary to determine representative average tendon stress values that can be compared to the epoxy sleeve system estimates (Section 4.3.3.2).
- 2.4 The effects of temperature variations and creep should be further studied to yield more accurate conclusions about the long-term stability of the epoxy sleeve system.

III Span Deflections

- 3.1 The electrical resistance method suggested for determining the time of contact between the base wire and the deflection meter assembly should be checked for stability in further field tests (Section 4.4.4.3).
- 3.2 The suggested base line methods for measuring vertical movements should be investigated to check the maximum span length that can still be used while maintaining $\approx 1/100$ in. long-term accuracy (the suggested method is described in Section 5.5).
- 3.3 An improved method for measuring vertical movements of long spans is recommended to be investigated. A combination of several base line legs or laser based systems should be tested for future field projects with longer span lengths.

IV Data Acquisition Systems

- 4.1 A modem can be coupled to the Campbell 21X Micrologger. Future field projects having an extensive number of sensors that can be regularly scanned with the 21X Micrologger (such as thermistors, thermocouples, electrical resistance strain gages, LVDTs, pressure transducers, etc) should consider the possibility of using a dedicated phone line inside the box girders. This would enable a very simple data retrieval procedure by using personal computers in the research laboratory. The number of trips to the actual structure and the effort for accessing the location of the Micrologger would thus be reduced considerably. However, expensive line stabilizers, surge suppressors, backup power units, and prevention for lightning strikes would have to be considered.

- 4.2 The automated data acquisition system (ADAS) designed during the development of the project --and fully described in Appendix B-- can be very useful for future field investigation projects. It is strongly recommended to fully develop a user-friendly software package for the suggested ADAS. If the system is standardized for future applications this could be very beneficial.

- 4.3 A much better but slightly more expensive compensation for leadwire effects --due to contact and cabling resistance variations-- can be incorporated in the developed ADAS. This can be accomplished by adding extra transformers to the main Wheatstone circuits. A good description of the needed changes was provided by Versnel and should be consulted as a reference [77].

APPENDIX A:

**SURVEY OF
SEGMENTAL CONCRETE
BOX GIRDER BRIDGES**

APPENDIX A:

Survey of Concrete Segmental Box Girder Bridges

I. Span-by-Span Method:

Bridge Name	Location	Country	Year Finished	Span Length [m]	Bridge Length [m]	Construction Method
1.1 America						
1 San Antonio Y Elevated Hwys.	San Antonio, TX	USA	1992	33	7240	SS-pc
2 Long Key	U.S. 1, FL	USA	1981	36	3706	SS-pc
3 Niles Channel	U.S. 1, FL	USA	1983	36	1390	SS-pc
4 Wiscasset	Wiscasset, ME	USA		37		SS-pc
5 Greenbelt Route	Washington, D.C.	USA	1989	41	586	SS
6 Sunshine Skyway (Approach)	Tampa, FL	USA	1987	41		SS-pc
7 Channel Five	U.S. 1, FL	USA	1983	41	1402	SS-pc
8 Seven Mile	U.S. 1, FL	USA	1982	41	10931	SS-pc
**Note: Largest segmental concrete bridge in the world.						
9 I110-Biloxi	Biloxi, MS	USA	1990	43	2837	SS-pc
10 MARTA Rapid Transit	Atlanta, GA	USA	1983	44	3080	SS-pc
11 Glenwood Canyon	Glenwood Canyon, CO	USA		45		SS-pc
12 I-295 James River (Approach)	Richmond, VA	USA	1989	46	275	SS-pc
13 Wando River (Approach)	Wando River, SC	USA	1989	46	2103	SS
14 Golden Valley Interchange	North of Reno, Nevada	USA	1988	47	47	SS-cip
15 Escambia Bay	Escambia Bay, FL	USA		52		SS-pc
16 Sheepscot River		USA	1982	55	379	SS
17 Denny Creek - U.S. I-90	Snoqualmie Pass, WA	USA	1980	57	1103	SS-cip
**Note: First span-by-span segmental concrete bridge in the US.						
1.2 Europe and Australia						
1 Tangenziale Milano		Italy		24	8000	SS
2 Untermarchtal	Danube River	Germany	1954		334	SS
3 Krahenberg	Andernach	Germany	1964	32	1100	SS-cip
4 Bolzano Elevated Motorway I	Bolzano	Italy	1974	35	2580	SS-pc
5 Pleichach Viaduct	Wurzburg - Fulda	Germany	1964	36	350	SS-cip
6 Elzthalbrucke	Eifel	Germany	1965	38	379	SS-cip

7	Hartel	Rotterdam	Holland	1968	39	281	SS	
8	Kettiger Hang	Andernach	Germany	1955	39		SS	
9	Bolzano Elevated Motorway II	Bolzano	Italy	1974	40	80	SS-pc	
10	Loisach River	Ohlstadt	Germany		41	1244	SS-cip	
11	Hammersmith Flyover		UK	1961	43	688	SS	
12	Bolzano Elevated Motorway III	Bolzano	Italy	1974	51	51	SS-pc	
13	Commonwealth Avenue I	Canberra	Australia	1964	55	622	SS-pc	
14	Beckenried Viaduct - Hwy. N-2	Basel to Chiasso	Switzerland	1981	55	3150	SS-cip	
**Note: Longest bridge of the Swiss highway network. Constructed with innovative "Stepping Formwork System".								
15	Orwell River (approach viaducts)	Eastern England	UK	1983	59	884	SS-cip	
16	Guadiana Viaduct	Beja - Serpa	Portugal		60	340	SS-cip	
**Note: First usage of the span-by-span technique on a dual structure.								
17	Rheinbrücke (approach)	Dusseldorf-Flehe	Germany		60	780	SS-cip	
18	Gruyere Viaduct		Switzerland	1979	61	2000	SS-cip-pc	
19	Section Five		UK		62	1158	SS	
20	Commonwealth Avenue II	Canberra	Australia	1964	64	256	SS-pc	
21	Commonwealth Avenue III	Canberra	Australia	1964	73	146	SS-pc	
22	Bendorf -east app- Rhine River	North of Koblenz	Germany	1964	94	289	SS	
23	Mancunian Way		UK	1967		976	SS	
24	Ahrtal		Germany	1976		1500	SS	
**Note: First segmental bridge built with overlying type of steel truss								
1.3 Other Countries								
1	Bubiyian	Bubiyian Island	Kuwait	1989	54	2383	SS-pc	

II. Incremental Launching Method:

No.	Bridge Name	Location	Country	Year Finished	Span Length [m]	Bridge Length [m]	Construction Method
2.1 America							
1	Wabash River - U.S. I-74	Covington, IN	USA	1978	57	289	IL
2	Caguana River	Puerto Rico	Puerto Rico	1991	70	385	IL
3	Rio Caroni		Venezuela	1963	96	480	IL
**Note: First incrementally launched segmental concrete bridge in the world. Designed by F. Leonhardt and W. Baur.							
2.2 Europe and Australia							
1	Neckarburg Valley - Neckar River	Rottweil	Germany	1977	30	365	IL

**Note: Main span is an arch bridge, box-girder spans were incrementally launched from one end.

2 Val Restel Viaduct	Italy			32	320	IL
3 Shepherds House	Reading, England	UK	1973	37	85	IL
4 Marolles		France	1972	40	105	IL
5 Luc Viaduct	Luc	France		41	278	IL
6 Oli Viaduct	Oli	France	1976	41	615	IL
**Note: Railroad bridge						
7 Paillon		France	1976	41	351	IL
8 Nuel Viaduct		France	1976	41	246	IL
9 Borriglone Viaduct		France	1976	41	246	IL
10 Var Viaduct		France	1976	42	337	IL
11 Querlin Guen		Germany		42	426	IL
12 C6a at IP5-Guarda		Portugal	1987	43	604	IL
13 Tet Viaduct		France		43	201	IL
14 Muhlbacktalbrucke	Southwest Stuttgart	Germany		43	580	IL
15 Steinaggertal		Germany	1981	48	470	IL
16 Aichtal		Germany	1983	51	1161	IL
**Note: The world's longest structure built by the incremental launching method						
17 Koches Valley		Germany		52	476	IL
18 Ravensbosch Valley	Valkenburg	Holland		56	420	IL
19 Creil Viaduct - Oise River	Creil	France	1978	59	336	IL
20 Charix Viaduct		France		64	542	IL
21 Poncein Viaduct -2-		France	1987	79	290	IL
22 Gronachtal		Germany	1978	80	528	IL
23 Gutachtal		Germany	1980	101	752	IL
24 Inn		Germany	1965	102	450	IL
25 Markbriet Valley		Germany	1980	109	928	IL
**Note: Temporary supports were used to achieve these lengths.						
26 Donau	Wörth	Germany	1980	168	404	IL
**Note: Temporary supports were used to achieve these lengths.						

2.3 Other Countries

1 Kimonkro	Ivory Coast		1978	36	216	IL
2 Tai Po Bypass - Bridge No. 10	Tai Po	Hong Kong	1985	42	242	IL
3 Tai Po Bypass - Bridge No. 11	Tai Po	Hong Kong	1985	42	158	IL

4	Tai Po Bypass - Bridge No. 12	Tai Po	Hong Kong	1985	42	200	IL
5	Tai Po Bypass - Bridge No. 13	Tai Po	Hong Kong	1985	42	116	IL
6	Olifant's River	Sishen-Saldanha	South Africa		45	1035	IL
7	Shatt al Arab		Iraq			760	IL

III. Progressive Placement Method:

3.1 America

No.	Bridge Name	Location	Country	Year Finished	Span Length [m]	Bridge Length [m]	Construction Method
1	Vail Pass, Miller Creek West	I-70, CO	USA	1979	47	158	PP-cip
2	Linn Cove Viaduct	Blue Ridge Parkway, NC	USA	1981	55	379	PP-pc
3	Vail Pass, Miller Creek East	I-70, CO	USA	1979	59	139	PP-cip
4	Vail Pass, Black Gore Creek	I-70, CO	USA	1979	69	228	PP-cip

3.2 Europe and Australia

1	Rombas Viaduct		France		45	327	PP
2	Bendorf -east- Rhine River	North of Koblenz	Germany	1964	58	217	PP
3	Ounasjoki	Rovaniemi	Finland	1967	70	217	PP

3.3 Other Countries

-none-

IV. Precast Balanced Cantilever Method:

4.1 America

No.	Bridge Name	Location	Country	Year Finished	Span Length [m]	Bridge Length [m]	Construction Method
1	Turkey Run State Park	Parke Co., IN	USA	1977	55	110	BC-pc
2	Sugar Creek - FAS Rte. 1620	Parke Co., IN	USA	1976	55	113	BC-pc
3	Vernon Fork		USA	1976	58	119	BC-pc
4	Muscatuck River - U.S. 50	N. Vernon, IN	USA	1975	58	116	BC-pc
5	JFK Memorial Causeway	Corpus Christy, TX	USA	1973	61	122	BC-pc
**Note: First segmental concrete bridge built in the USA.							
6	Vail Pass/Side Hill	Denver, CO	USA	1979	64	268	BC-pc
7	Albemarle Sound	Edenton, NC	USA	1990	68	148	BC-cip
8	Kishwaukee River	Rockford, IL	USA	1981	76	357	BC-pc

9	Lievre River - Hwy. 35	Notre Dame du Laus, Quebec	Canada	1967	79	159	BC-pc
**Note: First precast balanced cantilever prestressed concrete bridge built in North America.							
10	Rio-Niteroi	Rio De Janeiro	Brazil	1974	80	8240	BC-pc
11	Bear River	Digby, Nova Scotia	Canada	1972	81	609	BC-pc
12	Islington Avenue	Toronto, Ontario	Canada	1979	83	491	BC-pc
13	New Baldwin	Old Saybrook - Old Lyme, CT	USA	1992	84	769	BC-pc
14	Overstreet	Western Florida	USA		88	215	BC-pc
15	North Main St. Viaduct		USA	1979	88	1005	BC-pc
16	Escatawpa		USA		91		BC-pc
17	Kentucky River	Frankfort, KY	USA	1979	98	256	BC-pc
18	Columbia River N. - U.S. I-205	Portland,OR - Vancouver,WA	USA	1983	110	274	BC-pc
19	Zihwaukee - U.S. I-75	Saginaw, MI	USA	1981	119	2558	BC-pc
20	Rio Ulua		Honduras		120	240	BC-pc
21	Dauphin Island	Dauphin Island, AL	USA	1982	122	936	BC-pc
22	Wando River		USA	1989	122	244	BC-pc
4.2 Europe and Australia							
1	Kleinpolderplein Interchange	Rotterdam	Holland		35	2000	BC-pc
2	B-3 South Viaducts	Paris	France		38	2000	BC-pc
3	Choisy-le-Roi	Paris	France	1965	55	130	BC-pc
**Note: First precast balanced cantilever prestressed concrete bridge with epoxied match-cast joints. Designed by Muller.							
4	L-32 Tauernautobahn	Salzburg - Villach	Austria		55	1167	BC-pc
5	Saint Andre de Cubzac	Dordogne River - Bordeaux	France	1974	58	577	BC-pc
6	Sirník	Bratislava	Czechoslovakia	1965	60		BC-pc
7	Courbevoie	Paris	France	1966	60	140	BC-pc
8	Conflans	Seine - Marne Rivers, Paris	France	1972	60	140	BC-pc
9	Glacieres Viaduct		France	1987	61	215	BC-pc
10	Sylans Viaduct	Nantua-Bellegarde Gorge	France	1987	61	1268	BC-pc
11	Byker Viaduct	Newcastle	UK	1965	69	345	BC-pc
**Note: UK's first prestressed concrete segmental railway bridge.							
12	Deventer		Netherlands		74		BC-pc
13	Ussy - Marne River	Ussy	France	1950	75		BC-pc
**Note: Designed by E. Freyssinet.							
14	Pierre Benite - 2	Lyon	France		75	250	BC-pc
15	Oleron Viaduct	Oleron Island - Atlantic West	France	1964	79	2173	BC-pc

**Note: First application of launching-gantry concept for placing segments in cantilever.

16 Paris Belt (Downstream)	Paris	France	81	313	BC-pc
17 Pierre Benite - 1	Lyon	France	84	196	BC-pc
18 Trent Viaduct - River Trent	South Humber side Motorway	UK	85	267	BC-pc
19 Paris Belt (upstream)	Paris	France	90	270	BC-pc
20 River Torridge		Britain	90	650	BC-pc
21 Loire River	Blois	France	91	396	BC-pc
22 Eastern Scheldt	Oosterschelde	Holland	91	3199	BC-pc
23 Sallingsund	Northern Jutland	Denmark	93	1683	BC-pc
24 Saint André de Cubzac	Dordogne River - Bordeaux	France	95	625	BC-pc
25 Chillon Viaduct	Lake Geneva	Switzerland	104	2210	BC-pc
26 Saint Cloud - Seine River	Paris	France	106	1103	BC-pc
27 Brielse Maas		Holland	113	275	BC-pc
28 Hartel	Rotterdam	Holland	114	266	BC-pc
29 Ravensway - Rhine River	Amsterdam	Holland	151		BC-pc
30 Calix Viaduct	Caen	France	156	1183	BC-pc
31 Ottmarshelm	East France	France	172	430	BC-pc
32 B-3 South Viaducts	East Paris	France	174		BC-pc
33 Captain Cook - Brisbane River	Brisbane	Australia	183	555	BC-pc
4.3 Other Countries					
1 Ojat		USSR	64		BC-pc
2 Irtysch		USSR	110		BC-pc
3 Lichaer Factory		USSR	148		BC-pc

V. Cast in Situ Balanced Cantilever Method:

No.	Bridge Name	Location	Country	Year Finished	Span Length [m]	Bridge Length [m]	Construction Method
5.1 America							
1	Rio do Peixe	Herval	Brazil	1930	69		BC-cip
**Note: First application of the balanced cantilever method of construction in concrete bridges in the world. Reinf. concrete structure. Designed by E. Baumgart.							
2	Kipapa Stream	Oahu, HI	USA	1977	76	582	BC-cip
3	Napa River - U.S. I-29	Napa, CA	USA	1977	76	679	BC-cip
4	Knight Street - Fraser River North	Vancouver, British Columbia	Canada	1973	79	159	BC-cip
5	Lake Washington		USA		81		BC-cip

6	Genesee River		USA	1980	82	631	BC-cip
7	Eel River	Rio Dell, CA	USA	1976	91	435	BC-cip
8	H-3 Windward Viaduct	Hawaii	USA		91		BC-cip
9	Cline Avenue		USA	1982	97	97	BC-cip
10	Knight Street - Fraser River South	Vancouver, British Columbia	Canada	1973	110	213	BC-cip
11	Saint Adele (River of the Mules)	Adele, Quebec	Canada	1964	111	162	BC-cip
**Note: First cast-in-place concrete segmental bridge in North America.							
12	Red River		USA	1981	113	548	BC-cip
13	River of Matapedia - Rte. 132	Milnikel, Quebec	Canada	1979	122	244	BC-cip
14	Incienco		Guatemala		122	250	BC-cip
15	Pine Valley Creek	San Diego, CA	USA	1974	137	523	BC-cip
**Note: First cast-in-place balanced cantilever segmental concrete bridge built in the United States.							
16	Rio Tocantins		Brazil		140	256	BC-cip
17	Setubal		Argentina		140	298	BC-cip
18	Bennett Bay		USA	1990	159	527	BC-cip
19	Illinois River - HWY 36	West Central Illinois	USA	1990	168	308	BC-cip
20	West Seattle Freeway - main spans	Seattle, WA	USA	1985	180	408	BC-cip
21	St. Maurice River - Rte. 55	Grand'Mere, Quebec	Canada	1978	181	285	BC-cip
22	Columbia River N. - U.S. I-205	Portland, OR - Vancouver, WA	USA	1983	183	476	BC-cip
23	Pelotas River	Southern Brazil	Brazil	1966	189	249	BC-cip
24	Gastineau Channel		USA	1981	189	390	BC-cip
25	James River		USA		192		BC-cip
26	Acosta - St. John's River	Jacksonville, FL	USA		192	501	BC-cip
27	Parrots Ferry	Sonora, CA	USA	1979	195	393	BC-cip
28	Uruguay River		Uruguay/Argentina	1975	209		BC-cip
29	Schubenacadie River	South Mainland, Nova Scotia	Canada	1979	213	440	BC-cip
30	Dr. C.L. Gosse		Canada	1979	214	440	BC-cip
31	Houston Ship Channel	Houston, TX	USA	1981	229	458	BC-cip
**Note: Longest spanning balanced cantilever segmental concrete bridge in America.							
32	Koror-Babelthuap	Palau Island Chain (Pac. Trust)	USA	1978	241	385	BC-cip
5.2 Europe and Australia							
1	Chazey - Ain River	Chazey	France	1955	58	140	BC-cip
2	Lacroix Falgarde	Ariege River	France	1962	61	122	BC-cip
3	Lahn River	Balduinstein	Germany	1951	62		BC-cip

**Note: First "modern" application of the balanced cantilever method for prestressed concrete bridges. Designed by U. Finsterwalder.						
4	Kotosová	Bratislava	Czechoslovakia	1960	63	BC-cip
5	Puteaux - Seine River	Paris	France	1977	65	BC-cip
6	Bradano Viaduct	Turin	Italy	1959	66	BC-cip
7	Nové Mesto	Bratislava	Czechoslovakia	1962	70	BC-cip
8	Savines	Savines	France		77	BC-cip
9	Saint Jean - Garonne River	Bordeaux	France	1965	77	BC-cip
10	Vallon du Moulin a Poudre	Bouguen, Brest	France	1963	82	BC-cip
11	Oise River	Autoroute A1 @ Oise River	France	1968	83	BC-cip
12	Tibre River	Rome (vicinity)	Italy	1970	90	BC-cip
13	Stenungsund		Sweden	1960	94	BC-cip
14	Bezons - Seine River	Near Paris	France	1942	95	BC-cip
15	Oissel - Seine River	Oissel	France		100	BC-cip
16	Donzere	Donzere	France		100	BC-cip
**Note: Longest spanning balanced cantilever reinforced concrete bridge in the world. Designed by Caquot.						
17	Arret Darre Viaduct		France	1987	100	BC-cip
18	Siegtal	Sieger	Germany	1969	105	BC-cip
19	Tunsta		Sweden	1956	107	BC-cip
20	Källösund		Sweden	1960	107	BC-cip
21	Givors - Rhone River	Givors	France		110	BC-cip
22	Vejle Fjord	East Vejle Harbor	Denmark	1979	110	BC-cip
23	Nibelungen - Rhine River	Worms	Germany	1953	114	BC-cip
24	Coblentz - Moselle River	Coblentz	Germany	1953	123	BC-cip
25	Puente del Azufe	Rio Sil	Spain		130	BC-cip
26	Lutrive (N9 National Motorway)	Laussane	Switzerland	1973	132	BC-cip
27	Magnam Viaduct	French Riviera	France		132	BC-cip
28	Alnö		Sweden	1965	134	BC-cip
29	Arnhem - Rhine River	Arnhem	Holland		137	BC-cip
30	Kochertal	Nürnberg - Heilbron	Germany	1979	138	BC-cip
31	Tricastin	Rhone River	France		143	BC-cip
32	Bonhomme - Blavet River		France		146	BC-cip
33	Poncín Viaduct -1-		France	1987	155	BC-cip
34	Felsenau Crossing	Bern	Switzerland	1975	156	BC-cip
**Note: Two thin and narrow hollow box walls helped supporting the main spans. Designed by C. Menn.						

35 Biaschina	Ticino	Switzerland	1986	160	645	BC-cip
36 Gennevilliers - Seine River	Gennevilliers	France	1976	172	636	BC-cip
**Note: Longest spanning balanced cantilever prestressed concrete bridge in France.						
37 Ganter Valley	Simplon Road	Switzerland	1976	174	678	BC-cip
**Note: A pair of cable stays covered in concrete were used in the main span. Designed by C. Menni.						
38 Orwell River	Eastern England	UK	1983	190	402	BC-cip
**Note: UK's largest prestressed concrete span.						
39 Bendorf -west- Rhine River	North of Koblenz	Germany	1964	208	525	BC-cip
40 Danube River at Beska		Yugoslavia		210	420	BC-cip
41 Selbjorn		Norway	1980	212		BC-cip
42 Mooney Mooney Creek		Australia		220	480	BC-cip
43 Gateway	Brisbane	Australia	1986	260	520	BC-cip

**Note: Longest spanning balanced cantilever prestressed concrete bridge in the world.

5.3 Other Countries

1 Yui-Ko		Japan	1967	70	130	BC-cip
2 Tamagawa Railroad		Japan	1968	80	404	BC-cip
3 Yagiya Highway		Japan	1964	84	116	BC-cip
4 Amakusa No. 4		Japan	1966	146	510	BC-cip
5 Amakusa No. 3		Japan	1966	160	360	BC-cip
6 Urado Bay		Japan	1972	230	600	BC-cip
7 Hikoshima		Japan	1975	236		BC-cip
8 Hamana Ohashi	Hamana	Japan	1976	240	630	BC-cip

VI. Cable Stayed:

No.	Bridge Name	Location	Year Finished	Span Length [m]	Bridge Length [m]	Construction Method
6.1 America						
1	Yakima River	Benton City, WA	1957	52	122	CS-cip
**Note: Reinforced concrete structure. Designed by Hadley.						
2	Barranquilla	Barranquilla	1974	140	279	CS-cip
**Note: Designed by R. Morandi.						
3	I-295 James River	Richmond, VA	1989	192	239	CS-pc
**Note: Designed by Figg and Muller Engineers, Inc.						
4	Neches River	Port Arthur, TX	1991	195	323	CS-pc

**Note: First cable stayed bridge in the State of Texas.							
5	Lake Maracaibo	Lake Maracaibo	Venezuela	1962	235	1495	CS-cip-pc-dis
**Note: First "modern" cable stayed segmental concrete bridge in the world. Designed by R. Morandi.							
6	Cochrane	Alabama	USA		237		CS-cip
7	General M. Belgrano - Parana River	Chaco/Corrientes	Argentina	1973	245	572	CS-cip-pc-dis
**Note: Designed by Amman and Whitney.							
8	East Huntington	East Huntington, W. VA.	USA	1983	275	600	CS
**Note: Designed by A. Grant and F. Leonhardt.							
9	Coatzacoalcos II						
10	Pasco-Kennewick, Columbia River	Pasco, WA	Mexico	1985	288	698	CS
**Note: Designed by Arvid Grant - F. Leonhardt and Andr�.							
11	Encarnaci�n - Posadas	Encarnaci�n - Posadas	Paraguay-Argentina	1989	330	660	CS
**Note: Designed by Leonhardt and Andr�.							
12	Talmadge Memorial	Savannah River, GA	USA	1990	335	622	CS-pc
13	Sunshine Skyway	Tampa, FL	USA	1987	366	695	CS
**Note: Designed by Figg and Muller Engineers, Inc.							
14	Dame Point	Jacksonville, FL	USA	1989	396	793	CS
**Note: Longest spanning cable stayed segmental concrete bridge in America.							
6.2 Europe and Australia							
1	Tempul Aqueduct	Guadalete River, Jerez	Spain	1925	60	101	CS-cip
**Note: First concrete structure in the world to utilize cable stays. Designed by E. Torroja.							
2	Danube Canal	Viena	Austria	1974	119	230	CS-cip-pc
3	Nal�n River	Langreo	Spain	1989	130		CS-cip
4	Fernando Reig	Alcoy	Spain	1987	132		CS-pc
5	Magliana	Rome	Italy	1967	145	199	CS-cip-pc-dis
6	Rio Ebro	Navarra	Spain	1978	146	197	CS-pc
**Note: Designed by C. Fern�ndez Casado S.A.							
7	Viaduct Sur L'Is�re	Bourg Les Valence	France		148		CS-cip
8	Mainbrucke	Hoechst	Germany	1972	148	242	CS-cip
**Note: Designed by Dyckerhoff and Widmann.							
9	Meuse River @ Ben-Ahin	Ben-Ahin (Meuse River)	Belgium	1988	168	342	CS-cip
10	Carpineto	Provenza	Italy	1977	181	242	CS-cip
11	Polcevera Viaduct	Genoa	Italy	1967	210	639	CS-cip-pc-dis
**Note: Designed by R. Morandi.							

12 Centenario	Seville	Spain	1991	264	470	CS-pc
13 Arade	North Portimao	Portugal	1974	256	457	CS
14 Waal River	Tiel	Holland	1977	267	607	CS-cip-pc
15 Brotonne	Normandy	France	1989	320	594	CS-cip-pc
**Note: Designed by Campenon-Bernard, Mathivat and Müller.						
16 International Guadiana	Castro Marim - Ayamonte	Portugal-Spain	1983	324	637	CS
17 Barrios de Luna	León	Spain	1977	440	402	CS-cip
**Note: Current longest spanning concrete bridge in the world. Designed by C. Fernández Casado S.A.						
6.3 Other Countries						
1 Kwang Fu	...	Taiwan	1963	134	276	CS-pc
2 Dnieper River	Kiev	USSR	1980	144	410	CS-pc
3 Kabejima	...	Japan	1971	210	477	CS
4 Wadi Kuf	...	Libya		282		CS-cip-pc-tis

VII. Segmental Arches:

No.	Bridge Name	Location	Country	Year Finished	Span Length [m]	Bridge Length [m]	Construction Method
7.1 America							
1	George Westinghouse	Pittsburgh, PA	USA	1931	134		SA
**Note: Used box-girders and arch forms. Held the longest concrete span record in the United States for 40 years.							
2	Caracas Viaduct 3	Caracas	Venezuela	1952	138	213	SA
3	Caracas Viaduct 2	Caracas	Venezuela	1952	146	253	SA
4	Caracas Viaduct 1	Caracas	Venezuela	1952	152	309	SA
5	Friendship - Parana River	Ciudad del Este - Foz do Iguacu	Paraguay - Brazil	1965	290	552	SA
**Note: Arch was made of reinforced concrete, cast-in-situ, 3-celled box-girders.							
7.2 Europe and Australia							
1	Thur River	Billwil	Switzerland	1904	35	70	SA
**Note: Similar to Inn River bridge. Designed by R. Maillart. Two arches.							
2	Inn River	Zuoz	Switzerland	1901	38		SA
**Note: First reinforced concrete box-girder arch bridge in the world. Two-celled box-girders used in the arch. Designed by R. Maillart.							
3	Rhine River	Tavanasa	Switzerland	1905	51		SA
**Note: Designed by R. Maillart.							
4	Luzancy - Marne River	East of Paris	France	1946	55		SA-pc
**Note: First application of modern segmental construction of prestressed concrete bridges. Designed by E. Freyssinet.							

5 Arve River	Vessy	Switzerland	1936	56	SA
**Note: Designed by R. Maillart.					
6 Danube River	Leipheim	Germany	1937	85	316
**Note: Designed by E. Mörsch and P. Bonatz.					
7 Gueroz	Schiers	Switzerland	1932	90	SA
8 Salginatobel		Switzerland	1930	90	SA
9 Villeneuve		France	1919	96	SA
10 Reichenau - Rhine River	Reichenau	Switzerland	1964	100	SA
**Note: Prestressed concrete hollow-box deck girder, designed by C. Menn.					
11 Schwarzwasserbrücke		Switzerland	1979	114	SA
12 Mosel River		Germany	1934	119	324
13 Niesenbachbrücke		Austria	1973	120	SA
14 Krummbachbrücke		Switzerland	1977	124	SA
15 Teufelstal		Germany	1938	138	250
16 Trellins		France	1987	140	233
17 Aare River		Switzerland	1940	150	SA
18 Neckarburg - Neckar River	Rottweil	Germany	1977	154	365
19 Plougastel - Elorn Estuary	Brest	France	1930	180	559
**Note: Longest spanning concrete bridge in the world for 10 years. Arches built with innovative cantilever springings. Designed by E. Freyssinet.					
20 Tranebergsund		Sweden	1934	181	SA
21 Rip	North of Sidney	Australia		183	SA
22 Pag	Island of Pag	Yugoslavia	1967	193	SA-cip
23 Martin Gil Viaduct - Rio Esla	Zamora	Spain	1939	210	SA-cip
**Note: Built in longitudinal strips, or rings. Steel formwork built by suspension system similar to Joseph Melan's Golden Gate Bridge in 1889 in Calif. Railroad Bridge, designed by E. Torroja.					
24 Krk Island - shorter arch-	Island of Krk - Adriatic Sea	Yugoslavia	1978	244	SA-cip-pc
25 Sibeniik	Sibenik	Yugoslavia	1966	246	SA-cip
26 Sandö		Sweden	1943	264	SA
**Note: Longest spanning concrete bridge in the world for 20 years					
27 Arrabida		Portugal	1963	270	SA
28 Gladesville - Parramata River	Gladesville - Drummoyne	Australia	1964	305	SA-pc
29 Krk Island - longer arch-	Island of Krk - Adriatic Sea	Yugoslavia	1979	390	SA-cip-pc
7.3 Other Countries					
1 Akayagawa		Japan	1978	126	SA

2 Hokawazu	Japan	1974	170	SA
3 Van Staden	South Africa	1970	200	SA
4 Bloukraans	Capetown - Port Elizabeth South Africa	1984	272	SA

451

**Note: Decks of prestressed concrete twin T-beams, arch is 3-celled box-girder.

Graphical representation of maximum span length variations with time:

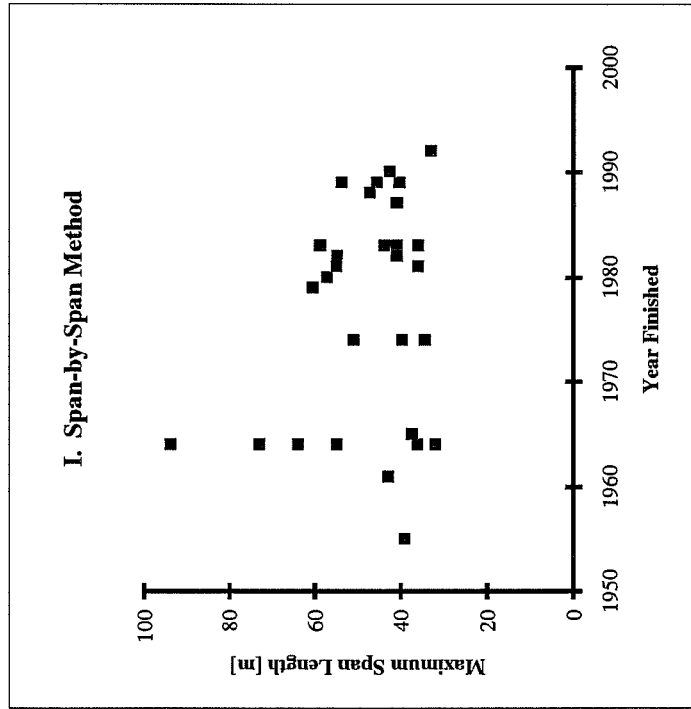


Figure A.1

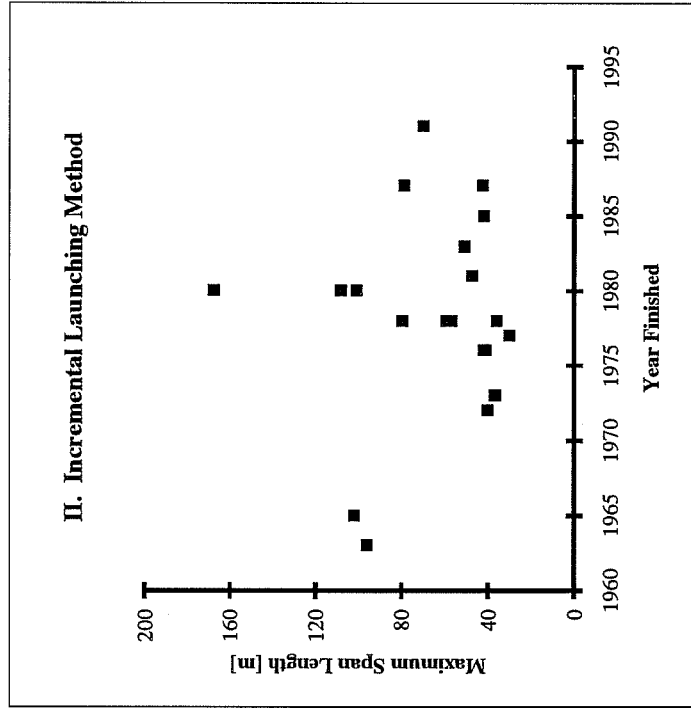


Figure A.2

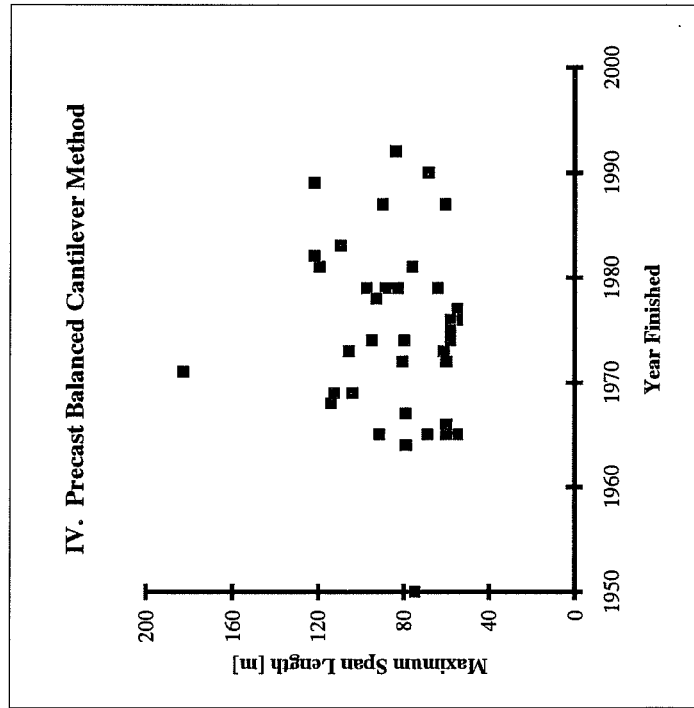


Figure A.4

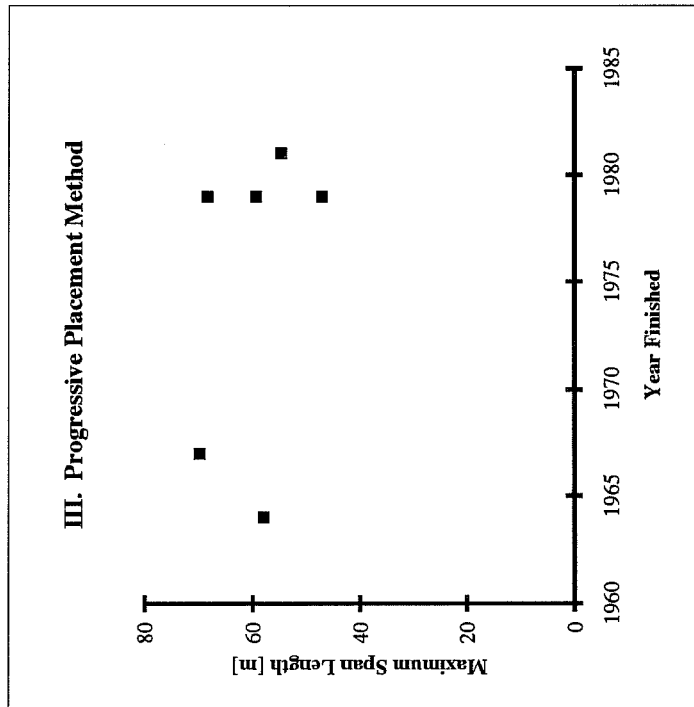


Figure A.3

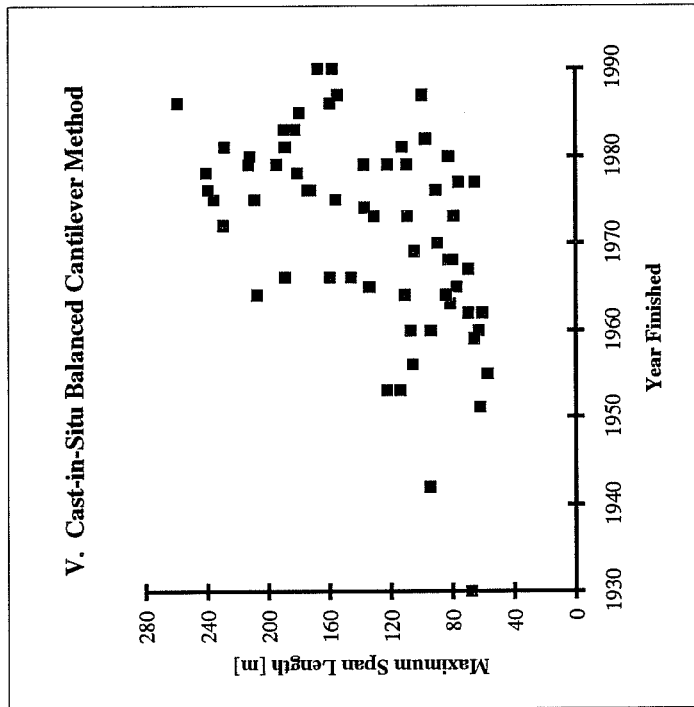


Figure A.5

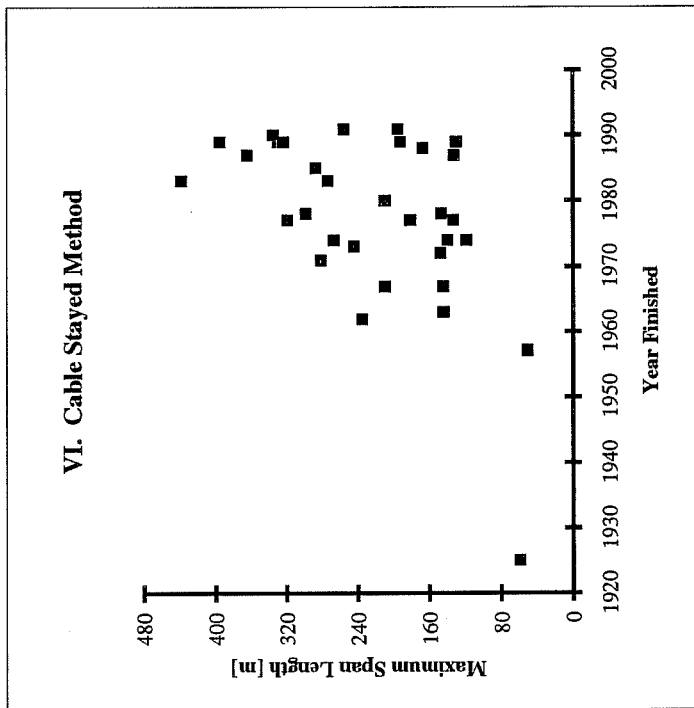


Figure A.6

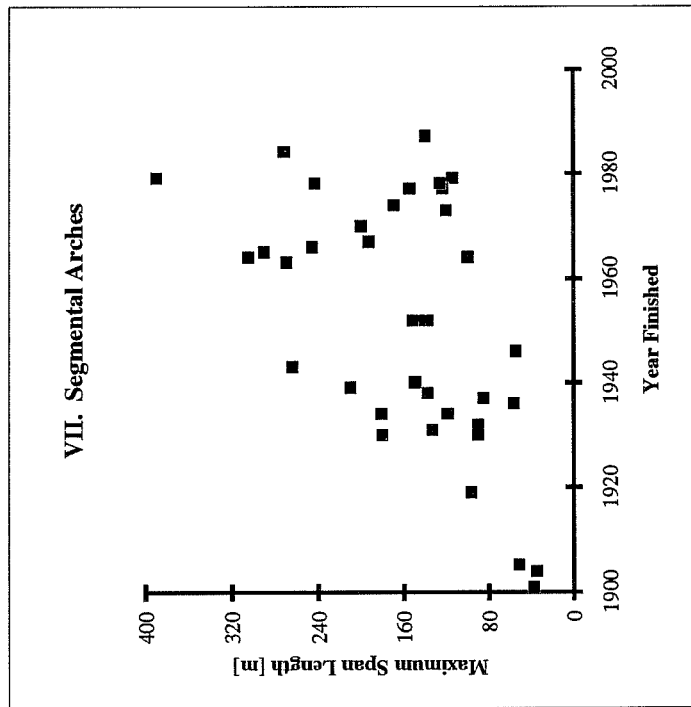
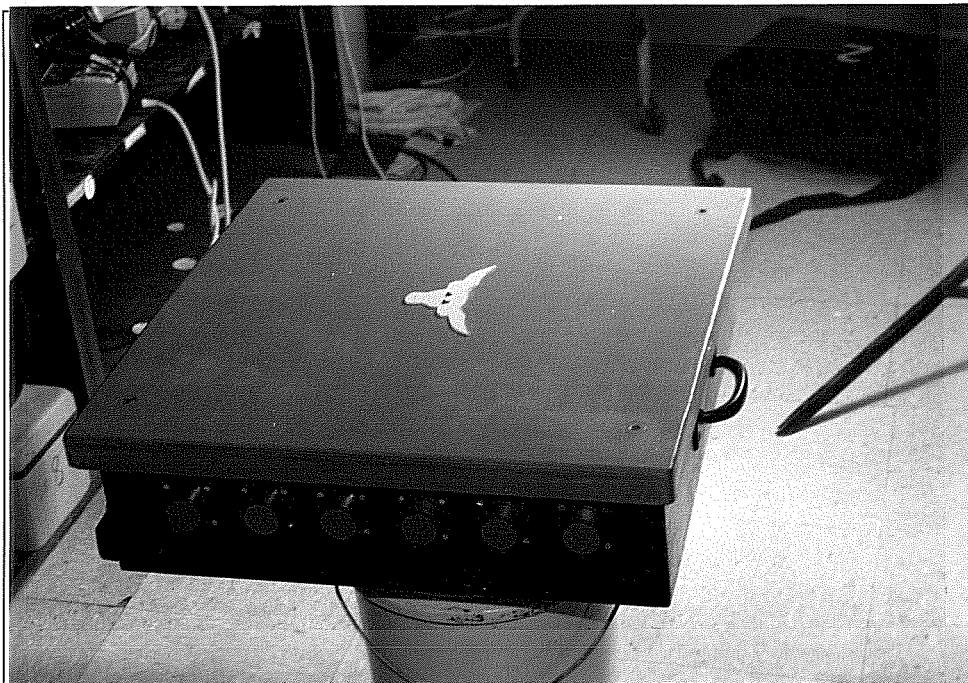


Figure A.7

APPENDIX B:

**SCHEMATIC OF
DATA ACQUISITION SYSTEM
Box Type A-43 & A-44**

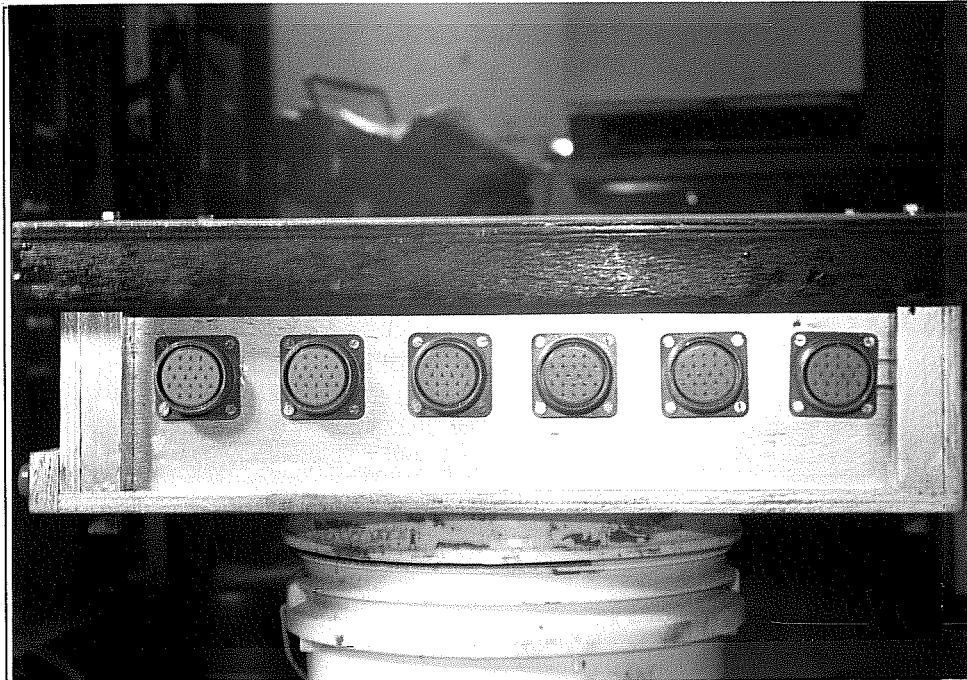
I. General Pictures of Finished Data Acquisition System



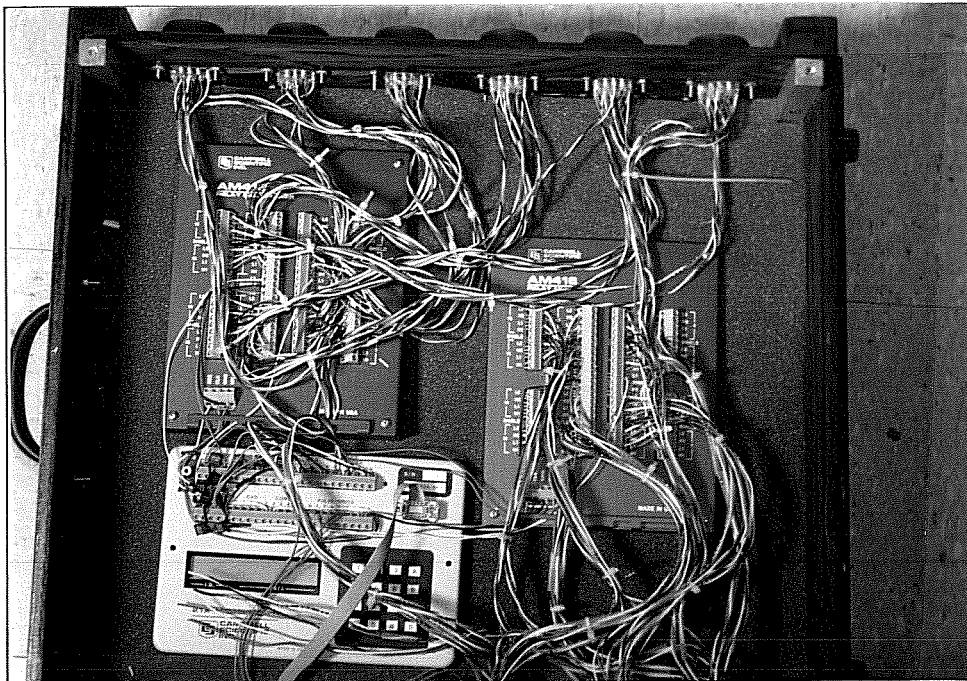
a. General Perspective



b. Side Panel A (indicators side)

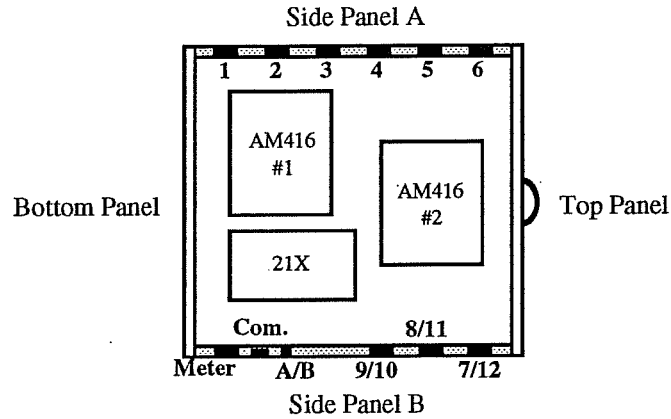


c. Side Panel B (connectors side)

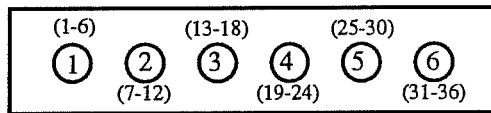


d. Plan View of Electrical Connections

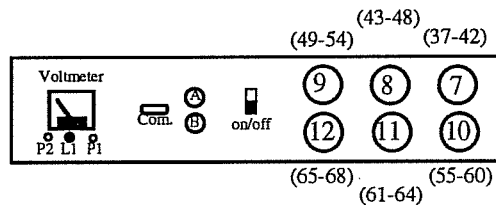
II. Plan View:



III Side Panel A:



IV. Side Panel B:



Description:

L1: Scan light

P1: Switch activating scan light

P2: Switch activating voltmeter

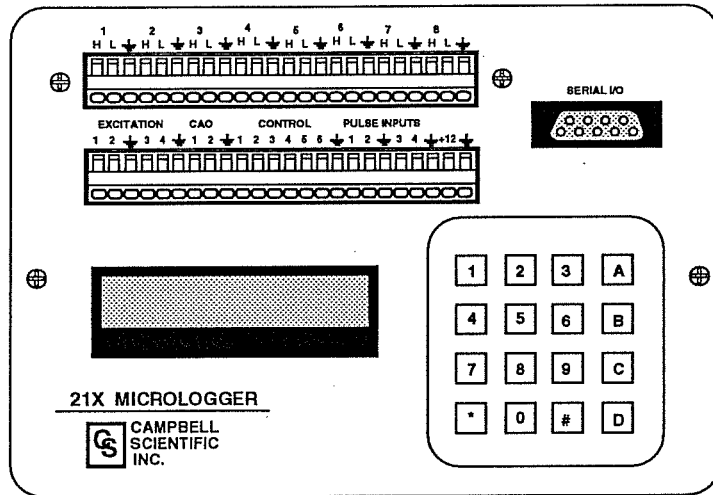
Com.: Standard 9-contact serial receptacle (type RS232)

A/B: Amphenol 2-contact receptacles (type MS-3102A-14S-9S)

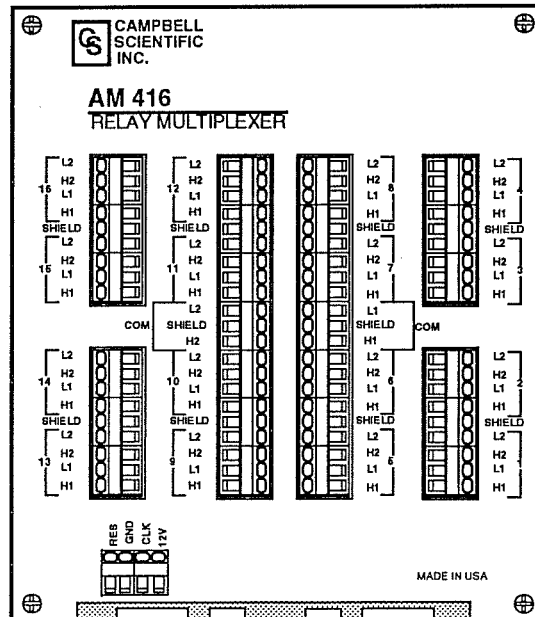
1 - 12: Amphenol 20-contact receptacles (type MS-3102A-28-16S)

* Channel numbers in parentheses

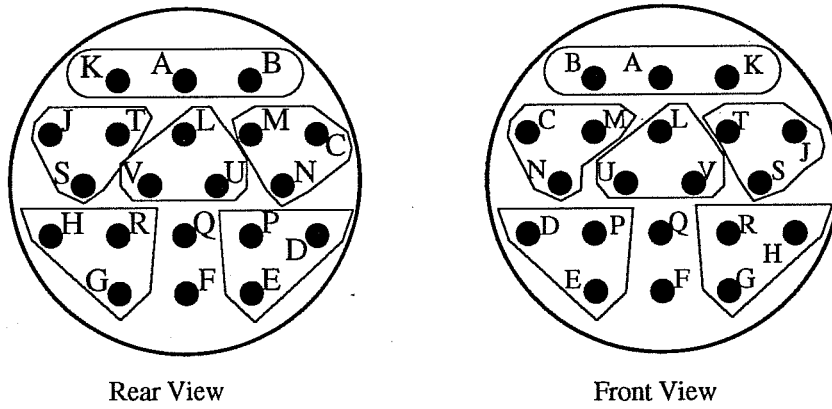
V. Data-logger 21X



VI. Multiplexer AM416



VII. Typical Wiring of Connectors #1 through #10



Amphenol 20-contact receptacle

Strain Gage
Channel Number

1 K --> S-
 A --> E+
 B --> E-

2 J --> S-
 T --> E+
 S --> E-

3 L --> S-
 V --> E+
 U --> E-

Strain Gage
Channel Number

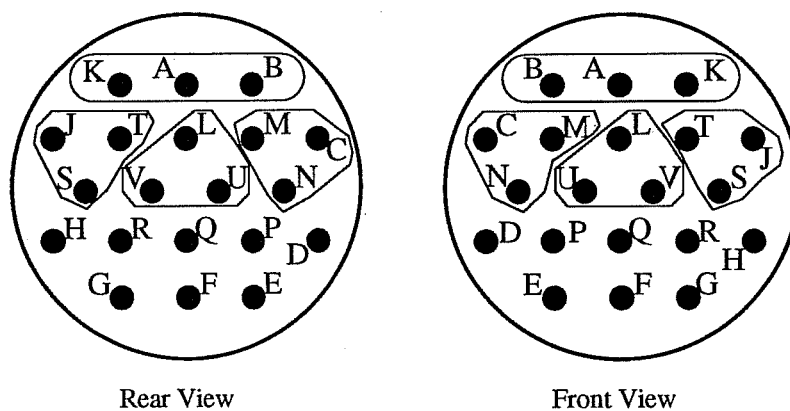
4 M --> S-
 C --> E+
 N --> E-

5 H --> S-
 R --> E+
 G --> E-

6 P --> S-
 D --> E+
 E --> E-

Q --> not connected
F --> not connected

VIII. Wiring of Connector #11

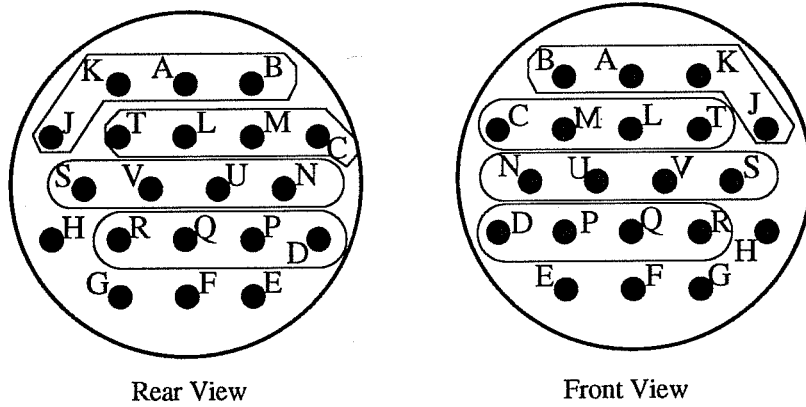


Amphenol 20-contact receptacle

Strain Gage
Channel Number

- | | | |
|-----------|----------------------------------|--|
| 61 | K --> S-
A --> E+
B --> E- | |
| 62 | J --> S-
T --> E+
S --> E- | H -->
R -->
G -->
P --> not connected
D -->
E -->
Q -->
F --> |
| 63 | L --> S-
V --> E+
U --> E- | |
| 64 | M --> S-
C --> E+
N --> E- | |

IX. Wiring of Connector #12



Amphenol 20-contact receptacle

**Strain Gage
Channel Number**

65 A --> E+
 B --> S-
 J --> E-
 K --> S+

66 M --> E+
 C --> S-
 T --> E-
 L --> S+

**Strain Gage
Channel Number**

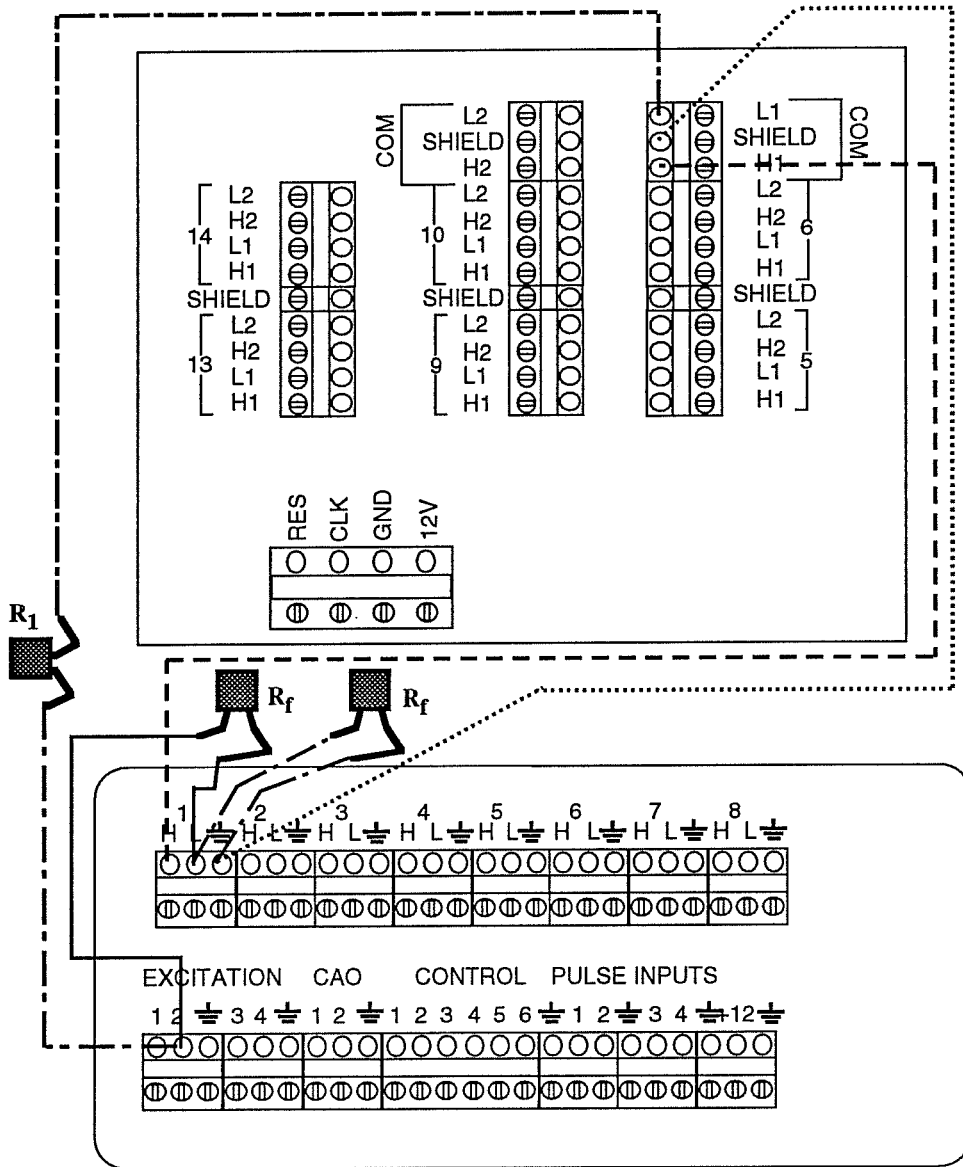
67 U --> E+
 N --> S-
 S --> E-
 V --> S+

68 P --> E+
 D --> S-
 R --> E-
 Q --> S+

H --> Control #4
 G --> Control #5
 F --> Pulse Input #3
 E --> Pulse Input #4

X. Internal connection circuit between Campbell and Multiplexers

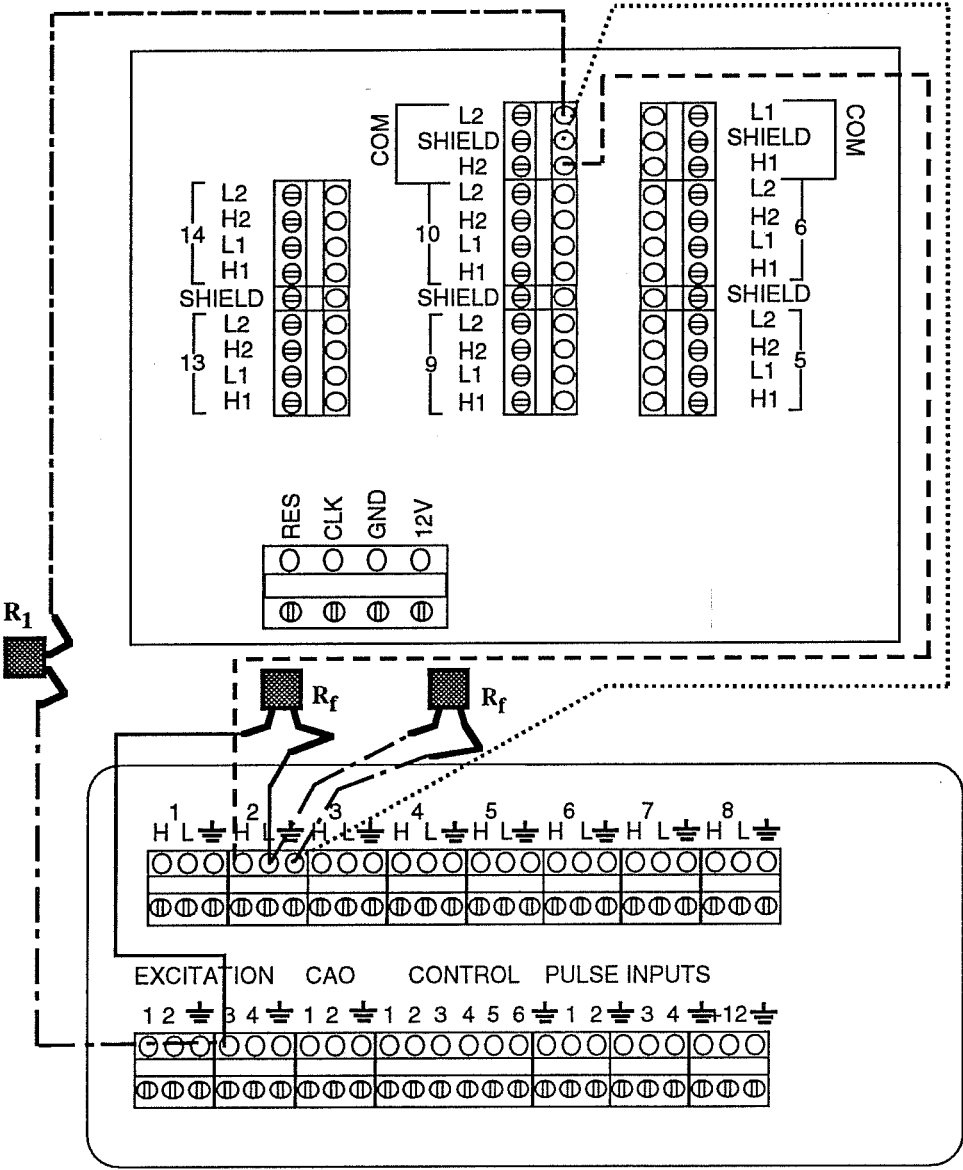
10.1 Quarter bridge completion circuit with Multiplexer #1, channels H1-L1:



Notes:

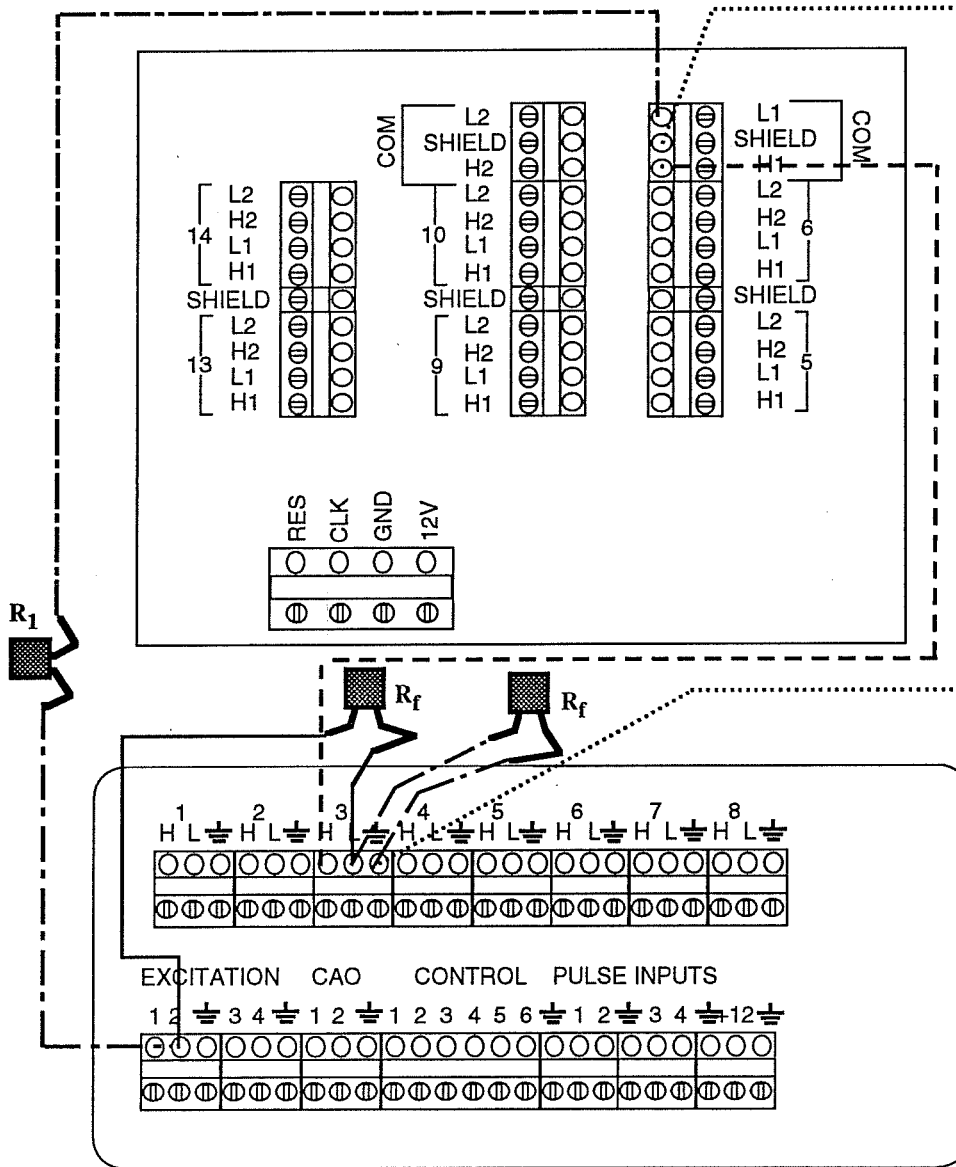
- R_f : 350 Ω (0.01%) Precision Resistor - 1st. Wheatstone arm
- R_1 : 350 Ω (0.01%) Precision Resistor - 2nd. Wheatstone arm

10.2 Quarter bridge completion circuit with Multiplexer #1, channels H2-L2:



Notes:
 R_f : 350 Ω (0.01%) Precision Resistor - 1st. Wheatstone arm
 R_1 : 350 Ω (0.01%) Precision Resistor - 2nd. Wheatstone arm

10.3 Quarter bridge completion circuit with Multiplexer #2, channels H1-L1:

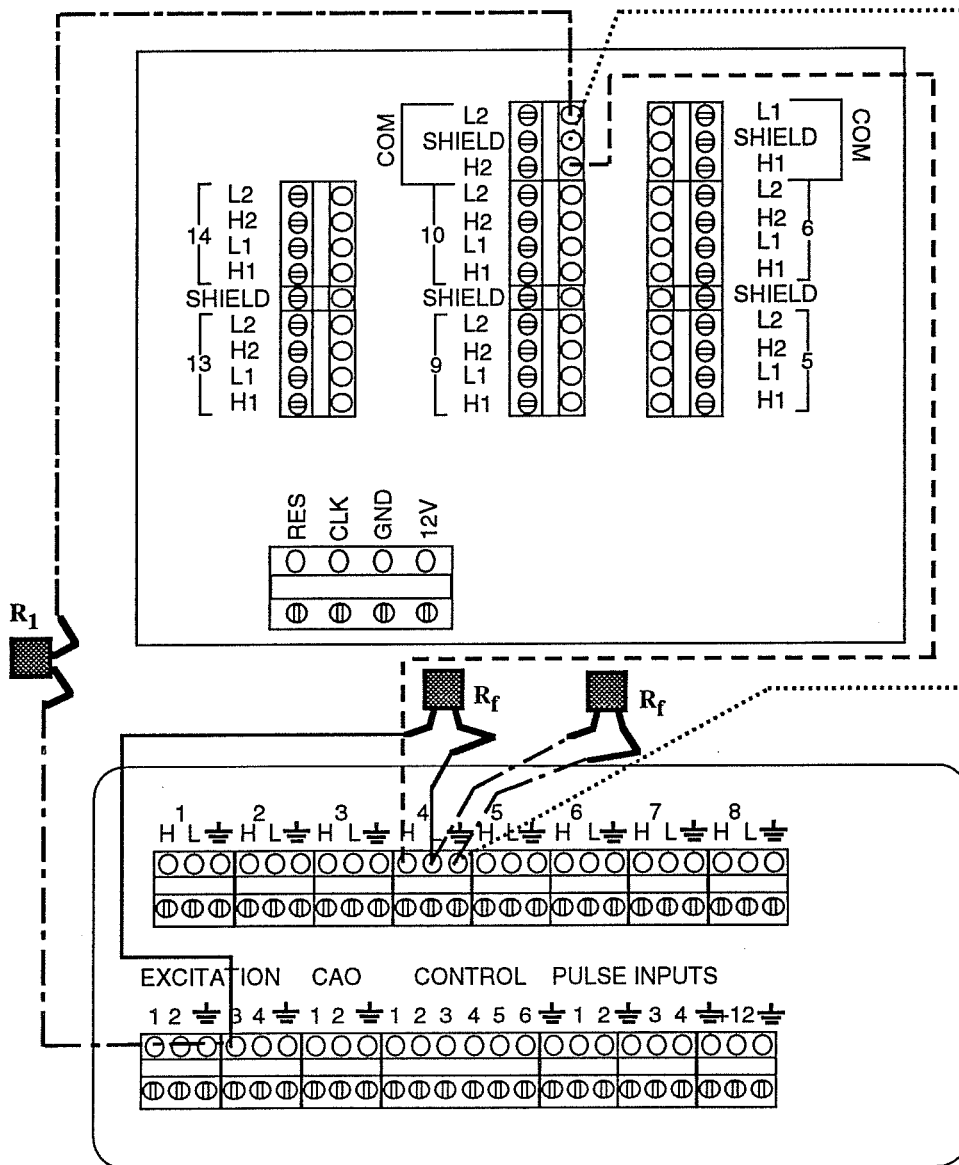


Notes:

R_f : 350 Ω (0.01%) Precision Resistor - 1st. Wheatstone arm

R_1 : 350 Ω (0.01%) Precision Resistor - 2nd. Wheatstone arm

10.4 Quarter bridge completion circuit with Multiplexer #2, channels H2-L2:

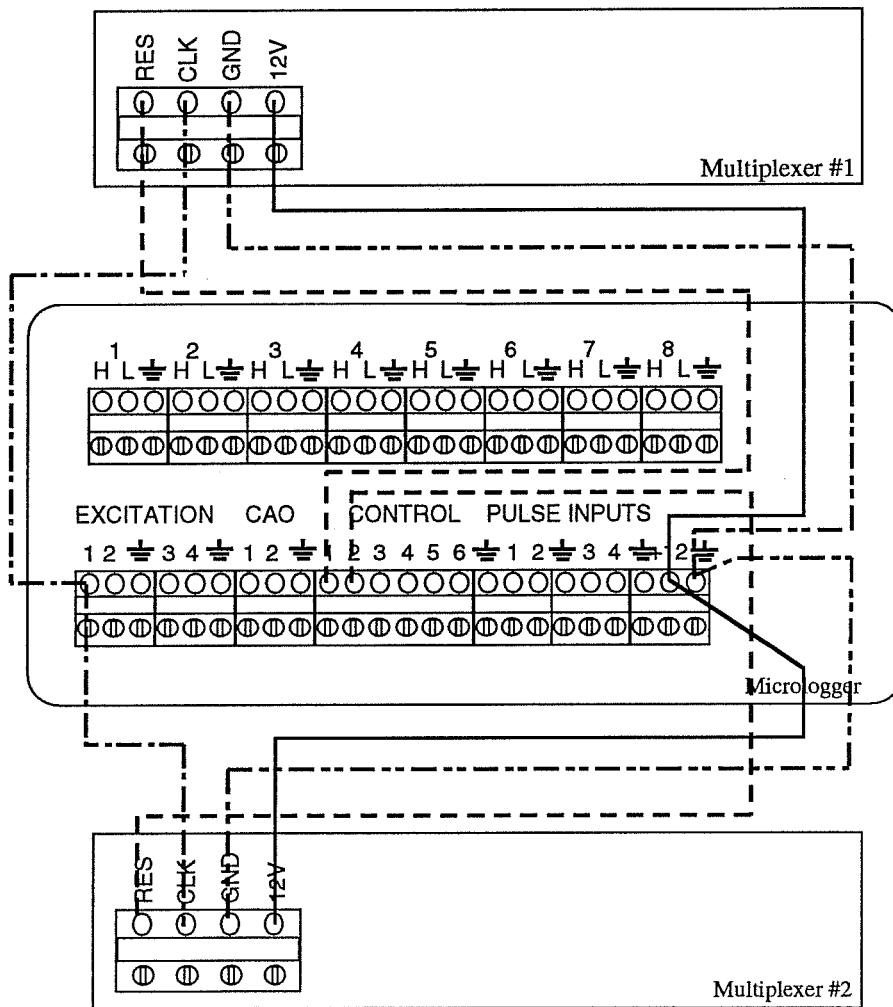


Notes:

R_f : 350 Ω (0.01%) Precision Resistor - 1st. Wheatstone arm

R_1 : 350 Ω (0.01%) Precision Resistor - 2nd. Wheatstone arm

10.5 Typical connections between Micrologger 21X and AM416 Multiplexers:



XI. Detailed Internal Wiring between Multiplexers, Datalogger and Connectors

11.1 Multiplexer #1:

Connector Number	Channel Number	Connector Letter Code	Wire Type	Wire Color	Multiplexer Channel				
1	1	K	S-	Red	1- 1H				
		A	E+	White	1- 1L				
		B	E-	Black	1/2- Ground				
	2	2	J	S-	Red	1- 2H			
			T	E+	White	1- 2L			
			S	E-	Black	1/2- Ground			
	3	3	L	S-	Red	2- 1H			
			V	E+	White	2- 1L			
			U	E-	Black	1/2- Ground			
	4	4	M	S-	Red	2- 2H			
			C	E+	White	2- 2L			
			N	E-	Black	1/2- Ground			
	5	5	H	S-	Red	3- 1H			
			R	E+	White	3- 1L			
			G	E-	Black	3/4- Ground			
	6	6	P	S-	Red	3- 2H			
			D	E+	White	3- 2L			
		6	6	E	E-	Black	3/4- Ground		
				2	7	K	S-	Red	4- 1H
						A	E+	White	4- 1L
						B	E-	Black	3/4- Ground
	8	8	J		S-	Red	4- 2H		
			T		E+	White	4- 2L		
			S		E-	Black	3/4- Ground		
9	9	L	S-		Red	5- 1H			
		V	E+		White	5- 1L			
		U	E-		Black	5/6- Ground			
10	10	M	S-		Red	5- 2H			
		C	E+		White	5- 2L			
		N	E-		Black	5/6- Ground			
11	11	H	S-	Red	6- 1H				
		R	E+	White	6- 1L				
		G	E-	Black	5/6- Ground				
12	12	P	S-	Red	6- 2H				
		D	E+	White	6- 2L				
		E	E-	Black	5/6- Ground				

Connector Number	Channel Number	Connector Letter Code	Wire Type	Wire Color	Multiplexer Channel
3	13	K	S-	Red	7- 1H
		A	E+	White	7- 1L
		B	E-	Black	7/8- Ground
	14	J	S-	Red	7- 2H
		T	E+	White	7- 2L
		S	E-	Black	7/8- Ground
	15	L	S-	Red	8- 1H
		V	E+	White	8- 1L
		U	E-	Black	7/8- Ground
	16	M	S-	Red	8- 2H
		C	E+	White	8- 2L
		N	E-	Black	7/8- Ground
	17	H	S-	Red	9- 1H
		R	E+	White	9- 1L
		G	E-	Black	9/10- Ground
	18	P	S-	Red	9- 2H
		D	E+	White	9- 2L
		E	E-	Black	9/10- Ground
4	19	K	S-	Red	10- 1H
		A	E+	White	10- 1L
		B	E-	Black	9/10- Ground
	20	J	S-	Red	10- 2H
		T	E+	White	10- 2L
		S	E-	Black	9/10- Ground
	21	L	S-	Red	11- 1H
		V	E+	White	11- 1L
		U	E-	Black	11/12- Ground
	22	M	S-	Red	11- 2H
		C	E+	White	11- 2L
		N	E-	Black	11/12- Ground
	23	H	S-	Red	12- 1H
		R	E+	White	12- 1L
		G	E-	Black	11/12- Ground
	24	P	S-	Red	12- 2H
		D	E+	White	12- 2L
		E	E-	Black	11/12- Ground

Connector Number	Channel Number	Connector Letter Code	Wire Type	Wire Color	Multiplexer Channel
5	25	K	S-	Red	13- 1H
		A	E+	White	13- 1L
		B	E-	Black	13/14- Ground
	26	J	S-	Red	13- 2H
		T	E+	White	13- 2L
		S	E-	Black	13/14- Ground
	27	L	S-	Red	14- 1H
		V	E+	White	14- 1L
		U	E-	Black	13/14- Ground
	28	M	S-	Red	14- 2H
		C	E+	White	14- 2L
		N	E-	Black	13/14- Ground
	29	H	S-	Red	15- 1H
		R	E+	White	15- 1L
		G	E-	Black	15/16- Ground
30	P	S-	Red	15- 2H	
	D	E+	White	15- 2L	
	E	E-	Black	15/16- Ground	
6	31	K	S-	Red	16- 1H
		A	E+	White	16- 1L
		B	E-	Black	15/16- Ground
	32	J	S-	Red	16- 2H
		T	E+	White	16- 2L
S	E-	Black	15/16- Ground		

11.2 Multiplexer #2:

6	33	L	S-	Red	1- 1H
		V	E+	White	1- 1L
		U	E-	Black	1/2- Ground
	34	M	S-	Red	1- 2H
		C	E+	White	1- 2L
		N	E-	Black	1/2- Ground
	35	H	S-	Red	2- 1H
		R	E+	White	2- 1L
		G	E-	Black	1/2- Ground
	36	P	S-	Red	2- 2H
		D	E+	White	2- 2L
		E	E-	Black	1/2- Ground

Connector Number	Channel Number	Connector Letter Code	Wire Type	Wire Color	Multiplexer Channel
7	37	K	S-	Red	3- 1H
		A	E+	White	3- 1L
		B	E-	Black	3/4- Ground
	38	J	S-	Red	3- 2H
		T	E+	White	3- 2L
		S	E-	Black	3/4- Ground
	39	L	S-	Red	4- 1H
		V	E+	White	4- 1L
		U	E-	Black	3/4- Ground
	40	M	S-	Red	4- 2H
		C	E+	White	4- 2L
		N	E-	Black	3/4- Ground
	41	H	S-	Red	5- 1H
		R	E+	White	5- 1L
		G	E-	Black	5/6- Ground
42	P	S-	Red	5- 2H	
	D	E+	White	5- 2L	
	E	E-	Black	5/6- Ground	
8	43	K	S-	Red	6- 1H
		A	E+	White	6- 1L
		B	E-	Black	5/6- Ground
	44	J	S-	Red	6- 2H
		T	E+	White	6- 2L
		S	E-	Black	5/6- Ground
	45	L	S-	Red	7- 1H
		V	E+	White	7- 1L
		U	E-	Black	7/8- Ground
	46	M	S-	Red	7- 2H
		C	E+	White	7- 2L
		N	E-	Black	7/8- Ground
	47	H	S-	Red	8- 1H
		R	E+	White	8- 1L
		G	E-	Black	7/8- Ground
48	P	S-	Red	8- 2H	
	D	E+	White	8- 2L	
	E	E-	Black	7/8- Ground	
9	49	K	S-	Red	9- 1H
		A	E+	White	9- 1L
		B	E-	Black	9/10- Ground

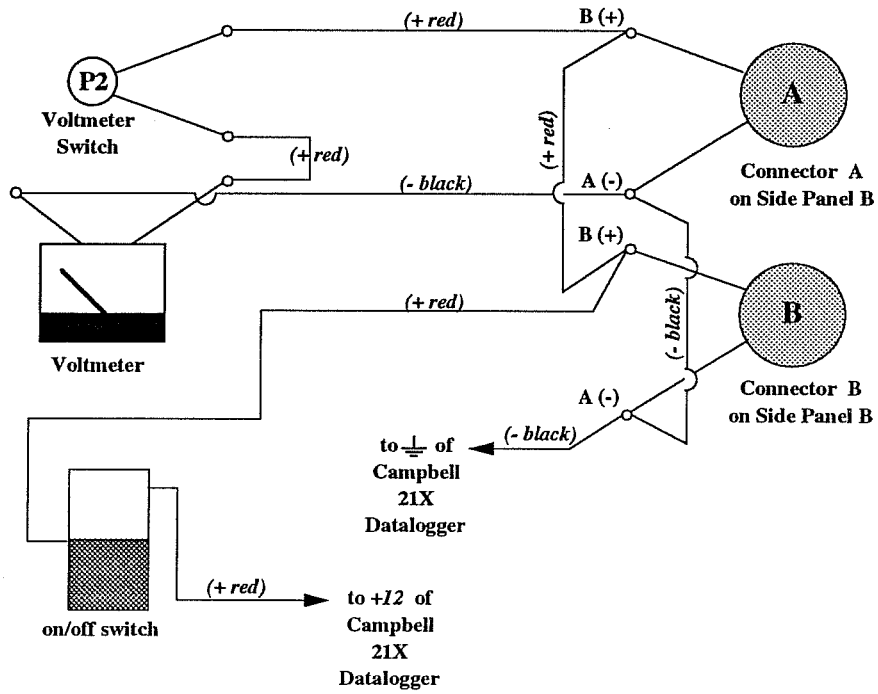
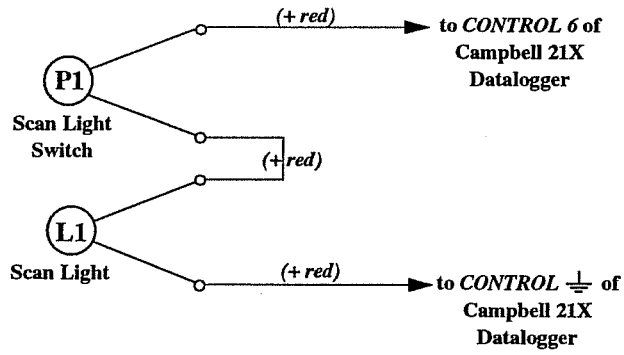
Connector Number	Channel Number	Connector Letter Code	Wire Type	Wire Color	Multiplexer Channel
9	50	J	S-	Red	9- 2H
		T	E+	White	9- 2L
	51	S	E-	Black	9/10- Ground
		L	S-	Red	10- 1H
		V	E+	White	10- 1L
		U	E-	Black	9/10- Ground
	52	M	S-	Red	10- 2H
		C	E+	White	10- 2L
		N	E-	Black	9/10- Ground
	53	H	S-	Red	11- 1H
		R	E+	White	11- 1L
		G	E-	Black	11/12- Ground
	54	P	S-	Red	11- 2H
		D	E+	White	11- 2L
E		E-	Black	11/12- Ground	
10	55	K	S-	Red	12- 1H
		A	E+	White	12- 1L
		B	E-	Black	11/12- Ground
	56	J	S-	Red	12- 2H
		T	E+	White	12- 2L
		S	E-	Black	11/12- Ground
	57	L	S-	Red	13- 1H
		V	E+	White	13- 1L
		U	E-	Black	13/14- Ground
	58	M	S-	Red	13- 2H
		C	E+	White	13- 2L
		N	E-	Black	13/14- Ground
	59	H	S-	Red	14- 1H
		R	E+	White	14- 1L
		G	E-	Black	13/14- Ground
	60	P	S-	Red	14- 2H
		D	E+	White	14- 2L
		E	E-	Black	13/14- Ground
11	61	K	S-	Red	15- 1H
		A	E+	White	15- 1L
		B	E-	Black	15/16- Ground
	62	J	S-	Red	15- 1H
		T	E+	White	15- 1L
		S	E-	Black	15/16- Ground

Connector Number	Channel Number	Connector Letter Code	Wire Type	Wire Color	Multiplexer Channel
11	63	L	S-	Red	16- 1H
		V	E+	White	16- 1L
		U	E-	Black	15/16- Ground
	64	M	S-	Red	16- 2H
		C	E+	White	16- 2L
		N	E-	Black	15/16- Ground

11.3 Campbell 21X:

Connector Number	Channel Number	Connector Letter Code	Wire Type	Wire Color	Multiplexer Channel
12	65	A	E+	Red	E4
		B	S-	White	5L
		J	E-	Black	5- Ground
	66	K	S+	Green	5H
		M	E+	Red	E4
		C	S-	White	6L
	67	T	E-	Black	6- Ground
		L	S+	Green	6H
		U	E+	Red	E4
	68	N	S-	White	7L
		S	E-	Black	7- Ground
		V	S+	Green	7H
		P	E+	Red	E4
		D	S-	White	8L
		R	E-	Black	8- Ground
Other connections: (same connector #12)		Q	S+	Green	8H
		H	(-)	Red	Control-4
		G	(-)	Red	Control-5
		E	(-)	Green	Pulse In-3
		F	(-)	Green	Pulse In-4

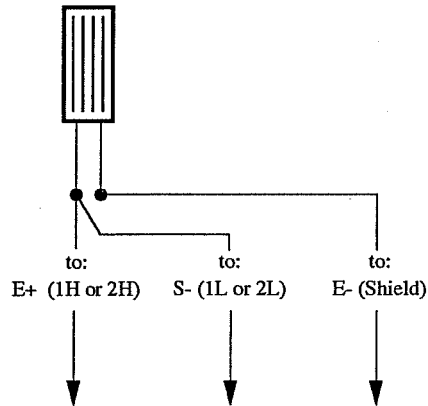
XII. Detailed Internal Wiring between Switches, Battery Connectors, and Datalogger



XIII. Wiring from Data Acquisition Box to Typical Sensors

13.1 Electrical Resistance Strain Gages (only for 350W)

--all three leadwire, quarter-bridge Wheatstone circuits--



Available Combinations:

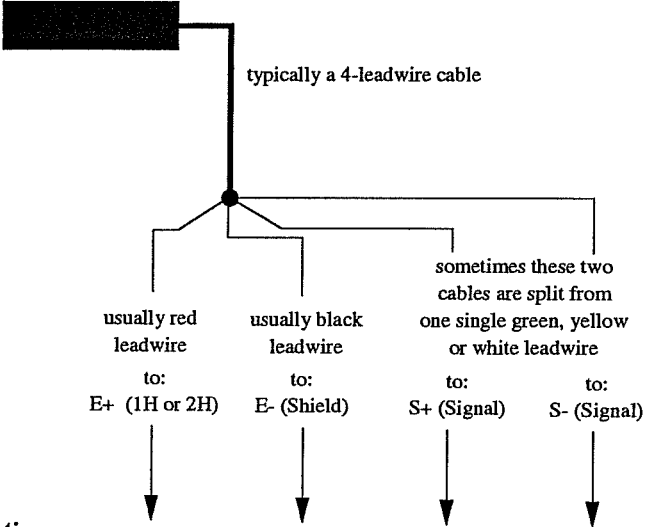
Connector Number	Connector Labels		
#1 through #10 (channels 1 thru 60)	A	K	B
	T	J	S
	V	L	U
	C	M	N
	R	H	G
	D	P	E
#11 (channels 61 thru 64)	A	K	B
	T	J	S
	V	L	U
	C	M	N

Notes:

* a total of 64 channels are available for this type of sensor.

** four additional channels can be employed if the completion circuits (one for each channel) are prepared externally from the data acquisition box. These additional sensors can then use Channels 65 through 68.

13.2 Pressure Transducer, Linear Potentiometers (LVDTs)
 --electrical resistance, 3 or 4-leadwire, full-bridge Wheatstone circuits--



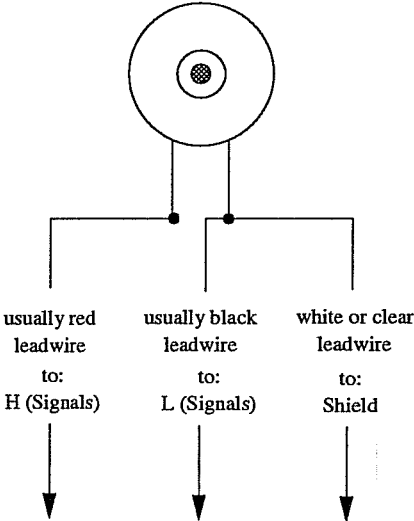
Available Combinations:

Connector Number	Connector Labels			
#12 (channels 1 thru 4)	A	J	K	B
	M	T	L	C
	U	S	V	N
	P	R	Q	D

Notes:

* a total of 4 channels are available for this type of sensor.

13.3 LI-200SZ Pyranometer



Available Combinations:

Connector Number	Connector Labels		
#12 (channels 1 thru 4)	K	B	J
	L	C	T
	V	N	S
	Q	D	R

Notes:

* a total of 4 channels are available for this type of sensor.

13.4 Other Sensors

a. Thermocouples

The Campbell 21X Micrologger was originally designed to measure up to 8 differential thermocouple channels (of the type T, E, K, or J). Each AM-416 Multiplexer was originally designed to handle up to 32 additional differential thermocouple channels (only if each group of 16 or all 32 channels are of the same thermocouple type T, E, K, or J)⁽¹⁾. The reference junction of the differential thermocouple measurements made by the Campbell 21X is the panel temperature (since each 21X has an internal sensor that determines the panel temperature).

However, with the new portable data acquisition boxes, thermocouple measurements are no longer available. This is because an added thermocouple junction will exist at the connections between the external thermocouple wires and the connectors located in the portable data acquisition box side panels.

b. Thermistors

Measurements of this type of sensor consist of electrical resistance readings. Single-ended channels can be used (up to 16 on each 21X and up to 64 on each AM-416). The new portable data acquisition boxes can still perform thermistor measurements using the available channels on connector #12. Up to eight thermistors can thus be used on each data acquisition box. The same wiring suggested by accompanying Campbell Instruments literature should be used. Campbell Scientific, Inc. offers two types of thermistors fully compatible to their dataloggers (the *107-* and the *108-Thermistors* sold for \$40.00 and \$44.00 respectively according to mid-1990 price sheet).

c. Relative Humidity

Campbell Scientific, Inc. offers the *207 Temperature and RH Probe* (\$200.00 each on mid-1990 price sheet) that can still be used with the new portable data acquisition box. The same

⁽¹⁾ If thermocouples were grounded at about the same ground potential of the 21X, then single-ended thermocouple measurements can be performed and the available number of channels will double from the previously given numbers (each 21X could thus handle up to 16 single-ended channels and each AM-416 up to 64 single-ended channels).

instructions provided in the Campbell literature applies to the available channels of connector #12.

d. Wind Speed and Direction

These sensors can still be used with each portable data acquisition box. The Campbell Scientific *014A Wind Speed Sensor* and the *024A Wind Direction Sensor* cost \$275.00 and \$393 in mid-1990.

APPENDIX C:

**SPECIAL PROVISIONS FOR
BRIDGE INSTRUMENTATION**
(Included in the San Antonio Y Bid Package)

SPECIAL PROVISIONS FOR BRIDGE INSTRUMENTATION

A team of investigators from the University of Texas at Austin will be instrumenting and monitoring three of the spans. The exact spans will be determined after the contractor has finalized his erection schedule. The following section describes special services required of the contractor and indicates possible delays and work stoppages involved in the field study.

1. Casting Yard Operations

A. Reinforcing steel for the up station joint segment and the up station deviator segment of one of the spans to be instrumented must be made available to the investigators no less than one week prior to casting of the segments to allow time for placement of gages. The gaged reinforcing bars will subsequently be placed in the reinforcing cages and special attention will be required to ensure that the gages not be damaged. The completed cage shall be made available for a check of the condition of the strain gages, and time shall be allowed for the replacement of the damaged gages.

B. Thermocouples will be placed in four segments of two of the specified spans. The thermocouples will be placed in the forms after the reinforcing cage is in place. Approximately one hour will be required for installation. A small work area for the investigators will be required adjacent to the casting bed for additional equipment.

C. In addition to normal quality assurance requirements, the investigators will require 12 concrete compression cylinders for each instrumented segment in each of the three spans to be instrumented.

D. The contractor shall place the segments designated for further instrumentation in these three spans in storage so as to be fully accessible to the investigators for the placement of additional instrumentation. The bottom surface of the boxes need not be accessible but the top surface and the interior must be fully accessible.

E. The investigators will place four small blockout forms in the webs and bottom slabs of one segment of one span. The blockouts will be positioned over the tendon ducts to allow access to the tendons during erection.

2. Erection Site Operations

A. While erecting each of the three spans selected for monitoring the contractor shall stop work on the span for up to 72 hours to allow for testing equipment installation. This stop shall take place after all epoxying and temporary post-tensioning has been performed, after all web and external tendons have been placed in the ducts and after all tendons have been seated with a small initial stress of approximately 15ksi. At this point the investigators will require up to 3 days to prepare for stressing operation measurements.

B. The contractor shall provide current calibration charts for all rams used during stressing operations. The contractor shall also provide a manifold on his hydraulic system with a Parker-

Hannifin 3000 series female quick-disconnect connection which is required for the connection of an electronic pressure transducer.

C. The contractor shall allow the following pauses for instrumentation readings during stressing operations.

Span AA-43*	- after stressing of T1 left and right-	45 min.
	after stressing of T2 and T3 left and right-	45 min.
	after stressing of T4 left and right-	45 min.
	after stressing of T6 and T7 left and right-	45 min.
Span AA-44*	- after stressing of T1 left and right-	45 min.
	after stressing of T2 and T3 left and right-	45 min.
	after stressing of T4 left and right-	45 min.
	after stressing of T6 and T7 left and right-	45 min.
Span CC-11*	- after stressing of T1 left and right-	45 min.
	after stressing of T2 left and right-	45 min.
	after stressing of T4 left and right-	45 min.
	after stressing of T5 left and right-	45 min.

* possible spans to be instrumented. The exact span designations will be determined after the contractor's schedule has been finalized.

D. The external tendons which have been instrumented will require special grouting procedures. These will be presented in detail after the exact spans are designated.

E. The contractor will make reasonable efforts to cooperate with the investigators to avoid damaging the instrumentation systems.

REFERENCES

1. Dunker, K. F. and Rabbat, B. G., "Performance of Highway Bridges," *Concrete International*, Journal of the American Concrete Institute, Vol. 12, No. 8, August 1990, pp. 40-43.
2. Powell, L. C., Breen, J. E., and Kreger, M. E., "State of the Art for Externally Post-Tensioned Bridges with Deviators," The University of Texas at Austin, Center for Transportation Research, Research Report 365-1, June 1988.
3. Podolny, W., and Muller, J., *Construction and Design of Prestressed Concrete Segmental Bridges*, John Wiley and Sons, Inc., 1982.
4. Billington, D. P., *The Tower and the Bridge*, Princeton University Press, Princeton, NJ, 1983.
5. Lin, T. Y., and Burns, N. H., *Design of Prestressed Concrete Structures*, 3rd. Edition, John Wiley and Sons, Inc., 1981.
6. Morice, P. B., and Cooley, E. H., *Prestressed Concrete - Theory and Practice*, Sir Isaac Pitman and Sons, Ltd., London, 1958.
7. Fischer, A., "The Roots of Science in Ancient China," *Mosaic Magazine*, April 1982, pp. 9-15.
8. Leonhardt, F., *Brücken - Ästhetik und Gestaltung*, The MIT Press, Cambridge, MA, 1984.
9. Billington, D. P., *Robert Maillart's Bridges - The Art of Engineering*, Princeton University Press, 1979.
10. Schlaich, J., and Scheef, H., *Concrete Box-Girder Bridges*, Structural Engineering Documents 1e, International Association for Bridge and Structural Engineering, 1982.
11. Kulka, F., Thoman, S. J., and Lin, T. Y., "Feasibility Study of Standard Sections for Segmental Prestressed Concrete Box-Girder Bridges," U.S. Department of Transportation, Federal Highway Administration, Report No. FHWA/RD-82/024, July 1982.
12. Ziadat, G. S., and Waldron, P., "Segmental Construction of Concrete Bridges: A State-of-the-Art Report," Report No. UBCE/C/86/1, University of Bristol, Department of Civil Engineering, December 1986.
13. Virlogeux, M. P., "External Prestressing: from Construction History to Modern Technique and Technology," American Concrete Institute, Special Publication SP-120, 1990, pp. 1-60.

14. Virlogeux, M. P., "Les Ossatures Mixtes Métal-Béton Précontraint," *Annales de L'Institut Technique du Bâtiment et des Travaux Publics*, Publication No. 458, Association Française pour la Construction (AFPC), Centre d'Études Supérieures et de Documentation des Annales de l'Institut Technique du Bâtiment et des Travaux Publics (ITBTP-CESDA), October 1987, pp. 4-30.
15. Mathivat, J., "Evolution récente des ponts en béton précontraint," *International Association for Bridge and Structural Engineering, IABSE Periodica 4/1988*, IABSE Surveys S-41/88, 1988.
16. Lacombe, H., "Prestressed Concrete Triangular Trusses," *International Association for Bridge and Structural Engineering, 12th Congress, Vancouver, September 1984*, pp. 9-14.
17. Breen, J., "Latest developments in modern technology in prestressed concrete in North America," *Fédération Internationale de la Précontrainte, FIP-XIth International Congress on Prestressed Concrete, June 1990, Hamburg, Germany*, pp. T6-T10.
18. "Segmental Bridges Divide Industry", *Engineering News Record*, November 2, 1989, pp. 24-27.
19. Tai, J. C., and Lo, G. K., "Design and Construction of the I-205 Columbia River Bridge - North Channel," *International Conference on Short and Medium Span Bridges, 1982, Toronto, Canada*, pp. 275-288.
20. Munn, W. D., "Multiple Methods Raise New Segmental Bridge," *Highway and Heavy Construction*, December 1989, pp. 38-41.
21. Matt, P., "Latest developments in modern technology in Europe", *Fédération Internationale de la Précontrainte, FIP-XIth International Congress on Prestressed Concrete, June 1990, Hamburg, Germany*, pp. T3-T5.
22. Wolff, R., and Franze, L., "Glass Fiber Tendons for Prestressed Concrete Bridges," *13th IABSE Congress, Helsinki, June 1988*.
23. "Aesthetics and Design: A High Tech Construction Solution in San Antonio," *Technical Quarterly, Texas State Department of Highways and Public Transportation, Transportation Planning Division, Vol. 5, Issue 4, July 1990*.
24. American Concrete Institute, *External Prestressing in Bridges*, Special Publication SP-120, 1990.
25. Raspaud, B., "Le Pont de Bubiyan - Conception de la Structure et Methodes," *Association Française pour la Construction, Bulletin Technique*, May 1983, pp. 13-23.
26. Mathivat, J., "The Present Evolution of Prestressed Concrete Bridges", *Association Française pour la Construction, Bulletin Technique*, September 1987, pp. 75-86.

27. Menn, C., *Prestressed Concrete Bridges*, Birkhäuser Verlag, Basel-Boston-Berlin, 1990.
28. Magnel, G., *Prestressed Concrete*, McGraw-Hill Book Company, Inc., New York, 1954.
29. Bruggeling, A. S. G., "Structural Concrete: Science into Practice," Heron, Delf University of Technology, Vol. 32, No. 2, 1987.
30. Bruggeling, A. S. G., "An Engineering Model of Structural Concrete," Introductory Report for the IABSE Colloquium: Structural Concrete, International Association for Bridge and Structural Engineering, Stuttgart, 1991.
31. Breen, J. E., "Why Structural Concrete," Introductory Report for the IABSE Colloquium: Structural Concrete, International Association for Bridge and Structural Engineering, Stuttgart, 1991.
32. Henneberger, W., and Breen, J. E., "First Segmental Bridge in the U. S.," Civil Engineering, American Society of Civil Engineers, June 1974, pp. 54-57.
33. Grant, A., "Incremental Launching of Concrete Structures," Journal of American Concrete Institute, August 1975, pp. 395-402.
34. "Design and Construction of the Caguana River Bridge," American Segmental Bridge Institute, ASBI Newsletter, Vol. 5, Spring 1990.
35. Torroja, E., *Philosophy of Structures*, University of California Press, Berkeley - Los Angeles, 1967.
36. "William Brothers Construction Co. Nears Completion of Neches Bridge," American Segmental Bridge Institute, ASBI Newsletter, Vol. 6, Summer 1990.
37. Matt, P., Voumard, J. M., Marti, P., and Thürlimann, B., "Main River Span Structure of the Gateway Bridge," Concrete International, American Concrete Institute, May 1988, pp.34-43.
38. Schupack, M., "Corrosion Protection of Unbonded Tendons," Concrete International, American Concrete Institute, Vol. 13, No. 2, February 1991, pp. 51-57.
39. Dolan, C. W., "Developments in Non-Metallic Prestressing Tendons," Prestressed Concrete Institute, PCI Journal, Vol. No. 5, September/October 1990, pp. 80-88.
40. AASHTO, "Interim Specifications for Segmental Bridges," American Association of State Highway and Transportation Officials, 1989.
41. Holman, R. J., "Development of an Instrumentation Program for Studying Behavior of a Segmental Box Girder Bridge," Joint Highway Research Project No. C-36-56T, Report JHRP-77-4, Purdue University, Lafayette, Indiana, March 1977.

42. Shiu, K. N., Aristizabal-Ochoa, J. D., and Russell, H. G., "Instrumentation of Denny Creek Bridge," Report to State of Washington Department of Transportation, Agreement Y-1837, Construction Technology Laboratories, Portland Cement Association, Skokie, IL, August 1981.
43. Hawkins, N. M., Clark, J. H., "Investigation of Thermal and Live Load Stresses in Denny Creek Viaduct," University of Washington, Report No. 63-1080, Olympia, WA, June 1983.
44. Richardson, J. E., "Field-Measured Post-Tension Prestress Loss in Stress-Relieved Strands," California Department of Transportation (CALTRANS), Report No. FHWA/CA/SD-84/02, Sacramento, CA, June 1984.
45. Ziadat, G. S., and Waldron, P., "Measurement of Time-Dependent Behaviour in the River Torridge Bridge," Report No. UBCE/C/87/4, University of Bristol, November 1987.
46. Baber, T. T., and Hilton, M. H., "Field Monitoring of the I-295 Bridge Over the James River Bridge -- Instrumentation Installation and Construction Period Studies," Interim Report, Virginia Transportation Research Council (Jointly Sponsored by the University of Virginia and the Virginia Department of Transportation), Charlottesville, Virginia, Report No. VTRC 88-R23, April 1988.
47. Shields, J., and Saiidi, M. S., "Direct Field Measurement of Prestress Losses in Box Girder Bridges," Report No. CCEER-89-4, Civil Engineering Department, University of Nevada at Reno, December 1989.
48. Kokubu, M., "Deflections of Prestressed Concrete Bridges in Japan," Magazine of Concrete Research, Vol. 24, No. 80, September 1972, pp. 117-126.
49. Kokubu, M., Goto, Y., Ozaka, Y., Okamura, H., and Momoshima, S., "Measurements of Creep and Shrinkage in Actual Prestressed Concrete Bridges," International Association for Bridge and Structural Engineering, Symposium: Design of Concrete Structures for Creep, Shrinkage, and Temperature Changes, Madrid 1970, pp.19-26.
50. Russell, H. G., Shiu, K. N., Gamble, W. L., and Marshall, V. L., "Evaluation and Verification of Time-Dependent Deformations in Postensioned Box-Girder Bridges," Transportation Research record 871, National Research Council, Washington, D.C., 1982, pp. 66-70.
51. Pfeil, W., "Twelve Years Monitoring of a Long Span Prestressed Concrete Bridge," Concrete International, American Concrete Institute, Vol. 3, No. 8, August 1981, pp.79-84.
52. Favre, R., and Markey, I., "Long-Term Monitoring of Bridge Deformation," Workshop Proceedings, U.S. - European Workshop on Bridges, Baltimore, 1990.

53. Markey, I., "Hydrostatic Levelling System for the Measurement of Bridge Deformation," Publication No. 134, Institut de Statique et Structures - Béton Armé et Précontraint (IBAP), Ecole Polytechnique Fédérale de Lausanne, November 1989.
54. Favre, R., Charif, H., and Markey, I., "Observation a Long Terme de la Déformation des Ponts," Institut de Statique et Structures - Béton Armé et Précontraint (IBAP), Ecole Polytechnique Fédérale de Lausanne, Projet de Recherche 86/88, October 1990.
55. Marshall, V., and Gamble, W. L., "Time Dependent Deformations in Segmental Prestressed Concrete Bridges," Research Report No. UILU-ENG-81-2014, SRS-495, University of Illinois at Urbana-Champaign, Department of Civil Engineering, Urbana, IL, October 1981.
56. American Society for Testing Materials, "Standard Test Method for Compressive Strength of Cylindrical Concrete Specimens," Specification C39-72, Philadelphia, PA, 1972.
57. Neville, A. M., *Creep of Plain and Structural Concrete*, London, 1983.
58. ACI Committee 209, "Prediction of Creep, Shrinkage, and Temperature Effects in Concrete Structures," Design for Creep and Shrinkage of Concrete Structures, Special Publication SP-76, American Concrete Institute, Detroit, Michigan, 1982.
59. Bakoss, S. L., Burfitt, A. J., and Cridland, L., "The Measurement of Strain in Concrete with the Embedment Type Vibrating Wire Gauge," The New South Wales Institute of Technology, School of Civil Engineering, Civil Engineering Monograph No. C.E. 76/2 M.E., Sydney, Australia, 1976.
60. Dunnicliff, J., *Geotechnical Instrumentation for Monitoring Field Performance*, John Wiley and Sons, Inc., New York, 1988.
61. Perry, C. C., and Lissner, H. R., *The Strain Gage Primer*, McGraw-Hill Book Company, Inc., New York, Second Edition, 1962.
62. Loh, Y. C., Internal Stress Gages for Cementitious Materials, SESA, Proceedings Vol. 11, No. 2, 1954, pp.13- 28.
63. Barker, W. R., and Reese, L. C., "Instrumentation for Measurement of Axial Load in Drilled Shafts," Center for Highway Research, The University of Texas at Austin, Research Report No. 89-6, November 1969.
64. Vijayvergiya, V. N., *Load Distribution for a Drilled Shaft in Clay Shale*, Ph.D. Dissertation, The University of Texas at Austin, Austin, Texas, November 1968.
65. Gamble, W. L., "Long-Term Behavior of a Prestressed I-Girder Highway Bridge in Champaign County, Illinois," University of Illinois at Urbana-Champaign, Structural

Research Series No. 470, Report No. UILU-ENG-79-2019, Research Project No. FHWA/IL/UI/180, August 1979.

66. Johnson, M. J., *Fiber Optic Interferometer Sensor for Strain Measurements in High Magnetic Fields and Cryogenic Environments*, M. S. Thesis, The University of Texas at Austin, May 1991.
67. Butter, C. D., and Hocker, G. B., "Fiber Optics Strain Gauge," *Applied Optics*, Vol.17, No. 18, September 1978, pp. 2867-2869.
68. Miessler, H. J., and Levacher, F. K., "Monitoring Stressing Behaviour with Integrated Optical Fiber Sensors," 13th IABSE Congress, Helsinki, International Association for Bridge and Structural Engineering, June 1988.
69. Wolff, R., and Miessler, H. J., "New Materials for Prestressing and Monitoring Heavy Structures," *Concrete International*, American Concrete Institute, Vol. 11, No. 9, pp. 86-89, September 1989.
70. Preston, H. K., "Testing of 7-Wire Strand for Prestressed Concrete -- The State of the Art," *Journal of the Prestressed Concrete Institute*, Vol. 30, No. 3, May-June 1985, pp. 134-155.
71. Koretsky, A. V., and Pritchard, R. W., "Critical Assessment of the International Estimates for Relaxation Losses in Prestressing Strands," University of Queensland, Department of Civil Engineering, Research Report No. CE25, St. Lucia, Australia, June 1981.
72. Comité Euro-International du Béton - Fédération Internationale de la Précontrainte, *CEB-FIP Model Code for Concrete Structures 1990*, Switzerland, 1990.
73. Yates, D. L., *A Study of Fretting Fatigue in Post-Tensioned Concrete Beams*, M. S. Thesis, The University of Texas at Austin, May 1988.
74. McGregor, R. J. G., *Evaluation of Strength and Ductility of a Three Span Externally Post-Tensioned Box Girder Bridge Model*, Ph. D. Dissertation, The University of Texas at Austin, August 1989.
75. Fellenius, B. H., "Ignorance is Bliss," *Geotechnical News*, Vol. 2, No. 4, December 1984, pp. 14-15.
76. Littlejohn, G. S., "Acceptance Criteria for the Service Behaviour of Ground Anchorages," *Ground Engineering*, Vol. 14, No. 3, April 1981, pp. 26-36.
77. Versnel, W. J., "Compensation of Leadwire Effects with Resistive Straingauges in Multi-Channel Straingauge Instrumentation," *Experimental Stress Analysis: Proceedings of the VIIIth International Conference on Experimental Stress Analysis*, Amsterdam, The Netherlands, May 12-16, 1986; Compiled by: Wieringa, H.; Published by: Dordrecht; Boston: Martinus Nijhoff, 1986; pp. 455-464.

78. Hanna, T. H., *Field Instrumentation in Geotechnical Engineering*, Trans Tech Publications, First Edition, 1985.
79. Pauw, A., and Breen, J. E., "Field Testing and Analysis of Two Prestressed Concrete Girders," The University of Missouri Bulletin, Volume 60, Number 52, Columbia Missouri, November 1959.
80. Poston, R. W., Bradberry, T. E., and Breen, J. E., "Load Tests of a Pretensioned Girder Bridge near Happy, Texas," Research Report No. 921-1F, Center for Transportation Research, The university of Texas at Austin, April 1985.
81. Bradberry, T. E., *Time dependent Deformation of Long Span Prestressed Concrete Beams Having Low Relaxation Strands*, M.S. Report, The University of Texas at Austin, May 1986.
82. White, C. D., *Observations and Evaluation of the Composite Wing Girder Bridge at Bear Creek*, M. S. Thesis, The University of Texas at Austin, May 1984.
83. Imbsen, R. A., Vandershaf, D. E., Schamber, R. A., and Nutt, R. V., "Thermal Effects in Concrete Bridge Superstructures," NCHRP Research Report No. 276, Transportation Research Board, Washington, D.C., September 1985.
84. Post, J., Tahamassebi, B., and Frank, K. H., "Estimating Fatigue Life of Bridges," The University of Texas at Austin, Center for Transportation Research, Report No. 464-1F, March 1988.
85. Texas Department of Highways and Public Transportation, Material Specification D-9-6110, Epoxy Adhesive Type V.
86. ASTM, "Corrosion Resistance of Coated Steel Specimens (Cyclic Method)," American Society of Testing Materials, Designation D-2933-74 (Reapproved 1986).
87. Pauw, A., and Breen, J. E., "Structural and Economic Study of Precast Bridge Units - Instrumentation," Technical Report No. 1, The University of Missouri, Department of Civil engineering, 1957.
88. Orsat, P., and Bertel, J. C., "Measurement of Forces Actually Applied on Rebars Anchor-Bolts or Strands with Tensiomag," International Association of Bridge and Structural Engineering, IABSE Proceedings, 5th Annual International Bridge Conference (IBC), June 13-15, 1988, Pittsburgh, Pennsylvania, pp. 51-56.
89. Measurements Group, *Manual of Technical Reports*, Strain Gage Technical Data, Strain Gage Listings, Technical Tips and Instruction Bulletins.
90. Measurements Group, "Optimizing Strain Gage Excitation Levels," Technical Note TN-502, 1979.

91. Radloff, B. J., *Bonding of External Tendons at Deviators*, M. S. Thesis, The University of Texas at Austin, December 1990.
92. Telephone conversations with Mr. Frank Dominico of Sika, Inc., during August and September of 1990.
93. Zumbrennen, L. G., *Behavior of Statically Loaded Prestressed Concrete Girders With 0.5 Inch Diameter Debonded Strands*, M. S. Thesis, The University of Texas at Austin, May 1991.
94. Lutz, B. A., *Measurement of Development Length of 0.5 Inch and 0.6 Inch Diameter Prestressing Strand In Fully Bonded Concrete Beams*, M. S. Thesis, The University of Texas at Austin, May 1991.
95. Falconer, B. A., *Post-Tensioning Anchorage Zones in Bridge Decks*, M. S. Thesis, The University of Texas at Austin, May 1990.
96. Measurements Group, "Surface Preparation for Strain Gage Bonding," Instruction Bulletin B-129-6, Raleigh, North Carolina, 1976.
97. Measurements Group, "Strain Gage Applications with M-Bond AE-10/15 and M-Bond GA-2 Adhesive Systems," Instruction Bulletin B-137-13, Raleigh, North Carolina, 1979.
98. Bryant, A. H., Wood, J. A., and Fenwick, R. C., "Creep and Shrinkage in Concrete Bridges," RRU Bulletin 70, National Roads Board, Wellington, New Zealand, 1984.
99. Comité Euro-International du Béton - Fédération Internationale de la Précontrainte, *CEB-FIP Model Code for Concrete Structures 1978*, 1978.
100. ACI Committee 209, "Effects of Concrete Constituents, Environment, and Stress on the Creep and Shrinkage of Concrete," Special Publication SP-27, American Concrete Institute, Detroit, Michigan, 1971.
101. Telephone conversations and electronic FAX transmittals with Mark Hatfield, Applications Engineer, Campbell Scientific, Inc., June/July 1990.
102. American Society for Testing Materials, "Standard Test Method for Creep of Concrete in Compression," Specification C512-87, Philadelphia, PA, August 1987.
103. Nanni, A., Yang, C. C., Pan, K., Wang, Y., and Michael, R. R. Jr., "Fiber-Optic Sensors for Concrete Stress/Strain Measurements," American Concrete Institute, ACI Materials Journal, Vol. 88, No. 3, May-June 1991, pp. 257-264.
104. The final completion bridge circuitry between the 21X-data-logger and each AM416-multiplexer was designed with the assistance of Joahan Ernest, Electronic Shop Assistant for FSEL, August/September 1990.

BIBLIOGRAPHY INDEX

I. General	379
II. Prestressed Concrete and Historical Reviews.....	379
III. Future Trends of Box Girder Bridges (Construction and Materials)	380
IV. Aesthetics in Bridges.....	382
V. Analysis and Design of Prestressed Concrete Bridges.....	382
VI. Construction Methods of Segmental Concrete Bridges	384
VII. Temperature Effects.....	388
VIII. Creep and Shrinkage of Concrete Bridges	389
IX. Performance of Instrumentation Systems for Structural Engineering	390
X. Experimental Tests.....	392
XI. Full-Scale Instrumentation Systems.....	394
XII. Bridge Surveillance and Maintenance Programs.....	497

BIBLIOGRAPHY

Other
Sections

I. General

- 1.1 Timby, E. K., "Major Bridge Projects from the Point of View of Owners," International Association for Bridge and Structural Engineering, IABSE-Periodica 2/1980, IABSE-Journal J-11/80, pp. 21-44.
- 1.2 Herr, L. A., and Sears, F. D., "Bidding and Contract Arrangement in Bridge Construction," Journal of Prestressed Concrete Institute, Vol. 25, No. 4, July/August 1980, pp. 38-40.
- 1.3 Alberdi Jr., T., "Value Engineering vs Alternate Designs in Bridge Bidding," Journal of Prestressed Concrete Institute, Vol. 25, No. 4, July/August 1980, pp. 41-47.
- 1.4 Kulka, F., "Alternate Designs for Long Span Bridges," Journal of Prestressed Concrete Institute, Vol. 25, No. 4, July/August 1980, pp. 48-58.
- 1.5 Sutter, J. J., "Construction Options in Bidding Concrete Bridges," Journal of Prestressed Concrete Institute, Vol. 25, No. 4, July/August 1980, pp. 59-65.
- 1.6 Kulka, F., Thoman, S. J., and Lin, T. Y., "Feasibility Study of Standard Sections for Segmental Prestressed Concrete Box-Girder Bridges," U.S. Department of Transportation, Federal Highway Administration, Report No. FHWA-RD-82/024, July 1982.
- 1.7 Peters, G. L., "Concrete Segmental Bridges: Past, Present, and Future," Paper presented at the American Segmental Bridge Convention (ASBI), San Diego, CA, December 1989.
- 1.8 Dunker, K. F., and Rabbat, B. G., "Performance of Highway Bridges," Concrete International, Journal of the American Concrete Institute, Vol. 12, No. 8, August 1990, pp. 40-43.
- 1.9 Desjardins, R. J., "Bidding Alternate Designs for Bridge Construction," Modern Steel Construction, American Institute of Steel Construction (AISC), Vol. 31, No. 3, March 1991, pp. 17-21.

VI

II. Prestressed Concrete and Historical Reviews

- 2.1 Magnel, G., *Prestressed Concrete*, McGraw-Hill Book Company, Inc., New York, 1954.

- 2.2 Morice, P. B., and Cooley, E. H., *Prestressed Concrete - Theory and Practice*, Sir Isaac Pitman and Sons, Ltd., London, 1958.
- 2.3 Billington, D. P., *Robert Maillart's Bridges - The Art of Engineering*, Princeton University Press, NJ, 1979.
- 2.4 Lin, T. Y., and Burns, N. H., *Design of Prestressed Concrete Structures*, 3rd. Edition, John Wiley and Sons, Inc., 1981. V
- 2.5 Fischer, A., "The Roots of Science in Ancient China", *Mosaic Magazine*, April 1982, pp. 9-15.
- 2.6 Billington, D. P., *The Tower and the Bridge*, Princeton University Press, Princeton, NJ, 1983.
- 2.7 Bruggeling, A. S. G., "Structural Concrete: Science into Practice," *Heron*, Delf University of Technology, Vol. 32, No. 2, 1987. III
- 2.8 Bruggeling, A. S. G., "An Engineering Model of Structural Concrete," Introductory Report for the IABSE Colloquium: Structural Concrete, International Association for Bridge and Structural Engineering, Stuttgart, 1991. III
- 2.9 Breen, J. E., "Why Structural Concrete," Introductory Report for the IABSE Colloquium: Structural Concrete, International Association for Bridge and Structural Engineering, Stuttgart, 1991. III

III. Future Trends of Box Girder Bridges (Construction and Materials)

- 3.1 Lacombe, H., "Prestressed Concrete Triangular Trusses," International Association for Bridge and Structural Engineering, 12th Congress, Vancouver, September 1984, pp. 9-14.
- 3.2 Wittfoht, E. H., "Outstanding and Innovative Construction Methods in Concrete Structures - Recent and Future Trends," FIP 86/4, 1986. VI
- 3.3 Virlogeux, M. P., "Les Ossatures Mixtes Métal-Béton Précontraint," *Annales de L'Institut Technique du Bâtiment et des Travaux Publics*, Publication No. 458, Association Française pour la Construction (AFPC), Centre d'Études Supérieures et de Documentation des Annales de l'Institut Technique du Bâtiment et des Travaux Publics (ITBTP-CESDA), October 1987, pp. 4-30.
- 3.4 "Swiss Cheese Box Girders," *Civil Engineering, Magazine of the American Society of Civil Engineers*, Vol. 58, No. 3, March 1988, pp. 40-43.

- 3.5 Franze, L., and Wolff, R., "Glass Fiber Tendons for Prestressed Concrete Bridges," 13th IABSE Congress, Helsinki, June 1988.
- 3.6 Powell, L. C., Breen, J. E., and Kreger, M. E., "State of the Art for Externally Post-Tensioned Bridges with Deviators," The University of Texas at Austin, Center for Transportation Research, Research Report 365-1, June 1988. **V, X**
- 3.7 Mathivat, J., "Evolution récente des ponts en béton précontraint," International Association for Bridge and Structural Engineering, IABSE Periodica 4/1988, IABSE Surveys S-41/88, 1988.
- 3.8 Wolff, R., and Miesslerer, H. J., "New Materials for Prestressing and Monitoring Heavy Structures," Concrete International, American Concrete Institute, Vol. 11, No. 9, pp. 86-89, September 1989. **IX**
- 3.9 American Concrete Institute, *External Prestressing in Bridges*, Special Publication SP- 120, 1990. **V, VI, X, XI**
- 3.10 Matt, P., "Latest developments in modern technology in Europe", Fédération Internationale de la Précontrainte, FIP-XIth International Congress on Prestressed Concrete, June 1990, Hamburg, Germany, pp. T3-T5.
- 3.11 Breen, J., "Latest developments in modern technology in prestressed concrete in North America," Fédération Internationale de la Précontrainte, FIP-XIth International Congress on Prestressed Concrete, June 1990, Hamburg, Germany, pp. T6-T10.
- 3.12 Boudot, J., Radiguet, B., and Pham, T., "The Sylans and Glacieres-Viaducts (France) - Prestressing of Concrete Trusses," Fédération Internationale de la Précontrainte, FIP-XIth International Congress on Prestressed Concrete, June 1990, Hamburg, Germany, pp. 309-317.
- 3.13 Jartoux, P., "Freysinet Stay Cables," Fédération Internationale de la Précontrainte, FIP-XIth International Congress on Prestressed Concrete, June 1990, Hamburg, Germany, pp. 99-111.
- 3.14 Jartoux, P., and Lacroix, R., "Development of External Prestressing Evolution of the Technique," Fédération Internationale de la Précontrainte, FIP-XIth International Congress on Prestressed Concrete, June 1990, Hamburg, Germany, pp. 91-98.
- 3.15 Dolan, C. W., "Developments in Non-Metallic Prestressing Tendons," Prestressed Concrete Institute, PCI Journal, Vol. No. 5, September/October 1990, pp. 80-88.
- 3.16 Schupack, M., "Corrosion Protection of Unbonded Tendons," Concrete International, American Concrete Institute, Vol. 13, No. 2, February 1991, pp. 51-57.

IV. Aesthetics in Bridges

- 4.1 Leonhardt, F., *Brücken - Ästhetik und Gestaltung*, The MIT Press, Cambridge, MA, 1984. II
- 4.2 Muller, J. M., and Figg McCallister, L., "Esthetics and Concrete Segmental Bridges in the United States," *Concrete International*, Vol. 10, No. 5, May 1988, pp. 25-33.
- 4.3 Schlaich, J., "Introduction - the engineer and aesthetics," *Fédération Internationale de la Précontrainte, FIP-XIth International Congress on Prestressed Concrete*, June 1990, Hamburg, Germany, pp. A3-A4.
- 4.4 Menn, C., "Aesthetics and economy in bridge design," *Fédération Internationale de la Précontrainte, FIP-XIth International Congress on Prestressed Concrete*, June 1990, Hamburg, Germany, pp. A5-A10.
- 4.5 Lin, T. Y., "Bridge pier follows force flow," *Fédération Internationale de la Précontrainte, FIP-XIth International Congress on Prestressed Concrete*, June 1990, Hamburg, Germany, pp. A15-A19.
- 4.6 Lee, D. J., "On the artistic design of bridges," *Fédération Internationale de la Précontrainte, FIP-XIth International Congress on Prestressed Concrete*, June 1990, Hamburg, Germany, pp. A20-A27.

V. Analysis and Design of Prestressed Concrete Bridges

- 5.1 Podolny, W., and Muller, J., *Construction and Design of Prestressed Concrete Segmental Bridges*, John Wiley and Sons, Inc., New York, 1982. VI
- 5.2 Schlaich, J., and Scheef, H., *Concrete Box-Girder Bridges*, Structural Engineering Documents 1e, International Association for Bridge and Structural Engineering, 1982. II
- 5.3 Mathivat, J., *The Cantilever Construction of Prestressed Concrete Bridges*, John Wiley and Sons, Inc., New York, 1983. VI
- 5.4 Thürlimann, B., "Considerations for the Design of Prestressed Concrete Bridges," *International Association for Bridge and Structural Engineers, IABSE-Periodica 4/1983, IABSE Proceedings P-70/83*, pp. 237-252.
- 5.5 Virlogeux, M., and M'Rad, A., "Etude d'une Section de Poutre en Elasticité non Linéaire - Application au Béton Armé ou Précontraint, et Aux Sections Mixtes," *Annales de l'Institut du Batiment et des Travaux Publics*, No. 444, May 1986.

- 5.6 Guyon, Y., *Limit-State Design of Prestressed Concrete*, John Wiley and Sons, New York, 1988.
- 5.7 Smith, M. J., and Goodyear, D., "A Practical Look at Creep and Shrinkage in Bridge Design," *Journal Prestressed Concrete Institute*, Vol. 33, No. 3, May/June 1988, pp. 108-121.
- 5.8 Beaupre, R., Powell, L. C., Breen, J. E., and Kreger, M. E., "Deviation Saddle Behavior and design for Externally Post-Tensioned Bridges," Research Report No. 365-2, Center for Transportation Research, The University of Texas at Austin, July 1988.
- 5.9 Shushkewich, K. W., "Approximate Analysis of Concrete Box Girder Bridges," *Journal of Structural Engineering*, American Society of Civil Engineers, Vol. 114, No. 7, July 1988, pp. 1644-1657.
- 5.10 "Box Segmentals Refining Design," *Civil Engineering*, American Society of Civil Engineers, Vol. 59, No. 10, October 1989, pp. 62-64.
- 5.11 Poineau, D., "Durability Assessment from the Design Phase to Execution," IABSE Symposium, Lisbon 1989, pp. 449-460.
- 5.12 Kuesel, T. R., "Whatever Happened to Long-Term Bridge Design," *Civil Engineering*, American Society of Civil Engineers, Vol. 60, No. 2, February 1990, pp. 57-60.
- 5.13 Virlogeux, M., "Non-Linear Analysis of Externally Prestressed Structures," *Fédération Internationale de la Précontrainte*, FIP-XIth International Congress on Prestressed Concrete, June 1990, Hamburg, Germany, pp. 165-193.
- 5.14 Shushkewich, K. W., "Strengthening Concrete Box Girder Bridges," *Journal of Structural Engineering*, American Society of Civil Engineers, Vol. 116, No. 6, June 1990.
- 5.15 Menn, C., *Prestressed Concrete Bridges*, Birkhäuser Verlag, Basel-Boston-Berlin, 1990.
- 5.16 Wium, D. J. W., and Buyukozturk, O., "Problems in Designing Prestressed Segmental Concrete Bridges," *Transportation Research Record 950*, Second Bridge Engineering Conference, Volume 2, Transportation Research Board, ????, pp. 68-75.

X

II

VI. Construction Methods of Segmental Concrete Bridges

- 6.1 Gerwick Jr., B. C., "Bridge Over the Eastern Scheldt," *Journal of the Prestressed Concrete Institute*, Vol. 11, No. 1, February 1966, pp. 53-59.
- 6.2 Pierce, L. F., "Oregon gets a segmental post-tensioned bridge," *Civil Engineering*, American Society of Civil Engineers, Vol. 42, No. 3, March 1972, pp. 67-69.
- 6.3 Henneberger, W., and Breen, J. E., "First Segmental Bridge in the U. S.," *Civil Engineering*, American Society of Civil Engineers, Vol. 44, No. 6, June 1974, pp. 54-57.
- 6.4 Bezzone, A. P., "Pine Valley Creek Bridge a First," *Civil Engineering*, American Society of Civil Engineers, Vol. 44 No. 8, August 1974, pp. 72-75.
- 6.5 Muller, J., "Ten years experience in precast segmental construction," *Journal Prestressed Concrete Institute*, Vol. 20, No. 1, January/February 1975, pp. 28-61.
- 6.6 PCI Committee on Segmental Construction, "Recommended Practice for Segmental Construction in Prestressed Concrete," *Journal of Prestressed Concrete Institute*, Vol. 20, No. 2, March/April 1975, pp. 22-41.
- 6.7 PCI Bridge Committee, "Tentative Design and Construction Specifications for Precast Segmental Box Girder Bridges," *Journal Prestressed Concrete Institute*, Vol. 20, No. 4, July/August 1975, pp. 34-40.
- 6.8 Grant, A., "Incremental Launching of Concrete Structures," *Journal of American Concrete Institute*, August 1975, pp. 395-402.
- 6.9 Gentilini, B, and Gentilini, L., "Precast Prestressed Segmental Elevated Urban Motorway in Italy," *Journal Prestressed Concrete Institute*, Vol. 20 No. 5, September/October 1975, pp. 26-43.
- 6.10 Baur, W., "Bridge erection by launching is fast, safe, and efficient," *Civil Engineering*, American Society of Civil Engineers, Vol. ? No. ?, March 1977, pp. 60-63.
- 6.11 Ballinger, C. A., Podolny Jr., W., and Abrahams, M. J., "A Report on the Design and Construction of Segmental Prestressed Concrete Bridges in Western Europe - - 1977," U. S. Department of Transportation, Federal Highway Administration, Report No. FHWA-RD-78-44, July 1978.
- 6.12 Podolny Jr., W., "An Overview of Precast Prestressed Segmental Bridges," *Journal Prestressed Concrete Institute*, Vol. 24, No. 1, January/February 1979, pp. 56-87.

- 6.13 "Record length bridge designed for utter simplicity (Long Key Bridge)," *Engineering News Record*, April 24, 1980, pp. 30-32.
- 6.14 Lovell, J. A. B., "The Islington Avenue Bridge," *Journal of Prestressed Concrete Institute*, Vol. 25, No. 3, May/June 1980, pp. 32-66.
- 6.15 Barker, J. M., "Construction Techniques for Segmental Concrete Bridges," *Journal of Prestressed Concrete Institute*, Vol. 25, No. 4, July/August 1980, pp. 66-86.
- 6.16 Figg, E. C., "Segmental Bridge Design in the Florida Keys," *Concrete International*, American Concrete Institute, Vol. 2, No. 8, August 1980, pp. 17-22.
- 6.17 Wittfoht, E. H., "Bridges - Construction Technique and Methods (Concrete and Steel)," *IABSE Periodica* No. 2, International Association for Bridge and Structural Engineering, 1980, pp. 48-64.
- 6.18 Faessel, P., Teyssandier, J. P., and Virlogeux, M., "Conception et Construction du Pont D'Ottmarsheim," Report No. 391, *Annales de L'Institut Technique du Batiment et des Travaux Publics*, February 1981.
- 6.19 Smyth, W. J. R., "Byker Viaduct - Britain's First Prestressed Segmental Railway Bridge," *Journal Prestressed Concrete Institute*, Vol. 26, No. 2, March/April 1981, pp. 92-109.
- 6.20 "Concrete's the Choice for Long-Span Bridges," *Concrete International*, American Concrete Institute, Vol. 3, No. 8, August 1981, pp. 19-25.
- 6.21 "Lehnenviadukt Beckenried: Stepping Formwork System Helps Construct Switzerland's Longest Bridge," *Concrete International*, American Concrete Institute, Vol. 3, No. 8, August 1981, pp. 26-33.
- 6.22 Podolny Jr., W., "The Evolution of Cable-Stayed Bridges," *Concrete International*, American Concrete Institute, Vol. 3, No. 8, August 1981, pp. 34-42.
- 6.23 Candrlic, V., "In Yugoslavia... Cantilever Construction of Large Prestressed Concrete Arches," *Concrete International*, American Concrete Institute, Vol. 3, No. 8, August 1981, pp. 43-48.
- 6.24 Harwood, A. C., "Construction of the Columbia River Crossing," *Concrete International*, American Concrete Institute, Vol. 3, No. 8, August 1981, pp. 49-54.
- 6.25 Pickard, S. S., "Houston Ship Channel Bridge," *Concrete International*, American Concrete Institute, Vol. 3, No. 8, August 1981, pp. 55-62.

- 6.26 Quinn, S. B., "Concrete Usage - Houston Ship Channel Bridge Project," Concrete International, American Concrete Institute, Vol. 3, No. 8, August 1981, pp. 63-68.
- 6.27 "Bloukrans Bridge: Africa's Largest Concrete Arch Bridge," Concrete International, American Concrete Institute, Vol. 3, No. 8, August 1981, pp. 69-73.
- 6.28 Fletcher, M. "Orwell Bridge: UK's Largest Prestressed Concrete Span," Concrete International, American Concrete Institute, Vol. 3, No. 8, August 1981, pp. 74-78.
- 6.29 Kane, T. A., Carpenter, J. E., and Clark, J. H., "The West Seattle Bridge: Concrete Answer to Urban Transportation Problem," Concrete International, American Concrete Institute, Vol. 3, No. 8, August 1981, pp. 85-92.
- 6.30 Lamberson, E. A., and Barker, J. M., "Kishwaukee River Bridges," Concrete International, American Concrete Institute, Vol. 3, No. 8, August 1981, pp. 93-101.
- 6.31 Billington, D., "Swiss bridge design spans time and distance," Civil Engineering, American Society of Civil Engineers, Vol. 51, No. 11, November 1981, pp. 42-46.
- 6.32 Prakash Rao, D. S., "New Developments in Bridge Engineering in West Germany," Concrete International, American Concrete Institute, Vol. 4, No. 5, May 1982, pp. 46-52.
- 6.33 Tai, J. C., and Lo, G. K., "I-205 Over Columbia Bridge: Geometric Control for Cast-in-Place and Precast Segmental Box Girder Construction," Transportation Research Record 871, Transportation Research Board, Washington D.C. 1982, pp. 1-8.
- 6.34 Tai, J. C. and Lo, G. K., "Design and Construction of the I-205 Columbia River Bridge - North Channel," International Conference on Short and Medium Span Bridges, Toronto, 1982, pp. 275-288.
- 6.35 Podolny Jr., W., and Mireles, A. A., "Kuwait's Bubiyan Bridge - a 3-D Precast Segmental Space Frame," Journal Prestressed Concrete Institute, Vol. 28, No. 1, January/February 1983, pp. 58-107.
- 6.36 Placidi, M., "Construction of Structures Set into Site by Displacement," International Association for Bridge and Structural Engineers, IABSE-Periodica 2/1983, IABSE Proceedings P-62/83, pp. 89-100.

- 6.37 Raspaud, B., "Le Pont de Bubiyan - Conception de la Structure et Methodes," Association Française pour la Construction, Bulletin Technique, May 1983, pp. 13-23.
- 6.38 Matt, P., "Status of Segmental Bridge Construction in Europe," Journal Prestressed Concrete Institute, Vol. 28, No. 3, May/June 1983, pp.104-125.
- 6.39 Quinn, S., "Record Concrete Box Girder Spans Houston Ship Channel," Civil Engineering, American Society of Civil Engineers, Vol. 53, No. 11, November 1983, pp. 46-50.
- 6.40 Wium, D. J. W., and Buyukozturk, O., "Precast Segmental Bridges - Status and Future Directions," Civil Engineering for Practicing and Design Engineers, Vol. 3, 1984, pp. 59-79.
- 6.41 "Dauphin Island Bridge," Journal of the Prestressed Concrete Institute, Vol. 29, No. 1, January/February 1984, pp. 128-147.
- 6.42 Arnold, C. J., "Salvaging the Zilwaukee," Civil Engineering, American Society of Civil Engineers, Vol. 56, No. 4, April 1986, pp. 46-49.
- 6.43 "Cable Stays Catch On," Civil Engineering, American Society of Civil Engineers, Vol. 56, No. 6, June 1986, pp. 58-61.
- 6.44 "Skyway bridge boasts a record and innovations," Engineering News Record, Vol. 217, No. 11, September 11, 1986, pp. 20-22.
- 6.45 Hurd, M. K., "Segmental box-girder bridge construction," Concrete International, American Concrete Institute, Vol. 8, No. 9, September 1986, pp. 19-27.
- 6.46 Ziadat, G. S., and Waldron, P., "Segmental Construction of Concrete Bridges: A State-of-the-Art Report," Report No. UBCE/C/86/1, University of Bristol, Department of Civil Engineering, December 1986. **V, VII, VIII**
- 6.47 "Zilwaukee Bridge," Concrete International, American Concrete Institute, Vol. 10, No. 5, May 1988, pp. 68-75.
- 6.48 Matt, P., Voumard, J. M., and Thürlimann, B., "Main River Span Structure of the Gateway Bridge," Concrete International, American Concrete Institute, Vol. 10, No. 5, May 1988, pp. 34-43.
- 6.49 Cézard, C., and Servant, C., "Charix Viaduct," International Association for Bridge and Structural Engineering, IABSE 13th Congress, Helsinki, June 6-12, 1988, pp. 63-70.

- 6.50 Percheron, J. C., "Stay Cable Advanced Technology - Wandre Bridge," International Association for Bridge and Structural Engineering, IABSE 13th Congress, Helsinki, June 6-12, 1988, pp. 59-62.
- 6.51 "Structures in Portugal," International Association for Bridge and Structural Engineering, IABSE-Periodica 1/1989, IABSE Structures C-48/49, February 1989.
- 6.52 Moreton, A. J., "Segmental Bridge Construction in Florida - A Review and Perspective," Journal of Precast/Prestressed Concrete Institute, Vol. 34, No. 3, May/June 1989, pp. 38-77.
- 6.53 Hurd, M. K., "Cable-Stayed bridge completed across James River," Concrete Construction, Vol. 34, No. 9, September 1989.
- 6.54 Florida Department of Transportation, *Post-Tensioning Manual - A Guide to Post-Tensioning of Bridges*, October 1989.
- 6.55 Florida Department of Transportation, *Segmental Manual - A Guide to the Construction of Segmental Bridges*, October 1989.
- 6.56 "Segmental Bridges Divide Industry," Engineering News Record, November 2, 1989, pp. 24-27.
- 6.57 Munn, W. D., "Multiple Methods Raise New Segmental Bridge," Highway and Heavy Construction, December 1989, pp. 38-41.
- 6.58 Ingerslev, L., C., F., "Construction of the Bahrain Causeway," Concrete International, American Concrete Institute, Vol. 12, No. 5, May 1990, pp. 25-33.
- 6.59 Moreton, A., "Florida Bridges Beat the Clock," Civil Engineering, American Society of Civil Engineers, Vol. 12, No. 5, May 1989, pp. 74-77.
- 6.60 Percheron, J. C., and Jartoux, P., "Tampico Bridge, México," Fédération Internationale de la Précontrainte, FIP-XIth International Congress on Prestressed Concrete, June 1990, Hamburg, Germany, pp. 117-120.

VII. Temperature Effects

- 7.1 Shiu, K. N., "Seasonal and Diurnal Behavior of Concrete Box- Girder Bridges," Transportation Research Record 982, Transportation Research Council, Washington, D.C., pp. 50-56.
- 7.2 Elbadry, M. M., and Ghali, A., "Nonlinear Temperature Distribution and its Effect on Bridges," International Association for Bridge and Structural Engineers, IABSE-Periodica 3/1983, IABSE Proceedings P-66/83, November 1983.

- 7.3 Imbsen, R. A., Vandershaf, D. E., Schamber, R. A., and Nutt, R. V., "Thermal Effects in Concrete Bridge Superstructures," NCHRP Research Report No. 276, Transportation Research Board, Washington, D.C., September 1985.
- 7.4 Shiu, K. N., and Russell, H. G., "Effects of Time-Dependent Concrete Properties on Prestress Losses," Second International Conference on Short and Medium Span Bridges, Proceedings Volume 2, August 1986, Ottawa, Canada, pp. 3-17.
- 7.5 Priestley, M. J. N., "The Thermal Response of Concrete Bridges," *Concrete Bridge Engineering: Performance and Advances*, Book Edited by R. J. Cope, Elsevier Applied Science, 1987, pp. 143-187.
- 7.6 "Brits control bath water," *Engineering News Record*, p. 12, July 5, 1990. VI
- 7.7 Mirambell, E., and Aguado, A., "Temperature and Stress Distributions in Concrete Box Girder Bridges," *Journal of Structural Engineering*, American Society of Civil Engineers, Vol. 116, No. 9, September 1990, pp. 2388-2409.

VIII. Creep and Shrinkage of Concrete Bridges

- 8.1 Kokubu, M., Goto, Y., Ozaka, Y., Okamura, H., and Momoshima, S., "Measurement of Creep and Shrinkage in Actual Prestressed Concrete Bridges", IABSE Symposium, Madrid, 1970, pp. 19-26. XI
- 8.2 Luciani, L., "Experimental Observations of Prestressed Structures with Reference to Long Term Deformations", IABSE Symposium, Madrid, 1970, pp. 21-27. XI
- 8.3 Keijer, U., "Long-Term Deformations of Cantilever Prestressed Concrete Bridges", IABSE Symposium, Madrid, 1970, pp. 27-34. XI
- 8.4 Jávora, T., "Measurements of Creep, Shrinkage and Temperature Changes in Prestressed Concrete Bridges", IABSE Symposium, Madrid, 1970, pp. 49-57. XI
- 8.5 Price, W. I. J., and Tyler, R. G., "Effects of Creep, Shrinkage and Temperature on Highway Bridges in the United Kingdom," IABSE Symposium, Madrid, 1970, pp. 81-93.
- 8.6 Crespo, A., Croci, G., Morabito, G., Perinetti, U., and Ferretti, A.S., "Mesures de température et de déformations sur un pont bâti en encorbellement," IABSE Symposium, Madrid, 1970, pp. 995-102. XI
- 8.7 Borges, F., Marecos, J., and Trigo J. T., "Creep Effects in some Arch and Cantilever Bridges," IABSE Symposium, Madrid, 1970, pp. 103-114. XI

- 8.8 Le Bourdelles, Y., "Mesures de déformations faites pendant la construction d'un pont en béton précontraint par encorbellement," IABSE Symposium, Madrid, 1970, pp. 146-151.
- 8.9 Zetlin, L., Thornton, C. H., and Lew, I. P., "Design of Concrete Structures for Creep, Shrinkage and Temperature Changes," IABSE Symposium, Madrid, 1970, pp. 269-280.
- 8.10 Marshall, V., and Gamble, W. L., "Time-Dependent Deformations in Segmental Prestressed Concrete Bridges", Research Report No. UILU-ENG-81-2014, Department of Civil Engineering, University of Illinois at Urbana-Champaign, October 1981.
- 8.11 ACI Committee 209, "Prediction of Creep, Shrinkage, and Temperature Effects in Concrete Structures," Design for Creep and Shrinkage of Concrete Structures, Special Publication SP-76, American Concrete Institute, Detroit, Michigan, 1982.
- 8.12 Neville, A. M., *Creep of Plain and Structural Concrete*, London, 1983.
- 8.13 Bryant, A. H., Wood, J. A., and Fenwick, R. C., "Creep and Shrinkage in Concrete Bridges," RRU Bulletin 70, National Roads Board, Wellington, New Zealand, 1984.

XI

XI

IX. Performance of Instrumentation Systems for Structural Engineering

- 9.1 Pauw, A., and Breen, J. E., "Structural and Economic Study of Precast Bridge Units - Instrumentation," Technical Report No. 1, The University of Missouri, Department of Civil engineering, 1957.
- 9.2 Perry, C. C., and Lissner, H. R., *The Strain Gage Primer*, McGraw-Hill Book Company, Inc., New York, Second Edition, 1962.
- 9.3 Reese, L. C., Brown, J. C., and Dalrymple, H. H., "Instrumentation for Measurements of Lateral Earth Pressure in Drilled Shafts," Research Report 89-2, Center for Highway Research, The University of Texas at Austin, September 1968.
- 9.4 Barker, W. R., and Reese, L. C., "Instrumentation for Measurement of Axial Load in Drilled Shafts," Center for Highway Research, The University of Texas at Austin, Research Report No. 89-6, November 1969.
- 9.5 Bakoss, S. L., Burfitt, A. J., and Cridland, L., "The Measurement of Strain in Concrete with the Embedment Type Vibrating Wire Gauge," The New South Wales Institute of Technology, School of Civil Engineering, Civil Engineering Monograph No. C.E. 76/2 M.E., Sydney, Australia, 1976.

- 9.6 Dreyer, H., "Long-Term Measurements in Rock Mechanics by Means of Maihak Vibrating Wire Instrumentation," *Field Measurements in Rock Mechanics, Proceedings of the International Symposium, Zurich, Volume One, April 4-6, 1977*, pp. 109-122.
- 9.7 Kovári, K., Amstad, Ch., and Fritz, P., "Integrated Measuring Technique for Rock Pressure Determination," *Field Measurements in Rock Mechanics, Proceedings of the International Symposium, Zurich, Volume One, April 4-6, 1977*, pp. 289-316.
- 9.8 Butter, C. D., and Hocker, G. B., "Fiber Optics Strain Gauge," *Applied Optics*, Vol. 17, No. 18, September 1978, pp. 2867-2869.
- 9.9 Littlejohn, B. S., "Acceptance Criteria for the Service Behaviour of Ground Anchorages," *Ground Engineering*, Vol. 14, No. 3, April 1981, pp. 26-36.
- 9.10 Sabnis, G. M., Harris, H. G., White, R. N., and Mirza, M. S., *Structural Modeling and Experimental Techniques*, Prentice-Hall, Inc., Englewood Cliffs, N. J., 1983.
- 9.11 "Suggested Method for Surface Monitoring of Movements Across Discontinuities," ISRM, *International Journal of Rock Mechanics and Mining Sciences and Geomechanics Abstracts*, Vol. 21, No. 5, October 1984, pp. 265-276.
- 9.12 Fellenius, B. H., "Ignorance is Bliss," *Geotechnical News*, Vol. 2, No. 4, December 1984, pp. 14-15.
- 9.13 Preston, H. K., "Testing of 7-Wire Strand for Prestressed Concrete -- The State of the Art," *Journal of the Prestressed Concrete Institute*, Vol. 30, No. 3, May-June 1985, pp. 134-155.
- 9.14 Construction Technology Laboratory, "Monitoring with Microcomputers During Construction," *CTL Review*, Vol. 8, No. 3, Fall 1985.
- 9.15 Hanna, T. H., *Field Instrumentation in Geotechnical Engineering*, Trans Tech Publications, First Edition, 1985.
- 9.16 Versnel, W. J., "Compensation of Leadwire Effects with Resistive Straingauges in Multi-Channel Strain Gauge Instrumentation," *Experimental Stress Analysis: Proceedings of the VIIIth International Conference on Experimental Stress Analysis, Amsterdam, The Netherlands, May 12-16, 1986*; Compiled by: Wieringa, H.; Published by: Dordrecht; Boston: Martinus Nijhoff, 1986; pp. 455-464.
- 9.17 Hicklenton, A., "Developments in Fibre Optic Sensors," *New Electronics Journal*, Vol. 20, No. 17, September 1, 1987, pp. 39-40.

- 9.18 Brevet, P., Bot, H., Fleury, A., and Michel, D., "Mise en oeuvre de la précontrainte," *Bulletin de Liaison des Laboratoires des Ponts et Chaussées*, Laboratoire Central des Ponts et Chaussées, No. 153, January 1988, pp. 47-55.
- 9.19 Orsat, P., and Bertel, J. C., "Measurement of Forces Actually Applied on Rebars Anchor-Bolts or Strands with Tensiomag," *International Association of Bridge and Structural Engineering, IABSE Proceedings, 5th Annual International Bridge Conference (IBC)*, June 13-15, 1988, Pittsburgh, Pennsylvania, pp. 51-56.
- 9.20 Dunnicliff, J., *Geotechnical Instrumentation for Monitoring Field Performance*, John Wiley and Sons, Inc., New York, 1988.
- 9.21 Sabris, G. M., Harris, H., White, R. N., and Mirza, S.M., *Structural Modeling and Experimental Techniques*, Prentice-Hall Inc., Englewood Cliffs, NJ, 1988.
- 9.22 Miessler, H. J., and Lessing, R., "Monitoring of Load Bearing Structures with Fiber Optical Sensors," *International Association for Bridge and Structural Engineers, IABSE Symposium, Lisbon*, 1989, pp. 853-858.
- 9.23 Overman, T. R., Hanson, N. W., Rabbat, B. G., Morgan, B. J., Zwiers R. I., and Shiu, K. N., "Techniques for Measuring Existing Long Term Stresses in Prestressed Concrete Bridges - Volume III - Executive Summary," *Construction Technology Laboratories, Report No. FHWA-RD-88-159*, February 1990.
- 9.24 Johnson, M. J., *Fiber Optic Interferometer Sensor for Strain Measurements in High Magnetic Fields and Cryogenic Environments*, M. S. Thesis, The University of Texas at Austin, May 1991.

X. Experimental Tests of Segmental Box Girder Bridges

- 10.1 Kashima, S. and Breen J. E., "Construction and Load Tests of a Segmental Precast Box Girder Bridge Model," *Research Report No. 121-5*, Center for Transportation Research, The University of Texas at Austin, February 1975.
- 10.2 McClure, R. M., and Larson, T. D., "An Experimental Segmental Bridge," *Research Project No. 72-9*, Pennsylvania State University, August 1975.
- 10.3 Ross, E. L., Conway, J. C., McClure, R. M., "Photoelastic Model Studies for an Experimental Segmental Bridge," *The Pennsylvania Transportation Institute, The Pennsylvania State University, Report No. 75-3/FHWA-PA-81-011*, Research Project 75-3, Interim Report, June 1980.
- 10.4 Koretsky, A. V., and Pritchard, R. W., "Critical Assessment of the International Estimates for Relaxation Losses in Prestressing Strands," *University of Queensland, Department of Civil Engineering, Research Report No. CE25*, St. Lucia, Australia, June 1981.

- 10.5 Koseki, K., *Shear Strength of Joints in Precast Segmental Bridges*, M. S. Thesis, The University of Texas at Austin, August 1981.
- 10.6 Fouré, B., "Essais de flexion sur des poutres en béton précontraintes par des câbles extérieurs," Dossier de Recherche 91-017, Centre Experimental de Recherches et D'Etudes du Batiment et des Travaux Publics (CEBTP), Service D'Etude des Structures, January 1984.
- 10.7 Wium, D. and Buyubozturk, O., "Behavior of Precast Segmental Concrete Bridges," Research Report R84-06, Order No. 766, Massachusetts Institute of Technology, Department of Civil Engineering, May 1984.
- 10.8 Bruneau, J., Causse, G., Raspaud, B., and Radiguet, B., "Test Loading of a Concrete Truss", IABSE 12th Congress, International Association for Bridge and Structural Engineering, Vancouver, September 1984, pp. 71-79.
- 10.9 Soongswang, K., *Ultimate Strength of Segmental Box Girders with Unbonded Tendons*, Ph.D. Dissertation, University of Florida, May 1987.
- 10.10 Abdel-Halim, M., McClure, R. M., and West, H. H., "Overload Behavior of an Experimental Precast Prestressed Concrete Segmental Bridge," *Journal of the Prestressed Concrete Institute*, Vol. 32, No. 6, November/December 1987, pp. 102-123.
- 10.11 Yates, D. L., *A Study of Fretting Fatigue in Post-Tensioned Concrete Beams*, M. S. Thesis, The University of Texas at Austin, May 1988.
- 10.12 Buyukozturk, O., Bakhoun, M. M., and Beattie, S. M., "Shear Behavior and Strength of Joints in Precast Concrete Segmental Bridges," Copy of Report Submitted to the *Journal of Structural Engineering of the American Society of Civil Engineers* for possible publication, Massachusetts Institute of Technology, January 1989.
- 10.13 Moore, J. A., *Stay Cable Anchorage System Tests*, M. S. Thesis, The University of Texas at Austin, May 1989.
- 10.14 McGregor, R. J. G., *Evaluation of Strength and Ductility of a Three Span Externally Post-Tensioned Box Girder Bridge Model*, Ph.D. Dissertation, The University of Texas at Austin, August 1989.
- 10.15 Fouré, B. and Martins, P.C. de R., "Flexural Behaviour up to Failure of Externally Prestressed Concrete Beams," *Fédération Internationale de la Précontrainte*, FIP-XIth International Congress on Prestressed Concrete, Hamburg, Germany, June 1990, pp. 195-255.

- 10.16 MacGregor, R. J. G., Kreger, M. E., and Breen, J. E., "Strength and Ductility of a Three-Span Externally Post-Tensioned Segmental Box Girder Bridge Model," External Prestressing in Bridges, American Concrete Institute, Publication SP-120, 1990, pp. 315-338.
- 10.17 Virlogeux, M., "Shear Strength of Beams Made of Precast Segments," Fédération Internationale de la Précontrainte, FIP-XIth International Congress on Prestressed Concrete, Hamburg, Germany, June 1990, pp. 217-236.
- 10.18 Mazurek, D., and DeWolf, J. T., "Experimental Study of Bridge Monitoring Technique," Journal of Structural Engineering, American Society of Civil Engineers, Vol. 116, No. 9, September 1990, pp. 2532-2549.
- 10.19 Radloff, B. J., *Bonding of External Tendons at Deviators*, M.S. Thesis, The University of Texas at Austin, December 1990.
- 10.20 Hindi, A. N., *Enhancing the Strength and Ductility of Post-Tensioned Segmental Box Girder Bridges*, Ph.D. Dissertation, The University of Texas at Austin, December 1990.

XI. Full-Scale Instrumentation Systems

- 11.1 Pauw, A., and Breen, J. E., "Field Testing and Analysis of Two Prestressed Concrete Girders," The University of Missouri Bulletin, Volume 60, Number 52, Columbia Missouri, November 1959.
- 11.2 Kokubu, M., "Deflections of Prestressed Concrete Bridges in Japan," Magazine of Concrete Research, Vol. 24, No. 80, September 1972, pp. 117-126.
- 11.3 Marécos, J. and Castanheta, M. N., "Observations and Testing of a Prestressed Bridge," Memoria No. 439, Laboratorio Nacional de Engenharia Civil, Misnistério das Obras Publicas, Lisboa, Portugal, 1974.
- 11.4 Holman, R. J., "Development of an Instrumentation Program for Studying Behavior of a Segmental Box Girder Bridge," Joint Highway Research Project No. C-36-56T, Report JHRP-77-4, Purdue University, Lafayette, Indiana, March 1977.
- 11.5 Gamble, W. L., "Long-Term Behavior of a Prestressed I-Girder Highway Bridge in Champaign County, Illinois," University of Illinois at Urbana-Champaign, Structural Research Series No. 470, Report No. UILU-ENG-79-2019, Research Project No. FHWA/IL/UI/180, August 1979.
- 11.6 Gamble, W. L., "Field Investigation of Prestressed Reinforced Concrete Highway Bridges", Research Report No. UILU-ENG-80- 2012, University of Illinois at Urbana-Champaign, May 1980.

- 11.7 Russell, H. G., "Field Instrumentation of Concrete Structures", *Full Scale Testing of Structures*, ASTM STP 702, W. R. Schiever, Ed., American Society for Testing Materials, 1980, pp. 63-77.
- 11.8 Pfeil, W., "Twelve Years Monitoring of a Long Span Prestressed Concrete Bridge," *Concrete International*, American Concrete Institute, Vol. 3, No. 8, August 1981, pp.79-84.
- 11.9 Shiu, K. N., Aristizabal-Ochoa, J. D., and Russell, H. G., "Instrumentation of Denny Creek Bridge," Report to State of Washington Department of Transportation, Agreement Y-1837, Construction Technology Laboratories, Portland Cement Association, Skokie, IL, August 1981. **VII, VIII**
- 11.10 Marshall, V., and Gamble, W. L., "Time Dependent Deformations in Segmental Prestressed Concrete Bridges," Research Report No. UILU-ENG-81-2014, SRS-495, University of Illinois at Urbana-Champaign, Department of Civil Engineering, Urbana, IL, October 1981. **VII, VIII**
- 11.11 Sokal, Y. J. and Tyrer, P., "Time Dependent Deformation in Prestressed Concrete Girders: Measurement and Prediction", Research Report No. CE30, University of Queensland, Department of Civil Engineering, November 1981.
- 11.12 Russell, H. G., Shiu, K. N., Gamble, W. L., and Marshall, V. L., "Evaluation and Verification of Time-Dependent Deformations in Postensioned Box-Girder Bridges," Transportation Research record 871, National Research Council, Washington, D.C., 1982, pp. 66-70. **VII, VIII**
- 11.13 Hawkins, N. M., Clark, J. H., "Investigation of Thermal and Live Load Stresses in Denny Creek Viaduct," University of Washington, Report No. 63-1080, Olympia, WA, June 1983. **VII, VIII**
- 11.14 Blight, G., "The Value of Field Measurement in Civil Engineering," *Civil Engineer in South Africa*, Vol. 25, No. 11, November 1983, pp. 597-603.
- 11.15 White, C. D., *Observations and Evaluation of the Composite Wing Girder Bridge at Bear Creek*, M.S. Thesis, The University of Texas at Austin, May 1984.
- 11.16 Richardson, J. E., "Field-Measured Post-Tension Prestress Loss in Stress-Relieved Strands," California Department of Transportation (CALTRANS), Report No. FHWA/CA/SD-84/02, Sacramento, CA, June 1984.
- 11.17 Poston, R. W., Bradberry, T. E., and Breen, J. E., "Load Tests of a Pretensioned Girder Bridge near Happy, Texas," Research Report No. 921-1F, Center for Transportation Research, The university of Texas at Austin, April 1985.

- 11.18 Bradberry, T. E., *Time dependent Deformation of Long Span Prestressed Concrete Beams Having Low Relaxation Strands*, M.S. Report, The University of Texas at Austin, May 1986.
- 11.19 Kelly, D., *Time Dependent Deflections of Pretensioned Beams*, M. S. Thesis, The University of Texas at Austin, August 1986.
- 11.20 Ziadat, G. S., and Waldron, P., "Measurement of Time-Dependent Behaviour in the River Torridge Bridge," Report No. UBCE/C/87/4, University of Bristol, November 1987. **VII, VIII**
- 11.21 Baber, T. T., and Hilton, M. H., "Field Monitoring of the I-295 Bridge Over the James River Bridge -- Instrumentation Installation and Construction Period Studies," Interim Report, Virginia Transportation Research Council (Jointly Sponsored by the University of Virginia and the Virginia Department of Transportation), Charlottesville, Virginia, Report No. VTRC 88-R23, April 1988.
- 11.22 Improta, P. J., "Bridges Surveying by Monitoring Their Dynamic Behavior," International Conference on Monitoring, Surveillance and Predictive Maintenance of Plants and Structures, October 18, 1989, pp. 207-215. **XII**
- 11.23 Markey, I., "Hydrostatic Levelling System for the Measurement of Bridge Deformation," Publication No. 134, Institut de Statique et Structures - Béton Armé et Précontraint (IBAP), Ecole Polytechnique Fédérale de Lausanne, November 1989.
- 11.24 Shields, J., and Saiidi, M. S., "Direct Field Measurement of Prestress Losses in Box Girder Bridges," Report No. CCEER-89-4, Civil Engineering Department, University of Nevada at Reno, December 1989.
- 11.25 Bakht, B., and Jaeger, L. G., "Bridge Testing - A Surprise Every Time," Journal of Structural Engineering, Vol. 116, No. 5, May 1990, pp. 1370-1383.
- 11.26 Saiidi, M. S., Shields, J., and Johnson, R., "Monitoring Prestress Forces in a Box Girder Bridge," NATO Advanced Research Workshop, Baltimore, Maryland, April-May 1990.
- 11.27 Specht, M., and Rosler, M., "The Marienfelde Bridge as a Research Project," Fédération Internationale de la Précontrainte, FIP-XIth International Congress on Prestressed Concrete, Hamburg, Germany, June 1990, pp. B165-B168.
- 11.28 Mazurek, D. F., and DeWolf, J. T., "Experimental Study of Bridge Monitoring Technique," Journal of Structural Engineering, American Society of Civil Engineers, Vol. 116, No. 9, September 1990, pp. 2532-2549.
- 11.29 Favre, R., and Markey, I., "Long-Term Monitoring of Bridge Deformation," Workshop Proceedings, U.S. - European Workshop on Bridges, Baltimore, 1990.

- 11.30 Favre, R., Charif, H., and Markey, I., "Observation a Long Terme de la Déformation des Ponts," Institut de Statique et Structures - Béton Armé et Précontraint (IBAP), Ecole Polytechnique Fédérale de Lausanne, Projet de Recherche 86/88, October 1990.

XII. Bridge Surveillance and Maintenance Programs

- 12.1 Park, S.H., *Bridge Inspection and Structural Analysis: Handbook of Bridge Inspection*, Trenton, NJ, 1980.
- 12.2 Reel, R. S., and Conte, D. F., "Ontario Structure Inspection System," Second International Conference on Short and Medium Span Bridges, Proceedings, Volume 1, August 17-21, 1986, Ottawa, Canada, pp. 309-323.
- 12.3 Andrey, D., *Maintenance des ouvrages d'art: Méthodologie de Surveillance*, Research Report OFR-32/82, Ecole Polytechnique Fédérale de Lausanne, Ph.D. Dissertation, June 1987.
- 12.4 Heath, J.A., "Bridge Inspection for Segmental Concrete Box Girders," Proceedings 5th International Bridge Conference (IBC), June 1988, pp. 126-130.
- 12.5 Poineau, D., "Durability Assessment from the Design Phase to Execution," International Association for Bridge and Structural Engineering, IABSE Symposium, Lisbon, 1989, pp. 449-460.
- 12.6 Gordon, S., "Durability of Highway Bridges," International Association for Bridge and Structural Engineering, IABSE Symposium, Lisbon, 1989, pp. 19-31.
- 12.7 Florida Department of Transportation, *Inspection Manual - A Guide to the Inspection of Segmental Bridges*, May 1990.
- 12.8 Tarricone, P., "Bridges Under Surveillance," Civil Engineering, American Society of Civil Engineers, Vol. 16, No. 5, May 1990, pp. 48-51.

VITA

José Antonio Arréllaga Acosta was born in Asunción, Republic of Paraguay, on February 23, 1964, the son of Víctor Hugo Arréllaga Moreno and María Mercedes Acosta de Arréllaga. José was raised in Asunción, where he initiated his studies in Civil Engineering at the *Facultad de Ciencias Físicas y Matemáticas de la Universidad Nacional de Asunción*. In 1985 he transferred to The University of Texas at Austin and continued with his studies until receiving a Bachelor of Science degree in Civil Engineering in December of 1988. He began his studies for the Masters degree in structural engineering in January of 1989. Currently, José is a partner of a recently formed private consulting engineering firm. José married María F. McGivney in 1990.

Permanent Address: 2002 Bremen St.
 Austin, Texas 78703

This thesis was typed by the author.